

THE CRYSTALLINE ETHER

Third revised and corrected version of the book

*WHAT IF THE UNIVERSE WAS A LATTICE
AND WE WERE ITS TOPOLOGICAL SINGULARITIES ?*

*WHAT IF THE FUNDAMENTAL PRINCIPLES OF THE UNIVERSE
WERE ONLY NEWTON'S AND THERMODYNAMICS LAWS ?*



GÉRARD GREMAUD

May 2021

THE CRYSTALLINE ETHER

Third simplified and illustrated version of the book:

***What if the Universe was a lattice
and we were its topological singularities?***

***And what if the only fundamental principles of the Universe
were Newton's and thermodynamics laws?***

Gérard Gremaud
May 2021



Books published by Gérard Gremaud

Honorary professor of Swiss Federal Institute of Technology of Lausanne (EPFL), Switzerland (gerardgremaud.ch)

L'éther cristallin

- <http://gerardgremaud.ch/>, troisième version revue et corrigée, mai 2021, 334 pages

The crystalline ether

- <http://gerardgremaud.ch/>, third version revised and corrected, May 2021, 318 pages

Théorie de l'éther cristallin

- <http://gerardgremaud.ch/>, troisième version revue et corrigée, mai 2021, 674 pages

Theory of the crystalline ether

- <http://gerardgremaud.ch/>, third version revised and corrected, May 2021, 664 pages

Et si l'Univers était un réseau et que nous en étions des singularités topologiques?

- <http://gerardgremaud.ch/>, deuxième version revue et corrigée, mai 2020, 324 pages

- [Editions Universitaires Européennes](http://www.editions-universitaires-europeennes.com/), première version, avril 2020, 328 pages, ISBN 978-613-9-56428-6

- [ResearchGate](https://www.researchgate.net/publication/354444444), première version, mars 2020, 324 pages

What if the Universe was a lattice and we were its topological singularities?

- <http://gerardgremaud.ch/>, second version revised and corrected, May 2020, 316 pages

- [ResearchGate](https://www.researchgate.net/publication/354444444), first version, March 2020, 316 pages

Univers et Matière conjecturés comme un Réseau Tridimensionnel avec des Singularités Topologiques

- <http://gerardgremaud.ch/>, deuxième version revue et corrigée, mai 2020, 668 pages

- [Amazon](http://www.amazon.com/), Charleston (USA), première version, deux éditions, 2016, 664 pages, ISBN 978-2-8399-1940-1

- [ResearchGate](https://www.researchgate.net/publication/354444444), première version, 2015, DOI: 10.13140/RG.2.1.2266.5682

Universe and Matter conjectured as a 3-dimensional Lattice with Topological Singularities

- <http://gerardgremaud.ch/>, second version revised and corrected, May 2020, 654 pages

- [Amazon](http://www.amazon.com/), Charleston (USA), first version, two editions, 2016, 650 pages, ISBN 978-2-8399-1934-0

- [ResearchGate](https://www.researchgate.net/publication/354444444), first version, 2015, DOI: 10.13140/RG.2.1.3839.4325

Théorie eulérienne des milieux déformables – charges de dislocation et désinclinaison dans les solides

- [Presses polytechniques et universitaires romandes](http://www.pur-editions.com/) (PPUR), Lausanne 2013, 751 pages, ISBN 978-2-88074-964-4

Eulerian theory of newtonian deformable lattices – dislocation and disclination charges in solids

- [Amazon](http://www.amazon.com/), Charleston (USA) 2016, 312 pages, ISBN 978-2-8399-1943-2

On n'a peut-être pas encore prêté assez d'attention [à] l'utilité dont cette étude [de la Géométrie] peut être pour préparer comme insensiblement les voies à l'esprit philosophique, et pour disposer toute une nation à recevoir la lumière que cet esprit peut y répandre [...]. Bientôt l'étude de la Géométrie conduira [...] à la vraie Philosophie qui par la lumière générale et prompte qu'elle répandra, sera bientôt plus puissante que tous les efforts de la superstition.

Jean le Rond D'Alembert, article "Géométrie" de *L'Encyclopédie*, 1772

Si toute la connaissance scientifique disparaissait dans un cataclysme, quelle phrase unique pourrait préserver le maximum d'information pour les générations futures? Comment pourrions-nous leur transmettre au mieux notre compréhension du monde? Je propose: "Toutes choses sont faites d'atomes, petites particules animées d'un mouvement incessant, qui s'attirent lorsqu'elles sont distantes les unes des autres, mais se repoussent lorsqu'on les force à se serrer de trop près". Cette seule phrase contient, vous le verrez, une quantité énorme d'information sur le monde, pour peu que l'on y mette un peu d'imagination et de réflexion.

Richard P. Feynman

The more the universe seems comprehensible, the more it also seems pointless. But if there is no solace in the fruits of our research, there is at least some consolation in the research itself [...] The effort to understand the universe is one of the very few things that lifts human life a little above the level of farce, and gives it some of the grace of tragedy.

Steven Weinberg, from "*The First Three Minutes*"

Imagination is more important than knowledge. For knowledge is limited to all we now know and understand, while imagination embraces the entire world, and all there ever will be to know and understand.

Albert Einstein

Pensons, il en restera toujours quelque chose!
(Think, there will always be something left!)

Snoopy

Table of contents

Introduction

Storytelling of this book	1
In search of a Theory of Everything	4

1 - Eulerian theory of deformable Newtonian lattices

Coordinate systems to describe the deformation of a medium	7
What is a solid lattice?	10
Definition of local quantities in Euler coordinates	13
Distortions of a solid lattice	15
Geometro-kinetics of a lattice in Euler coordinates	19
Geometro-compatibility of lattice distortions	20
Contortions of a solid lattice	23
Geometro-compatibility of lattice contortions	26
Newtonian dynamics and Eulerian thermokinetics	26
Physical properties specific to the medium	29
Potentialities of the Eulerian representation of deformable media	33

2 - Dislocation and disclination charges in a lattice

Macroscopic concept of plastic distortion charges	35
Definition of density and flow tensors of plastic charges	39
Macroscopic concept of plastic contortion charges	42
Quantified dislocations in a lattice	46
Dissociation of quantified dislocations	50
Quantified dislocation membranes	53
Quantified disclinations in a lattice	54
Solid lattices with axial symmetry	59
Quantified dislocation and disclination loops in a lattice	62
Clusters of dislocations, disclinations and dispirations	66
Flow of dislocation charges	69
Force of Peach and Kohler acting on a line of dislocation	73
Potentialities of the Eulerian representation of charged lattices	74

3 - The «Cosmological Lattice» and its properties

The «cosmological lattice» and its Newton's equation	79
Transverse and longitudinal perturbations in the cosmological lattice	81

<i>Curvature of the wave rays by a singularity of expansion and black holes</i>	85
<i>Cosmological expansion-contraction of a sphere of perfect lattice and dark energy</i>	88

4 - Maxwell's equations of electromagnetism

<i>Separability of Newton's equation partly «rotational» and partly «divergent»</i>	97
<i>«Maxwellian» behavior of the rotational part of Newton's equation</i>	99
<i>Analogy between rotation charges and electric charges</i>	100
<i>Analogy between anelasticity of the lattice and dielectricity of the matter</i>	101
<i>Analogy between mass transport in the lattice and magnetism in the matter</i>	102
<i>The complete analogy with the physical quantities of the electromagnetism theory</i>	103
<i>The effects of volume expansion of the lattice in the absolute frame of GO</i>	103
<i>Are there "magnetic monopoles" in this analogy?</i>	103
<i>Are there "vector electric charges" in this analogy?</i>	104
<i>The importance of this analogy</i>	106

5 - Topological singularities within the cosmological lattice

<i>Separability of Newton's equation in three partial equations in the presence of a topological singularity</i>	107
<i>Applications and potentialities of the separability of Newton's equation</i>	109
<i>Elastic energy, kinetic energy and inertial mass of a dislocation</i>	110
<i>Spherical singularities of rotation and curvature charges</i>	113
<i>Charge, fields, energies and mass of a twist disclination loop (BV)</i>	114
<i>«Coulomb-type» interaction between localized topological singularities with rotation charges</i>	117
<i>Charge, fields, energies and mass of a loop of prismatic edge dislocation (BC)</i>	117
<i>Charge, fields, energies and mass of a slip loop of dislocation (BM)</i>	118
<i>"Topological bricks" to build the world of elementary particles</i>	120
<i>The various physical properties transported by loop singularities</i>	121

6 - Lorentz transformation and special relativity

<i>Mobile charges and Lorentz transformations</i>	124
<i>Contraction of lengths in the direction of movement</i>	125
<i>Time dilation of a mobile cluster of topological singularities</i>	126
<i>Lorentz transformation for a mobile «object» linked by the rotation fields</i>	128
<i>Uniqueness of the Lorentz transformation according to the background expansion</i>	129
<i>Relativistic energies of the screw and edge dislocations</i>	130
<i>Equations of the relativistic dynamics of a screw or edge dislocation</i>	133
<i>Relativistic energies of loop singularities and spherical charges of rotation</i>	134
<i>About the probable explanation of the paradox of the electron energy</i>	136
<i>Peach and Koehler force and relativistic force of Lorentz</i>	137
<i>About the role of «ether» played by the cosmological lattice</i>	137
<i>Experiment of Michelson-Morley in the cosmological lattice</i>	141

<i>The relativistic composition of velocities and the absence of an absolute notion of simultaneity for the local observers HS</i>	141
<i>Doppler-Fizeau effects between moving singularities in the cosmological lattice</i>	144
<i>About the famous paradox of the Twins of Special Relativity...</i>	
<i>... which is only one in the minds of the HS observers</i>	147

7 - Gravitational fields of the topological singularities

<i>Expansion perturbations by a singularity with a given distorsion energy</i>	149
<i>Expansion perturbations by a singularity with a given curvature charge</i>	153
<i>Expansion perturbations by a singularity with a given rotation charge</i>	155
<i>About the gravitational fields of macroscopic singularities</i>	158
<i>Macroscopic vacancy located in the lattice, real gravitational black hole</i>	159
<i>Macroscopic interstitial located in the lattice, true anti-singularity of the macroscopic vacancy</i>	162
<i>About the possible analogy between vacancy singularities and black holes and between interstitial singularities and neutron stars</i>	163
<i>Perturbations of the expansion associated with the twist disclination loop (BV)</i>	165
<i>Perturbations of the expansion associated with the edge prismatic loop (BC)</i>	166
<i>Perturbations of the expansion associated with the mixed slip dislocation loop (BM)</i>	168
<i>About the various properties of the elementary topological loops</i>	169

8 - Newtonian gravitation and general relativity

<i>Newtonian gravitational interaction of clusters of twist disclination loops</i>	171
<i>The local rulers and clock of an HS observer</i>	174
<i>Analogies and differences from general relativity</i>	181
<i>About the formal analogy between the 3D spatial curvature equation of the cosmological lattice and the Einstein's equation of the 4D field of curvature in general relativity</i>	183
<i>About the dependence of the topological singularities on the expansion of the lattice</i>	185
<i>All of the gravitational interactions between the various singularities of the lattice</i>	188

9 - Cohesion of the edge-screw dispirations and the weak force

<i>Long-range and short-range interactions between a twist disclination loop (BV) and an edge dislocation loop (BC)</i>	193
<i>Coupling energy of a screw-edge dispiration loop (BVC) formed by a twist disclination loop (BV) and an edge dislocation loop (BC)</i>	195
<i>About the analogy with the weak interaction of Standard Model of elementary particles</i>	196

10 - Matter-antimatter asymmetry and its cosmological evolution

<i>About the constitution and the asymmetry of matter and anti-matter</i>	200
<i>Effects of the cosmological expansion of the lattice on gravitational interactions</i>	201

<i>A plausible scenario of cosmological evolution of topological singularities in a perfect cosmological lattice</i>	204
<i>About the famous «dark matter» of astrophysicists</i>	210
<i>About the Hubble's constant</i>	211
<i>About the «redshift» of galaxies</i>	212
<i>About the «cooling» mechanism of the cosmic microwave background</i>	214

11 - Quantum Physics

<i>Relativistic wave equation of gravitational expansion field fluctuations beyond the quantum decoherence limit</i>	215
<i>Gravitational perturbations of a massive singularity at relativistic speed</i>	219
<i>Schrödinger's equation of gravitational perturbations of a massive singularity moving at non-relativistic speed in a variable potential</i>	221
<i>The standing wave equation of a singularity placed in a static potential</i>	223
<i>About the interpretation of the wave function of gravitational fluctuations</i>	224
<i>Superposition of topological singularities, bosons, fermions and exclusion principle</i>	227
<i>Demystifying quantum physics</i>	230

12 - Spin of the topological loops

<i>About the non-existence of a static internal field of perturbations of expansion within a loop of twist disclination (BV)</i>	233
<i>Classic rotation of a twist disclination loop (BV)</i>	235
<i>Quantification of the angular momentum of the screw loop</i>	236
<i>About the completely classic interpretation of the spin of a particle</i>	238
<i>About the problem of the spin value of a topological loop</i>	239
<i>About the link between the concepts of bosons, fermions and spin</i>	240
<i>About the very important consequences of the existence of spin on the cosmological behavior of the lattice</i>	240

13 - Standard model of particles and strong force

<i>The current Standard Model of elementary particles</i>	241
<i>Leptons and quarks</i>	242
<i>Fundamental interactions and gauge bosons</i>	243
<i>Electromagnetic interaction and quantum electrodynamics</i>	243
<i>Weak interaction and electroweak theory</i>	243
<i>Strong interaction and quantum chromodynamics theory</i>	245
<i>Particle masses and Higgs boson</i>	247
<i>The problems of the standard model which already have solutions in the theory of the perfect cosmological lattice</i>	248
<i>The problems of the standard model which have not yet been explained in the theory of the perfect cosmological lattice</i>	249
<i>A "colored" face centered cubic lattice with specific stacking and rotation rules to explain the first family of quarks and leptons of the standard model</i>	250

Existence of quarks due to combining a screw disclination loop with an edge dislocation loop	253
Existence of intermediate gauge bosons	255
Weak interaction between quarks via intermediate bosons	256
Existence of localized "baryons" and «mesons, formed by 3 and 2 dispirations	257
The strong force and its asymptotic behavior	260
Strong interaction between quarks via the gluon gauge bosons	260
The constitution of neutrino and anti-neutrino leptons	261
The constitution of electron and positron leptons	263
Weak interaction of leptons and intermediate bosons of the standard model	265
An attempt to explain the three families of quarks and leptons	266
About the possibility of invoking the stacking fault energy between axial dense planes	267
The constitution of neutrino families	268
The constitution of electron families	270
The constitution of quark families	270
About the interest of the analogy between the «colored» cosmological lattice and the standard model	272
Still open questions about the «colored» cosmological lattice model and its analogy with the standard model	274

14 - Photons, Vacuum Fluctuations, Multiverses and Gravitons

Transverse rotation wave packets: the photons	277
About the possible properties of transverse rotation wave packets	280
Localized longitudinal gravitational fluctuations	282
Random microscopic fluctuations and quantum vacuum fluctuations	284
Is it possible to form stable oscillatory gravitational fluctuations?	285
Stable macroscopic gravitational oscillations in an infinite cosmological lattice and Multiverses	286
Quantified microscopic gravitational oscillations: the "gravitons"	288

Conclusion

About the central role of Newton's equation of the cosmological lattice	291
About the perfectly innovative role of the curvature charge	292
About the importance of the microscopic structure of the cosmological lattice	293
Still unclear points about the Crystalline Ether	294
About the unifying power of our Crystalline Ether Theory	295
About the epistemology and the consequences of this essay	295

Glossary

297

Mathematical and physical symbols

301

THE CRYSTALLINE ETHER

Introduction

Storytelling of this book

"What if the Universe was a crystal?" was the question that came to my mind little by little forty years ago when I was preparing a course for physics students in their fourth year of study. At that time, with a degree in physics-engineering and a doctorate in physics, I was pursuing research in *dislocation dynamics* at the Swiss Federal Institute of Technology of Lausanne, and as part of this research activity, I also had to participate in teaching. The course I was responsible for was directly related to my research and was called *physics of dislocations*. Dislocations are defects in arrangement in the crystal structure of solids, such as metals. And it is the movements of these structural defects which explain a good part of the macroscopic properties of deformation of crystalline solids, hence the importance of describing them theoretically and studying them experimentally.

When preparing for my course for the first time, I decided to teach a very theoretical mathematical approach to dislocations developed by M. Zorawski¹. Unfortunately, this approach is very complicated, because it uses Riemann differential geometry to describe the spatio-temporal evolution of dislocations in local infinitesimal frames, approach involving all the very heavy mathematical artillery of general relativity (metric tensor and symbols of Christoffel). This first version of my course was a bitter failure. This approach not only hid the whole reality of the behavior of dislocations behind an armada of very complicated mathematical objects (tensors), but it also very quickly provoked strong repulsion from students, but also from the professor.

During the second year of teaching this course, I therefore decided to completely change my approach to dislocations, basing it on a more usual description of the deformations of solids, using the classic Lagrange coordinate system and formalizing at best the physical properties of the medium, which is generally not very well done in most courses in the theory of continuous media.

By teaching this theory from year to year, and by perfecting the presentation of my course each time, I saw intriguing analogies appear with other theories of physics. The first analogy that appeared was surprising, as it involved *Maxwell's theory of electromagnetism*. And the analogy became over the years more and more clear and obvious, because it was not limited only to an analogy with one of the two pairs of Maxwell's equations in a vacuum, but it was also generalized to the various phenomenologies encountered in electromagnetism, such as *dielectric polarization* and *magnetization of matter*, as well as *charges and electric currents*.

It is by taking inspiration from the literature that I also showed in my course that it was

¹ M. Zorawski, «*Théorie mathématique des dislocations*», Dunod, Paris, 1967.

possible to calculate *the rest energy* E_0 of dislocations, which corresponds to the elastic energy of deformation E_{def} stored in the lattice by their presence and their kinetic energy E_{cin} , which corresponds to the kinetic energy of the particles of the lattice mobilized by their movement, which then allowed them to be assigned a *mass* M_0 of *virtual inertia* which satisfies relationships perfectly similar to the famous equation $E_0 = M_0 c^2$ of Einstein's special relativity, but which was obtained here in a completely classic way, that is to say without appealing to a principle of relativity. In addition, the dynamics of high velocity dislocations also satisfied the principles of special relativity and Lorentz transformations.

The analogy with Maxwell's equations was already very astonishing by the simple fact that it was initially postulated that the solid lattice satisfied a very simple dynamic, purely Newtonian, in the laboratory of the experimenter, while the dislocations, responsible for the plastic deformations of the solid, were necessarily subject to a relativistic dynamic within the solid, obligation due to the set of Maxwell equations governing the deformations of the medium. Therefore, I came to the very paradoxical conclusion that the relativistic dynamics of dislocations is in fact nothing more than a consequence of the perfectly classic Newtonian dynamics of the elastic solid lattice in the laboratory of the experimenter.

The numerous analogies which appeared during the preparation of my course between the theory of deformable solid media and the theories of electromagnetism and special relativity were sufficiently surprising and remarkable to not fail to tickle any open and somewhat scientific mind. But it was clear that these analogies were far from perfect. It was therefore very tempting to analyze these analogies in more depth and try to find out how to perfect them. This is what led me to work on this subject, in my spare time and for forty years, and finally to propose several theoretical books developing on the one hand an original approach to the deformation of solids² using coordinates of Euler instead of the coordinates of Lagrange, and on the other hand a revolutionary approach of the Universe³ based on the deepening, the improvement and the understanding of the analogies between the theory of the deformation of crystalline solids and the great theories of modern physics such as Maxwell's equations, special relativity, Newtonian gravitation, general relativity, modern cosmology, quantum physics and the standard model of elementary particles.

It is quite remarkable to be able to deduce all the great theories of modern physics from a logical development based exclusively on the simple concepts that are, from a physical point of view, the three main principles of classical physics, namely Newtonian dynamics (Newton's equation), the first principle of thermodynamics (conservation of the total energy of a system) and the second principle of thermodynamics (the existence of a physical quantity, entropy, measuring the disorder of a system), and from a mathematical point of view, the detailed

² G. Gremaud, *"Théorie eulérienne des milieux déformables – charges de dislocation et désinclinaison dans les solides"*, Presses polytechniques et universitaires romandes (PPUR), Lausanne (Switzerland) 2013, 751 pages, ISBN 978-2-88074-964-4

G. Gremaud, *"Eulerian theory of newtonian deformable lattices – dislocation and disclination charges in solids"*, Amazon, Charleston (USA) 2016, 312 pages, ISBN 978-2-8399-1943-2

³ G. Gremaud, *"Univers et Matière conjecturés comme un Réseau Tridimensionnel avec des Singularités Topologiques"*, Amazon, Charleston (USA) 2016, 664 pages, ISBN 978-2-8399-1940-1

G. Gremaud, *"Universe and Matter conjectured as a 3-dimensional Lattice with Topological Singularities"*, Amazon, Charleston (USA) 2016, 650 pages, ISBN 978-2-8399-1934-0

description of the spatio-temporal evolution of a lattice thanks to an original geometry based on Euler coordinates.

But if the basic principles of my approach are very simple and quite classic, the developments leading to find the great theories of modern physics from these principles are long, quite difficult and very theoretical, with many mathematics formulas. They are therefore not an easy approach, even for physicists, and especially if these are not versed in the field of solid state physics and their deformations. This is why I undertook to write this new book in which I have the ambition to make known, if possible with the minimum of mathematics, the ins and outs of my approach, in order to familiarize physicists and all people passionate about knowing the Universe at the simplicity and elegance of my original approach to it on some simple and very classic basic concepts.

I must note here that the existence of analogies between the mechanics of continuous media and the physics of defects and the theories of electromagnetism, special relativity and gravitation is by far not my own idea. Indeed, it had already been the subject of numerous publications before I was concerned about it. Excellent reviews on this subject have been published, notably by Whittaker⁴ in 1951 and by Unzicker⁵ in 2000.

For example, Nye⁶ initiated in 1953 the use of differential geometries to introduce topological defects such as dislocations in deformable continuous media, and for the first time made the connection between the dislocation density tensor and the curvature of the lattice. On the other hand, Kondo⁷ in 1952 and Bilby⁸ in 1954 have independently shown that dislocations can be identified with a crystalline version of 1922 Cartan's concept⁹ of twisting a continuum.

And this approach was formalized in great detail by Kröner¹⁰ in 1960, who also proposed in 1980 that the existence of extrinsic point defects, which can be considered as extra-material, could be identified with the presence of matter in the universe¹¹ and be introduced consequently in the form of Einstein equations, which would lead to a purely Riemannian differential geometry in the absence of dislocations. He also proposed that intrinsic point defects (vacancies, interstitials) could be approached by a non-metric part of an affine connection. Finally, he also considered that the introduction of other topological defects such as disclinations could call on even more complex higher-order geometries, such as Finsler or Kawaguchi geometries.

⁴ S. E. Whittaker, «A History of the Theory of Aether and Electricity», Dover reprint, vol. 1, p. 142, 1951.

⁵ A. Unzicker, «What can Physics learn from Continuum Mechanics?», arXiv:gr-qc/0011064, 2000

⁶ J.F. Nye, *Acta Metall.*, vol. 1, p. 153, 1953

⁷ K. Kondo, *RAAG Memoirs of the unifying study of the basic problems in physics and engineering science by means of geometry, volume 1. Gakujutsu Bunken Fukyu- Kay, Tokyo, 1952*

⁸ B. A. Bilby, R. Bullough and E. Smith, «Continuous distributions of dislocations: a new application of the methods of non-riemannian geometry», *Proc. Roy. Soc. London, Ser. A* 231, p. 263–273, 1955

⁹ E. Cartan, *C.R. Akad. Sci.*, 174, p. 593, 1922 & *C.R. Akad. Sci.*, 174, p. 734, 1922

¹⁰ E. Kröner, «Allgemeine Kontinuumstheorie der Versetzungen und Eigenspannungen», *Arch. Rat. Mech. Anal.*, 4, p. 273–313, 1960

¹¹ E. Kröner, «Continuum theory of defects», in «physics of defects», ed. by R. Balian et al., *Les Houches, Session 35*, p. 215–315. North Holland, Amsterdam, 1980.

Kröner's analogies between the mechanics of continuous media and the great modern theories of physics are undoubtedly the most famous. However, none of this previous research had gone as far in highlighting analogies as the approach presented in this book.

In search of a Theory of Everything

One of the fundamental problems of modern physics is the search for a Theory of Everything capable of explaining the nature of space-time, what matter is and how matter interacts. Since the 19th century, physicists have sought to develop theories of unified fields, which should consist of a coherent theoretical framework capable of taking into account the various fundamental forces of nature. Some attempts to find a unified theory include:

- *The "Great Unification"* which brings together the electromagnetic interaction forces, the weak forces and the strong forces,
- *Quantum Gravity, Quantum Loop Gravitation, and String Theories*, which seek to describe the quantum properties of gravity,
- *Supersymmetry*, which proposes an extension of space-time symmetry connecting the two classes of elementary particles, bosons and fermions,
- *The Theories of Strings and Superstrings*, which are theoretical structures integrating gravity, in which the point particles are replaced by one-dimensional strings whose quantum states describe all the types of elementary particles observed,
- *M Theory*, which unifies five different versions of string theories, with the surprising property that extra-dimensions are required to ensure its consistency.

However, none of these approaches is yet capable of explaining in a consistent manner and at the same time the electromagnetism, relativity, gravitation, quantum physics and the elementary particles observed. Many physicists believe that the 11-dimensional M Theory is the Theory of Everything. However, there is not a broad consensus on this point and there is currently no candidate theory capable of calculating experimental quantities known as the fine structure constant or the mass of the electron. Particle physicists hope that the future results of current experiments - the search for new particles in large accelerators and the search for dark matter - will still be necessary to define a Theory of Everything.

But these researches seem to have really stagnated for about 40 years, and many physicists now have serious doubts about the suitability of these theories. On this subject, I strongly advise readers to consult among others the books of Smolin¹², Woit¹³ and Hossenfelder¹⁴. Since the 1980s, thousands of theoretical physicists have published thousands of scientific articles that are generally accepted in peer-reviewed journals, even if these papers have contributed absolutely nothing new to the explanation of the Universe and solve none of the current

¹² Lee Smolin, «*The trouble with Physics*», Penguin Books 2008, London, ISBN 978-0-141-01835-5
 Lee Smolin, «*La révolution inachevée d'Einstein, au-delà du quantique*», Dunod 2019, ISBN 978-2-10-079553-6
 Lee Smolin, «*Rien ne va plus en physique., L'échec de la théorie des cordes*», Dunod 2007, ISBN 978-2-7578-1278-5

¹³ Peter Woit, «*Not Even Wrong, the failure of String Theory and the continuing challenge to unify the laws of physics*», Vintage Books 2007, ISBN 9780099488644

¹⁴ Sabine Hossenfelder, «*Lost in Maths*», Les Belles Lettres 2019, ISBN 978-2-251-44931-9

mysteries of physics. An enormous amount of energy has been mobilized to develop these theories, which are becoming very remote from the physical reality of our world. It is a race to publish more and more esoteric articles and to search for a form of "mathematical beauty" at the expense of "physical reality". Moreover, huge amounts of money have been invested in this research, to the detriment of fundamental research in other areas of physics, in the form of building increasingly complex machines. And, to the despair of experimental physicists, the results obtained have brought almost nothing new to high-energy physics, contrary to the "visionary" and optimistic predictions of the theorists.

In this book, the problem of unifying physical theories is dealt with in a radically different way. Instead of trying to build a unified theory by tinkering with an assembly of existing theories, making them more complex, even adding strange symmetries and additional dimensions for their "mathematical beauty", I start exclusively from the most classic fundamentals concepts of physics that are Newton's equation and the first two principles of thermodynamics. Using these fundamental principles, and by developing an original geometry based on the Euler coordinates, I come, by a purely logical and deductive path, to suggest that the Universe could be a crystal, a three-dimensional lattice, elastic and massive, and that the constituent elements of Ordinary Matter could be structural defects (hereinafter called topological singularities) of this crystal lattice, namely various loops of dislocation and disclinations which we will describe in detail. For an isotropic face-centered cubic lattice satisfying Newton's law, and with specific assumptions on its elastic properties, I find that the behaviors of this lattice and its topological singularities gather "all" the physics known today, by making appear spontaneously *very strong and often perfect analogies with all the great current physical theories* of the Macrocosm and the Microcosm, such as *Maxwell's Equations, Special Relativity, Newtonian Gravitation, General Relativity, Modern Cosmology and Quantum Physics*.

But this approach does not only find analogies with other theories of physics, it also proposes quite original, new and simple explanations to many physical phenomena that are still quite obscure and poorly understood at the present time by physics, such as the meaning and deep physical interpretation of *cosmological expansion, electromagnetism, special relativity, general relativity, quantum physics, and particle spin*. It also offers explanations of what *quantum decoherence, dark energy, dark matter, black holes*, and many other phenomena really are.

The detailed development of this approach also leads to some very innovative ideas, among which the most important is *the appearance of the curvature charge*, which is an unavoidable consequence of the treatment of a solid lattice and its topological singularities in Euler coordinates. This concept does not appear at all in all modern theories of physics, whether in general relativity, quantum physics or in the Standard Model, whereas in our approach this concept provides explanations for many obscure points of these theories, such as *weak force, matter-antimatter asymmetry, the formation of galaxies, the segregation between matter and antimatter within galaxies, the formation of gigantic black holes in the heart of galaxies, the apparent disappearance of antimatter in the Universe, the formation of neutron stars, the concept of dark matter, the bosonic or fermionic nature of particles*, etc.

Finally, by studying face-centered cubic lattices with special symmetries called axial, symbolically represented by "colored" 3D lattices, one can identify a lattice structure whose

loops of topological singularities perfectly coincide with the complex zoology of all elementary particles of the Standard Model, and one also finds simple physical explanations of the weak and strong forces of the Standard Model, with all their specific properties.

This approach, published in my second book *"Universe and Matter Conjectured as a Three-Dimensional Network with Topological Singularities"*³, does not pretend to present a Theory of All which would already be fully developed and usable, but it should and could by against proving to be extremely fruitful in giving simple explanations to modern physical theories whose deep meaning it is difficult, if not impossible, to understand, but also and above all to define close links and unifying bridges between the various major theories of modern physics.

The aim of this book is therefore to make this approach known to an informed and interested public, by approaching it in the simplest possible way, on the basis of numerous figures, by explaining it *"with the hands"* and by trying to avoid as much as possible the development of the underlying mathematical equations. On the other hand, I think that it is important to highlight the most fundamental equations of theory in figures, but without it being necessary to understand them. Regarding the organization of the content of the book, I tried to follow as closely as possible the plan of the initial theoretical book, so that those interested could refer directly to the complete mathematical treatments it contains.

In this book, I begin by autonomously summarizing the theory² published initially in 2013, which methodically laid the foundations for an original approach to solid lattices by Euler coordinates, and which also introduced in detail the concept of charge of dislocation and disclination within a crystal lattice, a concept which makes it possible to quantify structural defects, topological singularities, which can appear on the microscopic scale of such a lattice.

On the basis of this original approach of solid lattices and their topological singularities, I deduce a set of fundamental and phenomenological equations which makes it possible to treat in a very rigorous way the macroscopic spatio-temporal evolution of a solid Newtonian lattice deforming in the absolute space of the laboratory of an observer outside this lattice.

I then introduce an imaginary lattice, with rather special elastic and structural properties, the concept of which was imagined and published in 2016 in my second book¹, and which I termed a *"cosmological lattice"*. Initially, this lattice was imagined with a simple cubic structure, which forced me to do some perilous acrobatics to describe the three families of elementary particles of the standard model. But in this new version of 2021, I introduce a *face-centered cubic lattice*, which I poetically call the *crystalline ether*, which was suggested to me by my friend Willy Benoit, and which allows to describe much more judiciously the three families of elementary particles of the standard model. With a few well-chosen conjectures, the Newton equation of this lattice and the topological singularities that it may contain present a set of very surprising properties, which will progressively show strong and surprising analogies with all the major current physical theories, as summarized in the table of contents .

Chapter 1

Eulerian theory of deformable Newtonian lattices

To describe the spatio-temporal evolution of the deformation of a solid lattice, it is first necessary to define a reference system for making space and time measurements in the laboratory. For this, we have the choice between several possible coordinate systems, and we will choose here *the Euler coordinate system* for several reasons which will be explained in detail. Following this choice, it becomes possible to describe how the deformation of a lattice can be characterized by *distortions* and *contortions*. But to quantify these distortions and contortions, it will be necessary to use mathematical objects called *scalars*, *vectors* and *tensors*. We will therefore try to explain simply these mathematical objects, and why we systematically use *a vector representation of tensors*, which has undeniable advantages over the purely tensorial representation, if only by the possibility of using powerful formalism of a mathematical tool called *vector analysis*. This crucial choice makes it possible to fairly easily obtain equations which ensure the solidity of the lattice, known as *geometro-compatibility equations*, and equations which make it possible to describe the kinetics of the deformation, known as *geometro-kinetic equations*.

The basic concepts of physics, namely *Newtonian dynamics* and *Eulerian thermokinetics*, can then be introduced in this topological context. With all these ingredients, it then becomes possible to describe a number of specific behaviors of deformable solid lattices, such as *elasticity*, *anelasticity*, and *self-diffusion*.

Coordinate systems to describe the deformation of a medium

If an observer, who we will call hereafter *Great Observer GO*, wishes to describe in his laboratory the evolution of a certain continuous medium which moves in space by translation and rotation, and which, moreover, can deform at over time (figure 1.1), it must first define the kinetic behavior of the medium. Taking as *a basic axiom* that the evolution of the medium in space and time satisfies *the principle of additivity of velocities*, namely that the velocity of an object moving at velocity v_1 with respect to another moving object at velocity v_2 in the laboratory will have a velocity $v_1 + v_2$ in the laboratory, we will then have to deal with kinetics satisfying *the transformation of Galileo*, and called *Galilean kinetics*. In this case, the observer **GO** can describe this spatio-temporal evolution on the basis of an absolute reference system placed in his laboratory. This frame of reference is composed of *an orthonormal Euclidean coordinate system* $Ox_1x_2x_3$, that is to say of three rules of unit length, oriented perpendicularly to each other and represented by three arrows which are called the base vectors $(\vec{e}_1, \vec{e}_2, \vec{e}_3)$ of the coordinate system, and of a universal clock ensuring that time t is measured identically everywhere in the laboratory (figures 1.1 and 1.2).

To describe the spatio-temporal evolution of a deformable continuous medium, the observer then has several possibilities among which *the Lagrange coordinate system*, used to describe

the deformation of solids, and *the Euler coordinate system*, used in general to describe the hydrodynamics of fluids.

To simply and completely describe the spatio-temporal evolution of a solid continuous medium, the observer **GO** can use *the Lagrange coordinate system*. First, it performs a marking of the solid material medium at the initial instant $t = 0$ using a grid of points P_0 .

Then, he can define a stationary reference frame $Ox_1x_2x_3$ in his laboratory. By providing this fixed frame $Ox_1x_2x_3$ with unit length rules $(\vec{e}_1, \vec{e}_2, \vec{e}_3)$, and by orienting it judiciously with respect to the initial position of the medium at the instant $t = 0$, it can measure the position of all the points P_0 of the medium at the initial instant $t = 0$ using of arrows, vectors¹ \vec{r} .

At a point $t > 0$ in time, a point P_0 in the middle will have moved to P , and the observer can then connect the point P_0 to the point P using an arrow, the vector \vec{u} which is called *the displacement vector* of point P_0 . As this vector depends on the initial position \vec{r} of the point P_0 and time t , the set of vectors $\vec{u}(\vec{r}, t)$ identifying all the points of the medium is called *the displacement field* of the medium in Lagrange coordinates.

The Lagrange coordinate system is therefore based on the description of the evolution in space and time of *the vectors* $\vec{u}(\vec{r}, t)$ of *the displacement field* defined above, knowing the

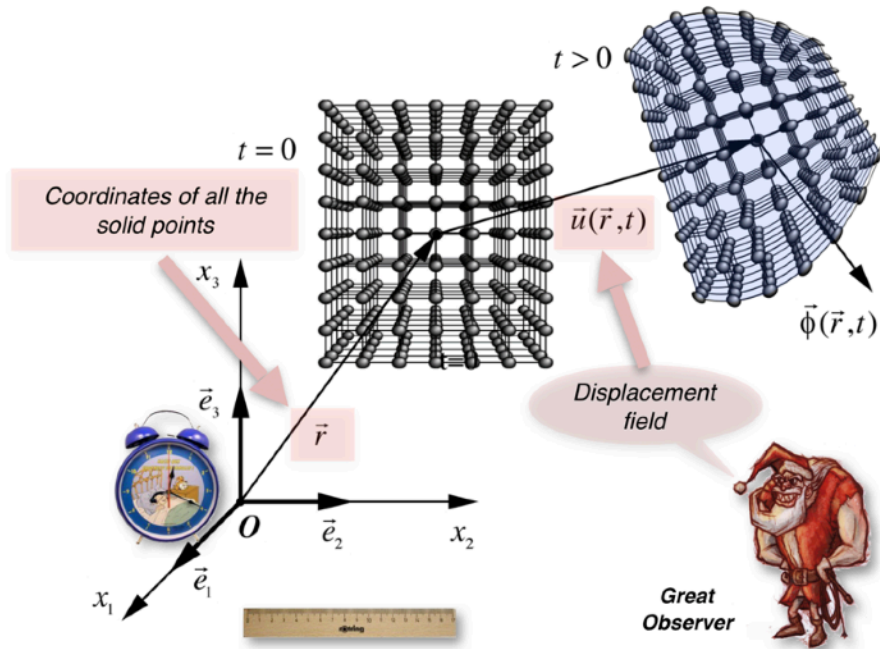
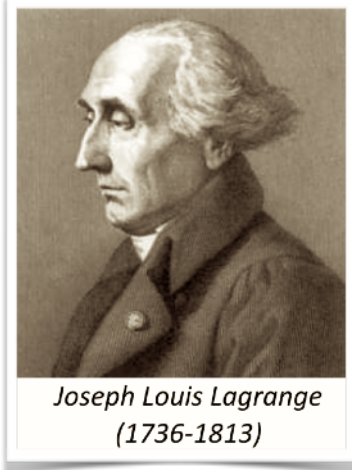


Figure 1.1 - The Lagrange coordinates

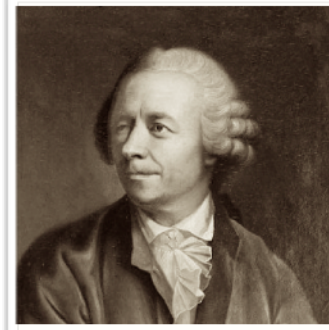
¹ **Vector:** a vector is a mathematical object corresponding to an arrow oriented in space. A vector actually represents a physical quantity described by three numbers which correspond respectively to the lengths of the three projections of the arrow on the axes $Ox_1x_2x_3$ of the coordinate system. We speak of a vector field when a vector physical quantity takes different values at all points in space and over time.

coordinates \vec{r} of all the points of the initial solid in the fixed frame $Ox_1x_2x_3$ of the laboratory of the observer, as illustrated in figure 1.1.

By using previously the expression of *continuous medium*, one appealed to an intuitive concept, namely that a medium presents, on the *macroscopic scale* where it is observed, neither discontinuous structure in the static state, nor appearance of discontinuities, such as tears, local ruptures or cavity formations during its spatio-temporal evolution.

From the macroscopic observation of the behavior of the medium, and in particular of *the continuity of the displacement field* \vec{u} , it is possible to attribute qualifiers to the medium observed. If the medium presents a perfectly continuous displacement field during its spatio-temporal evolution, it is qualified as *solid medium*. It then has the macroscopic property of having its own form which is difficult to modify.

If, on the other hand, the medium has a discontinuous displacement field \vec{u} , forming over time an inextricable entanglement, it is qualified as a *fluid medium*. This has the macroscopic property of flowing and must therefore be kept in a container whose shape it follows. In this case, the displacement field \vec{u} of the Lagrange coordinates loses all physical significance, and only *the vector velocity* $\vec{\phi}(\vec{r}, t)$ of the fluid located at the instant t at the space coordinate \vec{r} of the absolute reference frame retains a physical meaning. This definition of the movements of the medium by the observer **GO** is called *the Euler coordinate system*.



Leonhard Euler
(1707-1783)

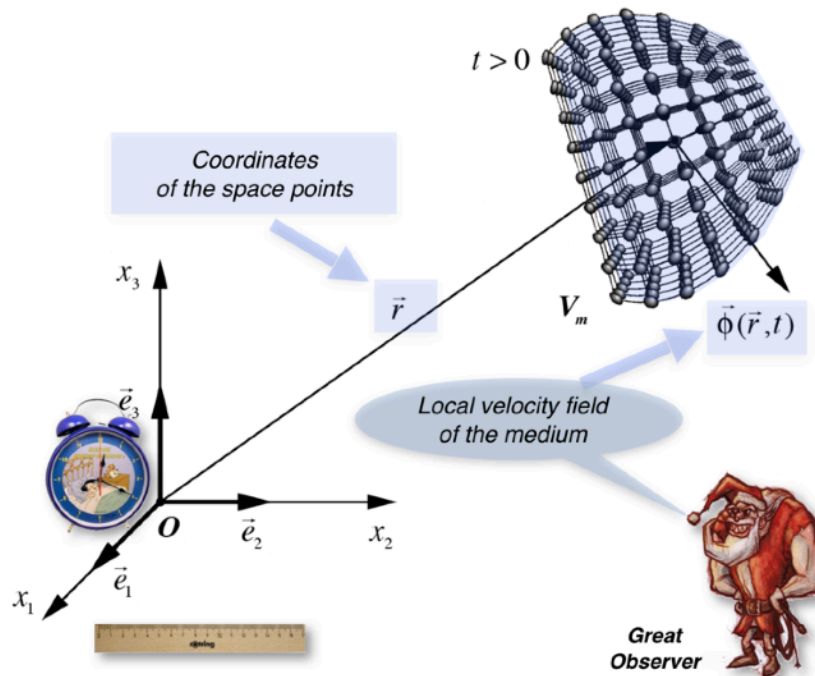


Figure 1.2 - The Euler coordinates

The Euler coordinate system is therefore based on the description of the evolution in space and time of the vectors of *the velocity field* $\vec{\phi}(\vec{r}, t)$ of the points of the fluid or solid medium located at the space \vec{r} and time t coordinates in the absolute coordinate system $Ox_1x_2x_3$ of the observer **GO** laboratory (figure 1.2).

What is a solid lattice?

The concept of continuous medium defined above only applies when this medium is observed *on a macroscopic scale*. Indeed, an enlargement of the same medium on *a sufficiently microscopic scale* will reveal a discontinuous collection of objects, to which we will attribute in the following *the generic name of particles* (for example corpuscles, atoms, molecules, etc.). We logically conclude that the global phenomenological properties observed at the macroscopic scale where the medium appears continuous are in fact *statistical effects* resulting from the large number of particles interacting with each other at the microscopic scale.

The enlargement of the medium also makes it possible to define certain important microscopic characteristics of the medium, such as *its structure*, that is to say the way in which the particles which compose it are assembled, and *its chemical composition*, that is to say the nature of the particles that compose it.

A continuous medium will be said to be solid when, on the microscopic scale, it corresponds to a collection of particles such that the identity of the nearest neighbors of a given particle does not change over time. In other words, each particle is connected to its closest neighbors by *elastic bonds* which prevent it from moving at a great distance from these. Consequently, only relative movements at a short distance from its closest neighbors are allowed to it via the elasticity of the bonds. Under the effect of these bonds, it is said that the particles then form a *solid lattice*.

It is possible to define different classes of solid lattices, according to the arrangement of the particles with respect to each other. If the arrangement of the particles presents a well-established order, which is repeated at great distance by translation of an elementary cell, we speak of a lattice of *crystal structure*. For example, the three-dimensional lattices drawn in figures 1.1 and 1.2 are obtained by the translation of a cubic unit cell, and they present a perfect order both at long distance and at short distance. The same is true of the two-dimensional lattice shown in figure 1.3a, which is obtained by translation in space of a hexagonal cell.

Certain solid lattices can present arrangements of particles having no order at long distance, but only *a certain order at short distance*. We speak in this case of an *amorphous lattice structure*. The two-dimensional example shown in figure 1.3 (b) represents an amorphous lattice of particles, obtained by tiling the surface with pentagons, hexagons and irregular heptagons, whose sides have a fixed length. The short-range order of the amorphous lattice is reflected in the fact that each of the particles has exactly three closest neighbors.

There can also exist solid lattices whose arrangement of particles does not present an order by translation at long distance, but *a certain order by rotation*. In this case, we are talking about *a lattice of quasi-crystalline structure*, the example of which in figure 1.3 (c) clearly shows the absence of order by long-distance translation. This lattice is obtained by two-dimensional tiling using two different types of rhombuses with different angles at the top (in this case, we speak of *Penrose tiling*). At first glance, this lattice seems amorphous. But the more detailed analysis of

figure 1.3 (d) shows that the particles are aligned on parallel lines between them. The distances between particles aligned on a straight line, as well as the distances between parallel straight lines, are not regular. There are in fact five preferred directions for the orientation of these alignments of particles. This two-dimensional quasi-crystalline structure therefore has a form of symmetry *by rotation of order five*, which is prohibited in the case of a crystalline structure obtained by translation of a basic pattern.

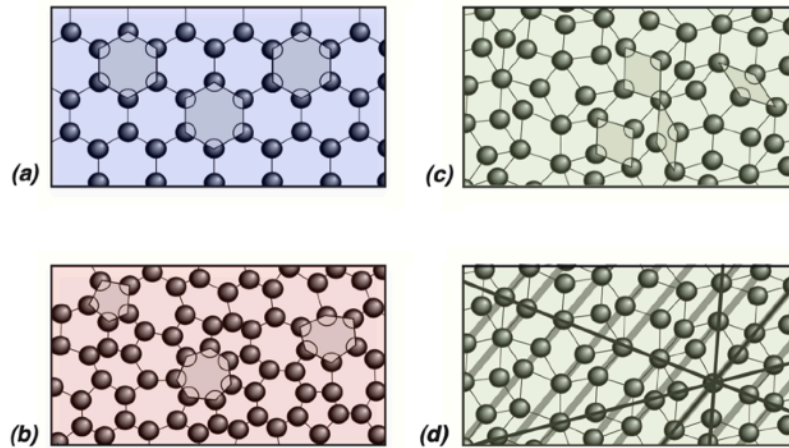


Figure 1.3 - Two-dimensional crystalline lattice (a), amorphous lattice (b) and quasi-crystalline lattice (c) , (d)

The examples given in figure 1.3 are two-dimensional representations. It is therefore still necessary to generalize these concepts to three-dimensional space. In three dimensions, the crystal lattices are formed by the translation of a three-dimensional elementary cell which is called *the unit cell of the lattice* (figure 1.4). The crystal lattices can be classified according to the operations of rotational symmetry, reflection and inversion with respect to a point which it is possible to apply to the elementary unit cell of the lattice. These symmetry operations lead to the existence of fourteen different lattices, called *Bravais lattices*, which are shown in Figure 1.4. These fourteen Bravais lattices can be further broken down into *seven crystalline systems* (triclinic, monoclinic, orthorhombic, tetragonal, rhombohedral, hexagonal and cubic) by considering the way in which space is paved by the elementary unit cell. For some of these seven crystalline systems, there may be different types of lattices (*P*, *C*, *I* or *F*), which correspond to the different patterns of filling of the elementary unit cell with particles.

It is interesting to note that the pattern of filling of a unit cell by the particles can lead to different values of the number of alternative sites specific to each unit cell and which can contain a bound particle. For example, in the case of the cubic structures represented in figure 1.4, the number of sites specific to a unit cell is 1 for the simple cubic system, 2 for the centered cubic system and 4 for the cubic system with centered faces.

In the case of non-ordered solid media, such as amorphous media, quasi-crystalline media or polycrystalline media with very fine grains, the notion of lattice unit cell no longer has any meaning. On the other hand, the concept of lattice site retains a precise physical meaning, even if there is no single elementary unit cell.

In the case of an ordered solid lattice, structural defects may appear in the regular assembly of the lattice particles. These structural defects have various origins, such as irregularities in the chemical species of the objects making up the lattice, or topological singularities, that is to say irregularities in the topological structure of the lattice, such as dislocations or disclinations which will be discussed later, and they can be classified into point, linear or planar defects according to their topology in the lattice.

It is also by observations of the dynamics at the microscopic scale, during the macroscopic spatio-temporal evolution of the lattice, that it will be possible to understand the objective reasons for certain macroscopic behaviors. For example, we will see that there are close links between the macroscopic deformation properties of ordered lattices and the lattice unit cell distortions induced by the presence of mobile topological singularities within the lattice, such as dislocations or disclinations.

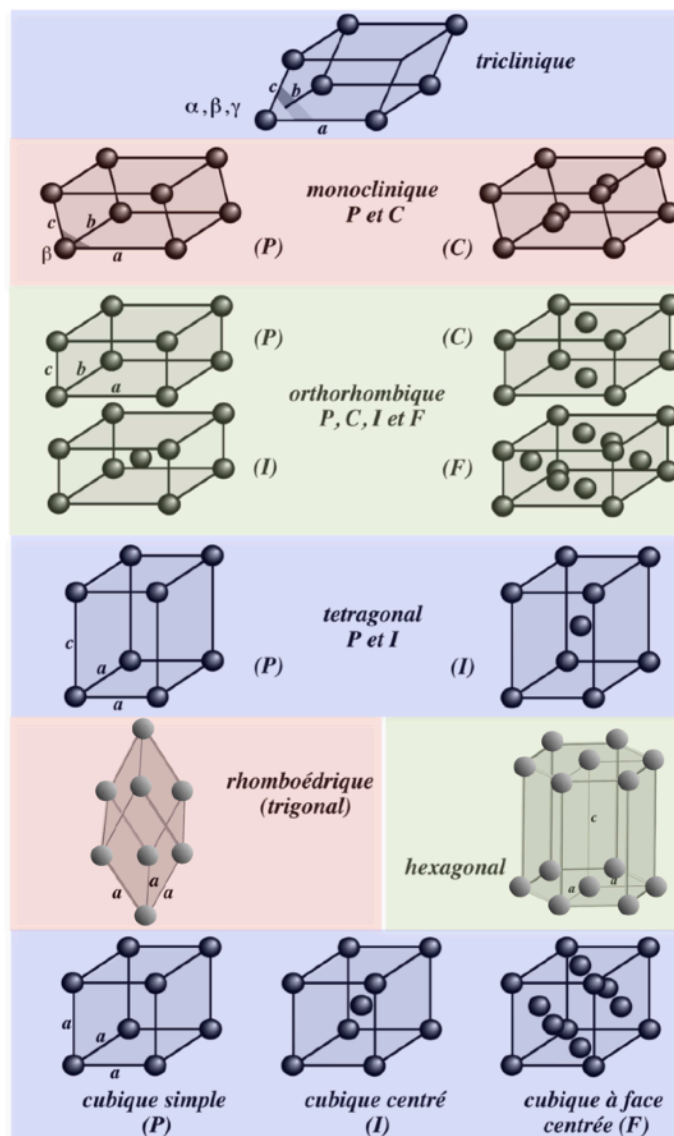


**Figure 1.4 - The seven crystalline systems
and the fourteen Bravais lattices**

In conclusion, a complete description of the spatio-temporal evolution of a lattice which can be considered as continuous on the macroscopic scale cannot absolutely do without the description of the phenomena occurring on the microscopic scale. The search for a theory describing the macroscopic spatio-temporal evolution of a deformable continuous lattice must therefore be based on the definition of mean macroscopic fields (scalar, vector and tensorial in nature) deduced from a statistical description of the dynamics at the microscopic scale of a multitude of objects interacting with each other.

To describe a solid lattice, it is therefore perfectly possible to use the Lagrange coordinate system or the Euler coordinate system. However, using Lagrange coordinates to describe deformable solids presents a number of inherent difficulties. From a mathematical point of view, mathematical objects (tensors) describing the deformations of a continuous solid in Lagrange coordinates are always very complicated (of order greater than one in the spatial derivatives of the components of the displacement field), which leads to a mathematical formalism very difficult to manage when a solid presents strong distortions (deformations and rotations). To these mathematical difficulties are added physical difficulties when it comes to introducing certain known properties of solids. Indeed, the Lagrange coordinate system becomes practically unusable, for example when it is necessary to describe the temporal evolution of the microscopic structure of a solid lattice (phase transitions) and of its structural defects (point defects, dislocations, disclinations, joints, etc.), or if it is necessary to introduce certain physical properties of the medium (thermal, electrical, magnetic, chemical, etc.) resulting in the existence in real space of scalar, vector or tensorial fields. Given the complexity of the calculations obtained in the case of the Lagrange coordinate system, which is however generally used to describe solids, it was desirable to try to develop the description of solids using the Euler coordinate system, which is generally used to describe fluids. This approach to deformable solids by Euler coordinates, which is ultimately much simpler and much more rigorous than that obtained with Lagrange coordinates, was developed and published in 2013 in the book "*Eulerian theory of deformable media*"².

Definition of local quantities in Euler coordinates

In the case of a collection of particles in space in the liquid or solid state, each particle i has its own velocity represented by a vector \vec{v}_i (figure 1.5). To determine *an average local velocity* of the particles, you need to fix a small volume element V_f centered on the space coordinate \vec{r} , then measure the velocities \vec{v}_i of all the particles contained in the fixed volume V_f .

If the instantaneous number of particles in this volume V_f is equal to N , and that N is sufficiently large, the average velocity $\vec{\phi}$ at the place \vec{r} and at the time t is defined by the average of the velocities \vec{v}_i taken on all the particles contained in V_f .

If an average velocity $\vec{\phi}$ other than zero is measured, it also means that, for each particle, it is possible to find a *fluctuation* $\Delta\vec{v}_i$ at average velocity $\vec{\phi}$ by the relation $\Delta\vec{v}_i = \vec{v}_i - \vec{\phi}$.

² G. Gremaud, "Théorie eulérienne des milieux déformables – charges de dislocation et désinclinaison dans les solides", Presses polytechniques et universitaires romandes (PPUR), Lausanne (Switzerland) 2013, 751 pages, ISBN 978-2-88074-964-4

G. Gremaud, "Eulerian theory of newtonian deformable lattices – dislocation and disclination charges in solids", Amazon, Charleston (USA) 2016, 312 pages, ISBN 978-2-8399-1943-2

In the case of a solid lattice, the existence of an average velocity $\vec{\phi}(\vec{r}, t)$ other than zero implies that the solid lattice of particles is subjected to a *collective movement*. The velocity $\vec{\phi}(\vec{r}, t)$ therefore represents the average local velocity of movement of the particles linked to the lattice sites, therefore the average velocity of the lattice sites (figure 1.2), while the $\Delta\vec{v}_i$ are the velocity fluctuations of the particles linked to the lattice around each of these sites. For example, in a real solid, such fluctuations are due to the disordered movements of *the thermal agitation* of the particles, which are in direct relation with *the temperature of the medium*.

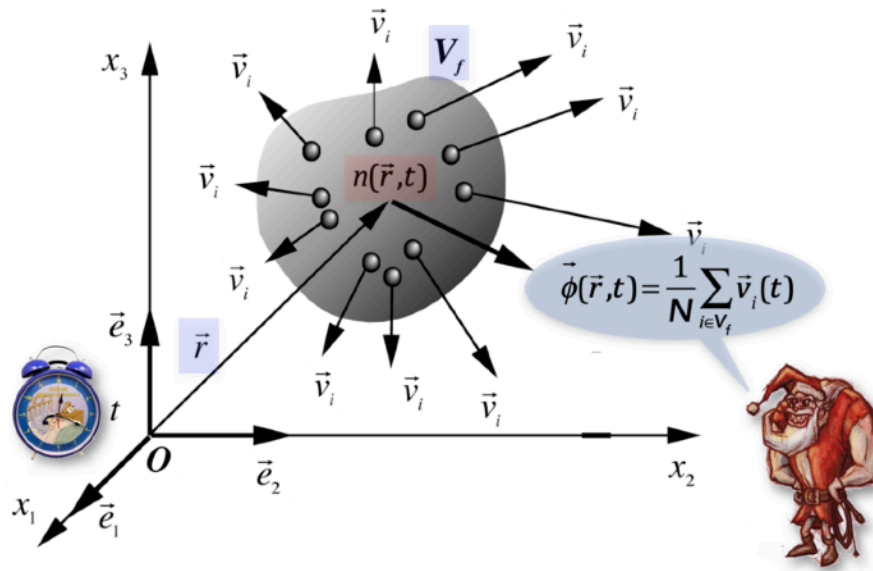


Figure 1.5 - Velocity and average local densities of a medium

Apart from the average local velocity $\vec{\phi}(\vec{r}, t)$ of a solid lattice, there is another quantity which will be called upon to play a fundamental role in Euler coordinates: it is *the volume density* of elementary substitutional sites of the lattice, which will be written with the symbol n , and which represents *the number of lattice sites contained in the volume unit* of the lattice. In the case of figure 1.5, this number n represents then the number of particles contained in the volume V_f when one chooses a volume V_f equal to the unit. This choice implies then to define all the physical quantities characterizing the solid lattice like average values taken on each site in the lattice. It is also clear that, in the case of unordered lattices, the quantity n can also be related to the density of elementary sites of the unordered lattice.

The *volume density* $n(\vec{r}, t)$ of substitutional sites of the solid lattice presents a direct link with the notion of volume expansion of the medium, since $n \rightarrow 0$ for intense expansions and $n \rightarrow \infty$ for intense contractions. This notion of expansion of the lattice volume can be expressed even better by introducing a quantity v defined as the inverse of n , that is to say $v = 1/n$. Indeed, this quantity v has for dimension a volume. It represents *the average volume occupied by a solid lattice site*. This volume v translates well the notion of volume expansion of the medium, since $v \rightarrow \infty$ for intense expansions and $v \rightarrow 0$ for intense contractions.

But it is even more interesting to introduce a dimensionless value using *the natural logarithm* of v thanks to the relation $\tau = -\ln(n/n_0) = \ln(v/v_0)$. There appears then a *dimensionless*

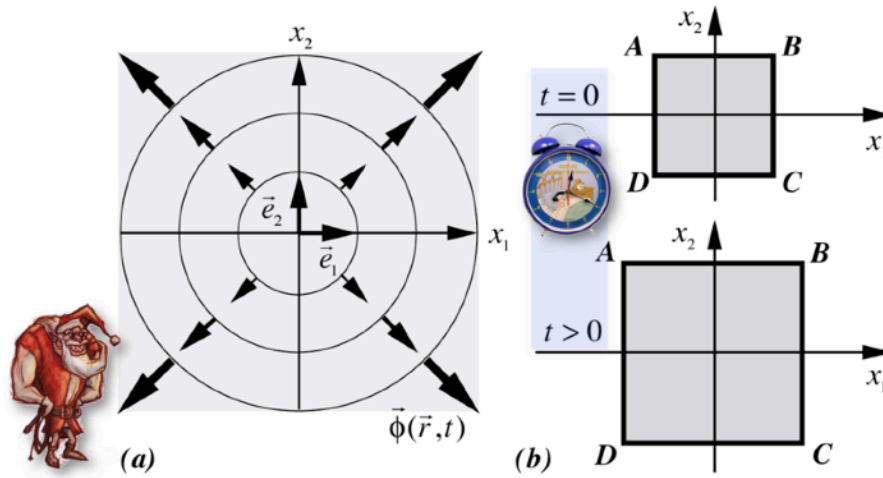


Figure 1.6 - Volumic expansion of the medium

scalar³ $\tau(\vec{r}, t)$ which will be called *scalar of volume expansion*, depending on the coordinates of space \vec{r} and time t within the lattice, and this time perfectly measuring the notion of volume expansion of the lattice, since $\tau \rightarrow \infty$ for intense expansions (when $v \rightarrow \infty$), $\tau \rightarrow -\infty$ for intense contractions (when $v \rightarrow 0$) and $\tau \rightarrow 0$ when $v \rightarrow v_0$. By the construction of the scalar τ , the constants v_0 and n_0 introduced here can be adjusted so that the scalar τ is zero when the lattice is in the state of expansion of rest. Figure 1.6 illustrates an example of velocity fields which leads to a uniform volume expansion of the medium which goes from a certain value of τ at the instant $t=0$ to a greater value of τ at the instant $t>0$, without the volume expansion τ depending on the place where it is measured.

Distortions of a solid lattice

In the presence of a non-zero velocity field $\vec{\phi}(\vec{r}, t)$ in space, a lattice can present movements which do not lead to any deformation, such as *the global translation* of the medium (figure 1.7a) or *the global rotation* of the medium (figure 1.7b).

But there can also exist non-zero velocity fields $\vec{\phi}(\vec{r}, t)$ in space which lead to *real deformations* of the medium, such as for example *the volume expansion* of the medium described above (figure 1.6), *the pure shear* with zero volume expansion of the medium (figure 1.8) or *the zero volume expansion elongation* of the medium (figure 1.9). There may also appear much more complicated velocity fields leading for example to local rotations with non-uniform shearing of the medium (Figure 1.10a) or to non-uniform expansions of the medium which lead to an expansion which depends not only on time, but also space coordinates (figure 1.10b).

In the presence of a non-homogeneous velocity field $\vec{\phi}(\vec{r}, t)$ in space, a lattice can therefore present, in addition to a global translation and a global rotation, movements corresponding to all kinds of deformation. To explain in detail the behaviors of global and local rotation and the

³ **Scalar:** a scalar is a mathematical object corresponding to a physical quantity described by a single number. We speak of a scalar field when a scalar physical quantity takes different values at all points in space and over time.

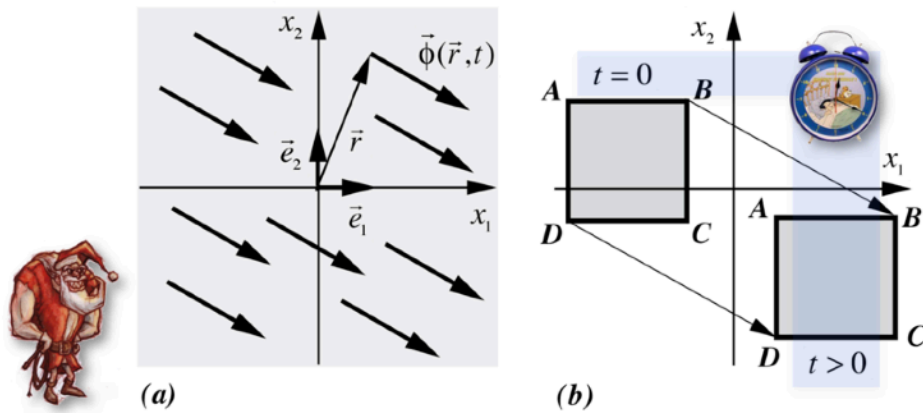


Figure 1.7a - Global translation of the medium

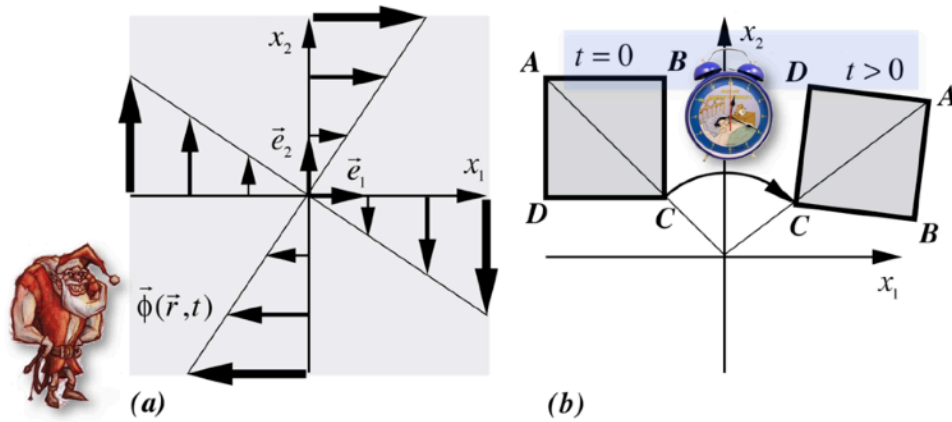


Figure 1.7b - Global rotation of the medium

behaviors of deformations, which will be called generically *distortions of the lattice*, it is necessary to introduce topological quantities having to translate these distortions.

An elegant way of proceeding in Euler coordinates is to note that the scalar volume expansion field τ defined above is already a scalar topological quantity which perfectly describes the volume expansion of the medium. We can then show that this scalar is in fact deductible from a more complicated topological quantity, namely *a tensor⁴ of second order* which is called *the tensor of distortion* β_{ij} . A tensor of order two is a mathematical object represented by an array 3 of 3 of nine different numbers (figure 1.11).

These nine numbers are then sufficient to describe perfectly *the set of global and local rotations and deformations* of the solid lattice. But as the manipulation of this tensor is mathematically quite complicated, and especially since it generally camouflages the real physical behavior of the medium, we choose an entirely original way of representing it in the

⁴ **Second order tensor:** second order tensor is a mathematical object represented by an array 3 of 3 of nine different numbers. A tensor of order two actually represents a physical quantity described by nine numbers. It can be very convenient to represent a tensor of order two using three vectors in the Euler co-ordinate system. We speak of a tensor field of order two when a tensorial physical quantity takes different values at all points in space and over time.

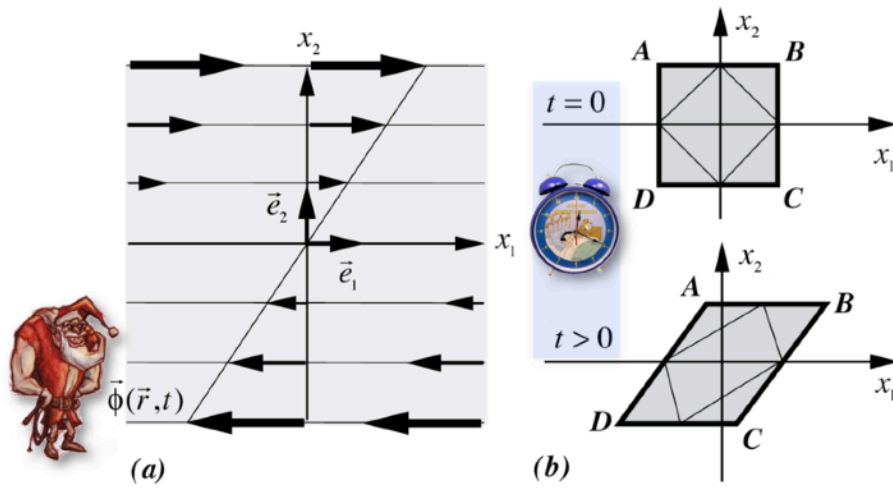


Figure 1.8 - Pure shear of the medium

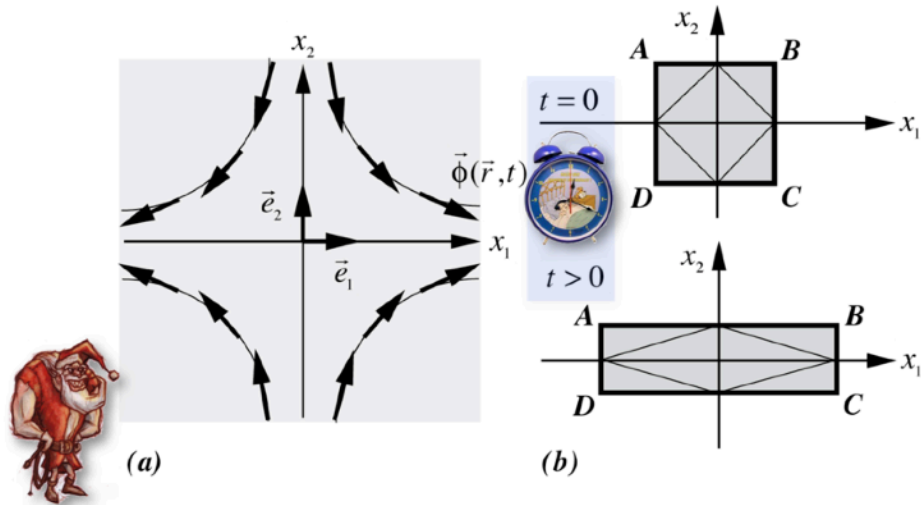


Figure 1.9 - Elongation of the medium without volumic expansion

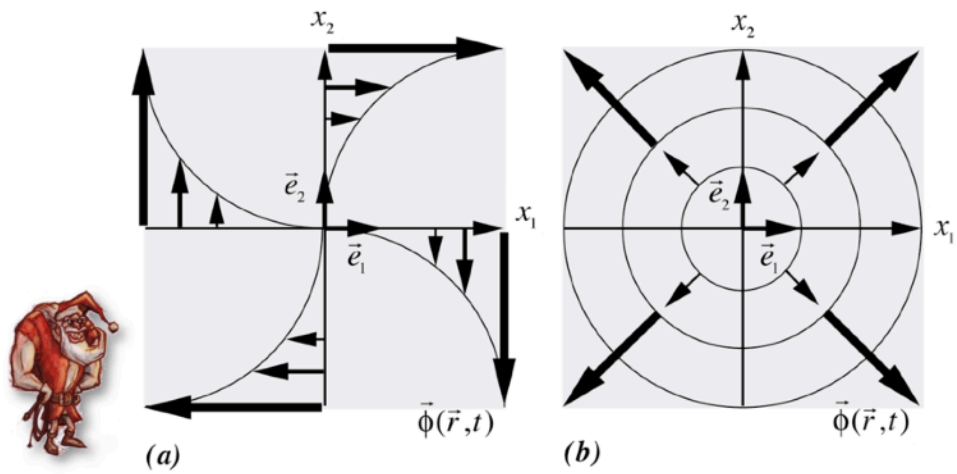


Figure 1.10 - Non-uniform local rotations (a) and expansions (b) of the medium

form of three vectors. Thus, the tensor field of lattice distortion β_{ij} will be represented for convenience by a *field of three vectors* $\vec{\beta}_1, \vec{\beta}_2, \vec{\beta}_3$, remembering that a vector is an arrow oriented in space composed of three numbers. This *vectorial representation of the tensor fields* is completely original and extremely powerful, because it makes it possible mathematically to call upon the spatial operators of *the vector analysis*, and it then considerably simplifies the physical interpretation of the tensor fields.

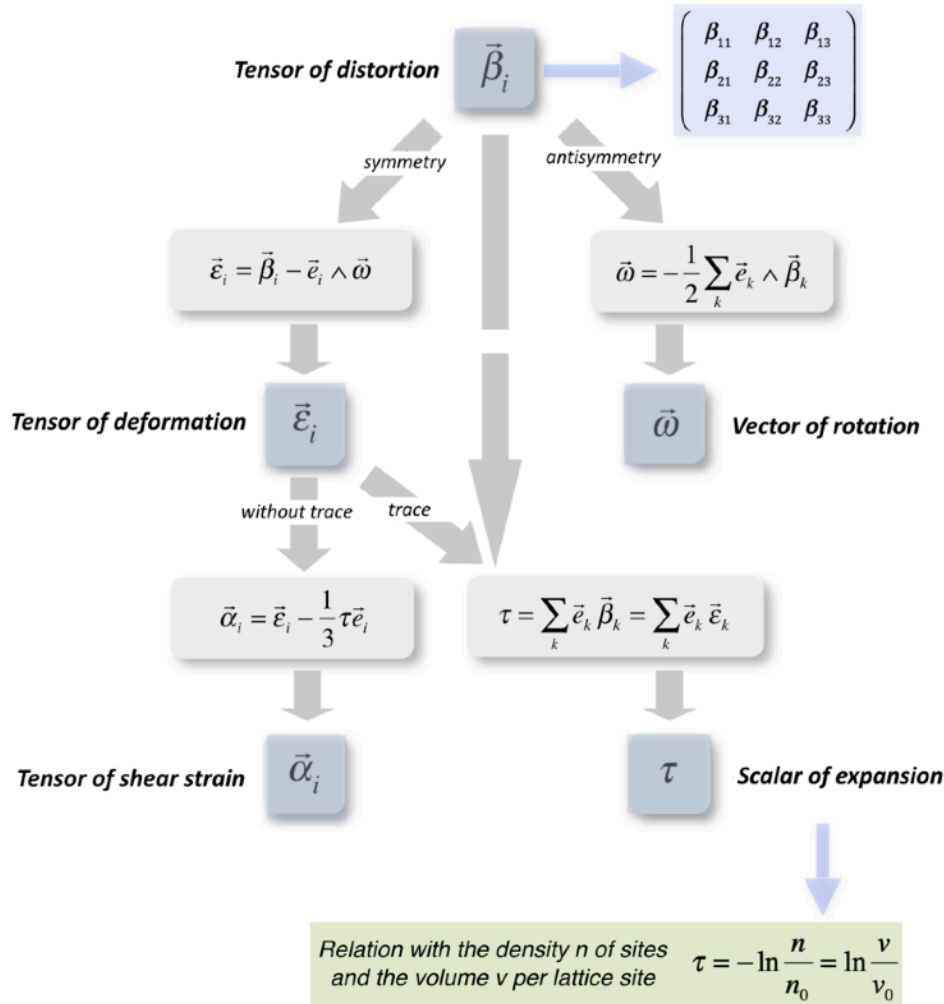


Figure 1.11 - The decompositions of the tensor of distortion

It is possible to apply *symmetry operations* on the *distortion tensor* $\vec{\beta}_i$ to extract the details of the rotations and the deformations of the medium. The operation of carrying out the sum of the diagonal elements of the tensor, namely $\beta_{11} + \beta_{22} + \beta_{33}$, provides a *scalar* called *the trace of the tensor* and which is in fact nothing other than the scalar of volume expansion τ .

The operation of taking the symmetrical part of the distortion tensor provides a symmetric tensor of second order $\vec{\epsilon}_i$, called *the strain tensor*, which represents all the deformations of the medium, but without the global rotations of the medium.

The operation of taking the anti-symmetrical part of the distortion tensor provides an axial vector $\vec{\omega}$, called *the rotation vector*, which represents all the local and global rotations within

the medium.

Finally, by removing its trace from the strain tensor $\vec{\varepsilon}_i$, we obtain a symmetric tensor of second order without trace $\vec{\alpha}_i$, called *the shear tensor*, which represents the set of shears of the medium. These operations of symmetry are described in figure 1.11, where, for the fine connoisseurs of vectorial computation, one made explicitly appear the mathematical operations of symmetry used, as well as the relation existing between the scalar of volume expansion, the density of sites of the network and the volume per network site.

Geometro-kinetics of a lattice in Euler coordinates

In Euler coordinates, we describe the evolution of the solid network in space and time using *the vectors of the velocity field* $\vec{\phi}(\vec{r}, t)$ of the points of the lattice located at the space and time coordinates \vec{r} and t in the absolute reference frame $Ox_1x_2x_3$ of the laboratory of the observer **GO** (Figure 1.2). However, if there is a non-homogeneous velocity field within the lattice, there must necessarily appear a spatio-temporal evolution of the distortions within this lattice. In Euler coordinates, the relationships between the velocity field $\vec{\phi}(\vec{r}, t)$ and the evolution of the distortion tensor $\vec{\beta}_i$, the rotation vector $\vec{\omega}$ and the volume expansion scalar τ will be called *the geometro-kinetic equations*. These equations are shown in figure 1.12.

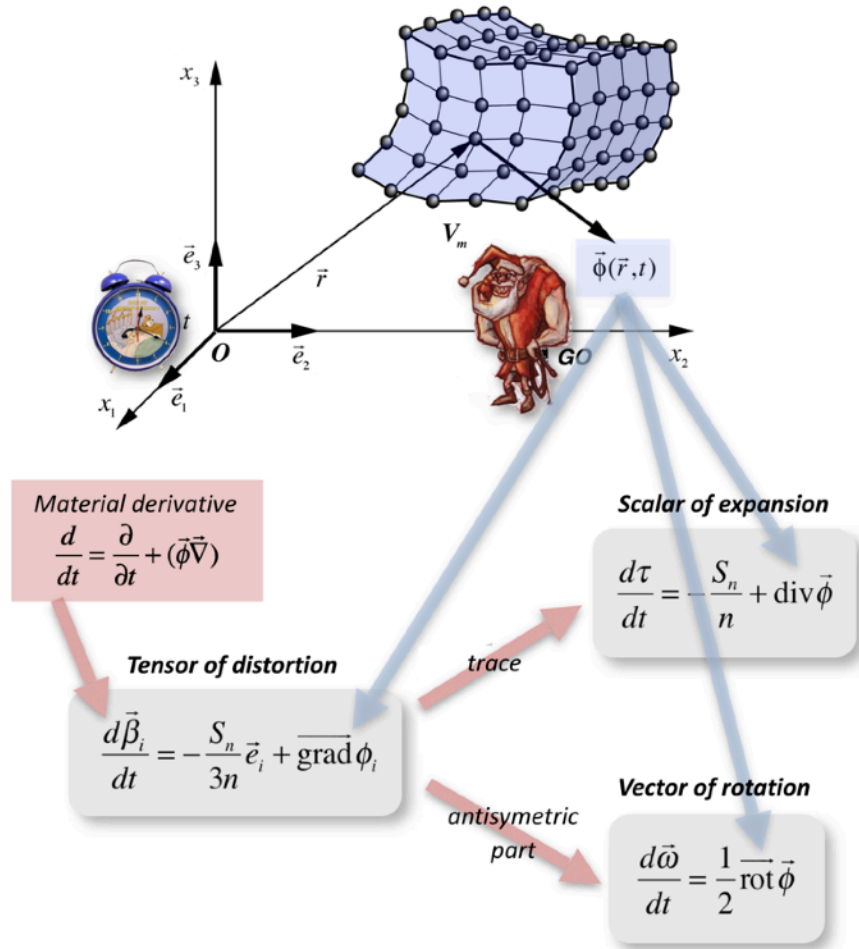


Figure 1.12 - The geometro-kinetic equations

Geometro-kinetic equations actually link *the temporal variations of the distortions* of the solid, which are calculated along the trajectory of the particles of the medium using a *mathematical operator of time* called *the material derivative*⁵, with *the spatial variations of the velocity field* $\vec{\phi}(\vec{r}, t)$ of the medium, which are calculated using mathematical space operators from vector analysis applied to the velocity field, and which are called *the gradient*⁶ in the case of the distortion tensor, *the curl*⁷ in the case of the rotation vector and *the divergence*⁸ in the case of the scalar of volume expansion. In these geometro-kinetic equations, there also appears a quantity S_n which corresponds to the possibility of the existence of a mechanism which can create or destroy lattice sites. This quantity S_n is called *the source of lattice sites*, and corresponds to the number of lattice sites created or destroyed per unit of time and per unit of volume of the lattice. The mechanisms leading to such sources of lattice sites will be discussed later.

Geometro-compatibility of lattice distortions

We have previously shown that the description of solids in Lagrange coordinates is characterized by a displacement field $\vec{u}(\vec{r}, t)$. Indeed, in Lagrange coordinates (figure 1.1), the solid is described by a vector \vec{r} locating the initial position of all its points in the reference frame $Ox_1x_2x_3$ of the observer **GO**. The Lagrange displacement vector field then makes it possible to locate in space at the instant t the position of all the points of the solid initially located at the coordinate \vec{r} in the coordinate system $Ox_1x_2x_3$.

It is intuitively clear that the description of the distortions of a solid in Euler coordinates should also make it possible to find such a displacement field. Indeed, in Euler coordinates (figure 1.2), the deformed solid is described at instant t in the absolute frame of reference of the observer **GO**. For a point **A** of the solid located at the coordinate \vec{r} of this frame of reference it must be possible to define a displacement vector $\vec{u}_E(\vec{r}, t)$ which connects this point **A** to the place **A'** where the same point **A** of the solid was located at the initial instant $t = 0$.

There is a close link between the particle time derivative of the distortion tensor $\vec{\beta}_i$ and the gradient of the components of the velocity field $\vec{\phi}(\vec{r}, t)$ as shown in the geometro-kinetic equation reported in figure 1.12. However, the velocity field $\vec{\phi}(\vec{r}, t)$ itself must be closely related to the temporal variation, called the temporal derivative, of the displacement field $\vec{u}_E(\vec{r}, t)$. It is therefore deduced that there must necessarily be a close link between the distortion tensor $\vec{\beta}_i$ and the gradient of the displacement field \vec{u}_E if the latter exists, and that the distortion tensor $\vec{\beta}_i$ is very probably *the gradient tensor* $\vec{\beta}_i = -\text{grad } u_{Ei}$ of the components of the displacement field \vec{u}_E .

⁵ **Material derivative operator:** it is a *mathematical operator of time* allowing to calculate the temporal variations of a physical quantity *along the trajectory of the particles* of a medium (see glossary).

⁶ **Gradient operator:** the *gradient of a scalar field* f is a mathematical space operator providing a *vector field* \vec{u} (see glossary).

⁷ **Curl operator:** the *curl of a vector field* \vec{u} is a mathematical space operator providing *another vector field* \vec{v} (see glossary).

⁸ **Divergence operator:** the *divergence of a vector field* \vec{u} is a mathematical space operator providing a *scalar field* g (see glossary).

Even if this reasoning seems complicated, it spontaneously leads to a mathematical condition on the distortion tensor $\vec{\beta}_i$ so that there really exists a displacement field \vec{u}_E . Indeed, in vector analysis, we demonstrate an unavoidable mathematical property, namely that the curl of a gradient is necessarily zero. Consequently, for there really exists a displacement field \vec{u}_E in coordinates of Euler, it is *necessary* that the curl of the tensor of distortion $\vec{\beta}_i$ is null, therefore that $\overrightarrow{\text{rot}} \vec{\beta}_i = 0$.

This equation is called *the geometro-compatibility condition* of the distortion tensor $\vec{\beta}_i$, and it ensures that there is indeed a continuous displacement field \vec{u}_E in Euler coordinates. Note again that if we take the trace of the geometro-compatibility equation for $\vec{\beta}_i$, in other words the sum of the diagonal elements of the tensor $\overrightarrow{\text{rot}} \vec{\beta}_i$, we find a new geometro-compatibility condition which then applies to the rotation vector $\vec{\omega}$, namely that the divergence of the vector of rotation $\vec{\omega}$ must be null so that there exists a field \vec{u}_E of continuous displacement in coordinates of Euler. These two geometro-compatibility equations are essential to ensure that a solid does not tear and that there do not appear any cavities during its space-time evolution. The various operations performed on the distortion tensors are summarized in figure 1.13.

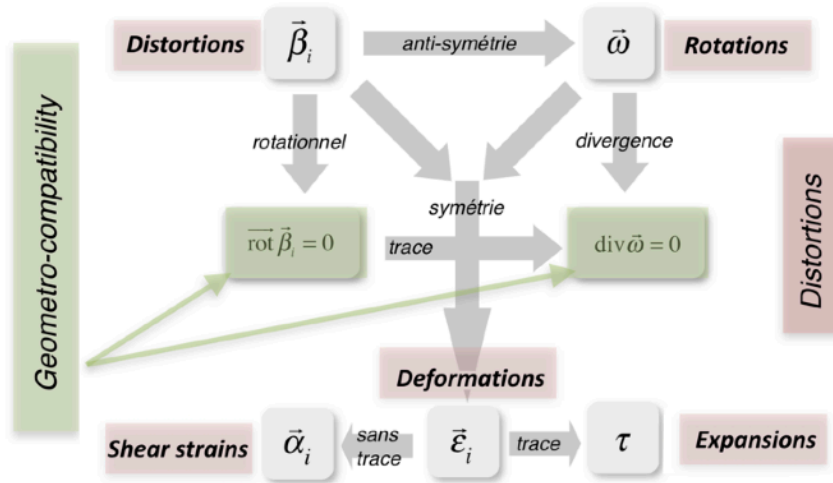


Figure 1.13 - The complete system of distortions of a solid lattice

The physical interpretation of these two *geometro-compatibility conditions* can be illustrated quite easily by the drawings shown in figures 1.14 and 1.15. The compatibility condition $\overrightarrow{\text{rot}} \vec{\beta}_i = 0$ for the distortion tensor $\vec{\beta}_i$ implies that the displacement field \vec{u}_E has good continuity properties. To show it, it suffices to consider a closed contour C within the medium, and to transfer the vectors of displacement \vec{u}_E along this contour (figure 1.14). If the medium presents a field of distortions satisfying the condition of compatibility $\overrightarrow{\text{rot}} \vec{\beta}_i = 0$, the vector of closure \vec{B} , called dislocation of the medium, is null, which effectively means from a topological point of view, that *there are no discontinuities of displacements*, called *dislocations*, in the medium.

The existence of a displacement field \vec{u}_E without discontinuities makes it possible to ensure *the topological connectivity* of the medium, that is to say from a physical point of view the fact

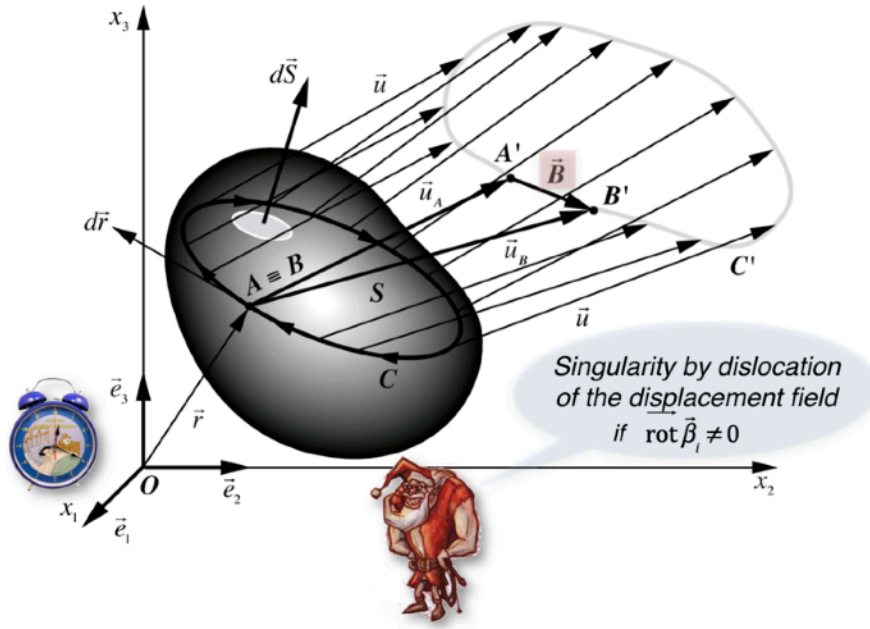


Figure 1.14 - Singularity by dislocation of the displacement field

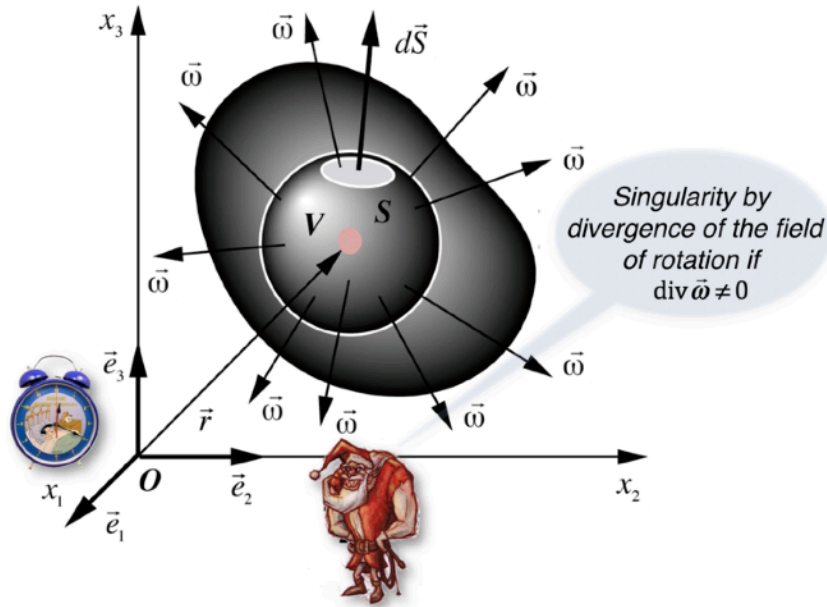


Figure 1.15 - Singularity by divergence of the rotation field

that there was no localization of the distortions, such as tears followed by a sliding of the jaws relative to each other, as well as *the topological compactness* of the medium, that is to say from a physical point of view the fact that it does not appear cavity formations or overlaps within the medium. In summary, the condition $\overline{\text{rot}} \vec{\beta}_i = 0$ ensures *the solidity of the medium*.

To find the meaning of the compatibility condition $\text{div} \vec{\omega} = 0$ for the rotation vector $\vec{\omega}$, we draw the rotation vector $\vec{\omega}$ on a closed surface S surrounding a volume V of solid (figure 1.15). The compatibility condition for the rotation vector $\vec{\omega}$ then stipulates that the flow of the

rotation field crossing the closed surface S is zero, which implies that *there is no divergent singularity of the rotation field* within the solid, such as that shown in the drawing in figure 1.15.

Contortions of a solid lattice

In a solid lattice, the fields $\vec{\beta}_i, \vec{\varepsilon}_i, \vec{\alpha}_i, \vec{\omega}, \tau$ represent the set of distortions, deformations, shears, rotations and volume expansions that the lattice unit cells undergo locally. If each unit cell is subjected to a field of distortion, which can vary from one cell to another, it must also appear effects of flexion and torsions on a more macroscopic scale of the solid medium, related to the lattice continuity.

These "curvatures" of the solid will be called the contortions of the lattice. In a geometro-compatible medium, they depend in fact only on deformations of the lattice, and are therefore deduced as spatial variations of the deformation field $\vec{\varepsilon}_i$ in the manner illustrated by the diagram in figure 1.16. A *contortion tensor* $\vec{\chi}_i$ then appears, which can be broken down by

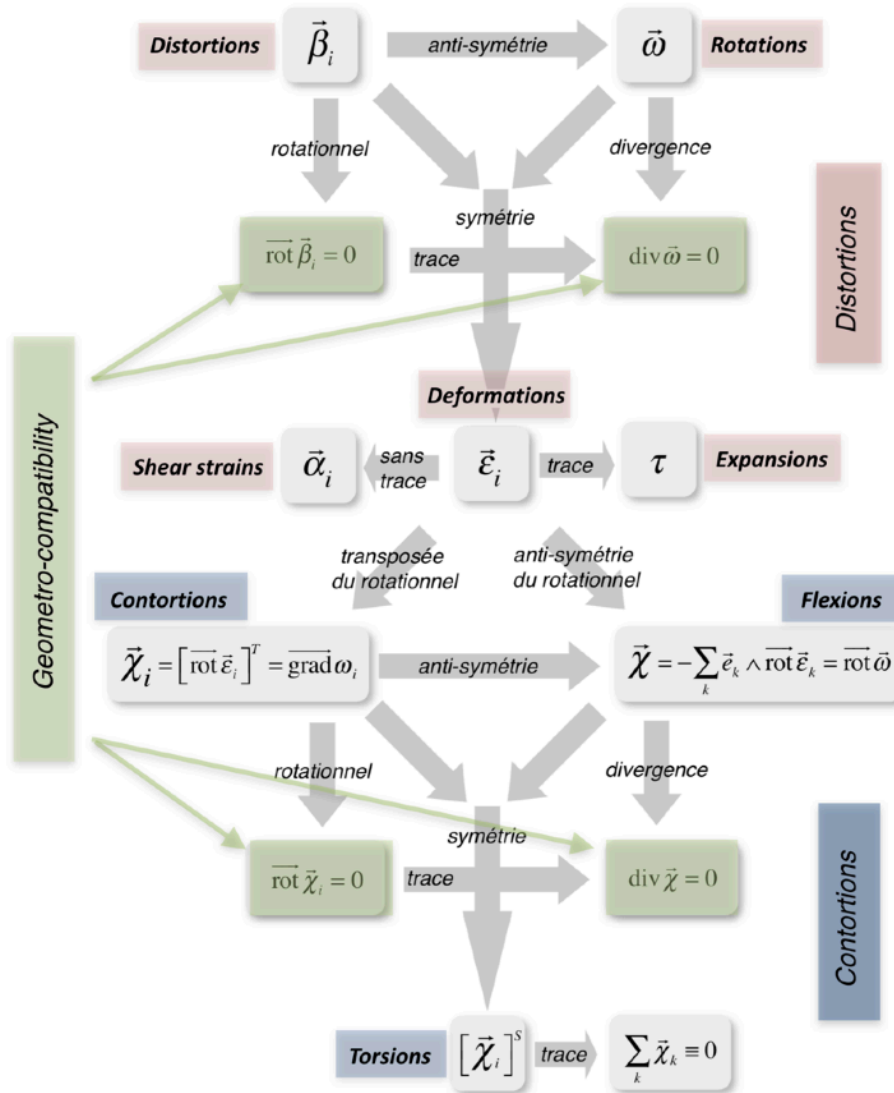


Figure 1.16 - The complete system of distortions and contortions of a solid lattice

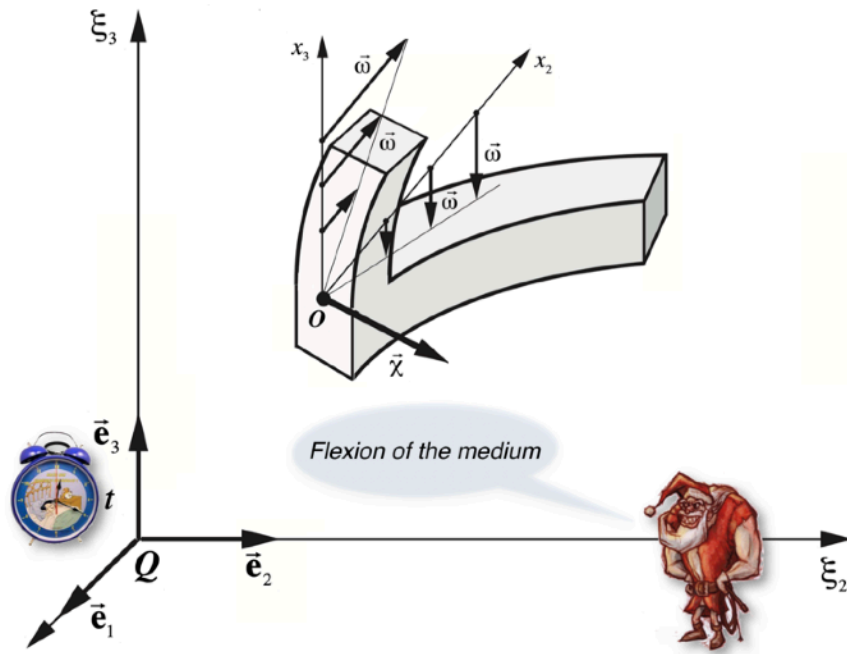


Figure 1.17 - Flexion of the medium

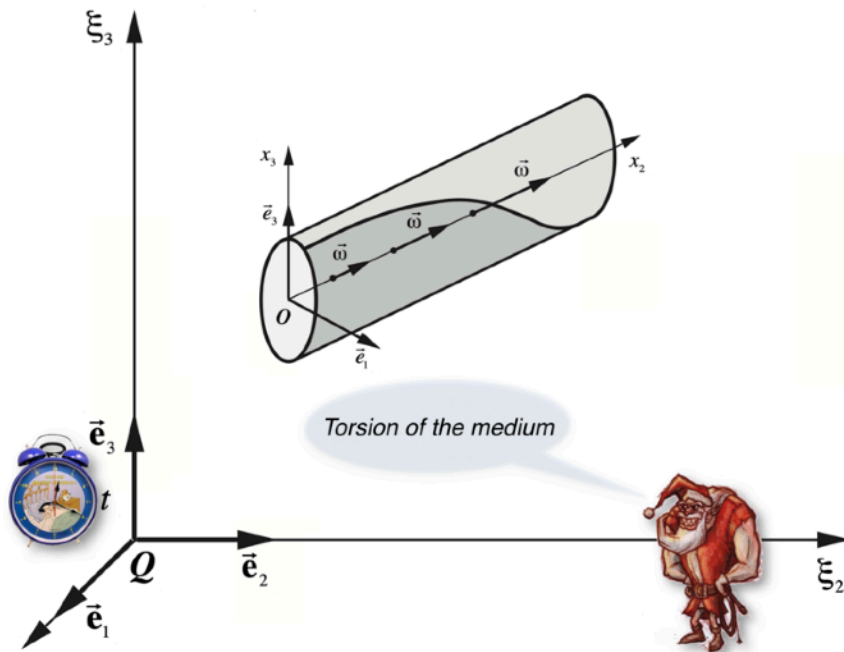


Figure 1.18 - Torsion of the medium

symmetries into a *flexion vector* $\vec{\chi}$ and a *transverse symmetric tensor (without trace) of torsion* $[\vec{\chi}_i]^s$.

In a geometro-compatible medium, the contortions of the lattice are also closely linked to the spatial derivatives of the rotation vector $\vec{\omega}$ as shown by the mathematical relationships giving the contortion tensor $\vec{\chi}_i$ and the flexion vector $\vec{\chi}$ in figure 1.16. These must therefore also

measure variations in rotations within the solid, such as *twists* or *bends*. We can therefore define more precisely the meaning of these tensors $\vec{\chi}_i$ and $\vec{\chi}$ using two typical examples of spatial variations of $\vec{\omega}$.

In the first example, a bent medium presents a rotation vector parallel to the axis Ox_3 , and which increases in the direction of the axis Ox_2 , as represented in figure 1.17. In this case, there is a non-diagonal component $\chi_{23} = \partial\omega_3 / \partial x_2 \neq 0$ of the tensor $\vec{\chi}_i$ which is not zero, and this component is associated with the *bending of the solid* as well illustrated by the figure 1.17.

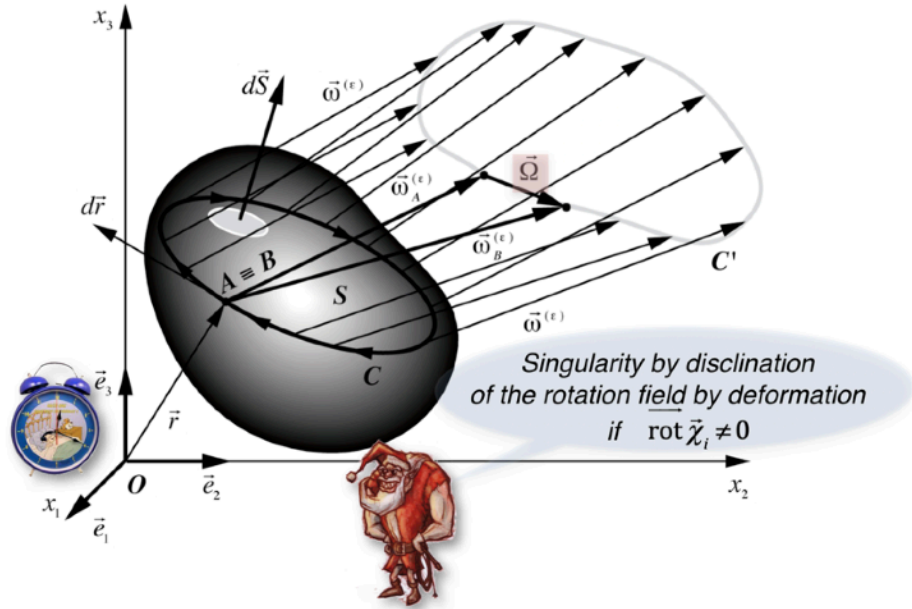


Figure 1.19 - Singularity by disclination of the rotation field by deformation

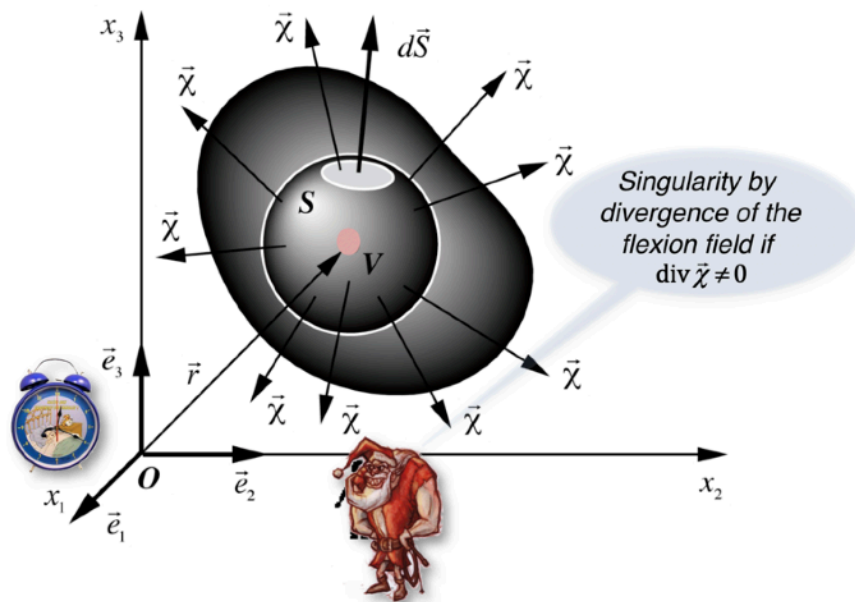


Figure 1.20 - Singularity by divergence of the flexion field

But in the case illustrated in figure 1.17, the vector $\vec{\omega}$ seems to turn around the axis Ox_1 so that there is a *non-zero flexion vector* $\vec{\chi} = -\text{rot} \vec{\omega}$ parallel to this axis as illustrated in figure 1.17.

In the second example (figure 1.18), we represent an increase along axis Ox_2 of a rotation vector parallel to axis Ox_2 . For once it is a *diagonal component* $\chi_{22} = \partial\omega_2 / \partial x_2 \neq 0$ of the tensor $\vec{\chi}_i$ which necessarily becomes non-zero. And we see that this corresponds to a torsion of the solid medium.

In these two examples, it has been illustrated that spatial variations in the rotation vector $\vec{\omega}$ do indeed lead to bending or twisting of the solid medium. But in a geometro-compatible medium, these same bends and twists are also deductible directly from the strain tensor $\vec{\varepsilon}_i$.

Geometro-compatibility of lattice contortions

In the table of figure 1.16, we note that there are also two geometro-compatibility conditions for the contortion tensor $\vec{\chi}_i$ and the flexion vector $\vec{\chi}$ respectively, in a very similar way as in the case of the distortion tensor and the rotation vector.

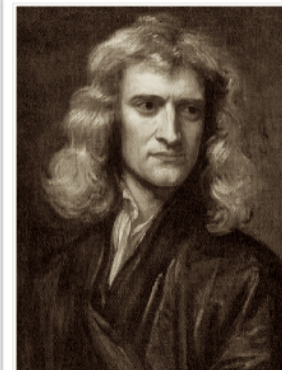
The condition of compatibility $\text{rot} \vec{\chi}_i = 0$ of the contortion tensor $\vec{\chi}_i$ can be interpreted by considering a closed contour C within the medium and by plotting the local rotation vector $\vec{\omega}^{(\varepsilon)}$ deduced from the strain tensor along this contour (figure 1.19). The condition of compatibility implies then that the closure vector $\vec{\Omega}$, called *the Frank vector*, is zero, which means from a topological and physical point of view that *there are no discontinuities of rotations by deformation*, which are called *disclinations* in the medium.

The condition of compatibility $\text{div} \vec{\chi} = 0$ of the flexion vector $\vec{\chi}$ is interpreted by considering a closed surface S surrounding a volume V of medium (figure 1.20). The compatibility condition for the flexion vector $\vec{\chi}$ then stipulates that the flow of the bending field crossing the closed surface S is zero, which implies that *there is no diverging singularity of the flexion field* within the solid, such as that shown in the drawing in figure 1.20.

Newtonian dynamics and Eulerian thermokinetics

It has been shown previously that a solid collection of particles in space can present a collective movement which corresponds to the global movements of translation, of global and local rotation and of deformation of the medium in the space of the observer, and that, in Euler coordinates, these movements are described by an average local speed $\vec{\phi}(\vec{r}, t)$. To go further in the description and prediction of these movements, we must now introduce the physical principles to which the environment obeys.

We suppose then that the solid lattice considered behaves in a Newtonian way in the absolute reference frame of **GO**, in other words that the dynamics of the particles of the medium satisfy Newton's law $\vec{f} = m\vec{a}$ which implies that the acceleration \vec{a} of a particle is related to the force \vec{f} that we apply to it via *the mass of inertia* m of the particle. In addition, we also admit that the physical



Isaac Newton
(1643-1727)

behaviors of the particle lattice obey the first two principles of thermodynamics, which have never been faulted, namely that energy is a conserved quantity, and that there exists a quantity called *entropy* which measures the state of disorder of the lattice.

We are going to introduce here rigorously the Newtonian dynamics and the thermokinetics of the lattice in Eulerian coordinates, starting from these three completely classic and well-known basic physical axioms. With this axiomatic and rigorous approach, we are led to define average quantities per site of the lattice, as well as sources and flows of physical quantities, which must satisfy three principles of continuity shown in figure 1.21.

Admitting the axiom that the individual movement of each particle of the lattice satisfies a *Newtonian dynamic*, namely the Newton's law $\vec{f} = m\vec{a}$, to the movement of each particle at velocity $\vec{\phi}$ must correspond a *momentum* and a *kinetic energy*. Per particle, according to Newtonian mechanics, the momentum is written $\vec{p} = m\vec{\phi}$ and the kinetic energy is written $e_{cin} = m\vec{\phi}^2 / 2$. These expressions of the momentum and the kinetic energy of a particle of the medium calls upon a conservative scalar physical quantity, specific to the particle: its *mass of inertia* or *inert mass* m . In Euler coordinates, we show that the conservation of the mass of inertia leads to a *principle of continuity for the mass of inertia* which is reported in figure 1.21.

This principle links the local temporal variation $\partial \rho / \partial t$ of the quantity of mass contained in the volume unit of the medium, which is called *the mass density* ρ of the medium, to: (i) the existence of a volume source of mass S_m , associated with creation or annihilation of mass within the medium and which is generally zero due to the principle of conservation of mass, (ii) the temporal variation $d\tau/dt$ of the scalar of volume expansion of the medium along the trajectory of its particles, (iii) the existence of a source S_n of lattice sites and (iv) the existence of a *mass transport flow* \vec{J}_m , i.e. a mass displacement by another physical process within the lattice, such as the self-diffusion which we will talk about later.

The movements of random fluctuations $\Delta \vec{v}_i$ of the medium particles corresponding to thermal agitation and the attractive or repulsive interactions that may exist between the particles of the medium must correspond respectively to an *internal thermal energy* and an *internal potential energy*. It is precisely the subject of the axiom of *the first principle of phenomenological thermodynamics*, which postulates the existence, for a given physical system, of a function U depending on the state of the system, called *the internal energy of the system*, which is such that, for any infinitesimal transformation of the system (any infinitesimal variation of one of the physical quantities of the system), we have the relation $dU = \delta W + \delta Q$, where dU represents the variation of the internal energy of the system, δQ represents the set of heat exchanges between the system and the outside world, and δW all of the work exchanges between the system and the outside world.

In the case of a solid lattice moving at velocity $\vec{\phi}$, the total energy is linked both to its internal energy and to its kinetic energy of global movement at velocity $\vec{\phi}$. In Euler coordinates, we show that the conservation of the energy of the deforming solid leads to a *principle of continuity*



for the total energy which is shown in figure 1.21. By expressing the average internal energy u and the average kinetic energy e_{cin} per lattice site, the continuity principle of energy states that the sum of the variations of internal energy u and kinetic energy e_{cin} taken along the trajectory of the particles depends on: (i) the existence of an external work source S_w^{ext} corresponding to a supply of mechanical energy from outside the medium, (ii) the work flow \vec{J}_w , i.e. exchanges of mechanical energy within the medium, (iii) the heat flow \vec{J}_q , that is to say heat exchanges within the medium, and (iv) the source S_n of lattice sites, that is to say the creation or annihilation of a certain number of lattice sites per unit of time.

The second principle of phenomenological thermodynamics postulates the existence, for a given physical system, of a function S depending on the state of the system, called the entropy of the system. This function in fact characterizes the state of disorder reigning within the system, and it is such that any infinitesimal transformation of the system satisfies the relation $dS \geq \delta Q / T$ where dS represents the variation of the entropy of the system, δQ represents the set of heat exchanges between the system and the outside world and T is the temperature of the system.

In Euler coordinates, we show that the second principle of phenomenological thermodynamics leads to a principle of continuity for the entropy which is reported in figure 1.21.

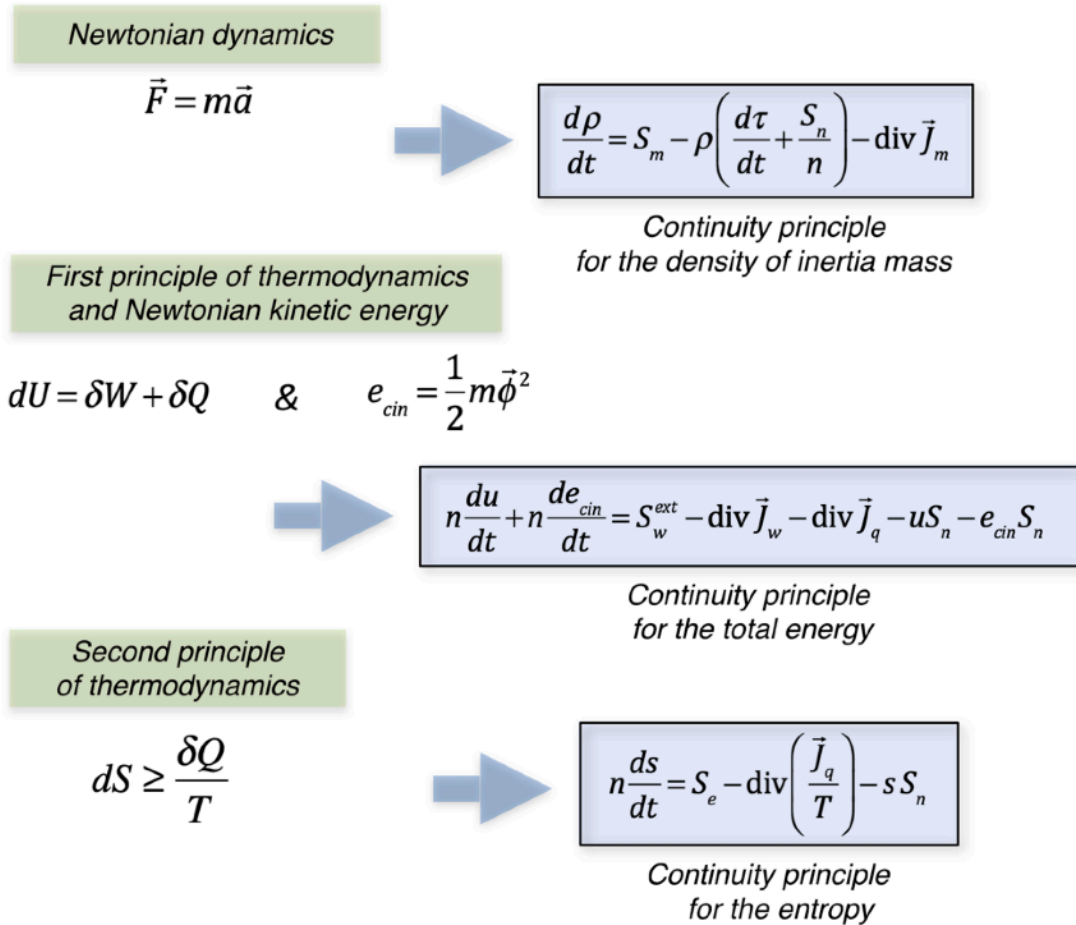


Figure 1.21 - The three Eulerian continuity principles deduced from the Newtonian dynamics and from the two basic principles of the thermodynamics

By expressing the average entropy s per lattice site, the principle of continuity of entropy stipulates that the variation of entropy s taken along the trajectory of particles depends on: (i) the existence of a volume source of entropy S_e , that is to say, the local creation of entropy within the medium, (ii) the heat flow \vec{J}_q within the medium, (iii) the temperature T of the medium which characterizes the state of thermal agitation of the medium particles and (iv) the source S_n of lattice sites.

These three physical principles are absolutely essential in solid media, and they are *the only fundamental physical principles absolutely necessary* for a complete description of Newtonian geometro-dynamics and of phenomenological thermodynamics of deformable media in Euler coordinates.

Physical properties specific to the medium

The equations of geometro-kinetics (figure 1.12) and geometro-compatibility (figure 1.16), as well as the three principles of continuity deduced from Newton's laws and phenomenological thermodynamics (figure 1.21) are the basic concepts for the treatment of deformable solid media in Euler coordinates, and remain the same whatever the solid considered. But we know very well that the physical properties and the macroscopic behaviors that we can observe on a solid medium can be very different from one medium to another. These physical properties are called *the phenomenological properties of the medium*. We will therefore now discuss the most important phenomenological physical properties of a solid lattice, namely *the mechanical properties of the lattice*, such as *elasticity* and *anelasticity*, and *the mass transport properties* within the lattice, such as *self-diffusion*.

It is common experience that you can bend a hacksaw blade strongly without great effort, and that it resumes all its straightness when you release the force that you applied to it. This typical phenomenological behavior is called *the elasticity of the solid*. The elasticity of the medium is due to the internal bonding forces between particles of the solid, so that bending the saw blade amounts to storing internal energy in the medium, in fact in the bonds between its particles, energy which is then used to return the blade to its original shape when released. Thus, to introduce this property of elasticity in the Eulerian equations of the medium, one will use *the average internal energy u per site of lattice* which one defined in the preceding paragraph, and one will express that this one depends on the deformations applied to the solid, in other words elastic deformation fields $\vec{\beta}_i^{el}$, $\vec{\varepsilon}_i^{el}$, $\vec{\alpha}_i^{el}$, $\vec{\omega}^{el}$, τ^{el} appearing in the solid when it is deformed. We express this situation by saying that internal energy u is a function $u(\vec{\beta}_i^{el}, s) = u(\vec{\varepsilon}_i^{el}, \vec{\omega}^{el}, s) = u(\vec{\alpha}_i^{el}, \vec{\omega}^{el}, \tau^{el}, s)$ depending on the state of elastic strain tensors, but also on the local entropy of the network, via *the average entropy s per lattice site*. This dependence on entropy reflects the effect on internal energy of the existence of a spatial and kinetic disorder within the medium, and in particular the effect of thermal agitation of the particles under the effect of heat.

When a solid is deformed, elasticity is an immediate response of the solid. But there can sometimes be another response from the solid which is generally added to the elastic response and which is delayed in time compared to the solicitation of the solid, but which is also recoverable with delay when the solicitation is released. Such a response of the solid is called *the anelasticity of the solid*. While the elastic response does not release thermal energy into the

solid, the anelastic response releases thermal energy when activated, and is said to be a dissipative process.

It is this type of process which dissipates the vibration energy of certain metals, such as cast iron for example, which are used in industry precisely for this property of damping vibrations and noise. When anelastic deformation phenomena are activated in a solid, these also store internal energy in the solid, energy which is then used by the solid to restore its initial shape, as in the case of elasticity. Anelastic deformations $\vec{\beta}_i^{an}, \vec{\varepsilon}_i^{an}, \vec{\alpha}_i^{an}, \vec{\omega}^{an}$ can therefore appear in a solid, which, as in the case of elastic deformations, also modify the function of the internal energy of the solid $u(\vec{\beta}_i^{el}, \vec{\beta}_i^{an}, s) = u(\vec{\varepsilon}_i^{el}, \vec{\varepsilon}_i^{an}, \vec{\omega}^{el}, \vec{\omega}^{an}, s) = u(\vec{\alpha}_i^{el}, \vec{\alpha}_i^{an}, \vec{\omega}^{el}, \vec{\omega}^{an}, \tau^{el}, s)$. This means that the internal energy of the solid is a function of the state of both elasticity and anelasticity of the solid. It will be noted here that, for the sake of simplification, it has been assumed that it does exist anelastic volume expansion, that is to say that $\tau^{an} = 0$.

In principle, the existence of a non-zero source S_n of lattice sites would violate the Newtonian principle of mass conservation, unless there is a phenomenon of *self-diffusion by intrinsic point defects within the lattice*. An *intrinsic point defect of the lacunar type*, simply called a *vacancy*, is a site of the particle solid lattice which has no particles (figure 1.22). It is therefore a "hole" in the lattice. An *intrinsic point defect of interstitial type*, called simply a *self-interstitial*, is a particle which is in the solid lattice, but which does not occupy a regular substitutional site of this lattice (figure 1.22). It is therefore an "additional" particle in the lattice.

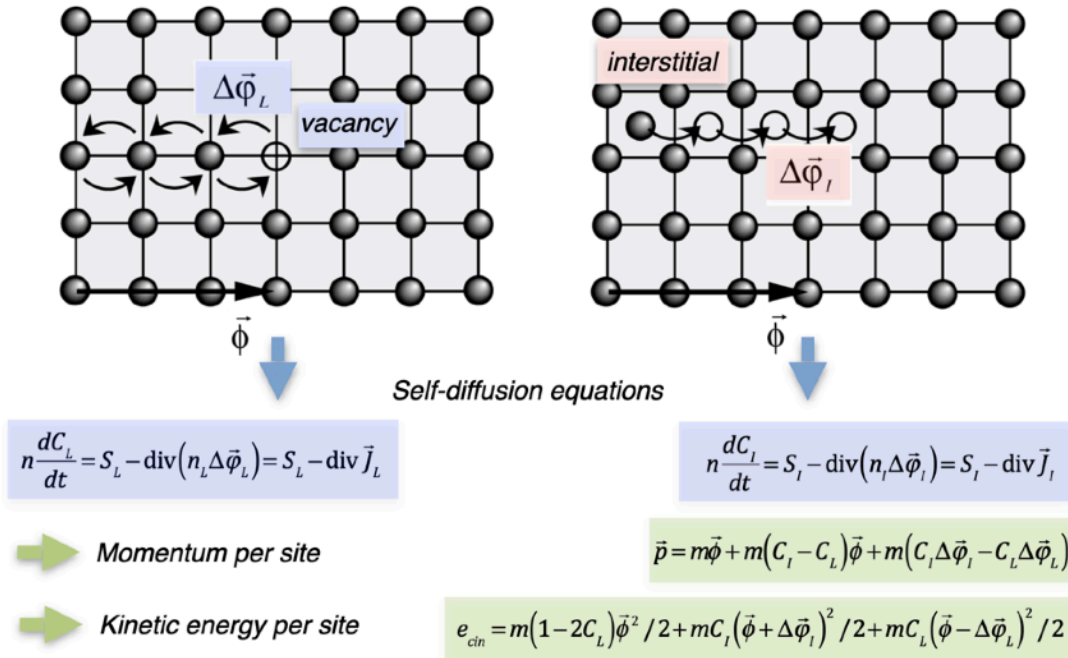


Figure 1.22 - Self-diffusion by vacancy and by self-interstitial

It is simple to understand how the presence of such intrinsic point defects can lead to the existence of mass transport phenomena by *lacunar and / or interstitial self-diffusion*. These two mass transport mechanisms can be illustrated in a lattice moving at absolute velocity $\vec{\phi}$ in the

space of the external observer **GO** (figure 1.22). The movement of a vacancy at velocity $\Delta\vec{\phi}_L$ relative to the lattice in a given direction leads to a relative mass flow in the opposite direction, at velocity $-\Delta\vec{\phi}_L$, while the movement of a self-interstitial at velocity $\Delta\vec{\phi}_I$ relative to the lattice in a given direction causes a mass flow in the same direction, at velocity $\Delta\vec{\phi}_I$.

To transcribe mathematically the existence of these point defects, we must first introduce the volume densities of vacancies and self-interstitials, i.e. the number $n_L = n_L(\vec{r}, t)$ of vacancies and $n_I = n_I(\vec{r}, t)$ of self-interstitials per volume unit of lattice. From these densities, it is possible to define *atomic concentrations of vacancies and auto-interstitials* with respect to the density n of network sites by relations $C_L = n_L / n$ and $C_I = n_I / n$. Contrary to appearances, there is a certain asymmetry between vacancies and auto-interstitials, which is expressed in the fact that the maximum atomic concentration of vacancies is always limited to 1, when all the sites of the lattice are locally unoccupied, while the atomic concentration of auto-interstitials depends on the number of interstitial sites accessible in each unit cell of a lattice with a given structure, and on the number of interstitials that it is possible to fit on each of these sites.

We can also introduce the *diffusion flows* \vec{J}_L and \vec{J}_I of vacancies and interstitials with respect to the lattice, defined by relations $\vec{J}_L = nC_L\Delta\vec{\phi}_L$ and $\vec{J}_I = nC_I\Delta\vec{\phi}_I$, and which measure the number of vacancies and interstitials that cross the unit surface per unit of time within the lattice. We can then deduce *the self-diffusion equations* reported in figure 1.22, which allow to calculate the temporal variations of the atomic concentrations of vacancies and auto-interstitials along the trajectory of the medium, on the one hand by the introduction of *volume sources of vacancies* S_L and *interstitials* S_I associated with the number of creations and annihilations of vacancies and interstitials per unit of time and per unit of volume, and on the other hand the introduction of *fluxes* \vec{J}_L and \vec{J}_I of vacancies and interstitials associated with the number of mobile vacancies and mobile interstitials crossing per unit time a unit surface within the lattice. The principle of mass conservation is then satisfied if the source of lattice sites is directly linked to the local creations and annihilations of vacancies and interstitials, that is to say linked to the sources S_L and S_I of vacancies and interstitials, via the relationship $S_n = S_L - S_I$.

In an elastic and anelastic network with self-diffusion, it is intuitively clear that the atomic concentrations C_L and C_I of vacancies and auto-interstitial must also influence the energy state of the lattice, so that the internal energy state function has to be written now as a function $u(\vec{\beta}_i^{el}, \vec{\beta}_i^{an}, C_L, C_I, s) = u(\vec{\varepsilon}_i^{el}, \vec{\varepsilon}_i^{an}, \vec{\omega}^{el}, \vec{\omega}^{an}, C_L, C_I, s) = u(\vec{\alpha}_i^{el}, \vec{\alpha}_i^{an}, \vec{\omega}^{el}, \vec{\omega}^{an}, \tau^{el}, C_L, C_I, s)$ of the set of thermodynamic variables that characterize the state of the medium.

The presence of vacancies and self-interstitials in the lattice will modify the expressions of kinetic energy and momentum expressed as an average value per particle or per lattice site, as shown in figure 1.22.

The function $u(\vec{\alpha}_i^{el}, \vec{\alpha}_i^{an}, \vec{\omega}^{el}, \vec{\omega}^{an}, \tau^{el}, C_L, C_I, s)$ which characterizes the internal energy state of the solid lattice is a phenomenological quantity of the considered medium, in the sense that it must be established for each medium and that it is specific to each medium. It is essentially this which will control the space-time behavior of the medium via *thermodynamic potentials*. Indeed, if we express the temporal variation of the internal energy along the trajectory of the medium, we obtain an equation which is called *the thermokinetic equation* of the medium, which is expressed from the relation $u(\vec{\alpha}_i^{el}, \vec{\alpha}_i^{an}, \vec{\omega}^{el}, \vec{\omega}^{an}, \tau^{el}, C_L, C_I, s)$ as shown in figure 1.23.

This thermokinetic equation reveals *mechanical potentials* $\vec{s}_k, \vec{m}, p, \vec{s}_k^{cons}, \vec{m}^{cons}$ called *the stress tensors* \vec{s}_k and \vec{s}_k^{cons} conjugated respectively to the elastic and anelastic shear tensors $\vec{\alpha}_i^{el}$ and $\vec{\alpha}_i^{an}$, *the moment vectors* \vec{m} and \vec{m}^{cons} conjugated respectively to the vectors of elastic and anelastic rotation $\vec{\omega}^{el}$ and $\vec{\omega}^{an}$, *the pressure* p conjugated to the scalar of volume expansion τ^{el} . These mechanical potentials represent the internal mechanical forces inside the medium, which tend to eliminate the deformations of the medium to restore the undeformed state of the solid medium. These mechanical potentials can be deduced from one another according to the graph shown in figure 1.23.

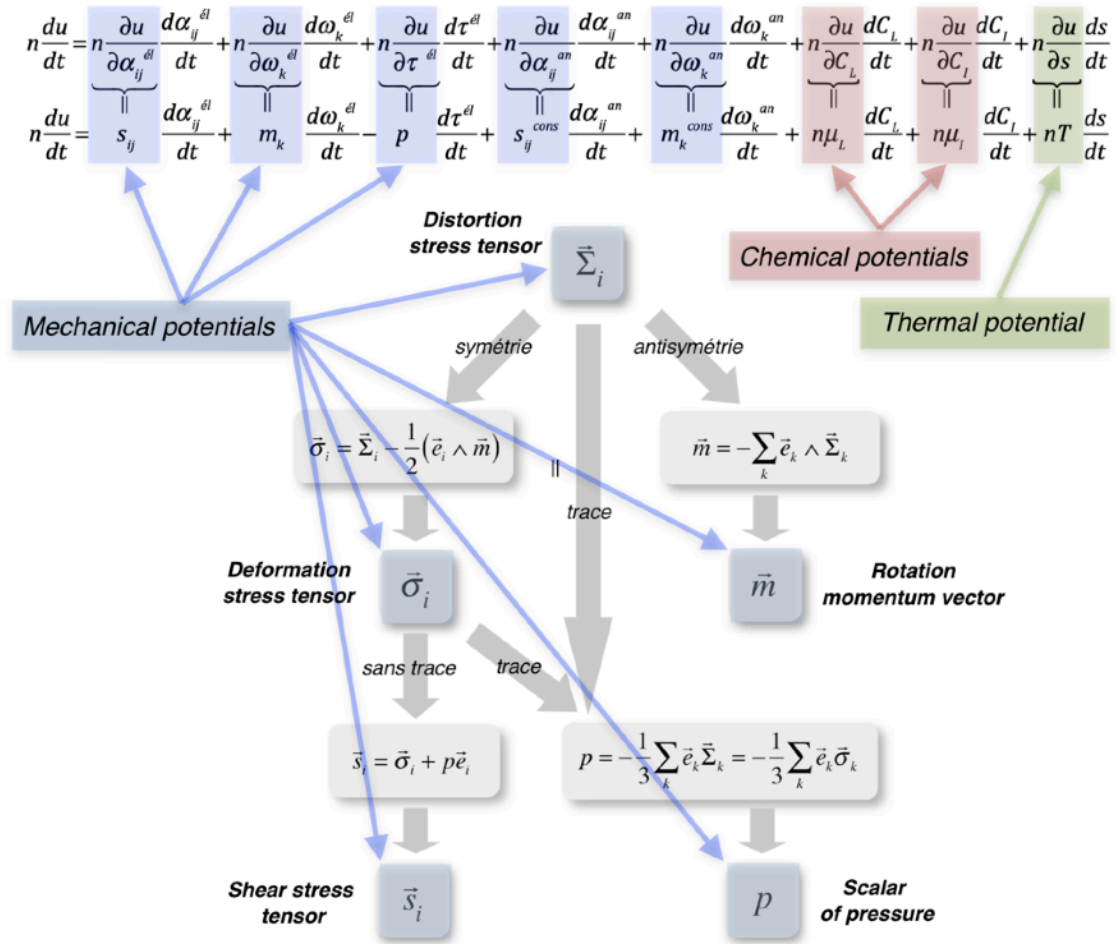


Figure 1.23 - Thermokinetics equations

The thermokinetic equation also reveals *the chemical potentials* μ_L and μ_I , conjugated with the atomic concentrations C_L and C_I of vacancies and auto-interstitials respectively. These chemical potentials represent in fact the internal chemical forces acting on the vacancies and the auto-interstitials within the medium, which tend to eliminate spatial variations in atomic concentrations C_L and C_I of vacancies and auto-interstitials, in order to restore the chemical equilibrium state inside the solid medium.

Finally, the thermokinetic equation still reveals a significant quantity of the medium, namely its temperature T , which is conjugated with its entropy s , and which measures the thermal agitation within the medium.

Potentialities of the Eulerian representation of deformable media

To end this chapter, we represent by a graph in figure 1.24 all the potentialities of the Eulerian representation to describe the spatio-temporal evolution of deformable Newtonian media, potentialities which are developed in detail in my first book written in French.

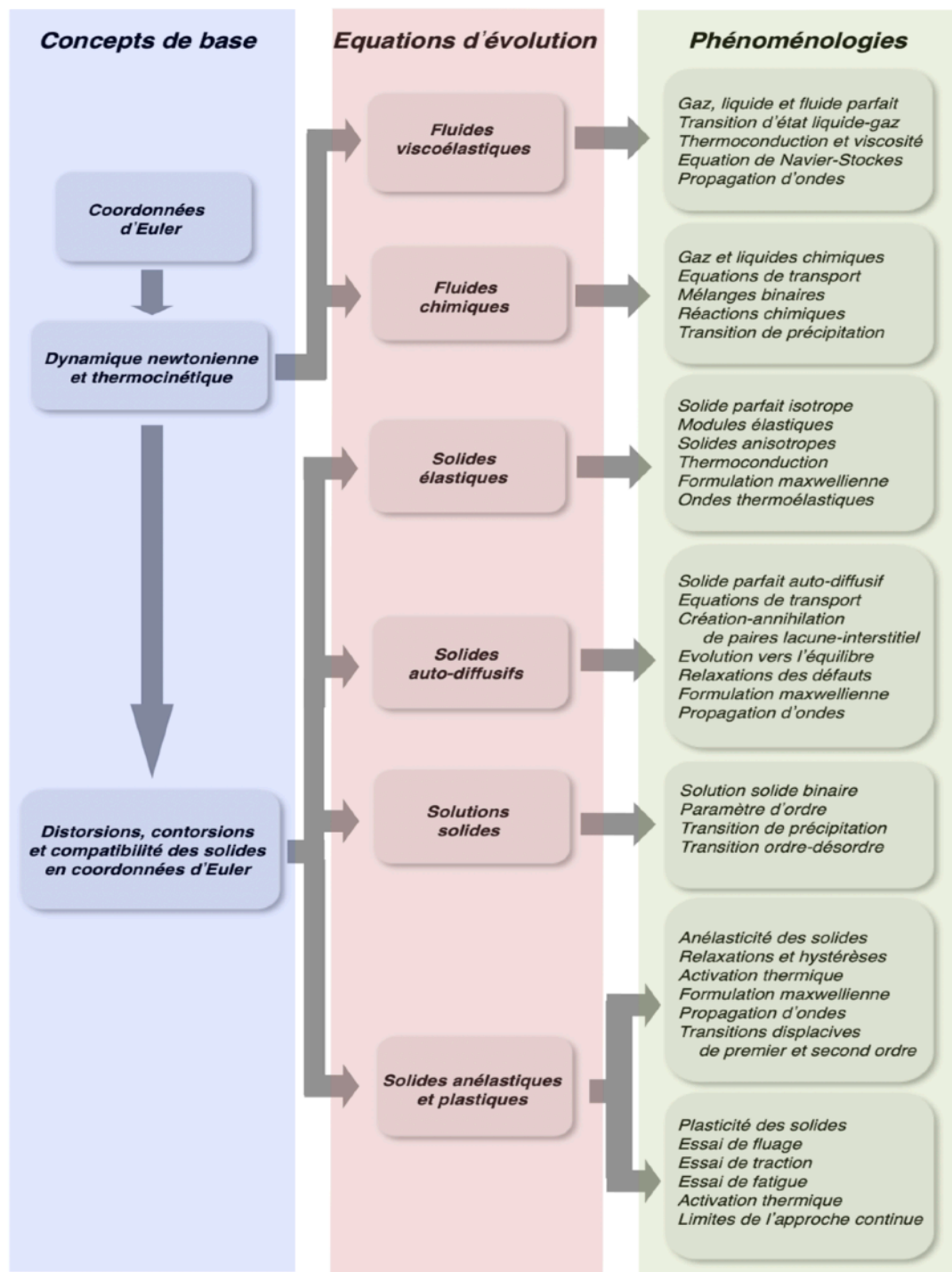


Figure 1.24 - The potentialities of the Eulerian representation of Newtonian deformable media

Chapter 2

Dislocation and disclination charges in a lattice

The description of structural defects, or topological singularities, which can appear within a solid, such as dislocations and disclinations, is a field of physics, initiated mainly by the idea of macroscopic defects of Volterra¹ in 1907, which has experienced very fast development during its very rich century of history, as Hirth² illustrated very well in 1985.

In this chapter, in order to describe the plasticity of solid lattices, we introduce an innovative concept of *density of dislocation and disclination charges* in Eulerian lattices, then we present a review of the macroscopic and microscopic topological singularities of the lattice which can be associated with dislocation and disclination charges. We then discuss the movement of dislocation charges within the lattice, by introducing the notion of dislocation charge flow, and we deduce the force acting on a dislocation charge, called *the Peach and Koehler force*. Finally, we present the potentialities inherent in this original approach of topological singularities within solid lattices in Euler coordinates.

Macroscopic concept of plastic distortion charges

In the previous chapter, we introduced the elastic and anelastic behaviors of a solid. There is yet another behavior that we will deal with now. If you take an aluminum bar and bend it slightly, it returns to its initial state if you release the stress that was applied to it, and this is elastic behavior. On the other hand, if it is folded very strongly and the stress is released, it no longer returns to its original state, but remains definitively folded. We speak in this case of *plastic behavior* and *plasticity* of the aluminum bar.

The description of the plasticity of a solid lattice is sometimes undertaken phenomenologically using a plastic distortion tensor $\vec{\beta}_i^{pl}$. However, this approach is extremely limited, in particular by the fact that there is no unequivocal relationship between the local state of plastic deformation and the microscopic state of the network of structural defects responsible for this plastic deformation. This is the reason why the way of expressing the presence of plastic distortions in a lattice must be approached so that it is possible to take into account the microscopic state of the network of structural defects. A very elegant way of carrying out this modification is to introduce the concepts of *densities and fluxes of dislocation charges*, responsible for *the plastic distortions* of the solid, as well as *densities of disclination charges*, responsible for *the plastic contortions* of the solid.

The concept of *charges of plastic distortions of the solid*, which will henceforth be called simply *dislocation charges* by language shortcuts, is intuitively simple to grasp, if one uses the approach¹ developed in 1907 by the Italian physicist Vito Volterra. The latter had the idea of

¹ V. Volterra, «L'équilibre des corps élastiques», *Ann. Ec. Norm. (3)*, XXIV, Paris, 1907

² J.-P. Hirth, «A Brief History of Dislocation Theory», *Metallurgical Transactions A*, vol. 16A, p. 2085, 1985

considering a pipe of solid material and imagining, either that it is cut and that it is subjected to a certain distortion before being glued, or that one removes part of it before being glued again, as shown by the examples in figure 2.1. In these two examples, the deformations undergone by the solid after gluing are irreversible and irrecoverable, therefore of *plastic nature*.

On the other hand, it is intuitively clear that internal forces have developed inside the solid after gluing. These appeared during the elastic deformation which was imposed on the rest of the solid to make the two jaws to be bonded coincide. In fact, everything happens exactly as if a localized topological discontinuity had appeared in the center of the pipe after gluing, discontinuity which would be the source of an *elastic distortion field* in the macroscopically continuous medium which composes the pipe. And this distortion field, by its presence, is itself a source of a field of conjugate stresses, which can be called *internal stress field*.

Mathematically, the discontinuity due to gluing should be able to be translated in terms of a local density of “*plastic charges*”, source of an elastic distortion field, and therefore of an internal stress field, in a completely similar way that in electromagnetism where the presence of a local density ρ of electric charges is responsible for the appearance of an electric displacement field \vec{D} , as shown by Maxwell's equation $\rho = \text{div } \vec{D}$, and consequently of a conjugated electric field \vec{E} , since $\vec{D} = \epsilon_0 \vec{E}$. The aim of this chapter will therefore be to show how it is possible to mathematically translate the phenomena of plasticity inside a solid, not only by introducing densities of plastic charges, but also flows of plastic charges, by analogy with the flow of electric charges \vec{j} appearing in the equation $\vec{j} = -\partial \vec{D} / \partial t + \text{rot } \vec{H}$ of Maxwell's electromagnetism, in which \vec{H} represents the magnetic field.

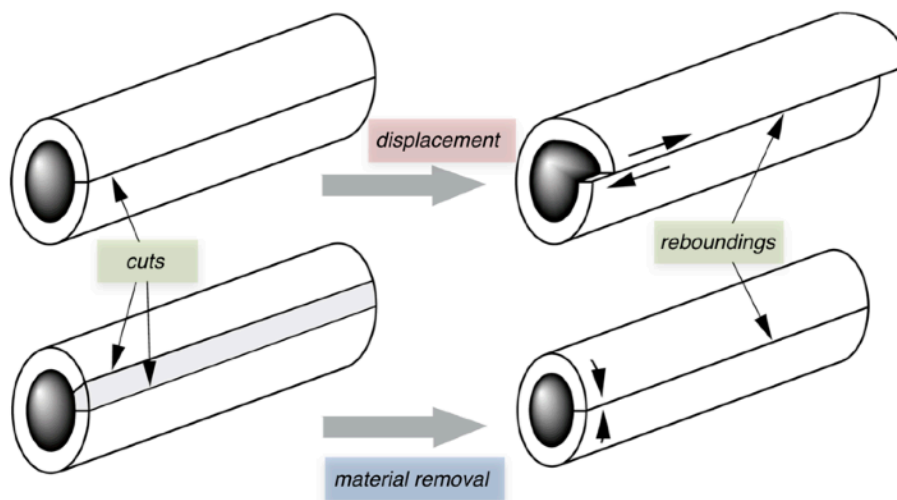


Figure 2.1 - The famous "Volterra pipes"

In figure 1.2, one saw that the condition of compatibility $\vec{\text{rot}} \vec{\beta}_i = 0$ prohibits the singularity by dislocation of the field of displacement \vec{u}_E . Consequently, if the compatibility condition was no longer zero, therefore if $\vec{\text{rot}} \vec{\beta}_i = \vec{\lambda}_i \neq \vec{0}$, the course on the closed contour C will result in the existence of a quantity \vec{B} , which is called *macroscopic Burgers vector*, defined on the contour C and which corresponds to the macroscopic translation necessary to accommodate the medium to the presence of *density charges* $\vec{\lambda}_i$, in order to ensure compatibility of total deformations and rotations (the absence of voids and overlaps of matter within the solid).

The discontinuity \vec{B} is called a *macroscopic dislocation* of the solid, in the sense of Volterra, and one will consequently call *density of dislocation charges* the tensorial density of charges $\vec{\lambda}_i$ responsible for plastic distortions.

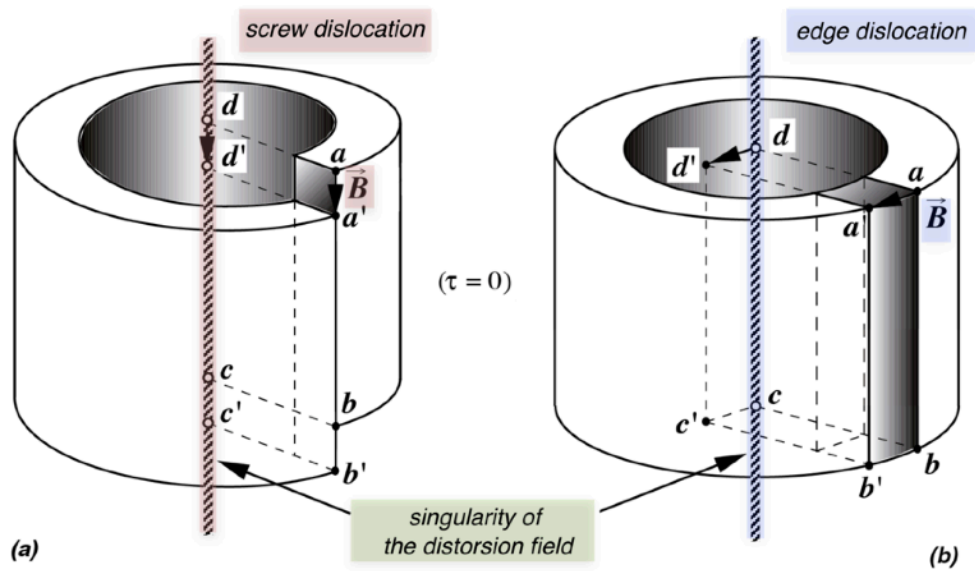


Figure 2.2 - Realization de screw (a) and edge (b) dislocations by cutting and gluing

Such macroscopic dislocation is carried out in a continuous solid by locally cutting this solid and by moving the two jaws of the cut parallel to each other, before gluing them again. This process is illustrated schematically in figure 2.2a using a pipe of material which is cut along the plane $abcd$ and which is glued after parallel sliding of the interfaces in the direction of the cut. There then appears a *one-dimensional topological singularity* of the distortion field located on the axis cd . This macroscopic singularity, characterized by a translation vector \vec{B} parallel to the line of singularity, is called *screw dislocation*.

On the other hand, if the two jaws are glued together by parallel translation of the jaws, perpendicular to the plane of the cut, and with the addition or subtraction of a parallelepiped of material (figure 8.2b), there appears another one-dimensional topological singularity of the distortion field, located on the axis cd . This macroscopic singularity, characterized by a translation vector \vec{B} perpendicular to the line of singularity, is called *edge dislocation*. Another way of proceeding to achieve an edge-type dislocation, but without adding or subtracting material, is to glue the two jaws together after parallel translation of the jaws in the plane of the cut, perpendicular to the direction of the cut, as shown in figure 2.3. Under the *sine qua non* condition that

the elastic volume expansion of the medium remained zero during the plastic deformation process, the Burgers vector \vec{B} , obtained by the course on a contour C surrounding the singularity, corresponds exactly to the macroscopic translation which has undergone the jaw $abcd$.

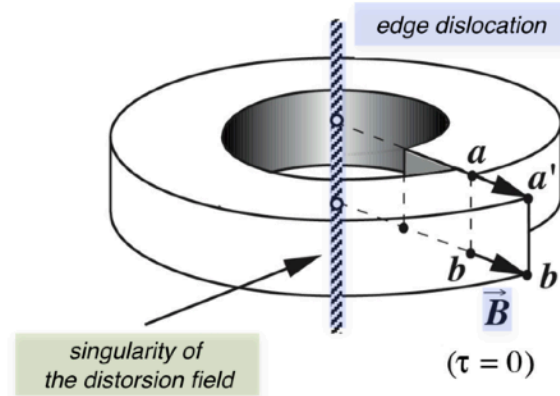


Figure 2.3 - Other realization of an edge dislocation
by cutting and gluing

Under the condition that the elastic volume expansion τ of the medium remained zero during the plastic deformation process, the Burgers vector \vec{B} , obtained by the course on the contour C surrounding the singularity, then corresponds exactly to the macroscopic translation which the jaw $a'b'cd$ underwent. As the vector \vec{B} must remain constant if we vary the diameter of the integration contour C or if we move this contour vertically, we deduce that *the dislocation charges must be confined to the immediate vicinity of the axis of the pipe, and that their tensor density must be a constant along this axis.*

One can also imagine that within a continuous solid one cuts a vacuum within the material in the shape of a torus, as illustrated by the section represented in figure 2.4a, then that one cuts the median plane located in the center torus. The two jaws ab and $a'b'$ thus formed can then be moved relative to each other, then glued.

The first possible case is to move the two jaws parallel to the cutting plane by a distance \vec{B} as shown in figure 2.4b. After gluing, the medium is deformed by shearing and the torus contains a *macroscopic dislocation of slip loop type*, composed of edge, screw and mixed dislocation portions.

You can also insert additional material in the form of a thin disc with a thickness \vec{B} between the two jaws and weld this disc to the two jaws (figure 2.4c). We then obtain a deformation of the medium responsible obviously for a curvature of the medium on both sides of the torus. The torus is then the site of a *macroscopic dislocation, of the prismatic loop type*. In this case, the prismatic loop is said to be *interstitial*, because it contains additional material, and it is composed of a single edge dislocation which closes on itself. A very similar case is obtained if, instead of adding a disc of material, we subtract a thin disc of material with a thickness \vec{B} , as illustrated in figure 2.4d. We also obtain a *macroscopic dislocation, of the prismatic loop type*, but this loop is said to be *lacunar*, because it lacks a certain amount of matter. Within the torus, there is also a single edge dislocation which closes on itself.

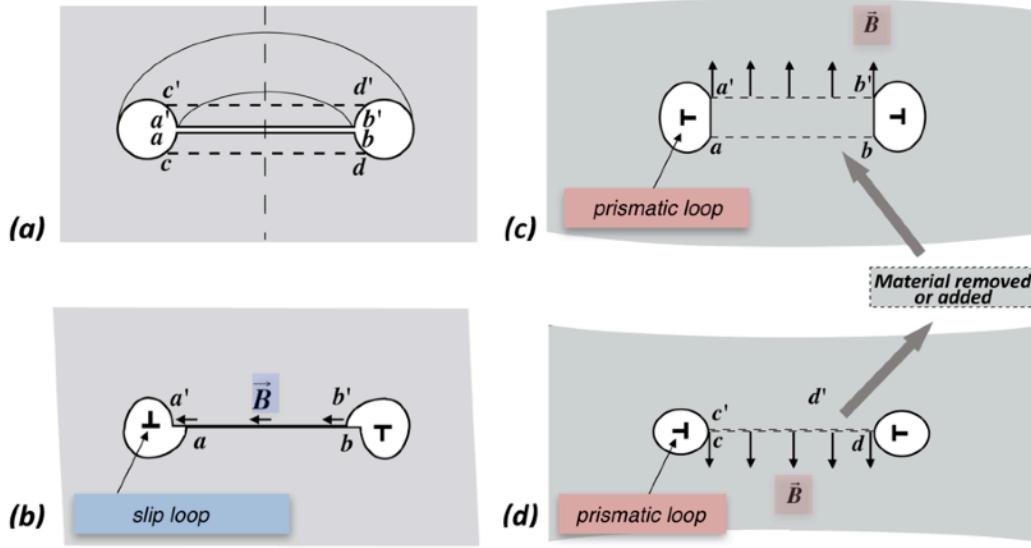


Figure 2.4 - Initial cutting of a torus and its median plane to form loops (a) and making a slip dislocation loop by sliding the jaws (b) and prismatic dislocation loops by addition (c) or subtraction (d) of material.

All the singularities thus obtained are obviously responsible for a field of distortion within the solid. Consequently, they require a non-zero formation energy. They are stabilized within the solid by re-bonding the two jaws of the cut, therefore by the bonds within the solid.

Definition of density and flow tensors of plastic charges

In figure 1.12, we represented the geometro-kinetic equations of the medium, which in fact connect the temporal variations of the distortions of the solid, calculated along the trajectory of the medium particles using the *material derivative*, with the spatial variations of the velocity field $\vec{\phi}(\vec{r}, t)$ of the medium particles, calculated using the gradient of the components of the velocity field in the case of the distortion tensor. And in figures 1.13 to 1.15, we had introduced the geometro-compatibility equations, which ensured the continuity of the Eulerian field of displacement within the solid, therefore the absence of discontinuities of displacements like dislocations. In the presence of displacement discontinuities, like those which we have just described on the macroscopic scale, it becomes necessary to redefine the geometro-kinetic equations and the geometro-compatibility equations of the medium, in order to take into account the presence of these topological singularities of distortion.

Using the definition of the distortion tensor, as it was obtained in the previous chapter in the presence of plastic deformation, the total distortions $\vec{\beta}_i^{tot}$ are the sum of elastic, anelastic and plastic distortions, such as $\vec{\beta}_i^{tot} = \vec{\beta}_i^{el} + \vec{\beta}_i^{an} + \vec{\beta}_i^{pl}$. Another notation for these distortions can be introduced, which makes it possible to separate the contributions of plastic deformation from the contributions of elastic and anelastic deformation, by simply writing that $\vec{\beta}_i^{tot} \rightarrow \vec{\beta}_i + \vec{\beta}_i^{pl}$ with $\vec{\beta}_i = \vec{\beta}_i^{el} + \vec{\beta}_i^{an}$, as illustrated in figure 2.5 (a).

This simple change of name makes it possible to introduce, by analogy with the equations of

electromagnetism, the concept of *tensor density* $\vec{\lambda}_i$ of charges, responsible for plastic distortions, by assuming *a priori* the relation $\vec{\lambda}_i = -\overrightarrow{\text{rot}} \vec{\beta}_i^{pl}$ of definition of $\vec{\lambda}_i$ from the plastic distortion tensor $\vec{\beta}_i^{pl}$, as well as the concept of *tensor flow* \vec{J}_i of charges, responsible for the temporal variation of plastic distortions, by supposing *a priori* the relation $\vec{J}_i = d\vec{\beta}_i^{pl} / dt$ of definition of \vec{J}_i , starting from the temporal derivative $d\vec{\beta}_i^{pl} / dt$ of the tensor of plastic distortion $\vec{\beta}_i^{pl}$. It should also be noted here that the concept of charge flow is defined as a *flow with respect to the lattice*, because it is deduced from the material derivative of $\vec{\beta}_i^{pl}$, that is to say from the temporal derivative of $\vec{\beta}_i^{pl}$ *taking along the trajectory of the solid lattice*.

The geometro-kinetic equation for the distortion tensor $\vec{\beta}_i$ in figure 1.12 already contained a source S_n of lattice sites, which actually represented a source of plasticity related to the volume expansion of the lattice. The geometro-kinetic equation for the distortion tensor $\vec{\beta}_i$ obtained in figure 2.5 (a) generalizes this fact, by including the source of lattice sites in the concept of *tensor flow* \vec{J}_i of plastic charges.

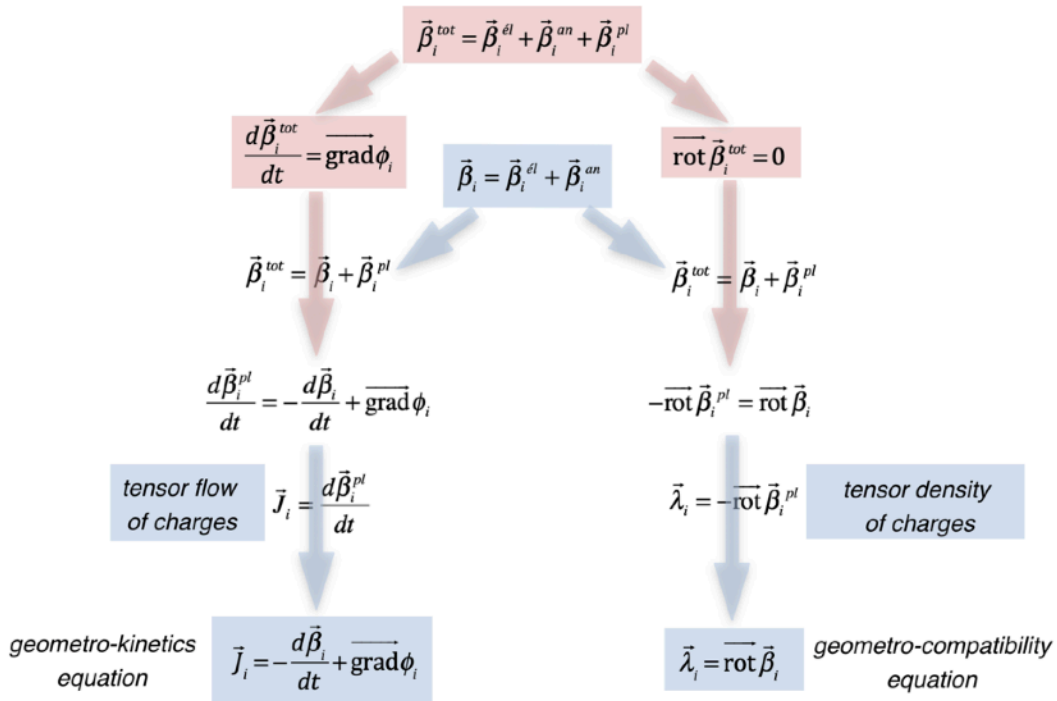


Figure 2.5(a) - Introduction of the tensor of density and flux of plastic charges in the presence of elasticity, elasticity and plasticity

The introduction of these new tensors of density and flow of charges is not free, because these answer at best the requirement to find a way to express the presence of plastic distortions in a solid so that it is possible to take into account the microscopic state of the network of structural defects in the solid. It will also be verified *a posteriori*, during the interpretation of these tensors in the rest of this chapter, that this way of proceeding is indeed judicious. With this approach to the phenomena of plasticity by tensors \vec{J}_i and $\vec{\lambda}_i$, the topological equations describing the geometro-kinetics and the geometro-compatibility of the distortion tensor

$\vec{\beta}_i = \vec{\beta}_i^{el} + \vec{\beta}_i^{an}$ of an elastic, anelastic and plastic solid are now written in a much more general way, as illustrated in figure 2.5(a).

This new version of topological distortion tensors and geometro-kinetic equations is in fact nothing more than a simple change of terminology for plastic distortions, based on an analogy with the two Maxwell equations of electromagnetism $\rho = \text{div } \vec{D}$ and $\vec{j} = -\partial \vec{D} / \partial t + \text{rot } \vec{H}$. Finding all the potentialities contained in this formulation of topological equations will therefore be the subject of the rest of this chapter.

The density $\vec{\lambda}_i$ of dislocation charges and the flow \vec{J}_i of dislocation charges are tensor quantities, on which it is possible to apply symmetry operations to reduce their tensor order, i.e. to make them vector quantities and scalar quantities. These symmetry operations are shown in figure 2.5 (b).

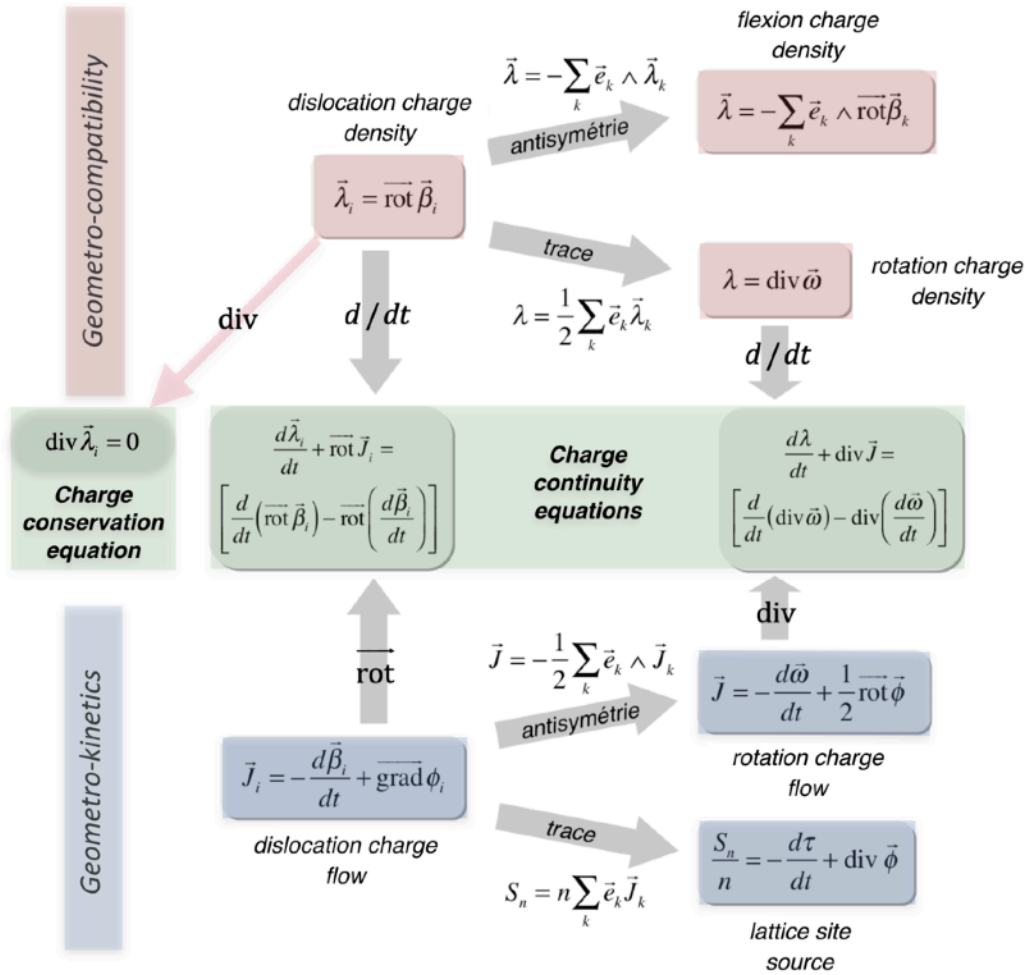


Figure 2.5(b) - Breakdowns of charge densities and charge flows, and charge continuity and charge conservation equations

Concerning the geometro-compatibility equations, we note that the tensorial density $\vec{\lambda}_i$ of dislocation charges contains a vector density $\vec{\lambda}$ of bending charges and a scalar density λ of rotation charges. We will return later to the interpretation of vector bending charges, but we can already give an interpretation of the effects of scalar rotation charges. Indeed, if we consider

figure 1.15, we know that the compatibility condition $\text{div } \vec{\omega} = 0$ prohibits the singularity by divergence of the rotation field, which means that, if $\text{div } \vec{\omega} = \lambda \neq 0$ within the volume V , there can appear a field of rotation vectors which diverge, of the same way that the local presence of a non-zero density of electric charges at a place in space induces a diverging electric field.

Concerning the geometro-kinetic equations, we note that the tensor flow \vec{J}_i of dislocation charges contains a *vectorial flow* \vec{J} of rotation charges and that it re-appears the *scalar volume source* S_n of lattice sites.

The mathematical combination of the material derivative of the geometro-compatibility equations with the rotational or the divergence of the geometro-kinetic equations makes it possible to deduce *the continuity equations* of figure 2.5(b) for the plastic distortion charges, which link the temporal evolution of the densities of charge along the trajectory of the medium to the spatial variations of the charge flows. These continuity equations reveal rather surprising terms of sources of plastic charges, in the sense that these terms are associated with *the possible existence of a non-commutativity of the temporal operator of material derivative with the space operators*. Finally, as regards the tensorial density $\vec{\lambda}_i$ of dislocation charges, we note that it is linked to the curl of $\vec{\beta}_i$, so that it obligatorily satisfies the relation $\text{div } \vec{\lambda}_i = 0$ of the vector analysis which we will call *the conservation equation of the dislocation charges*, equation which will be called thereafter to play a considerable role in the topological interpretation of the charges of dislocation.

Macroscopic concept of plastic contortion charges

In Figure 1.16, we reported the complete system of distortions and contortions of a solid lattice in Euler coordinates, in the case of a geometro-compatible solid. The same diagram, if it is drawn in the case of a solid with a non-zero density of dislocation charges $\vec{\lambda}_i$, becomes clearly more complex as illustrated in figure 2.6.

Apart from the tensor density $\vec{\lambda}_i$ of dislocation charges, the vector density $\vec{\lambda}$ of bending charges and the scalar density λ of rotation charges, which we will call 1st order charges associated with plastic distortions, there appear to be 2nd order charges, associated with plastic contortions, which will be called *the tensor density* $\vec{\theta}_i$ *of disclination charges* and *the scalar density* θ *of curvature charges*.

We also note that the expressions of *contortions* $\vec{\chi}_i$, *flexions* $\vec{\chi}$ and *torsions* $[\vec{\chi}_i]^S$ of the solid lattice become much more complicated since they now call in their respective expressions for the existence of *charge densities of contortion*, of *flexion* and of *torsion of 1st order*, deduced as combinations of the charge densities of dislocation $\vec{\lambda}_i$, of *flexion* $\vec{\lambda}$ and of *rotation* λ .

In figure 1.19, one saw that the condition of compatibility $\text{rot } \vec{\chi}_i = 0$ prohibited the singularity by disclination of the field of rotation $\vec{\omega}^{(e)}$ deduced from the deformation tensor. Consequently, *if the compatibility condition is no longer zero*, then if $\text{rot } \vec{\chi}_i = \vec{\theta}_i \neq 0$, the course on the closed contour C will result in the existence of a nonzero closure vector $\vec{\Omega}$, called the *Frank vector*. This means from a topological and physical point of view that there will be *discontinuities of rotations by deformation*. The discontinuities $\vec{\Omega}$ are called *disclinations* within the solid lattice.

Concerning the geometro-compatibility equations for 2nd order charges, we can also give an interpretation of the effects of the scalar charges θ of curvature. Indeed, if we consider figure 1.20, we know that the condition of compatibility $\text{div } \vec{\chi} = 0$ prohibits the singularity by

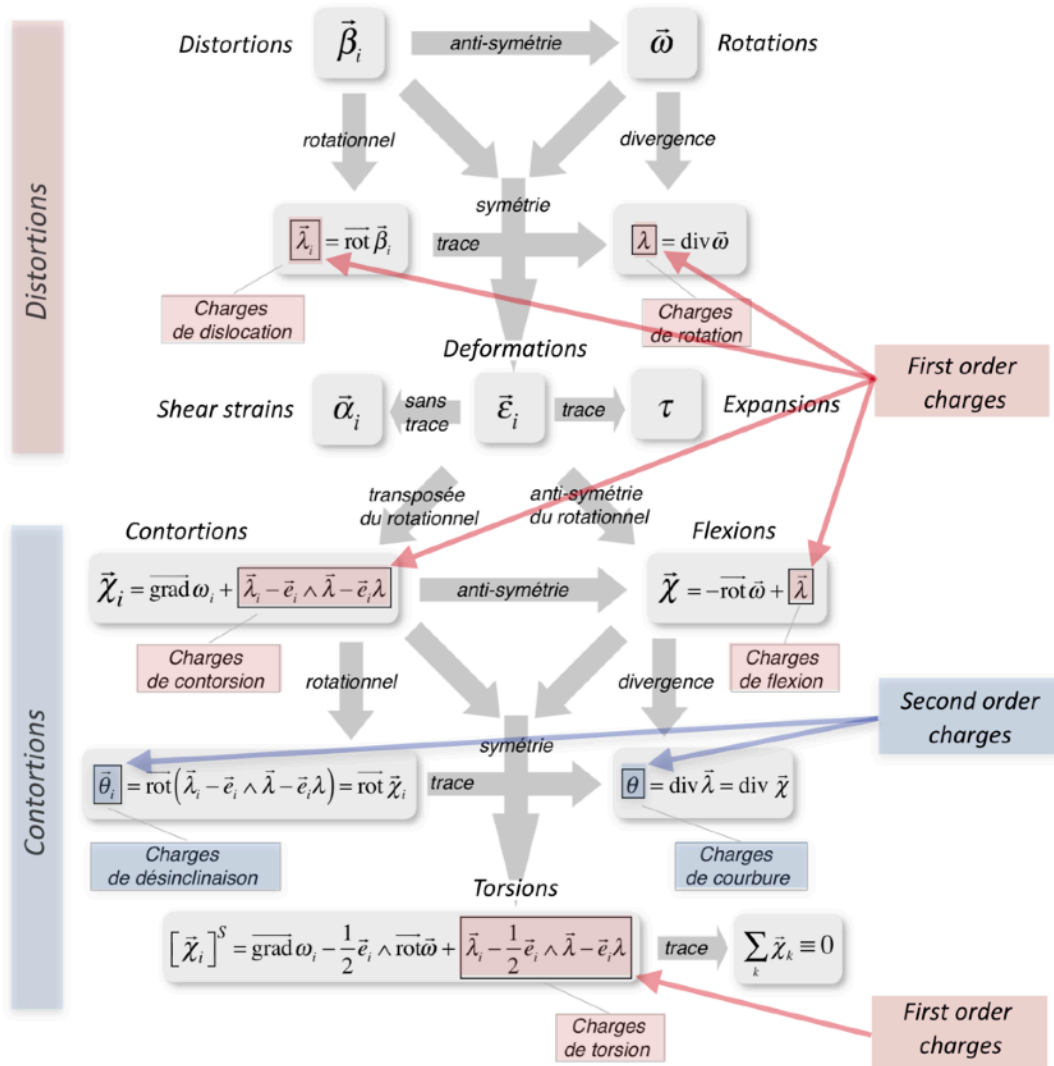


Figure 2.6 - The system of distortions and contortions in the presence of plastic charges

divergence of the flexion field, which means that, if $\text{div } \vec{\chi} = \theta \neq 0$ within the volume \mathbf{V} , it can appear a field of vectors of curvature which diverge, in the same way as the local presence of a density of non-zero electric charges at a place in space induces a diverging electric field.

The operations by symmetry and by vector analysis operators, making it possible to deduce from the tensor charge density $\vec{\lambda}_i$ of dislocation all the charge densities reported in figure 2.6, are summarized in figure 2.7.

It is quite simple to imagine carrying out a macroscopic scale disclination in a solid continuous medium by locally cutting this solid and turning the two jaws of the cut relative to each other, before putting them glue back together. This process is illustrated schematically in figure 2.8 using a pipe of material which is cut according to **abcd** and which is glued in two different ways:

- either by shearing the plane **a'b'cd** of one of the jaws without adding or subtracting material (figure 2.8a), which leads to a *unidimensional topological singularity* located on the axis **cd**, called *twist disclination*,

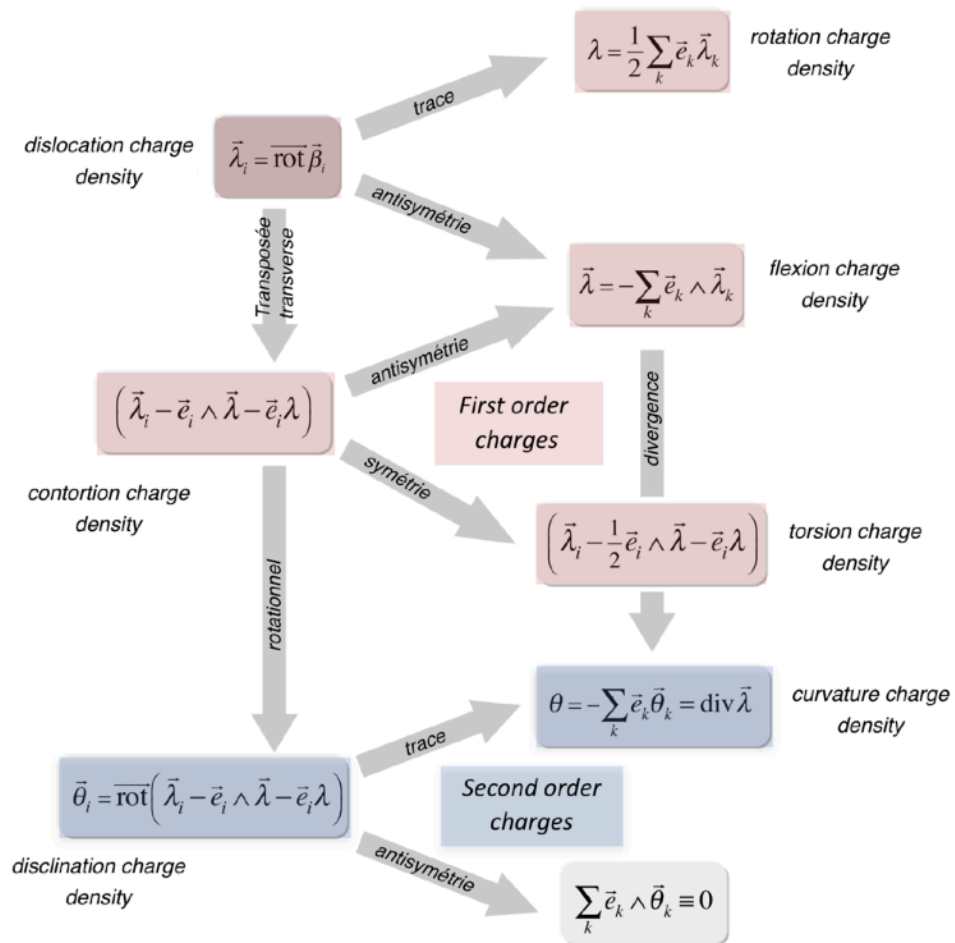


Figure 2.7 - Deduction of all charge densities from the dislocation charge density

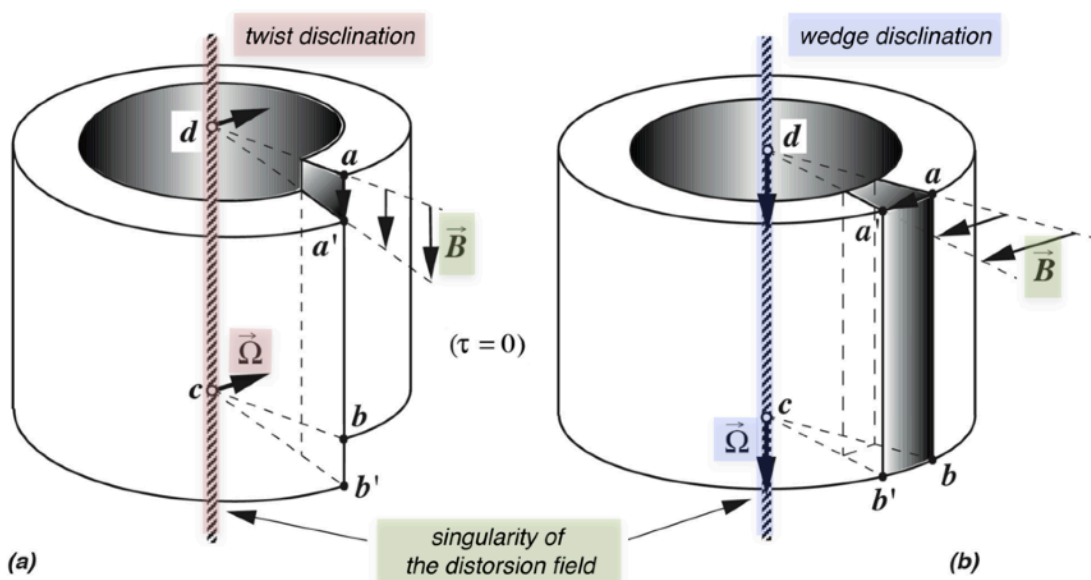


Figure 2.8 - Realization of twist (a) and wedge (b) disclinations by cutting and gluing

- either by rotation of one of the interfaces around the edge cd with addition or subtraction of material (figure 2.8b), which leads to a *one-dimensional topological singularity* located on the axis cd , called *wedge disclination*.

Under the condition that the elastic volume expansion τ of the medium remained zero during the plastic deformation process, the vector $\vec{\Omega}$, obtained by the course on the outline C surrounding the singularity, then corresponds exactly to the macroscopic rotation which the jaw $a'b'cd$ underwent. As the vector $\vec{\Omega}$ must remain constant if one varies the diameter of the integration contour C or if one displaces this contour vertically, one deduces that *the charges of disclination must be confined in the immediate vicinity of the axis cd of the pipe, and that their tensor density must be a constant along this axis*.

The topological singularities thus obtained are responsible for a distortion field within the solid. Consequently, they require a non-zero formation energy. They are stabilized within the solid by re-bonding the two jaws of the cut, therefore by the bonds within the solid.

By comparing figures 2.2 and 2.8, we can see an astonishing resemblance between screw dislocations and disclinations, as well as between edge dislocations and disclinations. This resemblance is not accidental, since the operations used to generate these discontinuities are very similar. It is interesting to note in particular that the macroscopic disclinations also present a displacement vector \vec{B} going from a to a' (figure 2.8), just like the macroscopic dislocations (figure 2.2). However, this vector \vec{B} , in the case of disclintions, increases linearly with the diameter of the integration loop that is used to calculate it. This means that in the presence of a macroscopic disclination, associated with a density of disclinations charges distributed along the

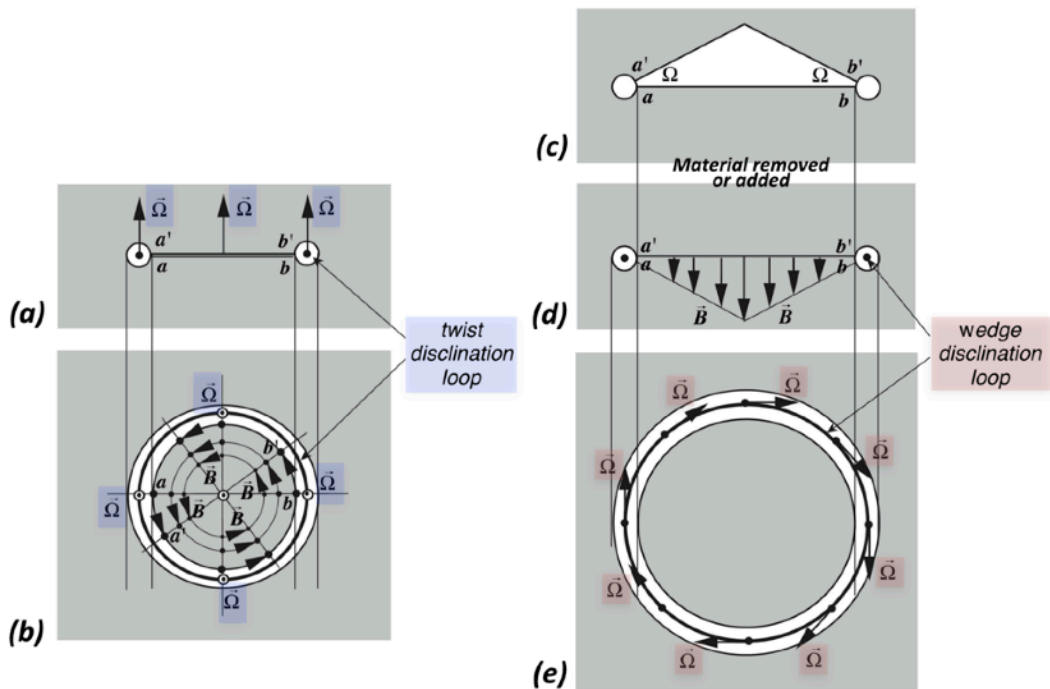


Figure 2.9 - Realization of a twist disclination loop by rotation of jaws (a) and (b) and a wedge disclination loop by removal (or addition) of a piece of conical material (c), (d) and (e)

axis cd of the pipe, there must also exist a density of dislocation charges. But this, instead of being located on the axis of the pipe as it is the case for a macroscopic dislocation, will be found homogeneously *on a surface* located in the cutting plane $abcd$ (figure 2.8), such that the Burgers vector \vec{B} increases linearly with the diameter of the integration loop C .

One can also imagine that within a continuous solid one cuts a void of material in the form of a torus, as illustrated by the section represented in figure 2.4a, then that one cuts the median plane located in the center of the torus. The two jaws ab and $a'b'$ thus formed can then be moved relative to each other, then glued. We can proceed as in figure 2.9a, and move the two jaws in parallel by a rotation $\vec{\Omega}$ of one relative to the other in the cutting plane. After re-bonding, the medium is deformed by rotation $\vec{\Omega}$ and the torus then contains a *macroscopic disclination loop of the twist type*.

Note here that the field of displacement of the medium on either side of the cutting plane is tangential to this plane and that the curvilinear vector of displacement \vec{B} on the cutting plane increases from a zero value in the center to a value maximum on the edges of the torus. At the level of the torus, the local displacement field \vec{B} looks like it can be mistaken for the displacement field of a screw dislocation closed on itself, but it is in fact a *pseudo-dislocation* because *the curvilinear Burgers vector*, tangential to the dislocation line is not preserved in this case, as shown in figure 2.9b.

One could also remove a piece of medium in the center of the torus, of lenticular or conical shape and with an angle Ω at the base, as illustrated in figure 2.9c. In this case, the gluing plane has a local displacement field \vec{B} corresponding to perpendicular Burgers vectors whose lengths have a circular symmetry (figure 2.9d). At the level of the torus, the deformation required for re-bonding is a rotation $\vec{\Omega}$ tangential to the torus, which would therefore correspond to a *macroscopic wedge disclination loop*, but which is in fact a *pseudo-disclination* since the vector of Frank, always tangential to the line of disclination, is not preserved along the line (figure 2.9d).

Quantified dislocations in a lattice

Having described the macroscopic dislocations and disclinations that can appear in a continuous medium, we can now ask ourselves how it is possible to introduce these topological defects on the microscopic scale of a solid lattice. It is clear that the presence of a lattice must necessarily imply a form of quantification of these defects, in the form of topological singularities of the lattice.

It was not until 1934 that the search for this type of singularity in solid lattices really started, and therefore that the theory of lattice dislocations was born, following three famous papers published independently and each describing in its own way the edge dislocation. These are the publications of Orowan³, Polanyi⁴ and Taylor⁵. Then it was in 1939 that Burgers⁶ described

³ E. Orowan, *Z. Phys.*, vol. 89, p. 605, 614 and 634, 1934

⁴ M. Polanyi, *Z. Phys.*, vol. 89, p. 660, 1934

⁵ G. I. Taylor, *Proc. Roy. Soc. London*, vol. A145, p. 362, 1934

⁶ J. M. Burgers, *Proc. Kon. Ned. Akad. Wetenschap.*, vol. 42, p. 293, 378, 1939

screw and mixed dislocations. And it was finally in 1956 that the first experimental observations of dislocations in metals were reported, simultaneously by Hirsch, Horne and Whelan⁷ and by Bollmann⁸, thanks to the electron microscope. As for the disclinations, it was in 1904 that Lehmann⁹ observed them for the first time in molecular crystals, and it was in 1922 that Friedel¹⁰ gave their first physical description. Then, from the middle of the twentieth century, the physics of defects in solids took on a considerable scale.

As the tensor density $\vec{\lambda}_i$ of dislocation charges must satisfy the conservation equation $\text{div } \vec{\lambda}_i \equiv 0$, it is impossible for it to appear in point form and it must be in the form of *three non-diverging vector fields*. This strong condition implies that the tensor density $\vec{\lambda}_i$ of dislocation charges must always occupy a *non-zero volume domain* within the solid medium, which must have a form of *tubular cord*, which has necessarily to cross the solid right through, or have a *shape of an O-ring*.

The area of charges $\vec{\lambda}_i$ of tubular or toric shape can be modeled in the form of a *line of dislocation*, commonly called *dislocation*, representable by a *central one-dimensional fiber* located at the center of the string of non-zero density $\vec{\lambda}_i$ of charges. This *line of dislocation* must then necessarily either cross the solid right through, or form a closed on itself dislocation loop.

The closely related domains of non-zero density of dislocation charges can be modeled in the simplest way in the *form of thin strings*. If the dislocation string is sufficiently thin (of sufficiently small section), the density charge $\vec{\lambda}_i$ can be represented by a single quantity confined to the immediate vicinity of the central fiber of the cord, which will be called *dislocation line*, by introducing the concept of *linear tensor charge* $\vec{\Lambda}_i$ of dislocation, namely a set of three vectors defined on the central fiber.

We can then show that the rectilinear strings appearing in a solid lattice are *quantified* on the microscopic scale of the lattice (figures 2.10 and 2.11), and that these strings then represent *elementary plastic singularities* of the distortion fields, in other words "*elementary particles*" of the plastic deformation of the lattice.

If we consider the case of an ordered lattice of particles on a microscopic scale, we can introduce dislocations by cutting the bonds on a lattice plane, parallel displacement of the jaws and reconstruction of the bonds, as illustrated in figures 2.10 and 2.11 in the case of a simple cubic lattice.

The Burgers vector \vec{B} of the singularities thus obtained, that is to say the microscopic discontinuity of the displacements of the lattice due to the presence of the dislocation, is deduced by considering a closed circuit C on the lattice of the real solid, surrounding the singularity, and by searching for the closing vector \vec{B} of the corresponding open circuit *in the undistorted virtual network*.

Thanks to figures 2.10 and 2.11, we can see that the microscopic lattice singularities have an

⁷ P. B. Hirsch, R. W. Horne, M. J. Whelan, *Phil. Mag.*, vol. 1, p. 667, 1956

⁸ W. Bollmann, *Phys. Rev.*, vol. 103, p. 1588, 1956

⁹ O. Lehmann, «*Flussige Kristalle*», Engelman, Leipzig, 1904

¹⁰ G. Friedel, *Ann. Physique*, vol. 18, p. 273, 1922

essential characteristic: *their Burgers vector is quantified*, that is to say that its components B_i can only be integer multiples of the step a of the virtual lattice, thus of the lattice in homogeneous volume expansion of value τ .

The nature of the microscopic plastic singularity can change according to the respective directions which take, in the system of local coordinates, the Burgers vector \vec{B} and the unit vector \vec{t} tangent to the line:

- when \vec{B} is parallel to \vec{t} (figure 2.10), the *linear charge of rotation* $\vec{\Lambda}_i$ of dislocation presents a non-zero trace ($\Lambda \neq 0$), therefore a *charge of rotation*, and a null antisymmetric part ($\Lambda \neq 0$). One speaks in this case of *screw dislocations*, and of *linear charge Λ of rotation of the screw dislocation*, and one symbolically represents this by a screw located on the line of dislocation.

Like $\Lambda = -\vec{B}\vec{t} / 2$, when the screw dislocation has a *right rotation*, identical to the direction of rotation of a normal screw or a corkscrew, Λ is positive and the vectors \vec{t} and \vec{B} are

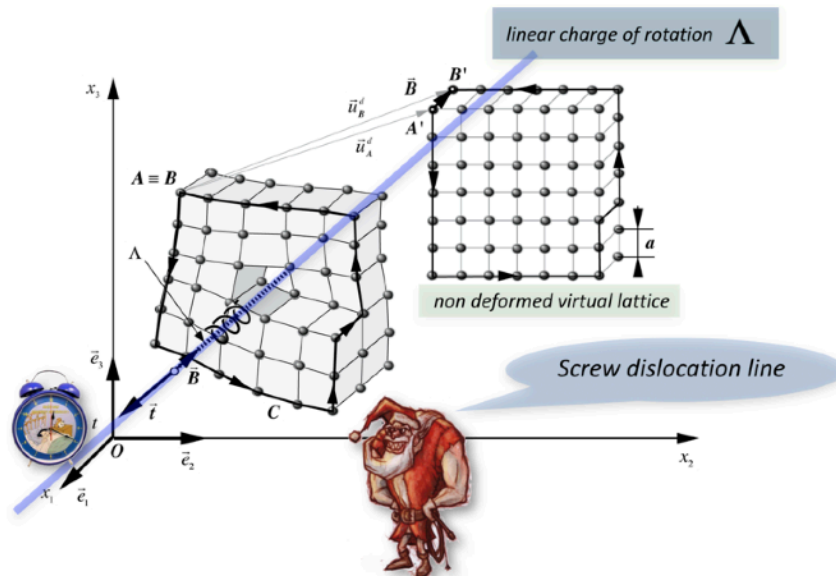


Figure 2.10 - Screw dislocation line quantified in a cubic lattice

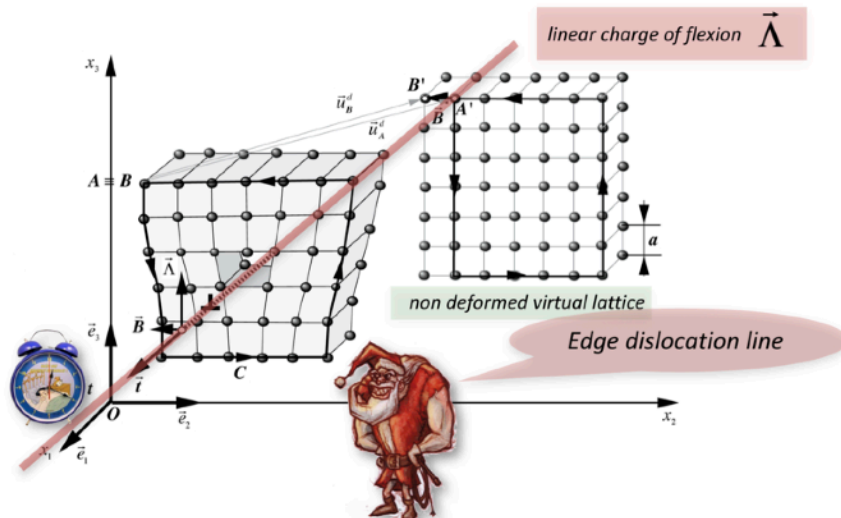


Figure 2.11 - Edge dislocation line quantified in a cubic lattice

oriented in opposite directions. On the other hand, if the screw dislocation has a *left rotation*, therefore in the opposite direction of rotation to that of a normal screw or a corkscrew, Λ is negative and the vectors \vec{t} and \vec{B} are oriented in the same direction (figure 2.12). Note that the choice of a given direction \vec{t} is perfectly arbitrary since only the sign of Λ is fixed.

- when \vec{B} is perpendicular to \vec{t} (figure 2.11), the *linear charge* $\vec{\Lambda}_i$ of dislocation presents a null trace ($\Lambda = 0$), therefore no charge of rotation, but a non-zero antisymmetric part ($\vec{\Lambda} \neq 0$). One speaks in this case of *edge dislocations*, and of *linear charge* $\vec{\Lambda}$ of flexion of the edge dislocation, and one symbolically represents this one by a sign \perp on the line of dislocation, oriented so as to represent the additional plane of particles. The vector $\vec{\Lambda}$ always has the direction of the additional plane of the edge dislocation (figure 2.13).

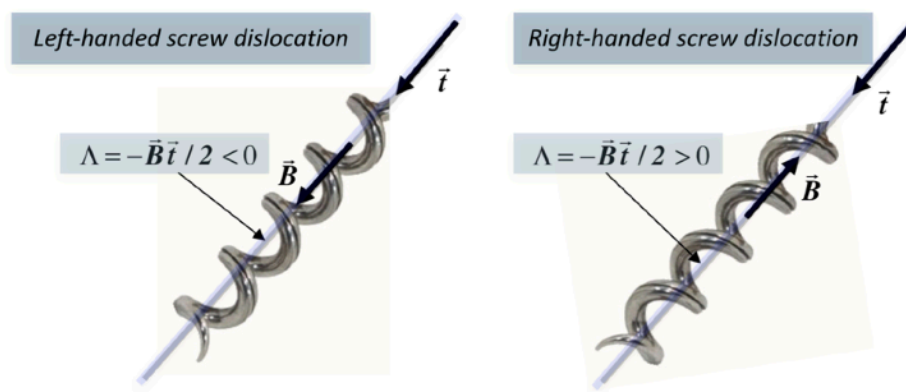


Figure 2.12 - Burgers vectors of screw type dislocations, «left-handed» and «right-handed» respectively

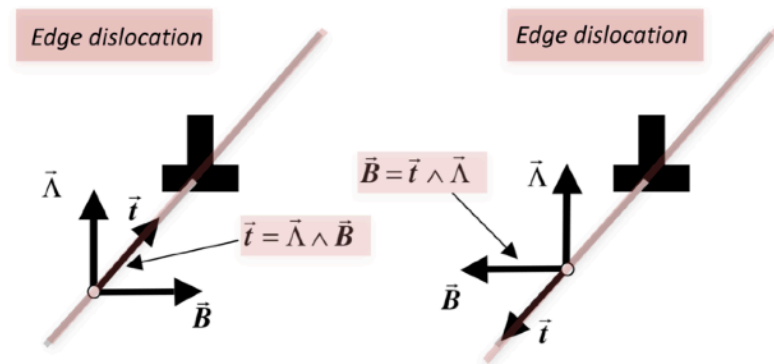


Figure 2.13 - Burgers vectors of edge type dislocations

- when \vec{B} is neither parallel nor perpendicular to \vec{t} , the *linear dislocation charge* $\vec{\Lambda}_i$ has a non-zero trace ($\Lambda \neq 0$), but also a non-zero asymmetric part ($\vec{\Lambda} \neq 0$), so that it behaves at the same time as a source of elastic and anelastic rotations *and* flexions. We speak in this case of *mixed dislocations*.

In a discrete network, a dislocation can perfectly change direction. In other words, along the dislocation line, the tangent vector \vec{t} is not necessarily preserved. In this case, as the Burgers vector \vec{B} is kept in the local frame, this means that the dislocation must change in nature. For

example, in figure 2.14, a simple cubic lattice model is shown in which a screw dislocation enters the left face, turns becoming mixed within the lattice and emerges as an edge dislocation on the right adjacent face.

Quantified dislocations are the most basic vectors of the plastic deformation of a lattice. In this sense, we could call them the "*elementary particles*" of plastic deformation. Besides, any dislocation string has its "*anti-string*". Indeed, it is easy to see that two parallel dislocations of the same direction \vec{t} and vectors of Burgers \vec{B} and $-\vec{B}$ respectively annihilate completely if they come to meet within the lattice.

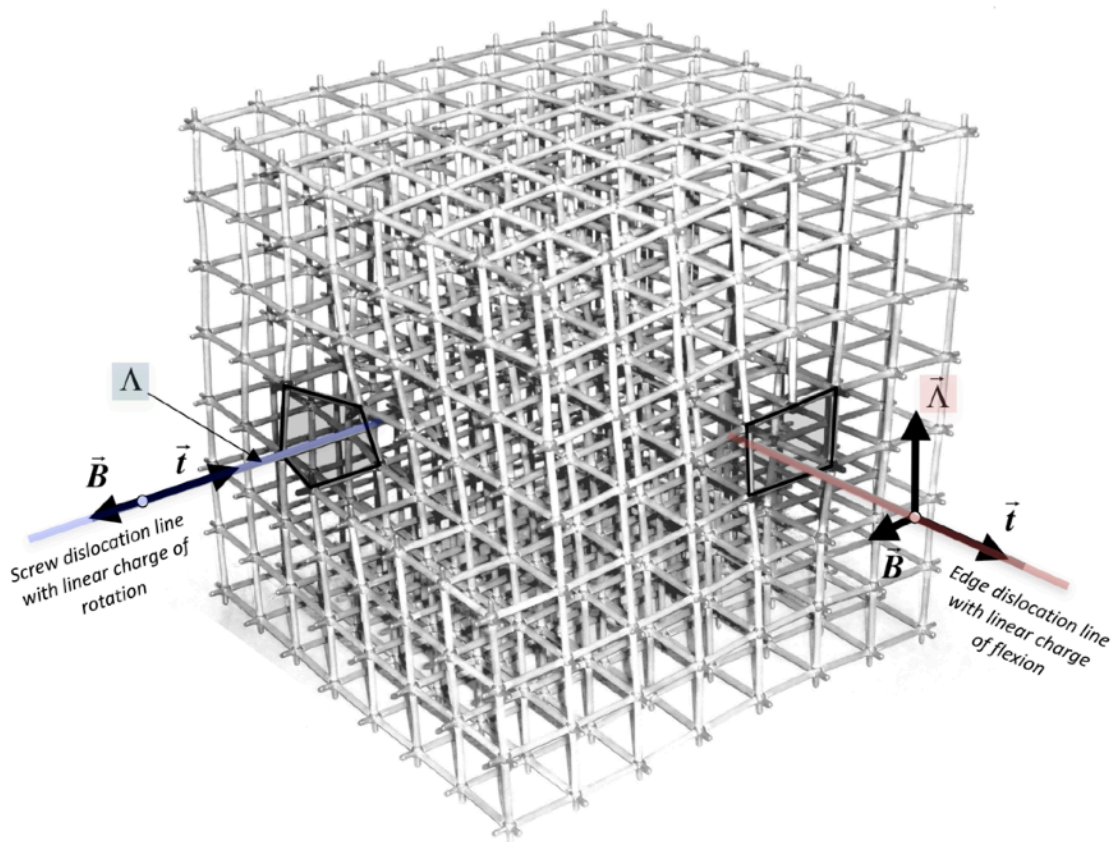


Figure 2.14 - Dislocation passing from screw to edge type in a cubic lattice

We also note that screw dislocations, carrying a scalar linear charge $\Lambda \neq 0$, are sources of a *field of divergent local rotations*, which is, as we have seen, the analog of the electric field. So, at a distance R from the string, the norm of the rotation field is simply $|\vec{\omega}| = |\Lambda| / 2\pi R$.

As for the corner dislocations, which carry a flexion charge $\bar{\Lambda} \neq 0$, they are sources of a *lattice flexion*, therefore of a *local curvature of the lattice* in their vicinity as well illustrated by the dislocation emerging from the cubic crystal in the figure. 2.14.

Dissociation of quantified dislocations

The dislocations appearing in structures a little more complex than the simple cubic lattice, such as for example cubic lattices with centered faces, cubic centered or hexagonal, *generally*

present much more complicated core structures. It can thus appear, essentially for energetic reasons, and according to the crystalline system considered, a dissociation of the core of the dislocation into two or more partial dislocations, of which the individual Burgers vectors are fractions of the translation vectors of the lattice.

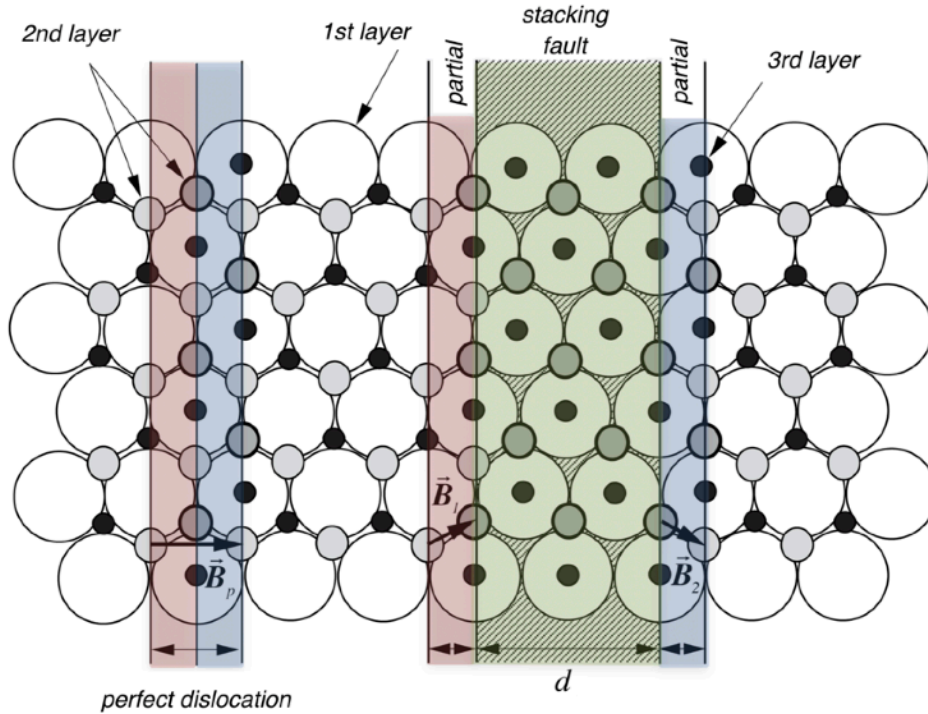


Figure 2.15 - Dissociation of a perfect dislocation into two partials and a stacking fault ribbon in a face-centered cubic lattice

For example, in face-centered cubic metals (CFC), the stacking of atoms is characterized by sequences *abc abc abc ...* (figure 2.15). The Burgers vector \vec{B}_p of a perfect dislocation must in principle connect two nodes of the lattice. But for energy reasons, the most favorable Burgers vectors are those that have a minimum length, because the distortion energy stored in the lattice by a dislocation is proportional to the square of its Burgers vector. Thus in the case of figure 2.15, the dislocations have interest to dissociate on their gliding plane in two partial of Burgers vectors \vec{B}_1 and \vec{B}_2 , so that $\vec{B}_p = \vec{B}_1 + \vec{B}_2$. In the case of this dissociation, we have indeed $\vec{B}_1 \vec{B}_2 > 0$, so that $\vec{B}_p^2 = \vec{B}_1^2 + \vec{B}_2^2 + 2\vec{B}_1 \vec{B}_2 > \vec{B}_1^2 + \vec{B}_2^2$. The two partial obtained in figure 2.15 by this dissociation are called *Shockley type*. The distance between the two partials is then controlled by a competition between the decrease in energy associated with the increase of the distance between the partials which repel each other, and the increase in energy due to the formation of an energy ribbon of crystalline stacking fault (*abc ac abc abc ...*) located between the two partial dislocations, as shown in figure 2.15.

Since the stacking fault ribbon has an energy γ per unit area, the total energy $E_t(d)$ per unit dislocation length for a dissociated dislocation over a distance d is written $E_t(d) = \gamma d + E_d(d)$, where $E_d(d)$ is the energy of the two partials as a function of the

distance d separating them, which is a monotonic function decreasing from E_0 for $d = 0$ to

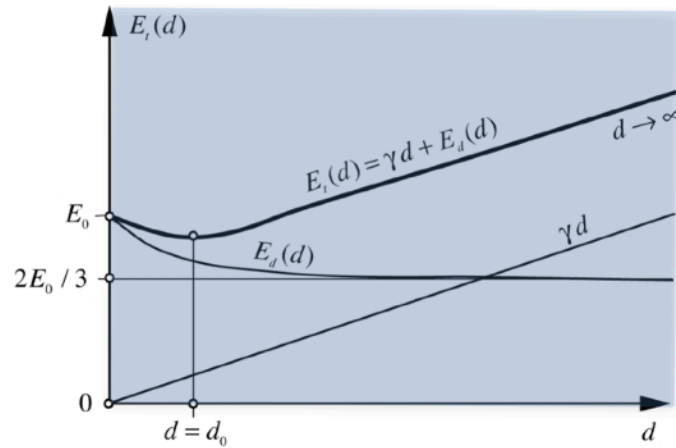


Figure 2.16 - Total energy of two partial dislocations depending on the distance between them, source of a "strong force" of attraction between them

$2E_0 / 3$ for $d \rightarrow \infty$ in the case of Shockley partials illustrated in figure 2.15.

The energy $E_t(d)$ therefore presents a minimum for the distance $d = d_0$ (figure 2.16), which is the equilibrium distance between the two partials, controlled by the competition between the energy decrease associated with the distance increase between the repulsive partials, and the energy increase due to the formation of a stacking-fault ribbon between the two partials. We see here appear a behavior of the energy $E_t(d)$ which induces an interaction force between the two partial which one could qualify as "strong force", in the sense that the energy of the pair of partial presents a minimum which fixes the equilibrium position d_0 , but that it continues to increase if we try to increase the separation distance beyond d_0 . The qualifier "strong force" is proposed here because the attractive behavior of the interaction force between partial at long distance presents a very interesting analogy with the strong force acting between quarks in the Standard Model of elementary particles.

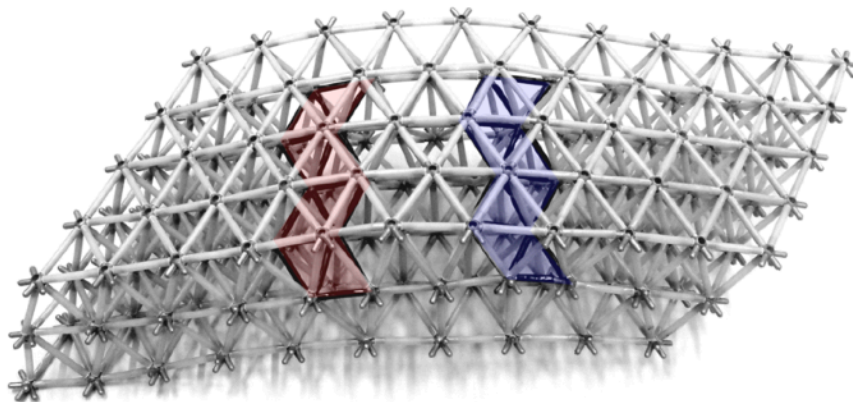


Figure 2.17 - Model of a mixed dislocation in a face centered cubic lattice presenting a dissociation into two partials, as well as kinks on the two partial dislocations

By way of exemplary illustration, figure 2.17 shows the model of a mixed dislocation, with an edge and a screw nature at the same time, dissociated into two partials in a cubic face centered structure. We can clearly see the existence of a stacking defect between the two partials. And since this is a mixed dislocation, the two partials show a series of kinks in it. In addition, we can even observe the bending of the network induced by the edge part of the dissociated dislocation.

All of the consequences linked to the structure of the lattice are obviously too specific for each conceivable crystal structure to be dealt with in detail here. But they can be approached in any book dealing with dislocations in crystalline structures.

Quantified dislocation membranes

A thin interface which contains dislocation charges and which separates two media containing no charges is called a *charged membrane*. These membranes can be any surfaces in space (*infinite surfaces, closed spheroidal or toric surfaces, ribbons or hollow tubes, thin plates, etc.*), with the only topological condition that, on any point of the membrane, the equation of conservation of the dislocation charges $\text{div } \vec{\lambda}_i \equiv 0$ is satisfied and that the disclination charges derive from the dislocation charges through the relation $\vec{\theta}_i = \overrightarrow{\text{rot}} [\vec{\lambda}_i - \vec{e}_i \wedge \vec{\lambda} - \vec{e}_i \lambda]$.

If a dislocation charged membrane is very thin, it is possible to introduce the notion of *surface tensor charge of dislocation* $\vec{\Pi}_i$. The existence of a *surface charge of dislocation* $\vec{\Pi}_i$ in the membrane leads to a discontinuity of the tangential components of the distortion vectors $\vec{\beta}_i$ on either side of it, and it is subject to the condition that *there is a gradient of the components of the Burgers vector on the surface of the membrane*.

Two-dimensional modeling of a thin membrane obtained with surface charges is generally called a *joint*. The joint is then entirely characterized by the data of the surface tensor $\vec{\Pi}_i$ of dislocation charges, the vectors of which are *tangent to the surface of the membrane*, which is in fact a direct consequence of the equation of conservation $\text{div } \vec{\lambda}_i \equiv 0$ of the dislocation charges. But it can also be characterized by the data of the anti-symmetrical part $\vec{\Pi}$ (the surface charge of flexion of the joint) and of the trace Π (the surface charge of rotation of the joint) of the load tensor $\vec{\Pi}_i$, as in the case of the one-dimensional lines of dislocation. This point is perfectly illustrated in figure 2.18, in which three thin membranes are presented whose Burgers vectors, growing linearly along the axis Ox_1 , are oriented respectively along the axes Ox_3 , Ox_1 , and Ox_2 . Since these thin dislocation membranes actually disorient or accommodate the solid grains on either side of the membrane, they are generally called *grain boundaries*.

We can for example consider that these membranes are in fact charged by edge dislocations or screw dislocations oriented parallel to the axis Ox_2 . We can then simply represent each individual dislocation by a linear vector charge $\vec{\Lambda}$ if it is an edge dislocation or by a scalar linear charge Λ if it is a screw dislocation. We then verify that:

- the thin edge type membrane with a Burgers vector perpendicular to the surface and increasing along the axis Ox_1 (figure 2.18a) can be entirely characterized by a *vector surface charge* $\vec{\Pi}$ of flexion, the vector of which is tangent to the plane of the membrane, directed according to Ox_1 , and worth $\vec{\Pi} = \vec{\Lambda} / d$. As this type of edge membrane makes it possible to disorient the solid grains located on either side of the membrane, it is called a *disorientation*

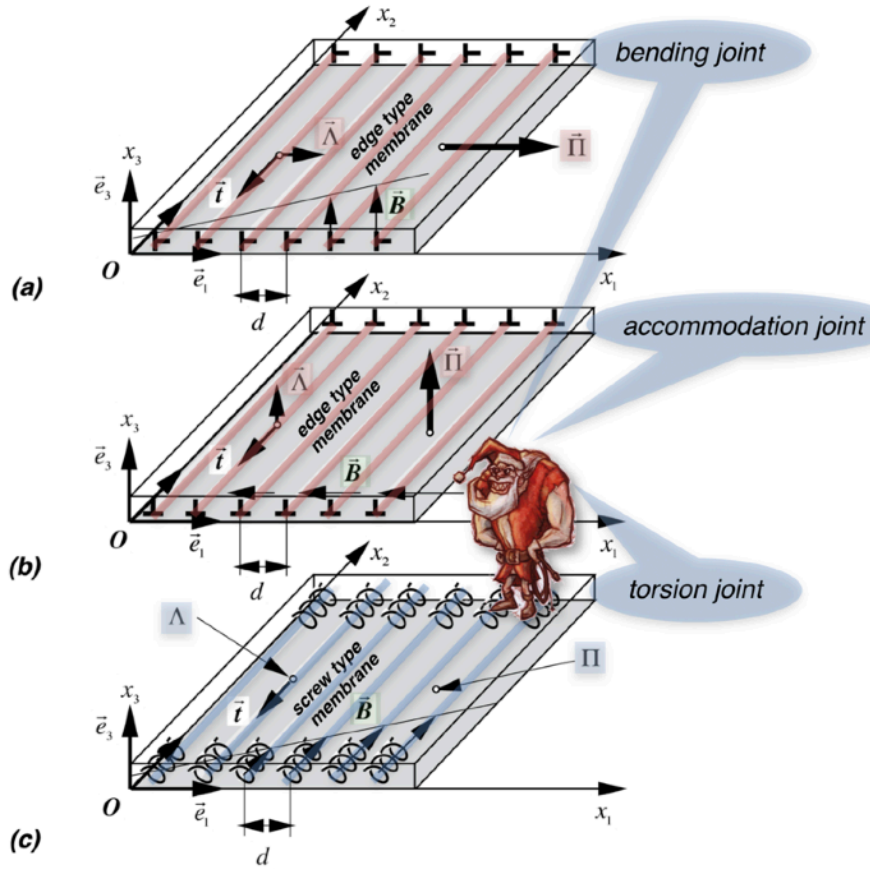


Figure 2.18 - Edge type dislocation membranes:
bending joint (a) and accommodation joint (b)
or screw type dislocation membranes: torsion joint (c)

joint, and in this particular case, as the disorientation corresponds to a flexion of the solid, we speak of a *bending joint*.

- the thin edge-type membrane with a Burgers vector parallel to the surface and increasing along the axis Ox_1 (figure 2.18b) can be entirely characterized by a *vector surface charge* $\vec{\Pi}$ of *flexion*, whose vector is perpendicular to the membrane, and being equal $\vec{\Pi} = \vec{\Lambda} / d$. As this type of edge membrane in fact makes it possible to modify in the direction Ox_1 the density of the crystalline planes of the solid grains situated on either side of the membrane, it can be qualified as an *accommodation joint*.

- the thin screw type membrane with a Burgers vector parallel to the membrane and increasing along the axis Ox_1 (figure 2.18c) is entirely characterized by the *scalar surface charge* Π of *rotation*, being equal $\Pi = \Lambda / d$. This type of screw membrane also corresponds to a disorientation joint between the solid grains located on either side of the membrane. In this particular case, as the disorientation corresponds to a rotation of the grains relative to one another, we speak of a *torsion joint*.

Quantified disclinations in a lattice

As the charges of disclination always derive from dislocation charges through relationship $\vec{\theta}_i = \text{rot} \left[\vec{\lambda}_i - \vec{e}_i \wedge \vec{\lambda} - \vec{e}_i \lambda \right]$, there can be no dislocation strings in an isolated state. But strings

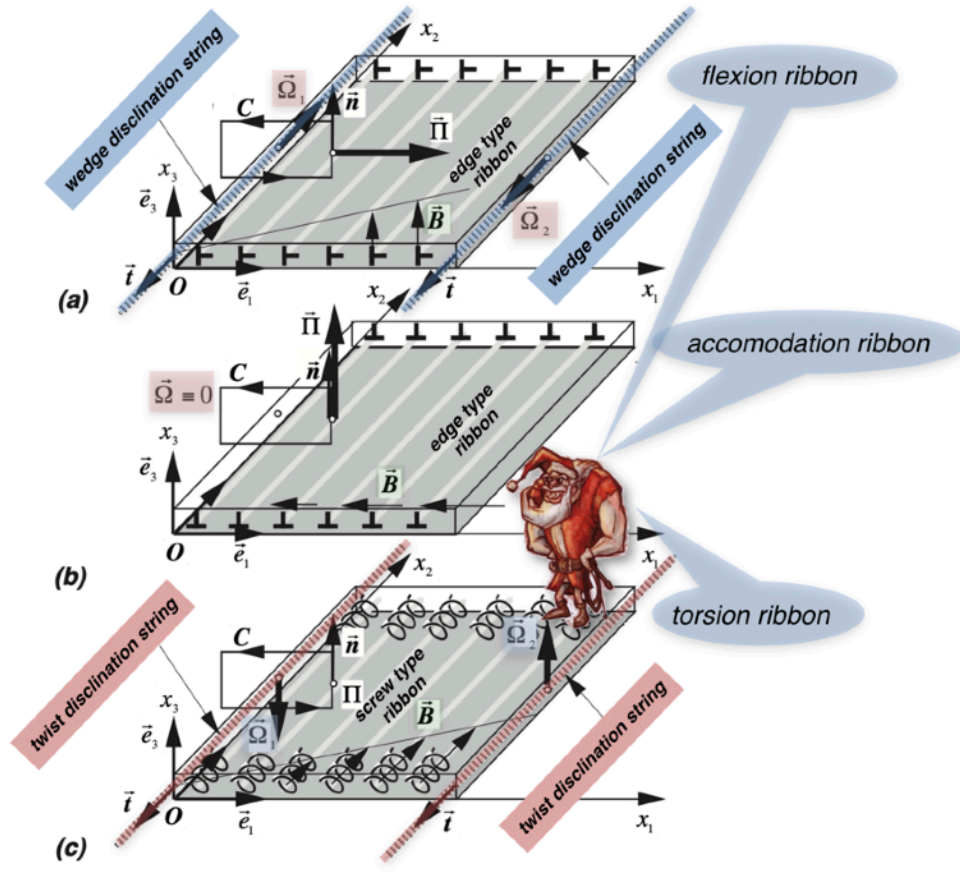


Figure 2.19 - Dislocation ribbons bordered by disclination lines of wedge type (a) and twist type (c).
 The dislocation ribbon (b) is not bordered by disclination lines

of disclination can appear in the presence of a large dislocation charge domain, such as a dislocation membrane in the form of a ribbon.

We can consider for example the case of flat ribbons charged with dislocations, which abruptly stop along the axis Ox_1 , as shown in figure 2.16. The boundaries which border these dislocation ribbons are then lines of disclination, because it appears on these boundaries singularities by disclination of the field of rotations by deformations, as described in figure 1.19, having a non-zero Frank vector $\vec{\Omega}$. In this figure, we see the following points:

- the edge-type dislocation ribbon with a Burgers vector perpendicular to the membrane and increasing along the axis Ox_1 (figure 2.19a) corresponds to a *localized bending joint*. It is bordered by two wedge type disclinations whose Frank vectors are parallel to the axis Ox_2 , and which are respectively worth $\vec{\Omega}_1 = -\vec{\Omega}_2 = -\vec{\Pi} \wedge \vec{n} = -|\vec{\Pi}| \vec{t}$,
- the edge-type dislocation ribbon with a Burgers vector parallel to the membrane and increasing along the axis Ox_1 (figure 2.19b) corresponds to a *localized accommodation joint*. As there is then no discontinuity in the rotational field by deformations, it is not bordered by any disclination and $\vec{\Omega}_1 = \vec{\Omega}_2 \equiv 0$,
- the screw-type dislocation ribbon with a Burgers vector parallel to the membrane and increasing along the axis Ox_1 (figure 2.19c) corresponds to a *localized torsional joint*. It is

bordered by *two twist-type disclinations* whose Frank vectors are parallel to the axis $\mathbf{O}x_3$, and which are worth respectively $\bar{\Omega}_1 = -\bar{\Omega}_2 = -\Pi\bar{\mathbf{n}}$.

It will be noted that the disclination of figure 2.19a corresponds to the macroscopic disclination represented in figure 2.8b, while that the disclination of figure 2.19c corresponds to the macroscopic disclination of figure 2.8a. The quantification on a cubic lattice of a ribbon of disclination similar to that of figure 2.19c is illustrated in figure 2.20, in which one has reported the two disclinations bordering a quantized dislocation ribbon composed of three aligned lattice screw dislocations.

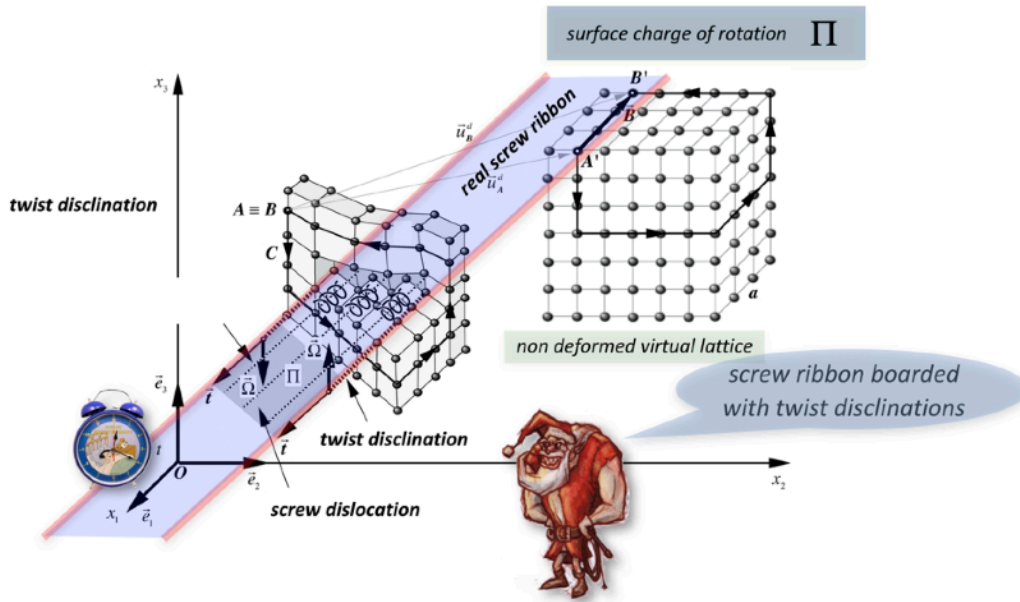


Figure 2.20 - Quantized two-dimensional dislocation ribbon composed of three screw lattice dislocations

Although there cannot be isolated disclinations, it is possible to imagine structured solid media which would contain rectilinear disclinations quantified on their lattice in the case of wedge disclinations, as shown in figure 2.21. In this figure, we have represented two wedge disclinations with Frank vectors $\Omega = \mp 90^\circ$ in a simple cubic lattice, and we have also reported the curvature vector $\bar{\chi}$ due to the charge Θ .

We can then imagine that there could be different families of quantified wedge disclinations by considering solid media with different arrangements of the particles in a secant plane of the disclination line. For the example, we will consider here simple arrangements like the arrangement on a quadratic network. But we could obviously also consider more complex arrangements, such as three-dimensional centered cubic, hexagonal or face centered cubic structures.

In the case of a quadratic arrangement, there can exist at most 3 different quantified wedge disclinations, which will be called $C1$, $C2$ and $C3$, with angles of rotation Ω of $+90^\circ$, $+180^\circ$ and $+270^\circ$, to which correspond 3 quantified wedge anti-disclinations, $\bar{C}1$, $\bar{C}2$ and $\bar{C}3$, with rotation angles of -90° , -180° and -270° (figure 2.22).

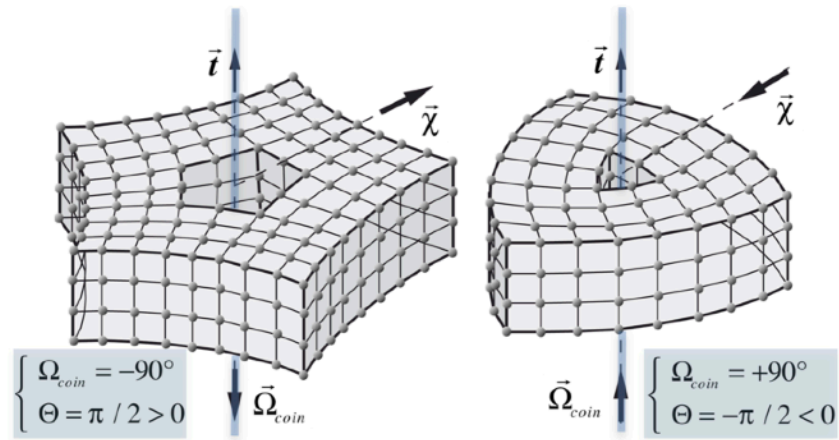


Figure 2.21 - Examples of quantified wedge disclination $\Omega = \mp 90^\circ$ in a simple cubic lattice

$C1 : \Omega = +90^\circ : \Theta = -\pi/2$	$\bar{C}1 : \Omega = -90^\circ : \Theta = +\pi/2$
$C2 : \Omega = +180^\circ : \Theta = -\pi$	$\bar{C}2 : \Omega = -180^\circ : \Theta = +\pi$
$C3 : \Omega = +270^\circ : \Theta = -3\pi/2$	$\bar{C}3 : \Omega = -270^\circ : \Theta = +3\pi/2$

Figure 2.22 - Family of quantified wedge disclinations in a quadratic planar arrangement

In the case of figures 2.22, we have reported the disclinations with a calculated size so that the volume expansion τ is identical in all the figures. Note also that the tilt of $+270^\circ$ in the quadratic arrangement could exist or not exist depending on the imaginary medium considered, because their existence is linked to the possibility of connecting two bonds of the same "particle" in the solid structured medium that we consider.

It has been shown that there cannot be isolated disclinations with non-zero Frank vector. Consequently, it is necessary to combine several disclinations close to one another so that the Frank vector obtained on a contour surrounding all these disclinations is zero.

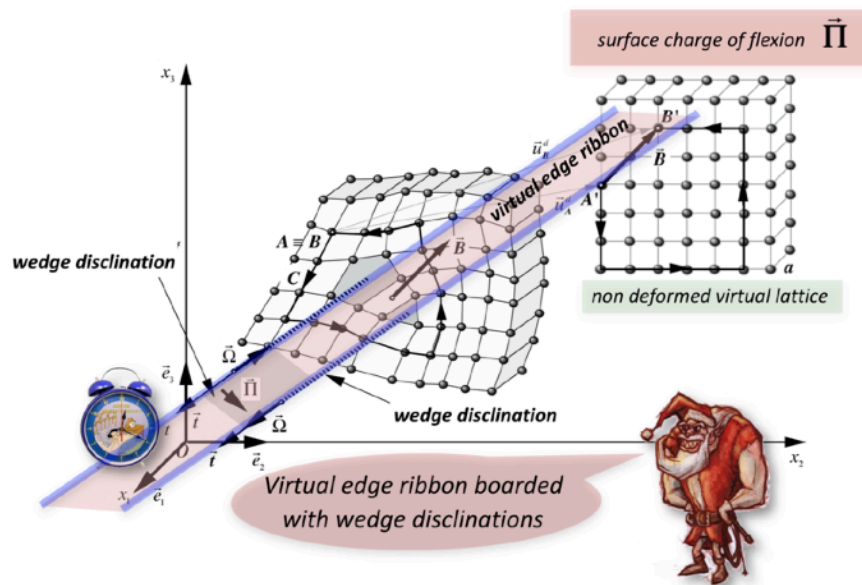


Figure 2.23 - Doublet of quantified wedge disclinations with virtual edge dislocation ribbon

The example shown in figure 2.23 illustrates this fact perfectly: by coupling two quantified wedge disclinations of type $C1$ and $\bar{C}1$ in a simple cubic structure, the total Frank vector becomes zero, and a virtual edge dislocation ribbon appears between the two disclinations, of non-zero global Burgers vector \bar{B} . The edge-type dislocation ribbon is similar to that shown in figure 2.19a and therefore contains a vector surface charge $\bar{\Pi}$ of flexion. But this real flexion charge $\bar{\Pi}$ is not associated with real quantized dislocations of the lattice, but *with a virtual ribbon of edge dislocation*. In the case of this wedge disclination doublet, it is fairly easy to imagine that the distortion energy increases extremely quickly if the two disclinations are moved away, so that these two disclinations can be considered to be linked by a "strong force", that is to say an attractive force which increases when an attempt is made to distance the two disclination.

We can find the multiplets of zero Frank vector disclinations which it is possible to construct on the basis of the quantified wedge disclinations that we have described in the case of the simple quadratic lattice. The basic zero vector Frank multiplets, i.e. those which can no longer be further decomposed into two or more zero Frank vector multiplets, are shown in figure 2.24. We note that, in a simple quadratic lattice, there can exist 3 doublets, 4 triplets and 2

quadruplets.

In table 2.24, the multiplets composed with disclinations $C3$ of $+270^\circ$ are grayed out, because they might not exist, for example in structured media which do not allow two bonds of the same "particle" to be connected together.

3 doublets	
$+90^\circ / -90^\circ$	
$+180^\circ / -180^\circ$	
$+270^\circ / -270^\circ$	

4 triplets	
$+90^\circ / +90^\circ / -180^\circ$	$-90^\circ / -90^\circ / +180^\circ$
$+90^\circ / +180^\circ / -270^\circ$	$-90^\circ / -180^\circ / +270^\circ$

2 quadruplets	
$+90^\circ / +90^\circ / +90^\circ / -270^\circ$	$-90^\circ / -90^\circ / -90^\circ / +270^\circ$

Figure 2.24 - The multiplets of quantified wedge disclinations in a quadratic planar structure

Solid lattices with axial symmetry

Mixed strings resulting from the combination of a string or a line of disclination with a string or a line of dislocation are called *strings* or *lines of dispiration*, or simply *dispirations*. Note that the term "dispiration" is an Anglicism and that there is no French translation of this term.

One can imagine lattices which have a certain axial symmetry of the particles composing it, like the cubic networks **(a)** and **(b)** illustrated in figure 2.25. This axial symmetry of the particles can simply present a privileged direction of the particles in the planes of the structure, as in case **(a)**, which has an alternating structure of successive layers **a, b, a, b, a, b,...** The axial symmetry can also have a preferential direction and way as in case **(b)** which has an alternating structure of successive layers **a, b, c, d, a, b, c, d, ...**

Moreover, in case **(b)**, the direction of rotation of the axes of the particles along the vertical axis produces an oriented medium, which is qualified as right-handed (clockwise) in case **(b)** illustrated in figure and left-handed (counter-clockwise) in the case where the planes rotate in the opposite direction.

If it is forbidden to break the axial orientation of the particles in a plane, it is not possible to introduce a vertically oriented screw dislocation with any Burgers vector. Indeed, if the distance between the horizontal planes is worth a , in order to ensure the continuity of the orientation of the particles, and also of their direction in the case **(b)**, it is necessary that the length of the vector of Burgers \vec{B}_{vis} of the dislocation vis is equal to $\pm 2a$ in case **(a)**, and $\pm 4a$ in case **(b)**.

In media with axial symmetry such as those shown in figure 2.25, we have just explained that the screw dislocations must have Burgers vectors \vec{B}_{vis} whose lengths are multiples of the

length of the lattice pitch. In this case, the screw dislocations may have an interest in splitting into partial with Burgers vectors of length a , forming respectively 2 or 4 partial in cases **(a)** and **(b)** respectively. Between the partial dislocations, *ribbons of connection faults* are formed between axial planes **ab**, **bc**, **cd**, etc. The partial separation distance then depends on the energy γ per unit area of the connection fault.

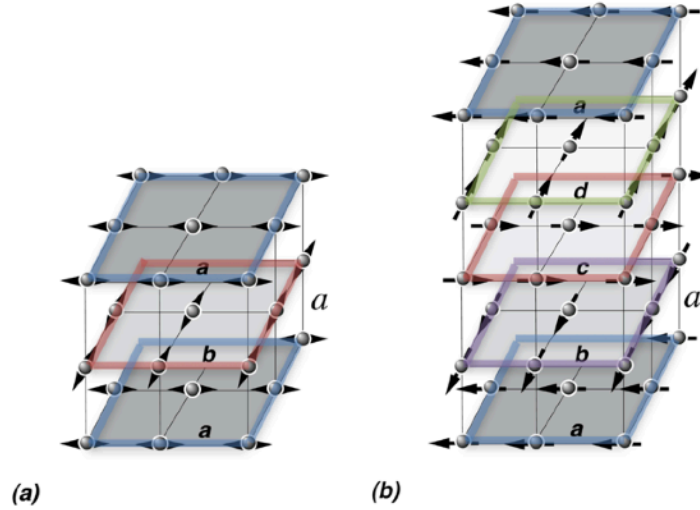


Figure 2.25 - Cubic lattices with axial symmetry, simple in case **(a)**, and oriented of dextrorotatory type (right-handed) in **(b)**

If the connection fault ribbon has an energy γ per unit area, the total energy $E_t(d)$ per unit length of a dissociated screw dislocation over distances d is written:

- $E_t(d) = \gamma d + E_d(d)$ in case **(a)**, where $E_d(d)$ is the energy of the two partials as a function of the distance d separating them, which is a monotonic function decreasing from E_0 for $d = 0$ to $E_0/3$ for $d \rightarrow \infty$,
- $E_t(d) = 3\gamma d + E_d(d)$ in case **(b)**, where $E_d(d)$ is the energy of the four partials as a function of the distance d separating them, which is a monotonic function decreasing from E_0 for $d = 0$ to $E_0/3$ for $d \rightarrow \infty$.

The energy $E_t(d)$ therefore has a minimum similar to that shown in figure 2.16 for the distance $d = d_0$, which is the equilibrium distance between the two or the four partial, controlled by the competition between the decrease in energy associated with the increase in distance between the partials and the increase in energy due to the formation of an energy ribbon due to lack of connection between the partials. This behavior of the energy $E_t(d)$ induces a force of interaction between the partials which one can quite qualify as *strong force*, in the sense that the energy of the triplet of partials will increase if one tries to increase the distance of separation beyond d_0 . This strong force therefore presents in its behavior an interesting analogy with the strong force acting between quarks in the Standard Model of elementary particles.

We can immediately imagine that there must also be connection conditions ensuring the continuity of the axial symmetry if we want to introduce a disclination in such a network. In fact, to ensure this continuity, it will necessarily be associated with the disclination a screw dislocation with the correct Burgers vector \vec{B} . It therefore appears here a structural necessity to

introduce dispirations in such environments.

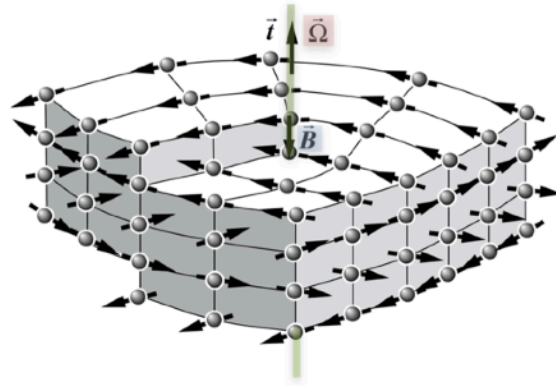


Figure 2.26 - Dispiration of $+90^\circ$ introduced into the axial lattice of figure 2.25 (b) showing the need to add a translation vector \vec{B} to ensure axial continuity

Figure 2.26 illustrates this point perfectly. Indeed, to introduce an disclination $\Omega = +90^\circ$ in the medium represented in figure 2.25(b), it is necessary to add to it a correctly oriented screw dislocation, of Burgers vector \vec{B} and of length a , which ensures the continuity of the axial orientation of the particles on the planes of the medium.

Note that screw dislocation of Burgers vector of opposite direction and length $3a$ could also have ensured the continuity of the axial orientation of the particles on the planes of the medium, so that there are two different dispirations with rotations $\Omega = +90^\circ$, both with a linear charge of

	Θ	$\Lambda_{(a)}$	$\Lambda_{(b)}^{(dextrogyre)}$	$\Lambda_{(b)}^{(lévoogyre)}$
<i>vis</i>	0	$\pm 2a$	$\pm 4a$	$\pm 4a$
<i>C1</i>	$-\pi/2$	$\pm a$	$+a, -3a$	$-a, +3a$
$\bar{C}1$	$+\pi/2$	$\pm a$	$-a, +3a$	$+a, -3a$
<i>C2</i>	$-\pi$	$0, \pm 2a$	$+2a, -2a$	$+2a, -2a$
$\bar{C}2$	$+\pi$	$0, \pm 2a$	$+2a, -2a$	$+2a, -2a$
<i>C3</i>	$-3\pi/2$	$\pm a$	$-a, +3a$	$+a, -3a$
$\bar{C}3$	$+3\pi/2$	$\pm a$	$+a, -3a$	$-a, +3a$

Tableau 2.27 - Linear charges of curvature Θ and rotation Λ of the dispirations in the cubic structures of figure 2.25 (a) and (b)

curvature of $\Theta = -\pi/2$, but differentiated by their Burgers vector \vec{B} associated with a linear charge of rotation Λ being equal to $\Lambda = a$ or $\Lambda = -3a$.

It is not too difficult to find out which linear torsion charges Λ should be associated with the different wedge dispirations of linear charge of curvature Θ that can be introduced into the cubic structures shown in figure 2.25.

In Table 2.27, these loads are reported for the cubic structures of figures 2.25(a) and (b). In case (a), the structure shows no difference between a *righthanded orientation* and a *lefthanded orientation* of the particles in the lattice. On the other hand, there appears to be a difference between these two orientations in case (b), which implies a change in sign of the charge Λ between the *righthanded* and *lefthanded* environments.

Quantified dislocation and disclination loops in a lattice

To satisfy the conservation equation $\text{div} \vec{\lambda}_i = 0$, a dislocation or a disclination string cannot be abruptly interrupted within the medium. On the other hand, such a string closing on itself to form a localized loop always satisfies the conservation equation. In this section, we will therefore present this type of loops as well as their properties in a solid lattice.

For a circular dislocation loop of radius R , the tensor linear charge $\vec{\Lambda}_i$ of the dislocation can be related to its Burgers vector using the relation $\vec{\Lambda}_i = -\vec{t} B_i$ where \vec{t} represents the unit vector tangent to the dislocation line.

Three types of dislocation loops then appear according to the orientation of the Burgers vector with respect to the normal \vec{n} to the surface of the loop, as shown in Figure 2.28:

- the *slip loops* (figure 2.28a) when $\vec{B} \perp \vec{n}$, having both edge portions (where $\vec{B} \parallel \vec{m}$), screw portions (where $\vec{B} \parallel \vec{t}$) and mixed portions. Their Burgers vector can take any orientation in the plane perpendicular to \vec{n} . They are obtained by the process described in figure 2.4b,

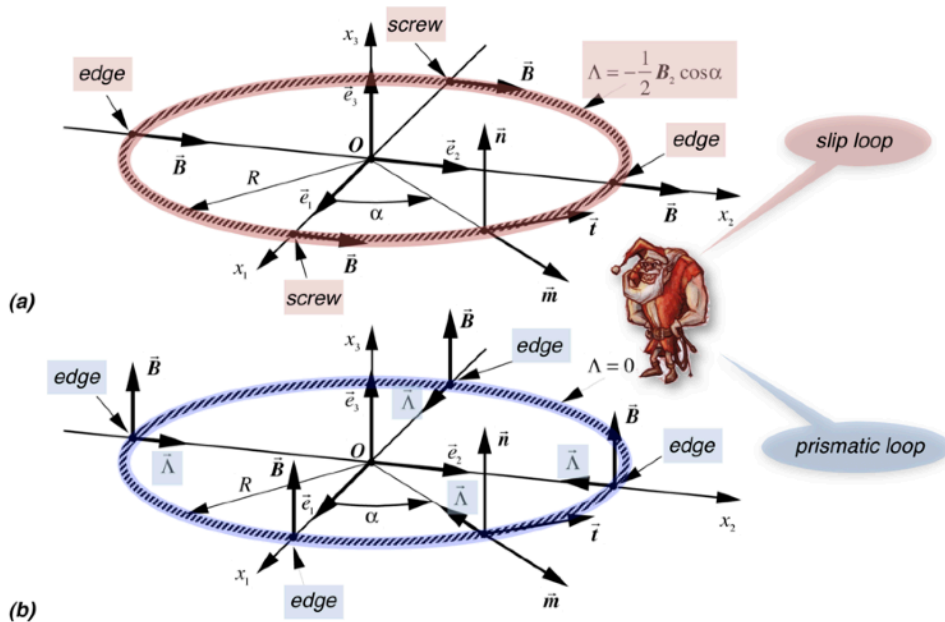


Figure 2.28 - Slip dislocation loop (a) and prismatic dislocation loop (b)

- the *prismatic loops* (figure 2.28) when $\vec{B} \parallel \vec{n}$, which have their Burgers vector in the imposed direction of the unit vector \vec{n} perpendicular to the plane of the loop, and which are obtained by the process described in figure 2.4c and d.
- the *mixed loops* when \vec{B} has a component in the direction of \vec{n} and a component in the plane of the loop.

We will see later that it is useful to introduce the notions of *global scalar charges of rotation* q_λ and *global scalar charges of curvature* q_θ , which will in fact be very important for characterizing the topological effects at long distance of topological singularities. These global scalar charges are perfectly analogous to the electrical charge of an electron, for example.

We can define a *global scalar charge* q_λ of rotation of a dislocation loop as the integral (the sum) of its *scalar linear density* Λ of torsion charge taken on the contour of the loop:

- in the case of the prismatic loop (figure 2.28b), the *global scalar charge* q_λ is null because the linear density Λ of torsion load is null everywhere on the contour of the loop.
- in the case of the slip loop (figure 2.28a), the linear density Λ of torsion charge evolves along the loop according to the cosine of the angle α , becoming positive, null, negative and null on a complete turn, so that the global scalar charge q_λ of rotation is also zero ($q_\lambda = 0$) for this type of loop. On the other hand, as the linear density Λ of torsion charge is positive for $\alpha = 0$ and negative for $\alpha = 180^\circ$ in the case of the *slip dislocation loop* shown in figure 2.28a, we deduce that the slip dislocation loops have a *dipolar momentum of rotation charges*.

We can also define a *global scalar charge* q_θ of curvature of a dislocation loop as the integral (the sum) of its scalar linear density Θ of curvature charge taken on the contour of the loop:

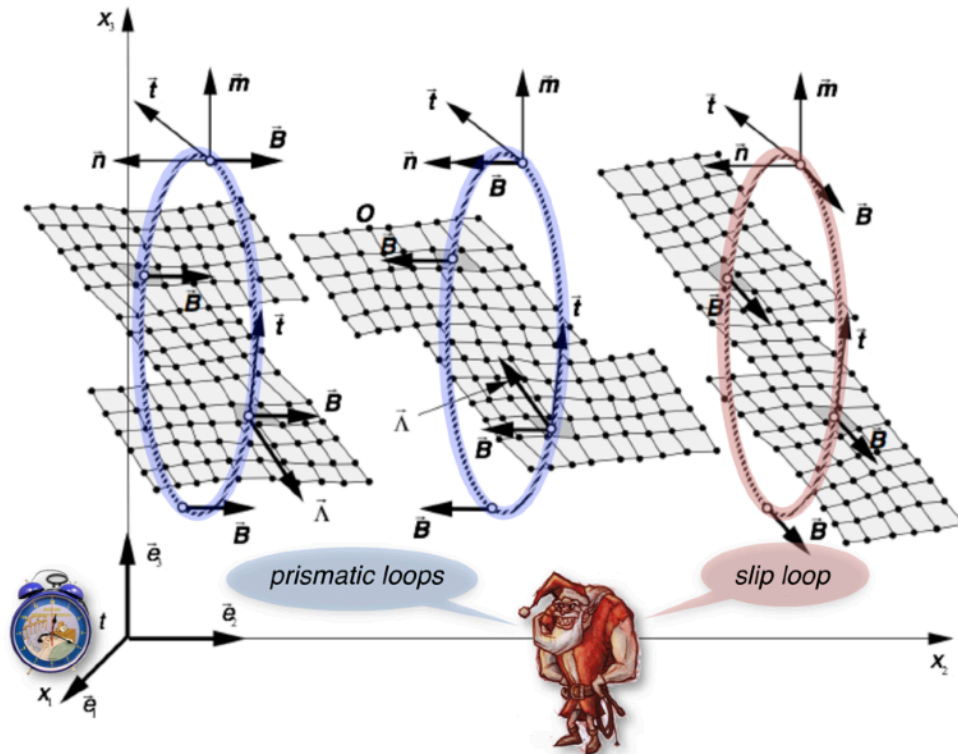


Figure 2.29 - Quantified loops of dislocations in a cubic lattice

$q_\lambda = \pi R^2 \Pi$. This global charge q_λ is actually the rotation charge of the twist disclination loop as seen from a long distance from the loop. This means that such a loop can behave as the source of a divergent field $\vec{\omega}$ of rotation within the solid medium.

Note that it is possible to see a disclination loop somewhat differently. Indeed, the fact of carrying out the rotation of the two planes one with respect to the other induces a displacement along the string *similar to that of a screw dislocation*. The Burgers vector and the linear charge of this *screw pseudo-dislocation* would then be worth $\Lambda_{vis} = -\vec{B}_{vis} \cdot \vec{t} / 2 = R\Pi/2$, so that the global charge of this pseudo-loop would be written $q_\lambda = 2\pi R \Lambda_{vis} = \pi R^2 \Pi$. One thus obtains the same value of the global charge q_λ as that obtained by considering the surface charge, which makes it possible to consider either this singularity as a *twist disclination loop* or as a *pseudo-loop of screw dislocation*.

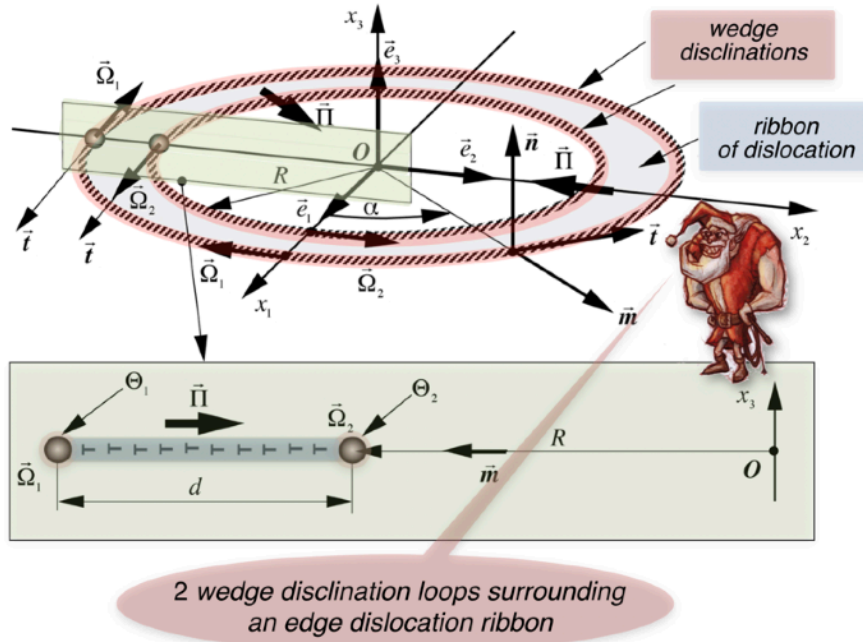


Figure 2.31 - loop of doublet of wedge disclinations linked by a dislocation ribbon

In figure 2.9, we have shown the macroscopic realization of a *wedge disclination loop*. But what are its main characteristics? For this, we consider a loop consisting of a doublet of wedge disclinations linked by a virtual dislocation ribbon, as shown in figure 2.31, in particular in the illustration of a section along a plane perpendicular to the plane of the loops. The linear densities of scalar charge of curvature Θ_1 and Θ_2 of the two disclinations are given by $\Theta_1 = -\vec{\Omega}_1 \cdot \vec{t} = -\vec{\Pi} \cdot \vec{m}$ and $\Theta_2 = -\vec{\Omega}_2 \cdot \vec{t} = -\vec{\Pi} \cdot \vec{m} = -\Theta_1$.

We deduce that the existence of these two densities Θ_1 and Θ_2 on either side of the dislocation ribbon generates a dipolar flexion field $\vec{\chi}_{dipolaire}$, located essentially in the vicinity of the two disclinations. This dipolar field is illustrated in figure 2.32 in the case of a doublet of quantized disclinations of $\pm 90^\circ$ in a cubic structure. We can clearly see the positive and negative curvatures around the two disclinations.

It is then interesting to see that the dislocation ribbon of surface flexion charge $\vec{\Pi}$ can be reduced, by integration over the distance d separating the two disclinations, to a linear charge $\vec{\Lambda}$ of virtual edge dislocation distributed over a radius loop $R + d/2$. Thus, this loop of a doublet of disclinations can be considered similar to a loop of edge dislocation with a linear charge $\vec{\Lambda}$ such as $\vec{\Lambda} = \vec{\Pi}d = -d\Theta_1\vec{m}$.

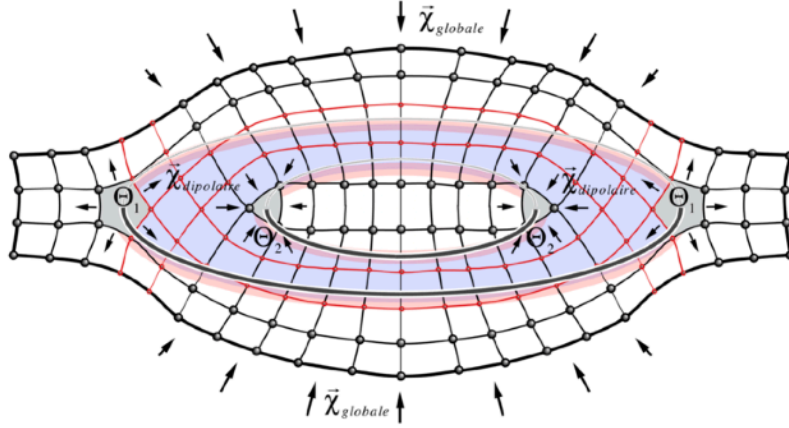


Figure 2.32 - local dipolar field of flexion due to charges Θ_1 and Θ_2 and divergent field of flexion due to the charge q_θ of two loops of wedge disclinations

Such a loop of doublets of disclinations then has a global scalar charge q_θ of curvature linked to the virtual edge dislocation ribbon which it contains, and its value is written $q_\theta = 2\pi\vec{\Lambda}\vec{m} = 2\pi\vec{B}_3 = 2\pi d\vec{\Pi}\vec{m} = -2\pi d\Theta_1$. We can still imagine that the diameter of the internal disclination loop tends towards zero and that only the external disclination loop, of linear charge Θ_1 and radius d remains. In this case, the global charge of curvature q_θ remains unchanged and is always given by the same relation. This global charge of curvature q_θ is that which is due to the entire dislocation ribbon, and that which is seen at a sufficiently large distance from the loop so that it is no longer possible to distinguish this loop from a simple edge dislocation loop. The charge q_θ is then responsible for the global flexion $\vec{\chi}_{globale}$ of the lattice at long-distance, as illustrated in figure 2.32 in the case of a doublet of quantized disclinations of $\pm 90^\circ$ in a cubic structure.

Clusters of dislocations, disclinations and dispirations

Since the dislocation, disclination and dispiration strings containing non-zero densities of tensor charges can be closed on themselves in the form of loops, it is quite possible to imagine the existence of small very localized clusters of such loops within a solid medium. Such clusters are in principle entirely characterized by their tensor density $\vec{\lambda}_i$ of dislocation charges, which take a non-zero value within the strings, in the field of the cluster.

As the cluster is composed exclusively of loops closing in on themselves, there are no vectors \vec{B} and \vec{l} or $\vec{\Omega}$ with non-zero value on any contour surrounding the cluster without crossing it, which implies that there is no discontinuities of the virtual displacement field $\vec{u}^{(\delta)}$ nor

discontinuities of the local rotation field $\vec{\omega}^{(\delta)}$ in the part of the solid surrounding the cluster, and that, consequently, the solid remains perfect outside the cluster.

However, the presence of the cluster within the solid must certainly imply a field of elastic and anelastic distortions of the perfect solid surrounding the cluster and up to a certain distance from it, just like the presence of a density ρ of localized electric charges implies an electric displacement field \vec{D} remote from these electric charges.

To find this field, it is necessary to bring into play here the fact that there is, apart from the conservation equation $\text{div } \vec{\lambda}_i \equiv 0$ of the tensorial charge, no restriction on the scalar densities λ and θ of charges of rotation and flexion. Consequently, it is entirely possible that, depending on the nature of the charges making up the cluster, it may have non-zero global scalar charges of rotation Q_λ and curvature Q_θ , defined by the sums on all the closed loops of the global charges $q_{\lambda(i)}$ and $q_{\theta(i)}$ as defined above for each individual loop in the previous section. One can imagine, for example, that the charge of curvature of a cluster could be due to prismatic dislocation loops, of lacunar or interstitial nature (figure 2.29) and / or wedge disclinations loops (figure 2.31), and that the rotation charge could be due to twist disclination loop (figure 2.30).

These considerations then make it possible to find the fields of elastic and anelastic distortions implied at a great distance by the presence of a localized cluster of charges. The presence of a non-zero global scalar charge Q_λ of rotation in a localized cluster of charges behaves as the source of a divergent field of rotation $\vec{\omega}$ within the perfect solid surrounding the cluster of charges (figure 2.33). The field of rotation then presents a *topological singularity* at the place where the cluster of charge Q_λ is located, and its norm $|\vec{\omega}|$ presents a decrease in $1/R^2$ at long distance from the cluster.

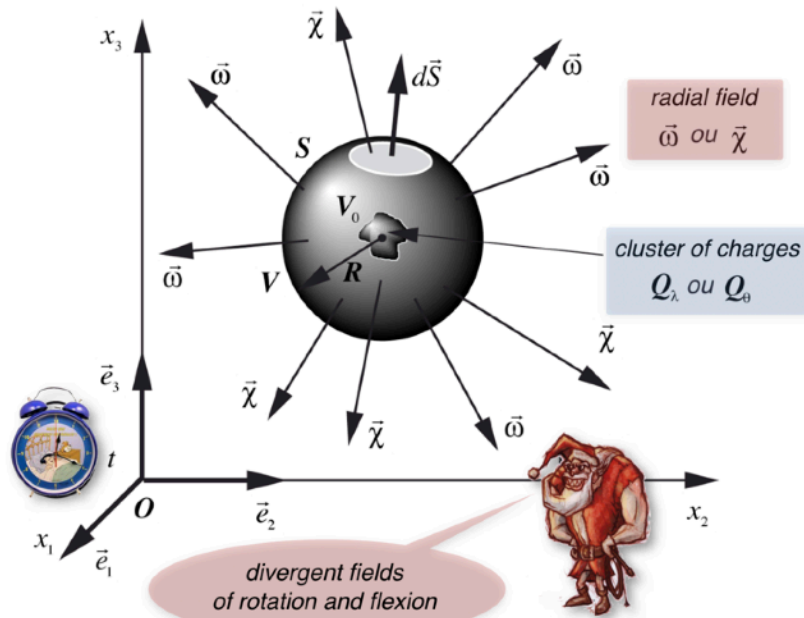


Figure 2.33 - Divergent fields of rotation and flexion in the vicinity of a cluster of charges

Everything in fact happens exactly as in electromagnetism, where a localized density ρ of electric charges, leading to a localized macroscopic electric charge Q , behaves like a singularity responsible for a field of electric displacement \vec{D} diverging in the surrounding space.

A macroscopic scalar load Q_θ of nonzero curvature behaves as *the source of a divergent field $\vec{\chi}$ of flexion* within the perfect solid surrounding the cluster of charges (figure 2.33). The bending field then presents a *topological singularity* at the place where the cluster of charges Q_θ is located, and its norm Q_θ also presents a decrease $1/R^2$ at long distance from the cluster. In other words, in the vicinity of a global localized load Q_θ of curvature, the solid presents curvatures by bending of spherical symmetry around the singularity.

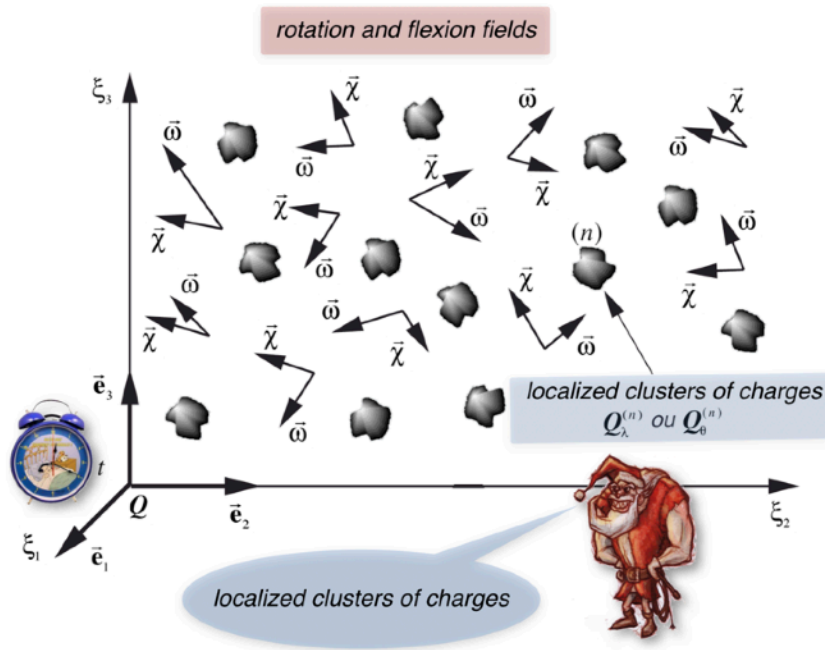


Figure 2.34 - Description of a solid containing localized clusters of charges

Let be a *hypothetical solid* in which the charges are confined in localized clusters, as illustrated for example in figure 2.34, and therefore in which *there are no dislocation and disclination strings propagating over great distances* compared to the scale at which solid is studied. It is clear that, depending on the complexity of the internal structure of these clusters, in other words the complexity of the entanglement of the loops making up these clusters, the description of the fields of distortion and contortion within the clusters themselves can be very complex. But if these clusters have stable internal structures and they can move individually within the solid, but without interacting enough between them to modify their internal structure, it is possible to greatly simplify the description of the distortion fields prevailing in this solid.

In this case indeed, and insofar one is essentially interested in describing the elastic and anelastic distortion and contortion fields in the domains of the perfect solid, that is to say at a certain distance from the outside the clusters of charges, the problem can be solved much more simply by considering only the scalar charge densities λ and θ inside the clusters, which can result at great distance by the existence of two macroscopic scalar charges $Q_{\lambda(n)}$ and $Q_{\theta(n)}$ for each cluster number (n) .

In fact, the knowledge of the distribution of charge density λ and θ inside a cluster makes it possible to find purely topological conditions, and consequently independent of the elastic properties of the solid considered, which are imposed on the fields of rotation $\vec{\omega}$ and flexion $\vec{\chi}$ reigning in the perfect solid outside the cluster. These conditions are simply expressed by the scalar equations of geometro-compatibility $\lambda = \text{div } \vec{\omega}$ and $\theta = \text{div } \vec{\chi}$. Depending on the inhomogeneity of the internal distribution of charge densities λ and θ in the cluster, it can then appear *dipolar or multipolar fields $\vec{\omega}$ and $\vec{\chi}$ at short and medium distance from each cluster.*

On the other hand, *at large distances from clusters of charges*, it is essentially the presence of macroscopic scalar charges $Q_{\lambda(n)}$ and $Q_{\theta(n)}$ which are different from zero which will be responsible for the appearance of monopolar radial fields of rotation $\vec{\omega}$ and flexion $\vec{\chi}$, as already illustrated in figure 2.33.

Thus, in this particular case of charges located in clusters, it is *the two invariant vector fields*, namely the fields of rotation $\vec{\omega}$ and flexion $\vec{\chi}$, which are affected at a certain distance from the clusters of charges. And it is quite remarkable that each of these clusters can be individually and completely characterized, as for its long-range effects on the fields of distortion and contortion, by its only two macroscopic scalar charges $Q_{\lambda(n)}$ and $Q_{\theta(n)}$, even so these clusters can have very complex core structures, of tensorial nature, therefore very strongly dependent on their spatial orientation in the local frame of reference.

In the analogy previously developed with electromagnetism, the field of rotation $\vec{\omega}$ is the analog of electric displacement \vec{D} , and the macroscopic charge of rotation $Q_{\lambda(n)}$ is the analog of the macroscopic electric charge Q of a corpuscle in electromagnetism. But is there also a similar analogy for the flexion field $\vec{\chi}$ and the overall charge $Q_{\theta(n)}$ of curvature?

A partially positive answer can be given here. Indeed, the presence of a cluster of macroscopic flexion charge $Q_{\theta(n)}$ is responsible for a non-zero and divergent vector flexion field $\vec{\chi}$ in its vicinity, therefore for a *spatial curvature of the solid lattice* surrounding this cluster, which results in the appearance of non-zero shear strain fields and volume expansion fields. Thus, the presence of a cluster of charges such as $Q_{\theta(n)} \neq 0$ implies, vis-à-vis the solid lattice, a result presenting a certain analogy with that stipulated by the theory of general gravitation of Einstein vis-à-vis the space-time in the presence of matter, namely that a cluster of matter located in a place of space is directly responsible for a curvature of the neighboring space-time. We will come back to this analogy in detail later.

Flow of dislocation charges

The macroscopic interpretation of the density tensors $\vec{\lambda}_i$ of dislocation charges as well as the conservation equation $\text{div } \vec{\lambda}_i \equiv 0$ which these tensors satisfy have revealed the notion of strings and loops of dislocation, disclination and dispiration. It has also been shown that at large distances from clusters of plastic charges, it is essentially the two invariant vector fields, namely the fields of rotation $\vec{\omega}$ and curvature $\vec{\chi}$, which are affected by the scalar components λ and θ of charges. It now remains to make the link between these quantities and the charge flows \vec{J}_i and \vec{J} introduced into the geometro-kinetic equations of figure 2.5.

Let us therefore consider a tube filled with a density $\vec{\lambda}_i$ of dislocation charges, which moves at *relative velocity \vec{V} with respect to the lattice*, where the velocity is measured perpendicular to the direction of the tube. We can show that the relation existing between the tensor density of

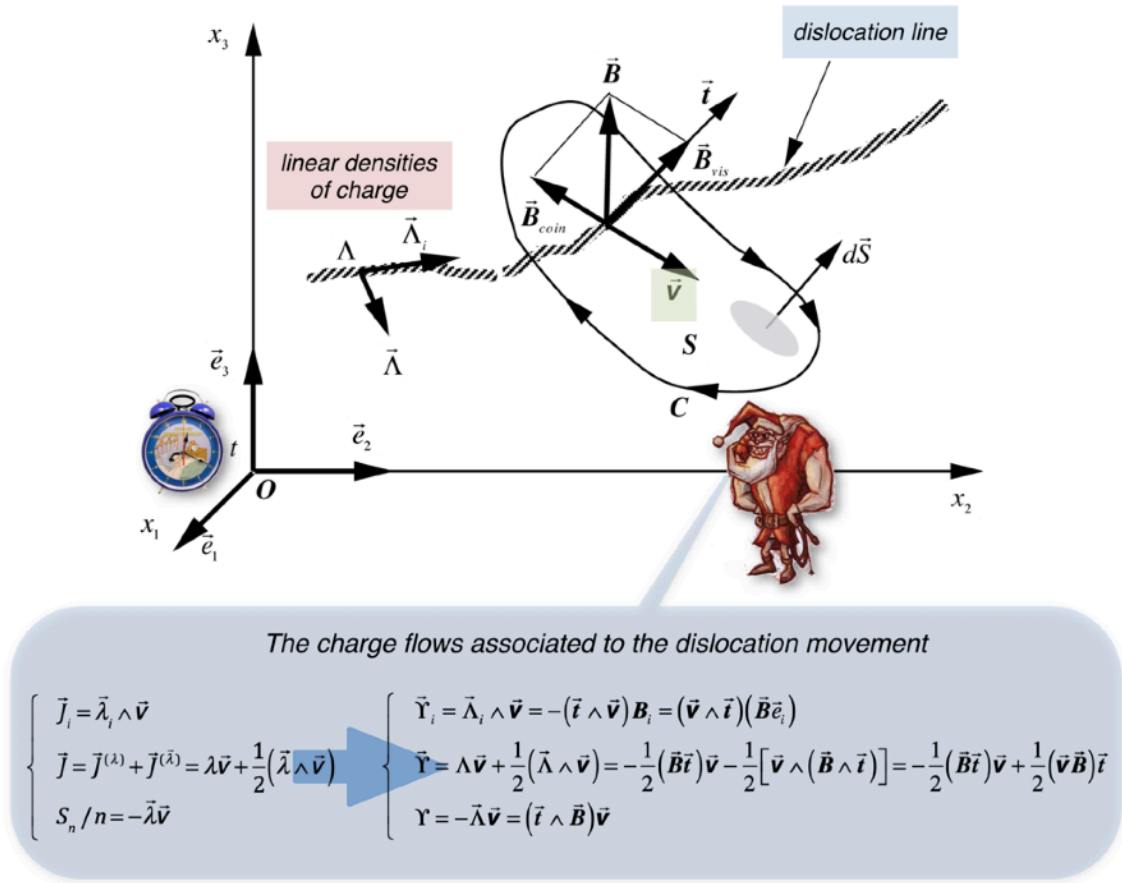


Figure 2.35 - The charge flows associated to a dislocation line moving at velocity \vec{v} in the frame $Ox_1x_2x_3$

charge $\vec{\lambda}_i$ in motion at speed \vec{v} with respect to the lattice and the tensorial flux \vec{J}_i of charges which is associated with this movement is then written $\vec{J}_i = \vec{\lambda}_i \wedge \vec{v}$, from which we also deduce the vector flux of charges $\vec{J} = \vec{J}^{(\lambda)} + \vec{J}^{(\tilde{\lambda})} = \lambda \vec{v} + (\vec{\lambda} \wedge \vec{v})/2$ and the scalar source of sites $S_n / n = -\vec{\lambda} \vec{v}$.

We can apply this relation to the case of dislocation lines. We consider a dislocation line like the one shown in figure 2.35, which moves to the velocity \vec{v} relative to the lattice. It is clear that, in the case of a line, the velocity \vec{v} can only be perpendicular at all points to the direction \vec{t} of the line. In the case of a line, one can integrate (summate) the vectorial flow \vec{J}_i of charges on the surface of the contour C surrounding the dislocation line and mobile with it. The integrations on the surface of the contour of the charge fluxes \vec{J}_i and \vec{J} will give the linear fluxes associated with the mobile dislocation, that is to say the total fluxes per length unit of dislocation, which will be represented by the symbols \vec{Y}_i and \vec{Y} . As the flows \vec{J}_i and \vec{J} have as dimension the inverse of a time (1/s), the linear flows \vec{Y}_i and \vec{Y} will have as dimension a surface per unit of time (m^2/s). As for the source S_n / n of network sites, its integral will also represent a surface per unit of time (m^2/s), and we will write it Υ . It then comes the relations reported in figure 2.35, which connect the linear fluxes \vec{Y}_i and \vec{Y} , as well as the linear source Υ of sites to the linear densities of charge $\vec{\Lambda}_i$, $\vec{\Lambda}$ and Λ of

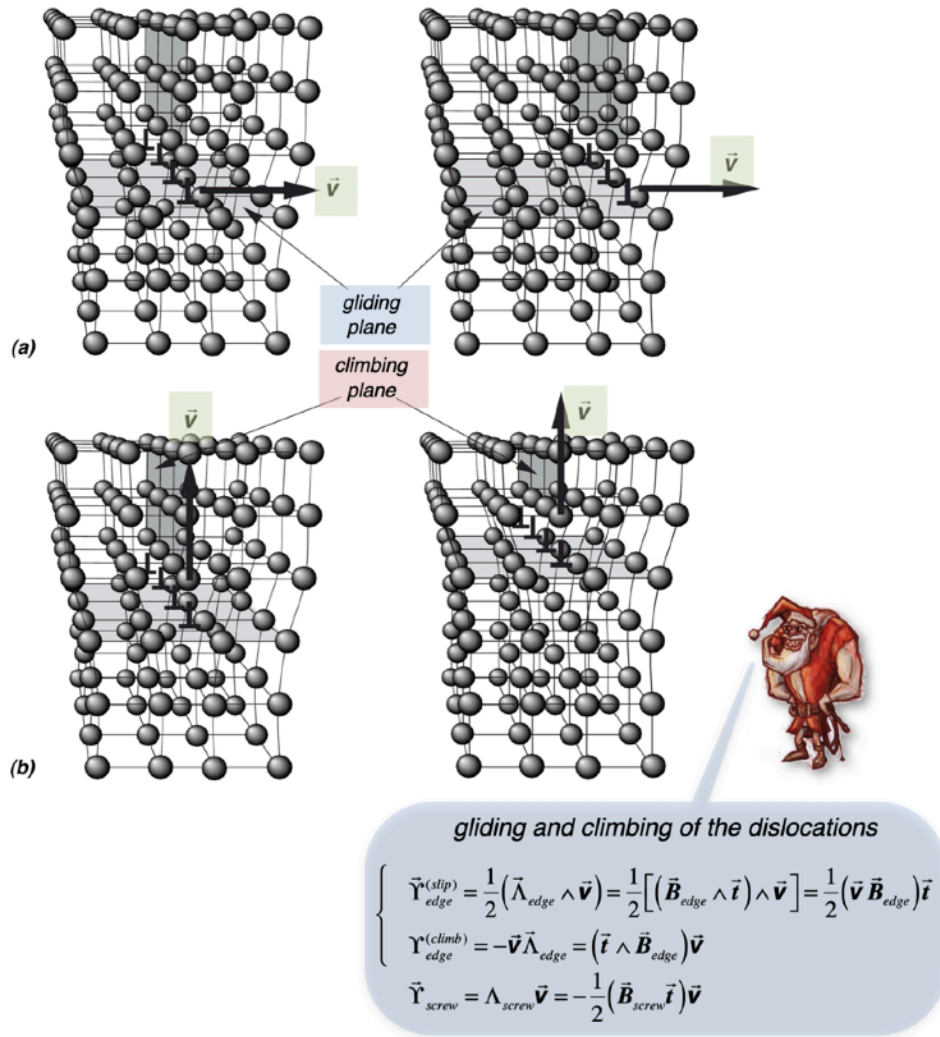


Figure 2.36 - The movements of gliding (a) and of climbing (b) of an edge dislocation

dislocations. We also deduce the relations directly linking the linear fluxes $\vec{\Upsilon}_i$, $\vec{\Upsilon}$ and Υ to the Burgers vector \vec{B} of the dislocation.

If the dislocation has only one screw component, the flux $\vec{\Upsilon}_{screw}$ will be given by the relation reported in figure 2.36. This relation shows that, as the velocity \vec{v} is always perpendicular to the direction \vec{t} of the line, the purely screw dislocations can move in all the directions perpendicular to the direction \vec{t} . In this case we speak of a *gliding movement of the screw dislocations*, and the planes on which the screw dislocation moves are called *gliding planes*.

In the case of a purely edge dislocation, two possible types of movement appear, leading to linear flows $\vec{\Upsilon}_{edge}^{(gliding)}$ and $\Upsilon_{edge}^{(climb)}$ whose mathematical expressions are shown in figure 2.36:

- the movement for which \vec{v} is perpendicular to $\vec{\Lambda}$, and which is responsible for a vector charge flow $\vec{\Upsilon}_{edge}^{(gliding)}$. This movement is shown in figure 2.36a. It corresponds to a conservative movement of *gliding* of the edge dislocation on its *gliding plane*, defined as the plane perpendicular to $\vec{\Lambda}$, therefore the plane which contains at the same time the Burgers vector \vec{B}_{edge} , the direction \vec{t} of the line and the velocity vector \vec{v} .

- the movement for which \vec{v} is parallel to $\vec{\Lambda}$, and which is responsible for a scalar charge flow $\Upsilon_{edge}^{(climb)}$. This movement is shown in figure 2.36b. It corresponds to a non-conservative

$$\left\{ \begin{array}{l}
 \dot{\vec{\beta}}_i^{pl} = \vec{J}_i = \vec{\lambda}_i \wedge \vec{v} \\
 \dot{\vec{\omega}}^{pl} = \vec{J} = \lambda \vec{v} + \frac{1}{2} (\vec{\lambda} \wedge \vec{v}) \\
 \dot{\vec{\epsilon}}_i^{pl} = \vec{J}_i - \vec{e}_i \wedge \vec{J} = \vec{\lambda}_i \wedge \vec{v} - (\vec{e}_i \wedge \vec{v}) \lambda - \frac{1}{2} \vec{e}_i \wedge (\vec{\lambda} \wedge \vec{v}) \\
 \dot{\vec{\tau}}^{pl} = \frac{S_n}{n} = -\vec{\lambda} \vec{v} \\
 \dot{\vec{\alpha}}_i^{pl} = \vec{J}_i - \vec{e}_i \wedge \vec{J} - \frac{1}{3} \vec{e}_i \frac{S_n}{n} = \vec{\lambda}_i \wedge \vec{v} - (\vec{e}_i \wedge \vec{v}) \lambda - \frac{1}{2} \vec{e}_i \wedge (\vec{\lambda} \wedge \vec{v}) + \frac{1}{3} \vec{e}_i (\vec{\lambda} \vec{v})
 \end{array} \right.$$

↓

$$\left\{ \begin{array}{l}
 \dot{\vec{\beta}}_i^{pl} = \Lambda [\vec{\lambda}_i \wedge \vec{v}] = \Lambda [(\vec{v} \wedge \vec{t})(\vec{B} \vec{e}_i)] \\
 \dot{\vec{\omega}}^{pl} = \Lambda \left[\Lambda_{vis} \vec{v} + \frac{1}{2} (\vec{\lambda}_{edge} \wedge \vec{v}) \right] = \Lambda \left[-\frac{1}{2} (\vec{B}_{screw} \vec{t}) \vec{v} + \frac{1}{2} (\vec{v} \vec{B}_{edge}) \vec{t} \right] \\
 \dot{\vec{\epsilon}}_i^{pl} = \Lambda \left[\vec{\lambda}_i \wedge \vec{v} + (\vec{v} \wedge \vec{e}_i) \Lambda_{screw} + \frac{1}{2} \vec{e}_i \wedge (\vec{v} \wedge \vec{\lambda}_{edge}) \right] \\
 = \Lambda \left[(\vec{v} \wedge \vec{t})(\vec{B} \vec{e}_i) + \frac{1}{2} (\vec{e}_i \wedge \vec{v})(\vec{B}_{screw} \vec{t}) - \frac{1}{2} (\vec{e}_i \wedge \vec{t})(\vec{v} \vec{B}_{edge}) \right] \\
 \dot{\vec{\tau}}^{pl} = \Lambda [-\vec{v} \vec{\lambda}_{edge}] = \Lambda [(\vec{t} \wedge \vec{B}_{edge}) \vec{v}] \\
 \dot{\vec{\alpha}}_i^{pl} = \Lambda \left[\vec{\lambda}_i \wedge \vec{v} + (\vec{v} \wedge \vec{e}_i) \Lambda_{screw} + \frac{1}{2} \vec{e}_i \wedge (\vec{v} \wedge \vec{\lambda}_{edge}) + \frac{1}{3} \vec{e}_i (\vec{v} \vec{\lambda}_{edge}) \right] \\
 = \Lambda \left[(\vec{v} \wedge \vec{t})(\vec{B} \vec{e}_i) + \frac{1}{2} (\vec{e}_i \wedge \vec{v})(\vec{B}_{screw} \vec{t}) - \frac{1}{2} (\vec{e}_i \wedge \vec{t})(\vec{v} \vec{B}_{edge}) - \frac{1}{3} \vec{e}_i [(\vec{t} \wedge \vec{B}_{edge}) \vec{v}] \right]
 \end{array} \right.$$

Orowan's relationships connect the macroscopic plastic deformation with the charge movements within the solid




Figure 2.37 - The Orowan's relation which connect the plastic distortions to the movements of the charges

movement of *climb* of the edge dislocation perpendicular to its gliding plane. Dislocation «*is climbing*» in the lattice, creating or destroying a lattice plan. This movement is therefore non-conservative in the sense that it destroys or builds the lattice, and it is this movement which is responsible for the existence of a source S_n of lattice sites in the geometro-kinetic equation of the volume expansion reported in figure 2.5, which is written as $S_n = -n \vec{v} \vec{\Lambda}_{coin} = n (\vec{t} \wedge \vec{B}_{coin}) \vec{v}$.

It is the movement of dislocation charges that is responsible for the macroscopic plastic deformation of a solid. From the knowledge of the dislocation charge flows \vec{J}_i , it is then possible to go back to the macroscopic plastic distortions $\dot{\vec{\beta}}_i^{pl}$ of the solid thanks to the famous Orowan relations. The total derivatives along the medium trajectory of the macroscopic plastic distortions $\dot{\vec{\beta}}_i^{pl}$, $\dot{\vec{\epsilon}}_i^{pl}$, $\dot{\vec{\alpha}}_i^{pl}$, $\dot{\vec{\omega}}^{pl}$ and $\dot{\vec{\tau}}^{pl}$ of the charged solid are reported in figure 2.37, as a function of the volume densities of charges $\vec{\lambda}_i$, $\vec{\lambda}$ and λ , as a function of the linear densities of charges $\vec{\gamma}_i$, $\vec{\gamma}$ and γ associated with the movement of dislocation lines, and finally as a function of the Burgers vectors of dislocations in place of the linear densities of charge of the dislocation lines.

integrating the relation giving \vec{f}_{PK} on the surface of a section of the string. It then comes, neglecting for the moment the term containing the vector \vec{A} , the expressions of the Peach and Koehler force acting on a dislocation line which are shown in figure 2.38, expressed respectively from the linear charge densities $\vec{\lambda}_i$, $\vec{\Lambda}$ and Λ of the dislocations, and from the Burgers vector \vec{B} of the dislocation.

The dimension of the force \vec{F}_{PK} acting on the dislocation is a force per unit of length (N/m). This is actually *the force per unit length of the line* in the presence of the stress fields \vec{s}_k, \vec{m}, p . The writing of the Peach and Koehler force \vec{F}_{PK} using the stress tensors p, \vec{m}, \vec{s}_k is very interesting, because it allows to make a much clearer representation than with the notation usually used in the literature which exclusively uses the symmetrical stress tensor $\vec{\sigma}_k$. Indeed, suppose a solid in which the volume expansion is zero, and therefore which would have a negligible pressure p . In this case, we know that we can replace the shear strain tensor $\vec{\alpha}_k$ with the rotation vector $\vec{\omega}$, so that the force becomes a gliding force which can be written $\vec{F}_{PK} = \Lambda \vec{m} + (\vec{m} \wedge \vec{\Lambda})/2$, in which the term $\Lambda \vec{m}$ is the force acting on the screw component of the dislocation and the term $(\vec{m} \wedge \vec{\Lambda})/2$ is the force acting on the edge component of the dislocation. As the component m_k of the moment of rotation is associated with the components σ_{ij} and σ_{ji} of the shear strain tensor, one can immediately make a very clear representation of the forces acting on a dislocation. The same goes for the pressure force $\vec{\Lambda}p$, which acts only on the edge component $\vec{\Lambda}$ of the dislocations and which corresponds, given its direction (figure 2.36), to a *climbing force on the dislocations*.

In the case of a localized charge \vec{Q}_λ of rotation, one obtains the force of Peach and Koehler by integrating the force on all the volume of the localized charge. The result is shown in figure 2.38. In this case, the dimension of $\vec{F}_{PK} = \vec{Q}_\lambda \vec{m}$ is that of a pure force, expressed in (N), and which is the analog of the electric force $\vec{F}_{\text{electrique}} = q\vec{E}$ acting on a localized electric charge in electromagnetism.

Potentialities of the Eulerian representation of charged lattices

The tensor density $\vec{\lambda}_i$ and the tensor flux \vec{J}_i of dislocation charges defined in this chapter make it possible to find the set of fundamental and phenomenological equations of spatio-temporal evolution which must be satisfied by an anelastic and self-diffusing solid lattice containing dislocation charges. This development is done with many details in my first book. We will only describe here very briefly two important aspects which can be treated in the context of the Eulerian representation of solid media containing plastic charges.

It is possible to combine all the results described so far to obtain the complete space-time evolution equations of a solid self-diffusing lattice, presenting phenomenological behaviors of elasticity and anelasticity, and containing dislocation charge densities and flows. As figure 2.39 shows, this system of equations is quite complex, especially at the level of the large number of phenomenological state equations and phenomenological dissipation equations necessary for a complete description of all possible phenomena in such an environment, and which we will not tackle in this book.

The concepts of densities and flow of dislocation charges make it possible to describe the phenomena of plasticity and anelasticity at the microscopic level of the discrete solid lattice, by introducing into it an evolutionary microstructure of plastic charges which should make it

Fundamental equations	
<p>Equations topologiques</p> $\begin{cases} \vec{J}_i = -\frac{d\vec{\beta}_i}{dt} + \text{grad}\vec{\phi}_i & (1) \\ \vec{J} = -\frac{1}{2}\sum_i \vec{e}_i \wedge \vec{J}_i = -\frac{d\vec{\omega}}{dt} + \frac{1}{2}\text{rot}\vec{\phi} & (2) \\ \frac{\vec{S}_i}{n} = \sum_i \vec{e}_i \vec{J}_i = -\frac{d\vec{\tau}}{dt} + \text{div}\vec{\phi} & (3) \end{cases}$ $\begin{cases} \vec{\beta}_i = \vec{\beta}_i^{(0)} + \vec{e}_i \wedge \vec{\omega}_0(t) = \vec{\beta}_i^{(0)} + \vec{e}_i \wedge \vec{\omega}_0(t) & (7) \\ \vec{\omega} = -\frac{1}{2}\sum_i \vec{e}_i \wedge \vec{\beta}_i = \vec{\omega}^{(0)} + \vec{\omega}^{(1)} + \vec{\omega}_0(t) & (8) \\ \vec{\tau} = \sum_i \vec{\beta}_i \vec{e}_i = \vec{\tau}^{(0)} + \vec{\tau}^{(1)} + \vec{\tau}_0(t) \text{ (ar hypothèse)} & (9) \\ \vec{e}_i = \vec{\beta}_i - \vec{e}_i \wedge \vec{\omega} = \vec{\beta}_i^{(0)} - \vec{e}_i \wedge \vec{\omega}^{(0)} = \vec{e}_i^{(0)} + \vec{e}_i^{(1)} & (10) \\ \vec{\alpha}_i = \vec{e}_i - \frac{1}{3}\vec{\tau}\vec{e}_i = \vec{\alpha}_i^{(0)} + \vec{\alpha}_i^{(1)} & (11) \\ d/dt = \partial/\partial t + (\vec{\phi}\vec{\nabla}) & (12) \\ \vec{\phi} = \vec{\phi} - \vec{\phi}_0(t) - \vec{\omega}_0(t) \wedge \vec{r} & (13) \end{cases}$ <p>Equations dynamique</p> $n \frac{d\vec{p}}{dt} = \rho \vec{g} + \sum_i \vec{e}_i \text{div} \vec{\beta}_i - \frac{1}{2} \left(\frac{d\vec{\omega}}{dt} \wedge \vec{\omega} + \vec{\omega} \wedge \frac{d\vec{\omega}}{dt} \right) + \frac{d\vec{C}_L}{dt} \quad (14)$ $\begin{cases} n = 1/v = n_0 e^{-\tau} & (15) \\ \vec{p} = m(\vec{\phi} + C_L \vec{\phi}_i - C_L \vec{\phi}_i) = m(\vec{\phi} + m(C_L - C_L) \vec{\phi} + \frac{m}{n} (\vec{J} - \vec{J}_i)) = \frac{1}{n} [\rho \vec{\phi} + m(\vec{J} - \vec{J}_i)] & (16) \\ \rho = mn(1 + C_L - C_L) & (17) \end{cases}$ <p>Equations de diffusion</p> $\begin{cases} n \frac{dC}{dt} = (S_{i,j} + S_{i,j}^{(1)}) - C_i (S_{i,j}^{(1)} - S_{i,j}^{(2)}) - \text{div} \vec{J}_L & (18) \\ n \frac{dC}{dt} = (S_{i,j} - S_{i,j}^{(1)}) - C_i (S_{i,j}^{(1)} - S_{i,j}^{(2)}) - \text{div} \vec{J}_i & (19) \\ \vec{J}_L = nC_i \Delta \vec{\phi}_i = nC_i (\vec{\phi}_i - \vec{\phi}) = nC_i (\vec{\phi}_i - \vec{\phi}) & (20) \\ \vec{J}_i = nC_i \Delta \vec{\phi}_i = nC_i (\vec{\phi}_i - \vec{\phi}) = nC_i (\vec{\phi}_i - \vec{\phi}) & (21) \end{cases}$ <p>Equations thermiques</p> $nT \frac{ds}{dt} = -(\mu_i^* + \mu_i^*)S_{i,j} - (\mu_i^* + h^*)S_{i,j}^{(1)} - (\mu_i^* - h^*)S_{i,j}^{(2)} + T\vec{J}_i \cdot \vec{X}_i + T\vec{J}_i \cdot \vec{X}_i + \vec{X}_i \frac{d\vec{p}}{dt} + \vec{m} \frac{d\vec{\omega}}{dt} + \vec{X}_i \vec{J}_i + \vec{m} \vec{J} - \text{div} \vec{J}_e \quad (22)$ $\begin{cases} \mu_i^* = \mu_i - \frac{1}{2}m(\vec{\phi}_i^2 - 2\Delta\vec{\phi}_i^2) & (23) \\ \mu_i^* = \mu_i + \frac{1}{2}m\vec{\phi}_i^2 & (24) \\ \vec{X}_i = \frac{1}{T} \left(-\frac{1}{3} \text{grad} \mu_i + m \frac{d}{dt} (\vec{\phi}_i - 2\Delta\vec{\phi}_i) - m\vec{g} \right) & (25) \\ \vec{X}_i = \frac{1}{T} \left(-\frac{1}{3} \text{grad} \mu_i - m \frac{d}{dt} (\vec{\phi}_i) + m\vec{g} \right) & (26) \\ \vec{X}_i = \frac{1}{T} \left(-\frac{1}{3} \text{grad} \mu_i - m \frac{d}{dt} (\vec{\phi}_i) + m\vec{g} \right) & (27) \\ h^* = f + Ts + p + \frac{1}{2}m\vec{\phi}^2 - \mu_i C_L - \mu_i C_i & (28) \end{cases}$ <p>Equations liées aux charges</p> $\begin{cases} \frac{d\vec{S}_i}{dt} = \vec{S}_i^{(1)} - (\vec{\nabla}\vec{\phi}) \cdot \vec{S}_i = \vec{S}_i^{(1)} + \text{rot}(\vec{\nabla} \wedge \vec{S}_i) = \vec{S}_i^{(1)} - \text{rot} \vec{J}_i & (29) \\ \frac{d\vec{S}}{dt} = \vec{S}^{(1)} - (\vec{\nabla}\vec{\phi}) \cdot \vec{S} = \vec{S}^{(1)} + \text{rot}(\vec{\nabla} \wedge \vec{S}) - \vec{\nabla} \text{div} \vec{S} = \vec{S}^{(1)} - 2 \text{rot} \vec{J}^{(1)} - \vec{\nabla}\vec{\theta} & (30) \\ \frac{d\vec{S}}{dt} = \vec{S}^{(1)} - (\vec{\nabla}\vec{\phi}) \cdot \vec{S} = \vec{S}^{(1)} - \text{div}(\vec{\nabla}\vec{S}) = \vec{S}^{(1)} - \text{div} \vec{J}^{(1)} & (31) \end{cases}$ <p>Equations related to the charges</p> $\begin{cases} \vec{J} = \sum_i \vec{e}_i \vec{J}_i & (32) \\ \vec{J} = \sum_i \vec{e}_i \vec{J}_i & (33) \\ \vec{S}_i \cdot \vec{n} = -\vec{J}_i \cdot \vec{n} & (34) \end{cases}$ $\begin{cases} \vec{S}^{(1)} = -\sum_i \vec{e}_i \wedge \vec{S}_i^{(1)} & (35) \\ \vec{S}^{(2)} = \frac{1}{2} \sum_i \vec{e}_i \vec{S}_i^{(1)} & (36) \end{cases}$ $\vec{J}_{re} = \sum_i (\vec{e}_i \wedge \vec{X}_i) + \vec{X}_i \vec{m} + \frac{1}{2}(\vec{m} \wedge \vec{X}_i) + \vec{X}_i \vec{p} + \vec{V} \wedge \vec{A} \quad (37)$	
Phenomenological equations	
<p>Fonctions et équations d'état</p> $f = f(\alpha_i^e, \alpha_i^m, \omega_i^e, \omega_i^m, \tau^e, \tau^m, C_L, C_i, T) \quad (38)$ $\begin{cases} s_i = n \left(\frac{\partial f}{\partial \alpha_i^e} + \frac{\partial f}{\partial \alpha_i^m} \right) - \frac{n}{3} \delta_i \sum_j \frac{\partial f}{\partial \alpha_{ij}^e} = s_i(\alpha_{ij}^e, \omega_{ij}^e, \tau^e, \alpha_{ij}^m, \omega_{ij}^m, C_L, C_i, T) & (39) \\ m_i = n \frac{\partial f}{\partial \omega_i^e} = m_i(\alpha_{ij}^e, \omega_{ij}^e, \tau^e, \alpha_{ij}^m, \omega_{ij}^m, C_L, C_i, T) & (40) \\ p = -n \frac{\partial f}{\partial \tau^e} = p(\alpha_{ij}^e, \omega_{ij}^e, \tau^e, \alpha_{ij}^m, \omega_{ij}^m, C_L, C_i, T) & (41) \end{cases}$ $\begin{cases} s_i^{(1)} = n \left(\frac{\partial f}{\partial \alpha_i^e} + \frac{\partial f}{\partial \alpha_i^m} \right) = s_i^{(1)}(\alpha_{ij}^e, \omega_{ij}^e, \tau^e, \alpha_{ij}^m, \omega_{ij}^m, C_L, C_i, T) & (42) \\ m_i^{(1)} = n \frac{\partial f}{\partial \omega_i^e} = m_i^{(1)}(\alpha_{ij}^e, \omega_{ij}^e, \tau^e, \alpha_{ij}^m, \omega_{ij}^m, C_L, C_i, T) & (43) \end{cases}$ $\begin{cases} x = -\frac{\partial f}{\partial T} = x(\alpha_{ij}^e, \omega_{ij}^e, \tau^e, \alpha_{ij}^m, \omega_{ij}^m, C_L, C_i, T) & (44) \\ \mu_L = \frac{\partial f}{\partial C_L} = \mu_L(\alpha_{ij}^e, \omega_{ij}^e, \tau^e, \alpha_{ij}^m, \omega_{ij}^m, C_L, C_i, T) & (45) \\ \mu_i = \frac{\partial f}{\partial C_i} = \mu_i(\alpha_{ij}^e, \omega_{ij}^e, \tau^e, \alpha_{ij}^m, \omega_{ij}^m, C_L, C_i, T) & (46) \end{cases}$ <p>Equations de dissipation: auto-diffusion et création-annihilation de paires</p> $\begin{cases} \vec{J}_e = \vec{J}_e(\vec{X}_e, \vec{X}_L, \vec{X}_i, n, T, C_L, C_i, ...) & (47) \\ \vec{J}_i = \vec{J}_i(\vec{X}_e, \vec{X}_L, \vec{X}_i, n, T, C_L, C_i, ...) & (48) \\ \vec{J}_i = \vec{J}_i(\vec{X}_e, \vec{X}_L, \vec{X}_i, n, T, C_L, C_i, ...) & (49) \\ S_{i,j} = S_{i,j}(\mu_i^* + \mu_i^*, n, T, C_L, C_i, ...) & (50) \end{cases}$ <p>Equations de dissipation: anélasticité</p> $\begin{cases} \vec{S}_i = \vec{S}_i^{(1)}(\alpha_{ij}^e, \omega_{ij}^e, \tau^e, \alpha_{ij}^m, \omega_{ij}^m, C_L, C_i, T, ...) & (51) \\ \vec{m} = \vec{m}^{(1)}(\omega_{ij}^e, \omega_{ij}^m, T, ...) + \vec{m}^{(2)}(\omega_{ij}^e, \omega_{ij}^m, T, ...) & (52) \end{cases}$ <p>Equations de dissipation: flux de charges plastiques dislocatives</p> $\begin{cases} \vec{J}_i = \vec{X}_i \wedge \vec{V} = \vec{J}_i(\vec{X}_e, \vec{X}_L, \vec{X}_i, n, T, ...) & (53) \\ \vec{J} = -\frac{1}{2} \sum_i \vec{e}_i \wedge \vec{J}_i = \vec{J} \wedge \vec{V} + \frac{1}{2}(\vec{X}_i \wedge \vec{V}) = \vec{J}(\vec{X}_e, \vec{X}_L, \vec{X}_i, n, T, ...) & (54) \\ \frac{\vec{S}_i}{n} = \frac{1}{n} \left(\vec{J}_i - \vec{X}_i \vec{p} - \frac{1}{2}(\vec{X}_i \wedge \vec{V}) \right) & (55) \\ \vec{S}_i^e = \vec{S}_i^e \left(\left[\mu_i^* + \frac{1}{2}m\vec{\phi}_i^2 \right], p, \vec{X}_i, n, T, C_L, C_i, ... \right) & (56) \\ \vec{S}_i^m = \vec{S}_i^m \left(\left[\mu_i^* - \frac{1}{2}m\vec{\phi}_i^2 \right], p, \vec{X}_i, n, T, C_L, C_i, ... \right) & (57) \\ \vec{g}^* = f + p + m\vec{\phi}^2/2 - \mu_i C_L - \mu_i C_i & (58) \end{cases}$ <p>Equations de dissipation: sources de charges plastiques dislocatives</p> $\begin{cases} \vec{S}_i^{(1)} = -\sum_i \vec{e}_i \wedge \vec{S}_i^{(1)} = \vec{S}_i^{(1)}(...) & (60) \\ \vec{S}_i^{(2)} = \frac{1}{2} \sum_i \vec{e}_i \vec{S}_i^{(1)} = \vec{S}_i^{(2)}(...) & (61) \end{cases}$ <p>Additional equations</p> <p>Continuité de la masse</p> $\frac{\partial \rho}{\partial t} = -\text{div}[\rho \vec{\phi} + m(\vec{J} - \vec{J}_L)] = -\text{div}(\rho \vec{\phi}) \quad \text{dans } Q_{\Sigma_1 \cup \Sigma_2}^{\vec{e}, \vec{e}} \quad (62)$ <p>Flux de travail et force de surface</p> $\begin{cases} J_n = \mu_i^* \vec{J}_L + \mu_i^* \vec{J}_i - \phi_i \vec{X}_i - \frac{1}{2}(\vec{\phi} \wedge \vec{m}) + p \vec{\phi} & (63) \\ \vec{F}_i = \sum_j \vec{e}_j (\vec{X}_j \cdot \vec{S}_i) - \frac{1}{2}(\vec{X}_i \wedge \vec{V}) - \vec{X}_i \vec{p} & (64) \end{cases}$ <p>Additional equations</p> $\begin{cases} S_i = -\frac{1}{T}(\mu_i^* + \mu_i^*)S_{i,j} - \frac{1}{T}(\mu_i^* + h^*)S_{i,j}^{(1)} - \frac{1}{T}(\mu_i^* - h^*)S_{i,j}^{(2)} + \vec{J}_i \cdot \vec{X}_i + \vec{J}_i \cdot \vec{X}_i + \vec{X}_i \frac{d\vec{p}}{dt} + \vec{m} \frac{d\vec{\omega}}{dt} + \vec{X}_i \vec{J}_i + \vec{m} \vec{J} + \vec{J}_i \text{grad} \left(\frac{1}{T} \right) & (65) \end{cases}$ <p>Bilan énergétique</p> $\begin{cases} n\vec{\phi} \left(\frac{d\vec{p}}{dt} - m\vec{\phi} \frac{dC_L}{dt} + m\vec{\phi}_L \frac{dC_L}{dt} \right) + \left(\vec{X}_i \frac{d\vec{p}}{dt} + \vec{m} \frac{d\vec{\omega}}{dt} - p \frac{d\vec{\tau}}{dt} \right) + \left(\vec{X}_i \vec{J}_i + \vec{m} \vec{J} - p \frac{\vec{S}_i}{n} \right) = \rho \vec{g} \vec{\phi} - \text{div} \left[-\phi_i \vec{X}_i - \frac{1}{2}(\vec{\phi} \wedge \vec{m}) + p \vec{\phi} \right] & (66) \end{cases}$	

Figure 2.39 - Synoptic representation of fundamental and phenomenological equations necessary for the description of the spatio-temporal evolution of a solid medium presenting elasticity, anelasticity and self-diffusion, and containing mobile plastic charges.

possible to translate the non-Markovian behaviors of plasticity. In addition, the approach using plastic charges at the microscopic level of the discrete solid lattice also makes it possible in principle to find exact local expressions for the dissipative equations linked to plastic charges.

By introducing the simplest solid which it is possible to consider, namely the isotropic perfect solid, one can obtain *the Newton's equation* of this solid. We can then show that this solid is perfectly described by *equations similar to Maxwell's equations* when *the volume expansion is homogeneous within the solid*.

One can also calculate the fields of distortions, the energies and the interactions of the dislocations in this perfect solid. In the case of stationary dislocations in the solid lattice, *the static distortions of the lattice* induced by them store elastic energy within the lattice. This stored energy can then be considered as *the rest energy of the dislocations*. In the case where the dislocations are mobile in the lattice, the displacements of the lattice induced by the movement of the dislocations are associated with kinetic energy. At low speed, this kinetic energy is directly linked to the rest energy of these dislocations via relations similar to *the famous expression of Einstein* $E_0 = M_0 c^2$, which makes it possible to introduce in a completely classic way the concept of *mass of inertia of the dislocations*.

From the distortion fields induced by the dislocations and from the Peach and Koehler force, we can also describe the interactions that can occur between dislocations.

Finally, we can also introduce *the string model*, which will allow us to deal with the dynamics of a dislocation that moves in the lattice while being deformed. The string model has proven to be extremely useful and efficient in dealing with plasticity and anelasticity problems due to the movement of dislocations and occurring in common solids, such as metals for example. But it is not within the purview of this book to deal in detail with the problem of these phenomena, which can be addressed in many books dealing with this particular subject. However, to arouse the interest of the reader, we have plotted the equation of the string of a dislocation in figure 2.40a, and, by way of example, two typical applications:

- *the thermally activated interaction of a dislocation with a field of punctual obstacles*: to introduce this type of interactions into the string model, it is necessary to know the spatial distribution of obstacles in the solid, as well as the internal stress fields generated by them. These stress fields due to obstacles can be expressed and visualized at the level of the gliding plane of the dislocation, as illustrated in figure 2.40b, where it appears many Peach and Koehler forces $\sum f_n(x_1, u(x_1, t))$ combining to act on the dislocation. But the string equation in figure 2.40b in the presence of interactions with obstacles is a purely mechanical equation, which cannot take into account temperature effects, such as the migration of obstacles by diffusion or the crossing of obstacles by thermal activation. Introducing the effects of temperature into the string equation is theoretically possible by developing a *"Brownian" image* of the dislocation, that is, by introducing a term of local thermal fluctuations $F_{fluctuation}(x_1, u(x_1, t), t)$ into the string equation, as illustrated in figure 2.40c, modeled on the term of thermal fluctuations in the model of *the Langevin equation*. It is clear that such an approach to the dynamics of dislocation quickly proves to be very complex.

In general, these problems of dislocation interactions with obstacles are approached in a much more pragmatic way, by developing, on the basis of the string model, simplified models judiciously adapted to the problem to be treated. To deepen this subject, one will find examples

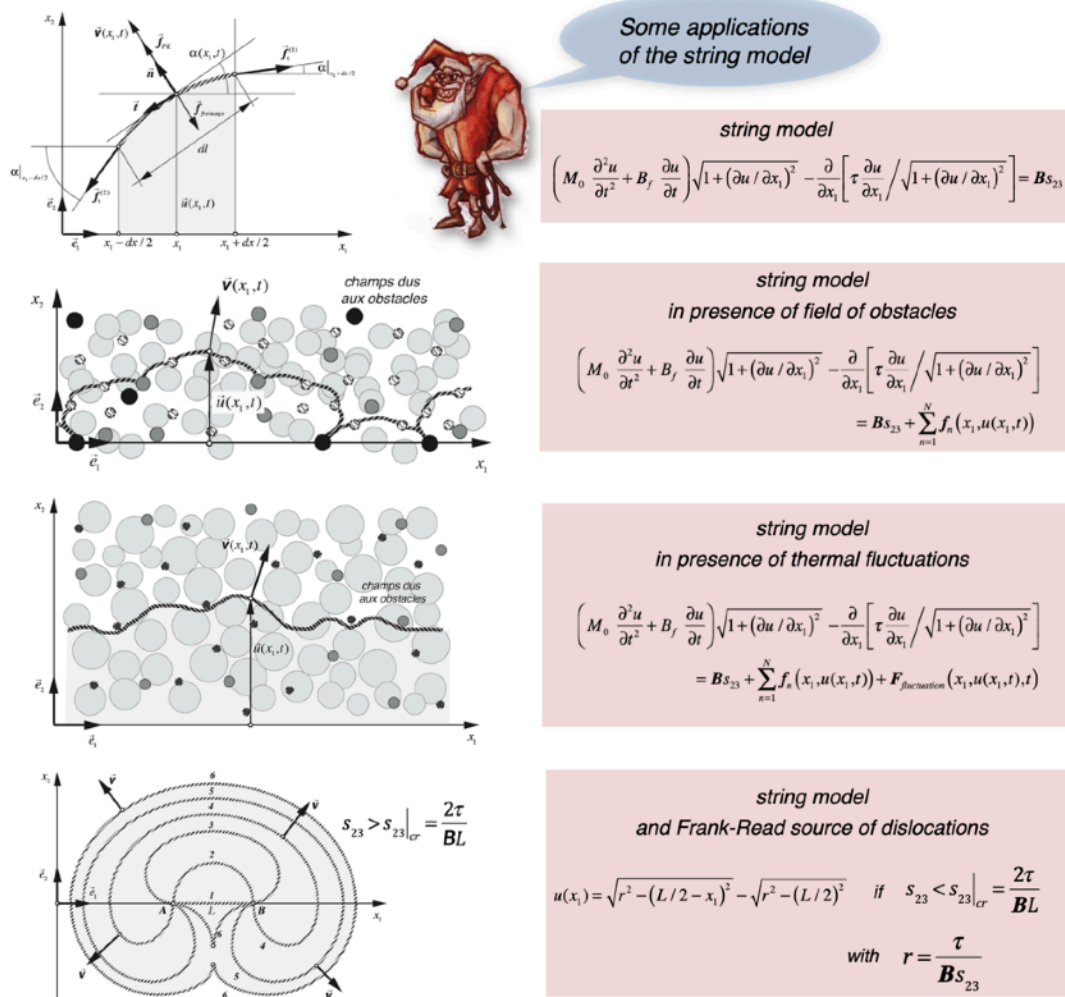


Figure 2.40 - The string model and some of its applications

of mechanisms of interaction of dislocations with obstacles, illustrated by experimental results and theoretical models, in many books dealing with dislocations, or in a more summarized way in review articles such as "Dislocation-point defect interactions"¹¹ and "dislocation-lattice interactions"¹².

- *the source of Frank-Read dislocations*: we now suppose a dislocation segment of length L anchored on its gliding plane at two points **A** and **B** located on the axis Ox_1 in $x_1 = 0$ and $x_1 = L$, as illustrated in figure 2.40d. Such anchoring points can be due to the existence of strong and localized interactions of the dislocation with obstacles (other dislocations, precipitates, etc.). Using the string equation in the static case, it is fairly easy to show that the deformation of the dislocation segment under the effect of a static stress is a portion of a circle whose radius depends on the stress s_{23} applied to the solid. In fact, the radius of curvature of

¹¹ G. Gremaud, chap.3.3, dans «Mechanical spectroscopy», Trans Tech Publications, Zürich, 2001, p.178-246

¹² W. Benoit, chap. 3.2, dans «Mechanical spectroscopy», Trans Tech Publications, Zürich, 2001, p. 158-177

the segment is inversely proportional to the static shear stress s_{23} , which means that the latter decreases as s_{23} increases. However, it is clear that there is a minimum limit for the radius of curvature, which intervenes for a critical stress $s_{23}|_{cr}$ such that the radius of curvature becomes equal to $L/2$. For any value s_{23} greater than $s_{23}|_{cr}$, there can be no static solution for the deformation of the string segment. There then appears a complex dynamic solution to the equation of the string, which in fact corresponds to a *Frank-Read source mechanism*.

The initial straight segment shown by (1) in Figure 2.40d curves between the two anchor points until it forms a semicircle (2). Then it continues to extend beyond the anchoring points, steps (3), (4) and (5), until the strand of the segment leaving from **A** joins the strand of segment leaving from **B** (6). At this point, as the two strands have the same Burgers vector, they bind together by forming on the one hand a new segment (1) growing between the anchoring points **A** and **B**, and on the other hand a closed loop (6) which will not stop growing. This mechanism therefore constitutes a phenomenon of uninterrupted source of dislocation loops. It is essentially this phenomenon, which is very well observed by electron microscopy, which explains why it is possible to carry out significant plastic deformations of certain solids such as metals. And it is indeed this type of phenomenon which can be responsible for the existence of a non-zero source of dislocation charges in the equation of continuity of the density of dislocation charges in Figure 2.5, which induces a non-commutativity of the operator of material derivative with the operators of space.

Chapter 3

The «Cosmological Lattice» and its properties

By the introduction of an elastic strain energy of the lattice, called the *elastic internal energy*, expressed *per unit volume of the lattice* and dependent at the same time on *the volume expansion, the shear strains and especially on the local rotations within the lattice*, we obtain an imaginary lattice, which we will call "*cosmological lattice*". This lattice has a very particular *Newton's equation*, in which appears in particular *a new term of force*, which is directly related to the energy of distortion due to the topological singularities contained in the lattice, and which will be called thereafter to play a fundamental role in analogies with Gravitation and with Quantum Physics.

The propagation of waves in the cosmological lattice presents very interesting features. The propagation of transverse waves with linear polarization is always associated with longitudinal wavelets, and the propagation of pure transverse waves can only be done by *waves with circular polarization*, which will then have a direct link with the existence of photons. On the other hand, the propagation of longitudinal waves can disappear in favor of the appearance of *localized modes of longitudinal vibration* in the case where the volume expansion of the lattice is less than a certain critical value, which will subsequently have a direct link with quantum physics.

A curvature of the wave rays also appears in the vicinity of a singularity of the volume expansion of the lattice. This phenomenon makes it possible to find the conditions which the expansion field associated with a topological singularity must satisfy so that a trap appears which captures all the transverse waves, in other words a "*black hole*".

A finite cosmological lattice in absolute space can exhibit *a dynamic volume expansion and / or contraction*, provided that it contains a certain amount of kinetic energy, a phenomenon quite similar to the cosmological expansion of the Universe. According to the signs and the values of the elastic modules, several types of cosmological behaviors of the lattice are possible, some of which present the phenomena of *big bang, rapid inflation* and *acceleration of the speed of expansion*, and which can be followed in some cases of a *re-contraction of the lattice* leading to a *big-bounce* phenomenon. We deduce that it is the elastic energy contained in the lattice and due to the expansion which is responsible for these phenomena, and in particular for *the increase in the speed of expansion*, phenomenon which is observed on the current Universe by astrophysicists and which is attributed by them to a hypothetical "*dark energy*".

The «cosmological lattice» and its Newton's equation

Let us introduce an imaginary solid lattice, which will be arbitrarily called "*cosmological lattice*" and whose *internal energy of distortion is expressed per volume unit* in the form of a development of the volume expansion τ , the elastic and anelastic shears $\vec{\alpha}_i^{el}$ and $\vec{\alpha}_i^{an}$, but also directly from the vectors of elastic and anelastic rotation $\vec{\omega}^{el}$ and $\vec{\omega}^{an}$. Our initial

conjecture is therefore *a priori* the following: the internal energy of the "cosmological lattice" is expressed as a function $U^{def} = U^{def}[\tau, \tau^2, (\vec{\alpha}_i^{el})^2, (\vec{\omega}^{el})^2, (\vec{\alpha}_i^{an})^2, (\vec{\omega}^{an})^2]$ of the state of distortion per unit volume of the lattice.

Such a lattice in fact corresponds to the most general isotropic perfect lattice that one can imagine if one makes his energy depend both linearly on the volume expansions and quadratically on the volume expansions, shear strains and rotations by torsional deformation. Still in the spirit of simplification, we can also assume that there is no elasticity by volume expansion in this lattice. The state function per unit volume of this cosmological lattice is therefore written in the form of the expression presented in figure 3.1, in which appears four elastic constants K_0, K_1, K_2, K_3 and two anelastic constants K_1^{an}, K_2^{an} which completely characterize the elasticity and the anelasticity of this lattice.

Conjecture 1 - The internal energy of lattice distortion is expressed per volume unit of lattice, as a second order development in the distortion tensors

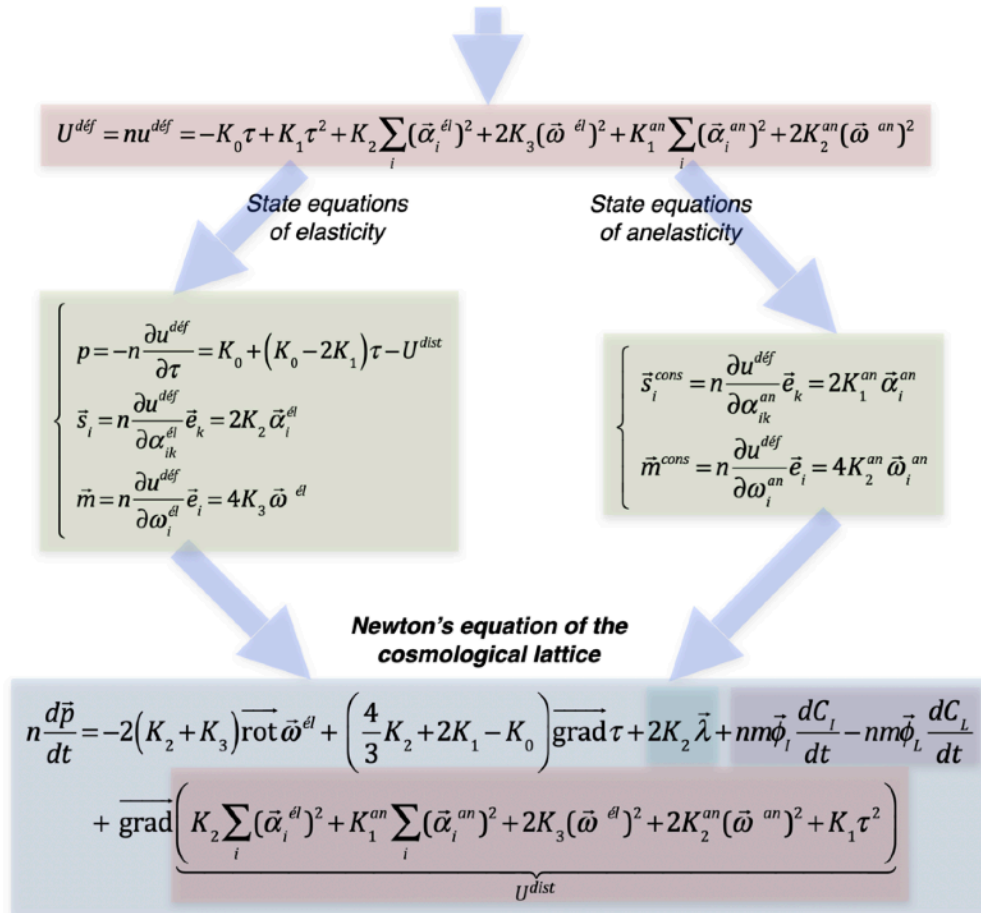


Figure 3.1 - The first conjecture which leads to the cosmological lattice and its Newton's equation

One then deduces from it five *equations of state of elasticity and anelasticity*, respectively for the scalar of pressure p , the symmetrical transverse tensors of shear stresses \vec{s}_i and \vec{s}_i^{cons} as well as the moment vectors \vec{m} and \vec{m}^{cons} , which are also reported in the figure 3.1. These state equations can be used to carry out a rather tedious computation which finally provides *the*

equation of Newton of the cosmological lattice reported in figure 3.1. This equation is indeed a Newton's equation because it provides *the temporal variation of the amount of momentum per lattice site*, taken along the trajectory of the lattice, according to the spatial variations of the tensors of distortion, via the elastic and anelastic constants.

We will see later that this Newton's equation will play an absolutely central role on the behavior of the cosmological lattice. It is quite complicated, in particular by the presence of *the density $\bar{\lambda}$ of flexion charge*, of terms related to *the diffusion of intrinsic point defects* and especially of *the new term of force* depending directly on *the volume density of internal distortion energy U^{dist}* , which is directly related to the energy of distortion, namely the quadratic terms of the deformation energy U^{def} , due to the topological singularities contained in the lattice, and which will be called thereafter to play a fundamental role in the analogies with Gravitation and with Quantum Physics.

The fact of introducing a rotational energy with terms in $\bar{\omega}^{el}$ and $\bar{\omega}^{an}$ into the expression of the internal energy of the cosmological lattice, as well as the fact of developing its internal energy per unit of volume and not per site of lattice, are not not at all elementary to understand, and really make this lattice *a perfectly imaginary lattice* of which there is absolutely no equivalent among the usual solids.

Rather than embarking now on a superfluous search for interpretation of the “hidden face” of this imaginary lattice, it seems preferable to start by exploring in detail the consequences that this hidden face implies in terms of the behaviors that the cosmological lattice can present. It is therefore to this task that devolves the rest of this book, which will be devoted to extracting the substantial core from this hidden face. To do this, we will show that it is *the Newton's equation* that we have just deduced which has spectacular properties and which is at the heart of the very many analogies that we will develop in the following with the great theories of physics, namely Maxwell's Electromagnetism, Lorentz Transformation, Einstein's Special Relativity, Newton's Gravitation, Einstein's General Relativity, and even Quantum Physics and the Standard Model of Elementary Particles.

Transverse and longitudinal perturbations in the cosmological lattice

We will first be interested in the transverse and longitudinal perturbations that can reign within the cosmological lattice. There are quite surprising vibrational phenomena (figure 3.2), such as *the existence of a mode of propagation of linearly polarized transverse waves which are necessarily coupled to longitudinal wavelets*, while *circularly polarized transverse waves are free of these wavelets*. There is also the possibility of propagation of *longitudinal waves*. But, under certain conditions which strongly depend on the elastic moduli and the state of expansion of rest of the lattice, the mode of longitudinal propagation can disappear and be replaced by *a very astonishing mode of localized vibrations of expansion*, which will play by thereafter a key role in analogies with gravitation and quantum physics.

To discuss these various modes of mechanical perturbations in the cosmological lattice, we will make simplifying hypotheses, namely that there are no anelastic perturbations, therefore that $\bar{\alpha}_i^{an} = 0$ and $\bar{\omega}^{an} = 0$, that there are no vacancies and self-interstitials, therefore that $C_i = C_L \equiv 0$ and that there is no density $\bar{\lambda}$ of flexion charges, therefore that $\bar{\lambda} = 0$.

We will further assume that the state of the background volume expansion of the lattice is a constant τ_0 , so that the total volume expansion of the lattice is written $\tau = \tau_0 + \tau^{(p)}$, in which $\tau^{(p)}$ represents the mechanical perturbations of the expansion around the rest value τ_0 . To calculate the various perturbation modes, we inject the expression of the momentum of the perturbations, that is $\vec{p}^{(p)} = m\vec{\phi}^{(p)}$, into Newton's equation in figure 3.1. We can then describe four different perturbations modes:

Transverse perturbations in the cosmological lattice

Pure transverse waves with circular polarization

$$\vec{\omega}(x_j, t) = \omega_{i0}^{(p)} \exp[i(k_t x_j - \omega t)] \vec{e}_i \pm i \omega_{i0}^{(p)} \exp[i(k_t x_j - \omega t)] \vec{e}_k \quad \text{with} \quad c_t = \frac{\omega}{k_t} = \sqrt{\frac{K_2 + K_3}{mn}}$$

Transverse waves with linear polarization necessarily coupled to longitudinal wavelets

$$\begin{aligned} \omega_i^{(p)}(x_j, t) &\equiv \omega_{i0}^{(p)} \exp[i(k_t x_j - \omega t)] \\ \tau^{(p)}(x_j, t) &\equiv \tau_0^{(p)} \exp[i(2k_t x_j - 2\omega t)] \end{aligned} \quad \text{with} \quad \begin{aligned} c_t &= \frac{\omega}{k_t} = \sqrt{\frac{K_2 + K_3}{mn}} \\ \tau_0^{(p)} &\equiv -\frac{K_2 + K_3}{K_2/3 + 2K_1(1 + \tau_0) - K_0 - K_3} (\omega_{i0}^{(p)})^2 \end{aligned}$$

Longitudinal perturbations in the cosmological lattice

Pure longitudinal waves if $4K_2/3 + 2K_1(1 + \tau_0) - K_0 > 0$

$$\underline{\tau}^{(p)} = \tau_0^{(p)} \exp[i(k_l x_j - \omega t)] \quad \text{with} \quad c_l = \frac{\omega}{k_l} \equiv \sqrt{\frac{1}{mn} \left[\frac{4}{3} K_2 + 2K_1(1 + \tau_0) - K_0 \right]}$$

Eigen modes of localized vibrations if $4K_2/3 + 2K_1(1 + \tau_0) - K_0 < 0$

$$\underline{\tau}^{(p)} = \tau_0^{(p)} \exp[-x_j / \delta] \exp[i\omega t] \quad \text{with} \quad \delta = \frac{1}{\omega} \sqrt{\frac{1}{mn} \left[\frac{4}{3} K_2 + 2K_1(1 + \tau_0) - K_0 \right]}$$

Figure 3.2 - Transverse and longitudinal perturbations in the cosmological lattice

- the propagation of a linearly polarized transverse wave in the cosmological lattice, that is to say of a wave for which the vibration of the particles of the lattice is perpendicular to the direction of propagation of the wave. Such a wave satisfies a completely conventional wave equation provided that its amplitude is not too strong. But it must be accompanied by a *longitudinal wavelet* which propagates in the same direction and at the same velocity as that of transverse perturbation. The frequency of this longitudinal wavelet is twice the frequency of the transverse perturbations, and its amplitude is proportional to the square of the amplitude of the transverse perturbations. It will also be noted that the speed of propagation of the transverse perturbations strongly depends on the background volume expansion τ_0 of the lattice since the value of the lattice site density n which appears in the expressions of the speed of the

transverse waves is an exponential function $n = n_0 e^{-\tau_0}$ of the background volume expansion τ_0 of the lattice.

- *the propagation of a circularly polarized transverse wave* in the cosmological lattice, that is to say of a wave for which the vibration of the particles of the network rotates around the direction of propagation of the wave. It is said that such a wave has a *positive or negative helicity* depending on whether the direction of vibration of the particles rotates dextrorotatory or levorotatory at an angle of 360° over one wavelength. Circularly polarized transverse waves are pure, in the sense that they are not coupled to longitudinal wavelets.

- *the propagation of a longitudinal wave* in the cosmological lattice, that is to say of a wave for which the direction of vibration of the particles of the lattice is the same as the direction of propagation of the wave is quite complicated to compute, because *the propagation equations are strongly non-linear* and depend directly on the state of rest expansion τ_0 of the lattice. In this case, only very small perturbations $\tau^{(p)}$ within the lattice are considered, which makes it possible to linearize the wave equations. The celerity c_l of longitudinal waves of small amplitude which appears in figure 3.2 is expressed with the square root of an argument which must be positive for it to exist. As this argument depends both on the elastic constants K_0, K_1, K_2 and on the state of rest volume expansion τ_0 of the lattice, directly and exponentially via the expression $n = n_0 e^{-\tau_0}$, *the existence of a longitudinal wave propagation is subject to the condition $4K_2/3 + 2K_1(1 + \tau_0) - K_0 > 0$* .

- *the longitudinal perturbations in the form of localized eigen modes of vibrations of the volume expansion*. In the cosmological lattice, if the celerity c_l of the longitudinal waves becomes an imaginary number (this is what is called the square root of a negative number), *there is no longer any propagation of longitudinal waves*. In this case, we can rewrite the complex perturbation solution in the form shown in figure 3.2. There arises here a very surprising phenomenon, namely *the appearance of localized eigen modes of longitudinal vibrations*, which do not propagate at great distance, but which are on the contrary confined on distances of the order of δ . For high amplitudes of these localized modes of longitudinal perturbations, these will become non-linear and will therefore strongly depend on the amplitude $\tau^{(p)}$ of the perturbations. The appearance of these "strange" modes is obviously subject to the condition that $4K_2/3 + 2K_1(1 + \tau_0) - K_0 < 0$.

It is remarkable that in the cosmological lattice, the speed $c_t = \omega/k_t$ of the transverse waves depend exponentially on the state of expansion τ of the lattice via the value of a multiplicative term being worth $e^{\tau/2}/\sqrt{n_0}$. The same goes for the speed c_l of the longitudinal waves, although there is also a dependence on their speed through a term τ within the argument of the root.

It is also remarkable that the linearly polarized transverse waves are necessarily coupled to longitudinal wavelets in the cosmological lattice, and that the only transverse waves which are pure, not coupled to longitudinal wavelets, are then the transverse waves with right or left circular polarization, that is to say transverse waves of positive or negative helicity. Strangely, there is already a property specific to photons in the real universe, namely that photons are necessarily of non-zero helicity. As photons are quantum objects, we find here an astonishing peculiarity to which we will return.

The existence of domains of volume expansion of the cosmological lattice in which the

propagation of longitudinal waves is not possible, when $4K_2/3 + 2K_1(1 + \tau_0) - K_0 < 0$, corresponds well by analogy with the fact that there is no propagation of longitudinal waves in the theory of Einstein's General Relativity. Indeed, in the latter, the gravitational waves are transverse waves, defined as the propagation of perturbations of the space-time metric. These waves have a tensorial symmetry, with two independent polarizations perpendicular to the direction of propagation, contrary to the longitudinal perturbations which have a scalar symmetry.

The condition $4K_2/3 + 2K_1(1 + \tau_0) - K_0 < 0$ that there are no longitudinal waves implies the existence of a *critical background expansion* τ_{0cr} of the lattice, the limit between the expansion domains where it exists and where there are no longitudinal waves. In order for the cosmological lattice to present analogies with Einstein's General Gravitation, with electromagnetism and with the photons of quantum physics, it is necessary that there are no longitudinal waves, but that there are pure transverse waves of circular polarization. Hence the need to make a second conjecture which is shown in figure 3.3.

Conjecture 2 - So that the "cosmological lattice" presents analogies with Einstein's General Gravitation, with electromagnetism and with the photons of quantum physics, it is necessary that:

1) there are transverse waves with circular polarization

$$K_2 + K_3 > 0$$

2) there are no longitudinal waves

$$\begin{cases} \tau_0 < \tau_{0cr} = \frac{K_0}{2K_1} - \frac{2K_2}{3K_1} - 1 & (\text{si } K_1 > 0) \\ \tau_0 > \tau_{0cr} = \frac{K_0}{2K_1} - \frac{2K_2}{3K_1} - 1 & (\text{si } K_1 < 0) \end{cases}$$

Figure 3.3 - The second conjecture necessary for the cosmological lattice

This conjecture implies, so that there are no longitudinal waves, that the volume expansion τ_0 of the cosmological lattice is smaller or greater than the value of the *critical expansion* τ_{0cr} depending on whether the elastic modulus K_1 is positive or negative.

In the absence of longitudinal waves, the cosmological lattice then presents *localized eigen modes of longitudinal perturbations*, therefore local vibrations of the scalar τ of volume expansion. Such modes immediately make one think of the ideas of quantum fluctuations in gravitation on a very small scale since they affect the scalar τ which undeniably has a link with the gravitational field. But these localized perturbations of the scalar of volume expansion also make one think of the quantum fluctuations of the vacuum described by quantum physics. We can therefore, on the basis of this analogy between τ and the gravitational field, ask the following question: "is gravity that must be quantified on a very small scale, or is it gravitation,

on a very small scale, responsible for quantum physics? ” We will try to provide some answers to this topical question of the most relevant.

Curvature of the wave rays by a singularity of expansion and black holes

Among the surprising behaviors that a cosmological lattice can exhibit with regard to wave propagation, there appears a *non-dispersive curvature of the wave propagation rays by a gradient of volume expansion* due to the presence of a strong topological singularity of the expansion τ . This curvature can go as far as the formation of "*black holes*" absorbing all the waves passing in its proximity, or of impenetrable "*white holes*" repelling all the waves passing in its proximity.

The fact that the celerities of the transverse and longitudinal waves increase non-linearly with the value of the static volume expansion τ via the value of the site density $n = n_0 e^{-\tau}$ will cause a curvature of the rays of propagation of these waves if they pass in the direct vicinity from a singularity of volume expansion within the lattice, as illustrated in figure 3.4.

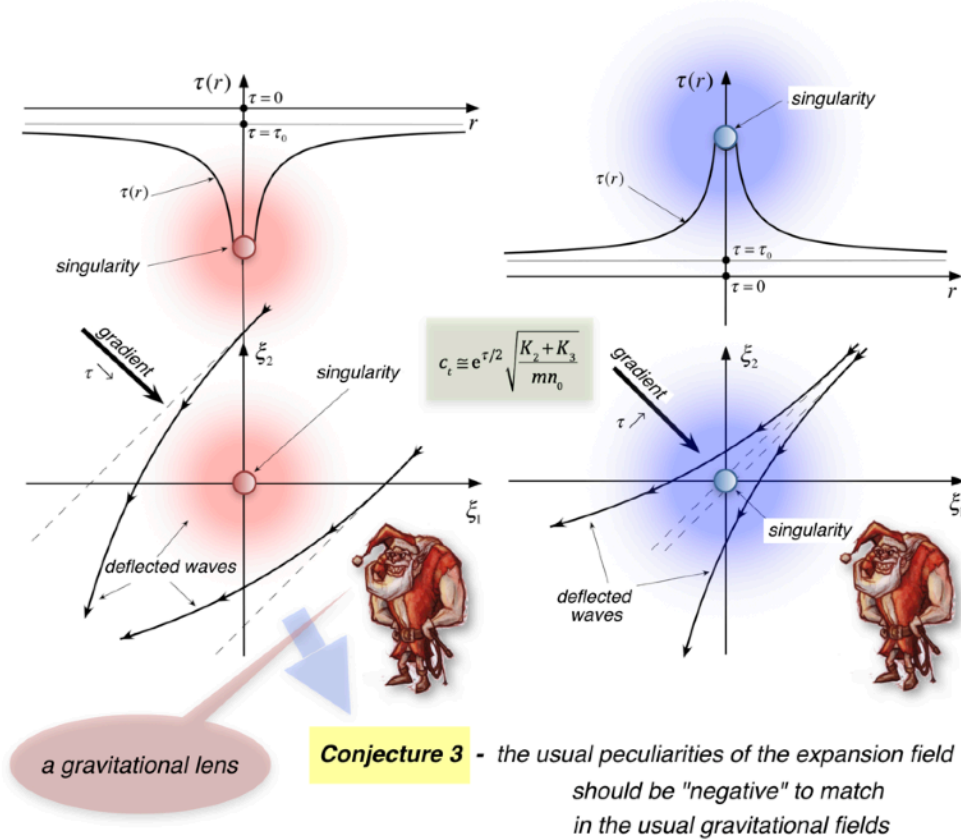


Figure 3.4 - The curvature of the wave rays in the vicinity of a singularity of the volume expansion of spherical symmetry

Indeed, imagine a motionless cosmological lattice in the absolute frame of reference of the **GO** observer and containing a singularity of volume expansion of spherical symmetry located at the center of the coordinate system $O\xi_1\xi_2\xi_3$. Let us also consider a longitudinal or transverse

wave, initially planar, arriving towards this singularity in a given initial direction. The speed of propagation increases or decreases as it approaches singularity, under the effect of lattice density $n = n_0 e^{-\tau}$. According to whether the singularity of τ is "positive" (passes through a maximum at the origin) or "negative" (passes through a minimum at the origin), there will appear a curvature of the rays of propagation of the waves, so that the wave seems repelled by a "positive singularity" or attracted by a "negative singularity».

This phenomenon does not depend on the shape of the field around the singularity, but only on its gradient, that is to say on *the slope of the function $\tau(r)$* . For a plane wave incident on the singularity, this phenomenon of acceleration or deceleration of the wave will then cause a deformation of the wave planes similar to the effect of a diverging lens in the case of a "positive singularity" or a converging lens in the case of a "negative singularity». In addition, as this phenomenon does not depend on the frequency of the wave, the singularity behaves like a converging or diverging lens of a *non-dispersive nature* in the cosmological lattice, that is to say which does not depend on the frequency of the incident wave.

Now imagine that in a motionless cosmological lattice in the absolute frame of reference of the **GO** observer, and containing a "negative singularity" of the volume expansion, of spherical symmetry, located at the center of the coordinate system, it passes a transverse wave ($c_t = c_t$) or a longitudinal wave ($c_l = c_l$). In the vicinity of the singularity, at a distance $r = r_{cr}$ from the origin of the singularity, the wave planes are always parallel to a line passing through the origin of the singularity, so that the radius of the transverse or longitudinal wave located in $r = r_{cr}$ is in fact a circle centered on the origin, as illustrated in figure 3.5. *The condition of existence* of this sphere of perturbations around the singularity effectively depends on the slope of $\tau(r)$ as explained in figure 3.5.

Thus, if a transverse or longitudinal wave passes at a distance satisfying this relationship $r \leq r_{cr}$, it becomes impossible for it to escape from the virtual sphere of radius r_{cr} . If the field of singularity has a monotonous gradient increasing from its origin, the curvature of the wave rays located inside this critical sphere will be further accentuated, so that all these waves will be definitively trapped by the singularity. By analogy with the "sphere of photons" surrounding a black hole in general relativity, one will call "sphere of transverse and longitudinal perturbations" the layer located at a distance $r = r_{cr}$ from the heart of the singularity. It is clear that the existence of such a *sphere of perturbations* is subject to the condition that it lies outside the "object" responsible for the negative singularity of the expansion field. If the radius of this "object" is R , we deduce that the condition $r_{cr} > R$ must also be part of the conditions of existence of a "black hole».

We saw in the previous section that the propagation of longitudinal waves in the perfect lattice is subject to the condition that the expression $4K_2/3 + 2K_1(1 + \tau_0) - K_0$ is positive. This condition takes the form of a condition on the background volume expansion τ_0 of the lattice, which must be greater or less than a critical value τ_{0cr} given in figure 3.3. If the propagation of longitudinal waves is possible in the lattice, then the longitudinal waves will also undergo the phenomenon of trapping at the limit $r = r_{cr}$. In the event that $K_1 > 0$, there is yet another phenomenon. Indeed, if the singularity presents a monotonic gradient increasing from its origin, there could exist a radius $r = r_{cr2}^{(l)} < r_{cr}$ surrounding it beyond which the value of $\tau(\bar{r})$ becomes less than τ_{0cr} . In this case, any longitudinal wave initially trapped at the limit $r = r_{cr}$

will then reach this second limit $r = r_{cr2}^{(l)} < r_{cr}$ beyond which it will not even be able to propagate, but will increase natural modes of longitudinal vibrations located inside this volume. In the case where $K_1 < 0$, this same phenomenon does not exist since the existence of a propagation implies that $\tau(r) < \tau_0 < \tau_{0cr}$ in this case.

The cosmological lattice presents a very interesting analogy with the theory of General Gravitation of Einstein since one can find there, in the vicinity of singularities of the volume expansion, *spheres of perturbations* very similar to the *sphere of photons surrounding a black hole*. We therefore deduce from this *non-dispersive effect of the curvature of the rays by the gradients of the volume expansion* that the scalar of volume expansion undoubtedly has a strong analog relationship with the gravitational field in General Relativity.

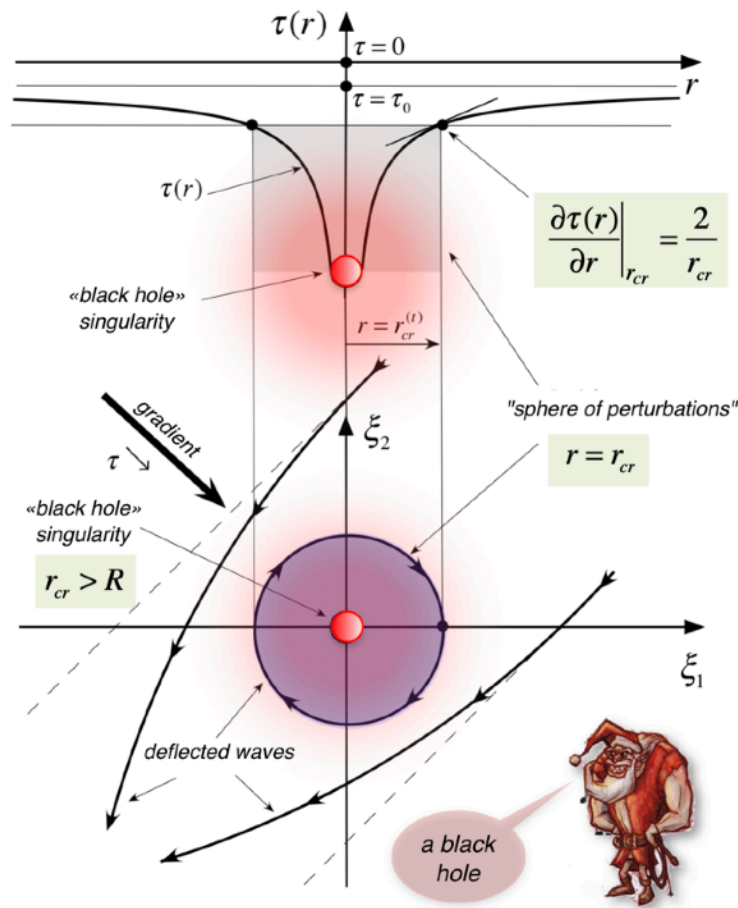


Figure 3.5 - The "sphere of perturbations", a real "black hole" in the vicinity of a negative singularity of τ

It is also interesting to note that only a negative singularity of τ has this property similar to that of a "black hole" capturing all the waves passing in its proximity, whereas a positive singularity of τ would behave like a "white hole" that is to say as an entity which would repel the waves, and which therefore could not be penetrated by waves. Hence the third conjecture for our analogy with Gravitation, reported in figure 3.4.

It is quite remarkable to note that the curvature of the waves by a gradient of volume expansion and the existence of a sphere of perturbations around a localized singularity of

volume expansion are exclusively due to the development of the internal energy per unit volume that we used for the cosmological lattice. Indeed, if we try to take a closer look at what would happen in the case of a perfect solid for which the internal energy would be written as a development expressed by lattice site, we would see that the speed of the transverse waves would be "invariant" whatever the state of expansion of the lattice, which obviously cannot lead to a non-dispersive curvature of the wave rays nor to the appearance of a sphere of perturbations. This analogy therefore justifies *a fortiori* the conjecture 1 that we had posed in figure 3.1, since it is this conjecture which allows the existence of the curvature of the waves and the sphere of disturbances in the cosmological lattice.

Cosmological expansion-contraction of a sphere of perfect lattice and dark energy

By considering a finite imaginary sphere of cosmological lattice, one can introduce the concept of "*cosmological evolution*" of the lattice, supposing that a certain amount of kinetic energy is injected into it. In this case, the lattice presents strong temporal variations of its volume expansion, which one can model in a very simplistic way by supposing that the volume expansion remains perfectly homogeneous in all the lattice during its evolution.

Let us imagine that, in the absolute reference frame $O\xi_1\xi_2\xi_3$, the **GO** observes a solid, of spherical shape, of radius R_U , made up of a lattice of cells (figure 3.6), and that this solid has a homogeneous background volume expansion which depends on time, but not on the position within the lattice, so that $\tau(t) = \tau_0(t) \neq \tau_0(\vec{\xi}, t)$. In this case, the **GO** will observe that the radius R_U of this solid sphere depends on time $R_U = R_U(t)$ and therefore that this sphere will

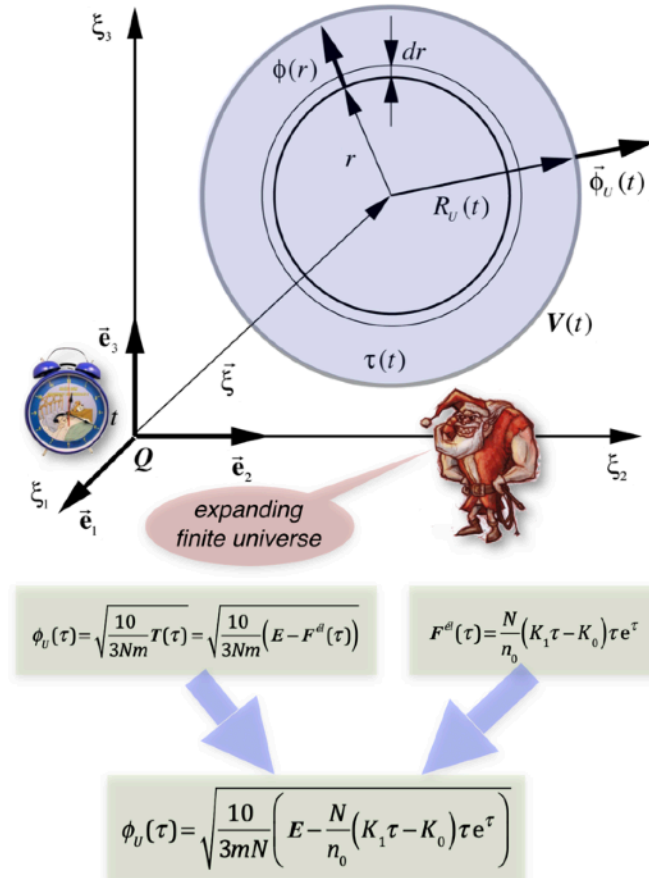


Figure 3.6 - "Cosmological" volume expansion $\tau(t)$ of an imaginary solid sphere

tend to expand or contract. This behavior, which one could qualify as “cosmological” by analogy to the cosmological theories of expansion of the Universe, necessarily implies the conservation of energy, namely that the total energy E of the solid, composed of the elastic energy $F^{el}(\tau)$ of expansion and the kinetic energy $T(\tau)$ of expansion, is a constant.

The total kinetic energy T of volume expansion is necessarily linked to the speed of expansion, which can be characterized by the velocity $\vec{\phi}_U(t)$ of the surface of the sphere (figure 3.6). The kinetic energy T can then be obtained by summing (by integration) over the whole sphere the kinetic energy of the lattice sites located in a spherical cap of radius r and thickness dr . The speed of expansion in the spherical cap is simply given by $\phi(r) = \phi_U r / R_U$ since the volume expansion was assumed to be homogeneous. From the expression of the kinetic energy T thus obtained as a function of $\vec{\phi}_U$ and of the total number N of sites contained in the sphere, the dependence of $\phi_U(\tau)$ is deduced as a function of $T(\tau)$. On the other hand, like $T(\tau) = E - F^{el}(\tau)$, we finally get the dependence of $\phi_U(\tau)$ as a function of $F^{el}(\tau)$. But the total elastic energy can be calculated quite easily from the state function U^{def} of the lattice since τ is homogeneous in the space of the sphere and the other distortion tensors are zero. With the expression of $F^{el}(\tau)$ calculated and reported in figure 3.6, one can directly expressed $\phi_U(\tau)$ as a function of τ and of the total energy E/N per lattice site. The expression shown in figure 3.6 shows that it is possible to plot ϕ_U as a function of τ , for various values of E/N . As this expression also depends on the two elastic constants K_0 and K_1 , we will get eight different graphs, shown in figure 3.8, depending on whether these two elastic constants are positive, zero or negative, knowing that the graph in the case where the two constants were zero has no sense.

As an example, consider the case of the lattice for which $K_0 > 0$ and $K_1 > 0$. The relations of figure 3.6 allow to deduce its “cosmological behavior” as represented in figure 3.7:

- if $E < 0$, the lattice presents a single possible trajectory, entirely located in the domain $\tau > 0$, and which corresponds to expand and contract indefinitely between two extreme values of τ ,
- if $0 < E < F_{max}^{el}$, the network presents two possible trajectories: the first corresponds to expand and contract indefinitely between a positive value and a negative value of τ , and the second corresponds to oscillate indefinitely between a negative value of τ and an expansion tending towards $\tau \rightarrow -\infty$,
- if $E > F_{max}^{el}$, the lattice presents a single very interesting possible trajectory. It pulsates indefinitely from a *big bang* to a *big crunch*. The big bang is followed by a phase of rapid expansion, followed by a deceleration, then again an expansion at increasing speed, and suddenly a reversal of the speed of expansion, to contract again by following in opposite direction every stages traveled during expansion. The contraction ends with a big crunch, which can only be followed by a bigbang since the lattice has then accumulated a total kinetic energy equal to E , phenomenon called “big bounce”.

In the case of this lattice, one also notes the existence of domains of volume expansion presenting different behaviors concerning the longitudinal waves: a domain where it coexists transverse and longitudinal waves, for $\tau > \tau_{0cr} = K_0 / 2K_1 - 2K_2 / 3K_1 - 1$, and a domain where there exists only transverse waves and localized longitudinal eigen vibration modes, for $\tau < \tau_{0cr} = K_0 / 2K_1 - 2K_2 / 3K_1 - 1$. And the area where there are no longitudinal waves

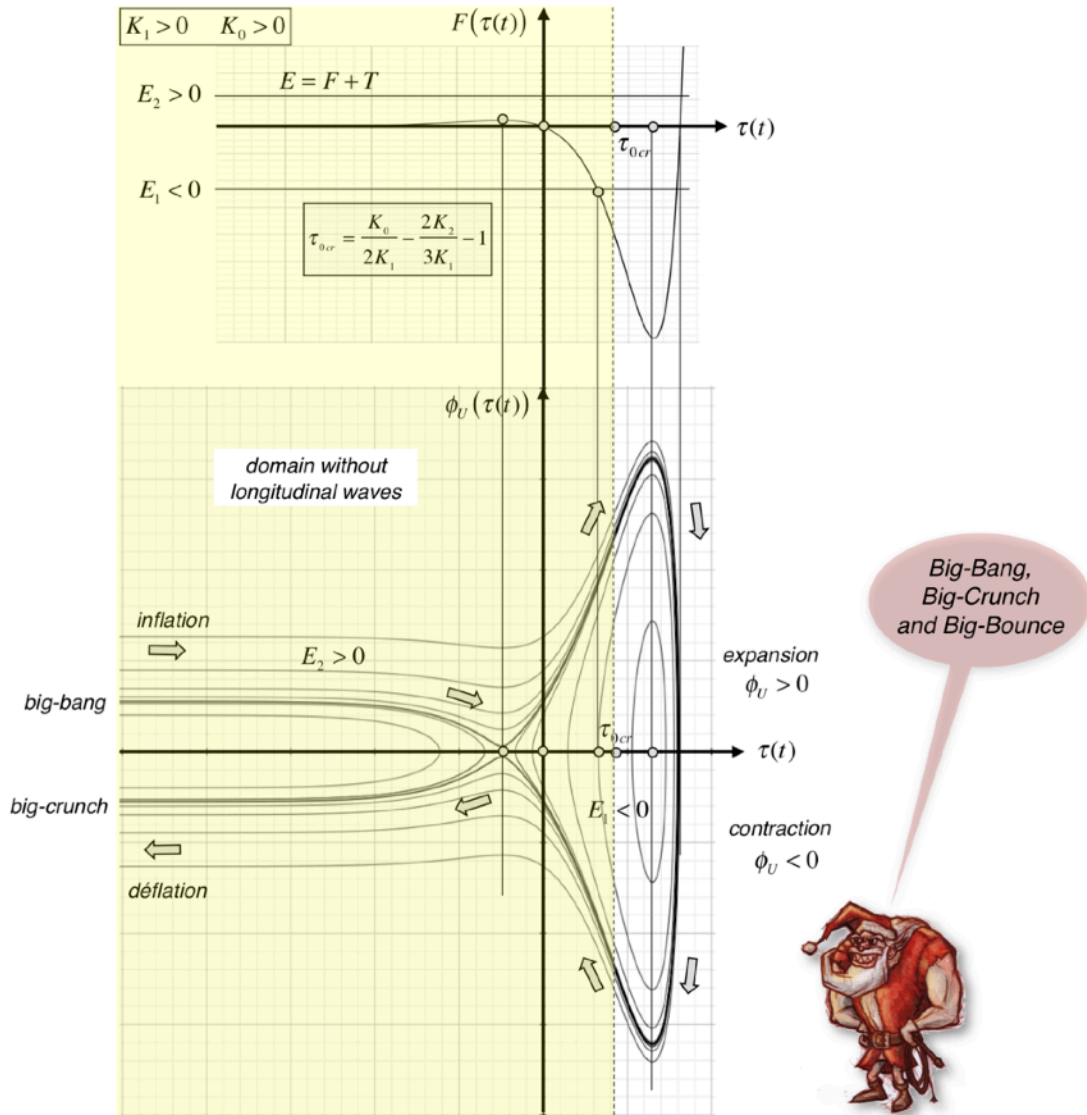


Figure 3.7 - «cosmological behaviour» of the elastic energy $F^{el}(\tau)$ of expansion and of the velocity $\bar{\phi}_U(\tau)$ of expansion of a cosmological lattice with $K_0 > 0$ and $K_1 > 0$

corresponds precisely to the area of big bang, inflation, slowing inflation, followed finally with an acceleration of expansion.

In Figure 3.8, we have reported the eight different behaviors that it is possible to obtain with a cosmological lattice, according to the values that the modules K_0 and K_1 can take. Also shown in this figure are the areas of expansion in which the longitudinal waves cannot exist.

We can see that there are *four really different "cosmological behaviors"*, three of which have much more convincing analogies with what we know about the cosmology of the real Universe:

- the cosmological lattices with $K_1 < 0$ which are shown in figures 3.8 (a), (c) and (d). These three types of lattices show a big bang followed by high-speed inflation, a slowdown in inflation and finally an expansion at increasing speed towards $\tau \rightarrow +\infty$, stages which follow one another in perfect order. The disappearance of longitudinal waves occurs in these lattices for expansions greater than a critical value τ_{0cr} which depends on the value of the shear modulus

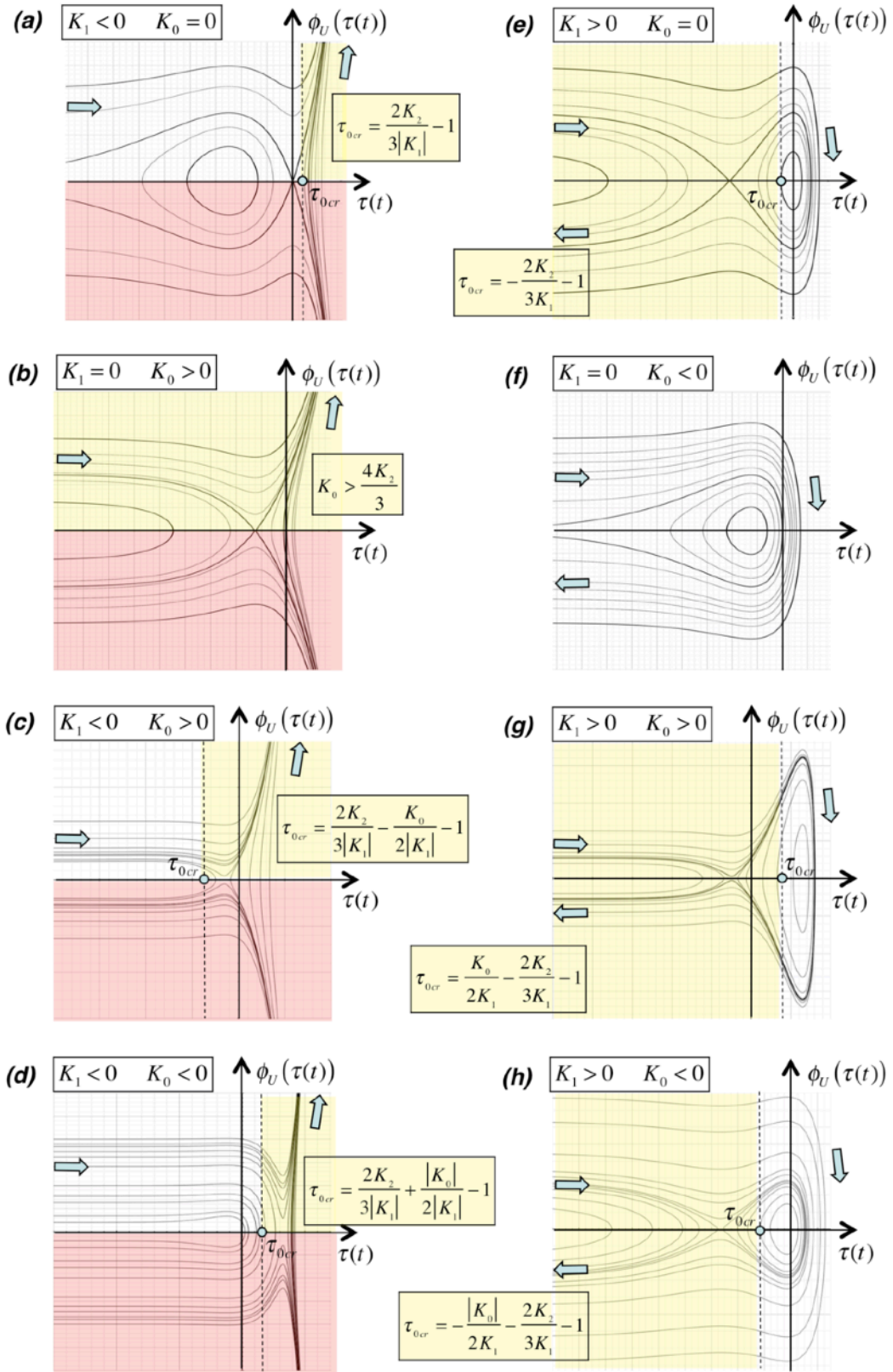


Figure 3.8 - All the possible cosmological behaviours of a cosmological lattice, according to the values of K_0 and K_1 : from (a) to (d) the solids with an infinite expansion, and from (e) to (h) the solids oscillating from big-bang to big-crunch

$K_2 > 0$,

- the cosmological lattice of figure 3.8 (b), with $K_1 = 0$ and $K_0 > 0$, for which there never exists longitudinal waves provided that $K_0 > 4K_2/3$, which makes it a very simple and very interesting case to describe the cosmological behavior of the real Universe,
- the cosmological lattices with $K_1 > 0$ or $K_1 = 0$ and $K_0 < 0$ which are shown in figures 3.8 (e), (g) and (h). These three types of lattices go well through the four stages of the cosmology of the real Universe, in the absence of longitudinal waves (a “big-bang” starting from a singularity of space-time, followed by a period of very rapid inflation, then a slowdown in inflation, followed by an expansion whose speed seems to increase well over time), before entering a phase of expansion during which the longitudinal waves appear, and which precedes a symmetrical phase of contraction returning to the state of singularity for $\tau \rightarrow -\infty$ (“big-crunch”). In this case, there is indeed a region of the diagram, for $\tau < \tau_{0cr}$, which lies in the domain where there are no longitudinal waves, and in which the lattice is expanding at increasing speed. Note that the lattice in figure 3.8 (g) could be an excellent candidate to describe the cosmological behavior of the real Universe, because all of its elastic moduli are positive,

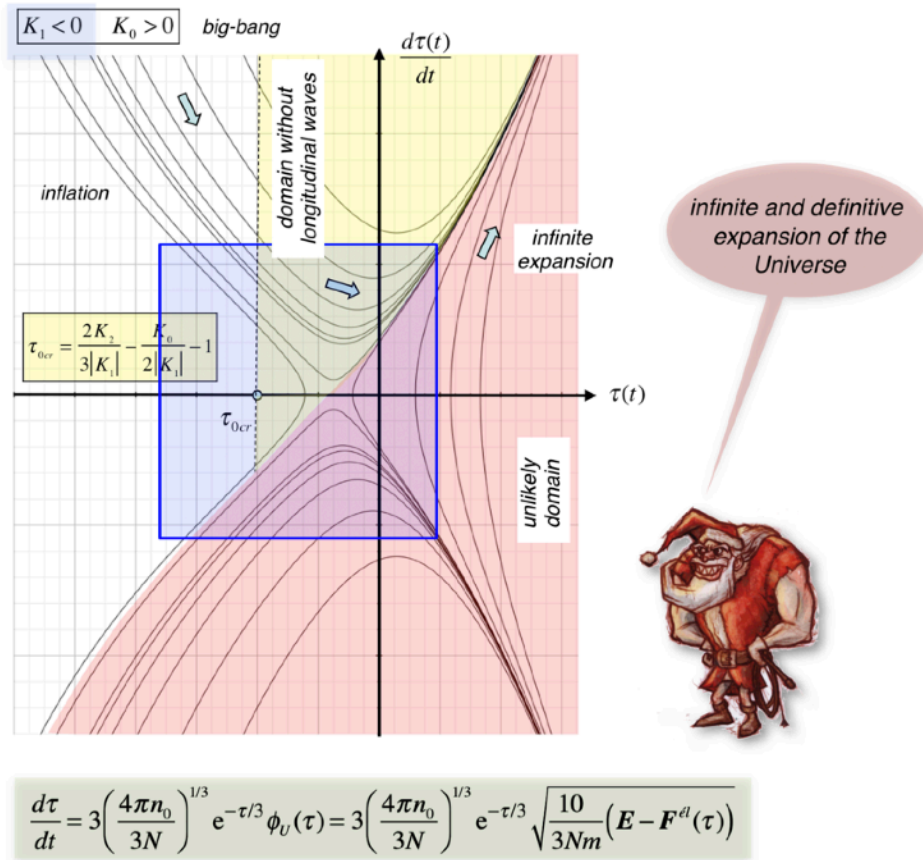


Figure 3.9 - «cosmological behavior» of the speed of cosmological expansion $d\tau / dt$ as a function of τ of an imaginary cosmological lattice with $K_1 < 0$.

- finally, the cosmological lattice of figure 3.8 (f), with $K_1 = 0$ and $K_0 < 0$, does not present the stages corresponding to the cosmological evolution of the real Universe, and it always presents longitudinal waves. It is not able to describe the cosmological behavior of the real Universe.

The “cosmological behavior” of a lattice can be illustrated even more clearly by calculating the speed $d\tau/dt$ of the volume expansion as a function of the volume expansion τ , as shown for case (c) with τ in figure 3.9, and for case (g) with $K_1 > 0$ in figure 3.10. The behavior of the speed $d\tau/dt$ of volume expansion as a function of τ can be deduced from the knowledge of $F^{el}(\tau)$ as shown by the relation reported in figure 3.9.

Figures 3.9 and 3.10 are very interesting, because they clearly show the existence of an initial stage of extremely rapid inflation of volume expansion τ in cosmological lattices since $d\tau/dt \rightarrow \pm\infty$ for $\tau \rightarrow -\infty$, just after the big-bang stage or just before the big-crunch stage, and that the speed of volume expansion or contraction goes through a minimum before accelerating again, just after the inflation stage or just after the re-contraction stage.

It goes without saying that the modeling used here to describe the “cosmological behaviors” of imaginary lattices is extremely simplified, and one could even qualify it as simplistic. In fact, it is essentially the initial hypothesis of a homogeneous volume expansion throughout the lattice that can be questioned, because with this hypothesis we eluded the two major problems which would lead in principle to much more complicated models: the fact that the solid is subjected to the Newtonian dynamics in the absolute space of the **GO**, and the fact that one should in

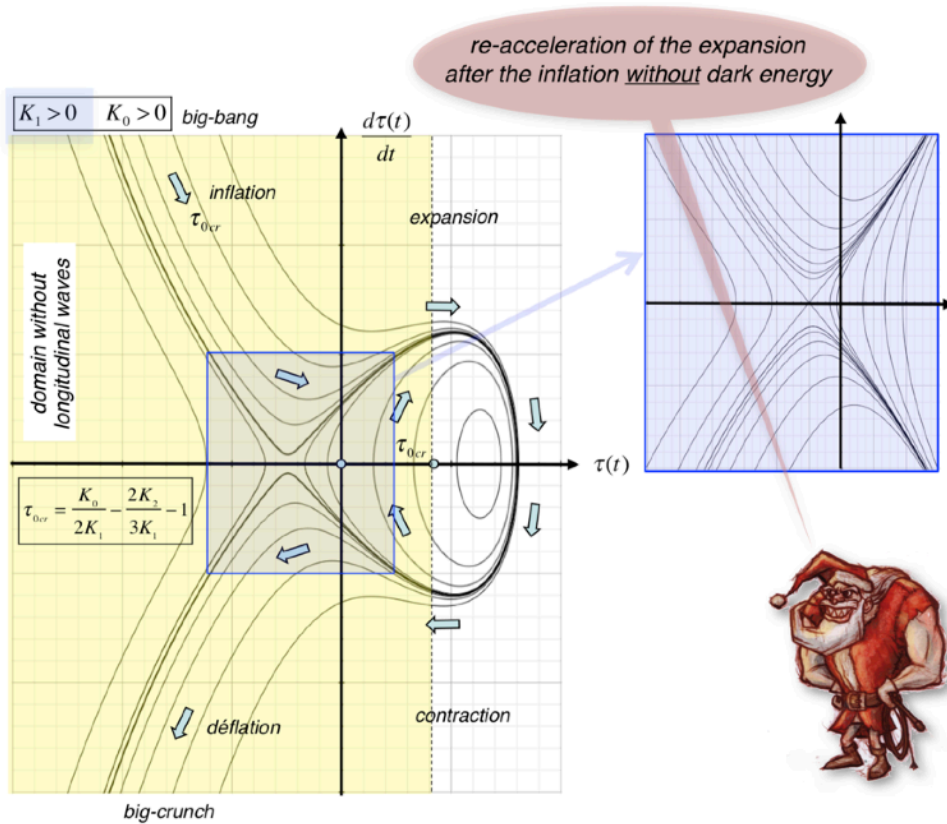


Figure 3.10 - «cosmological behavior» of the speed of cosmological expansion $d\tau/dt$ as a function of τ of an imaginary cosmological lattice with $K_1 > 0$.

principle have placed a condition on the nullity of the pressure at the external limit of the solid. But despite the extreme simplifications of our modeling, the global behaviors predicted in figures 3.8 to 3.10 must still remain fairly close to the behaviors that could have been obtained by a more realistic treatment of the problem.

It is obviously not possible to choose here the cosmological lattice which would come closest to the known cosmological evolution of the real Universe. But from a philosophical point of view and from a common sense point of view, the cosmological lattices of figures 3.8 (e) to (h), which present a big-bang followed by a big crunch, and therefore ultimately a big- bounce seem much more satisfactory for a Cartesian spirit than the lattices of figures 3.8 (a) to (d), which present an infinite and unique expansion. We can therefore make a "*philosophical*" conjecture here, shown in figure 3.11.

Conjecture 4 - *it is more "reasonable" for the mind to imagine that K_1 satisfies $K_1 > 0$ so that the expansion of the lattice is not infinite*

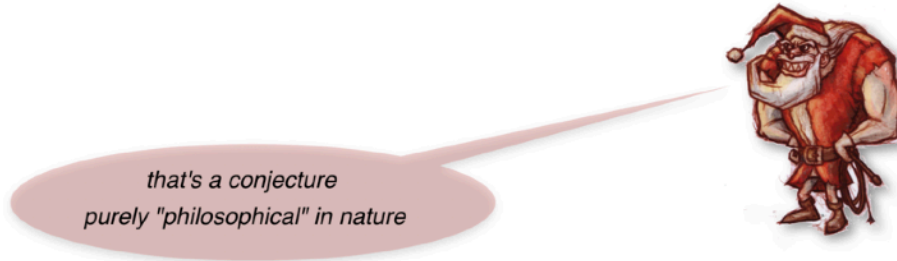


Figure 3.11 - the fourth common sense conjecture

As for the value of K_0 , nothing currently allows us to propose a positive, zero or negative value, because the cases illustrated in Figures 3.8 (e), (g) and (h) are all three very interesting.

Note also that the elastic energy $F^{el}(\tau)$ contained in the cosmological lattice could well correspond to the famous "*dark energy*" of the astrophysicists, introduced to explain the increase in the speed of the expansion of the Universe recently observed experimentally, since it is this elastic energy which is entirely responsible for the increase in the speed of the volume expansion via the relation reported in figure 3.9.

It is again remarkable to note that these behaviors of the volume expansion of a sphere of cosmological lattice are exclusively due to *the development of the internal energy per unit of volume* which we used for this one. Indeed, if we try to look at what would happen in the case of a perfect solid for which the internal energy would be written as a development expressed by lattice site, we would see that the behavior of expansion is radically different like shown in figure 3.12:

- if the modulus k_1 of the imaginary perfect solid is positive, this can only oscillate indefinitely between a state of minimum volume expansion τ_{min} and a state of maximum volume expansion τ_{max} , as illustrated by the first figure 3.12. If one reports in the diagrams $F^{el}(\tau)$ and $\vec{\phi}_U(\tau)$, the critical value $\tau_{0cr} = 1 + 2k_2 / 3k_1 > 1$ of τ_0 below which there are longitudinal waves in this perfect lattice, one notes that during its "*cosmological evolution*" the solid will pass

alternately from a domain ($\tau \leq \tau_{0cr}$) where there coexist transverse and longitudinal waves, with another domain ($\tau \geq \tau_{0cr}$) where there exist only transverse waves and localized modes of longitudinal vibrations. But in this domain without longitudinal waves, the speed of expansion can only slow down, which is in disagreement with the observations made on the current Universe.

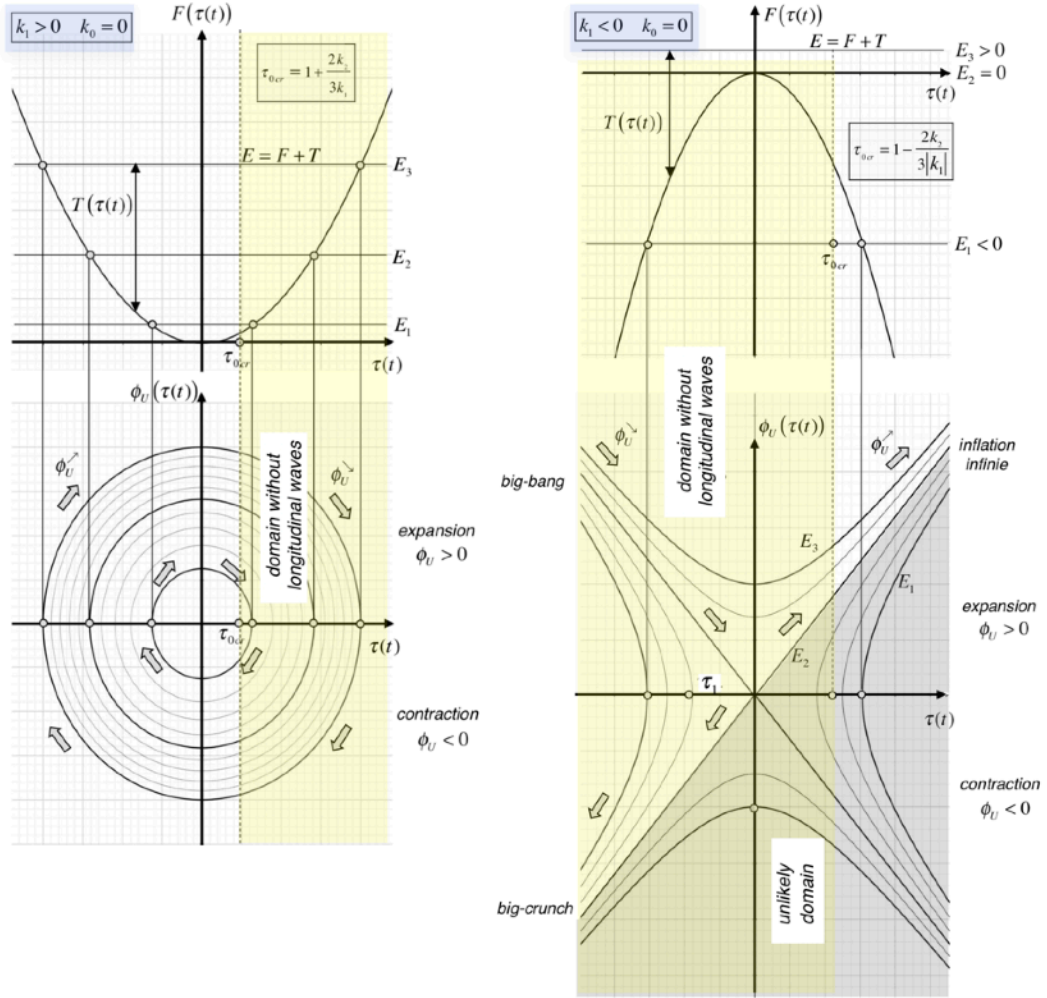


Figure 3.12 - «cosmological behaviors» of the elastic energy $F^{el}(\tau)$ of expansion and of the speed $\vec{\phi}_U(\tau)$ of expansion of an imaginary perfect solid whose internal energy would be written as a developement expressed by lattice site, for $k_1 < 0$ and $k_1 > 0$

- if the modulus k_1 of the imaginary perfect solid is negative, depending on the value of the total energy E , this solid could have several different "cosmological behaviors" as well illustrated by the second figure 3.12. If $E \leq 0$, it can contract and expand in a back and forth movement between $\tau \rightarrow -\infty$ and τ_1 , or then expand indefinitely from $\tau = 0$. Note that it is difficult to imagine a solid that would evolve by contracting since $\tau = \infty$, which is why these behaviors are reported in a gray area. If $E \geq 0$, it can expand indefinitely from $\tau \rightarrow -\infty$. In this

case, the longitudinal waves appear in the domain $\tau \geq \tau_{0cr} = 1 - 2k_2 / 3|k_1| < 1$.

The different "cosmological behaviors" deduced for an imaginary perfect solid can also be compared with the cosmological behavior which is currently attributed to our real Universe. Indeed, in the case of the real universe, we have a system which does not present longitudinal waves, as shown by the theory of general relativity, and which pursues, in the light of the last observations, a cosmological evolution in several stages: a "big-bang" based on a singularity of space-time, followed by a period of very rapid inflation, then a slowdown in inflation, followed, according to very recent experimental observations, by an expansion whose speed seems to increase over time. This last stage is the one that would correspond to the current state of our Universe.

Among the "*cosmological behaviors*" deduced from the *perfect solid*, only the perfect solid with $k_1 < 0$ presents any analogy with the cosmological behavior of the real Universe. Indeed, the perfect solid with $k_1 < 0$, in the case where E is greater than zero (second figure 3.12), traverses well the stages of big bang, inflation, slowing of inflation and expansion at increasing speed in the area where there are no longitudinal waves. But for this solid, the stage of expansion at increasing speed inevitably continues towards $\tau \rightarrow +\infty$, which does not satisfy our fourth conjecture dictated by common sense.

These results in the case of the perfect solid whose internal energy would be written as a development expressed by lattice site are far from satisfactory if we compare them with the known expansion of the universe. This therefore justifies *again* the conjecture 1 that we had posed in figure 3.1, since it is this one which allows the existence of the cosmological behaviors reported in figures 3.7 to 3.10, and especially which allows the existence of the curvature of the wave rays by the volume expansion gradients of figures 3.4 and 3.5.

Chapter 4

Maxwell's equations of electromagnetism

Maxwell's equations are the fundamental laws of electromagnetism formulated at the end of the 19th century by James Clerk Maxwell on the basis of the various theorems of Gauss, Ampère and Faraday which described electric and magnetic phenomena separately before Maxwell unified them. Maxwell's laws govern all classical phenomena related to electric and magnetic fields, and thereby represent one of the most beautiful applications of the concept of fields in physics. But Maxwell's equations of electromagnetism are a postulate deduced from experimental observations, and we admit them because they correspond to the experimental observations.

In this chapter, we theoretically demonstrate the existence of a set of equations to describe the rotations and shear strains of the cosmological lattice in the absence of variations in volume expansion, and we note that there is a complete and perfect analogy between this set of equations and Maxwell's set of equations. This analogy not only demonstrates that it is possible to theoretically deduce the set of these equations on the basis of some fundamental physical principles applied to the cosmological lattice, but it also makes it possible to consider the cosmological lattice as a physical support for the electromagnetic fields, and to give physical interpretations to the various physical quantities of electromagnetism.

We start by showing the separability of the volume expansion field from the other fields in Newton's equation of a cosmological lattice in the case where the concentrations of point defects are constants. Newton's equation can be separated into two parts, a so-called *rotational part* and a so-called *divergent part*.

In the case where the volume expansion field can be considered as quasi-constant, the rotational part then shows a set of equations for the field of macroscopic rotations and local rotations (associated with the shears of the lattice) perfectly identical to the set of *Maxwell's equations of electromagnetism*. This analogy with Maxwell's equations leaves no room for the existence of *magnetic monopoles*, but there is however the possibility of imagining the existence of *vector electric charges*.

Separability of Newton's equation partly «rotational» and partly «divergent»

Suppose that the volume expansion field within a cosmological lattice has a homogeneous background field τ_0 with an elastic expansion field τ^{el} superimposed on it, so that it can be written $\tau = (\tau_0 + \tau^{el})$. Supposing further that the atomic concentrations of vacancies and auto-interstitials are *homogeneous constants* throughout the lattice, and therefore that they do not depend on time ($dC_v/dt = dC_{vi}/dt = 0$), we can write Newton's equation of the lattice under the shape shown in figure 4.1.

Thanks to the hypothesis of homogeneity of the concentrations of vacancies and auto-interstitials, the linearity of the relationships in the various velocities shows that it is possible to

split them into two contributions by separating the speeds $\vec{\phi}$, $\vec{\phi}_L$ and $\vec{\phi}_I$ into a component, indexed "rot", associated with the deformations by shears and rotations on the one hand, and a component, indexed "div", associated with the deformations by volume expansion on the other hand. There thus come two contributions to Newton's equation as shown in figure 4.1:

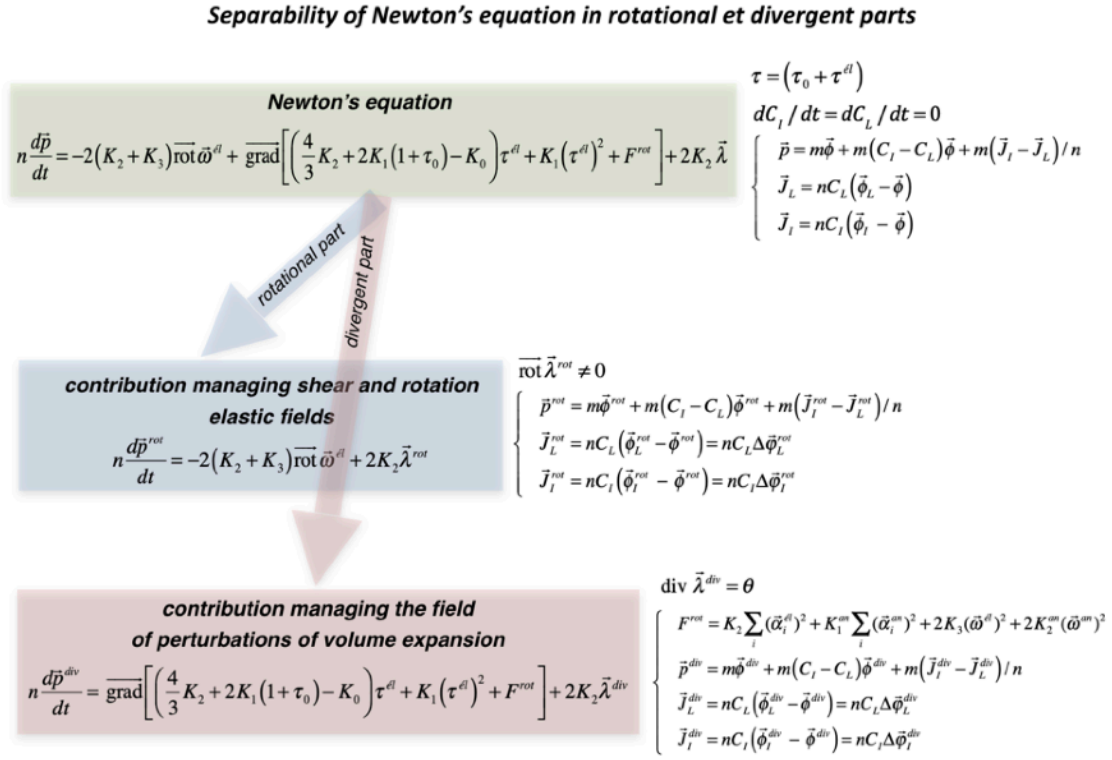


Figure 4.1 - Separability of Newton's equation in rotational and divergent parts under conditions of homogenous concentrations of vacancies and self-interstitials

- a contribution managing the elastic fields of shears and rotation, via the vector field of rotation $\vec{\omega}^{el}$. This contribution only depends on the volume expansion τ by the presence of the site density $n = n_0 e^{-(\tau_0 + \tau^{el})}$,
- a contribution managing the perturbation field of volume expansion, which is dependent on the previous solution via the energy density F^{rot} of deformation by elastic and anelastic shears and rotations.

The density of flexion charges has also been split into two parts: the "rotational" flexion charges and the "divergent" flexion charges, which satisfy two relationships also shown in figure 4.1, and which allow the equation of Newton for expansion τ^{el} to be related to the flexion charge density θ within the lattice.

This splitting of Newton's equation in the case where the concentrations of vacancies and interstitials are homogeneous constants makes it possible to solve the problems of spatio-temporal evolution of the cosmological lattice, by separating the resolution of the elastic fields of shears and rotation of that of the volume expansion field. But as the density of sites

$n = n_0 e^{-(\tau_0 + \tau^{el})}$ intervenes at the same time in the rotational and divergent parts, there exists a certain coupling between the results of the two partial equations of Newton. However, with additional simplifying assumptions, it may be possible to solve these two sets of equations completely independently. This is what we will show in the following, considering the specific case where the volume expansion field can be considered to be quasi-constant.

«Maxwellian» behavior of the rotational part of Newton's equation

Let us now assume that the average value $\langle \tau \rangle = \tau_0 + \langle \tau^{el} \rangle$ of the volume expansion within the cosmological lattice can be considered as a first approximation as constant and homogeneous, so that the density n of sites can also be considered on average as a homogeneous constant. With this hypothesis, Newton's equation is reduced to its purely rotational part.

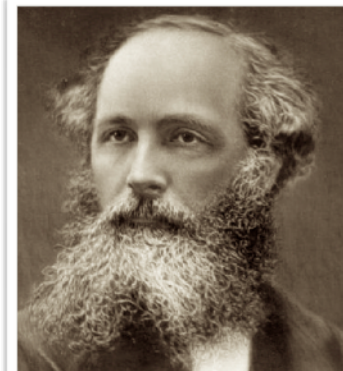
In this case, the torque vector \vec{m} derives from a virtual equation of state, *the virtual volume density of free energy of elastic rotation*, linked to shear deformations and pure elastic rotations, without volume expansions, which is written $F_{rotation}^{el}(\vec{\omega}^{el}) = 2(K_2 + K_3)(\vec{\omega}^{el})^2$. Still by assumption, we will also assume that *the lattice anelasticity* manifests itself only by shear and / or rotation, so that it can very well be represented here by an anelastic rotation vector $\vec{\omega}^{an}$.

The equations necessary for the complete description of the shears and elastic rotations of the cosmological lattice must still incorporate the topological equations for the elastic vector of rotation $\vec{\omega}^{el}$, namely the geometro-kinetic equation and the geometro-compatibility equation in the presence of dislocation charges. As the mass density ρ of inertia of the lattice is a constant $\rho = m(n + n_I - n_L) = mn(1 + C_I - C_L) = cste$, we deduce that $\text{div}(\vec{n}\vec{p}^{rot}) = -\partial\rho/\partial t = 0$. With all these considerations, we can finally deduce the complete set of equations reported in figure 4.2a, which describes the spatio-temporal evolution of the cosmological lattice in the presence of pure shears and local rotations.

The relationships thus obtained for the cosmological lattice in the local frame of reference $\mathcal{O}_{x_1x_2x_3}$ mobile with the medium are then compared with *the Maxwell equations of electromagnetism* (figure 4.2b) in an electrically charged,

conductive, magnetic and dielectric medium. We note that there is a very strong analogy between these two sets of equations, except for the fact that the evolution equations involve in principle the material derivative, while the Maxwell's equations involve the partial derivative with respect to time. However, it should be noted here that the material derivative in a local referential mobile with the medium can be replaced by the time partial derivative if the deformations remain sufficiently weak and / or slow in the vicinity of the origin of the local referential, this that we assumed in the table in figure 4.2a.

The analogy between the equations of a cosmological lattice taken with almost constant and homogeneous volume expansion and the Maxwell's equations of electromagnetism is quite remarkable, because it is absolutely complete, as the equations reported in the tables of figures 4.2a and b. The Maxwell's equations have a precise correspondence with the equations of the



James Clerk Maxwell
(1831-1879)

$$\begin{cases}
-\frac{\partial(2\vec{\omega}^{el})}{\partial t} + \text{rot} \vec{\phi}^{rot} \equiv (2\vec{J}) = \text{geometro-kinetic equation} \\
\text{div}(2\vec{\omega}^{el}) = (2\lambda) = \text{geometro-compatibility equation}
\end{cases}$$

$$\begin{cases}
\frac{\partial(n\vec{p}^{rot})}{\partial t} \equiv -\text{rot}\left(\frac{\vec{m}}{2}\right) + 2K_2 \vec{\lambda}^{rot} = \text{Newton's equation} \\
\text{div}(n\vec{p}^{rot}) = 0 = \text{conservation equation of the mass density}
\end{cases}$$

$$\begin{cases}
(2\vec{\omega}^{el}) = \frac{1}{(K_2 + K_3)} \left(\frac{\vec{m}}{2}\right) + (2\vec{\omega}^{an}) + (2\vec{\omega}_0(t)) = \text{phenomenology of elasticity and anelasticity} \\
(n\vec{p}^{rot}) = (nm) \left[\vec{\phi}^{rot} + (C_i - C_L) \vec{\phi}^{rot} + \left(\frac{1}{n} (\vec{J}_i^{rot} - \vec{J}_L^{rot})\right) \right] = \text{phenomenology of mass transport}
\end{cases}$$

$$\begin{cases}
\frac{\partial(2\lambda)}{\partial t} \equiv -\text{div}(2\vec{J}) = \text{continuity of rotation charges}
\end{cases}$$

$$\begin{cases}
-\left(\frac{\vec{m}}{2}\right)(2\vec{J}) \equiv \\
\vec{\phi}^{rot} \frac{\partial(n\vec{p}^{rot})}{\partial t} + \left(\frac{\vec{m}}{2}\right) \frac{\partial(2\vec{\omega}^{el})}{\partial t} - \text{div} \left(\vec{\phi}^{rot} \wedge \left(\frac{\vec{m}}{2}\right) \right) = \text{equation of energetic balance}
\end{cases}$$

$$\begin{cases}
c_t = \sqrt{\frac{K_2 + K_3}{mn}} = \text{celerity of transverse waves}
\end{cases}$$

Figure 4.2a - «Maxwellian» formulation of evolution equations of the cosmological lattice in a local frame $Ox_1x_2x_3$ mobile with the lattice

rotations in the cosmological network: the Maxwell-Ampère equation corresponds to the geometro-kinetic equation, the Maxwell-Gauss equation to the geometro-compatibility equation, the equation of Maxwell-Faraday to the Newton's equation and finally the Maxwell-Thompson equation to the mass density conservation equation.

In fact, our equations contain an additional term for a "rotational" flexion charge density $\vec{\lambda}^{rot}$ in the second pair of equations, which has no counterpart in Maxwell's equations. Assuming then a cosmological lattice in which $\vec{\lambda}^{rot}$ can be neglected, namely that $\vec{\lambda}^{rot} \approx 0$, the analogy between the equations of the cosmological lattice and the Maxwell's equations becomes perfect, and deserves to be commented on in more detail.

Analogy between rotation charges and electric charges

The equations in tables 4.2a and b show a complete analogy between the density λ of rotation charges and the density ρ of electric charges, which are involved in the geometro-compatibility equation and in the Maxwell-Gauss equation, as well as between the vector flux \vec{J} of rotation charges and the electric current density \vec{j} , which are involved in the geometro-kinetic equation and in the Maxwell-Ampère equation respectively.

$\left\{ \begin{array}{l} -\frac{\partial \vec{D}}{\partial t} + \text{rot } \vec{H} = \vec{j} = \text{equation of Maxwell - Ampère} \\ \text{div } \vec{D} = \rho = \text{equation of Maxwell - Gauss} \end{array} \right.$
$\left\{ \begin{array}{l} \frac{\partial \vec{B}}{\partial t} = -\text{rot } \vec{E} = \text{equation of Maxwell - Faraday} \\ \text{div } \vec{B} = 0 = \text{equation of Maxwell - Thompson} \end{array} \right.$
$\left\{ \begin{array}{l} \vec{D} = \epsilon_0 \vec{E} + \vec{P} + \vec{P}_0(t) = \text{phenomenology of dielectricity} \\ \vec{B} = \mu_0 \left[\vec{H} + (\chi^{\text{para}} + \chi^{\text{dia}}) \vec{H} + \vec{M} \right] = \text{phenomenology of magnetism} \end{array} \right.$
$\left\{ \begin{array}{l} \frac{\partial \rho}{\partial t} = -\text{div } \vec{j} = \text{continuity of electric charges} \end{array} \right.$
$\left\{ \begin{array}{l} -\vec{E} \cdot \vec{j} = \\ \vec{H} \frac{\partial \vec{B}}{\partial t} + \vec{E} \frac{\partial \vec{D}}{\partial t} - \text{div}(\vec{H} \wedge \vec{E}) \end{array} \right. = \text{equation of energetic balance}$
$\left\{ \begin{array}{l} c = \sqrt{\frac{1}{\epsilon_0 \mu_0}} = \text{celerity of light} \end{array} \right.$

Figure 4.2b - «Maxwellian» formulation of the electromagnetism equations

The equation of continuity of the rotation charges is written in these tables considering that the source of rotation charges $S^\lambda = \left[d(\text{div } \vec{\omega}^{\text{el}}) / dt - \text{div}(d\vec{\omega}^{\text{el}} / dt) \right]$ described in figure 2.5 is zero ($S^\lambda = 0$), and it then corresponds to the equation of continuity of the electric charges when it is assumed the absence of creation and annihilation of electric charges. We immediately imagine that there is certainly a link between the source S^λ of rotation charges due to the non-commutation of the operators of time and space, and the phenomena of creation-annihilation of electric charges.

Analogy between anelasticity of the lattice and dielectricity of the matter

The phenomenon of anelasticity introduced here by the term $2\vec{\omega}^{\text{an}}$ becomes, in comparison with Maxwell's equations of electromagnetism, the analog of dielectric polarization \vec{P} in the relation $\vec{D} = \epsilon_0 \vec{E} + \vec{P} + \vec{P}_0(t)$, giving the electric displacement \vec{D} according to the electric field \vec{E} and the polarization \vec{P} of matter. This analogy between the fields $2\vec{\omega}^{\text{an}}$ and \vec{P} is very strong since the possible phenomenological behaviors of these two quantities are completely similar, with in both cases relaxation, resonant or hysteretic behaviors described in

detail in the book¹. For example, in the case of pure relaxation, it is possible to link $\vec{\omega}$ to \vec{m} via a complex modulus, just as it is possible to link \vec{D} to \vec{E} via a complex dielectric coefficient in electromagnetism. In fact, a closer comparison would even show that the behaviors associated with thermal activation, and therefore temperature, also present analogies.

As for the term of homogeneous dielectric polarization $\vec{P}_0(t)$ that we have introduced here, it is analogous to a term of global rotation $2\vec{\omega}_0(t)$ of the lattice, therefore of the local frame in the absolute referential of the **GO**. This term of analogy therefore disappears if the local coordinate system $Ox_1x_2x_3$ is only in translation $\vec{\phi}_O(t)$ with respect to the absolute referential.

Analogy between mass transport in the lattice and magnetism in the matter

As the quantity $n\vec{p}^{rot}$ represents both the average momentum per unit volume of the solid and the average mass flow within the solid, we deduce that the mass flow within the solid is due both to a mass transport $nm\vec{\phi}^{rot}$ at velocity $\vec{\phi}^{rot}$ by the movement of the lattice, to a mass transport $nm(C_I - C_L)\vec{\phi}^{rot}$ at velocity $\vec{\phi}^{rot}$ by the driving movement of point defects by the lattice and to a mass transport $m(\vec{J}_I^{rot} - \vec{J}_L^{rot})$ due to the phenomenon of self-diffusion of vacancies and interstitials.

Each of these mass transports has an analog in Maxwell's equations of electromagnetism. Mass transport $nm\vec{\phi}^{rot}$ via the lattice is analogous to the basic term $\mu_0\vec{H}$ of *magnetic induction* in the vacuum. The mass transport $nm(C_I - C_L)\vec{\phi}^{rot}$ by entrainment of point defects by the lattice corresponds perfectly to the term $\mu_0(\chi^{para} + \chi^{dia})\vec{H}$ of magnetism, in which the magnetic susceptibility consists of two parts: the positive paramagnetic susceptibility χ^{para} , which therefore becomes the analog of the concentration of interstitials, and the negative diamagnetic susceptibility χ^{dia} , which is therefore analogous to the concentration of vacancies.

As for the phenomenon of self-diffusion by vacancies and interstitials, it appears in these equations by the term $n\vec{p}_{auto-diffusion}^{rot} = m(\vec{J}_I^{rot} - \vec{J}_L^{rot}) = mn(C_I\Delta\vec{\phi}_I^{rot} - C_L\Delta\vec{\phi}_L^{rot})$ connecting the last part of $n\vec{p}^{rot}$ to the velocities $\Delta\vec{\phi}_L^{rot}$ and $\Delta\vec{\phi}_I^{rot}$ of self-diffusion of point defects.

The term $(\vec{J}_I^{rot} - \vec{J}_L^{rot})/n = C_I\Delta\vec{\phi}_I^{rot} - C_L\Delta\vec{\phi}_L^{rot}$ associated with this mass transport by self-diffusion of point defects becomes, in comparison with Maxwell's equations of electromagnetism, the perfect analogue of the magnetization \vec{M} of matter in the relation giving magnetic induction \vec{B} . The analogy between the fields $C_I\Delta\vec{\phi}_I^{rot} - C_L\Delta\vec{\phi}_L^{rot}$ and \vec{M} is very strong since there are similar phenomenological behaviors of these two quantities, like relaxation behaviors described in the book¹, which derive from transport equations and which implicitly assume that the self-diffusion processes are of Markovian type, therefore that they do not depend on history, that is to say on the previous transport processes, which is the case of usual solids.

But nothing precludes a priori from imagining solid lattices for which the transport processes would not be of the Markovian type. As an example, we can imagine a hypothetical lattice in which the vacancies are very strongly anchored in the lattice, while the interstitials are almost

¹ G. Gremaud, "Théorie eulérienne des milieux déformables – charges de dislocation et désinclinaison dans les solides", Presses polytechniques et universitaires romandes (PPUR), Lausanne (Switzerland) 2013, 751 pages, ISBN 978-2-88074-964-4

G. Gremaud, "Eulerian theory of newtonian deformable lattices – dislocation and disclination charges in solids", Amazon, Charleston (USA) 2016, 312 pages, ISBN 978-2-8399-1943-2

free to move there. The momentum $n\vec{p}^{rot}$ within the solid would then be written $n\vec{p}^{rot} = nm\left[\vec{\phi}^{rot} + (C_I - C_L)\vec{\phi}^{rot} + C_I\Delta\vec{\phi}_I^{rot}\right]$, and the mass transport $n\vec{p}^{rot}$ would now contain a term $(2C_I - C_L)\vec{\phi}^{rot}$ associated with both the vacancies and the interstitials, whose coefficient $(2C_I - C_L)$ is analogous to magnetic susceptibility χ in electromagnetism, and which can take a positive or negative value depending on concentrations C_I and C_L of point defects. It would also contain the term $nmC_I\Delta\vec{\phi}_I^{rot}$ associated with a mass transport by inertial conservative movement of interstitials, perfectly analogous to the permanent magnetization \vec{M} of ferromagnetic and antiferromagnetic materials in electromagnetism.

The presence of a constant term $nmC_I\Delta\vec{\phi}_I^{rot}$ in $n\vec{p}^{rot}$ would then correspond very clearly to a non-Markovian type process, since the value of $\Delta\vec{\phi}_I^{rot}$ must essentially depend on the history of this hypothetical solid lattice. One could imagine for example that the movement of the interstitials is controlled by a dry type friction with the lattice, in which case there would exist a critical force of depinning of the interstitials, which would lead to the appearance of hysteresis cycles of $\Delta\vec{\phi}_I^{rot}(t)$ depending on $\Delta\vec{\phi}_I^{rot}(t)$, absolutely analogous to the hysteresis cycles of magnetization $\vec{M}(t)$ as a function of the magnetic field $\vec{H}(t)$ observed in ferromagnetic or antiferromagnetic materials.

The complete analogy with the physical quantities of the electromagnetism theory

The analogy reported in the tables of figures 4.2a and b between the equations of a cosmological lattice taken with almost constant and homogeneous volume expansion and the Maxwell's equations of electromagnetism is quite remarkable, because it is absolutely complete, and it also calls upon very similar relaxation and hysteretic processes in the two systems. The complete analogy which exists between the physical quantities of our approach and the electromagnetic quantities of Maxwell's approach of electromagnetism can be reported in tables of figures 4.3a and b.

The effects of volume expansion of the lattice in the absolute frame of GO

In this analogy, the existence of a uniform translation at non-zero velocity $\vec{\phi}_O(t)$ of the lattice, therefore of the local frame $Ox_1x_2x_3$ of reference with respect to the absolute frame $Q\xi_1\xi_2\xi_3$ of reference of **GO**, would have for analogy, in Maxwell's equations, a homogeneous magnetic field $\vec{H}_0(t)$ in space. This last remark implies that, if a solid lattice was expanding in the absolute frame of **GO** there should appear a field $\vec{\phi}_O(t)$ in the local frames $Ox_1x_2x_3$. This field $\vec{\phi}_O(t)$ should have for analogous a *locally homogeneous magnetic field* $\vec{H}_0(t)$ in space if the Universe was in expansion, and which would point in the direction of the movement of the local frame of reference of the observer compared to the absolute space.

Are there "magnetic monopoles" in this analogy?

The equation $\text{div}(n\vec{p}^{rot}) = 0$ reflects the fact that we consider a solid with a uniform and static volume expansion field. The existence of a non-zero and constant value of $\text{div}(n\vec{p}^{rot})$, such that $\text{div}(n\vec{p}^{rot}) = \text{div}\left[mn(1 + C_I - C_L)\vec{\phi}^{rot} \right] + \text{div}\left[m(\vec{J}_I^{rot} - \vec{J}_L^{rot}) \right] \neq 0$ would imply that there is a constant and divergent field of velocity $\vec{\phi}^{rot}$ of the lattice sites, and therefore, with the

$\left\{ \begin{array}{l} 2\vec{\omega}^{el} = \text{field of local elastic rotation} \\ n\vec{p}^{rot} = \text{field of rotational momentum density} \\ \vec{m}/2 = \text{field of rotation torque} \\ \vec{\phi}^{rot} = \text{field of rotational velocity} \end{array} \right.$
$\left\{ \begin{array}{l} 2\vec{J} = \text{flux of rotation charges (loops of twist disclinations)} \\ 2\lambda = \text{density of rotation charges} \\ \vec{\lambda}^{rot} = \text{density of rotational flexion charges} \end{array} \right.$
$\left\{ \begin{array}{l} 1/(K_2 + K_3) = \text{compliance shear and rotation module} \\ nm = \text{density of mass of the lattice} \end{array} \right.$
$\left\{ \begin{array}{l} 2\vec{\omega}^{an} = \text{field of local anelastic rotation} \\ (C_I - C_L) = \text{atomic concentrations of vacancies and interstitials} \\ (\vec{J}_I^{rot} - \vec{J}_L^{rot})/n = \text{flux of vacancies and interstitials} \end{array} \right.$
$\left\{ \begin{array}{l} \vec{\phi}^{rot} \wedge \vec{m}/2 = \text{Poynting's vector} \\ c_t = \sqrt{(K_2 + K_3)/mn} = \text{celerity of transverse waves} \end{array} \right.$

Figure 4.3a - Complete analogy between **the physical quantities of the cosmological lattice** and the electromagnetic quantities of the Maxwell's equations

assumption that $\tau = cste$, a non-zero source S_n of lattice sites, or that there would be a constant and divergent flow of self-diffusion $m(\vec{J}_I^{rot} - \vec{J}_L^{rot})$, which would necessarily require localized and non-zero sources of point defects S_L^{pl} and I or S_I^{pl} , which is very difficult to imagine.

Within the framework of the analogy with electromagnetism, a relation $\text{div}(n\vec{p}^{rot}) = cste \neq 0$ would have for analogy the relation $\text{div}\vec{B} = cste \neq 0$. However, this last relation reveals the well-known notion of *magnetic monopoles*, of *particles of unipolar magnetic charge*, proposed by certain theories, but never observed experimentally. According to our analogy with the cosmological lattice, magnetic monopoles could not be stable particles, but should correspond to localized and continuous sources of lattice sites or point defects, which is particularly difficult to imagine. We deduce from this that in our analogy, the existence of magnetic monopoles as electromagnetically isolated particles is not possible.

Are there "vector electric charges" in this analogy?

One can legitimately wonder what the analogy of the density of "rotational" flexion charges $\vec{\lambda}^{rot}$ could be in Maxwell's equations. If there existed a quantity analogous to $\vec{\lambda}^{rot}$ in Maxwell's

$\left\{ \begin{array}{l} \vec{D} = \text{electric field of displacement} \\ \vec{B} = \text{magnetic field of induction} \\ \vec{E} = \text{electric field} \\ \vec{H} = \text{magnetic field} \end{array} \right.$
$\left\{ \begin{array}{l} \vec{j} = \text{electric flux} \\ \rho = \text{density of scalar electric charges} \\ \vec{\rho} = \text{density of vectorial electric charges} \end{array} \right.$
$\left\{ \begin{array}{l} \epsilon_0 = \text{dielectric permittivity of vacuum} \\ \mu_0 = \text{magnetic permeability of vacuum} \end{array} \right.$
$\left\{ \begin{array}{l} \vec{P} = \text{dielectric polarisation of matter} \\ (\chi^{para} + \chi^{dia}) = \text{paramagnetic and diamagnetic susceptibility of matter} \\ \vec{M} = \text{magnetisation of matter} \end{array} \right.$
$\left\{ \begin{array}{l} \vec{H} \wedge \vec{E} = \text{Poynting's vector} \\ c = \sqrt{1/(\epsilon_0 \mu_0)} = \text{light celerity} \end{array} \right.$

Figure 4.3b - Complete analogy between the physical quantities of the cosmological lattice and the electromagnetic quantities of the Maxwell's equations

equations, we could hypothetically qualify it as the density $\vec{\rho}$ of "vector electric charges" by making the following analogy $\vec{\rho} \Leftrightarrow \vec{\lambda}^{rot}$. Maxwell's equations would then be written a little differently from known equations, with an additional charge term not in the equation $\text{div } \vec{B} = 0$ as suggested by magnetic monopole theories, but in the Maxwell-Faraday equation as follows $\partial \vec{B} / \partial t = -\text{rot } \vec{E} + \kappa \vec{\rho}$, in which κ is a new electrical coefficient, analogous to the module $2K_2$: $\kappa \Leftrightarrow 2K_2$.

In the static case, if such a vector charge really existed, the equation containing it would be written as follows $\text{rot } \vec{E} = \kappa \vec{\rho}$, and would have the analogous equation $\text{rot}(\vec{m}/2) = 2K_2 \vec{\lambda}^{rot}$ in the cosmological lattice. It would therefore imply for the displacement field that $\text{rot } \vec{D} = \epsilon_0 \kappa \vec{\rho}$, so that the density $\vec{\rho}$ of "vector electric charges" would be a source of a rotational electric field \vec{E} and of a rotational electric displacement field \vec{D} , just as the scalar density ρ of electric charges is a source of a divergent electric displacement field \vec{D} by the relation $\text{div } \vec{D} = \rho$. If we now compare the coefficients of the two theories, we obtain, from the analogies $\epsilon_0 \Leftrightarrow 1/(K_2 + K_3)$ and $\kappa \Leftrightarrow 2K_2$, that there is the following analogy $\epsilon_0 \kappa \Leftrightarrow 2K_2/(K_2 + K_3)$ between the coefficients of the two theories.

However, experimental observations have never revealed the existence of such "vectorial

electric charges". In fact, this can be explained quite simply by the fact that the topological singularities considered in the cosmological lattice will always be exclusively twist disclination loops, edge dislocation prismatic loops and mixed dislocation glide loops, and in the case of such loops, it is easy to see that the overall vectorial charge $\vec{q}_{\vec{\lambda}}$ obtained by integrating the linear flexion charge $\vec{\Lambda}$ on the contour of the loop is zero, so that the vectorial electric charge density $\vec{\rho}$ obtained as the average value of the sum of all the vectorial charges $\vec{q}_{\vec{\lambda}}$ contained per unit volume is necessarily zero, so that $\vec{\rho} = 0$. We can therefore introduce here a new conjecture for our approach, namely:

Conjecture 5 - *There are no localized electrical vector charges $\vec{q}_{\vec{\lambda}}$ in the cosmological lattice, so that the charge density $\vec{\rho}$ of vectorial electrical charges is necessarily zero in Maxwell's equations:*

$$\vec{\rho} = 0$$

no experimental observation of
vector electric charges



Figure 4.4 - *The fifth conjecture that concludes to the non-existence of "vector electrical charges"*

Note that there could perhaps be long "strings" of edge dislocation that would cross the entire cosmological lattice and that would indeed have a linear density $\vec{\Lambda}$ of vector electric charge, which would then effectively cause a non-zero density $\vec{\rho}$ of vector electric charge to appear in Maxwell's equations. But this is a somewhat extravagant hypothesis.

The importance of this analogy

In fact, the existence of an analogy between two theories is always very fruitful in physics, by the reciprocal contribution of each of the theories. In our case, it is clear that this analogy with the theory of electromagnetic fields will allow us in the following to use for the description of a lattice all the arsenal of theoretical tools developed since a very long time in field theory, such as for example the Lorentz transformation or the theory of delayed potentials.

In the other sense, the approach developed here is in fact a much more complex theory than classical electromagnetism, since it follows from a tensor theory which can be reduced to a vector theory by contraction on the tensor indices, and moreover, by choosing particular "restrained" cases of behavior of the solid lattice, such as the constancy and the homogeneity of the volume expansion. By taking into account the tensorial aspect of the theory of solid lattices and by renouncing to the "clamping" of the behaviors of these, the analogy will become particularly interesting and fruitful, as we will see later.

Chapter 5

Topological singularities within the cosmological lattice

Newton's equation can also be separated differently into *two partial Newton's equations* which allow on the one hand to calculate the elastic distortion fields associated with the topological singularities contained in the lattice, and on the other hand to calculate the perturbations of the volume expansion associated with the elastic distortion energies of these topological singularities. Using Newton's first partial equation, we can then describe the elastic distortion fields and energies of topological singularities within a cosmological lattice. It is thus possible to find conditions on the elastic modules of this lattice such that it is possible to attribute in a completely classic way a mass of inertia to the topological singularities, which always satisfies the famous «Einstein's formula» $E_0 = M_0 c^2$.

Separability of Newton's equation in three partial equations in the presence of a topological singularity

Suppose the existence of a localized singularity of dislocation charges of spherical, tubular or membrane shape, containing charge densities $\vec{\lambda}_i$, $\vec{\lambda}$ and / or λ , and suppose that one can neglect the anelasticity and the self-diffusion in the lattice, by assuming that $\vec{\alpha}_i^{an} = \vec{\omega}^{an} = 0$ and that $dC_i/dt = dC_L/dt = 0$. The presence of a localized singularity of dislocation charges can be introduced into this equation by considering that the fields prevailing in the lattice are of three different natures: the elastic fields due to the charges of the singularity, which will be indexed (*ch*), the fields independent of the singularity within the lattice, which are due for example to the other singularities, and which will be indexed (*ext*), the background field τ_0 of the volume expansion of the lattice and finally a perturbation field $\tau^{(p)}$ of the volume expansion due to the energy of distortion F_{dist} stored in the lattice by the elastic fields of the considered singularity. These fields represented in figure 5.1 can be introduced into Newton's equation, which can be developed by judiciously grouping the different terms, and we note that the Newton equation is in fact composed of three coupled equations which manage the different fields prevailing in the lattice, and which we have reported in figure 5.1.

Newton's third partial equation deals with *fields external to the singularity* associated with the velocity $\vec{\phi}^{ext}$. But this Newton's equation is not in fact perfectly independent of the other fields, due to the presence of $n = n_0 \exp\left[-\left(\tau_0 + \tau^{ch} + \tau^{ext} + \tau^{(p)}\right)\right]$ in the expression of the momentum associated with $\vec{\phi}^{ext}$. One can suppose, to simplify the problem of the treatment of the fields specific to the singularity, that the external field τ^{ext} can be regarded as constant, that is to say $\vec{\phi}^{ext} = 0$ and $\tau^{ext} = \tau^{ext}(\vec{r})$, in which case the equation put in its static form becomes perfectly independent of fields τ^{ch} and $\tau^{(p)}$.

As for the fields $\vec{\omega}^{ch}$, τ^{ch} and $\tau^{(p)}$, which are associated with the singularity, they then satisfy two other strongly coupled partial Newton's equations, which we will discuss now.

Separability of the Newton's equation in the presence of topological singularities

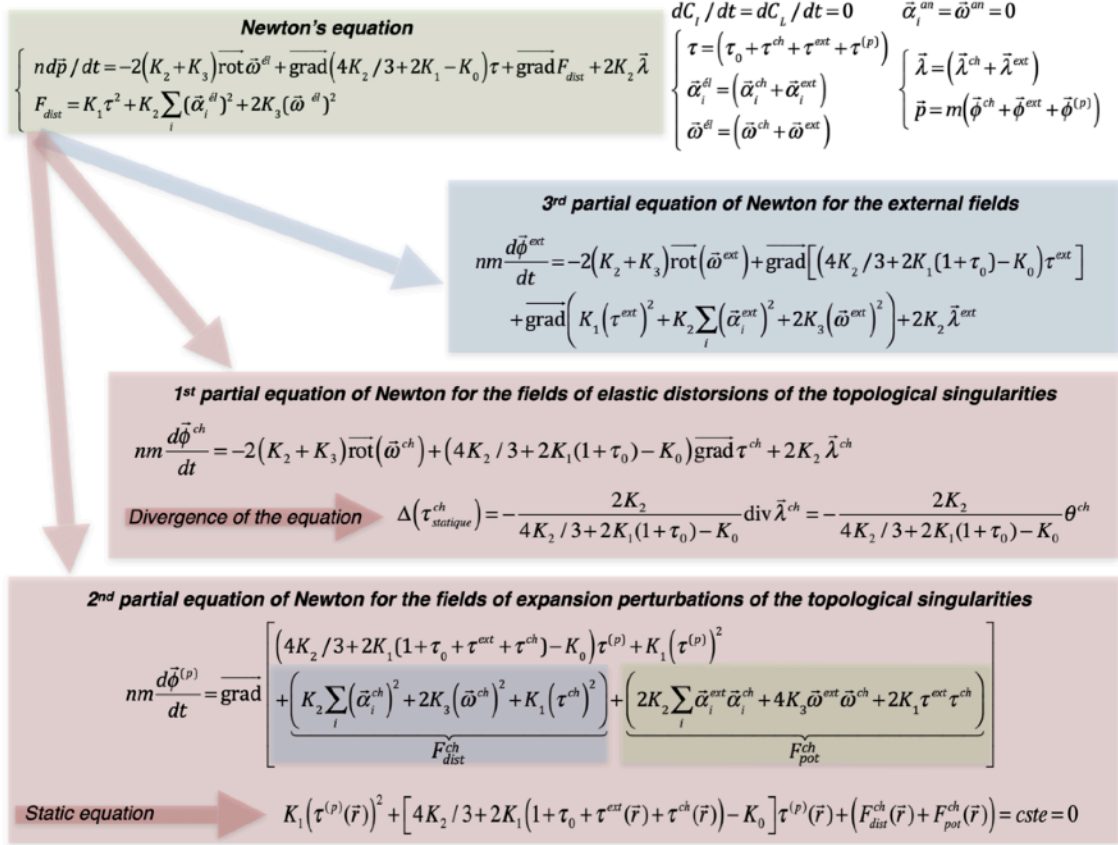


Figure 5.1 - Separability of the Newton's equation in three partial equations in the presence of topological singularities

Newton's first partial equation is concerned with the fields of elastic distortions $\vec{\omega}^{ch}$ and τ^{ch} associated with the charges contained in the singularity. This equation is coupled to the fields τ^{ext} and $\tau^{(p)}$ by the value $n = n_0 \exp \left[-(\tau_0 + \tau^{ch} + \tau^{ext} + \tau^{(p)}) \right]$ appearing in the expression of the momentum associated with $\vec{\phi}^{ch}$. In the static case, this coupling disappears, so that it makes it possible to deduce the static fields of elastic distortions $\vec{\omega}^{ch}$ and τ^{ch} generated by the topological singularity in a completely independent way from the fields τ^{ext} and $\tau^{(p)}$.

One notes also that this first partial equation of Newton depends on the density $\vec{\lambda}^{ch}$ of flexion charges of the singularity. The divergence of this equation in its static form then provides a static equation depending on the density θ^{ch} of curvature charges of the singularity, since the divergence of the density $\vec{\lambda}^{ch}$ of flexion charges is equal to the density θ^{ch} of curvature charges of the singularity, which is also shown in figure 5.1.

The second partial Newton's equation which can be extracted deals with the problem of the perturbations $\tau^{(p)}$ of the expansion field by the elastic energy stored in the lattice by the singularity. It is clear that this last equation is very strongly coupled to the fields $\vec{\omega}^{ext}$, τ^{ext} , $\vec{\omega}^{ch}$ and τ^{ch} deduced from the two other Newton's equations. First, there is a dynamic coupling via the term $n = n_0 \exp \left[-(\tau_0 + \tau^{ch} + \tau^{ext} + \tau^{(p)}) \right]$ appearing in the expression of the momentum associated with $\vec{\phi}^{(p)}$. There also appears a coupling term associated with the module K_1 in the form $2K_1(1 + \tau_0 + \tau^{ext} + \tau^{ch})$. But the main coupling terms are those due to the elastic energy

of the singularity and to the coupling energy of the singularity with the external fields, which appear in two particular contributions which have very precise meanings:

- the density of elastic energy F_{dist}^{ch} stored in the lattice by the elastic fields due to the singularity, in other words the energy density of distortion of the singularity,
- the energy density F_{pot}^{ch} of coupling of the singularity with the external fields, in other words the potential energy density of the singularity.

These two terms $F_{dist}^{ch}(\vec{r}, t)$ and $F_{pot}^{ch}(\vec{r}, t)$ are obtained by solving the first partial equation and the third partial equation. In the static case, if we have solved these two equations taken in the static state, and we therefore know the equilibrium values of the fields $\vec{\omega}^{ext}(\vec{r})$, $\tau^{ext}(\vec{r})$, $\vec{\omega}^{ch}(\vec{r})$ and $\tau^{ch}(\vec{r})$, the second partial equation becomes an equilibrium equation for the static field of perturbation whose solution is an equation of the second degree in $\tau^{(p)}(\vec{r})$, which is also reported in figure 5.1. The constant *cste* was introduced when passing from the gradient to the gradient argument. However, as $\tau^{(p)}(\vec{r})$ must necessarily be identically zero if the energy $F_{dist}^{ch}(\vec{r}) + F_{pot}^{ch}(\vec{r})$ is zero, this constant can only be zero.

Applications and potentialities of the separability of Newton's equation

The decomposition of Newton's equation into three partial equations that we have just presented reveals a partial equation (the 3rd) for the external fields, a partial equation (the 1st) for the elastic distortion fields associated with the presence of a topological singularity and a partial equation (the 2nd) for the expansion perturbation fields due to the elastic distortion energies associated with the topological singularity. The methodology to be used to solve the problem of fields associated with a topological singularity is then the following:

- in a first step, we must independently solve the first partial Newton's equation, in order to find the elastic distortion fields $\vec{\omega}^{ch}$ and τ^{ch} generated by the singularity, without taking into account the expansion perturbations due to energies $F_{dist}^{ch}(\vec{r}, t)$ and $F_{pot}^{ch}(\vec{r}, t)$ of the singularity,
- then, starting from the elastic fields $\vec{\omega}^{ch}$ and τ^{ch} obtained previously by the first partial Newton's equation, the additional perturbations $\tau^{(p)}(\vec{r}, t)$ of the expansion field due to the elastic energies $F_{dist}^{ch}(\vec{r}, t)$ and $F_{pot}^{ch}(\vec{r}, t)$ of the singularity are calculated using the second partial equation, or using the second degree equation in the static case.

At first glance this process seems quite complex, but it contains enormous potential with regard to the description and interpretation of the behaviors of topological singularities within the cosmological lattice. Indeed, we will show in the following that it becomes possible to deal with the following themes:

- the existing link between the "first partial Newton equation" for elastic distortion fields and Einstein's Special Relativity: the first partial Newton equation allowing to find the elastic distortion fields associated with topological singularities will allow us to calculate the fields and energies associated with screw dislocations, edge dislocations, screw dislocation loops, edge dislocation loops and mixed dislocation loops, and to show that these fields are subject to a relativistic dynamic, which will lead us to discuss the "ether role" that the cosmological lattice plays with respect to topological singularities, as well as analogies and differences with Einstein's Special Relativity.
- the link between Newton's second partial equation for expansion perturbation fields and Einstein's General Relativity and Quantum Physics: Newton's second partial equation for finding

the associated volume expansion perturbations is also very important. Indeed, we will see that this one, if applied to macroscopic clusters of singularities with a rather low mass density, leads to the existence of a static volume expansion field, which is deduced from Newton's second partial equation in its static form, and which allows to find the gravitational effects, and to discuss the analogies and differences of our approach with Newton's Gravitation, Einstein's General Relativity and the Modern Cosmology of the Universe. Then we will also see that this partial equation, if applied to microscopic singularities of high mass density, cannot present static solutions and must therefore be solved in its dynamic form, which allows us to find Quantum Physics, and to discuss the analogies and differences with Schrödinger's equations, the concepts of fermions and bosons, Heisenberg's uncertainty and Pauli's exclusion principles, and the notions of spin and magnetic moment of elementary particles.

The fact that the mass density of clusters of singularities plays a considerable role in the resolution of the second partial Newton equation in static or dynamic form is quite remarkable, as this will provide *an objective criterion for quantifying the quantum decoherence phenomenon which is the basis for a realistic explanation of the quantum phenomenon.*

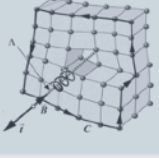
Elastic energy, kinetic energy and inertial mass of a dislocation

It is possible to calculate the distortion energy and the kinetic energy of a dislocation string in the cosmological lattice. The distortion energy is obtained by calculating the lattice distortions associated with the presence of the dislocation and by summing the elastic energy due to these distortions in the whole lattice. Similarly, the kinetic energy associated with the movement of a dislocation moving at low velocity \vec{V} compared to the celerity c_t of the transverse waves is obtained by calculating the velocities of all the points of the lattice associated with the movement of the dislocation and by summing the kinetic energy which is associated with these movements in the whole lattice. If these calculations are easy enough to do in the case of a screw dislocation, they become very difficult in the case of an edge dislocation. We will not dwell on it here and will give the results obtained in the cosmological lattice in figure 5.2. These complete calculations can be found in the theoretical book «*Universe and Matter conjectured as a 3-dimensional Lattice with Topological Singularities*» published in 2016.

In these relations, we note that the elastic and kinetic energies depend on the proper dimensions of the cosmological lattice, via the expression $\ln(R_\infty/a)$, in which R_∞ is *the external dimension of the cosmological lattice* and a is *the step of the cosmological lattice*, with obviously $R_\infty \gg a$. These energies also depend on the squares Λ^2 and $\bar{\Lambda}^2$ of the linear densities of charges of the screw and edge dislocations respectively.


By comparing the kinetic energy E_{cin}^{screw} stored in the lattice by the movement of the line of screw dislocation with the elastic potential energy E_{dist}^{screw} stored in the lattice by the presence of this same line, one finds the famous *expression of Einstein* $E_{dist}^{screw} = M_0^{screw} c_t^2$ *connecting the mass of inertia to the rest energy of the dislocation via the celerity of the transverse waves.* But this relation is found here *without in any way calling upon a relativistic dynamic of the line*, because it is due to the fact that the rest energy and the kinetic energy are nothing other than elastic potential energy (of shear and local rotation) and kinetic energy stored within the lattice by the dynamic deformation imposed on this lattice by the elastic distortion fields (shear and local rotation) of the mobile screw dislocation.

Screw and edge dislocation lines



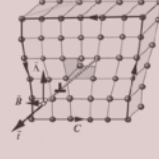
$$\begin{cases} E_{dist}^{screw} = \frac{(K_2 + K_3)\Lambda^2}{\pi} \ln \frac{R_\infty}{a} \\ E_{cin}^{screw} = \frac{mn\Lambda^2}{2\pi} \left(\ln \frac{R_\infty}{a} \right) \mathbf{v}^2 = \frac{1}{2} M_0^{screw} \mathbf{v}^2 \end{cases}$$

screw dislocation line



edge dislocation line

$$M_0^{screw} = \frac{E_{dist}^{screw}}{c_t^2}$$



$$\begin{cases} E_{dist}^{edge} \equiv \frac{\tilde{\Lambda}^2}{4\pi} \left(\frac{K_2}{K_2 + K_3} \right)^2 \left(\ln \frac{R_\infty}{a} \right) \left\{ K_1 \frac{1}{\mathbb{C}^2} + K_2 \left[4\zeta^2 - 8\zeta + \frac{2}{3} \left(\frac{1 - 3\mathbb{C} + 9\mathbb{C}^2}{\mathbb{C}^2} \right) \right] + 2K_3 \right\} \\ E_{cin}^{edge} \equiv \frac{mn\tilde{\Lambda}^2}{8\pi} \left(\frac{K_2}{K_2 + K_3} \right)^2 \left(\ln \frac{R_\infty}{a} \right) \left\{ 2\zeta^2 - 4\zeta + \frac{1 + 12\mathbb{C}^2}{4\mathbb{C}^2} \right\} \mathbf{v}^2 = \frac{1}{2} M_0^{edge} \mathbf{v}^2 \\ \text{with } \mathbb{C} \equiv \frac{4K_2 + 6K_1(1 + \tau_0) - 3K_0}{6(K_2 + K_3)} \end{cases}$$

$$M_0^{edge} \equiv \left\{ \frac{(K_2 + K_3) \left(2\zeta^2 - 4\zeta + \frac{1 + 12\mathbb{C}^2}{4\mathbb{C}^2} \right)}{K_1 \frac{1}{\mathbb{C}^2} + K_2 \left[4\zeta^2 - 8\zeta + \frac{2}{3} \left(\frac{1 - 3\mathbb{C} + 9\mathbb{C}^2}{\mathbb{C}^2} \right) \right] + 2K_3} \right\} \frac{E_{dist}^{edge}}{c_t^2}$$

Figure 5.2 - Elastic energy, kinetic energy and mass of inertia of a screw dislocation and an edge dislocation in the cosmological lattice

In the case of the edge dislocation, it is very different. It is observed in fact that the resting energy depends in a rather complicated way on the four elastic modules K_0, K_1, K_2, K_3 , in particular via a parameter \mathbb{C} , and that it also appears a parameter ζ which depends in fact on the boundary conditions of the lattice which are used to carry out the computations of energies. Likewise, the relation between the energy of distortion and the mass of inertia of an edge dislocation differs quite strongly from Einstein's relation via the term reported between braces, which depends on the parameter ζ and the modules K_0, K_1, K_2, K_3 , in particular via the module \mathbb{C} .

To ensure a complete analogy between the topological singularities of our approach and the particles of the real universe, it would be desirable that the edge dislocations also exactly satisfy Einstein's relation. However, for an edge dislocation satisfies this relation, the term between braces in the relation between the energy of distortion and the mass of inertia of the edge dislocation must be equal to 1.

Since the lattice under consideration is finite, the conditions at the lattice boundaries are free. We can then show that the value of the parameter ζ is the one that will minimize the distortion energy of the edge dislocation, and this condition implies that $\zeta = 1$. We can then show that, for the edge dislocations to also satisfy Einstein's relation, the modules K_0, K_1, K_2, K_3 must satisfy fairly strict conditions that we will issue in the form of a conjecture, conjecture 6 in figure 5.3, which states that the modules K_0 and K_3 are equal and positive, and modules K_1 and K_2 are also positive (or zero), but much smaller than the modules K_0 and K_3 .

Screw and edge dislocation lines in the perfect cosmological lattice

Conjectures 6 - the «perfect cosmological lattice»
satisfies the following relation ships:

$$\begin{cases} K_0 = K_3 > 0, \\ 0 < K_1 \ll K_0 = K_3 \\ 0 \leq K_2 \ll K_3 = K_0 \end{cases}$$

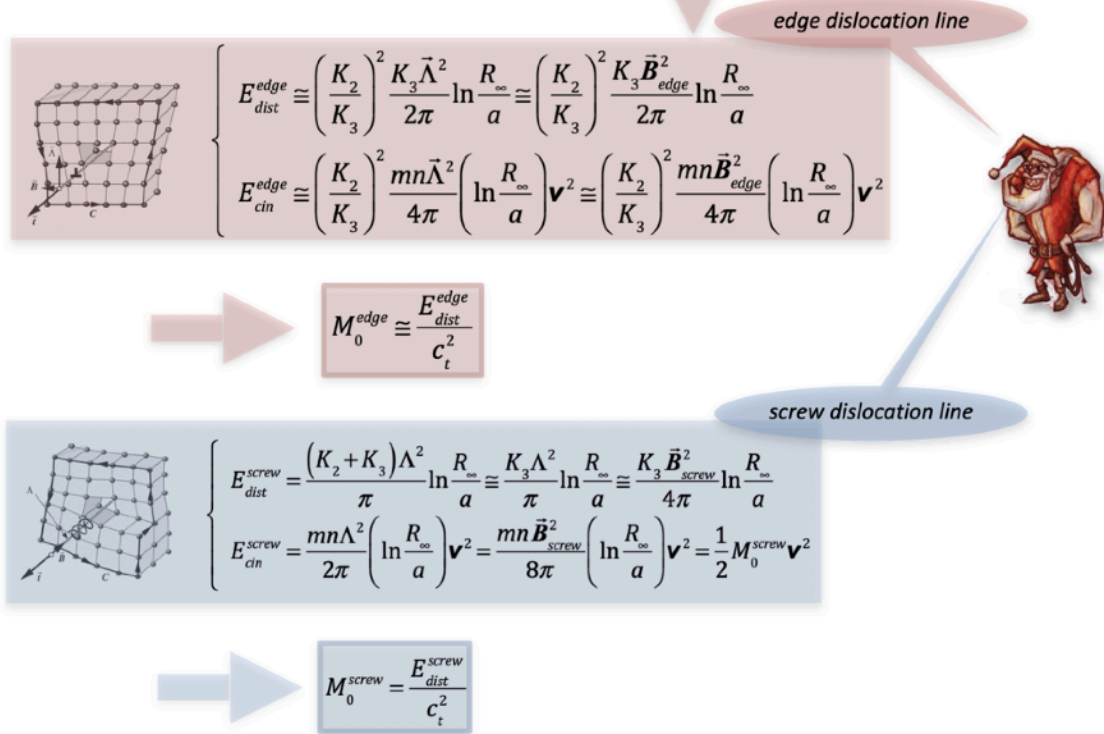


Figure 5.3 - Elastic energy, kinetic energy and mass of inertia
of a screw dislocation and an edge dislocation in the perfect cosmological lattice
satisfying the sixth conjecture

This set of conditions expressed by the sixth conjecture will ensure that the screw and edge dislocations both satisfy real Einstein's relations, which are deduced in a purely classical manner, without making appeal to a principle of special relativity, which are written $M_0^{screw} \cong E_{dist}^{screw} / c_t^2$ and $M_0^{edge} \cong E_{dist}^{edge} / c_t^2$ respectively. The cosmological lattice thus obtained will be qualified as a *perfect cosmological lattice*.

We note that the potential energy and the non-relativistic kinetic energy of an edge dislocation in *the perfect cosmological lattice* are both *extremely weaker* than the potential energy and the non-relativistic kinetic energy of a screw dislocation since, for a screw dislocation and an edge dislocation of Burgers vectors of the same norm $|\vec{B}_{edge}| = |\vec{B}_{screw}|$, we have $E_{dist}^{edge} \equiv 2(K_2/K_3)^2 E_{dist}^{screw} \lll E_{dist}^{screw}$ and $E_{cin}^{edge} \equiv 2(K_2/K_3)^2 E_{cin}^{screw} \lll E_{cin}^{screw}$. We will see later what important role can be attributed, in our analogy with the physical theories of the Universe, to the facts that edge dislocations exactly follow Einstein's relation and that they also present much weaker energies than screw dislocations in a perfect cosmological lattice satisfying the relationships of conjecture 6.

Spherical singularities of rotation and curvature charges

Imagine the existence within a perfect cosmological lattice of a localized macroscopic cluster of topological singularities, in the form of a sphere of radius $R_{cluster}$ containing a uniform density λ of rotation charges, as shown in figure 5.4. It is possible and quite simple to calculate the elastic rotation field $\vec{\omega}^{el}$ associated with this charge, both inside and outside the singularity. Let's introduce the global charge Q_λ given by the integration of the density λ in the volume of the cluster, or given by the sum of the elementary charges $q_{\lambda(i)}$ within the cluster, and the vector \vec{n} which represents the vector normal to the spherical surface. The result of these calculations is shown in figure 5.4. Outside the cluster, that is to say for $r > R_{cluster}$, the external field of rotation $\vec{\omega}_{ext}^{el}$ due to the cluster of charges is independent of the radius $R_{cluster}$ of the cluster. But the field $\vec{\omega}_{int}^{el}$ inside the cluster, that is to say for $r < R_{cluster}$, depends on $R_{cluster}$.

To calculate the elastic energy stored in the lattice by the presence of the field of rotation $\vec{\omega}^{el}$ of the singularity, in other words *the energy of elastic distortion $E_{dist}^{(Q_\lambda)}$ of the lattice due to the charge of the cluster*, one should in principle calculate the energy associated with the field of rotation, increased by the energy of the shear strain fields associated with the field of rotation. But in the case of *a perfect cosmological lattice*, we have the relationship $K_2 \ll K_3$ between the rotation and shear moduli, so that in principle we can neglect the energy associated with shear strain. The calculation provides the distortion energy $E_{dist ext}^{(Q_\lambda)}$ stored outside the singularity in a quasi-infinite medium, that is to say a medium for which $R_\infty \gg R_{cluster}$ and the elastic distortion energy $E_{dist int}^{(Q_\lambda)}$ stored inside the singularity. *The rest elastic energy $E_{dist}^{(Q_\lambda)}$ of the spherical cluster of rotational charge Q_λ and radius $R_{cluster}$* can therefore be written as the sum of the energies stored outside and inside the singularity. We see that it is finished and depends essentially on the radius $R_{cluster}$ and the charge Q_λ of the cluster.

A localized macroscopic topological singularity of radius $R_{cluster}$, apart from having a global charge Q_λ of rotation, can also have a global charge Q_θ of curvature. Indeed, such a singularity can be formed of a cluster of elementary topological singularities of the lattice, such as prismatic dislocation loops which each have an elementary charge $q_{\theta(i)}$ of curvature. If $Q_\theta > 0$, we are talking about *a cluster of vacancy nature* because lattice sites are missing within the cluster, and if $Q_\theta < 0$, we are talking about *a cluster of interstitial nature*, because there is then an excess of lattice sites within the cluster.

A localized curvature singularity is responsible for a non-zero and divergent flexion field in its vicinity. Indeed, if we know the density $\theta^{ch}(\vec{r})$ of curvature charges within the singularity, we

can easily calculate the divergent flexion field outside the singularity, linked to a spatial curvature of the lattice. The result of the calculation is shown in figure 5.4.

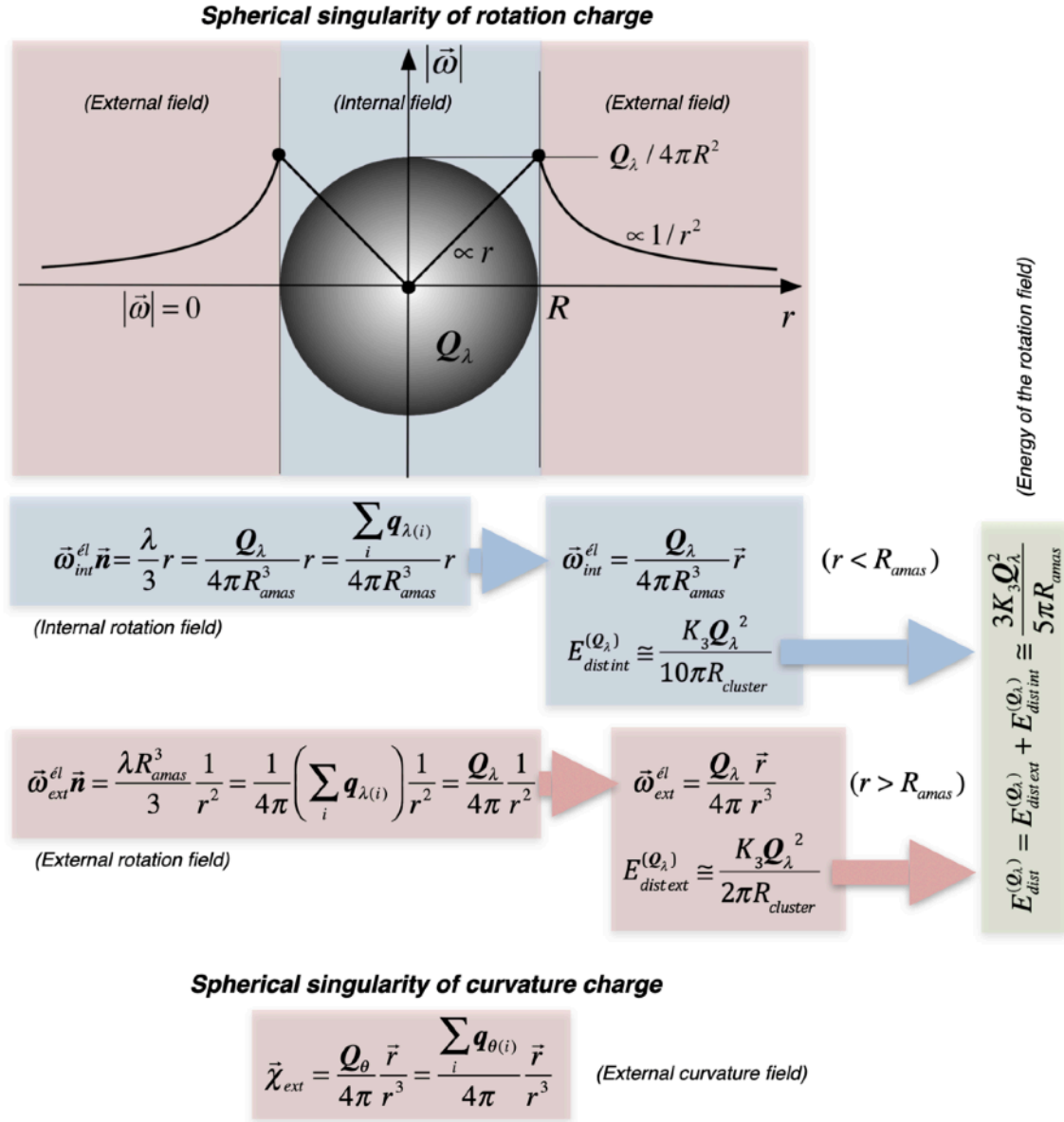


Figure 5.4 - Fields and energies of a spherical singularity of rotation charge or curvature charge

The vectors of this flexion field converge towards the singularity if this is of interstitial nature (excess of lattice sites within the singularity), and diverge from the singularity if it is of interstitial nature (depletion of lattice sites within the singularity). On the other hand, we also note that the flexion field due to the cluster of curvature charges does not depend on the radius $R_{cluster}$ of the cluster apart from the cluster.

Charge, fields, energies and mass of a twist disclination loop (BV)

The simplest topological singularity of a lattice which can have a localized charge q_λ of rotation, among all the topological singularities described above on the scale of a solid lattice, is

obviously the twist disclination loop ($\mathbf{BV} = \text{Boucle Vis in French}$) described in figure 2.30. Recall that such a loop is generated by a rotation $\vec{\Omega}_{BV}$ of the upper plane of a circular cut in the middle of an angle α_{BV} relative to the lower plane (figure 5.5). The fact that two planes which have been displaced with respect to each other by rotation are glued together, is the cause of the appearance of a surface charge Π_{BV} of rotation on the plane of the loop. We then have $\vec{\Omega}_{BV} = \alpha_{BV} \vec{n} = -\vec{n} \Pi_{BV}$, which implies that $\mathbf{q}_{\lambda BV} = \pi R_{BV}^2 \Pi_{BV} = -\pi R_{BV}^2 \Omega_{BV}$. This charge $\mathbf{q}_{\lambda BV}$ is in fact the global rotation charge of the twist disclination loop as seen from a long distance from the loop. This means that such a loop can effectively behave as the source of a divergent field of rotation $\vec{\omega}$ within the solid medium. Such a loop can also be seen a little differently. Indeed, the fact of carrying out the rotation of the two planes one relative to the other induces a curvilinear displacement $R_{BV} \alpha_{BV}$ along the loop similar to that of a screw dislocation. The curvilinear Burgers vector \vec{B}_{BV} and the linear charge Λ_{BV} of this screw pseudo-dislocation loop then has a value $\vec{B}_{BV} = R_{BV} \alpha_{BV} \vec{t}$, which leads to a linear pseudo-charge of the loop with a value $\Lambda_{BV} = -\vec{B}_{BV} \cdot \vec{t} / 2$ and to a global charge $\mathbf{q}_{\lambda BV} = 2\pi R_{BV} \Lambda_{BV} = -\pi R_{BV} \vec{B}_{BV} \cdot \vec{t}$ of the loop. The same global charge value is obtained as that obtained by considering the surface charge Π_{BV} , which makes it possible to consider this topological singularity indifferently as a twist disclination loop or as a screw pseudo-dislocation loop. Considering the loop as a screw pseudo-dislocation loop then makes it possible to show, in a rather complicated way, that there is a local rotation field of toric shape around the loop, which is confined up to a distance of the order $r_B \approx 2R_{BV}$ relative to the center of the loop, where R_{BV} is the radius of the loop. Outside this toric confinement space, the far field becomes equal to the divergent field of rotation due to the global charge $\mathbf{q}_{\lambda BV}$ of rotation of the loop.

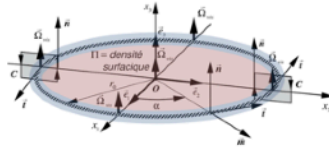
The distortion energy of a twist disclination loop is the energy which is stored by the rotations generated by the screw pseudo-dislocation of radius R_{BV} in a torus whose central fiber is the disclination loop and whose radius of the section roughly corresponds to R_{BV} , to which is added the energy of the external field of rotation of spherical symmetry for distances greater than $r \geq 2R_{BV}$. The calculation of the exact value of this energy is obviously very complex, in particular because the field of rotation cancels out exactly in the center of the loop. However, we can try to approximate the actual distortion energy of the loop, using the energy of a straight dislocation to calculate the energy of the curved dislocation. In the case where the radius R_{BV} of the loop is enormously larger than the core radius a of the screw pseudo-dislocation vis ($R_{BV} \gg a$), this approximation must approach the real value of the energy of distortion within the torus surrounding the loop, and we can correct it by introducing a constant A_{BV} correcting the value of the external radius of the torus to best approach the real value of the energy. We will therefore write the energy of distortion $E_{dist\ toric}^{BV}$ of the toric field from the energy of a screw dislocation per unit of length, like the energy contained in the torus surrounding the twist disclination loop. This value is reported in figure 5.5, in which a is the core radius of the screw pseudo-dislocation, of the order of magnitude of the step of the cosmological lattice in the presence of any expansion field τ , $A_{BV} R_{BV}$ is the range of the toric field of the loop and A_{BV} is a constant which can only be obtained by the exact calculation of the energy of the loop, but which must be very close to unity according to our previous discussion. To simplify the rest of our presentation, as the ratio $A_{BV} R_{BV} / a$ does not depend almost on the background expansion, we will consider it to be approximately constant, and introduce a constant ζ_{BV}

specific to the twist disclination loop, and being equal to $\zeta_{BV} = \ln(A_{BV} R_{BV} / a) \equiv cste$ with $A_{BV} \approx 1$ so to be able to write the energy of the toric field in the form shown in figure 5.5.

The loop of twist disclination (BV)

Conjecture 7 - the radius of a loop of twist disclination is much greater than the step of the cosmological lattice:

$$\ln(A_{BV} R_{BV} / a) \gg 1$$



$$\left\{ \begin{array}{l} q_{\lambda BV} = 2\pi R_{BV} \Lambda_{BV} = -\pi R_{BV} \vec{B}_{BV} \vec{t} \quad (\text{rotation charge}) \\ \vec{\omega}_{ext}^{BV} = \frac{q_{\lambda BV}}{4\pi} \frac{\vec{r}}{r^3} \quad (\text{divergent field of rotation}) \\ E_{dist}^{BV} \cong E_{dist\ tor}^{BV} \cong 2(K_2 + K_3) \zeta_{BV} R_{BV} \Lambda_{BV}^2 = \frac{1}{2} (K_2 + K_3) \zeta_{BV} R_{BV} \vec{B}_{BV}^2 \\ E_{cin}^{BV} \cong E_{cin\ tor}^{BV} \cong mn \zeta_{BV} R_{BV} \Lambda_{BV}^2 \mathbf{v}^2 = \frac{1}{4} mn \zeta_{BV} R_{BV} \vec{B}_{BV}^2 \mathbf{v}^2 \\ M_0^{BV} = \frac{E_{dist}^{BV}}{c_t^2} \\ \zeta_{BV} = \ln(A_{BV} R_{BV} / a) \quad (A_{BV} \approx 1) \end{array} \right.$$

Figure 5.5 - Charge, fields, energies and mass of a twist disclination loop

We can then compare this energy of the toric field of the loop with the energy associated with the spherical field of rotation at great distance from the loop, which occurs beyond the distance $2R_{BV}$ of the loop, which is due to its rotation charge $q_{\lambda BV}$, and which is simply worth $E_{dist\ ext}^{BV} \cong \pi K_3 R_{BV} \vec{B}_{BV}^2 / 4$. By comparing this value with the energy of the toric field reported in figure 5.5, we obtain the ratio $E_{dist\ tor}^{BV} / E_{dist\ ext}^{BV} \cong 2 \ln(A_{BV} R_{BV} / a) / \pi$. If we admit here a new and seventh conjecture, reported in figure 5.5, namely that *the radius of a twist disclination loop is much larger than the step of the cosmological lattice*, therefore that $\ln(A_{BV} R_{BV} / a) \gg 1$, the energy associated with the spherical external field of rotation becomes perfectly negligible with respect to the energy of the toric field of the loop. Therefore, the energy E_{dist}^{BV} of the twist disclination loop is essentially contained in the toroidal field of the loop, and we can write that $E_{dist}^{BV} \cong E_{dist\ tor}^{BV}$.

The non-relativistic kinetic energy of a moving twist disclination loop is the energy that is stored by the lattice movements generated by the moving screw pseudo-dislocation. Using the relation obtained in the case of a screw dislocation, and admitting the seventh conjecture, the kinetic energy E_{cin}^{BV} of the loop is fairly easily calculated, which is shown in figure 5.5. Again, the kinetic energy of the external rotational field is negligible compared to this kinetic energy, so we can consider that the kinetic energy of the loop is essentially confined to the toric field of the

loop. We therefore deduce that Einstein's relation applies perfectly to the twist disclination loop in the form $M_0^{BV} = E_{dist}^{BV} / c_t^2$.

We know from the separability of Newton's equation described at the beginning of this chapter that the existence of elastic distortion fields induces, via their energy, a perturbation field of expansion. We will return later in detail to this expansion perturbation field associated with the twist disclination loop.

“Coulomb-type” interaction between localized topological singularities with rotation charges

Assume first of all two loops of twist disclinations with rotation charges $q_{\lambda BV(1)}$ and $q_{\lambda BV(2)}$. There is an interaction force between these two loops, of electric type, and this interaction force can be deduced very generally using the Peach and Koehler force.

Indeed, the spherical external field of rotation generated by a charge $q_{\lambda BV(1)}$ located at the center of the coordinate system is given by the relation of figure 5.5. If a twist disclination of rotation charge $q_{\lambda BV(2)}$ is then at the position marked by a vector $\vec{r} = \vec{d}$ in the coordinate system, the interaction force acting on this charge on the part of the charge $q_{\lambda BV(1)}$ is the Peach and Koehler force, which is exerted in the direction of the vector \vec{d} and whose intensity is worth $F_{PK(2)}^{BV} = [(K_2 + K_3) / \pi] q_{\lambda BV(1)} q_{\lambda BV(2)} / d^2$.

Thus, the reciprocal force between the two charges is repulsive if $q_{\lambda BV(1)} q_{\lambda BV(2)} > 0$ and attractive if $q_{\lambda BV(1)} q_{\lambda BV(2)} < 0$. This force of interaction between the rotation charges of twist disclination loops is the perfect analog of the force of interaction $\vec{F}^{électrique} = q_{(1)} q_{(2)} \vec{d} / 4\pi\epsilon_0 d^3$ between two electric charges $q_{(1)}$ and $q_{(2)}$ in electromagnetism, and thus fits perfectly with the analogy developed in the previous chapter with the equations of Maxwell. As the previous relation of the force of Peach and Koehler is perfectly independent of the size of the loops, it can be generalized without problem to two macroscopic clusters of topological singularities which would have macroscopic charges of rotation $Q_{\lambda(1)}$ and $Q_{\lambda(2)}$ which would be distant from d , under the form $F_{PK(2)} = [(K_2 + K_3) / \pi] Q_{\lambda(1)} Q_{\lambda(2)} / d^2$. In this case of two macroscopic clusters, the "electrical" interaction force between them therefore does not depend on the respective radii $R_{amas(1)}$ and $R_{amas(2)}$ of the two clusters.

Charge, fields, energies and mass of a loop of prismatic edge dislocation (BC)

If we consider a prismatic loop of edge dislocation (**BC** = *Boucle Coin* in French) with a radius R_{BC} (figure 2.28), the distortions induced in the lattice are those of an edge dislocation. We can therefore calculate approximately the elastic distortion energy of this loop as the energy which is stored in the lattice by the elastic distortions generated by the edge dislocation in a torus centered on the loop.

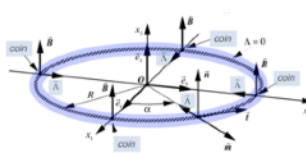
By using the same arguments as for the twist disclination loop, we deduce that, in a perfect cosmological lattice, the elastic energy of distortion of a prismatic loop is essentially contained in the toric fields surrounding the loop, and reported in the figure 5.6, in which A_{BC} is a constant close to unity, which should be calculated exactly by the exact integration of the energy of the fields within the torus, and where $\zeta_{BC} = \ln(A_{BC} R_{BC} / a)$ is a constant proper to the edge dislocation loop.

The prismatic loop of edge dislocation (BC)

Conjecture 7 - the radius of a prismatic loop of edge dislocation is much greater than the step of the cosmological lattice:

$$\ln(A_{BC} R_{BC} / a) \gg 1$$





$$\left\{ \begin{array}{l} \mathbf{q}_{\theta BC} = -2\pi \bar{\mathbf{n}} (\bar{\mathbf{t}} \wedge \bar{\mathbf{A}}_{BC}) = 2\pi \bar{\mathbf{A}}_{BC} \bar{\mathbf{m}} = -2\pi \bar{\mathbf{n}} \bar{\mathbf{B}}_{BC} \quad (\text{flexion charge}) \\ \bar{\chi}_{ext}^{BC} = \frac{\mathbf{q}_{\theta BC}}{4\pi} \frac{\bar{\mathbf{r}}}{r^3} \quad (\text{divergent field of flexion}) \\ E_{dist}^{BC} \equiv E_{dist\ tor}^{BC} \equiv \left(\frac{K_2}{K_3} \right)^2 K_3 \zeta_{BC} R_{BC} \bar{\Lambda}_{BC}^2 \equiv \left(\frac{K_2}{K_3} \right)^2 K_3 \zeta_{BC} R_{BC} \bar{\mathbf{B}}_{BC}^2 \\ E_{cin}^{BC} \equiv E_{cin\ tor}^{BC} \equiv \frac{1}{2} \left(\frac{K_2}{K_3} \right)^2 mn \zeta_{BC} R_{BC} \bar{\Lambda}_{BC}^2 \mathbf{v}^2 = \frac{1}{2} \left(\frac{K_2}{K_3} \right)^2 mn \zeta_{BC} R_{BC} \bar{\mathbf{B}}_{BC}^2 \mathbf{v}^2 \\ M_0^{BC} = \frac{E_{dist}^{BC}}{c_t^2} \\ \zeta_{BC} \equiv \ln(A_{BC} R_{BC} / a) \quad (A_{BC} \approx 1) \end{array} \right.$$

Figure 5.6 - Charge, fields, energies and mass of a prismatic loop of edge dislocation

Outside the loop, the fields due to the edge dislocation loop are reduced to a divergent flexion field of spherical symmetry. It is clear that this flexion field must be associated with a perturbation in the volume expansion field which must have a certain energy. We will come back to this problem later, and we will show that the energy associated with this flexion field is perfectly negligible compared to the distortion energy reported in figure 5.6, so that the energy of the edge dislocation loop is essentially contained in the toric fields in the immediate vicinity of the loop.

The non-relativistic kinetic energy of this loop is essentially the kinetic energy stored in the lattice by the dynamic distortions generated by the edge dislocation in the torus centered on the loop. Using the relations deduced previously for the edge dislocation, we deduce the approximate value of this kinetic energy, and we note that Einstein's relation applies perfectly to the non-relativistic kinetic energy of the prismatic dislocation loop since $M_0^{BC} = E_{dist}^{BC} / c_t^2$. As for the expansion perturbation field associated with this loop, we will come back to this in detail later.

Charge, fields, energies and mass of a slip loop of dislocation (BM)

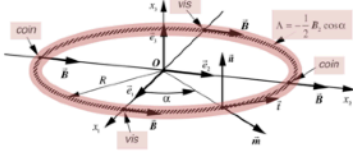
The slip loop of mixed dislocation (**BC** = *Boucle Mixte* in French) with a radius R_{BC} (figure 2.28), of a "vector" nature, is obtained by gliding (parallel translation to the plane of the loop) in the direction of the Burgers vector, so that the lattice does not present any "extra-matter" in this

case (figure 2.28). On the other hand, the presence of a screw component in the regions where $\vec{B}_{BM} \parallel \vec{t}$ induce a dipolar rotational field $\vec{\omega}_{dipolaire}^{BM}(r, \theta, \varphi)$ in the vicinity of the slip loop.

The slip loop of mixed dislocation (BM)

Conjecture 7 - the radius of a slip loop of mixed dislocation is much greater than the step of the cosmological lattice:

$$\ln(A_{BM} R_{BM} / a) \gg 1$$



$$\left\{ \begin{array}{l} q_{\lambda BM} = 0 \quad \& \quad q_{\theta BM} = 0 \\ \exists \text{ an external dipolar field of rotation } \vec{\omega}_{dipolar}^{BM}(r, \theta, \varphi) \\ \left\{ \begin{array}{l} E_{dist}^{BM} \cong E_{distore}^{BM} \cong \frac{1}{4} (K_2 + K_3) \zeta_{BM} R_{BM} \vec{B}_{BM}^2 \\ E_{cin}^{BM} \cong E_{cintore}^{BM} \cong \frac{1}{8} mn \zeta_{BM} R_{BM} \vec{B}_{BM}^2 v^2 \\ M_0^{BM} = \frac{E_{dist}^{BM}}{c_t^2} \cong \frac{1}{4c_t^2} (K_2 + K_3) \zeta_{BM} R_{BM} \vec{B}_{BM}^2 \\ \zeta_{BM} = \ln(A_{BM} R_{BM} / a) \quad (A_{BM} \approx 1) \end{array} \right. \end{array} \right.$$

Figure 5.7 - Charge, fields, energies and mass of a slip loop of mixed dislocation

If we consider a slip loop with a radius R_{BM} , the distortions induced in the short distance lattice are those of a screw dislocation for the angles $\alpha = 0$ and $\alpha = \pi$, and those of an edge dislocation for the angles $\alpha = \pi/2$ and $\alpha = 3\pi/2$. We can therefore consider that we pass continuously as a function of the angle α from a screw dislocation to an edge dislocation via mixed intermediate states. The distortion energy associated with the bent string is stored mainly in the torus centered on the loop. However, since the two edge parts and the two screw parts of the loop are respectively of opposite charges, the fields associated with the edge parts and the screw parts of the loop decrease very quickly at great distance from the loop. For example, the modulus of the rotation field in the plane of the loop and over a diameter passing through the screw parts of the loop behaves approximately as follows $|\vec{\omega}_{dist}^{BM}| \propto |\vec{B}_{BM}| R_{BM} / (4\pi r^2)$ at great distance ($r \gg R_{BM}$). If the radius R_{BM} of the loop is very much greater than the step of the lattice, we can roughly take into account this rapid decrease in the dipole field by imagining that the field in the vicinity of the string is that of a dislocation. We can thus roughly calculate the rest energy of such a loop by integrating the energies per unit length of string within the torus for the screw and edge components of the string as a function of the angle α . It therefore comes

approximately, in the perfect cosmological lattice, the expression of the energy reported in figure 5.7. An exact calculation of the energy should lead to the value A_{BM} of the constant proper to the geometry of the mixed loop, and which must approach the value 1.

It would also be necessary to take into account the energy of distortion associated with the dipolar field of rotation outside the loop. However, this is obviously lower than the distortion energy associated with the external field of rotation of a twist disclination loop, so that this energy can be perfectly neglected in comparison with the distortion energy contained in the torus. This again means that the energy of the mixed dislocation loop is essentially contained in the immediate vicinity of the dislocation loop.

The non-relativistic kinetic energy of the slip loop of dislocation is calculated approximately in the same way as its elastic distortion energy.

It can be seen that the energies E_{dist}^{BM} and E_{cin}^{BM} are in fact those supplied by the screw parts of the slip loop, and that these are essentially contained in the immediate vicinity of the dislocation loop. Einstein's relation therefore applies perfectly to the slip dislocation loop since $M_0^{BM} = E_{dist}^{BM} / c$. As for the expansion perturbation field associated with this loop, we will come back to this later in detail in chapter 24, where we will see that the energy associated with this field is negligible compared to the distortion energy contained in the torus.

"Topological bricks" to build the world of elementary particles

In Figures 5.4 to 5.7, we have reported all the results obtained for the three most basic types of loops that can be found in the perfect cosmological lattice. In our analogy with the real world, the three loops of disclination and dislocation which appear there could well constitute the most elementary topological bricks of the cosmological lattice, which could make it possible to work out loops of more complex structures which could be analogues of elementary particles of the Standard Model.

The twist disclination loop is the most basic topological singularity at the origin of an electrical charge. At a certain distance from the center of a twist disclination loop, greater than approximately $2R_{BV}$, the external rotation field of the disclination loop behaves exactly like the external field of a spherical charge of value $q_{\lambda BV} = 2\pi R_{BV} \Lambda_{BV}$.

One can then wonder what should be the radius R_{ch} of the spherical charge so that it has an elastic energy of global distortion equal to the energy of distortion of the loop. With the charge value $q_{\lambda BV}$ ensuring a long distance field similar to that of the twist disclination loop, the energy of a spherical charge of radius R_{ch} is worth $E_{dist}^{q_\lambda} \cong 12K_3 \pi R_{BV}^2 \Lambda_{BV}^2 / (5R_{ch})$. For this global energy of the spherical charge to be equal to that of the distortion loop of radius R_{BV} and linear charge Λ_{BV} , that is to say that $E_{dist}^{q_\lambda} \cong E_{dist}^{BV}$, the radius R_{ch} of the charge must satisfy the following relation $R_{ch} \cong R_{BV} 6\pi / [5 \ln(A_{BV} R_{BV} / a)]$, obtained by recalling that in the perfect cosmological lattice $K_2 \ll K_3$.

By using conjecture 7, we note that the radius of a spherical charge which would have an energy of the rotation field equal to the energy of the toric field of a twist disclination loop should be considerably smaller than the radius of the twist disclination loop. As the twist disclination loop is the most basic microscopic lattice singularity that it is possible to find which has a non-zero rotation charge $q_{\lambda BV}$, the twist disclination loop therefore corresponds to the most elementary structure of an electric charge in our analogy with the real world.

The prismatic dislocation loop is the most basic topological singularity responsible for a spatial curvature charge. When we compare the elastic distortion energy of a prismatic loop with the elastic distortion energy of a twist disclination loop, with the same radii and the same modules of their Burgers vector, we see that in the perfect cosmological lattice with $K_2 \ll K_3$, we have $M_0^{BC} \equiv 2(K_2/K_3)^2 M_0^{BV} \ll M_0^{BV}$. Thus, *the mass of inertia of the prismatic edge dislocation loop is considerably lower than the mass of inertia of the twist disclination loop.*

On the other hand, as the prismatic dislocation loop has a nonzero charge of curvature $q_{\theta BC} = -2\pi \vec{n} \vec{B}_{BC}$, which can be positive (loop of the lacunar type) or negative (loop of the interstitial type), it is necessarily associated with a flexion field $\vec{\chi}_{ext}^{BC}$ at long distance by lattice curvature, given by $\vec{\chi}_{ext}^{BC} = q_{\theta BC} \vec{r} / (4\pi r^3)$. Thus, the prismatic dislocation loop is the most basic microscopic lattice singularity which is the source of spatial curvature of the lattice by the divergent flexion field which is associated with it, while the twist disclination loop is the most basic microscopic lattice singularity which is a source of spatial torsion of the lattice by the divergent field of rotation associated with it.

As one tried at first sight an analogy between the rotation charge of the twist disclination loop and the electric charge of the electron of the physics of particles, then the loop of prismatic edge dislocation, which does not present a field of rotation and which is of rest mass much weaker than the twist disclination loop, could very well, at first glance, be identified by analogy *with the real-world neutrino*, which is actually an electrically neutral particle and of much lower mass than the electron.

If we accept this analogy, the neutrino would in this case be the source of a spatial curvature by flexion of the perfect cosmological lattice, in other words the source of a field of curvature of space, while the charge of the electron would be the source of a spatial torsion by rotation of the perfect cosmological lattice, corresponding to the electric field of electromagnetism. This analogy with the two basic leptons of particle physics is obviously very sketchy at the moment, and it could very well intervene in fact more complex combinations of these elementary loops in the form of loops of dispiration of complex structures to explain the different elementary particles of the real world.

The slip dislocation loop is the most basic topological singularity at the origin of an electric dipolar moment. Unlike the twist disclination loop and the prismatic dislocation loop, the slip dislocation loop has no field at a long distance like a divergent rotation field or a divergent flexion field. However, this loop has a dipolar moment of rotation $\vec{\omega}_{dipolar}^{BM}(r, \theta, \varphi)$ in its vicinity, linked to the two opposite rotation charges located on either side of the loop. Thus, the slip dislocation loop is the most basic microscopic lattice singularity that can be the source of a dipolar moment of rotation.

In our analogy with the real world, a slip dislocation loop in the perfect cosmological lattice could correspond to the most elementary structure which could generate an electric dipolar moment for an elementary particle. However, it turns out that the research and measurement of an electrical dipole moment of elementary particles is currently an important research subject of the Physics of elementary particles.

The various physical properties transported by loop singularities

From the previous discussion, it would therefore seem that the twist disclination loop could

transport the electric charge, the prismatic edge dislocation loop the curvature charge and the slip mixed dislocation loop the electric dipolar moment. We can add to these three properties another property which could be of enormous interest. In our analogy with the real world, it is quite difficult to imagine, to find the analog of the spin of a charged particle and the magnetic moment associated with it, that a symmetrical spherical singularity of rotation charge like that described in figure 5.4 can turn on itself. However, if we consider that the analog of an electrical charge is indeed the twist disclination loop shown in figure 5.5, the topology of this singularity, consisting of a screw pseudo-dislocation, makes it possible to imagine very naively that it can rotate around one of its diameters. In this case, the distribution of the rotation charge, analogous to a distribution of the electric charge in the form of a ring along the perimeter of the twist disclination loop, would necessarily impose the appearance of a magnetic moment of the loop associated with this real movement of rotation. We will come back to this subject later.

There is still a fifth fundamental and very important property of elementary particles which could be explained with our analogy. It is the fact of being able to calculate the elastic distortion energies E_{dist}^{loop} and the kinetic energies E_{cin}^{loop} of the loops, and to be able to deduce therefrom their inertia masses M_0^{loop} , and that these are contained essentially in the immediate vicinity of the loops. But it is also and above all the fact that they all satisfy, in the perfect cosmological lattice, the famous relation of Einstein, which is *a fundamental property of these loops which has been demonstrated without in any way appealing to a principle of special relativity*.

On the other hand, the mass of inertia of the loops is a property linked to the mass of inertia of the cosmological lattice in the absolute reference frame of the external observer **GO**. In an analogy with the real world, the mass of inertia of the topological lattice would then correspond to *the famous Higgs field* that had to be introduced into the Standard Model to explain the mass of elementary particles, and *the Higgs particle* would then be the only one real particle of the real world since it would correspond to a constituent particle of the perfect cosmological lattice, while the other elementary particles of the Standard Model would correspond to topological singularities of the perfect cosmological lattice.

There is certainly still a huge way to go to find an analogy which would provide, by judicious combination of the different elementary topological loops in the form of different dispirations of more or less complex structures, the set of elementary particles of the Standard Model and their physical properties. But the major problem that we will address in the following will be above all to find the analogies which explain the gravitational behavior of real world objects on a macroscopic scale (Newton's gravitation, General Relativity), as well as the quantum behavior of the real world at the microscopic scale (Quantum Physics).

We will retain for the moment in this chapter that several of the fundamental properties of elementary particles in our real world find a very simple and perfectly classic explanation using the analogy with the elementary loop singularities of a perfect cosmological lattice.

Chapter 6

Lorentz transformation and special relativity

Thanks to *Newton's first partial equation in the presence of topological singularities*, it was possible to obtain *the elastic distortion fields associated with the various elementary singularities of the cosmological lattice*. In this chapter, we will show that these elastic distortion fields satisfy *the Lorentz transformation*, and that they reveal *a new interpretation of the special relativity*.

We have deduced the kinetic energy associated with the movement of a dislocation or of a dislocation or disclination loop within the perfect cosmological lattice, by implicitly supposing that the distortion perturbations due to the moving charge are transmitted within the lattice with almost infinite speed compared to the speed of the charge within the lattice. However, it is well known that perturbations within a solid lattice are actually transmitted at the finite speeds of transverse or longitudinal perturbations. To take into account the propagation effects of perturbations with finite speed within the solid lattice when the speed of displacement of the charge becomes significant in comparison with the speed of propagation of transverse and / or longitudinal waves, we demonstrate here the Lorentz transformation to go from a stationary reference frame in the lattice to the mobile reference frame associated with the moving charge. This transformation is then applied to the singularities in movement at relativistic speed within a perfect topological lattice, namely the screw and edge dislocations, the localized charge of rotation, the twist disclination loop, the prismatic dislocation loop and the slip dislocation loop. We calculate their total energy, due to the sum of the potential energy stored by the lattice distortions generated by the presence of the charge and the kinetic energy stored in the lattice by the movement of their charge, and we show that those satisfy *a relativistic dynamic*. In addition, there is a very elegant explanation of the famous «*electron energy paradox*» which says that the mass associated with the electromagnetic fields of the electron does not satisfy the principles of special relativity.

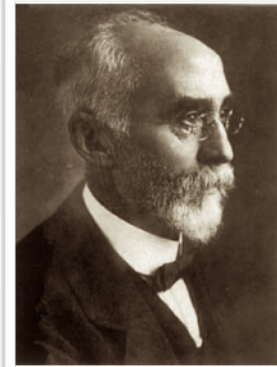
We then show that the Lorentz transformation also reveals *a term of relativistic force* acting on the rotation charges in motion, a term which is perfectly analogous to *the Lorentz force in electromagnetism*.

On these bases, we discuss the analogy between our approach and *the theory of Special Relativity*. We note that the cosmological lattice behaves in fact like *an ether*, in which the topological singularities satisfy exactly the same properties as those of Special Relativity, not only concerning *the contraction of the measuring rods and the dilation of time*, but also concerning *the Michelson-Morley experience and the Doppler-Fizeau effect*. But the existence of the cosmological lattice then makes it possible to interpret the concept of special relativity quite differently, and to explain for example very simply some somewhat obscure sides of special relativity, such as the famous «*paradox of twins*».

Mobile charges and Lorentz transformations

When topological singularities of charge densities $\vec{\lambda}_i$, $\vec{\lambda}$ or λ move in the frame $Ox_1x_2x_3$ fixed to the solid lattice at significant speeds compared to the celerities of propagation of transverse and / or longitudinal waves, it would obviously be very useful to be able to find the dynamic fields $\vec{\tau}(\vec{r},t)$, $\vec{\omega}(\vec{r},t)$ and $\vec{\alpha}_i(\vec{r},t)$ generated by these singularities in the frame $Ox_1x_2x_3$. Finding a solution of differential equations for singularities moving in the reference frame $Ox_1x_2x_3$ is not at all easy. On the other hand, using a mobile referential with the singularities, in which the singularities seem immobile, should allow us to calculate the static fields in $O'x_1'x_2'x_3'$ much more simply, then to obtain the dynamic fields in $Ox_1x_2x_3$ using transformation laws which have yet to be defined.

Consider for example an infinite screw dislocation along the axis Ox_1 and suppose that it moves at velocity \vec{v} in the direction of the axis Ox_2 . The choice of screw dislocation is not free, because it turns out that it is the only singularity which does not induce lattice distortions by volume expansion, but only a divergent field of rotation, which must greatly simplify the calculations. In the reference frame $O'x_1'x_2'x_3'$ moving with the dislocation string, the displacement field \vec{u}_{ext}^{screw} must be that of a static screw dislocation, as shown in figure 6.1.



Hendrik Anton Lorentz
(1853-1928)

In order to transform this static field in $O'x_1'x_2'x_3'$ into a dynamic field associated with the mobile screw dislocation in $Ox_1x_2x_3$, we must establish the transformation laws which will provide us with the dynamic fields in $Ox_1x_2x_3$. And the dynamic fields thus obtained must satisfy the space-time evolution equations in $Ox_1x_2x_3$. As there is translation of the coordinate system $O'x_1'x_2'x_3'$ with respect to the coordinate system $Ox_1x_2x_3$, the transformation laws must transform the coordinate x_2' of $O'x_1'x_2'x_3'$ into a coordinate which must depend on speed and time, in the form $(x_2 - vt)$, in the coordinate system $Ox_1x_2x_3$. We can *a priori* hypothesize that the transformation laws are written $x_2' = \alpha(x_2 - vt)$, $x_1' = \beta x_1$ and $x_3' = \beta x_3$ according to the three respective axes. With these transformation laws, the static displacement field \vec{u}_{ext}^{screw} becomes a dynamic field $\vec{u}_{ext}^{screw}(\vec{r},t)$ which depends on the factor $(x_2 - vt)$ and the constants α and β in $Ox_1x_2x_3$.

From the dynamic field $\vec{u}_{ext}^{screw}(\vec{r},t)$ thus obtained in $Ox_1x_2x_3$, one can directly calculate the fields of rotation $\vec{\omega}_{ext}^{screw}(\vec{r},t)$ and speed $\vec{\phi}_{ext}^{screw}(\vec{r},t)$ in $Ox_1x_2x_3$ via the rotational and the time derivative of $\vec{u}_{ext}^{screw}(\vec{r},t)$. But in the reference frame $Ox_1x_2x_3$, the fields thus obtained must satisfy the spatio-temporal evolution equations, namely the second pair of Maxwell's equations. For this requirement to be satisfied, the parameter α introduced into the transformation laws must necessarily be written $\alpha = \beta / (1 - v^2 / c_t^2)^{1/2} = \beta / \gamma_t$, in which it appears the well-known factor $\gamma_t = (1 - v^2 / c_t^2)^{1/2}$ of Lorentz transformations. By introducing this relation for α in the expressions obtained for $\vec{\phi}_{ext}^{screw}(\vec{r},t)$ and $\vec{\omega}_{ext}^{screw}(\vec{r},t)$, we obtain the expressions of the fields of the screw dislocation in $Ox_1x_2x_3$, as represented in figure 6.1. It is then remarkable that these fields, which perfectly satisfy the equations of spatio-temporal evolution in the reference frame $Ox_1x_2x_3$, do not depend absolutely on the parameter β , but only on the parameter γ_t of the

Lorentz transformations, so that the parameter β can be chosen freely, and we will admit here the value of 1, so that it is shown that the laws of spatial transformation are indeed the Lorentz laws represented in figure 6.1.

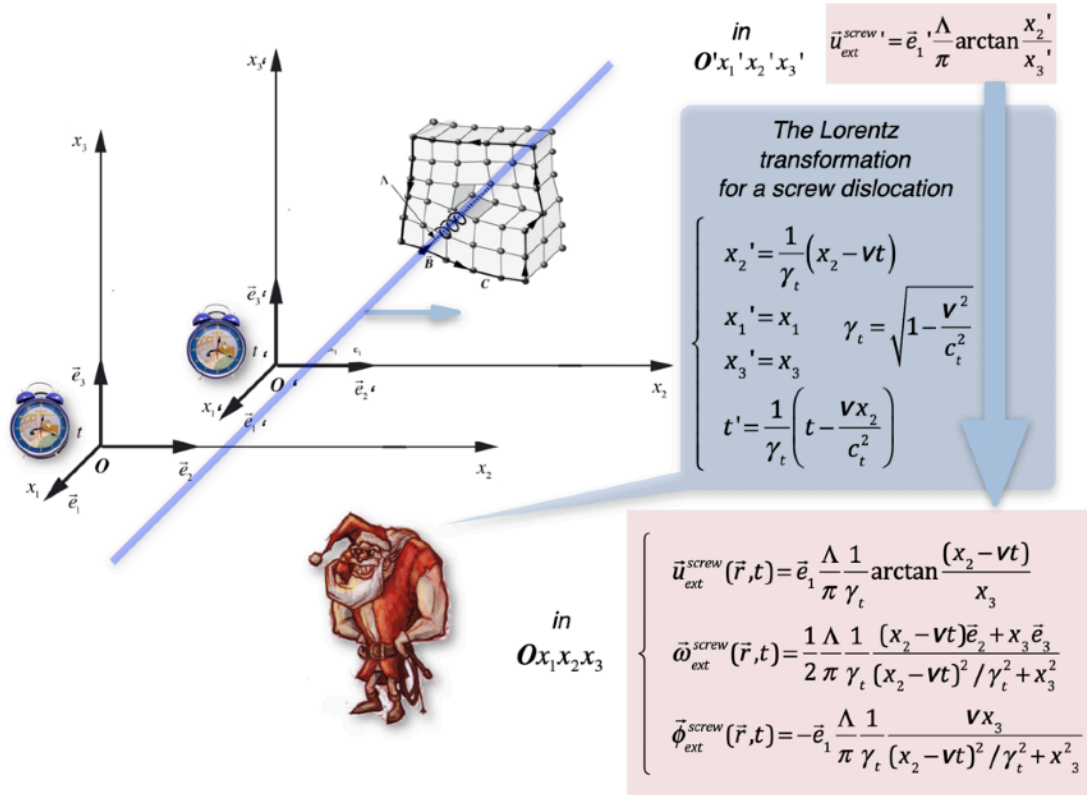


Figure 6.1 - The Lorentz transformation deduced using a moving screw dislocation

Contraction of lengths in the direction of movement

The expressions in figure 6.1 for dynamic fields $\vec{u}_{ext}^{screw}(\vec{r}, t)$, $\vec{\omega}_{ext}^{screw}(\vec{r}, t)$ and $\vec{\phi}_{ext}^{screw}(\vec{r}, t)$ are effective solutions of topological equations and Newton's equation for a screw dislocation moving in the reference frame $Ox_1x_2x_3$. It is interesting to take a look at the behavior of these fields as a function of the velocity \vec{v} of the dislocation. One can take for example the projection ω_2 of the external vector field of rotation in the direction of the movement of the dislocation, and report its value $\omega_2(t=0, x_3=0)$, taken at the instant $t=0$ and for the coordinate $x_3=0$, as a function of x_2 for different values of the ratio v/c_t , as illustrated in the figure 6.2. We then observe that the horizontal component of the rotation field seems to contract along the axis Ox_2 . It is easy to calculate that a certain value of $\omega_2(t=0, x_3=0)$ is observed at a distance Δx_2 from the origin which depends on the velocity \vec{v} of the dislocation, given by $\Delta x_2(v) = \Delta x_2(v=0)(1 - v^2/c_t^2)^{1/2}$, so that the field of rotation of the moving screw dislocation is *effectively contracted along the axis Ox_2 of a factor γ_t* .

Now imagine a cluster of rotation singularities which are linked to each other via their fields of rotation (it should be recalled here that the field of rotation corresponds to the electric field in

our analogy with the real world). If the cluster moves along the axis Ox_2 in the reference frame $Ox_1x_2x_3$ of the **GO**, the fields of rotation associated with this cluster must contract along the axis Ox_2 with a factor γ_t in order to satisfy the topological equations and the Newton equation of the lattice. The consequence is then that the cluster itself, which is linked by these fields of rotation, must contract along the axis Ox_2 . If this cluster represents an “object” for the great observer **GO** located outside the lattice, this “object” will contract along the axis Ox_2 . But if it is observed in its own frame of reference by a hypothetical observer who would be located inside the lattice, this “object” will remain exactly the same as it is at rest in the absolute frame of reference $Ox_1x_2x_3$, and its shape will not change in the reference frame $O'x_1'x_2'x_3'$ regardless of the speed of this “object” in $Ox_1x_2x_3$.

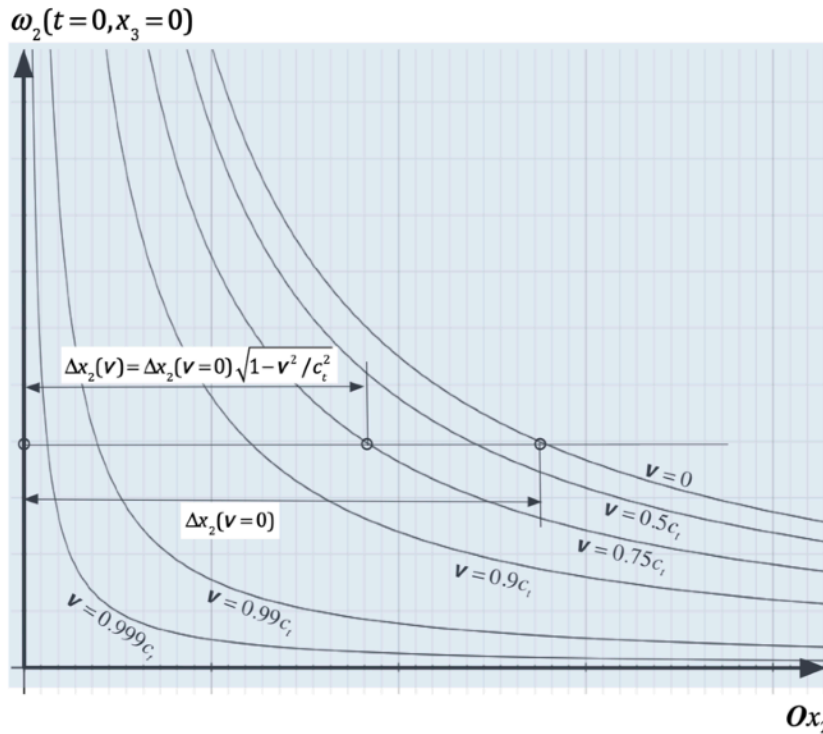


Figure 6.2 - Contraction of the component $\omega_2(t=0, x_3=0)$ of the rotation vector of a screw dislocation in $Ox_1x_2x_3$ in the direction of its movement, depending on its velocity \vec{v}

Time dilation of a mobile cluster of topological singularities

Now imagine that the observer measures the time T_0 it takes for a transversal wave to travel the distance d_0 in the absolute frame of reference $Ox_1x_2x_3$, be reflected on a mirror and return to its point of emission. It is clear that the observer measures a time equal to $T_0 = 2d_0 / c_t$. Such a time measurement system based on an “object” constituted by a cluster of singularities linked by the fields of rotation can be used by the observer **GO** as a time base, a clock giving the basic time lapse T_0 .

Imagine that the clock system, based on the same “object”, but now moving at a velocity \vec{v} along the axis Ox_1 in the base reference frame $Ox_1x_2x_3$, is observed by the **GO**. If the

transverse wave is emitted in the mobile reference frame $O'x_1'x_2'x_3'$ in the vertical direction within this frame of reference, this same wave is seen by the **GO** as a non-vertical wave in its frame of reference $Ox_1x_2x_3$, as illustrated in figure 6.3 (a). For the **GO** observer, the time T it takes for the wave to travel at celerity c_t , via the reflection on the mirror of the moving "object" is easily calculated using the triangle in the plane Ox_1x_3 , and we just gets that $T = T_0 / \gamma_t$. This means that the base time of the mobile clock in the reference frame $O'x_1'x_2'x_3'$, measured by the **GO** in its own reference frame $Ox_1x_2x_3$ seems dilated as a function of the velocity \vec{v} with a factor $1/\gamma_t$, and therefore that *the clock of the mobile "object" slows down compared to the GO's absolute clock*.

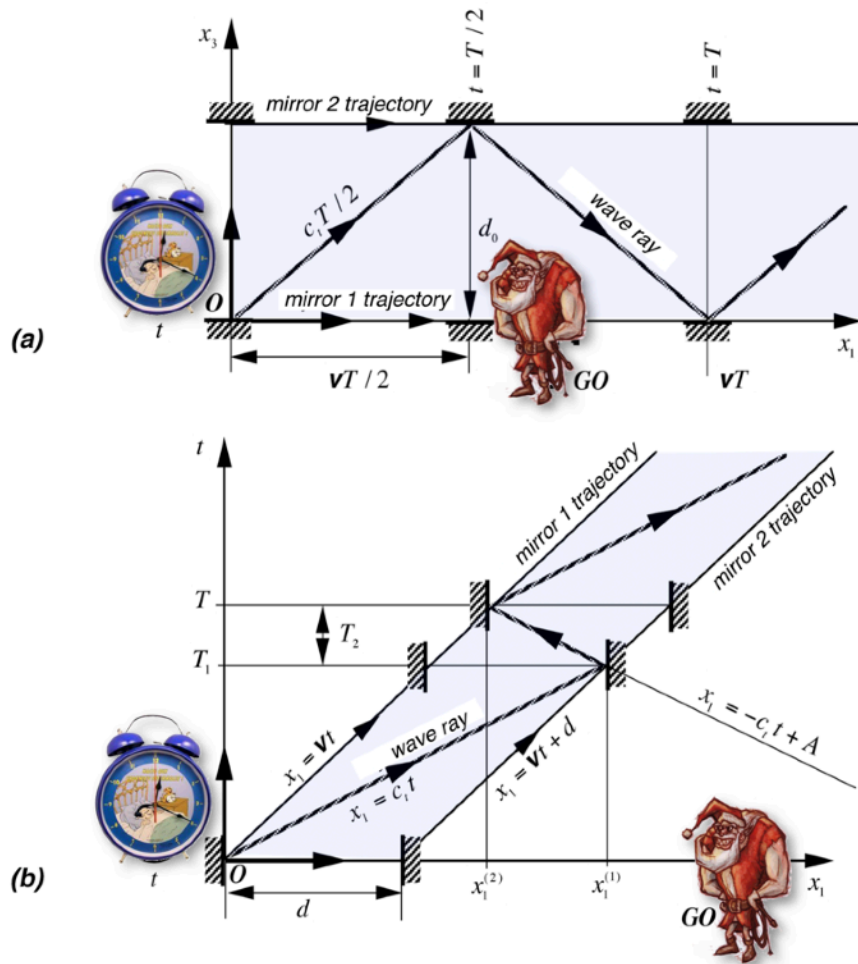


Figure 6.3 - (a) the trajectory of the transverse wave emitted vertically by the local clock of the mobile «object» in the frame, as observed by **GO** in his reference frame
(b) the trajectory of the transverse wave emitted horizontally by the local clock of the mobile «object» in the frame, as observed by **GO** in his reference frame

One can still wonder if the time in the reference frame $O'x_1'x_2'x_3'$ of the "object" remains isotropic in this reference frame, in other words if a clock based on a horizontal trajectory of the transverse wave, gives the same time as the vertical clock. If the horizontal clock is observed by the **GO** in its frame $Ox_1x_2x_3$, the wave path can be illustrated by the path diagram in figure 6.3

(b). In this diagram, the trajectories of the moving mirrors are represented by two lines with a slope \mathbf{v} , separated by a distance d in the direction $\mathbf{O}x_1$. The trajectories of the transverse wave lines are represented by two lines with slopes $+c_t$ and $-c_t$ respectively, for the two directions of propagation of the wave.

In this trajectory diagram, we can again geometrically calculate the time T required for the wave to travel a round-trip path via a reflection on a mirror of the mobile "object", knowing that the distance d between the two mirrors associated with the mobile "object" is contracted by a factor γ_t as we have seen previously, which provides the following relationship $d = \gamma_t d_0 = d_0 (1 - \mathbf{v}^2 / c_t^2)^{1/2}$ between the distance d and the distance d_0 at rest which separate the two mirrors, and we then obtain again $T = T_0 / \gamma_t$ as result of this calculation.

The two diagrams in figure 6.3 clearly show that the two mobile clocks, operating respectively with a vertical and horizontal wave propagation in the frame $\mathbf{O}'x_1'x_2'x_3'$ provide exactly the same local time, meaning that *there is indeed a local time t' and that this local time t' remains isotropic in the mobile frame of reference $\mathbf{O}'x_1'x_2'x_3'$* , regardless of the direction of movement of the "object" in the lattice.

In the mobile frame $\mathbf{O}'x_1'x_2'x_3'$, the length the wave has to travel along $\mathbf{O}'x_1'$ or $\mathbf{O}'x_3'$ inside the clock system is measured as a length d_0 , and the local time to go back and forth via reflection on a mirror is measured as being T_0 both in the case of a wave propagating vertically as horizontally. This means that the speed of the wave measured by an observer linked to the mobile frame of reference $\mathbf{O}'x_1'x_2'x_3'$ has exactly the same value c_t as that measured in the frame of reference $\mathbf{O}x_1x_2x_3$, regardless of the velocity $\mathbf{\bar{v}}$ of the frame of reference $\mathbf{O}'x_1'x_2'x_3'$ relative to the frame of reference $\mathbf{O}x_1x_2x_3$.

Imagine then that a transverse wave $\vec{\omega}' = \omega_0 \vec{e}_3 \sin[\omega'(x_1'/c_t - t')]$ propagates along $\mathbf{O}'x_1'$ in the frame of reference $\mathbf{O}'x_1'x_2'x_3'$ moving at speed $\mathbf{\bar{v}}$ in the direction $\mathbf{O}'x_1'$ relative to the frame of reference $\mathbf{O}x_1x_2x_3$. To express this wave in the frame of reference $\mathbf{O}x_1x_2x_3$, we use the space transformation $x_1' = (x_1 - \mathbf{v}t) / \gamma_t$ already obtained before and a new time transformation relation $t' = \varepsilon t + \delta x_1$, in which the parameters ε and δ have yet to be determined. By introducing these two relations in the expression of the wave in the frame $\mathbf{O}'x_1'x_2'x_3'$, this one must obligatorily take the simple form $\vec{\omega} = \omega_0 \vec{e}_3 \sin[\omega(x_1/c_t - t)]$ in the frame $\mathbf{O}x_1x_2x_3$, which implies that the constants must take the values $\delta = -\mathbf{v} / \gamma_t c_t^2$ and $\varepsilon = 1 / \gamma_t$, and that consequently the law of Lorentz for the transformation of time is written $t' = (t - \mathbf{v} x_1 / c_t^2) / \gamma_t$, as it has already been reported in figure 6.1.

Lorentz transformation for a mobile "object" linked by the rotation fields

The fact that the fields of rotation, and therefore the mobile "objects" linked by the fields of rotation, are actually contracted in the direction of movement by a factor $\gamma_t = (1 - \mathbf{v}^2 / c_t^2)^{1/2}$, that the isotropic time measured by the clocks of the mobile "object" is really dilated by a factor $1 / \gamma_t$ and that the velocities of the transverse waves measured in $\mathbf{O}x_1x_2x_3$ and in $\mathbf{O}'x_1'x_2'x_3'$ have exactly the same values c_t , mean that the transformation laws reported in figure 6.1, allowing to pass from one referential to the other, are *the same as the well-known Lorentz transformations of electromagnetism*.

It should be noted here that these transformations were used initially as simple mathematical tools making it possible to calculate with Maxwell's equations the electromagnetic fields

generated by mobile electric charges. Later, these transformations were used in special relativity by Einstein, by postulating that Lorentz relations are applicable *to any frame of reference moving at speed \mathbf{V} relative to another*, hence the term "relativity" which corresponds in fact *to axiomatically admitting the constancy of the speed of light in any frame of reference*.

Here, in the case of a solid lattice, the Lorentz transformation is obtained by a quite different approach based on the existence of a solid lattice in the absolute frame of reference $\mathbf{O}_{x_1x_2x_3}$ of **GO**, which is *the support (we then speak of ether) for the propagation of transverse waves*. This approach makes it possible to demonstrate the reality of the physical consequences of the Lorentz transformation, such as the spatial contraction and the dilation of time measured in $\mathbf{O}_{x_1x_2x_3}$ for mobile "objects" made up of topological singularities linked by fields of rotation. And this demonstration is based on the initial assumption that the **GO** can introduce a relative frame of reference $\mathbf{O}'_{x_1'x_2'x_3'}$ associated with the mobile "object" into its absolute frame of reference $\mathbf{O}_{x_1x_2x_3}$. The use of the Lorentz transformation in the case of the cosmological lattice is therefore limited only to transforming the fields between a mobile relative reference frame $\mathbf{O}'_{x_1'x_2'x_3'}$ with respect to the lattice and the absolute **GO** reference frame $\mathbf{O}_{x_1x_2x_3}$, which is fixed to the lattice. Consequently, there is absolutely no axiomatic hypothesis of "relativity" here stipulating that the Lorentz transformation is applicable to any referential moving relative to another. We will see that this remark is very important, because it implies a point of view radically different from that of Einstein's special relativity.

Uniqueness of the Lorentz transformation according to the background expansion

In conjecture 6, we stipulated that the module K_1 must be necessarily positive for the edge dislocations to satisfy the same Einstein relation as the screw dislocations in the cosmological Lattice. This conjecture therefore implies that the existence of longitudinal waves is subject to the fact that the background expansion of the cosmological lattice satisfies the hypothesis $\tau_0 > \tau_{0cr}$. In this particular case, as transverse and longitudinal waves can propagate within the lattice with different celerities c_t and c_l respectively, the fields associated with a mobile "object" which would be made up of topological singularities like edge dislocations which are linked both by fields of rotation and expansion, would become immensely more complicated to calculate. Indeed, supposing that the displacement of the linked charges in the reference frame $\mathbf{O}_{x_1x_2x_3}$ takes place at velocity $\vec{\mathbf{V}}$ in the direction \mathbf{O}_{x_1} , one should define two mobile reference frames $\mathbf{O}'_{x_1'x_2'x_3'}$ and $\mathbf{O}''_{x_1''x_2''x_3''}$ which move with the charges, by assigning to each of these reference frames the Lorentz transformation laws with velocities c_t and c_l respectively, therefore with two Lorentz factors $\gamma_t = (1 - \mathbf{V}^2 / c_t^2)^{1/2}$ and $\gamma_l = (1 - \mathbf{V}^2 / c_l^2)^{1/2}$.

We can imagine quite easily that the complete resolution of this type of problem for any density $\tilde{\lambda}_i$ of mobile charges in $\mathbf{O}_{x_1x_2x_3}$ can prove to be extremely complex, especially if there is still a non-homogeneous expansion field within the lattice, and especially as longitudinal perturbations can propagate like waves.

This is why we will treat in the following only the particular case, which is in fact the really interesting case for our analogy with the universe, of topological singularities which move in the perfect cosmological lattice presenting a homogeneous and constant background volume expansion which satisfies the relationship $\tau_0 < \tau_{0cr}$. In this case, we know that *the longitudinal waves do not exist*, meaning that any disturbance of the distortion fields can only propagate at

the speed of the transverse waves, and that the problem of determining the fields generated by mobile singularities can be solved by applying the unique Lorentz transformation for the frame of reference $O'x_1'x_2'x_3'$, the one shown in figure 6.1. The problem of expansion perturbation fields linked to topological singularities will be dealt with later, in the chapters dealing, on the one hand, with “*gravitational fields*” namely static perturbations of the expansion field due to topological singularities, and on the other hand “*quantum fields*” namely the dynamic perturbations of the expansion field due to mobile topological singularities when $\tau_0 < \tau_{ocr}$.

If we now consider mobile rotation charges, of charge density λ , which move within the lattice with velocity \vec{V} along the axis Ox_1 , the fields $\vec{\omega}$ generated by these charges will be dynamic fields which will evolve according to the movements of the charges. As the transmission of information of the mobile charges at any point of the solid lattice is done in this case at the speed c_t of the transverse waves, one can use the transformation of Lorentz deferred to figure 6.1 by associating a mobile reference frame $O'x_1'x_2'x_3'$ with the charges. It is interesting to show here the transformation relations concerning the pair of Maxwell equations managing the dynamics within the lattice, outside the charges, in the case where the volume expansion is homogeneous and constant ($n = cste$).

These relations of transformation of the fields of momentum $(n\vec{p})$ and torque \vec{m} in the frame of reference $Ox_1x_2x_3$ in the fields $(n\vec{p})'$ and \vec{m}' in the frame of reference $O'x_1'x_2'x_3'$ are obtained by fairly simple calculation, and are reported in figure 6.4. Thanks to these transformation relationships, we will be able to calculate the fields associated with movement within a solid lattice of different types of rotation charges, as well as their total energy, composed of their elastic potential energy and their kinetic energy.

Relativistic energies of the screw and edge dislocations

Let us consider an infinite cylindrical screw string and suppose that it moves at velocity \vec{V} in the direction of the axis Ox_1 . In the reference frame $O'x_1'x_2'x_3'$ in movement with the string, we can apply the transformation relations of figure 6.4 to find, from the expression of the static field $\vec{\omega}_{ext}$ of rotation of the dislocation as well as from the Lorentz transformation relations, the dynamic fields $\vec{\omega}_{ext}$ and $\vec{\phi}$ expressed in the reference frame $Ox_1x_2x_3$. We then deduce directly from these expressions the elastic energy density F_{dist}^{screw} of distortion and the kinetic energy density F_{cin}^{screw} in the frame of reference $Ox_1x_2x_3$. The total energy E_V^{screw} per unit length of the dislocation is obtained by integration of these energy densities in $Ox_1x_2x_3$. The total energy of the screw dislocation thus obtained is shown in figure 6.4, and its expression deserves a few comments:

- in fact, this expression is quite remarkable, because not only does it appear there the mass of inertia $M_0^{screw} \equiv E_{dist}^{screw} / c_t^2$ at rest of the screw dislocation that we had already obtained in a completely classic manner, but also it allows better understand the true physical origins of the relativistic terms of distortion energy E_V^{dist} and kinetic energy E_V^{cin} which appear there. Indeed, in this form, the term E_V^{dist} corresponds to *the relativistic correction of the elastic distortion energy E_{dist}^{vis} at rest*, while the term E_V^{cin} corresponds to *the relativistic correction of the non-relativistic kinetic energy $M_0^{vis} V^2 / 2$* ,

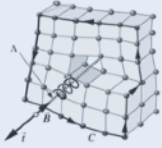
- in this case of screw dislocation, that is to say when the density λ of scalar charge is distributed in *an infinite rectilinear string*, the behavior of the total energy E_V^{screw} is a pure

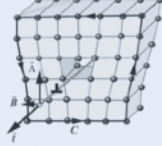
Relativistic transformations of the momentum and the torque

$$\left\{ \begin{array}{l} m_1' = m_1 \\ m_2' = (m_2 - 2\mathbf{v}np_3) / \gamma_t \\ m_3' = (m_3 + 2\mathbf{v}np_2) / \gamma_t \end{array} \right. \quad \left\{ \begin{array}{l} np_1' = np_1 \\ np_2' = (np_2 + \mathbf{v}m_3 / (2c_t^2)) / \gamma_t \\ np_3' = (np_3 - \mathbf{v}m_2 / (2c_t^2)) / \gamma_t \end{array} \right.$$



Total relativistic energies of rectilinear screw and edge dislocations



$$E_{\mathbf{v}}^{\text{vis}} = \underbrace{\frac{1}{\gamma_t} \left(1 - \frac{\mathbf{v}^2}{2c_t^2} \right) E_{\text{dist}}^{\text{vis}}}_{E_{\mathbf{v}}^{\text{dist}}} + \underbrace{\frac{1}{\gamma_t} \frac{1}{2} M_0^{\text{vis}} \mathbf{v}^2}_{E_{\mathbf{v}}^{\text{cin}}} = \frac{E_{\text{dist}}^{\text{vis}}}{\gamma_t} = \frac{M_0^{\text{vis}} c_t^2}{\gamma_t} = \frac{1}{\gamma_t} \frac{(K_2 + K_3) \Lambda^2}{\pi} \ln \frac{R_{\infty}}{R}$$


$$E_{\mathbf{v}}^{\text{coin}} = \underbrace{\frac{1}{\gamma_t} \left(1 - \frac{\mathbf{v}^2}{2c_t^2} \right) E_{\text{dist}}^{\text{coin}}}_{E_{\mathbf{v}}^{\text{dist}}} + \underbrace{\frac{1}{\gamma_t} \frac{1}{2} M_0^{\text{coin}} \mathbf{v}^2}_{E_{\mathbf{v}}^{\text{cin}}} = \frac{E_{\text{dist}}^{\text{coin}}}{\gamma_t} = \frac{M_0^{\text{coin}} c_t^2}{\gamma_t} = \frac{1}{\gamma_t} \left(\frac{K_2}{K_3} \right)^2 \frac{K_3 \bar{\Lambda}^2}{2\pi} \ln \frac{R_{\infty}}{R}$$

Figure 6.4 - The relativistic transformations of the momentum and the torque, and the total relativistic energies of rectilinear screw and edge dislocations

relativistic behavior, satisfying very exactly the famous relation of special relativity $E = E_0 / \gamma$, whereas a localized scalar load of rotation does not satisfy such a relation as we will see in the continuation,

- the total energy associated with the moving charge tends to an infinite value when the speed \mathbf{v} tends to the celerity c_t of the transverse waves as shown in figure 6.5. This behavior is generated by the presence of the term $\gamma_t = (1 - \mathbf{v}^2 / c_t^2)^{1/2}$ in the expression of energy, term which is due to the relativistic contraction of the field of rotation in the direction of the movement, imposed by the Lorentz transformation,
- the total energy $E_{\mathbf{v}}^{\text{screw}}$ associated with the moving charge is not at all energy stored in the singularity itself, but it is the movement of the singularity in the lattice which stores both potential energy $E_{\mathbf{v}}^{\text{dist}}$ of elastic distortion of the lattice and of the Newtonian kinetic energy $E_{\mathbf{v}}^{\text{cin}}$ of movement of the lattice in its vicinity,
- the fractions of the total energy being found in the form of potential elastic energy of rotation of the lattice and in the form of kinetic energy of the cells of the lattice depend on the value of the ratio \mathbf{v} / c_t as shown in figure 6.6. We see, among other things, that the energy fractions in potential form and in kinetic form become perfectly equal when the speed \mathbf{v} of a charge tends towards the celerity c_t of the transverse waves,
- the fact of obtaining exactly a relativistic behavior is due to the particularity that the term of kinetic energy $E_{\mathbf{v}}^{\text{cin}}$ is precisely compensated by an additional negative term in the potential energy $E_{\mathbf{v}}^{\text{dist}}$ in the case of a screw dislocation. We will see later that this compensation effect is not systematic, and that it essentially depends on the topology of the considered charge. We

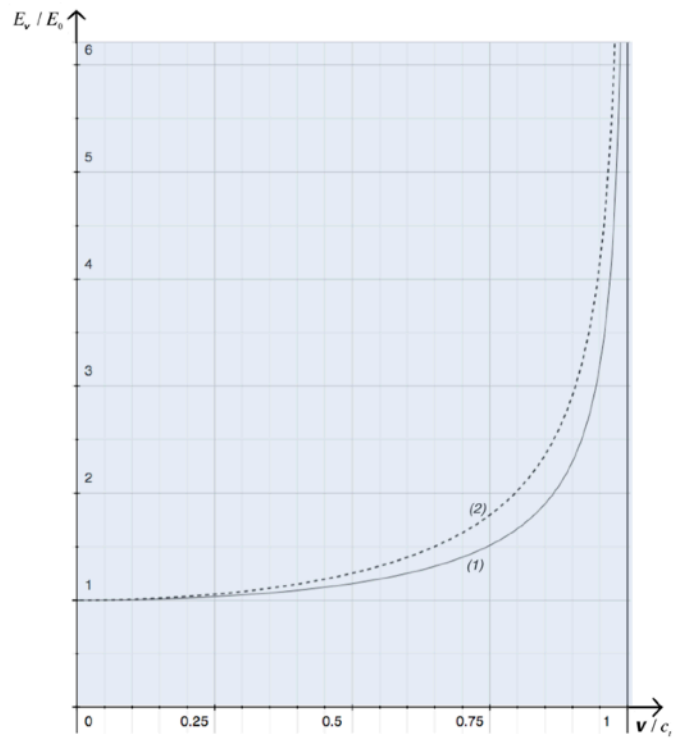


Figure 6.5 - Total energy of the charge compared to its rest energy, as a function of v / c_i , in the case of a screw or edge dislocation (1) or a spherical charge of rotation (2)

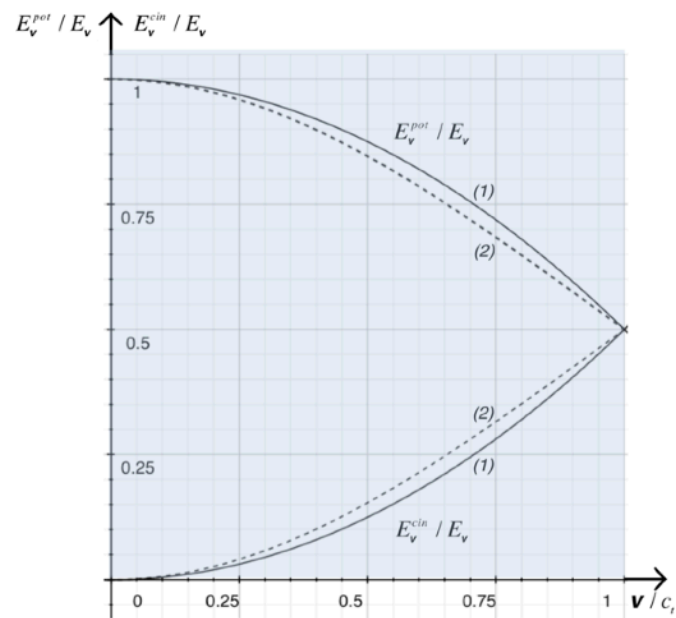


Figure 6.6 - Fractions of the total energy in potential and kinetic form, as a function of v / c_i , in the case of a screw or edge dislocation (1) or a spherical charge of rotation (2)

therefore have here a somewhat paradoxical situation, namely that *the relativistic dynamics of screw dislocations is a direct consequence of the purely Newtonian dynamics of the lattice* in the absolute space of **GO**, because it is the exact compensation of the term of Newtonian kinetic energy E_v^{cin} of the lattice by the additional negative term in the elastic potential energy E_v^{pot} which is responsible for it.

With regard to rectilinear edge dislocations, the supposition that the lattice is a perfect cosmological lattice satisfying conjecture 6, namely that $K_0 = K_3 > 0$, that $K_1 \ll K_0$ and that $K_2 \ll K_3$, and also satisfying the hypothesis $\tau_0 < \tau_{ocr}$, implies that edge dislocations in a perfect cosmological lattice are subject exactly to the same relativistic behaviors as screw dislocations. So we have in particular that $E_v^{coin} = E_{dist}^{coin} / \gamma_t$ where the energy of distortion also satisfies a real Einstein relation $E_{dist}^{edge} \equiv M_0^{edge} c_t^2$ as we have shown previously in a purely classical way. We thus obtain for the edge dislocation a completely similar expression of its total relativistic energy E_v^{edge} as in the case of the screw dislocation, as shown in figure 6.4.

Equations of the relativistic dynamics of a screw or edge dislocation

Suppose that a rectilinear screw or edge dislocation, which moves at high velocity \vec{v} in the perfect cosmological lattice, is subjected to a *Peach and Koehler force* \vec{F}_{PK} per unit of length. Due to the rectilinear geometry of the dislocation, the vectors \vec{v} and \vec{F}_{PK} can only be perpendicular to the line of dislocation. The power transmitted to the dislocation by the force \vec{F}_{PK} is obviously written $\vec{F}_{PK} \vec{v}$, and this power comes to increase the total energy E_v^{disloc} of the dislocation, so that the relativistic dynamic equation of the dislocation corresponds to equal the temporal variation of the total energy E_v^{disloc} taken along the trajectory with the power $\vec{F}_{PK} \vec{v}$ supplied to the dislocation by the Peach and Kohler force, as shown in figure 6.7.

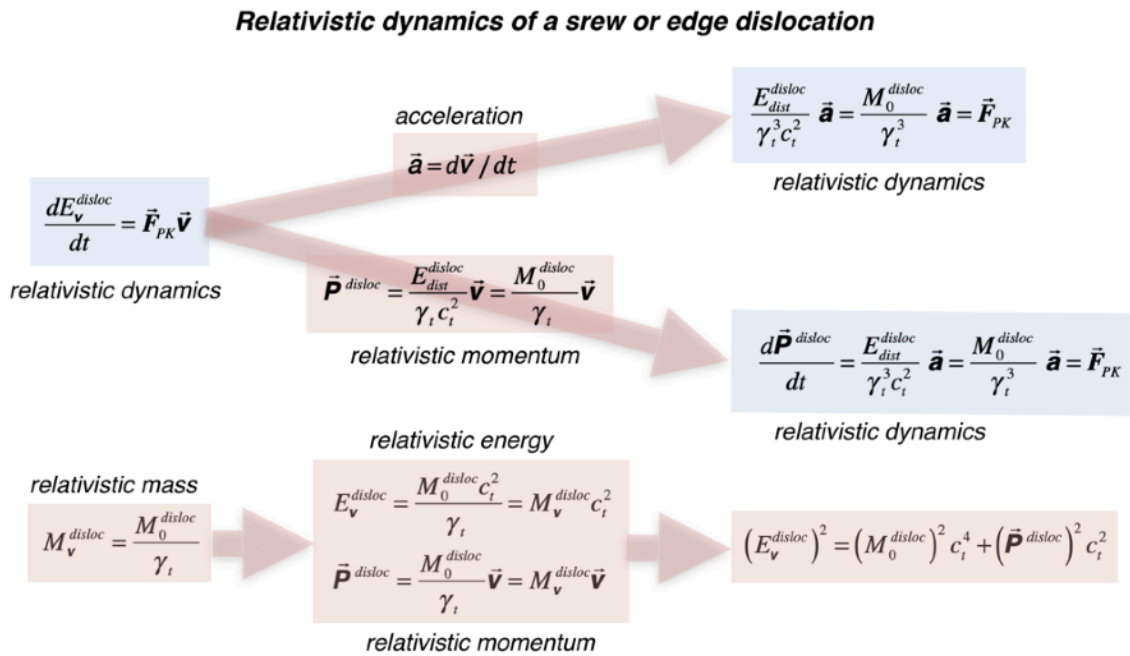


Figure 6.7 - Relativistic dynamic equations, relativistic momentum and relativistic mass of a screw or edge dislocation

But in the case of a rectilinear dislocation, the vectors \vec{v} and \vec{F}_{PK} are parallel, so that we can write a vector equation for the relativistic dynamics of the dislocation directly involving the acceleration $\vec{a} = d\vec{v}/dt$ of the dislocation. Note that the time derivative of the total energy, namely $dE_{\vec{v}}^{disloc}/dt = (\partial E_{\vec{v}}^{disloc}/\partial \vec{v})(d\vec{v}/dt) = \vec{a} \partial (E_{dist}^{disloc}/\gamma_t)/\partial \vec{v}$, must take into account the fact that the Lorentz factor γ_t also depends on the norm of \vec{v} . By introducing the relativistic momentum \vec{P}^{disloc} per unit length of the screw or edge dislocation, we can still write the relativistic dynamic equation in a different way which is shown in figure 6.7. The expression of the relativistic momentum \vec{P}^{disloc} allows us to introduce a generalized relativistic mass $M_{\vec{v}}^{disloc}$ of the dislocation in motion, which we can use to write the total energy $E_{\vec{v}}^{disloc}$ and the momentum \vec{P}^{disloc} of the dislocation. The relationships in figure 6.7 are perfectly identical to the dynamic relationships obtained in special relativity. We can also verify that the classical relation $E^2 = m^2 c^4 + p^2 c^2$ which is very known in special relativity also has its analog under the form $(E_{\vec{v}}^{disloc})^2 = (M_0^{disloc})^2 c_t^4 + (\vec{P}^{disloc})^2 c_t^2$.

A very interesting remark stands out here: the total relativistic energy $E_{\vec{v}}^{disloc}$ associated with the movement of the dislocation is the sum of the potential energy $E_{\vec{v}}^{dist}$ of elastic deformation of the lattice and the Newtonian kinetic energy $E_{\vec{v}}^{cin}$ of movement of the lattice.

But by associating the total relativistic energy $E_{\vec{v}}^{disloc}$ with this moving string, and knowing that the energy at rest of this string is given by E_{dist}^{disloc} , we could also consider that the energy of the moving string is equal to the sum of its rest energy E_{dist}^{disloc} and an energy of movement E_{mvt}^{disloc} which corresponds to the additional energy generated by its displacement within the medium, namely $E_{mvt}^{disloc} = E_{\vec{v}}^{disloc} - E_{dist}^{disloc} = (M_{\vec{v}}^{disloc} - M_0^{disloc})c_t^2 = M_0^{disloc}(1/\gamma_t - 1)c_t^2$.

In special relativity, this motion energy E_{mvt}^{disloc} is often called *the kinetic energy T of the particle*. But in the case of the dislocation considered here, we know that it is not really a kinetic energy since $E_{mvt}^{disloc} = E_{\vec{v}}^{disloc} - E_{\vec{v}}^{cin} - E_{dist}^{disloc} = E_{\vec{v}}^{cin} + (1/\gamma_t - \vec{v}^2/2\gamma_t c_t^2 - 1)E_{dist}^{disloc}$ is in fact a combination of real kinetic energy $E_{\vec{v}}^{cin}$ and potential energy $(1/\gamma_t - \vec{v}^2/2\gamma_t c_t^2 - 1)E_{dist}^{disloc}$ of the dislocation.

Finally, if we calculate the total energy for low speeds ($\vec{v} \ll c_t$), we obtain the relation $E_{\vec{v}}^{disloc} \cong E_{dist}^{disloc} + M_0^{disloc} \vec{v}^2/2 + \dots$ and we find the classical kinetic energy linked to the mass of inertia at rest M_0^{disloc} of the dislocation.

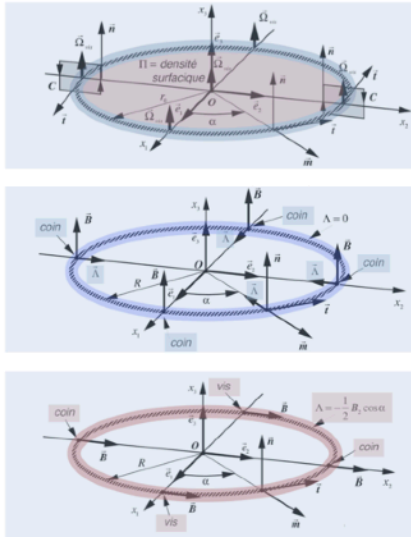
Relativistic energies of loop singularities and spherical charges of rotation

We saw in the previous chapter that the topological singularities in loops in a *perfect cosmological lattice* also all satisfy Einstein's relation $E_{dist}^{loop} = M_0^{loop} c_t^2$ which was obtained from a classical calculation of their elastic energy of distortion and their kinetic energy. This implies that the relativistic energy of the singularities in loops is deduced in an identical way that we deduced the relativistic energy of an edge dislocation above. Consequently, one deduces the relativistic energies indicated in figure 6.8 for the singularities in loops in a perfect cosmological lattice, namely *the twist disclination loop*, *the prismatic edge dislocation loop* and *the slip mixed dislocation loop*.

We also deduce that, in a perfect cosmological lattice, the relativistic dynamic equation of a loop singularity is perfectly identical to that of a screw or edge dislocation, as shown in figure 6.7, namely $d\vec{P}^{loop}/dt = \vec{F}^{loop}$ in which \vec{F}^{loop} is the force acting globally on the loop and \vec{P}^{loop} is the amount of relativistic momentum of the loop, given by $\vec{P}^{loop} = M_0^{loop} \vec{v} / \gamma_t$.

Let us now consider a localized spherical charge of rotation, like that described in figure 5.4, which moves along the axis Ox_1 at velocity \vec{v} . In the mobile frame of reference $O'x_1'x_2'x_3'$ with the charge, we can use the relativistic transformation relationships of momentum $n\vec{p}$ and torque \vec{m} of figure 6.4, as well as the Lorentz transformation relationships of figure 6.1 to deduce the potential energy density $F_{dist}^{Q_\lambda}$ and the kinetic energy density $F_{cin}^{Q_\lambda}$ in $Ox_1x_2x_3$. The total relativistic energy $E_v^{Q_\lambda}$ is then calculated by integration over the entire lattice volume, and we obtain the energy reported in figure 6.8, which again consists of a relativistic potential energy $E_{pot}^{Q_\lambda}$ and a relativistic kinetic energy $E_{cin}^{Q_\lambda}$.

Relativistic energies of loop singularities

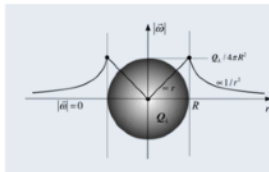


$$E_v^{BV} = \underbrace{\frac{1}{\gamma_t} \left(1 - \frac{v^2}{2c_t^2} \right) E_{dist}^{BV}}_{E_v^{dist}} + \underbrace{\frac{1}{\gamma_t} \frac{1}{2} M_0^{BV} v^2}_{E_v^{cin}} = \frac{E_{dist}^{BV}}{\gamma_t} = \frac{M_0^{BV} c_t^2}{\gamma_t}$$

$$E_v^{BC} = \underbrace{\frac{1}{\gamma_t} \left(1 - \frac{v^2}{2c_t^2} \right) E_{dist}^{BC}}_{E_v^{dist}} + \underbrace{\frac{1}{\gamma_t} \frac{1}{2} M_0^{BC} v^2}_{E_v^{cin}} = \frac{E_{dist}^{BC}}{\gamma_t} = \frac{M_0^{BC} c_t^2}{\gamma_t}$$

$$E_v^{BM} = \underbrace{\frac{1}{\gamma_t} \left(1 - \frac{v^2}{2c_t^2} \right) E_{dist}^{BM}}_{E_v^{dist}} + \underbrace{\frac{1}{\gamma_t} \frac{1}{2} M_0^{BM} v^2}_{E_v^{cin}} = \frac{E_{dist}^{BM}}{\gamma_t} = \frac{M_0^{BM} c_t^2}{\gamma_t}$$

Relativistic energy of a localized rotation charge



$$E_v^{Q_\lambda} = \underbrace{\frac{1}{\gamma_t} \left(1 - \frac{v^2}{3c_t^2} \right) E_{dist}^{Q_\lambda}}_{E_{pot}^{Q_\lambda}} + \underbrace{\frac{1}{\gamma_t} \frac{2v^2}{3c_t^2} E_{dist}^{Q_\lambda}}_{E_{cin}^{Q_\lambda}} = \frac{1}{\gamma_t} \left(1 + \frac{v^2}{3c_t^2} \right) \underbrace{\frac{3(K_2 + K_3)Q_\lambda^2}{5\pi R}}_{E_{dist}^{Q_\lambda}}$$

Figure 6.8 - relativistic energies of loop singularities
and of localized rotation charges

By the term γ_t in the denominator, we find here a behavior of the total energy $E_v^{Q_\lambda}$ of the charge similar to that of a relativistic behavior since it tends towards an infinite value when the speed \mathbf{v} tends towards the celerity c_t of the transverse waves as shown well by figure 6.5 in which one carried over $E_v^{Q_\lambda} / E_{dist}^{Q_\lambda}$ according to \mathbf{v} / c_t .

As in the case of a screw or edge dislocation, the total energy is found in the form of relativistic elastic potential energy $E_{pot}^{Q_\lambda}$ of rotation of the lattice and in the form of relativistic kinetic energy $E_{cin}^{Q_\lambda}$ of the cells of the lattice, and the fractions of each of these energies depend on the value of the ratio \mathbf{v} / c_t as shown in figure 6.6. It can be seen that these

fractions of energy in potential form and in kinetic form here also become perfectly equal when the speed \mathbf{v} of the localized charge tends towards the celerity c_t of the transverse waves.

However, the expression of total energy $E_{\mathbf{v}}^{Q_\lambda}$ is not this time in perfect agreement with classic relativistic behavior because $E_{\mathbf{v}}^{Q_\lambda} \neq E_{dist}^{Q_\lambda} / \gamma_t$. This disagreement is to be associated with the fact that the additional negative term in potential energy no longer exactly compensates for the kinetic energy term, since the kinetic energy term is twice greater than the absolute value of the additional term in potential energy. If we calculate the total energy $E_{\mathbf{v}}^{Q_\lambda}$ for low speeds ($\mathbf{v} \ll c_t$) by developing the term γ_t in the denominator, we obtain the following relation $E_{\mathbf{v}}^{Q_\lambda} \cong E_{dist}^{Q_\lambda} (1 + \mathbf{v}^2 / 2c_t^2 + \dots)(1 + \mathbf{v}^2 / 3c_t^2) \cong E_{dist}^{Q_\lambda} + 5E_{dist}^{Q_\lambda} \mathbf{v}^2 / 6c_t^2 + \dots$. In this case, the energy of the moving charge is therefore equal to its rest energy and to a second energy term proportional to the speed of the charge squared, and which can be assimilated to a *kinetic energy term of the charge*. One can consequently allot a *mass of inertia at rest* M_0 to the spherical charge of rotation, and the relation of Einstein is written $E_{dist}^{Q_\lambda} \cong 3M_0 c_t^2 / 5$. It can therefore be seen that the relationship between energy at rest and mass of inertia for a spherical rotation charge Q_λ deviates somewhat from Einstein's famous relation of special relativity, which states that $E_0 = M_0 c^2$.

About the probable explanation of the paradox of the electron energy

We find with the relation $E_{dist}^{Q_\lambda} \cong 3M_0 c_t^2 / 5$ for a localized singularity of rotation a famous paradox of classical electromagnetism. Indeed, the same type of calculation carried out in classical electromagnetism to find the energy stored by the electric field of a moving electron gives a result quite similar to this one, namely that $E_{electromagnetic}^{relativistic} \neq E_{electrical\ field}^{at\ rest} / \gamma$, and therefore that the mass associated with *the electromagnetic fields of the electron does not satisfy the principles of special relativity*. This famous result in electromagnetism has caused a lot of ink to flow and has been the subject of much discussion. Several models have been proposed to explain it, without much success elsewhere. We can consider in fact that it was never really understood within the framework of the classical theory of electromagnetism and special relativity. A detailed discussion of this subject can be found in the famous physics lesson of R. P. Feynman¹.

This famous *paradox of the electrical energy of the electron* could find here a simple explanation, if we suppose that the electron also has an annular structure² similar to a loop of twist disclination, or to a loop of screw pseudo-dislocation and that the electric field of the electron is the analog of the field of rotation. In fact, the expression of the relativistic energy of a twist disclination loop perfectly satisfies Einstein's expression $E_{\mathbf{v}} \cong E_0 / \gamma_t$, so that if the electron presented the topological structure of the twist disclination loop in a cosmological lattice, we would have a localized charge q_λ of rotation which would present a divergent field $\vec{\omega}^{el}$ of rotation at a great distance just as the electron presents a divergent electric field \vec{E}^{el} ,

¹ Richard P. Feynman, *The Feynman Lectures on Physics*, Addison-Wesley Publ. Company, 1970, chap. 28

² The idea of a ring-shaped electron was first proposed in 1915 by Parson (Smithsonian miscellaneous collections, nov. 1915) and then developed by Webster (Amer. Acad., janv. 1915) and Allen (Phil. Mag., 4, 1921, p. 113), and the proposal that an electron could be similar to a twist disclination loop was proposed in 1996 by Unziker (arXiv:gr-qc/9612061v2).

and which would satisfy at low speed ($\mathbf{v} \ll c_t$) the relation of the special relativity since for a screw loop one has well the relation $E_{dist}^{BV} = M_0^{BV} c_t^2$.

Peach and Koehler force and relativistic force of Lorentz

In Chapter 2, we introduced the *Peach and Koehler force* $\vec{f}_{PK} = \lambda \vec{m} + \vec{v} \wedge \vec{A}$ which acts through the field \vec{m} on the unit of volume of rotation charges with charge density λ . In this relation, the term $\lambda \vec{m}$ is the analog of the electric force $\vec{f} = \rho \vec{E}$ acting per unit of volume on a density ρ of electric charge in the Maxwell equations of electromagnetism, whereas the term $\vec{v} \wedge \vec{A}$ had been introduced to take account of the forces which do not produce work. For a density λ of charges moving at velocity \vec{v} along the axis Ox_1 , the force density acting in the frame $O'x_1'x_2'x_3'$ linked to the charge is therefore written, since the charge is immobile in this frame and that, consequently, $\vec{v} = 0$ in this frame, under the form $\vec{f}'_{PK} = \lambda \vec{m}'$. We can therefore find the force per unit of volume acting on the same charge density which moves at velocity \vec{v} in the stationary frame of reference $Ox_1x_2x_3$, using the relativistic transformation relations of momentum $n\vec{p}$ and torque \vec{m} , and we obtain quite easily the next expression $\vec{f}_{PK} = \lambda m_1 \vec{e}_1 + \lambda (m_2 \vec{e}_2 + m_3 \vec{e}_3) / \gamma_t + 2\lambda (\vec{v} \wedge n\vec{p}) / \gamma_t$ for this force. In the case where $|\vec{v}| \ll c_t$, γ_t becomes close to unity and the force per unit of volume in the stationary frame $Ox_1x_2x_3$ simply becomes equal to $\vec{f}_{PK} \cong \lambda \vec{m} + 2\lambda (\vec{v} \wedge n\vec{p})$, which is the perfect analog of the electromagnetic force of Lorentz $\vec{f}_L = \rho \vec{E} + \vec{j} \wedge \vec{B} = \rho (\vec{E} + \vec{v} \wedge \vec{B})$. The term $2\lambda (\vec{v} \wedge n\vec{p})$ in force \vec{f}_{PK} is nothing other than the term $\vec{v} \wedge \vec{A}$ we introduced in figure 2.38 to account for non-working forces, so that the vector \vec{A} now has a known value, which is worth $\vec{A} = 2\lambda n\vec{p}$.

We can then apply the relation giving \vec{f}_{PK} to the various topological singularities of the cosmological lattice:

- in the case of a rectilinear screw dislocation, the integration of the relation on the unit of length of the dislocation gives the force $\vec{F}_{PK} = \Lambda \vec{m} + 2\Lambda (\vec{v} \wedge n\vec{p})$ acting on the unit of length of dislocation. However, if a rectilinear screw dislocation moves in a solid, its velocity \vec{v} is necessarily perpendicular to the line of dislocation, and the force \vec{F}_{PK} will have action only if it is also perpendicular to the line, so that only the component $n\vec{p}$ in the direction of the string can give a force \vec{F}_{PK} capable of acting on the dislocation.

- in the case of a spherical rotation charge Q_λ , the relationship giving \vec{f}_{PK} can be integrated on the volume of the charge, and we obtain the total force acting on the rotation charge which is worth $\vec{F}_{PK} = Q_\lambda \vec{m} + 2Q_\lambda (\vec{v} \wedge n\vec{p})$.

- in the case of a twist disclination loop of charge $q_{\lambda BV} = 2\pi R \Lambda_{BV} = -\pi R \vec{B}_{BV} \vec{t}$, we can apply the relation giving \vec{f}_{PK} , which allows us to write $\vec{F}_{PK} = q_{\lambda BV} \vec{m} + 2q_{\lambda BV} (\vec{v} \wedge n\vec{p})$ for the force acting on the loop.

The last two relationships correspond directly to the expression of the electromagnetic force $\vec{F} = q(\vec{E} + \vec{v} \wedge \vec{B})$ acting on a moving electric charge q .

About the role of «ether» played by the cosmological lattice

We have seen that the displacement of a topological singularity in the frame of reference $Ox_1x_2x_3$ of a perfect cosmological lattice, at velocity \vec{v} in the direction of the axis Ox_1 , can be described in a frame $O'x_1'x_2'x_3'$ mobile with the singularity thanks to the Lorentz

transformation. At constant volume expansion, a cluster of mobile singularities within the lattice, formed for example by a set of localized singularities like dislocation and disclination loops interacting with each other via their fields of rotation, is subjected to exactly *the same Lorentz transformation, with all the properties which are allotted to it like the dilation of time and the contraction of the lengths*, since the field of rotation which provides the interactions between the singularities satisfies this transformation.

There is obviously a strong mathematical analogy between the Lorentz transformation applied here for the transmission of information and interactions via transverse waves within the cosmological lattice and the Lorentz transformation of the special relativity applied to describe the relativistic dynamics of moving objects in the Universe in relation to the speed of light. But there is also a very serious physical difference between these two theories, linked above all to the existence of an "*ether*" for topological singularities, which is in fact the lattice and which gives a privileged status to fixed singularities in the lattice comparatively to mobile singularities inside the network, whereas in theory of special relativity, all mobile objects have the same status, hence the famous name of "*relativity*". This essential difference makes it possible to shed entirely new and original light on the phenomena of relativity. This is what we will discuss later.

The dynamics of singularities within a cosmological lattice differs from special relativity by the very existence of the lattice which acts as an *absolute reference* for the movement of singularities and as an *ether* for the propagation of transverse and longitudinal waves. Unlike special relativity, the lattice can be described from the outside by a **GO** observer (*Imaginary Great Observer*) which has a universal clock and universal rulers in the absolute frame of reference $Q\xi_1\xi_2\xi_3$. This observer outside the lattice is not subject to any speed of information propagation constraint, so that he is the only one able to observe qualitatively, quantitatively and exactly *the notion of instantaneous events occurring within the lattice*.

We can also imagine a completely different type of observer. These are the local observers **HS** (*Homo Sapiens*), which are *an integral part of the lattice* and which would themselves consist of topological singularities of the lattice. These particular observers then have a very different status from the **GO** observer since they are *an integral part of the lattice* and that they can move around there. But these observers are required to transmit information from one point to another on the lattice at the finite speed of transverse waves or longitudinal waves. A **HS** observer therefore has no access to an absolute definition of the simultaneity of events such as that of the **GO**, but only has a relativistic definition of simultaneity, which depends in particular on its velocity \vec{V} of movement relative to the lattice and the local value of the volume expansion of the lattice.

For reasons of convenience, the external observer **GO** can obviously choose, as universal rulers and universal clock, the rulers and the clock of an **HS** observer stationary with respect to the lattice, and which would be located at a place on the lattice which would be stationary and of zero volume expansion ($\tau = 0$).

All **HS** observers are provided with a local reference frame which has rulers and its own clock, which seem immutable for this **HS**, while the length of its rulers and the speed of counting the time of its clock actually vary in the absolute reference frame of the **GO** as a function of the volume expansion of the lattice at the location where it is located (we will come back to this

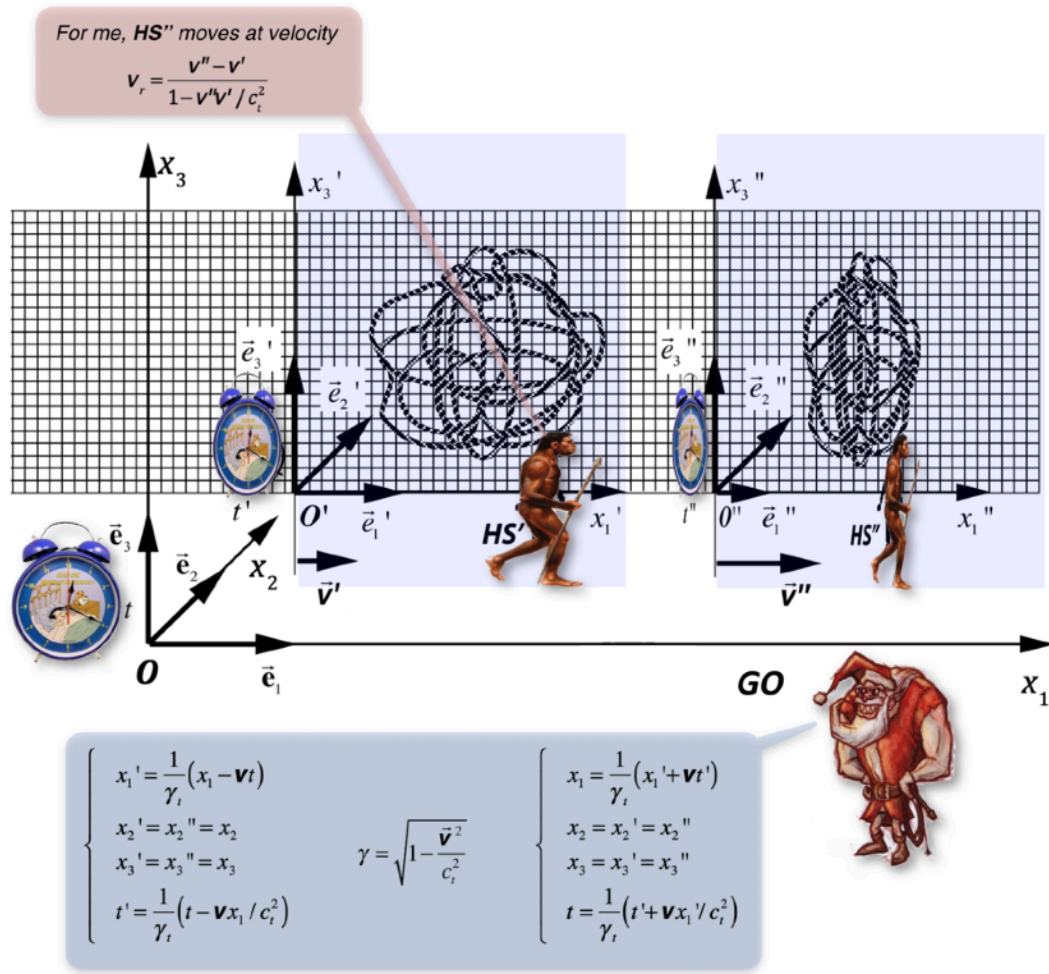


Figure 6.9 - The mobile Lorentz frames of the moving observers HS' and HS''

point in detail later) and its velocity \vec{v} relative to the lattice. Consequently, the HS does not have direct access to the value of the local volume expansion of the lattice or to its own velocity \vec{v} of displacement relative to the lattice. Only the GO has direct access to this type of information.

The Lorentz transformations that we have defined are therefore in reality tools of the GO , which can be used without problem to determine the rulers and local clocks of all the HS s attached to the lattice, or simply to calculate the various fields associated with topological singularities in motion within the lattice. And it can apply these transformations to any place on the lattice where it is possible to find a state of homogeneous and constant expansion, which may very well be different from zero expansion since the Lorentz transformations are based on the transmission speed of transverse waves, which is perfectly determined whatever the state of expansion of the lattice ($c_t(\tau) = c_{t0} e^{\tau/2}$). From this point of view, our interpretation of Lorentz transformations is quite far from the interpretation of special relativity, for which these transformations are tools that any HS observer can use to move from one referential to another referential in motion by compared to the first, and for which the speed of light is an absolute constant. The main consequences of these essential differences will be analyzed in detail later

in this chapter.

The Lorentz transformations imply that, for singularities moving at velocity \vec{V} in the direction Ox_1 , the ruler according to the direction Ox_1 is shortened by a factor γ_t , so that $\vec{e}_1' = \gamma_t \vec{e}_1$. To interpret this shortening of the ruler in the direction of movement, we have to imagine the architecture of the cluster as a set of topological singularities linked together by their interactions via their respective fields of rotation (figure 6.9). These singularities of the lattice move relative to the lattice at velocity \vec{V} in the direction Ox_1 , and the finiteness of the speed c_t of their interactions via the rotation field requires that the complete architecture of the cluster of singularity contracts in the direction Ox_1 .

But this contraction does not affect the lattice, which retains its original volume expansion state, which is shown in figure 6.9 for the case of two clusters of identical singularities which move at two different velocities, \vec{V}' and \vec{V}'' , measured compared to the lattice by the **GO** observer. Thus, the relativistic effects on the rulers of observers **HS'** and **HS''**, associated with the collective movement of singularities with respect to the lattice, have nothing to do with effects of volume expansion of the lattice, for which the modifications of the lengths observer rulers **HS'** and **HS''** will be associated with real variations in the cell parameter of the cosmological lattice as we will see later.

Note also that these two effects are cumulative, namely that the rulers of an **HS** observer can be contracted or expanded by variations in volume expansion of the lattice and still contracted by a movement of the cluster of singularities with respect to the lattice. In this way, the contraction-expansion of the rulers and the clock of an **HS** observer depends on both the local expansion of the lattice and the velocity \vec{V} of **HS** relative to the lattice.

In addition, in the Lorentz transformation applied by the **GO** observer, the value of $\gamma_t = (1 - \mathbf{V}^2 / c_t^2)^{1/2}$ is not only related to the velocity \vec{V} of **HS** with respect to the lattice, but also to the local celerity c_t of the transverse waves, which depends on the volume expansion of the cosmological lattice, since $c_t|_{\tau \neq 0} = c_{t0}|_{\tau=0} e^{\tau/2}$.

The phenomenon of slowing down of the clock of the observer **HS** which moves relative to the lattice has already been explained, with figures 6.3 (a) and (b). Imagine that there is an observer **HS'** who builds his own clocks in his reference frame $O'x_1'x_2'x_3'$, by fixing two mirrors facing each other at a distance d_0 from each other, mirrors which have the property of reflecting transverse waves. By sending a transverse wave between the two mirrors, **HS'** can perfectly use, as a time base, the period of time $T_0 = 2d_0 / c_t$ that elapses between a round trip of the wave between the two mirrors, because the distance d_0 and the celerity c_t of transverse waves are for him constants. If the **HS'** observer is initially at rest relative to the lattice, the **GO** can consider the time lapse $T_0 = 2d_0 / c_t$ as its own time base in $Ox_1x_2x_3$.

Now imagine that the observer **HS'** moves relative to the lattice with velocity \vec{V} in the direction Ox_1 , and that he places two clocks in quadrature, that is to say a clock having its two mirrors in the direction Ox_1' and a second clock having its two mirrors along the axis Ox_3' (or Ox_2'). In principle, in its frame $O'x_1'x_2'x_3'$, the time span $T_0 = 2d_0 / c_t$ measured by **HS'** with its two clocks is exactly the same.

Now let's take the **GO** point of view. We have shown that the base time of the mobile clock of the observer **HS'** in $O'x_1'x_2'x_3'$, measured by the observer **GO** in its absolute frame of reference $Ox_1x_2x_3$, appears dilated as a function of the velocity \vec{V} of a factor $1/\gamma_t$, in an

identical manner for the two clocks in quadrature, so that $T = T_0 / \gamma_t$. This means that a local time t' actually exists for the observer **HS'**, that this local time elapses more slowly for an observer **HS'** in movement relative to the lattice, and that this local time t' remains isotropic in $O'x_1'x_2'x_3'$, regardless of the direction of movement of the observer **HS'** within the lattice.

Concerning the dilation or contraction of time, there can also be coupling between the relativistic effects and the effects of volume expansion. We will see for example later that, in the case of a cosmological lattice, an observer **HS'** which would be placed in a zone of strong volume contraction ($\tau \ll 0$) would present a proper time very strongly slowed compared to the proper time of the **GO**. In addition, if it were still moving at a speed \mathbf{v} close to c_t with regard to the lattice, its proper time would be even more significantly slowed down compared to the **GO's** proper time.

Experiment of Michelson-Morley in the cosmological lattice

The network plays the same role vis-à-vis the singularities and the propagation of transverse waves as the famous "ether" supposedly propagating light waves and so much discussed at the beginning of the XXth century. The Michelson-Morley experiment, which consisted in trying to measure, using an interferometer, a difference in the speed of propagation of light waves in the direction of a displacement of the interferometer at velocity \vec{v} and transversely to the direction of this displacement, has gave negative results, and it was concluded at the time that there was no ether. But in the two examples above, the calculation proposed in the solid lattice with two local clocks in quadrature shows that the result is identical to that obtained by Michelson-Morley, namely that there is no time difference from travel in the two perpendicular directions, which the **HS** obviously interprets as the fact that the speed of propagation does not depend on the direction in which it is measured. But in the case that we have treated here, there is indeed an ether constituted by the lattice within which the singularities move, and which is perfectly known by the **GO**.

We deduce that, in the case of the solid lattice acting as an ether, the singularities which move at velocity \vec{v} have effectively their own clock which slows down since the **GO** measures a clock time T_0 with the **HS** clock stationary compared to the network, but a time $T = T_0 / \gamma_t$ with the clock of an **HS** which moves at velocity \vec{v} compared to the lattice.

On the other hand, if an **HS'** measures the speed c_t' of a transverse wave in its moving frame of reference $O'x_1'x_2'x_3'$, with its own rulers and clock, it finds exactly the same value as that measured by the **GO** in the lattice, since we have in the direction Ox_1' that $c_t' = 2d_0 / T = (2d / \gamma_t) / (T / \gamma_t) = 2d / T = c_t$.

The relativistic composition of velocities and the absence of an absolute notion of simultaneity for the local observers HS

In figure 6.9, two frames have been shown in translation along the axis Ox_1 at velocities \vec{v}' and \vec{v}'' measured by the **GO** observer. One may wonder how translates the relativity of the velocities measured by the **HS**, and in particular what is the relative velocity \vec{v}_r that the observer **HS'** measures in his reference frame $O'x_1'x_2'x_3'$ for the displacement of the reference frame $O''x_1''x_2''x_3''$ of the observer **HS''**. For **GO**, the point O'' of the frame of **HS''**

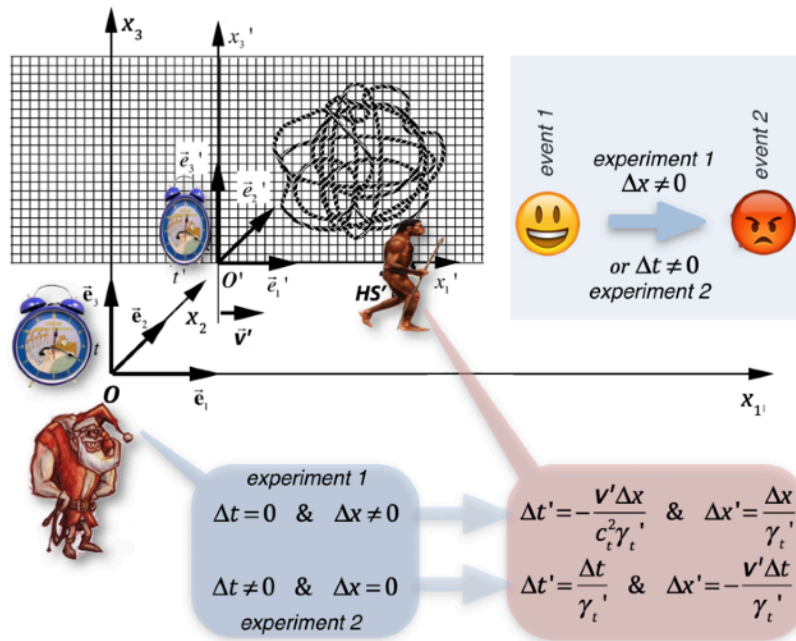


Figure 6.10 - The non-simultaneity of the events of **GO** for the moving observers **HS'**

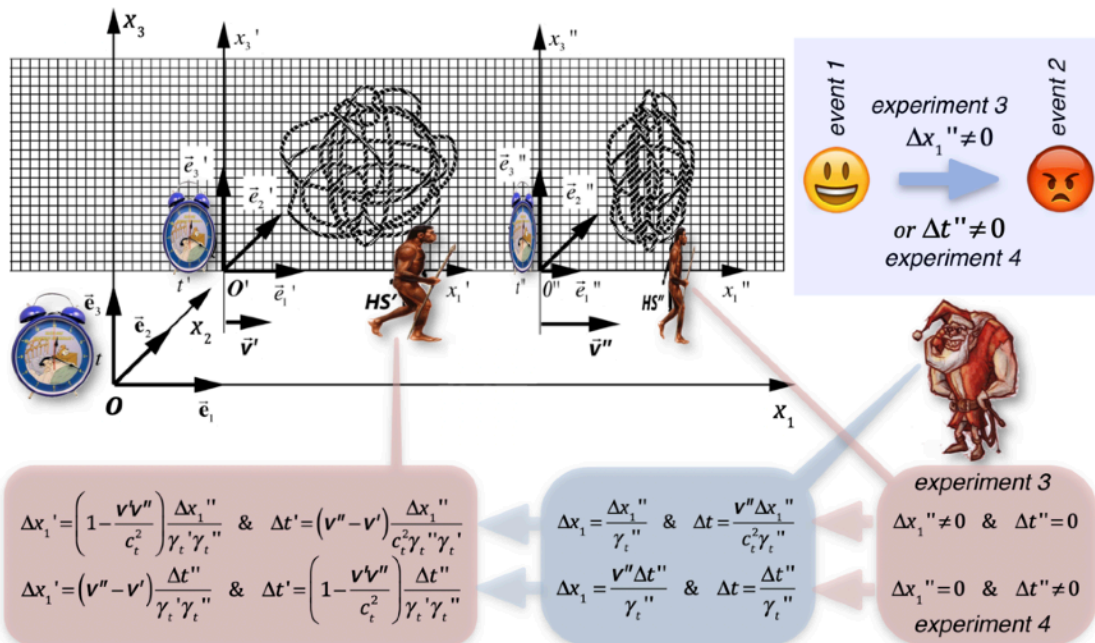


Figure 6.11 - The non-simultaneity of the events for the moving observers **HS'** and **HS''**

moves in $Ox_1x_2x_3$ from $x_1^{(1)}$ to $x_1^{(2)}$ in a time lapse that goes from t_1 to t_2 , so the norm of velocity \vec{v}'' is worth $v'' = (x_1^{(2)} - x_1^{(1)}) / (t_2 - t_1)$.

If HS' observes this same displacement, it finds a relative velocity \vec{v}_r whose norm is worth $v_r = (x_1^{(2)'} - x_1^{(1)'}) / (t_2' - t_1')$. This expression can then be transformed using the Lorentz relations of figure 6.9, and there comes the expression of the relative velocity \vec{v}_r of movement of the observer HS'' as measured by the observer HS' and expressed under the form $v_r = (v'' - v') / (1 - v''v' / c_t^2)$ according exclusively to the velocities \vec{v}' and \vec{v}'' measured by the GO . The relative velocity of the frame $O''x_1''x_2''x_3''$ measured by HS' corresponds to what is called *the classical relativistic composition of velocities*. By symmetry, the relative velocity of the frame $O'x_1'x_2'x_3'$ measured by HS'' will be given by exactly the same expression with a change of sign.

The observers linked to the lattice do not in fact have access to the absolute notion of simultaneity that the GO can have. To illustrate this point, we can imagine four very simple experiments:

1st experiment: let us consider two simultaneous events observed by GO in the frame of reference $Ox_1x_2x_3$ at the time $t = 0$ at the coordinates $x_1^{(1)} = 0$ and $x_1^{(2)} = \Delta x_1$, therefore distant from Δx_1 (figure 6.10). These two simultaneous events are then observed by an HS' in its reference frame $O'x_1'x_2'x_3'$ moving at velocity \vec{v} in the direction Ox_1 at the coordinates $(x_1^{(1)'} = 0, t_1' = 0)$ and $(x_1^{(2)'} = \Delta x_1 / \gamma_t, t_2' = -v\Delta x_1 / (c_t^2 \gamma_t))$, obtained by the Lorentz transformations reported in figure 6.9. We therefore observe that the two events are not observed as simultaneous by the HS' , but separated by a non-zero time interval $\Delta t' = t_2'$, and the distance measured by the HS' between the two events is equal to $\Delta x_1' = x_1^{(2)'} = \Delta x_1 / \gamma_t$ which is greater than the distance measured by the GO , and which is the consequence of the contraction of the ruler \vec{e}_1' of HS' in the direction Ox_1 .

2nd experiment: consider an event occurring at the origin of the GO reference frame $Ox_1x_2x_3$ and which extends from $t_1 = 0$ to $t_2 = \Delta t$, therefore over an absolute period of time Δt (figure 6.10). This event is then observed by an HS' in its coordinate system moving at velocity \vec{v} in the direction Ox_1 at the coordinates $(x_1^{(1)'} = 0, t_1' = 0)$ and $(x_1^{(2)'} = -v\Delta t / \gamma_t, t_2' = \Delta t / \gamma_t)$, obtained using the Lorentz relations of figure 6.9. We note that the event seems to move in the frame of HS' over a distance $\Delta x_1' = |x_1^{(2)'}| = v\Delta t / \gamma_t$, longer than the absolute course $v\Delta t$ of the frame $O'x_1'x_2'x_3'$ in the lattice, due to the contraction of the ruler \vec{e}_1' used by HS' , and that the lapse of time that the event lasts for HS' is worth, and therefore seems longer for HS' than for GO , which is at first sight rather strange since the clock of HS' rotates more slowly than that of GO . This phenomenon is due to the flight times taken by the transverse waves to reach the HS' in movement relative to the lattice. This last experiment clearly shows that the time intervals measured by HS' are relative intervals since they depend on the finite speed of propagation of information within the lattice.

3rd experiment: let us now consider two simultaneous events in the mobile coordinate system $O''x_1''x_2''x_3''$ of HS'' , at the coordinates $x_1^{(1)''} = 0$ and $x_1^{(2)''} = \Delta x_1''$, and occurring at the moment $t'' = 0$ (figure 6.11). In the stationary frame of reference $Ox_1x_2x_3$ with respect to the lattice, the coordinates of these two events become two distinct events in time, the intervals between them being written $\Delta x_1 = \Delta x_1'' / \gamma_t''$ and $\Delta t = v''\Delta x_1'' / (c_t^2 \gamma_t'')$. These relations can be used now to obtain the coordinates of the two events in the reference

frame of **HS'**, which can then be clarified in the form of a spatial distance $\Delta x_1'$ and a time interval $\Delta t'$ between the two events, represented in the figure 6.11. The two simultaneous events distant from $\Delta x_1''$ in the frame $O''x_1''x_2''x_3''$ of **HS''** become two non-simultaneous events in the frame $O'x_1'x_2'x_3'$ of **HS'**.

4th experiment: let us now consider *two successive events in the mobile coordinate system $O''x_1''x_2''x_3''$, occurring at the same place at the coordinate $x_1^{(1)''} = 0$ and occurring at times $t_1'' = 0$ and $t_2'' = \Delta t''$* (figure 6.11). In the motionless frame of reference $Ox_1x_2x_3$, the coordinates of these two events become two distinct events in space which can be used to obtain the coordinates of the two events in the reference frame $O'x_1'x_2'x_3'$ of **HS'**, which can be clarified in the form of a spatial distance $\Delta x_1'$ and a time interval $\Delta t'$ between the two events as shown in Figure 6.11. The two events occurring at the origin of the **HS''** frame $O''x_1''x_2''x_3''$ therefore become two separate events in the space of the **HS'** frame $O'x_1'x_2'x_3'$.

Doppler-Fizeau effects between moving singularities in the cosmological lattice

In figures 6.12 and 6.13, we have reported several experiments of exchanging signals at a given frequency between singularities in motion within the lattice via transverse waves. By taking the **GO** point of view, it is possible to easily describe these experiments which reveal the Doppler-Fizeau phenomenon. It is obviously assumed that all these experiments take place in a lattice with a homogeneous and constant value of the volume expansion, without which the description of these experiments would become much more complex.

1st experiment: an observer **HS'** in the reference frame $O'x_1'x_2'x_3'$ moving at velocity \vec{v}' relative to the lattice in the direction Ox_1 emits a wave at the frequency f_e' , measured with his own clock, towards an observer **HS** in a stationary frame of reference $Ox_1x_2x_3$ relative to the lattice (figure 6.12a). The transverse wave emitted in $O'x_1'x_2'x_3'$ is written simply $\vec{\omega} = \vec{\omega}_0 \sin(\omega' t' - k' x_1')$ with $f_e' = \omega' / 2\pi$ and $k' = \omega' / c_t$. In the reference frame $Ox_1x_2x_3$, the same wave is obtained by replacing the coordinates t' and x_1' of **HS'** by the coordinates t and x_1 of **HS**, using the Lorentz transformations of figure 6.9, and identifying the wave vector and the pulsation obtained with those of the expression of the wave $\vec{\omega} = \vec{\omega}_0 \sin(\omega t - k x_1)$ in the frame of reference $Ox_1x_2x_3$, and we find the relations giving ω and k from the values of ω' and k' in the frame of reference $O'x_1'x_2'x_3'$, in the form $\omega = (\omega' + k' v') / \gamma_t'$ and $k = (k' + \omega' v' / c_t^2) / \gamma_t'$. As $k' = \omega' / c_t$ and $f_e' = \omega' / 2\pi$, we deduce the relationship between the frequency f_e' of the signal sent by **HS'** and the frequency f_r of the received signal measured by **HS** with its own clock, as shown in figure 6.12a.

For $v' > 0$, that is to say when **HS'** approaches **HS**, the frequency f_r of the signal received by **HS** is higher than the frequency f_e' of the signal transmitted by **HS'**. This is the *Doppler-Fizeau effect*, and in the usual jargon of physicists, we speak of a "signal shifted towards blue". Otherwise, if **HS'** moves away from **HS** ($v' < 0$), the received signal is of frequency f_r lower than the frequency f_e' of the transmitted signal, and one speaks about a "signal shifted towards red". In the form shown in figure 6.12a, the relation shows the term $(1 - v' / c_t)^{-1}$ of the purely classical Doppler effect, but which applies to a transmitted frequency $\gamma_t' f_e'$, which is nothing other than the frequency of the signal transmitted by **HS'**, but measured by **HS** with its

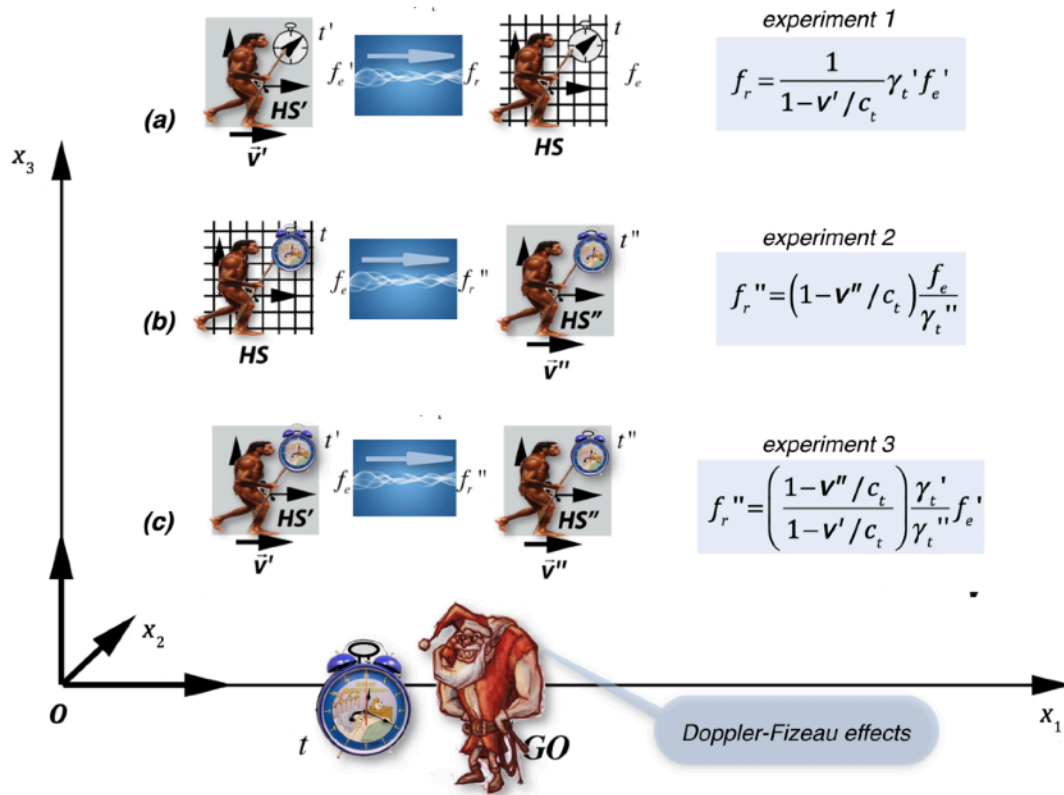


Figure 6.12 - Different measuring configurations of the Doppler-Fizeau effect

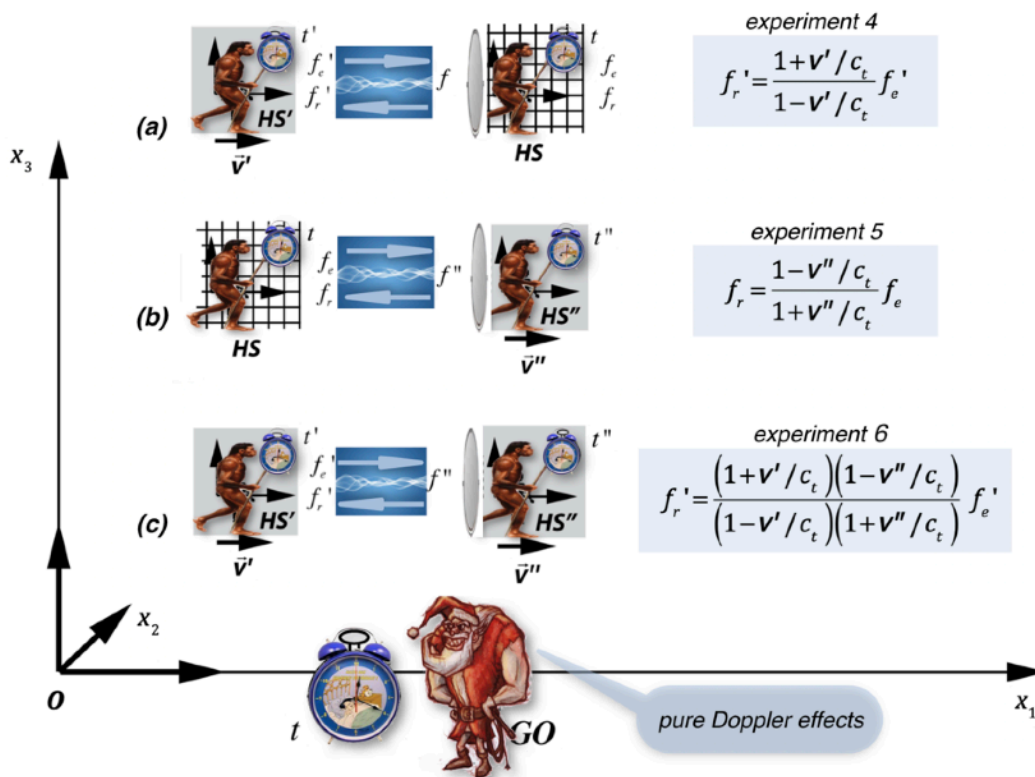


Figure 6.13 - Different measuring configurations of the pure Doppler effect

own clock, or by **GO** with the universal clock.

2nd experiment: an **HS** observer in the reference frame $Ox_1x_2x_3$ at rest with respect to the lattice transmits a signal with a frequency f_e , measured with his own clock, to an **HS''** observer which moves at velocity \vec{v}'' in the direction Ox_1 relative to the lattice (figure 6.12b). With the same type of calculation as in the case of the 1st experiment, it is possible to verify that the frequency f_r'' of the signal received by **HS''** and measured with its own clock takes the value shown in figure 6.12b.

For $v'' > 0$, that is to say when **HS''** moves away from **HS**, the frequency f_r'' of the signal received by **HS''** is lower than the frequency f_e of the signal transmitted by **HS**. Again, this is the *Doppler-Fizeau effect*. In this form, the expression of f_r'' makes appear the term $(1 - v''/c_t)$ of the *classic Doppler effect*, but which applies to a frequency f_e/γ_t'' , which is nothing other than the frequency of the signal emitted by **HS**, but as measured with the **HS''** clock.

3rd experiment: an observer **HS'** in the reference frame $O'x'_1x'_2x'_3$ moving at velocity \vec{v}' in the direction Ox_1 relative to the lattice emits a wave at the frequency f_e' , measured with its own clock, towards an observer **HS''** which moves at velocity \vec{v}'' in the direction Ox_1 relative to the lattice (figure 6.12c). The frequency f_r'' of the signal received by **HS''** and measured by him with his own clock is easily obtained by combining the two relations (6.12 a) and (6.12b) obtained previously. In this form, the expression of f_r'' shows in fact in parentheses the *classic Doppler effect* due to the movements of the two observers relative to the lattice, as well as the frequency $\gamma_t' f_e' / \gamma_t''$ which is nothing other than the frequency of the signal emitted by **HS'**, but measured with the **HS''** clock.

4th experiment: an observer **HS'** in the reference frame $O'x'_1x'_2x'_3$ moving at velocity \vec{v}' in the direction Ox_1 relative to the lattice emits a wave at the frequency f_e' , measured with its own clock, which is reflected on a mirror associated with a fixed reference frame with respect to the lattice, and receives the echo of this wave whose he measures the frequency f_r' , always with its own clock (figure 6.13a). It is easy to find the value of f_r' using the relations (6.12a) and (6.12b) previously obtained in which we introduce the frequency f received and re-emitted by the mirror in the **HS** reference frame. The combination of these two relationships then shows us that, in this case, the effect measured by **HS'** is a *pure classic Doppler effect*, which is perfectly logical since **HS'** uses its own clock to measure f_e' and f_r' .

5th experiment: an observer **HS** in the fixed reference $Ox_1x_2x_3$ with respect to the lattice emits a wave at the frequency f_e , measured with his own clock, which is reflected on a mirror associated with a reference frame $O''x''_1x''_2x''_3$ in movement in the direction Ox_1 at velocity \vec{v}'' compared to the fixed lattice, and receives the echo of this wave whose he measures the frequency f_r , always with its own clock (figure 6.13b). It is easy to find the value of f_r by again using the relations previously obtained in which the frequency f'' received and re-emitted by the mirror is introduced into the reference frame of **HS''**. The combination of the two relations (6.12a) and (6.12b) again shows us that, in this case, the effect measured by **HS** is a *pure classic Doppler effect*, since **HS** uses its own clock to measure f_e and f_r .

6th experiment: an observer **HS'** in the reference frame $O'x'_1x'_2x'_3$ in movement relative to the lattice at velocity \vec{v}' in the direction Ox_1 emits a wave at the frequency f_e' , measured

with its own clock, which is reflected on a mirror associated with a reference frame $O''x''_1x''_2x''_3$ in movement relative to the lattice at velocity \vec{v}'' in the direction Ox_1 , and receives the echo of this wave whose he measures the frequency f_r' , always with its own clock (figure 6.13c). Again, it is easy to find the value of f_r' by using twice the relationship (6.12c). We find again that, in this case, the effect measured by HS' is a *pure classic Doppler effect*, since HS' uses its own clock to measure f_e' and f_r' .

About the famous paradox of the Twins of Special Relativity...

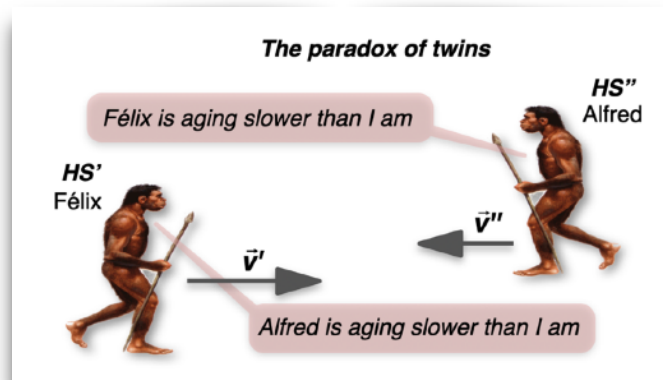
... which is only one in the minds of the HS observers

The existence of the lattice, therefore of an "ether", makes it possible to give a very simple and very elegant explanation to the famous *paradox of the Twins of Special Relativity*. We have already seen that a local observer HS'' in its mobile reference frame $O''x''_1x''_2x''_3$ at velocity \vec{v}'' relative to the lattice in the direction Ox_1 is in principle not able to measure this velocity since its clock and its own rulers do not change for him, which results also in the fact that Michelson-Morley type experiments do not provide useful informations to him. However, one may wonder whether Doppler-Fizeau type experiments with another HS' observer moving at velocity \vec{v}' relative to the lattice in the direction Ox_1 could provide him with more information. In relation to the HS' observer, the observer HS'' can perform three types of measurement:

- he can measure the relative speed \mathbf{v}_r of HS' with respect to it, given by the formula in figure 6.9, with a changed sign,
- he can measure the frequency ratio f_r''/f_e' of a certain known event occurring in his reference frame and in the reference frame of HS' , given in figure 6.12c,
- he can measure the frequency ratio f_r''/f_e'' of a signal which he has sent itself and which is reflected on a mirror in the frame of reference of HS' , given in figure 6.13c.

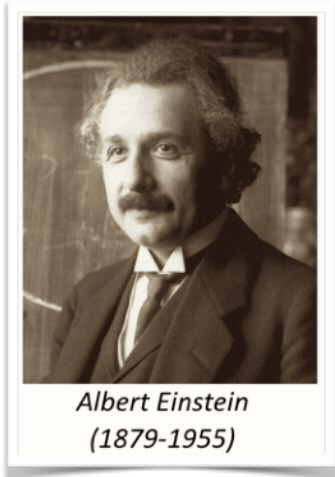
We can then show that these three experimental measurements do not allow HS'' to determine unequivocally \vec{v}' and \vec{v}'' . Indeed, the last two relationships are absolutely equivalent and therefore do not solve the problem. As for the first two relations, it is easy to show that this system is also indeterminate, because it provides the relation $f_r''/f_e' = \left[1 - (\mathbf{v}_r/c_t)^2\right]^{1/2}$, so that HS'' ultimately has no way of finding his velocity \vec{v}'' relative to the lattice using experiments of Doppler-Fizeau type.

This last relation is extremely interesting, because it shows that HS'' can deduce the relative speed \mathbf{v}_r of HS' compared to him by measuring the frequency ratio f_r''/f_e' of a certain known event occurring in his reference frame and in the reference frame of HS' and that for him, in his reference frame $O''x''_1x''_2x''_3$, this frequency ratio is of the relativistic type. But the observer HS' , in his reference frame $O'x'_1x'_2x'_3$, could make the same measurement, and he would then obtain exactly the same result. Thus, for HS observers who do not have



access to their absolute velocities relative to the lattice (*therefore relative to «ether»*), their principle of relativity is exactly *the same principle as that of Special Relativity*. In particular, by applying the Lorentz transformation, **HS''** will have the impression that **HS'** ages slower than

him, while **HS'** will also have the impression that it is **HS''** who ages slower than him. This strange situation at first sight is called *the paradox of twins in Special Relativity*.



Albert Einstein
(1879-1955)

But this paradox of twins is only one in the minds of the observers **HS'** and **HS''**. Indeed, for the **GO** which has access to the relative speeds of the **HS** observers compared to the lattice, it is perfectly clear that it is the observer **HS** which moves compared to the lattice which ages less quickly than the observer **HS** which remains fixed compared to the lattice. Thus, if a pair of **HS** twins carry out the famous *Langevin twin experiment*, namely that one of the twins sets off in a rocket at subluminal speeds and then returns to his twin which has remained at the starting point, the **GO** will be able to say unequivocally that the **HS** who has traveled at very high speed

compared to the lattice will be the youngest when they meet after the trip. And the **GO** knows perfectly well that this effect took place throughout the journey, *even during periods when the speed of the traveling twin has been constant in relation to the lattice*.

This interpretation of the paradox of twins based on the existence of the cosmological lattice, *therefore of an ether*, is entirely new and gives a very simple, logical and elegant answer to many questions and interpretations of the paradox of twins suggested by Special Relativity and by Einstein's General Relativity³.

³ See for example:

http://fr.wikipedia.org/wiki/Paradoxe_des_jumeaux

http://en.wikipedia.org/wiki/Twin_paradox

Chapter 7

Gravitational fields of the topological singularities

Thanks to *Newton's second partial equation*, one can obtain *the external fields of expansion perturbations*, i.e. *the external fields of gravitation* associated with a localized topological singularity. We find that these external gravitational fields can have three components, namely a generally dominant component associated with *the elastic energy of distortion*, that is to say *with the mass of the singularity*, and two components generally much weaker due respectively to *the charge of curvature* of the singularity and to *the charge of rotation* of the singularity.

In the process, we also come to show that the collapse of clusters of singularities of the vacancy type or of the interstitial type leads to fairly singular macroscopic topological singularities within the lattice: a hole in the lattice, a kind of *macroscopic vacancy*, in the case of the collapse of singularities of vacancy nature, or a piece of additional lattice, a kind of *macroscopic interstitial* within the lattice in the case of the collapse of singularities of interstitial nature. The description of the “gravitational” fields of these two types of macroscopic complementary singularities shows that the macroscopic vacancy singularity can behave like a real black hole, whereas the macroscopic interstitial singularity does not have this property. Subsequently, these macroscopic singularities will prove to be ideal candidates to explain the “black holes” of the Universe in the case of the macroscopic vacancies and the “neutron stars” of the Universe in the case of the macroscopic interstitials.

By applying the calculations of the external gravitational field of the topological singularities to the microscopic singularities in the form of twist disclination loops, prismatic edge dislocation loops or slip mixed dislocation loops, we deduce the set of gravitational properties of these loops. Several extremely interesting consequences will be deduced therefrom, in particular the existence, in the case of the prismatic edge dislocation loop, of an equivalent mass of gravitation different from the mass of inertia, which may even prove to be negative in the case of loops of an interstitial nature, a result which will have very significant consequences thereafter.

Expansion perturbations by a singularity with a given distortion energy

Let us consider a singularity localized at rest, of volume $V_{cluster}$, consisting of a loop or a cluster of numerous loops of dislocations and / or of disclinations, and let us suppose known the densities of distortion energy $F_{dist}^{cluster}(\vec{r})$ and potential energy $F_{pot}^{cluster}(\vec{r})$ within this singularity. The equilibrium of the expansion perturbation field $\tau_{int}^{(E)}(\vec{r})$ within this singularity is given by the solution of the second degree equation deduced from Newton's second partial equation in figure 5.1. We cannot do here an exact calculation of $\tau_{int}^{(E)}(\vec{r})$ since it would require dealing with a concrete case of singularity to know exactly the distributions of the densities of distortion energy $F_{dist}^{cluster}(\vec{r})$ and potential energy $F_{pot}^{cluster}(\vec{r})$ within this singularity. On the other hand, one can deal with this problem in an approximate way by introducing average values of the various fields concerned. We can start by introducing *the global energy at rest* $E_{dist}^{cluster} + V_{pot}^{cluster}$ of the

topological singularity by summing the distributions of the densities of distortion energy $F_{dist}^{cluster}(\vec{r})$ and potential energy $F_{pot}^{cluster}(\vec{r})$ within this singularity, so that we can define an average value $\bar{\tau}_{int}^{(E)}$ of the internal field of expansion perturbations. It is clear that this mean field is purely virtual, in other words that it does not really exist, but that it represents in fact a form of mean value of all the accidents of the perturbation field within the singularity, accidents which must be extremely marked especially if we have to deal with a cluster of very many topological singularities. The exact calculation of the mean perturbation field $\bar{\tau}_{int}^{(E)}$ is quite complicated, since it is subject to various assumptions regarding its conditions of existence. We will not enter here into a detailed discussion of these conditions of existence. The detailed calculations show that there are static or dynamic solutions for the expansion disturbance fields associated with the topological singularity, as shown in Figure 7.0.

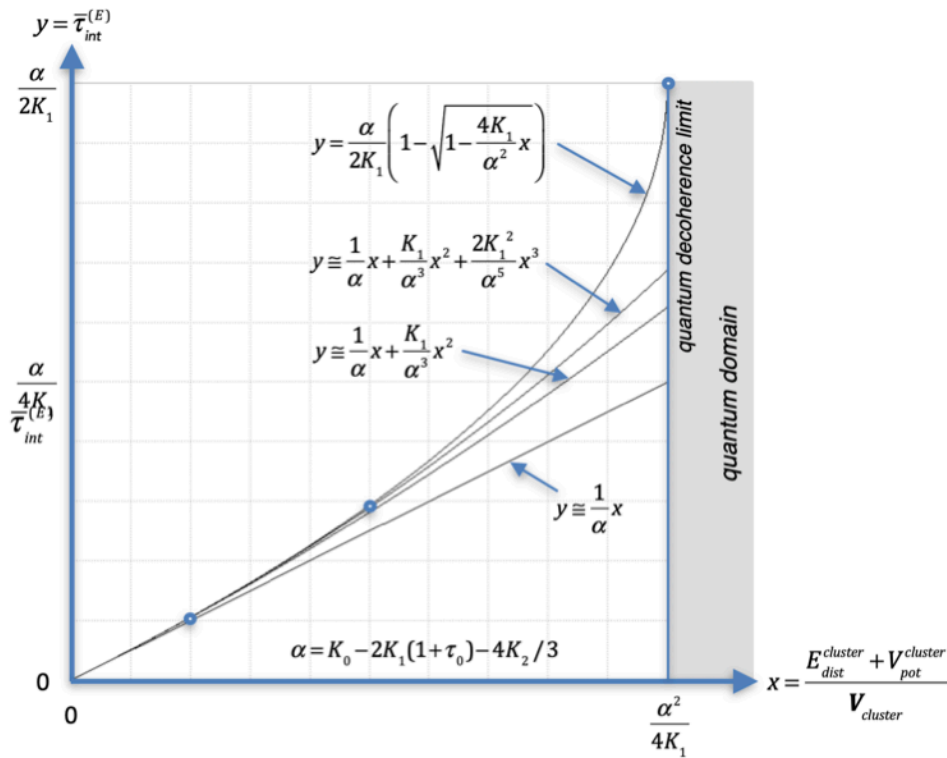


Figure 7.0 - the function $\bar{\tau}_{int}^{(E)}$ in the static solution domain for energy density values of the singularity below the critical value $\alpha^2 / 4K_1$, and domain of the quantum behaviour for values above the critical value.

The expansion field perturbations associated with a localized topological singularity are in fact an expression of the existence of a *static external "gravitational field"* at a long distance from this singularity, as long as it has an energy density or rotational load density below a certain critical value $\alpha^2 / 4K_1$.

In the case where this energy density becomes greater than this critical value $\alpha^2 / 4K_1$, the expansion field associated with this localized topological singularity becomes a *dynamic expansion perturbation*, which will bring to light the quantum behaviors of this singularity, which we will discuss in chapter 11. The critical value of the energy density then becomes an extremely important quantity since it corresponds in fact to a *quantitative value which defines*

the famous quantum decoherence limit, i.e. the limit of passage between a classical behaviour and a quantum behaviour of the topological singularity.

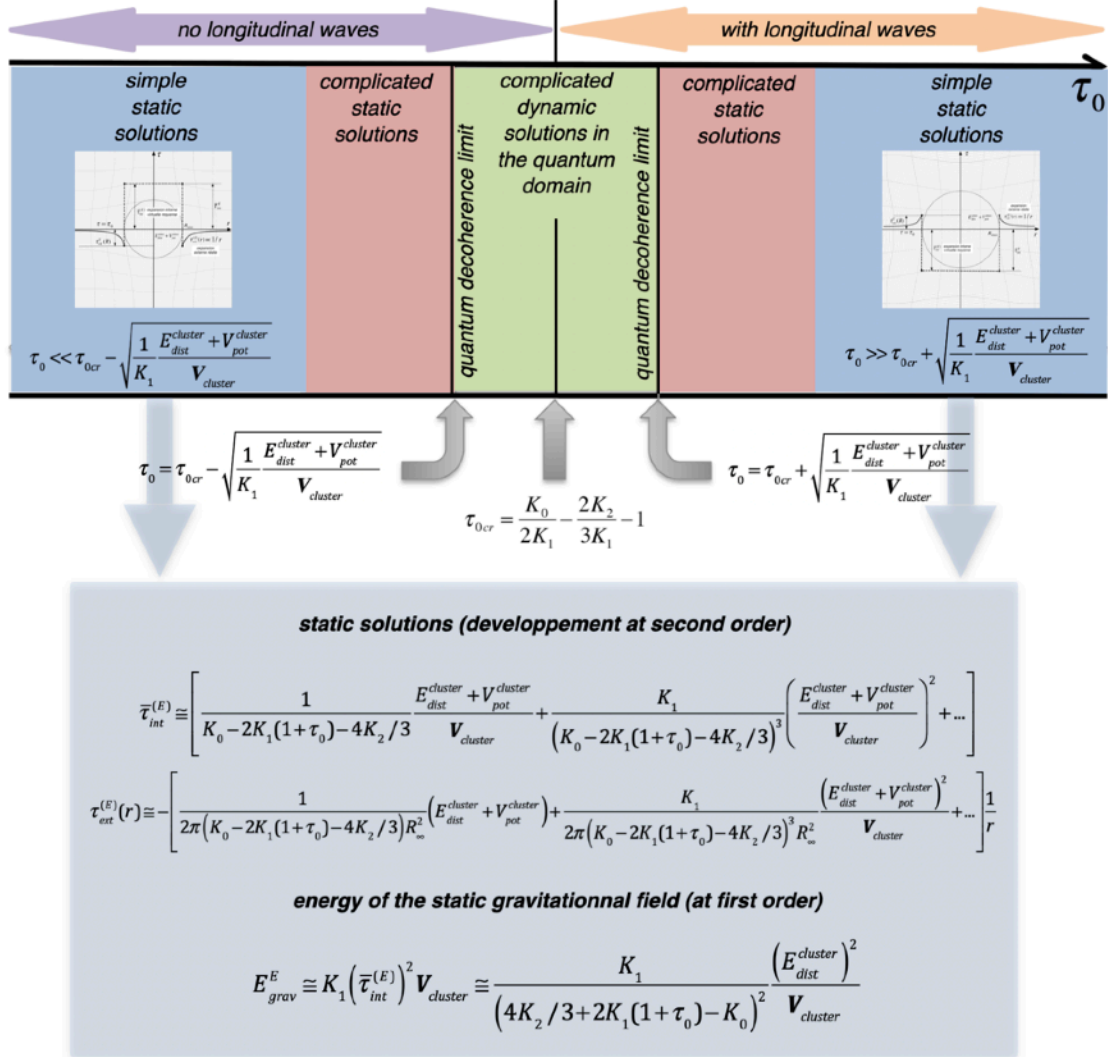


Figure 7.1 - the domains of solutions of expansion perturbations of a singularity with a given energy $E_{dist}^{cluster} + V_{pot}^{cluster}$ as a function of the background expansion

The background expansion domains of the lattice in which these solutions occur are given by conditions which are shown in figure 7.1. In a small domain centered on $\tau_0 = \tau_{0cr}$, there can only exist a dynamic solution of Newton's equation for the expansion perturbation, dynamic solution which allows to pass from the static solution of the domain $\tau_0 < \tau_{0cr}$ to the static solution in the domain $\tau_0 > \tau_{0cr}$ and vice-versa.

In the domains outside this small domain of dynamic solutions, there are static solutions for the perturbations of the volume expansion fields caused by the singularity. But here too, the calculations and the results obtained are quite complicated. But there are areas of lattice background expansion τ_0 that present simple static solutions. These domains are reported in figure 7.1, with the expressions of the internal and external perturbation fields which correspond to them. It is remarkable to note then that the average value $\bar{\tau}_{int}^{(E)}$ of the internal field of

perturbation of the expansion depends on *the global energy of rest* $E_{dist}^{cluster} + V_{pot}^{cluster}$ of the singularity and its volume $V_{cluster}$, while the field of external perturbations decreases in $1/r$ with the distance from the cluster, that it only depends on the total energy $E_{dist}^{cluster} + V_{pot}^{cluster}$ of it, and especially that *it does not depend on the volume or the radius of it*.

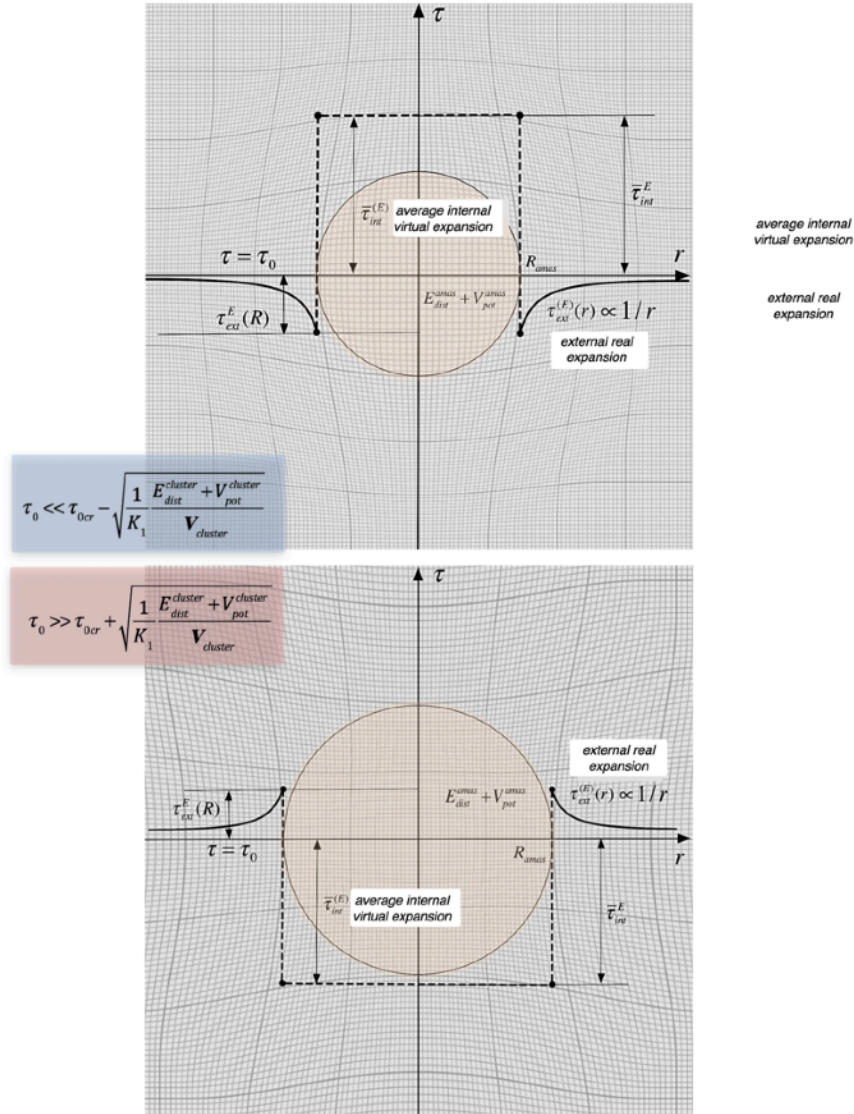


Figure 7.2 - the expansion field inside and outside a singularity
with a given energy $E_{dist}^{cluster} + V_{pot}^{cluster}$

These behaviors of the expansion perturbation field are reported in figure 7.2 as a function of the distance r from the center of the singularity, in both cases $\tau_0 \ll \tau_{0cr}$ and $\tau_0 \gg \tau_{0cr}$.

The total energy of the expansion field can also be calculated, and we see that it is positive, that it is proportional to the product of the volume of the singularity by the square of the internal field of expansion perturbations of the singularity, and that it depends only on the modulus of elasticity K_1 which, as we recall, must be much smaller than the modules K_0 and K_3 in the perfect cosmological lattice.

It is interesting to compare the gravitational energy of the singularity with its elastic energy of distortion, by calculating the approximate value of the ratio of the two. The expression $E_{grav}^E / E_{dist}^{cluster} \cong (K_1 / K_0^2) (E_{dist}^{cluster} / V_{cluster})$ comes for $\tau_0 \ll \tau_{0cr}$. Now, according to conjecture 6, the ratio K_1 / K_0^2 is extremely small, so that the gravitational energy of the singularity is certainly extremely smaller than the elastic energy of distortion of the singularity in the domain $\tau_0 \ll \tau_{0cr}$. We will come back to this point later.

With the conjectures 6 of the *perfect cosmological lattice*, if we are in the *expansion domain* $\tau_0 < \tau_{0cr}$ in which there are no longitudinal waves, the mean virtual internal field $\bar{\tau}_{int}^{(E)}$ of the singularity is positive. As for the real external field $\tau_{ext}^{(E)}(\vec{r})$ of the singularity, it is negative and therefore perfectly satisfies conjecture 3 of figure 3.4 deduced from the curvature of the wave rays in the vicinity of the singularity.

On the other hand, if one is in the *domain of expansion* $\tau_0 > \tau_{0cr}$ where there are longitudinal waves, the fields reported in figure 7.2 are reversed compared to the fields in the domain of expansion $\tau_0 < \tau_{0cr}$: the average virtual internal field $\bar{\tau}_{int}^{(E)}$ of the singularity becomes negative, and the real external field $\tau_{ext}^{(E)}(\vec{r})$ becomes positive, so that it no longer satisfies conjecture 2 deduced from the curvature of the wave rays in the vicinity of the singularity.

Expansion perturbations by a singularity with a given curvature charge

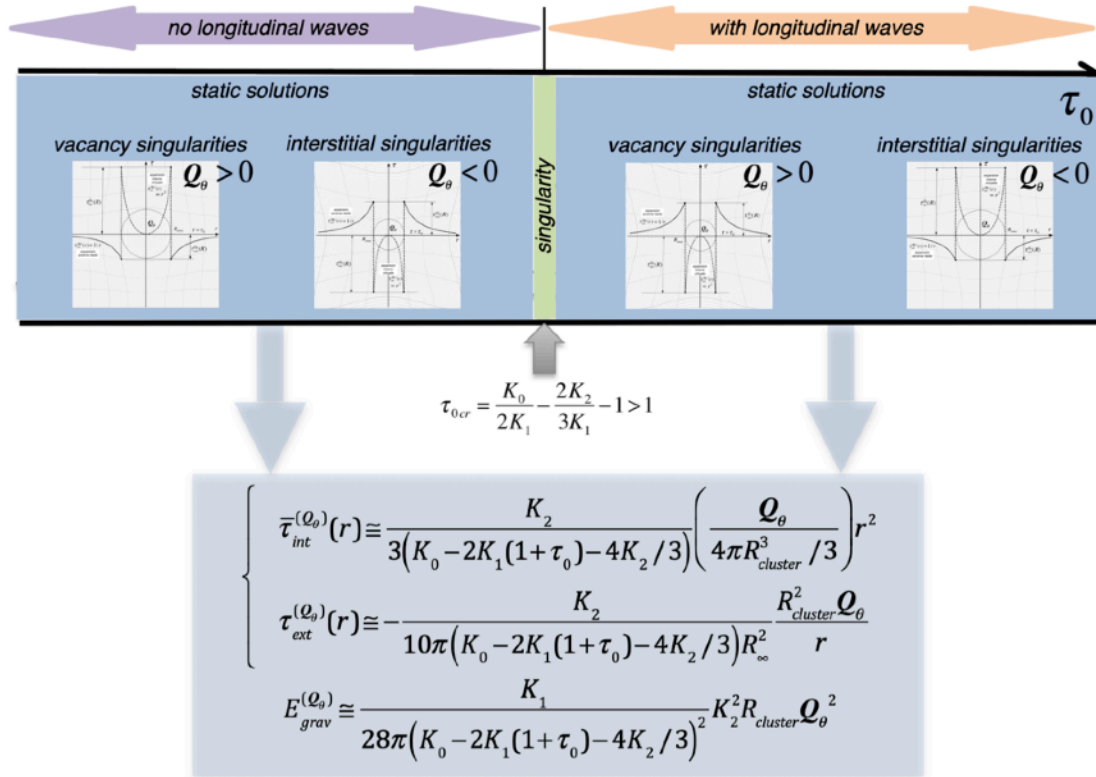


Figure 7.3 - the domains of solutions of expansion perturbations of a singularity with a given curvature charge Q_θ as a function of the background expansion

A localized singularity of radius $R_{cluster}$, apart from having a given rest energy, can also have an overall charge of curvature Q_θ . Indeed, such a singularity can consist of a cluster of discrete topological singularities of the lattice, such as prismatic dislocation loops which each have a n elementary charge of curvature $q_{\theta BC(i)}$. If $Q_\theta > 0$, we will speak of a *singularity of a vacancy nature* because there are missing lattice sites within the cluster, and if $Q_\theta < 0$, we will speak of a *singularity of interstitial nature*, because there is then excess of lattice sites within the cluster. A curvature singularity is responsible for a non-zero and divergent flexion field in its vicinity as we have shown in figure 2.33.

To find the perturbations of the expansion field due to this singularity, we start from the static equilibrium equation obtained by the divergence of Newton's first partial equation in figure 5.1. The equilibrium equation of the expansion field of such a singularity then requires knowing the density $\theta^{cluster}(\vec{r})$ of curvature charges within the singularity. Generally not knowing this density which is specific to a given singularity, we use to simplify the approximation of a homogeneous

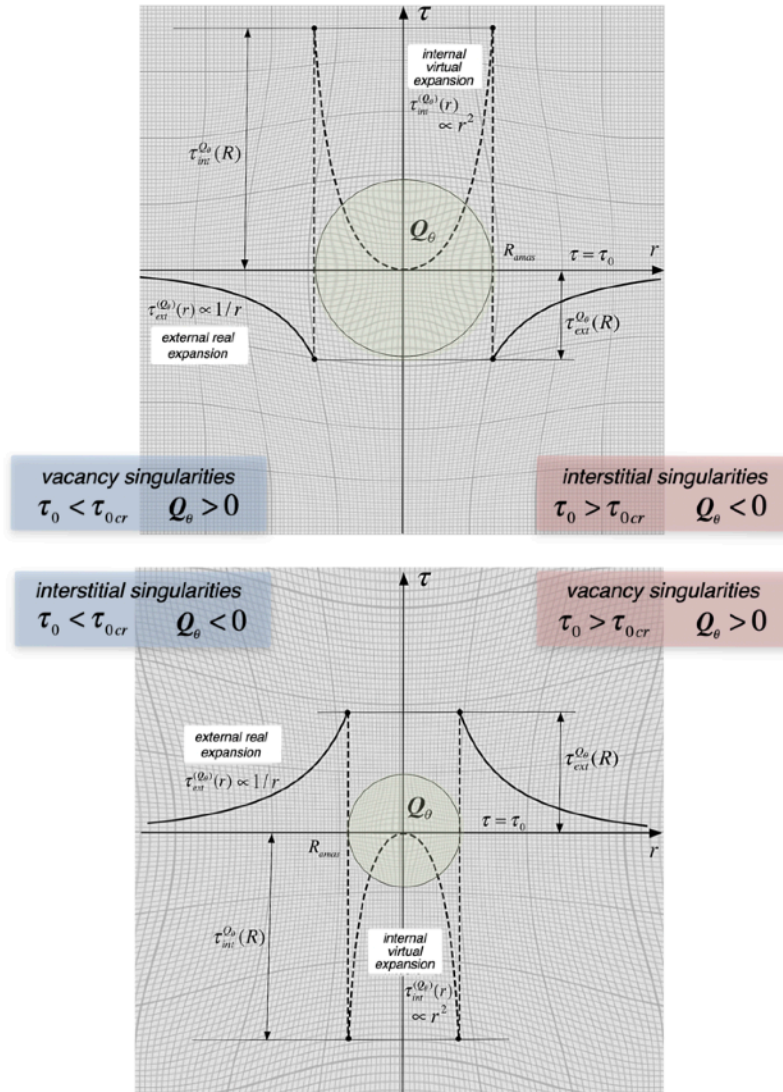


Figure 7.4 - the expansion field inside and outside a singularity with a given curvature charge Q_θ

average curvature charge density within the singularity, such as $\bar{\theta}^{cluster} = Q_\theta / (4\pi R_{cluster}^3 / 3)$. We then obtain a simplified equation of equilibrium for the virtual internal field whose solution $\tau_{int}^{(Q_\theta)}(r)$ is of spherical symmetry. As before, the exact calculation of the perturbation fields is quite complicated, because it is subject to various assumptions concerning its conditions of existence, in particular the condition that the total internal and external perturbation field is of zero mean value, so that the value of the mean field within the lattice is equal to the background expansion τ_0 of the lattice. Under these conditions, we obtain the internal and external fields reported in figure 7.3, as well as the energy associated with this expansion perturbation field.

These expressions imply that, if these fields exist, that is to say if $K_2 \neq 0$, these present an infinite singularity when the background expansion τ_0 reaches the critical value τ_{0cr} which cancels the denominator, and we can show that a singularity of curvature necessarily goes through a black hole stage, for $\tau_0 \leq \tau_{0cr}$ in the case of singularities of a vacancy nature and for $\tau_0 \geq \tau_{0cr}$ in the case of singularities of interstitial nature.

The signs of the term $K_0 - 2K_1(1 + \tau_0) - 4K_2 / 3$ and of the module K_2 play an important role here. Using the conjectures 6 of the *perfect cosmological lattice*, we have that:

- if $K_2 / [K_0 - 2K_1(1 + \tau_0) - 4K_2 / 3] > 0$, that is to say if $\tau_0 < \tau_{0cr}$, *only the singularities of a vacancy nature*, with $Q_\theta > 0$, satisfy the conjecture 3 of figure 3.4 concerning the curvature by attraction of the wave rays in the vicinity of the singularity, while *the singularities of interstitial nature*, with $Q_\theta < 0$ repel the wave rays,
- if $K_2 / [K_0 - 2K_1(1 + \tau_0) - 4K_2 / 3] < 0$, that is to say if $\tau_0 > \tau_{0cr}$, *only the singularities of interstitial nature*, with $Q_\theta < 0$, satisfy conjecture 3 concerning the curvature by attraction of the wave rays in the vicinity of the singularity, while the singularities of vacancy nature, with $Q_\theta > 0$, repel the wave rays.

These behaviors of the expansion perturbation field are reported in figure 7.4 as a function of the distance r from the center of the vacancy or interstitial singularity, in the four possible cases, namely for $\tau_0 < \tau_{0cr}$ and $\tau_0 > \tau_{0cr}$, and for $Q_\theta < 0$ and $Q_\theta > 0$.

Expansion perturbations by a singularity with a given rotation charge

Now imagine the existence within the perfect lattice of a localized singularity of volume $V_{cluster}$ and global rotation charge Q_λ , composed of a cluster of elementary rotation charges $q_{\lambda BV(i)}$ or containing a density $\lambda(\vec{r})$ of rotation charges.

Such a singularity will therefore have an external field of expansion perturbations linked to the elastic energy of the singularity due to the field of internal rotation at the singularity, and which is deduced directly by the second relation of figure 7.1. This perturbation field therefore does not depend on volume $V_{cluster}$ or radius $R_{cluster}$ of the singularity with rotation charge.

But to this external field of expansion perturbation due to the internal energy of rotation of the singularity must also be added an external field of expansion perturbations which is generated by the external field of rotation of the singularity, and which appears as a result of the distortion energy $E_{dist(rot ext)}^{cluster}$ associated with the external rotation field $\vec{\omega}_{ext}^{el}$. The external rotation field of the singularity is given in figure 5.4, and it does not depend either on the volume V_{amas} nor on the radius $R_{cluster}$ of the rotation singularity. This external perturbation $\tau_{ext}^{(E_{dist(rot ext)})}(r)$ of the volume expansion field is deduced using the static version of Newton's second partial equation of figure 5.1, in which the energy density is due to the external elastic energy of the rotation field

of the singularity, and in which τ^{ext} and τ^{ch} are zero. The solution of the second degree equation thus obtained presents several solutions depending on the volume expansion domain τ_0 considered, as shown in figure 7.5

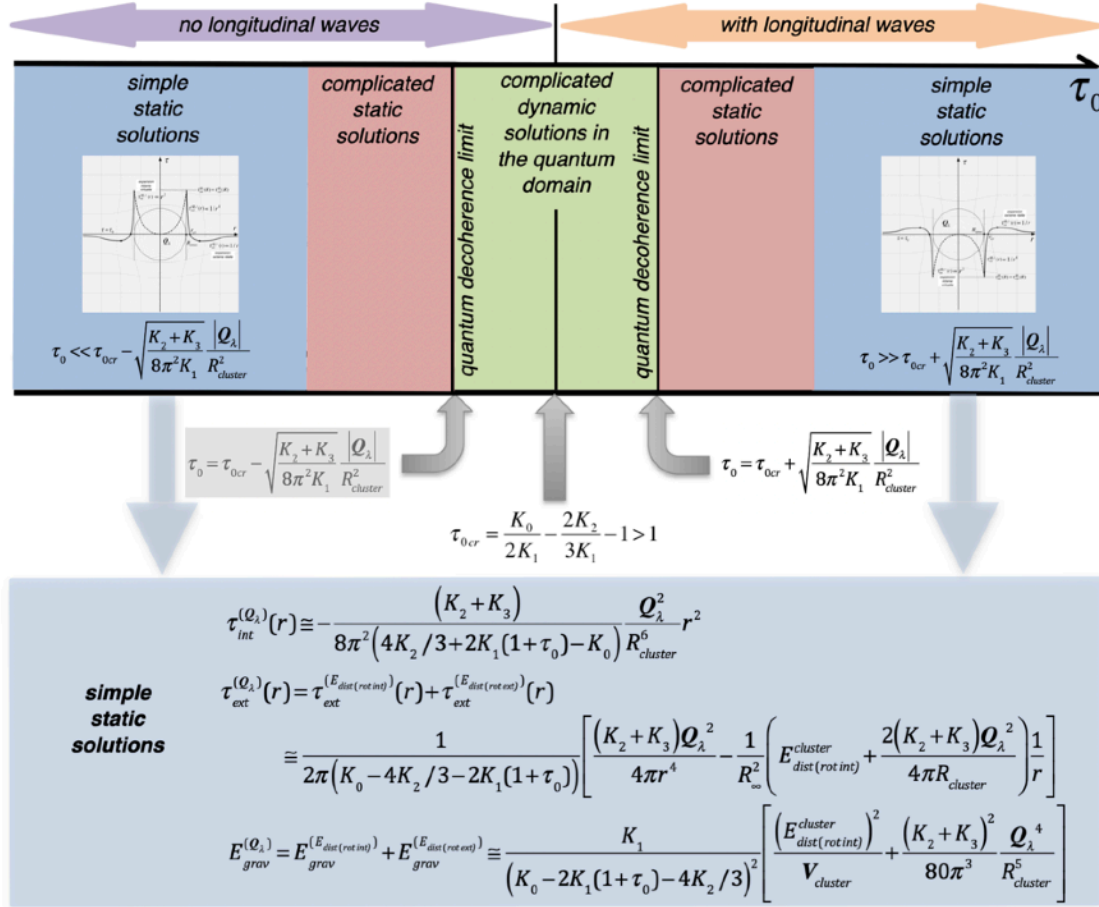


Figure 7.5 - the domains of solutions of expansion perturbations of a singularity with a given rotation charge Q_λ as a function of the background expansion

In a domain of volume expansion τ_0 centered on $\tau_0 = \tau_{0cr}$, there can only exist a *dynamic solution of Newton's equation for the perturbation of external expansion associated with the singularity of rotation*, which makes it possible to pass from the static solution of the domain $\tau_0 < \tau_{0cr}$ to the static solution in the domain $\tau_0 > \tau_{0cr}$ and vice versa. The transition limit from the dynamic solution to the static solution again corresponds to *the quantum decoherence limit*.

In the vicinity of this domain of dynamic solutions, there appear two domains of fairly complicated static solutions which will not be discussed here. Finally, it is for the extreme values of the background field τ_0 that fairly simple static solutions appear for the external field of perturbations due to the singularity of rotation. Once again assuming that the mean value of the expansion taken outside and inside the singularity is equal to τ_0 , we obtain the final expression of the external perturbation field $\tau_{ext}^{(Q_\lambda)}(r)$ reported in figure 7.5.

It can therefore be seen that the total external field of expansion perturbations of a singularity of rotation has a long-range component in $1/r$ associated with the internal and external elastic

energy of rotation of the singularity and a short-range component in $1/r^4$ associated directly with the energy of the external rotation field of the singularity. We superimposed very schematically the superposition of these two fields in figure 7.6, respectively in the cases where $\tau_0 < \tau_{0cr}$ and $\tau_0 > \tau_{0cr}$.

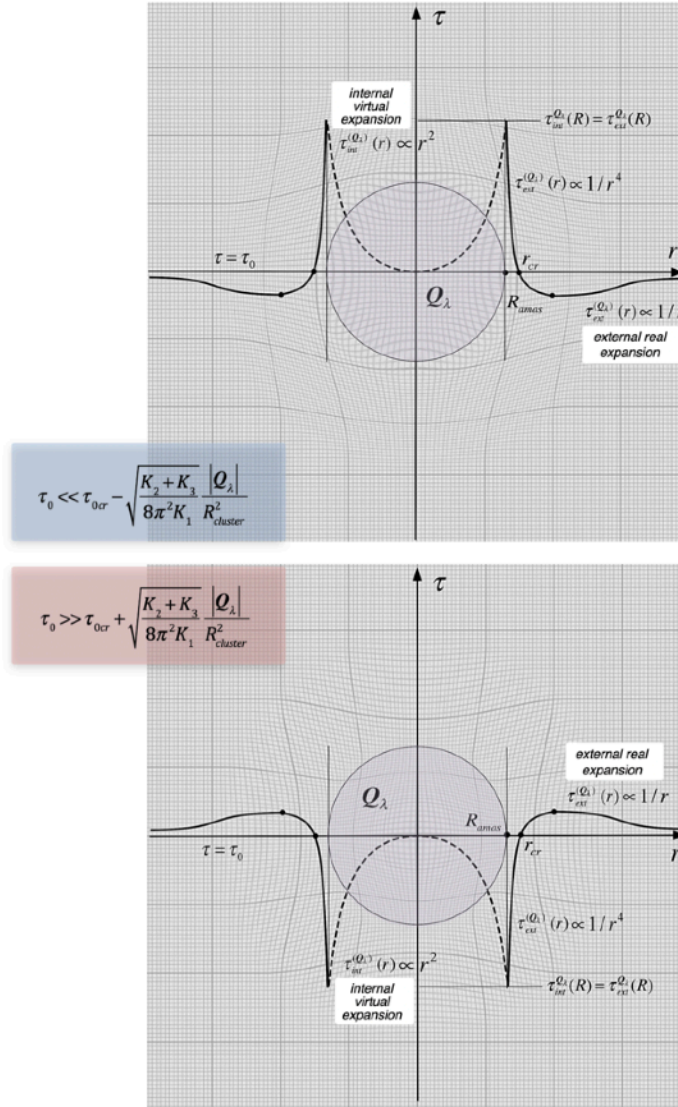


Figure 7.6 - the expansion field inside and outside a singularity with a given rotation charge Q_λ

In both cases (spherical singularity of rotation or twist disclination loop), it can be shown that there is a critical distance r_{cr} greater than the radius of the singularity ($r_{cr} > R_{cluster}$) for which the external expansion field is reversed. We also note that the perturbations of the expansion field at the interface of the singularity are positive in the expansion domain $\tau_0 < \tau_{0cr}$ and negative in the expansion domain $\tau_0 > \tau_{0cr}$.

On the other hand, as the energies of distortion (for example $E_{dist}^{(Q_\lambda)}$ in the case of a spherical load of rotation or $E_{distore}^{BV}$ in the case of a twist disclination loop) are always positive, there is no

asymmetry in the fields of expansion between charges and anti-charges of rotation. On the other hand, there appears to be an inversion of these fields when moving from the domain $\tau_0 < \tau_{0cr}$ to the domain $\tau_0 > \tau_{0cr}$.

In figure 7.5, one also reported the field of the internal perturbation of expansion, in the case of a spherical charge of rotation for which this field can be calculated in an exact way. We also reported the total energy of the gravitational perturbation field, also calculated in the case of a spherical charge of rotation.

About the gravitational fields of macroscopic singularities

Concerning the fields of "gravitational" nature of the macroscopic singularities which we have just described, it is very encouraging to note that there is a first field of expansion associated directly with *the energy $E_{dist}^{cluster} + V_{pot}^{cluster}$ of the cluster of topological singularities*, in a similar way to the gravitational field of Einstein's General Relativity which is also an emanation of *the energy-momentum tensor of matter*.

But there still appear in our approach two other "gravitational" fields of expansion which are associated respectively with *the global charge Q_θ of curvature* and *the global charge Q_λ of rotation* of the cluster of topological singularities. These fields have in fact no equivalent in Einstein's General Relativity.

The existence of the second "gravitational" expansion field, due to *the curvature charge Q_θ* , is subject to the condition that the shear modulus K_2 of the perfect lattice is not zero. There is therefore still the possibility of discussing the existence or not of this field according to the value which must be attributed to the module K_2 in our analogy with the real world, knowing that this module must in any case be very small vis-à-vis of the module K_3 , as already specified with conjecture 4.

The third "gravitational" expansion field is associated with *the rotation charge Q_λ* of the cluster of topological singularities considered. Within the framework of our analogy, this third expansion field must necessarily exist if the cluster has a non-zero charge Q_λ since the module K_3 must exist to satisfy the analogy with Maxwell's equations. But this field has no direct analogy in Einstein's General Relativity and Particle Physics theories.

Note again that the three preceding "gravitational" fields have non-zero gravitational energies. As these depend on the coefficient $K_1 / K_0^2 \ll 1$, which must be very small in the perfect cosmological lattice, the gravitational energy of the singularities is certainly negligible compared to the elastic energy of distortion of the singularities.

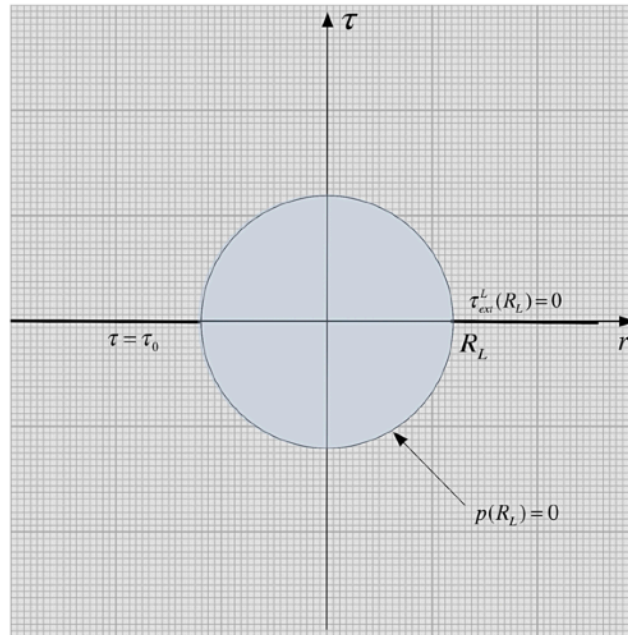
The fact that there appear two "gravitational" fields of volume expansion which apparently have no analogues in the theories of General Relativity of Einstein and in Particle Physics is very interesting to test our approach. We will return in the following chapters to the roles that the three fields of volume expansion could play respectively associated with the energies $E_{dist}^{cluster} + V_{pot}^{cluster}$ the charge of curvature Q_θ and the charge of rotation Q_λ of a localized singularity or of a localized cluster of topological singularities.

If the background expansion field τ_0 of the lattice increases or decreases so as to pass through the critical value τ_{0cr} , there appears a domain where there can no longer exist a static solution to Newton's equation, which means that *it must necessarily appear a dynamic solution which makes it possible to transform a static singularity of the domain $\tau_0 < \tau_{0cr}$ into a static*

singularity of the domain $\tau_0 > \tau_{0cr}$, and vice versa. The non-existence of a static solution to Newton's equation when the energy density and / or the rotational charge of the singularity becomes too large is mathematically a fact quite similar to what we already encountered in chapter 2 in the case of *Frank-Read sources of dislocations*, where there were no longer any static solutions to the deformation of an anchor dislocation string when the stress exceeded a certain critical limit value, and we will see below that the appearance of pure dynamic solutions for the expansion perturbation field have in fact a very close link with quantum physics.

Macroscopic vacancy located in the lattice, real gravitational black hole

Imagine that a cluster of vacancy type singularities, i.e. singularities carrying positive curvature charges, such as prismatic dislocation loops of the lacunar type for example, collapses on itself (under the effect for example of "gravitational attractive forces" which we will



$$\begin{cases} \tau_{ext}^{(L)}(r) \cong -\left(1 + \tau_0 + \tau^{external}(R_L)\right) \frac{R_L}{r} \\ R_L = \sqrt[3]{\frac{3N_L}{4\pi n_0 e}} \end{cases}$$

$$E_{grav}^{(L)} \cong 2\pi \left(K_0 - 2K_1 \tau_0\right) \left(1 + \tau_0 + \tau^{external}(R_L)\right) R_L^2$$

$$\cong \sqrt[3]{\frac{6\pi^2 N_L}{n_0 e}} \left(K_0 - 2K_1 \tau_0\right) \left(1 + \tau_0 + \tau^{external}(R_L)\right)$$

Figure 7.7a - the expansion field $\tau_{ext}^{(L)}(r)$ of a macroscopic vacancy of about 10'000 lattice sites for $\tau_0 = -\left(1 + \tau^{ext}(R_L)\right)$, and the expressions of its radius and its gravitational energy

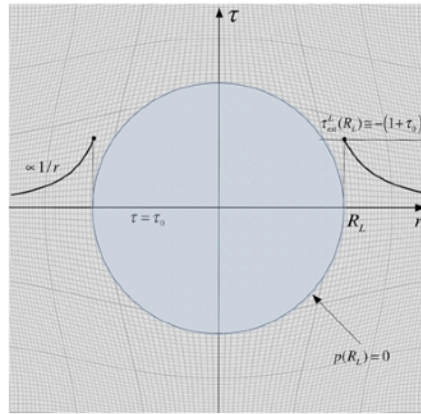


Figure 7.7b - the expansion field $\tau_{ext}^{(L)}(r)$ of a macroscopic vacancy of about 10'000 lattice sites for $\tau_0 < -(1 + \tau^{externe}(R_L))$, represented on the same scale as in figure 7.7a

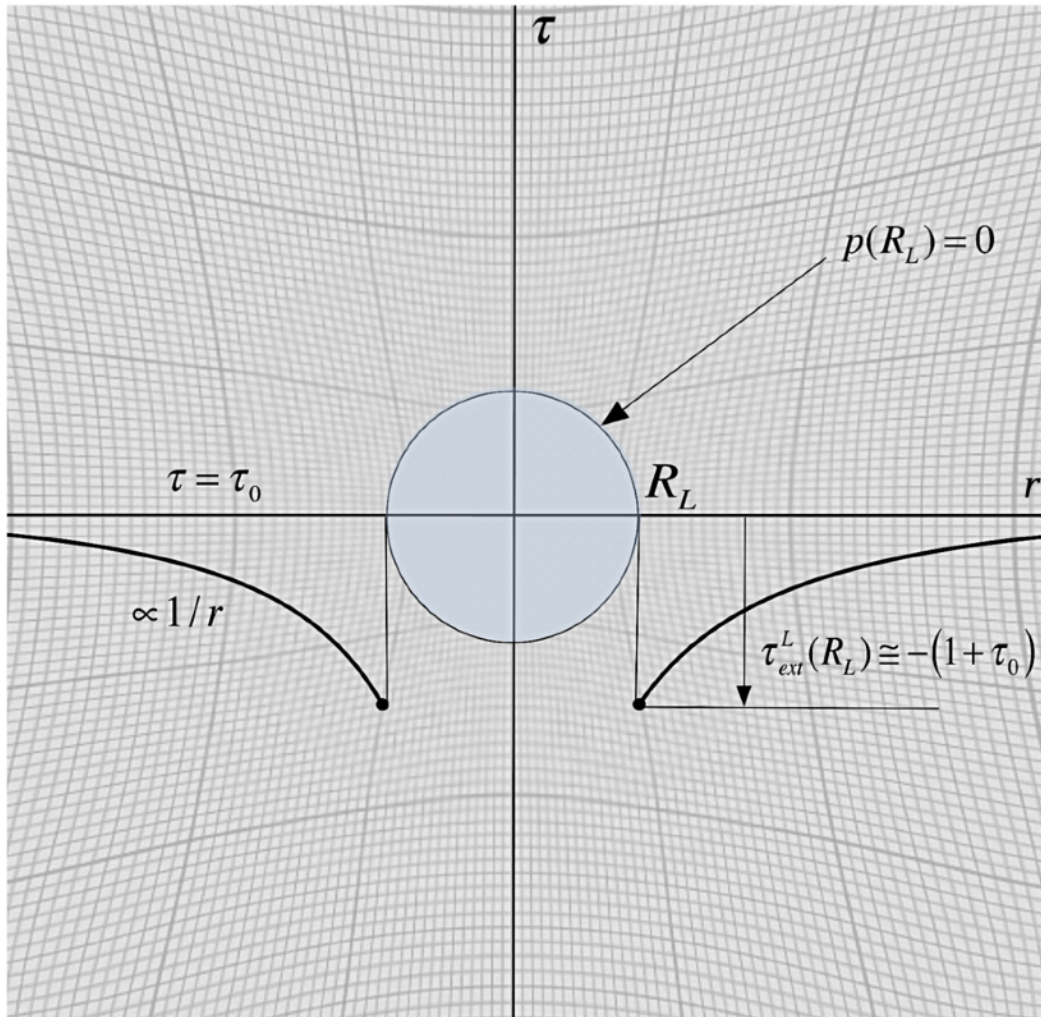


Figure 7.7c - the expansion field $\tau_{ext}^{(L)}(r)$ of a macroscopic vacancy of about 10'000 lattice sites for $\tau_0 > -(1 + \tau^{externe}(R_L))$, represented on the same scale as in figure 7.7a

describe later). If the initial cluster is neutral vis-à-vis the rotation charges, the individual singularities of the cluster combine, losing their own identity (dislocation or disclination loops) to form a single macroscopic hole within the lattice, as a kind of macroscopic vacancy formed by individual vacancies, as shown in figures 7.7a to 7.7c. This means that there is a local lack of N_L lattice sites. The radius of this macroscopic vacancy, assumed to be spherical, is then worth $R_{L0} = \sqrt[3]{3N_L / (4\pi n_0)}$, in the imaginary case where the lattice presented a homogeneous expansion of $\tau = 0$.

Within the real lattice, the presence of this macroscopic vacancy will generate a spherical volume expansion field $\tau_{ext}^{(L)}(r)$ that must be defined. On the surface of the singularity, the expansion field is equal to the sum of the field $\tau_{ext}^{(L)}(R_L)$ generated by the singularity, the background expansion field τ_0 of the lattice and an external expansion field $\tau^{external}(R_L)$ due to the other singularities located in the vicinity of the macroscopic vacancy. On the other hand, on the surface of the singularity, the total field must be arranged so that the pressure at the interface of the hole is zero. To obtain the field of expansion $\tau_{ext}^{(L)}(r)$ of the macroscopic vacancy as well as its real radius R_L , the condition of zero pressure at the interface can be injected into the equation of state of the pressure in figure 3.1. We obtain a second degree equation, which, under the assumption $K_0 \gg K_1$ of conjecture 6, has only one valid solution which is shown in figure 7.7a. We can then show that the mean expansion field in the presence of this macroscopic singularity is indeed equal to the background expansion τ_0 of the lattice.

On the other hand, we note that the real radius R_L of the macroscopic vacancy is a quantity which depends only on the number N_L of missing lattice sites.

In figures 7.7a to 7.7c, the expansion field associated to a macroscopic vacancy of approximately 10,000 substitutional sites has been plotted graphically, for three different values of the background expansion τ_0 of the lattice, and trying to respect at best the scale of the drawing.

The energy of a macroscopic vacancy associated with its field $\tau_{ext}^{(L)}(r)$ of expansion perturbations is calculated quite easily, and we obtain the relation reported in figure 7.7a. It can be seen that the energy of formation of the macroscopic vacancy depends only on the background expansion τ_0 of the lattice and that it is canceled ($E_{grav}^{(L)} \rightarrow 0$) for the values $\tau_0 \rightarrow -(1 + \tau^{external}(R_L))$ and $\tau_0 \rightarrow K_0 / (2K_1)$. Between these two values, namely in the interval $-(1 + \tau^{external}(R_L)) < \tau_0 < K_0 / 2K_1$, the energy of formation of the macroscopic vacancy is positive, whereas it becomes negative outside this interval. On the other hand, within the interval $-(1 + \tau^{external}(R_L)) < \tau_0 < K_0 / 2K_1$, the energy of formation of two macroscopic vacancies of N_L sites is higher than the energy of formation of a single macroscopic vacancy of $2N_L$ sites since $E_{grav}^{(L)}|_{2N_L} \equiv 2E_{grav}^{(L)}|_{N_L} / \sqrt[3]{4} < 2E_{grav}^{(L)}|_{N_L}$, so that two macroscopic vacancies will have an energy advantage to merge when the background expansion field is in this interval.

In the presence of a macroscopic vacancy, the first condition reported in figure 3.5 for the appearance of a black hole implies that the critical radius to make a black hole with a macroscopic vacancy is equal to $r_{cr} = (1 + \tau_0 + \tau^{external}(R_L))R_L / 2$. If we add the necessary condition that $r_{cr} > R_L$, there comes the condition $\tau_0 > 1 - \tau^{external}(R_L)$ on the background expansion τ_0 of the lattice to form a black hole.

We conclude that a macroscopic vacancy, whatever its size and its energy, necessarily becomes a black hole as soon as the background volume expansion τ_0 exceeds the value of

$1 - \tau^{external}(R_L)$. This conclusion is extremely interesting insofar as we have here the macroscopic stable topological singularity which we can consider as *the true black hole*, analogous to the black hole of general relativity, when $\tau_0 > 1 - \tau^{external}(R_L)$, represented in figure 7.7c. And this vacancy topological singularity behaves like a white hole which repels the wave rays when the condition $\tau_0 < -\left(1 + \tau^{external}(R_L)\right)$ is satisfied, as in figure 7.7b.

***Macroscopic interstitial located in the lattice,
true anti-singularity of the macroscopic vacancy***

Now imagine that a cluster of interstitial type singularities, i.e. singularities carrying negative curvature charges, such as interstitial type prismatic dislocation loops, collapses on itself under the effect of attractive gravitational forces described in the previous chapter. If the initial cluster is neutral vis-à-vis the rotation charges, the individual singularities of the cluster combine, losing their own identity (dislocation or disclination loops) to form a single piece of macroscopic local lattice embedded within the lattice, and formed of N_I sites, as shown in figure 7.8.

This means that there is an excess of N_I lattice sites locally forming a *macroscopic interstitial*. The radius of this macroscopic embedding, assumed to be spherical, then is worth $R_{I0} = \sqrt[3]{3N_I / (4\pi n_0)}$ in the imaginary case where $\tau = 0$.

We can obviously consider that this macroscopic interstitial of N_I lattice sites corresponds in fact to *the anti-singularity of the macroscopic vacancy* of $N_L = N_I$ sites, in the sense that the combination of these two singularities completely restores the original lattice, since the N_L missing sites of the lattice are filled by the N_I interstitials.

In the presence of such an embedding of a piece of lattice within the lattice, there is obviously no coherence of the two lattices, and the condition of equilibrium amounts to the fact that the pressures at the interface are equal on the part and other of the interface, so that $p_{ext}(R_I) = p_{int}$, which actually comes down to that $\tau_{int}^{(I)} = \tau_{ext}^{(I)}(R_I)$. As the external field $\tau_{ext}^{(I)}(r)$ satisfies the divergence equation $\Delta \tau_{ext}^{(I)}(r) \equiv 0$ drawn from Newton's first partial equation in figure 5.1, we deduce the solution for the external field, ensuring that the number of cells of lattices before introducing the singularity interstitial is equal to the number of cells of lattice after introduction of the singularity. Under this condition, one finds the fields of expansion perturbations outside and inside the macroscopic interstitial represented in figure 7.8.

Assuming that there exists in the vicinity of the macroscopic interstitial a field of expansion $\tau^{external}(R_I)$ due to the other singularities located in its vicinity, the real radius of the macroscopic interstitial will depend on the background expansion τ_0 , on its own internal field of expansion internal and on the external field $\tau^{external}(R_I)$ by the relation also reported in figure 7.8. We can use this expression of R_I to express the field of external perturbations a little differently, in a form which shows that the external field of expansion perturbations is simply proportional to the number of additional sites agglutinated in the lattice.

The "gravitational" energy of the expansion field associated with this macroscopic interstitial is then written, taking into account the external and internal fields, as shown in figure 7.8.

Although *the macroscopic interstitial is the anti-singularity of the macroscopic vacancy*, its formation energy is always positive as long as $\tau_0 < K_0 / 2K_1$, and infinitely smaller than the formation energy of the macroscopic vacancy, which reveals *a colossal asymmetry between the two complementary macroscopic singularities*.

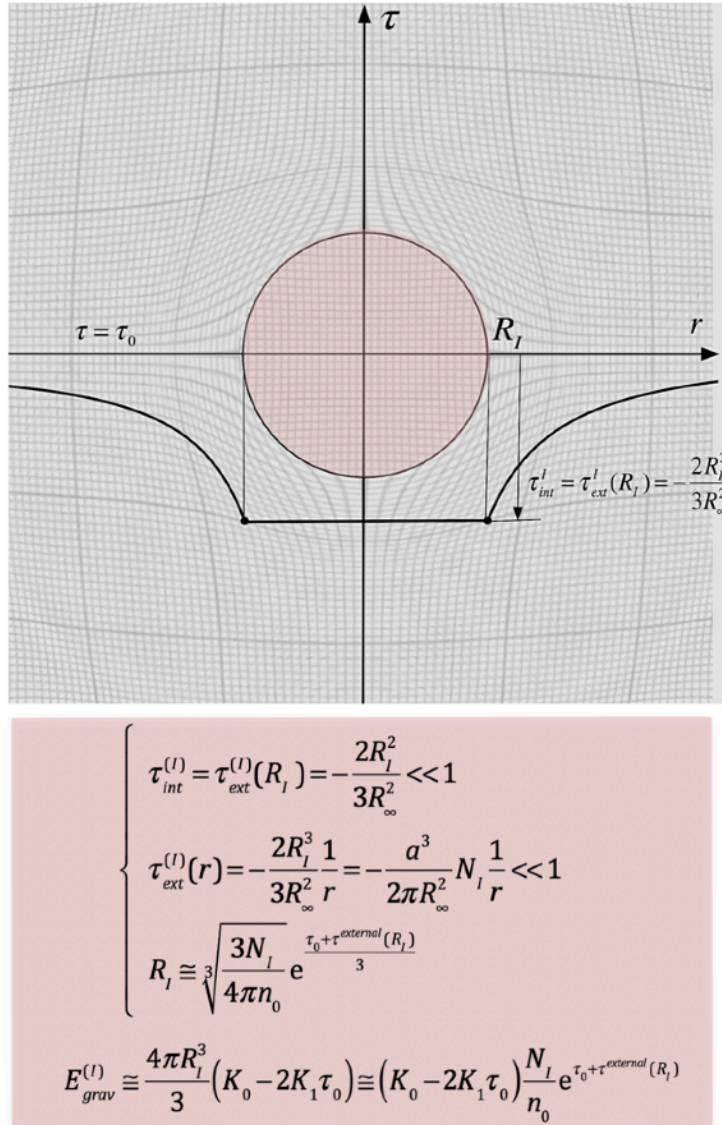


Figure 7.8 - the internal and external expansion fields of a macroscopic interstitial and the expressions of its radius and its gravitational energy

In the presence of a macroscopic lattice interstitial, the first condition in figure 3.5 for a macroscopic interstitial to form a black hole implies that the critical radius of formation would be given by $r_{cr} = R_l^3 / (3R_\infty^2)$, and the second condition, namely that $r_{cr} > R_l$, implies that $R_l > \sqrt{3}R_\infty$. Obviously, we deduce that a macroscopic lattice interstitial, whatever its size and energy, *can never behave like a black hole*. This conclusion is extremely interesting insofar as we have here a topological object presenting a considerable asymmetry with its anti-singularity, the macroscopic vacancy, which necessarily becomes a black hole as soon as $\tau_0 > 1 - \tau_{ext}^{external}(R_l)$.

About the possible analogy between vacancy singularities and black holes and between interstitial singularities and neutron stars

The macroscopic interstitial is the perfect anti-singularity of the macroscopic vacancy if

$N_I = N_L$ since the combination of the two singularities completely restores the perfect lattice. But there is a *colossal difference* between these two singularities, since their respective energies of formation are extremely different, and that the macroscopic vacancy becomes a black hole within the cosmological lattice as soon as $\tau_0 > 1$ while the macroscopic interstitial can never become black hole.

If we consider that these two topological objects can be formed by gravitational collapse of clusters of singularities, of a lacunar nature for the macro vacancy (for example lacunar prismatic dislocation loops) and of interstitial type for the macro interstitial (for example interstitial prismatic dislocation loops), we find by analogy the formation of black holes and neutron stars by gravitational collapse in the theory of gravitation. But if a sufficient initial mass of the cluster is a condition for arriving at a gravitational collapse, it would not be the initial mass of the cluster which conditions the evolution towards a black hole or towards a neutron star, but the very nature of the initial cluster.

Conjecture 8 - *the singularities of vacancy nature correspond by analogy to anti-matter and the singularities of interstitial nature to matter*

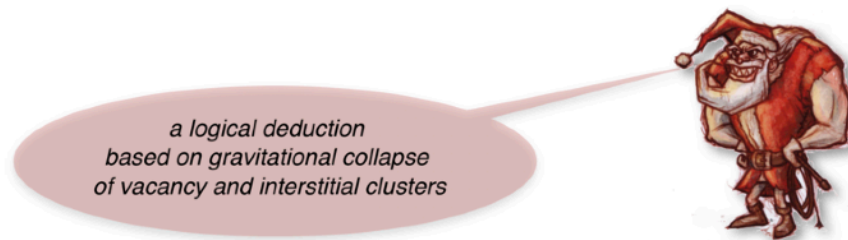


Figure 7.9 - *the eighth conjecture on the nature of matter and anti-matter*

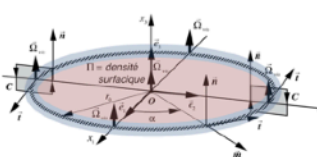
If we then accept the conjecture 8 plotted in the figure 7.9, namely that the singularities of a vacancy nature correspond by analogy to anti-matter and the singularities of interstitial nature to matter, the black holes would then be residues of collapses of clusters of anti-matter of a lacunar nature and the neutron stars of the residues of collapsed clusters of matter of interstitial nature.

In this analogy, black holes, by virtue of their constitution of "*vacancy holes*" cannot keep any memory of the initial cluster of vacancy singularities from which they come, except *the quantity of microscopic vacancies*, that is to say the number of missing lattice sites in the initial vacancy singularities. On the other hand, neutron stars, by virtue of their constitution of "*interstitial embedding*" of pieces of lattice that are not coherent with the surrounding lattice, could conserve, apart from *the quantity of microscopic interstitials*, that is to say the number of excess lattice sites in the initial interstitial singularities, at least also the memory of the kinetic moment of rotation of the initial cluster of interstitial singularities from which they originate, in the form of *a very rapid rotation of the embedding*, which would correspond well with the enormous rotational speeds observed in the case of neutron stars, also called *pulsars* because of the electromagnetic pulses which they emit at fixed frequency following their very fast rotation.

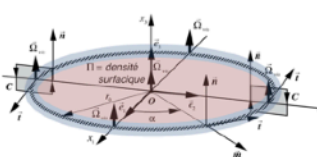
Perturbations of the expansion associated with the twist disclination loop (BV)

The twist disclination loop has already been described in detail in figure 5.5. Concerning its "gravitational" properties, namely its external fields with long and short range of perturbations of the expansion, one can directly deduce them using the relations of figure 7.5, and report them in figure 7.10, using elsewhere the mass of inertia M_0^{BV} of the loop in place of its distortion energy E_{dist}^{BV} thanks to the expression of Einstein's relation. As these fields are perturbations of the volume expansion, they correspond in our analogy with the real world to *gravitational fields*, acting respectively at long distance (LD) and at short distance (CD). In this form, the field of long distance expansion perturbations (LD) depends exclusively on the mass of inertia of the loop, and does not depend on the size of the loop, which further confirms our analogy between this field of expansion perturbations and a gravitational field.

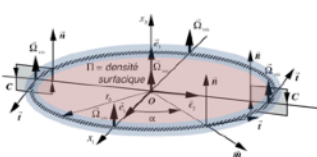
The twist disclination loop (BV)



$$\left\{ \begin{array}{l} \mathbf{q}_{\lambda BV} = -\pi R_{BV}^2 \Omega_{BV} = 2\pi R_{BV} \Lambda_{BV} = -\pi R_{BV} \vec{B}_{BV} \vec{t} \quad (\text{charge of rotation}) \\ M_0^{BV} = \frac{2}{c_t^2} (K_2 + K_3) \zeta_{BV} R_{BV} \Lambda_{BV}^2 = \frac{1}{2c_t^2} (K_2 + K_3) \zeta_{BV} R_{BV}^3 \Omega_{BV}^2 \end{array} \right.$$



$$\left\{ \begin{array}{l} \vec{\omega}_{ext}^{BV}(\vec{r}) = \frac{\mathbf{q}_{\lambda BV}}{4\pi} \frac{\vec{r}}{r^3} \quad (\text{divergent field of rotation}) \\ \tau_{ext LD}^{BV}(\vec{r}) \cong -\frac{c_t^2}{2\pi(K_0 - 2K_1(1 + \tau_0) - 4K_2/3)R_\infty^2} \frac{M_0^{BV}}{r} \\ \tau_{ext CD}^{BV}(r) \cong \frac{c_t^2}{2\pi(K_0 - 2K_1(1 + \tau_0) - 4K_2/3)} \frac{R_{BV} M_0^{BV}}{2\pi \zeta_{BV}} \frac{1}{r^4} \end{array} \right.$$



$$\left\{ \begin{array}{l} E_v^{BV} = \frac{1}{\gamma_t} \left(1 - \frac{\mathbf{v}^2}{2c_t^2} \right) E_{dist}^{BV} + \frac{1}{\gamma_t} \frac{1}{2} M_0^{BV} \mathbf{v}^2 = \frac{E_{dist}^{BV}}{\gamma_t} = \frac{M_0^{BV} c_t^2}{\gamma_t} \\ E_{dist}^{BV} \cong M_0^{BV} c_t^2 \quad \text{if } \mathbf{v} = 0 \\ E_{cin}^{BV} \cong \frac{1}{2} M_0^{BV} \mathbf{v}^2 \quad \text{if } \mathbf{v} \ll c_t \end{array} \right.$$

Figure 7.10 - The essential properties of a twist disclination loop (BV)

The expansion perturbation fields that we have just described obviously have an energy, which it would be desirable to compare with the elastic energy E_{dist}^{BV} of the screw loop. The total energy of the expansion perturbation field due to the elastic energy of the loop is deduced by the relation of figure 7.5 and is reported in figure 7.10. We can compare this energy with elastic energy, by relating it, and we get approximately $E_{grav}^{(q_{\lambda BV})} / E_{dist}^{BV} \propto (K_1 / K_0) (\vec{B}_{BV} / R_{BV})^2 \ll 1$, because $K_1 \ll K_0$. It is therefore deduced that the "gravitational" energy $E_{grav}^{(q_{\lambda BV})}$ of the twist disclination loop due to its elastic energy E_{dist}^{BV} is perfectly negligible compared to its elastic

energy in the perfect cosmological lattice.

In figure 7.10, we have reported all of the important properties that we have deduced so far for a twist disclination loop in a perfect cosmological lattice, namely its charge, its mass of inertia, its fields of rotation and disturbances of the long distance expansion, its elastic and kinetic energies, and finally its relativistic behavior. We see, among other things, that the mass of inertia M_0^{BV} of the loop does not only control the dynamic properties of the loop, like its kinetic energy E_{cin}^{BV} , but that it is also it which generates the gravitational fields $\tau_{ext LD}^{BV}(r)$ and $\tau_{ext CD}^{BV}(r)$ of external perturbations of expansion.

As the “gravitational” energy $E_{grav}^{(q_{\lambda BV})}$ of the expansion perturbation fields due to the rotation charge $q_{\lambda BV}$ of the twist disclination loop is perfectly negligible compared to the elastic energy E_{dist}^{BV} of the loop, this “gravitational” energy is not listed in the essential properties table.

As for the field of perturbations of the expansion within the torus itself surrounding the loop, and of the energy which is associated with this internal field, we will come back to this in detail later, when we will deal with the problem of spin and magnetic moment of the twist disclination loop.

Perturbations of the expansion associated with the edge prismatic loop (BC)

The prismatic edge dislocation loop we described in figure 5.6 has a curvature charge $q_{\theta BC}$, which makes it the elementary building block of *the lattice curvature charge* in our real world analogy. This charge is responsible for an external divergent flexion field, analogous to a geometric curvature field.

Knowing the elastic energy of the prismatic edge dislocation loop, we can use the relation of figure 7.1 to calculate the external field $\tau_{ext}^{(E)}(r)$ of expansion perturbations associated with the elastic energy E_{dist}^{BC} of the edge dislocation loop, here neglecting its energy potential V_{pot}^{BC} . One can also use the relation of figure 7.3 to calculate the external field $\tau_{ext}^{(q_{\theta BC})}(r)$ of expansion perturbations associated with the curvature charge $q_{\theta BC}$ of the loop. But using conjecture 5, that is $K_2 \ll K_3$, one can show that the first term $\tau_{ext}^{(E)}(r)$ is most likely far less than the second term $\tau_{ext}^{(q_{\theta BC})}(r)$. Thus, in the case of this loop, it is the expansion perturbation field due to the curvature charge which largely prevails over the expansion perturbation field due to the elastic distortion energy of the loop, unlike the twist disclination loop for which the energy of the perturbation field due to the distortion energy of the loop greatly outweighs the energy of the perturbation field due to the external field of rotation.

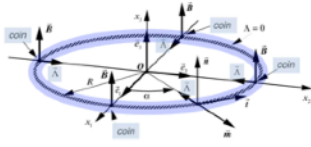
Apart from the mass of inertia M_0^{BC} of the edge loop, one can also introduce *an equivalent mass of curvature* $M_{curvature}^{BC}$ defined in figure 7.11, and which can be positive or negative depending on whether the edge loop is of a lacunar or interstitial nature. This mass of curvature then allows the gravitational field $\tau_{ext LD}^{BC}(r)$ to be written in the form shown in figure 7.11. According to the hypothesis of conjecture 5 ($K_2 \ll K_3$), the equivalent mass of curvature in the expression of the gravitational field satisfies the relationship $|M_{curvature}^{BC}| \gg M_0^{BC}$. In addition, the equivalent mass of curvature can be positive or negative. These two facts will imply very surprising results as we will see later.

The expansion perturbation fields that we have just described obviously have an energy, which it would be desirable to compare with the elastic energy E_{dist}^{BC} of the edge loop. The

energy $E_{grav}^{(E)}$ of the expansion perturbation field due to the elastic energy of the loop is deduced thanks to the relations of figure 7.1. This energy can be compared with elastic energy, and it then comes the ratio $E_{grav}^{(E)} / E_{dist}^{BC} \propto (K_1 K_2^2 / K_0^3) (\vec{B}_{BC} / R_{BC})^2 \lll 1$ as $K_1 K_2^2 \lll K_0^3$. We therefore deduce that the "gravitational" energy $E_{grav}^{(E)}$ of the edge dislocation loop due to its elastic energy E_{dist}^{BC} is perfectly negligible compared to its elastic energy in the perfect cosmological lattice.

Let's take a look at the energy $E_{grav}^{(q_{\theta BC})}$ associated with the expansion perturbation field due to the curvature charge of the edge loop. Using the relation of figure 7.3, one obtains the energy of the field of "gravitation" associated with the charge of curvature, which can be compared with the elastic energy E_{dist}^{BC} , and one obtains the ratio $E_{grav}^{(q_{\theta BC})} / E_{dist}^{BC} \propto K_1 / K_0 \lll 1$ as $K_1 \lll K_0$. We deduce again that the "gravitational" energy $E_{grav}^{(q_{\theta BC})}$ of the dislocation edge loop due to its curvature charge $q_{\theta BC}$ is perfectly negligible compared to its elastic energy E_{dist}^{BC} in the perfect cosmological lattice.

The prismatic edge dislocation loop (BC)



$$\left\{ \begin{array}{l} q_{\theta BC} = -2\pi \vec{n} (\vec{t} \wedge \vec{\Lambda}_{BC}) = 2\pi \vec{\Lambda}_{BC} \vec{m} = -2\pi \vec{n} \vec{B}_{BC} \quad \left\{ \begin{array}{l} > 0 \text{ if vacancy loop } (\vec{n} \vec{B}_{BC} < 0) \\ < 0 \text{ if interstitial loop } (\vec{n} \vec{B}_{BC} > 0) \end{array} \right. \\ \\ M_0^{BC} = \frac{E_{dist}^{BC}}{c_t^2} \cong \left(\frac{K_2}{K_3} \right)^2 \frac{K_3}{c_t^2} \zeta_{BC} R_{BC} \vec{\Lambda}_{BC}^2 = \left(\frac{K_2}{K_3} \right)^2 \frac{K_3}{c_t^2} \zeta_{BC} R_{BC} \vec{B}_{BC}^2 \\ \\ M_{curvature}^{BC} = -\frac{2\pi K_2}{5c_t^2} R_{BC}^2 \vec{n} \vec{B}_{BC} = \frac{K_2}{5c_t^2} R_{BC}^2 q_{\theta BC} \quad \left\{ \begin{array}{l} > 0 \text{ if vacancy loop } (q_{\theta BC} > 0) \\ < 0 \text{ if interstitial loop } (q_{\theta BC} < 0) \end{array} \right. \\ \\ |M_{curvature}^{BC}| \gg M_0^{BC} \end{array} \right.$$

$$\left\{ \begin{array}{l} \vec{\chi}_{ext}^{BC}(\vec{r}) = \frac{q_{\theta BC}}{4\pi} \frac{\vec{r}}{r^3} \\ \\ \tau_{ext}^{BC}(r) \cong -\frac{c_t^2}{2\pi(K_0 - 4K_2/3 - 2K_1(1 + \tau_0))R_w^2} \frac{M_{curvature}^{BC} + M_0^{BC}}{r} \end{array} \right.$$

$$\left\{ \begin{array}{l} E_v^{BC} = \frac{1}{\gamma_t} \left(1 - \frac{\mathbf{v}^2}{2c_t^2} \right) E_{dist}^{BC} + \frac{1}{\gamma_t} \frac{1}{2} M_0^{BC} \mathbf{v}^2 = \frac{E_{dist}^{BC}}{\gamma_t} = \frac{M_0^{BC} c_t^2}{\gamma_t} \\ \\ E_{dist}^{BC} \cong M_0^{BC} c_t^2 \quad \text{if } \mathbf{v} = 0 \\ \\ E_{cin}^{BC} \cong \frac{1}{2} M_0^{BC} \mathbf{v}^2 \quad \text{if } \mathbf{v} \ll c_t \end{array} \right.$$

Figure 7.11 - The essential properties of a prismatic edge dislocation loop (BC)

In figure 7.11, we have reported all the important properties that we have deduced so far for an edge dislocation loop in a perfect cosmological lattice, namely its curvature charge, its mass of inertia, its equivalent gravitational mass, its fields of flexion and of perturbations of the expansion of the long distance, its elastic and kinetic energies, and finally its relativistic behavior. One notes there that it is its elastic energy E_{dist}^{BC} , and as a consequence its mass of inertia M_0^{BC} which is deduced from it, which controls its dynamic properties, like its kinetic

energy E_{cin}^{BC} , but that it is its equivalent gravitational mass $M_{curvature}^{BC}$ of curvature which essentially controls its external gravitational field $\tau_{ext LD}^{BC}(r)$ of expansion perturbations at long-distance.

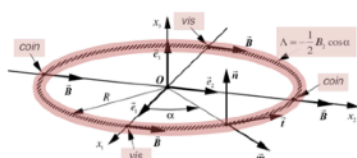
As the “gravitational” energies $E_{grav}^{(E)}$ and $E_{grav}^{(q_{\theta BC})}$ of the fields of expansion perturbations due to the elastic energy E_{dist}^{BC} and to the curvature charge $q_{\theta BC}$ of the dislocation edge loop are perfectly negligible compared to the elastic energy E_{dist}^{BC} of the loop, these “gravitational” energies do not appear in the table of essential properties.

On the other hand, the equivalent gravitational mass of curvature $M_{curvature}^{BC}$ is not only much greater than the mass of inertia M_0^{BC} , but it can even be negative in the case of edge loops of interstitial nature. This result turns out to be very surprising since it corresponds to the possible existence of a negative gravitational field, and it is in fact extremely promising by the novelty which it brings in our approach compared to the General Relativity of Einstein. The possible consequences of this astonishing result will be explored in detail in the rest of the book.

Perturbations of the expansion associated with the mixed slip dislocation loop (BM)

The mixed slip dislocation loop that we have described in figure 5.7 has neither rotation charge nor curvature charge, but on the other hand a dipolar moment of rotation field $\vec{\omega}_{dipolar}^{BM}(r, \theta, \varphi)$, analogous to an electric dipolar moment. Knowing the elastic energy of distortion of the mixed slip dislocation loop in a perfect cosmological lattice, we can use the relation of figure 7.1 to calculate the external field $\tau_{ext}^E(r)$ of expansion perturbations associated with this elastic energy E_{dist}^{BM} , by neglecting here the potential energy V_{pot}^{BM} . On the other hand, it also becomes interesting here to replace in the expression $\tau_{ext}^E(r)$ the distortion energy E_{dist}^{BM} by the mass of inertia M_0^{BM} of the loop using the relation $E_{dist}^{BM} = M_0^{BM} c_t^2$. *It comes the expression of $\tau_{ext}^E(r)$ reported in figure 7.12.*

The slip mixed dislocation loop (BM)

$$\left\{ \begin{array}{l} M_0^{BM} \equiv \frac{K_2 + K_3}{4c_t^2} \zeta_{BM} R_{BM} \vec{B}_{BM}^2 \\ \exists \text{ an external dipolar rotation field } \vec{\omega}_{dipolar}^{BM}(r, \theta, \varphi) \\ \tau_{ext}^{BM}(r) \equiv - \frac{c_t^2}{2\pi(K_0 - 4K_2/3 - 2K_1(1 + \tau_0))R_\infty^2} \frac{M_0^{BM}}{r} \end{array} \right.$$


$$\left\{ \begin{array}{l} E_v^{BM} = \frac{1}{\gamma_t} \left(1 - \frac{v^2}{2c_t^2} \right) E_{dist}^{BM} + \frac{1}{\gamma_t} \frac{1}{2} M_0^{BM} v^2 = \frac{E_{dist}^{BM}}{\gamma_t} = \frac{M_0^{BM} c_t^2}{\gamma_t} \\ E_{dist}^{BM} \equiv M_0^{BM} c_t^2 \quad si \quad v = 0 \\ E_{cin}^{BM} \equiv \frac{1}{2} M_0^{BM} v^2 \quad si \quad v \ll c_t \end{array} \right.$$

Figure 7.12 - The essential properties of a slip mixed dislocation loop (BM)

The expansion perturbation fields we have just found obviously have an energy, which it would be desirable to compare with the elastic energy E_{dist}^{BM} of the loop. The energy $E_{grav}^{(E)}$ of the expansion perturbation field due to the elastic energy of the loop is deduced thanks to the relations of figure 7.1, and can be compared directly with the elastic energy E_{dist}^{BM} to derive the ratio $E_{grav}^{(E)} / E_{dist}^{BM} \propto (K_1 / K_0) (\vec{B}_{BM} / R_{BM})^2 \ll 1$ as $K_1 \ll K_0$. We therefore deduce that the "gravitational" energy $E_{grav}^{(E)}$ of the mixed dislocation loop due to its elastic energy E_{dist}^{BM} is perfectly negligible compared to its elastic energy in the perfect cosmological lattice.

In figure 7.12, we have plotted the set of properties of a mixed slip dislocation loop in the perfect cosmological lattice. If this loop has neither rotation charge nor curvature charge generating external fields of rotation or flexion at long range, it is provided with an external field of dipolar rotation $\vec{\omega}_{dipolar}^{BM}(r, \theta, \varphi)$, at short range, analogous to an electric dipolar field. The external field of expansion perturbations is due to the elastic distortion energy of the loop, and depends on its mass of inertia M_0^{BV} .

On the other hand, since the "gravitational" energy $E_{grav}^{(E)}$ of the expansion perturbation fields due to the elastic energy E_{dist}^{BM} of the mixed dislocation loop is perfectly negligible compared to the elastic energy E_{dist}^{BM} of the loop, this "gravitational" energy is not included in the table of essential properties.

About the various properties of the elementary topological loops

We have demonstrated above all the essential properties of the three elementary loops that can be encountered in the perfect cosmological lattice, and we have notably established the expressions of the fields of perturbations of external expansion, which correspond to "gravitational fields" of expansion of the loops, and which will play a very important role thereafter.

We have shown that the energies $E_{grav}^{(E)}$, $E_{grav}^{(q_{\lambda BV})}$, $E_{grav}^{(q_{\theta BC})}$ of the "gravitational" fields associated with the elastic energies, the rotation charges and the curvature charges of the elementary loops are perfectly negligible with respect to the elastic energies associated with these loops, and that we can therefore perfectly ignore them in our calculations.

One can wonder if the elementary topological loops can be black holes. To do this, we apply the conditions of the black holes of figure 3.5 to the expansion fields $\tau_{ext LD}^{BV}(r)$, $\tau_{ext}^{BC}(r)$ and $\tau_{ext}^{BM}(r)$ respectively. By applying these conditions to the twist disclination loop in the case where $\tau_0 \ll \tau_{0cr}$, we obtain the following condition $|\vec{B}_{BV}| \geq 2R_\infty (2\pi / \zeta_{BV})^{1/2}$ so that this loop is a black hole, which would imply that the pseudo-vector of Burgers of the loop is of the order of magnitude of the radius of the lattice, which obviously makes no sense.

The same goes for the mixed slip dislocation loop, since the condition for it to be a black hole becomes $|\vec{B}_{BM}| > 4R_\infty (2\pi / \zeta_{BM})^{1/2}$. In the case of the prismatic edge dislocation loop, the condition is expressed differently since the gravitational mass is worth $M_{curvature}^{BC} + M_0^{BC}$. Like $|M_{curvature}^{BC}| \gg M_0^{BC}$, we get $R_{BC} |\vec{B}_{BC}| \geq 10K_0 R_\infty^2 / K_2$. But since the module K_2 must be much smaller than the module K_0 according to conjecture 6, this condition can obviously never be satisfied. Consequently, it is clear that the three elementary loops forming the basis of the microscopic topological singularities cannot be black holes in the domain $\tau_0 \ll \tau_{0cr}$.

In the analogy between our approach and the major theories of physics, the three types of elementary loops that we have discussed in this chapter have a number of amazing and

remarkable properties that we will list here:

- they are respectively the elementary bricks of *the electric charge*, *the curvature charge* and *the electric dipolar moment*, from which it might be possible to form dispirations, by more or less complicated combination of several loops, in order to find topological singularities which are analogues of the elementary particles of our real world,
- their rest energy and their kinetic energy are essentially *confined in the toric field surrounding the loops*,
- as the energy associated with the “gravitational” fields of expansion perturbations is perfectly negligible, *they perfectly satisfy Einstein's relation*, which is surprisingly obtained in our approach as a purely classical property of topological singularities within the lattice, without appeal to a principle of relativity,
- they perfectly satisfy *special relativity*, with a completely original explanation of relativistic energy $E_v^{loop} = E_v^{dist} + E_v^{cin} = E_{dist}^{loop} / \gamma_t = M_0^{loop} c_t^2 / \gamma_t$ as the sum of a relativistic term of elastic distortion energy and a relativistic term of kinetic energy,
- they satisfy *a relativistic dynamic equation* reported in figure 6.7,
- the twist disclination loop, carrying a rotation load similar to the electric charge, satisfies *Maxwell's equations* and *Lorentz force*,
- the three types of loops present a long distance field of perturbations of the volume expansion, which is the analog of *a gravitational field decreasing in $1/r$* and which *depends only on a gravitational mass $M_0^{loop} + M_{curvature}^{loop}$* of the loops composed of the mass of inertia and of the equivalent curvature mass of the loop, without directly depending on the size R_{loop} of the loops,
- the gravitational masses of the twist disclination loop and the mixed slip dislocation loop are strictly equal to their masses of inertia, while the gravitational mass of the prismatic edge dislocation loop consists of the mass of inertia and the mass of curvature of the loop, with a mass of curvature much higher than the mass of inertia, and which may even be negative in the case of loops of interstitial nature,
- the gravitational mass of the prismatic edge dislocation loop contains two terms: the first dominant term of mass of curvature $M_{curvature}^{BC}$ is positive or negative depending on whether the loop is of lacunar or interstitial type, and the second term of mass of inertia M_0^{BC} is always positive. This means that the gravitational mass is not symmetrical between a loop of vacancy nature and a loop of interstitial nature. There appears here *a weak asymmetry in the absolute value of the gravitational mass between an interstitial loop and its lacunar anti-loop*, which is expressed by the following three relationships:

$$M_{curvature}^{BC(I)} + M_0^{BC(I)} > 0 \ ; \ M_{curvature}^{BC(i)} + M_0^{BC(i)} < 0 \ ; \ \left| M_{curvature}^{BC(i)} + M_0^{BC(i)} \right| \lesssim M_{curvature}^{BC(I)} + M_0^{BC(I)}$$
- all these properties are perfectly analogous to the fundamental properties of elementary particles in the real world, except for the gravitational mass of the prismatic edge dislocation loops, loops which have in fact a strong analogy with neutrinos. This very special property of prismatic edge dislocation loops will be discussed in *the following chapters, in which we will discuss the gravitational interaction between loops*.

Chapter 8

Newtonian gravitation and general relativity

A detailed study of the gravitational interactions intervening between loops of twist disclination leads to a strong analogy with the gravitation of Newton, but presenting however some differences as regards the gravitational attraction at short range and especially the dependence of the constant of gravitation in the volume expansion of the lattice.

We are then interested in *the Maxwellian formulation* of the spatio-temporal evolution equations presented previously in chapter 4, which corresponded to the expression of local laws of physics, such as electromagnetism, as seen by the imaginary external observer **GO** (*Great Observer*). We show in this chapter that it is possible to imagine a local observer **HS** (*Homo Sapiens*) which would be intimately linked to the local coordinate system, because it itself consists of a cluster of topological singularities of the lattice. This observer can only know local rulers and clocks in his local coordinate system, which are influenced by the local expansion field so that they make Maxwell's equations invariant with respect to volume expansions. A relativistic notion of time then appears for the local observers **HS**, for whom the speed of the transverse waves is measured as a universal constant, whereas this depends very strongly on the local volume expansion if it is measured by the observer **GO** outside the lattice.

The gravitational interactions thus obtained have very strong analogies with *Newton's Gravitation* and with *Einstein's General Relativity*. Perfectly analogous points are discussed in detail, such as the perfect analogy with *Schwarzschild's metric* at a great distance from a massive object and *the curvature of the wave rays* by a massive object.

But we also show that our Eulerian approach of the cosmic lattice brings new elements to the theory of Gravitation, in particular modifications of the Schwarzschild metric at very short distance from a singularity, and a better understanding of the critical rays associated with black holes: *the radii of the perturbation sphere and of the point of no return are both similar and equal to the Schwarzschild radius*, while *the limit radius for which the dilation of the observer's time would tend towards infinity becomes zero*, so our approach is not limited to the description of a black hole beyond the Schwarzschild sphere.

While the clusters of singularities composed of loops of twist disclination satisfy Newton's gravitation, and most of the results of General Relativity, we will finally ask ourselves the question of how to behave, towards the gravitation, other topological singularities, such as edge dislocation loops, mixed dislocation loops, macroscopic vacancies and macroscopic interstitials. We will thus deduce all the long-range gravitational interaction forces between the various topological singularities and their behaviors.

Newtonian gravitational interaction of clusters of twist disclination loops

In the previous chapter, it was shown that the mass of inertia of twist disclination loops is

extremely higher than the mass of inertia of edge and mixed dislocation loops, so that perturbations of the expansion field will be mainly caused by the twist disclination loops. This is why we will start by analyzing the long-range expansion perturbation fields due to them.

For a screw loop, the mass of inertia depends on the square of the rotation charge $q_{\lambda BV}$ (see figure 7.10). If such a loop is in an expansion field τ , the dependence of the mass of inertia M_0^{BV} and the charge of rotation $q_{\lambda BV}$ of this loop is related to the dependence $c_t = c_{t0} e^{\tau/2}$ and the dependence of R_{BV} and Ω_{BV} in the local expansion. One could think a priori that the radius of the loop is linked to the pitch of the lattice, so that $R_{BV} = R_{BV0} e^{\tau/3}$, and that the angle of rotation Ω_{BV} must correspond to an angle satisfying *the symmetry of the lattice*, namely for example a multiple of $\pi/2$ for a cubic lattice, or a multiple of $\pi/3$ for a hexagonal lattice or for a face-centered cubic lattice, so that Ω_{BV} should not depend on the background expansion of the lattice.

However, we do not know at all the exact nature of the cosmological lattice, so that, for the sake of generality, we will assume *a priori* an unknown dependence of R_{BV} and Ω_{BV} on the background expansion of the lattice, as if the loop could undergo an extension of its radius and / or a torsion dependent on the local volume expansion of the lattice, writing by assumption that $R_{BV} = R_{BV0} e^{\alpha_{BV}\tau}$ and $\Omega_{BV} = \Omega_{BV0} e^{\beta_{BV}\tau}$, where α_{BV} and β_{BV} are constants which will have to be determined subsequently, as indicated in figure 8.1. On the basis of this assumption, one can deduce the dependencies in the lattice expansion τ of the charge $q_{\lambda BV}$ and the mass of inertia M_0^{BV} of a loop, then the dependencies in τ of the charge $Q_{\lambda}^{cluster}$, the mass of inertia $M_0^{cluster}$ and the energy $E^{cluster}$ of a cluster of rotation charges.

Two clusters of loops located at a distance d from each other will interact with each other via their "gravitational" fields of long-range expansion perturbations (figure 8.1). We can calculate the energies of the clusters (1) and (2) from their mass of inertia, by introducing into the energy the total value of the expansion at the heart of each cluster. Indeed, the two clusters distant from the distance d are respectively immersed in the expansion perturbation field of the other cluster. As we know that the elastic energy of a loop is essentially located in the vicinity close to the loop, one is assured that the elastic energy of the cluster is essentially located in the core of the cluster, so that their respective energy is influenced by the presence of the other cluster and so that there appears an increase ΔE_{grav} in the energy of the two interacting clusters, which depends on the distance d separating the two clusters. The total interaction force between the two clusters is then given by the derivative with respect to d of the energy variation ΔE_{grav} of the two clusters, which leads to an interaction force shown in figure 8.1. This expression shows the product of the gravitational masses divided by the squared distance separating the two clusters, which furiously recalls a term from Newton's law of gravitation. Let's introduce a "gravitational constant" G_{grav} function of the lattice constants α_{BV} and β_{BV} and of lattice elastic constants, but also of the local volume expansion τ of the lattice.

The total force $F_{grav}(d)$ of gravitational interaction between the two clusters takes a form that can be recognized when we develop the exponential terms it contains, since it shows *the expression of Newton's gravitational force* between the two loops, corrected by additional terms in the bracket, which are the results of second-order developments, so that they are certainly smaller than 1. For rather low mass densities of the clusters and large distances d between the clusters, the second order terms in the bracket can be neglected, so that *a perfect analogy with*

Newton's gravitational interaction $F_{grav}(d) \equiv G_{grav} M_{0(1)}^{cluster} M_{0(2)}^{cluster} / d^2$ of the real world is found, and G_{grav} becomes the "gravitational constant", which must be very small since it occurs R_∞^2 in the denominator.

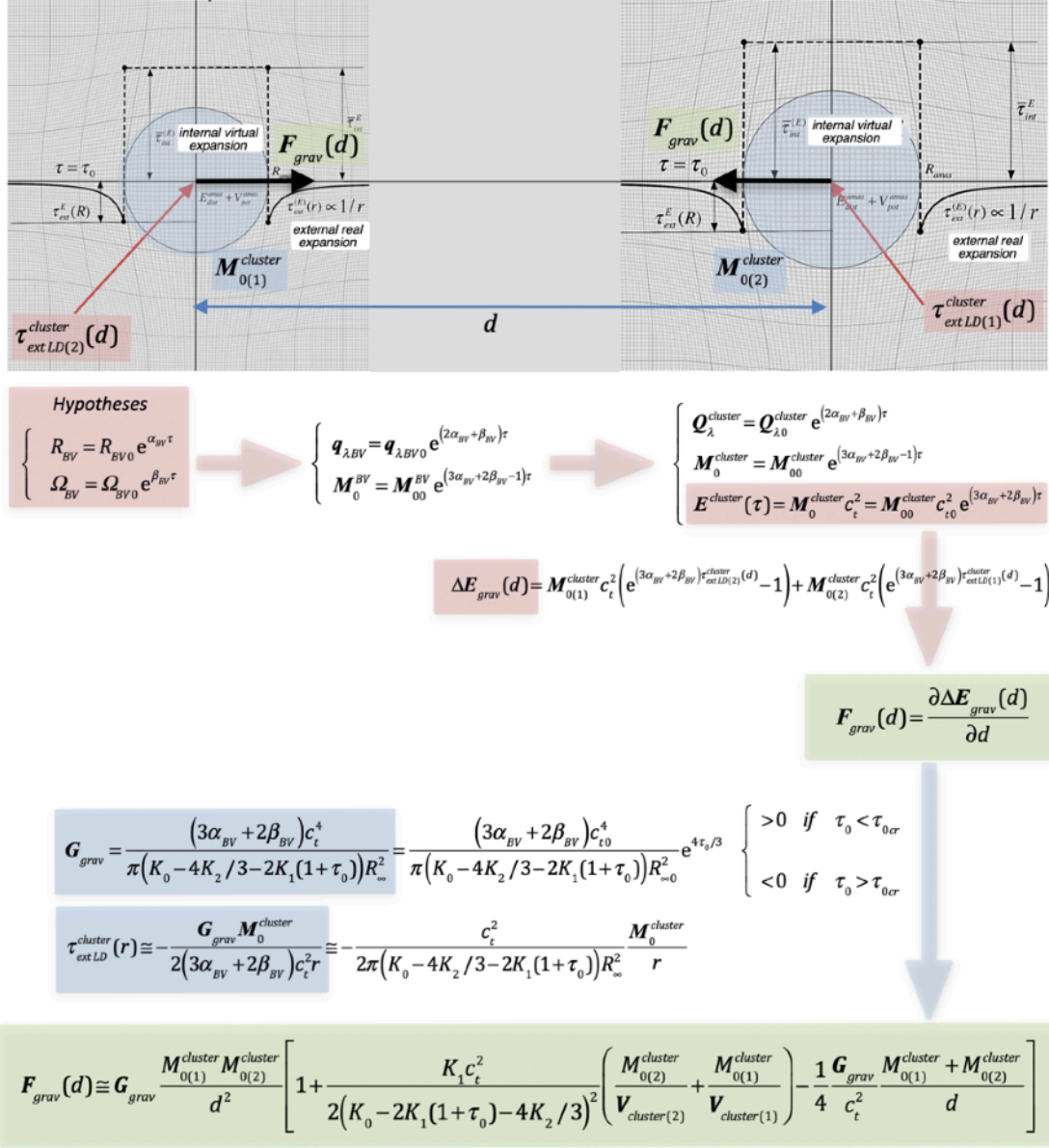


Figure 8.1 - The «gravitational» interaction force between two clusters of singularities with rotation charge

Let us then try to understand what the second-order terms actually represent in the full expression $F_{grav}(d)$ of Figure 8.1. The term dependent on cluster mass densities $M_{0(i)}^{cluster} / V_{cluster(i)}$ is a correction to the "gravitational constant" G_{grav} independent of the distance d between clusters, which actually comes from the non-linear behaviour of the function $\bar{\tau}_{int}^{(E)}(x)$ shown in Fig. 7.0 when the cluster mass density exceeds a certain critical value. As for the term dependent on d , it brings a correction to the interaction force when the distance between clusters becomes small. This term comes from the development of the

exponential terms of the energy variation ΔE_{grav} of the two clusters.

What first appears when looking at the expression of the "constant" of gravitation is that it is in fact in no way a constant since it depends on the average state of expansion τ_0 of the lattice via the values of c_t^4 and R_∞^2 , as well as by the value of τ_0 intervening in the denominator in factor of the module K_1 , which makes the value of G_{grav} positive if $\tau_0 < \tau_{0cr}$ and negative if $\tau_0 > \tau_{0cr}$. This strong dependence of G_{grav} on the background expansion of the lattice should undoubtedly play a key role in the evolution of the Universe during its cosmological expansion. We will come back to this subject later.

At a shorter distance d , there appears a *correction to Newton's law* expressed by a multiplicative term. This second-order term in the expression of the approximate law of gravitation will modify the interactions between two clusters when they are very close to each other. But unlike the results obtained in General Gravitation using the Schwarzschild metric, which predicts a small increase in the force of attraction at very short distances, the second-order corrective term in our approach leads to a small decrease in $1/d^3$ of the attraction force at very short distances.

For example, in the case of the planet Mercury which is quite close to the Sun, the calculation of the corrective term provides the value $G_{grav} M_{Sun} / (4c_t^2 d_{Mercury}) \cong 5,6 \cdot 10^{-7}$ with $M_{Sun} \cong 2 \cdot 10^{30} [kg]$, $d_{Mercury} \cong 5,8 \cdot 10^{10} [m]$, $G_{grav} \cong 6,6 \cdot 10^{-11} [m^3 / kg \cdot s^2]$, $c_t^2 \cong 10^{17} [m^2 / s^2]$ which gives for the period of revolution of Mercury 88 days ($7,6 \cdot 10^6$ seconds), an increase of 2.128 seconds compared to the value calculated with Newton's law of gravitation.

The local rulers and clock of an HS observer

Consider a local reference frame $Ox_1x_2x_3$ defined by the **GO** observer (*the imaginary Great Observer*) from its absolute frame of reference $Q\xi_1\xi_2\xi_3$. This local coordinate system $Ox_1x_2x_3$ is in fact a convenience used by **GO** to solve the problems of local evolution of the solid lattice, in particular in regions of the solid having a non-zero volume expansion, but which can be considered as constant and homogeneous in the vicinity of the origin of the coordinate system $Ox_1x_2x_3$, for example using *the Maxwellian formulation* described in chapter 4.

But now imagine that there is indeed another category of local observer that we called observer **HS** (*Homo Sapiens*) and which is really found in the local coordinate system $Ox_1x_2x_3$ because it is itself constituted from the topological singularities of the lattice, and in particular from elementary loops of twist disclination which interact with each other via their rotation field generated by their own rotation charge. In his local frame, the **HS** obviously does not have access to the global view of the lattice in the absolute reference frame, since he only knows the conditions of the local lattice in which he lives. The **HS** observer can therefore only define his own rulers \vec{e}_{yi} in his coordinate system $Oy_1y_2y_3$, by defining them from the linear dimensions of the objects contained in the lattice in which he lives. This is illustrated in figure 8.1 for two observers **HS** and **HS'** living in two different locations of the lattice, where the respective volume expansions of the lattice τ and τ' are different.

If the lattice locally exhibits a certain volume expansion τ , the **HS** rules should satisfy a relationship of the type $\vec{e}_{yi} = e^{a\tau} \vec{e}_i$ where the constant a is not defined a priori and must therefore be determined. This implies that the rulers of an **HS** will be of different length than those of the **GO** if the lattice is locally shrinking ($\tau < 0$) or expanding ($\tau > 0$). If a certain point

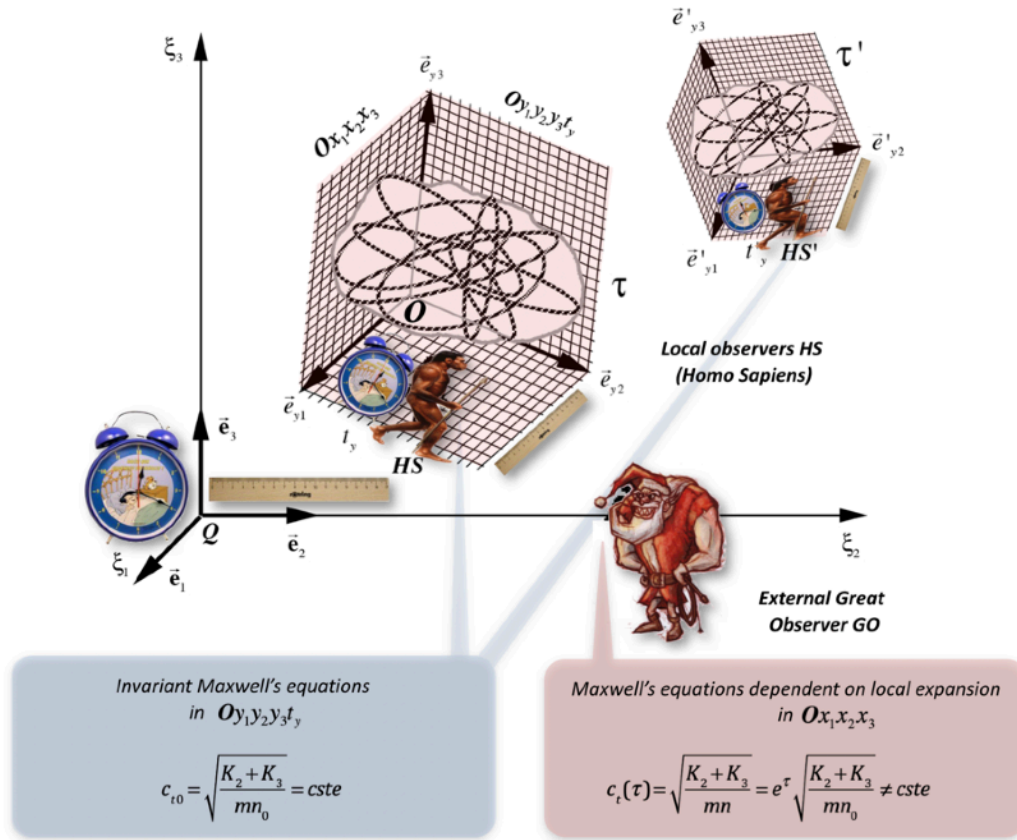


Figure 8.2 - Local rulers and clocks in the reference frames of HS and HS'

in space, identified by the vector \vec{r} , is observed simultaneously by the **GO** and by **HS**, the vector will be written $\vec{r} = \sum x_i \vec{e}_i = \sum x_i e^{-a\tau} \vec{e}_{yi} = \sum y_i \vec{e}_{yi}$ in $Ox_1x_2x_3$ and in $Oy_1y_2y_3$ respectively so that the coordinates of the point of the space is transformed by relationship $y_i = e^{-a\tau} x_i$.

On the other hand, the time measured in $Ox_1x_2x_3$ at $\tau \neq 0$ must also be different from the time measured when $\tau = 0$, so that **HS** own clock in its frame $Oy_1y_2y_3$ must indicate a time t_y different from the absolute time t of the **GO**, but linked to it by the relationship $t_y = e^{b\tau} t$. Regarding the **HS** clock, he will have to build it locally since it does not have access to the absolute time of the **GO**. It will then be logical for him to build a simplistic clock using one of his local rulers and the speed of the transverse waves which he can measure in the coordinate system of his own frame of reference. Consider a ruler of length d_0 measured by **GO** in a lattice with zero volume expansion. The length of the same ruler placed in the **HS** frame and measured by the **GO** becomes $d = d_0 e^{a\tau}$. To traverse the distance of this ruler, the transverse waves use a period of time Δt measured by the **GO**, and given by $\Delta t = \Delta t_0 e^{-b\tau}$. In the coordinate system $Ox_1x_2x_3$, placed in a volume expansion region τ other than zero, the initial length d_0 of the ruler therefore becomes equal to $d_0 e^{a\tau}$, and the travel time of the ruler becomes $\Delta t_0 e^{-b\tau}$, so that the speed of the transverse waves in the presence of the expansion τ is equal to $c_t = d / \Delta t = c_{t0} e^{(a+b)\tau} = c_{t0} e^{\tau/2}$. This implies that time will flow differently for **HS**

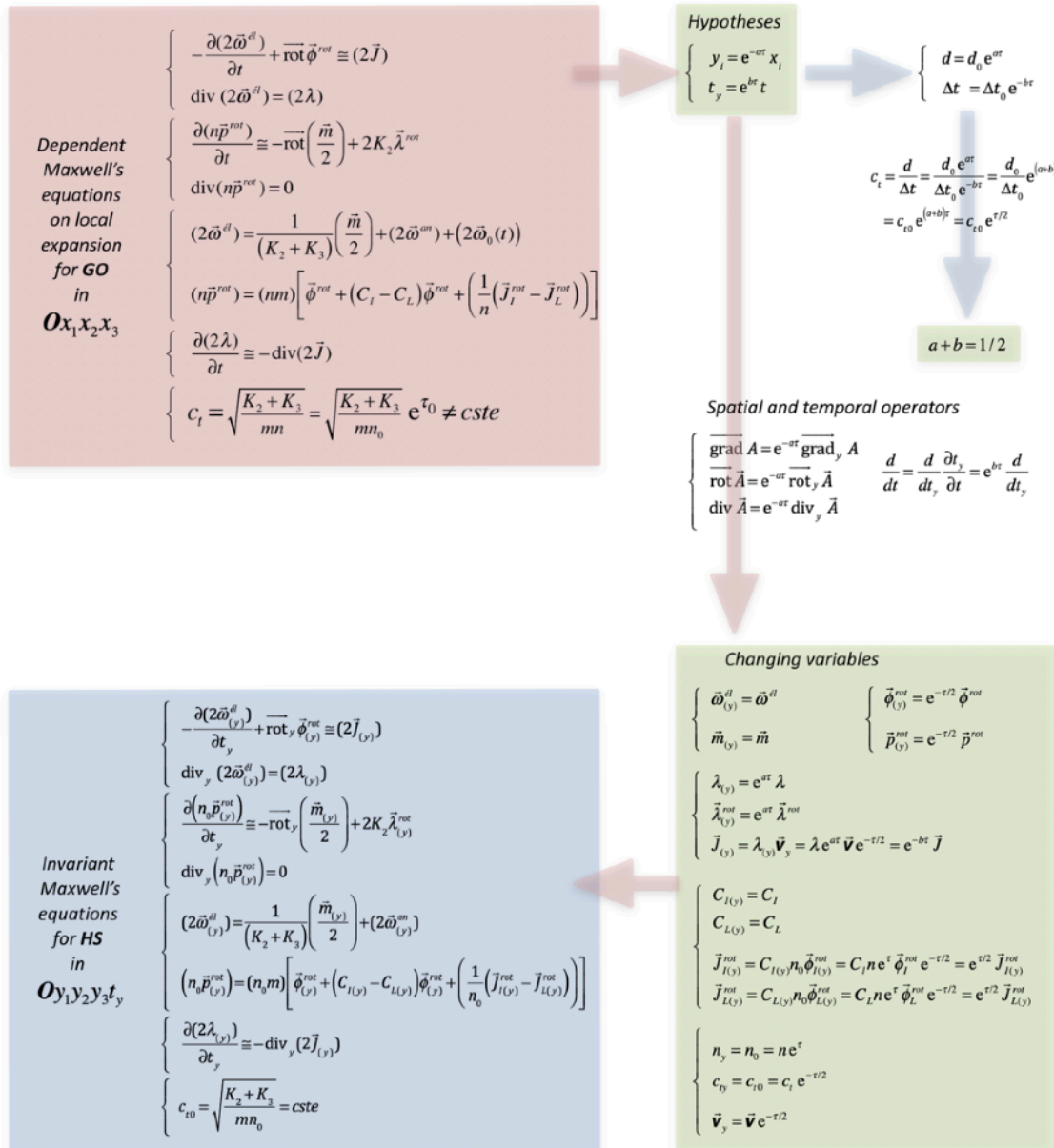


Figure 8.3 - The transition from the local frame $O_{x_1x_2x_3}$ of GO to the local frame $O_{y_1y_2y_3}$ of HS

in $O_{y_1y_2y_3}$ if the lattice is contracting or expanding. We then have the following relationship between the values of a and b due to the operation of the **HS** clock: $a + b = 1/2$.

In figure 8.3, one deduces all the expressions making it possible to pass from the local reference frame $O_{x_1x_2x_3}$ of the **GO** to the local reference frame $O_{y_1y_2y_3}$ of the **HS**. On the basis of the assumptions for the rulers and the clock of **HS**, one expresses the formulas of passage of the operators of time and space, and one applies them to the equations of Maxwell expressed in $O_{x_1x_2x_3}$ to obtain these same equations in $O_{y_1y_2y_3}$. By making a change of variables in the fields of rotation, torque, velocity and momentum, as well as on the quantities associated with the densities and fluxes of rotation charges and the quantities associated with the concentrations of vacancies and of interstitial and to the fluxes of these defects, we obtain the Maxwell's equations as formulated by **HS** in his local frame of reference $O_{y_1y_2y_3}$.

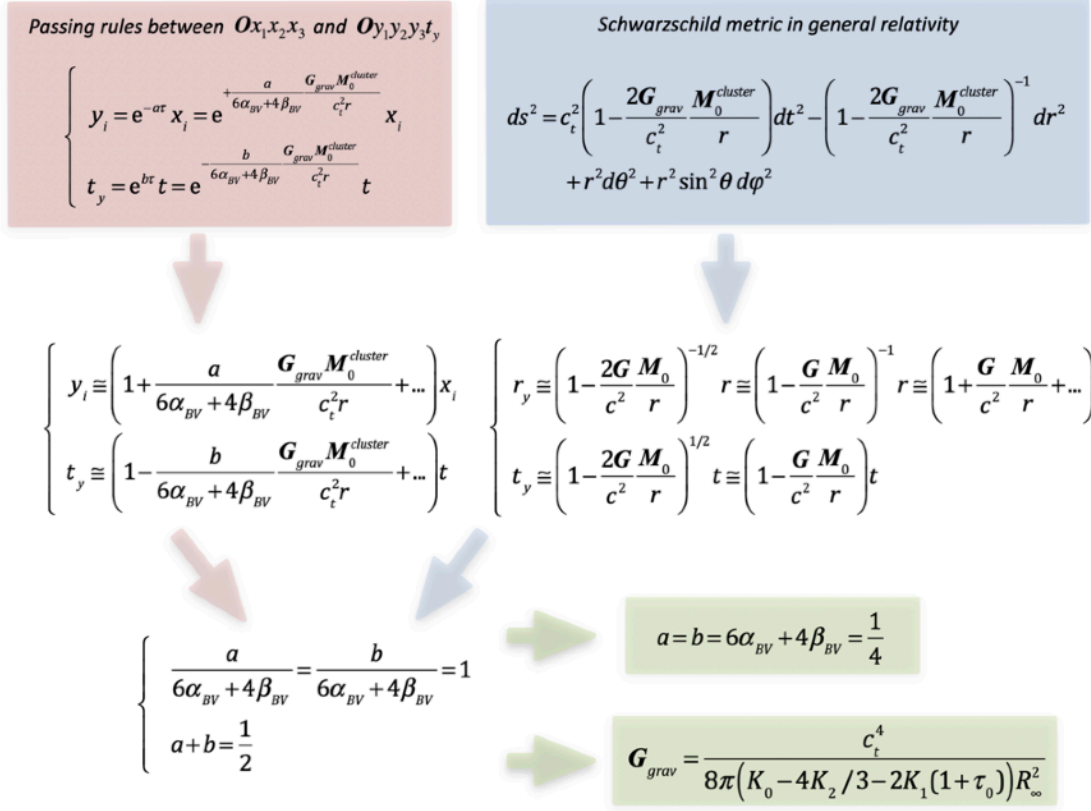


Figure 8.4 - Comparison of passing rules between the local frame $O_{x_1 x_2 x_3}$ of **GO and the local frame $O_{y_1 y_2 y_3}$ of **HS** with the transformation rules experimentally verified of the Schwarzschild metric in general relativity**

In these expressions of change of variables, it is perfectly logical to have posed $\vec{\omega}_{(y)}^{el} = \vec{\omega}^{el}$ and $\vec{m}_{(y)} = \vec{m}$ since these quantities are associated with measurements of angles of rotation, and to have chosen the relations $\vec{\phi}_{(y)}^{rot} = e^{-\tau/2} \vec{\phi}^{rot}$ and $\vec{p}_{(y)}^{rot} = e^{-\tau/2} \vec{p}^{rot}$, since these quantities are in fact associated with velocities. By this change in the variables, we then obtain a set of invariant Maxwell equations in the frame $O_{y_1 y_2 y_3 t_y}$ of the observer **HS** as illustrated in figures 8.2 and 8.3, i.e. equations which no longer depend on the local expansion τ . We note, among other things, that the speed of the transverse waves becomes an invariant constant for the **HS** observer, whatever the state of expansion of the lattice in which he lives. We also note that only the quantities associated with the densities and the flow of rotation charges are transformed in a dependent way in the parameter a , while all the other quantities are transformed in a logical and predictable way.

The fact that the Maxwell equations of the **HS** observers are invariant (independent of local expansion τ) implies that the local **HS** observers are perfectly incapable of measuring the local state of expansion of the lattice in which they live on the sole basis of electromagnetic measurements based on Maxwell's equations. In particular, the measurement of the speed of the transverse waves by the **HS** observers always provides an invariant value, whatever the local state of expansion of the lattice. Thus, local observers **HS** are essentially subject to the

physical laws corresponding to electromagnetism, and are only aware of the gravitational effects associated with the expansion field through indirect observations of their effects, such as the movement of the planets or the slowing down of their clocks in a gravitational field. This is why the **HS** will have to seek to explain the phenomena related to gravitation by ad-hoc theories (Newton's Gravitation, General Relativity) which seem a priori independent of the laws of electromagnetism, but which they will obviously seek to unify.

Figure 8.2 illustrates well here the existence of a strong analogy between our approach and *Einstein's General Relativity Theory*. Indeed, the rulers and the clock of an **HS** living in a certain place of the lattice depend on the local volume expansion τ of the lattice, in a way analogous to what stipulates the General Relativity for the rulers and the clock of an observer located in a given gravitational field. In the case illustrated in figure 8.2, we understand that the lattice plays the role of an "ether" which imposes the size of the rulers of the **HS** observer, while it is the celerity of the transverse waves within the lattice (in fact the speed of information transport) which imposes the speed of the **HS** clock.

On the other hand, the existence of three degrees of freedom on the parameters a , b , α_{BV} and β_{BV} is quite surprising, because it implies that there is still a possible choice at this level, which cannot be determined on the basis of our knowledge of the cosmological lattice. In fact, an arbitrary choice of "free" values of a , α_{BV} and β_{BV} should not lead to inconsistencies in the system, and the resulting cosmological lattice could be perfectly viable. Consequently, we can consider that the parameters a , α_{BV} and β_{BV} are really properties specific to the cosmological lattice, in fact intrinsic constants of the lattice, in the same way as are the elastic modules K_i or the mass m of inertia per cell of the lattice. The determination of these constants therefore necessarily involves experimentation, in other words by measuring the real properties of the cosmological lattice associated with these two constants.

By combining the various relations obtained in figure 8.3, we can write the transformation rules to pass from the local reference frame $Ox_1x_2x_3$ of the **GO** into the local reference frame $Oy_1y_2y_3t_y$ of an **HS** placed at a distance r in the gravity field of a cluster of mass M_0^{amas} , according to unknown parameters a , α_{BV} and β_{BV} , as shown in figure 8.4. These transformation equations can, at a certain sufficient distance r from a cluster of mass $M_0^{cluster}$, be written approximately by development of the exponentials.

In General Relativity, the dependencies of the radial ruler and the clock of an observer subjected to the gravitational field of an object of mass M_0^{amas} are deduced from *the Schwarzschild metric*. This is obtained in the case of a massive object with spherical symmetry by postulating an invariant metric with respect to the rotations, which is also shown in figure 8.4. From this Schwarzschild metric, we deduce that the radial ruler and the observer's clock depend symmetrically on the distance r separating him from the object of mass M_0 , with expressions similar to *the simplified expressions obtained in our approach*, but with a coefficient 1 in front of $G_{grav} M_0^{cluster} / c_t^2 r$. However, the dilation of time in a gravity field, represented by the second relation deduced from the metric of Schwarzschild, has



Karl Schwarzschild
(1873-1916)

been verified experimentally with very great precision¹, even on elevation differences as small as 1 meter on the surface of the earth, and this effect is currently taken into account in very precise navigation systems, such as *GPS*. This experimentally verified effect can therefore be used to adjust the determination of the parameters a , α_{BV} and β_{BV} , by ensuring that the long-distance relationships of our approach correspond to the relationships deduced from the Schwarzschild metric. By making this comparison, we get that $a = b = 6\alpha_{BV} + 4\beta_{BV} = 1/4$.

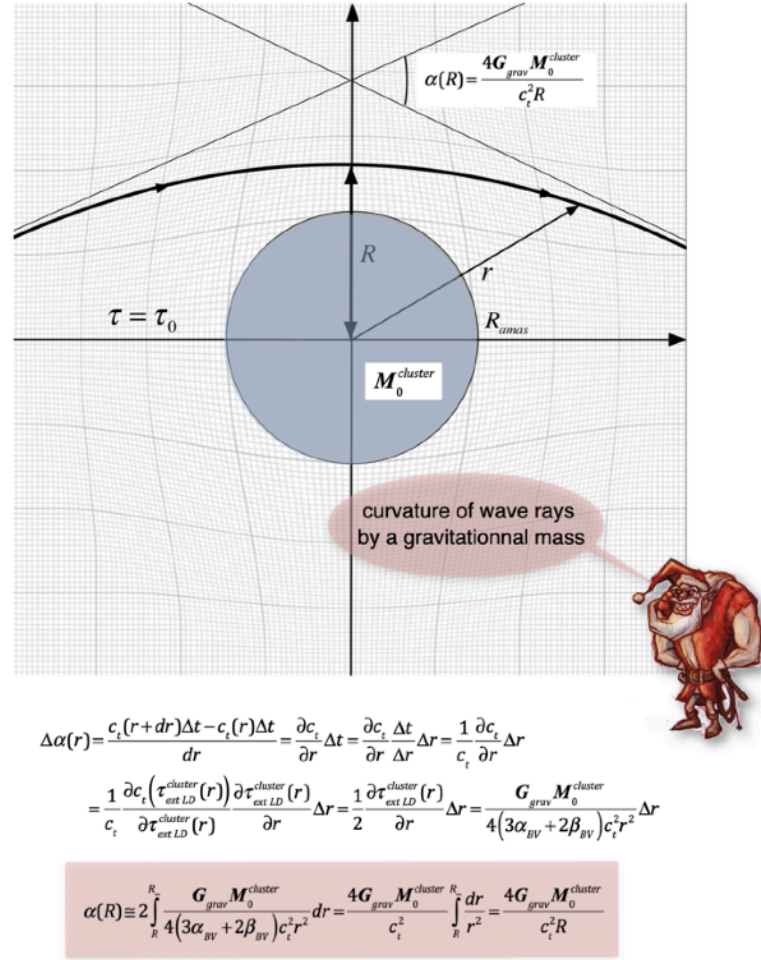


Figure 8.5 - curvature of transversal wave rays in the vicinity of a massive cluster

We can still verify the analogy of our approach with Einstein's General Relativity, for example by calculating the curvature of the rays of transverse waves in the vicinity of a massive cluster, as illustrated in figure 8.5, since the measurement of this effect at the beginning of the 20th century was the first experimental verification of Einstein's General Relativity.

In the vicinity of a massive cluster, the celerity $c_t(r)$ of the transverse waves depends on the distance r to the center of the cluster. This implies that the directions of two radii of waves perpendicular to a straight line passing through the center of the cluster, and passing to the

¹ see for example: C. W. Chou, D. B. Hume, T. Rosenband, D. J. Wineland : "Optical Clocks and Relativity", *Science*, vol. 329, 5999, pp. 1630-1633

distances r and $r + \Delta r$ from the cluster will have an infinitesimal angle $\Delta\alpha(r)$. We can use the dependence of the celerity $c_t(r)$ in the gravitational field $\tau_{ext LD}^{cluster}(r)$ to express $\Delta\alpha(r)$. As the wave will travel the path shown in figure 8.5, the tangents to infinity of the incident wave and of the deflected wave form a total angle $\alpha(R)$ depending on the minimum distance R of the wave from the center of the cluster. Half of the total angle $\alpha(R)$ can then be deduced approximately by integrating $\Delta\alpha(r)$ for distances r to the center of the cluster ranging from R to R_∞ , and the desired value of the deflection angle $\alpha(R)$ is obtained. It turns out that this value is exactly the same as that obtained in general relativity, which is logical since we used Schwarzschild's metric to calibrate the constants of our approach. General Relativity provides for a curvature worth $\alpha(R) \cong 4G_{grav} M_0^{cluster} / c_t^2 R$, and the calculation of this value in the case of a light ray with a grazing incidence with the sun gives a deflection angle of 1,75" of arc.

As for the experimental values of the deflection of light by the sun, measured by Eddington at the beginning of the 20th century (May 1919) during an eclipse of the sun, they gave approximately $1,98'' \pm 0,12''$ of arc (at Sobral in Brazil) and $1,61'' \pm 0,31''$ of arc (in Sao Tomé-et-Principe in the Gulf of Guinea), which corresponds fairly well to the value calculated theoretically by General Relativity, despite the many difficulties of the experimental measurements.

During the Lorentz transformation described in chapter 6, the transformation laws are symmetrical with respect to time and space, just like the transformation laws in General Relativity in the case of the Schwarzschild metric. Among all the possible results that one could have imagined for the parameters a , b , α_{BV} and β_{BV} , the results obtained from the time dilation and the curvature of the wave rays in weak gravity field conveniently provide symmetric transformation laws, since we get that $a = b$. We can therefore issue here a conjecture 9, which combines the effects of time dilation and curvature of the wave rays in a weak gravity field, and reported in figure 8.6

Conjecture 9 - *the metric of our theory in a weak gravitational field must be the same as Schwarzschild's metric in General Relativity*

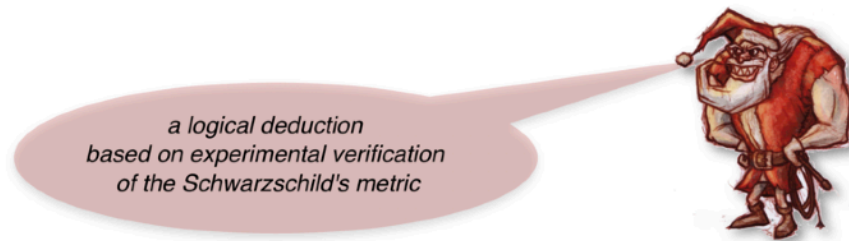


Figure 8.6 - *The ninth conjecture on the long distance metric of a massive object*

We still have a degree of freedom to choose the values of the parameters α_{BV} and β_{BV} , which must be linked by expression $3\alpha_{BV} + 2\beta_{BV} = 1/8$. However, knowing exactly the values of α_{BV} and β_{BV} is not important with regard to the gravitational properties of the loop, since the fact that $3\alpha_{BV} + 2\beta_{BV} = 1/8$ implies that the mass of inertia M_0^{BV} and the distortion energy E^{BV} of a loop, as well than the quantities G_{grav} , $\tau_{ext LD}^{cluster}(r)$ and $F_{grav}(d)$ do not explicitly depend on α_{BV} and β_{BV} .

The exact choice of parameters α_{BV} and β_{BV} obviously depends on the deep nature of the cosmological lattice, which is beyond the scope of this treaty. But the simplest solution to imagine would be that β_{BV} is equal to zero, because, in this case, the torsion Ω_{BV} of the twist disclination loop would become a constant independent of the expansion of the lattice, for example a multiple of $\pi/2$ for a cubic lattice, or a multiple of $\pi/3$ for a hexagonal lattice or for a face-centered cubic lattice, which obviously seems the most logical.

But a zero value of β_{BV} would also imply that α_{BV} would be worth $1/24$, and therefore that the radius $R_{BV} = R_{BV0} e^{\tau/24}$ of the loop would depend much less on the expansion of the lattice than the pitch $a = a_0 e^{\tau/3}$ of the lattice or the length $\vec{e}_{yi} = e^{\tau/4} \vec{e}_i$ of the **HS** observer ruler.

Unable to make an explicit safe choice of the values of the parameters α_{BV} and β_{BV} , we will leave this problem open, while remembering that there is this degree of freedom for the choice of their values, which must simply be linked by the expression $3\alpha_{BV} + 2\beta_{BV} = 1/8$.

Analogies and differences from general relativity

Let us assume that a twist disclination loop of inertia mass M_0^{BV} is at the confines of the lattice, and that a cluster of singularities with an inertia mass $M_0^{cluster} \gg M_0^{BV}$ is at the center of the lattice. The gravitational force acting on the loop is therefore written approximately $\mathbf{F}_{grav}^{BV}(r) \cong G_{grav} M_0^{cluster} M_0^{BV} / r^2$. Under the effect of this force, the twist disclination loop will undergo an acceleration in the direction of the cluster of singularities, and the potential gravitational energy of the loop will gradually transform into kinetic energy of the loop which will be worth $E_{kinetic}^{BV}(r) \cong G_{grav} M_0^{cluster} M_0^{BV} / d$, depending from its distance d from the cluster. But the kinetic energy of the loop is written $E_{kinetic}^{BV} = M_0^{BV} \mathbf{v}^2 / 2$ in the non-relativistic case so that the speed of the loop as a function of the distance d separating it from the cluster depends on the gravitational constant and the mass of inertia of the cluster: $\mathbf{v}^2(R) = 2G_{grav} M_0^{cluster} / d$. As the mass of inertia of the loop does not intervene in this relation, this relation remains valid even for relativistic speeds of the loop. However, we know that the total relativistic energy $\mathbf{v}^2(R) = 2G_{grav} M_0^{cluster} / d$ of the loop will tend towards infinity when its speed $\mathbf{v}(R)$ will tend towards the celerity c_t of the transverse waves, so that the following condition $\mathbf{v}^2(R) \leq c_t^2$ must be satisfied before reaching the speed limit. This condition implies the existence of a critical distance $d_{cr} = 2G_{grav} M_0^{cluster} / c_t^2$ for which the energy of the loop becomes infinite. This critical distance d_{cr} only depends on the mass $M_0^{cluster}$ of the cluster, and obviously only exists if the radius of the cluster is less than d_{cr} . It is called the *Schwarzschild radius* of the cluster and in fact corresponds to the limit beyond which the loop cannot irreversibly leave the cluster since it would then require infinite energy to do so. Thus, the mass $M_0^{cluster}$ of the cluster whose radius $R_{cluster}$ would satisfy the condition $R_{cluster} < d_{cr}$ would in fact be a *black hole* which would irreparably absorb any singularity which would have the misfortune to approach it at a distance $R \leq R_{Schwarzschild}$. This *Schwarzschild radius*² $R_{Schwarzschild} = 2G_{grav} M_0^{cluster} / c_t^2$ is obtained in exactly the same way in Relativity, so that it is identical in our approach and in General Relativity.

² Schwarzschild, K. (1916). On the gravitational field of a point mass according to Einstein's theory. Sitzber. Preuss. Akad. Wiss., Physik-Math. Kl., Vol. 189, pp.189-196. (translated by Helga and Roger Stuewer).

In our approach, we have already approached the notion of black hole by defining in figure 3.5 the conditions for a singularity of the gravitational field to behave like a black hole *with respect to transverse waves*, by defining the radius r_{cr} of the sphere of perturbations around the singularity, namely the sphere beyond which any transverse wave is trapped by the singularity. By then applying these conditions to the cluster of mass $M_0^{cluster}$ generating the gravitational field $\tau_{ext LD}^{cluster}(r)$ of figure 8.1, one obtains the expression of *the radius r_{sphere} of the sphere of perturbations* of the cluster in the form $r_{sphere} = 2G_{grav} M_0^{cluster} / c_t^2$, i.e. the same value than the radius of the Schwarzschild sphere. In General Relativity, we define *the sphere of photons*, i.e. the limit in the vicinity of a black hole from which no photon can escape from the black hole, whose radius is equal to $R_{photons sphere} = 3GM / c^2$, namely 3/2 of the Schwarzschild radius. We will come back to this disturbing difference with our approach.

In our approach, the proper time of an **HS** is actually written exactly as an exponential term proportional to $-1/r$. With this exponential expression, we see that the proper time of the observer **HS** which approaches at very short distance from a cluster *expands infinitely when the distance tends towards zero*. In General Relativity, it is said that the proper time of the **HS** seems to expand infinitely when the **HS** approaches a critical limit distance r_{cr} calculated on the basis of the Schwarzschild metric, when $t_y \rightarrow 0$, which leads to the critical distance $r_{cr} = G_{grav} M_0^{cluster} / c_t^2$. This limit distance is therefore smaller than the radius of the Schwarzschild sphere, the point of no return for a black hole. Now, it seems rather difficult to imagine that the time of an **HS** seems to stop when the **HS** reaches this critical distance, and it is surprising that this critical distance is half the radius of Schwarzschild, and not simply the radius of Schwarzschild itself, or else the zero radius as in our approach.

Perfect cosmological lattice		General Relativity
$\begin{cases} y_i = e^{\frac{G_{grav} M_0^{cluster}}{c_t^2 r}} x_i \\ t_y = e^{\frac{G_{grav} M_0^{cluster}}{c_t^2 r}} t \end{cases}$	Transformation laws	$\begin{cases} y_i = \left(1 + \frac{G}{c^2} \frac{M_0}{r} + \dots\right) x_i \\ t_y = \left(1 - \frac{G}{c^2} \frac{M_0}{r}\right) t \end{cases}$
$R_{Schwarzschild} = 2G_{grav} M_0^{cluster} / c_t^2$	Schwarzschild radius	$R_{Schwarzschild} = 2G_{grav} M_0^{cluster} / c_t^2$
$R_{photon sphere} = 2G_{grav} M_0^{cluster} / c_t^2$	Photon sphere radius	$R_{photon sphere} = 3G_{grav} M_0^{cluster} / c_t^2$
$R_{time dilation \rightarrow \infty} \rightarrow 0$	Radius of infinite dilation of time	$R_{time dilation \rightarrow \infty} \equiv G_{grav} M_0^{cluster} / c_t^2$
Curvature vector by flexion		Einstein's curvature tensor
$\vec{\chi} = -\frac{4K_2/3 + 2K_1}{2(K_2 + K_3)} \overrightarrow{\text{grad} \tau} + \frac{1}{2(K_2 + K_3)} \left(n \frac{d\vec{p}}{dt} - \overrightarrow{\text{grad} F^{def}} \right) + \frac{K_3}{K_2 + K_3} \vec{\lambda}$ <p>«Gravitational» field Energy-momentum vector Flexion charge</p>		$G = 8\pi T$ <p>Energie-momentum tensor</p>
Divergence of Newton's equation: equation of motion for "gravitational" distortions		Divergence of the energy-momentum tensor: gravitational motion equation
$\vec{\nabla} \cdot \vec{\chi} = \text{div} \left[\frac{1}{2(K_2 + K_3)} \left(n \frac{d\vec{p}}{dt} - \overrightarrow{\text{grad} F^{def}} \right) - \frac{4K_2/3 + 2K_1}{2(K_2 + K_3)} \overrightarrow{\text{grad} \tau} + \frac{K_3}{K_2 + K_3} \vec{\lambda} \right] = \theta$		$\vec{\nabla} \cdot T = 0$

Figure 8.7 - Comparative behavior of the perfect cosmological lattice with the general relativity of Einstein

In General Relativity, the simplest black holes are characterized by three critical radii: *the radius of the photon sphere* which is worth $R_{\text{photons sphere}} = 3GM / c^2$, *the radius of the horizon or point of no return*, also called *the Schwarzschild radius*, which is given by $R_{\text{Schwarzschild}} = 2GM / c^2$, and *the radius for which the dilation of the observer's time tends to infinity*, which is approximately equal to $R_{\text{time dilation} \rightarrow \infty} \cong GM / c^2$. The fact that there are three different radii for black holes in General Relativity is quite intriguing, as is the existence of a nonzero radius for which the dilation of the observer's time tends to infinity. It is mainly for this reason that it is said that it is not possible to describe by General Relativity the physics of objects that fall into a black hole beyond the Schwarzschild sphere.

In our approach, on the contrary, the radii of the perturbation sphere and of the point of no return are both similar to the Schwarzschild radius ($2GM / c^2$), which is very satisfying for the mind, since it thus only exists a single boundary representing *the horizon of a black hole*. On the other hand, there is no limit radius in our approach for which the dilation of the observer's time would tend towards infinity, so that our approach is not limited to the description of a black hole beyond the Schwarzschild sphere. Now our approach is equivalent to General Relativity as long as the gravitational field is weak and satisfies the condition $\tau_{\text{ext LD}}^{\text{cluster}}(r) < 1$. The reason is that these are the two experimentally verified effects, namely the time dilation and the curvature of wave rays in weak fields which were chosen to make our approach identical to that of General Relativity in weak gravitational field. On the other hand, our approach becomes different for strong gravitational fields, as shown by the compared expressions of the transformation laws in figure 8.7, which explains the differences that we have just described with regard to the different characteristic radii of black holes.

About the formal analogy between the 3D spatial curvature equation of the cosmological lattice and the Einstein's equation of the 4D field of curvature in general relativity

The local spatial curvature of the cosmological lattice, as measured by the **GO** observer, is characterized by *the curvature vector by flexion* $\vec{\chi} = -\text{rot } \vec{\omega} + \vec{\lambda}$, perfectly described in figure 2.6. It is remarkable to note that this flexion vector can be directly obtained from *the Newton's equation of the cosmological lattice* (figure 3.1). This gives the value of the flexion field in the cosmological lattice in the form shown in figure 8.7. We therefore deduce that the existence of a local topological curvature of the lattice seen by the **GO** via the flexion vector depends on three terms at the same time:

- the gradient of the local volume expansion, which is nothing other than the gradient of *the "gravitational" field* τ within the lattice,
- the temporal variations of the local momentum of the lattice and the gradient of the density of elastic energy F^{el} stored in the lattice, term which one could qualify as *"energy-momentum vector"* due to the singularities present in the lattice,
- the density $\vec{\lambda}$ of flexion charges within the lattice, which reflects the presence of *topological singularities within the lattice*, such as dislocations and / or disclinations.

On the other hand, for a local observer **HS**, both *its rulers and its clock depend on the local volume expansion*, so that an equation similar to the flexion field equation should necessarily

become a four-dimensional equation of curvature of space-time, which we are obviously not going to try to establish here.

The operation of *taking the divergence of the curvature field*, i.e. $\text{div } \vec{\chi} = \text{div } \vec{\lambda} = \theta$, allows writing a second equation shown in figure 8.7. This relationship shows that *the divergence of the flexion vector is equal to the density of curvature charges* due to the topological singularities contained in the lattice, and is therefore zero if there are no curvature charges. Moreover, in the case where there are no curvature charges, *the divergence of the bending vector is nothing other than the divergence of the Newton's equation of the lattice*, i.e. the equation of motion for the divergent part of the distortions, namely the “gravitational” distortions by volume expansion.

The first relation giving the spatial curvature of the lattice from the Newton's equation of the lattice is the three-dimensional analog of *the Einstein's four-dimensional field equation of General Relativity*³, which is written $\mathbf{G} = 8\pi\mathbf{T}$, in which \mathbf{G} is *the famous curvature tensor of Einstein (Einstein tensor)*, which is expressed in terms of *the Ricci curvature tensor* $\mathbf{G}_{\mu\nu} = \mathbf{R}_{\mu\nu} - g_{\mu\nu}R/2$, corresponding to a certain part of *the Riemann tensor* which describes the curvatures of space-time. As for the tensor \mathbf{T} , it is a “geometric object” called *the stress-energy tensor, or the energy-momentum tensor, or the stress-energy-momentum tensor*, which characterizes the matter contained in space.

This Einstein field equation shows how the energy-momentum tensor of matter generates an average curvature of space-time in its vicinity. Among other things, it allows you to calculate the static curvature field of a massive object, or the generation of gravitational waves by a massive mobile object. In addition, it also contains the equations of motion (“Newton's equations”) for matter whose energy-momentum tensor generates the curvature of space-time.

In the case of Einstein's field equation, it should also be noted that the energy-momentum tensor is a tensor with zero divergence $\vec{\nabla} \cdot \mathbf{T} = 0$, which ensures that the laws of conservation of energy and angular momentum are respected. This equation $\vec{\nabla} \cdot \mathbf{T} = 0$ therefore represents in fact *the equation of motion of matter* in General Relativity.

There is very clearly a strong analogy between Einstein's field equation $\mathbf{G} = 8\pi\mathbf{T}$ and the equation giving the flexion field $\vec{\chi}$ in the case of the cosmological lattice, described in table 8.7, because the latter also connects a “geometric vector” of spatial curvature to a kind of “energy-momentum vector” within the solid lattice, which contains at the same time the temporal variations of the local momentum of the lattice, the gradient of the local volume expansion, and the gradient of the density F^{el} of elastic energy stored in the lattice, quantities which are all influenced by the presence of torsion charges or flexion charges within the lattice. In addition, this equation for the field $\vec{\chi}$ of curvature by flexion derives directly from the Newton's equation of the lattice. However, unlike Einstein's field equation, which describes the curvatures of 4-dimensional space-time, this equation is deduced by the **GO** which is lucky to have an absolute clock, so that *there is no “curvature of time” for him*, and that, consequently, his equation of curvature is purely spatial in 3 dimensions. On the other hand, if we considered the way that “homo sapiens” **HS** observers should have to describe the gravitational behavior they observe, *they should take into account the “curvature of time”* since their clocks depend on the local state of expansion of the lattice where they are.

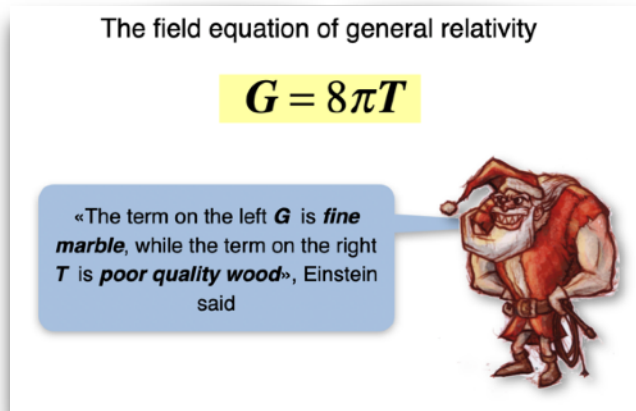
³ a very goof account of Einstein's General Relativity can be found in the book:
Ch. W. Misner, K. S. Thorne, J. A. Wheeler, **Gravitation**, W.H. Freeman and Co, San Francisco 1973

In the case of Einstein's field equation, the equation of the divergence $\vec{\nabla} \cdot \mathbf{T} = 0$ of the energy-momentum tensor represents *the equation of gravitational movements of matter* in General Relativity, just like the equation $\vec{\nabla} \vec{\chi} = \text{div } \vec{\chi} = \text{div } \vec{\lambda} = \theta$ of the divergence of the curvature represents the divergence of the Newton's equation of motion of the lattice, that is to say the equation of motion for the "gravitational" distortions of the lattice by volume expansion.

But the most important difference between Einstein's field equations and cosmological lattice equations is that *the concept of curvature charges associated with topological singularities does not exist in Einstein's equations*, which appears in the fact that the divergence of the energy-momentum tensor is always zero, so that there is no equation similar to the equation

$\text{div } \vec{\chi} = \text{div } \vec{\lambda} = \theta$ in General Relativity. We will see later in this book that the concept of curvature charges, absent in modern theories of relativity, quantum physics and particle physics, can explain a large number of facts misunderstood by modern theories of physics.

It is very tempting to say here that *the concept of curvature charges*, and that *the pure geometric equation* $\text{div } \vec{\chi} = \text{div } \vec{\lambda} = \theta$ answers the



question that Einstein asked when he said that, in the field equation $G = 8\pi T$, the term on the left, the curvature tensor of Ricci G , is made of *fine marble*, while the right term, the energy-momentum tensor T , is made of *poor quality wood*, meaning that the right term is only a phenomenological representation of the matter injected into the field equation, which is not derived directly from a prime principle as is the term on the left. In our approach, on the other hand, the right term of the equation for the flexion field is made of *fine marble*, since it is derived directly from a prime principle which is the Newton's equation of the lattice.

About the dependence of the topological singularities on the expansion of the lattice

In the case of a twist disclination loop (BV), we have seen that the dependences in volume expansion of the radius of the loop, its angle of twist, its rotational charge and its mass of inertia can be written by introducing the constants α_{BV} and β_{BV} , which makes it possible to deduce several important relationships for the twist disclination loop in the presence of a background expansion field τ_0 and / or an external expansion field τ^{external} generated by other singularities, relations which are reported in the table of figure 8.8.

In the case of a prismatic edge dislocation loop (BC), we do not know a priori the dependencies in volume expansion of the radius of the loop, the Burgers vector and the charge of curvature. We therefore introduce new expansion constants α_{BC} and β_{BC} in such a way that we can write the relations for the radius R_{BC} of the loop, for the Burgers vector \vec{B}_{BC} and for the curvature charge $q_{\theta BC}$ in the form shown in table 8.8. These expansion constants α_{BC} and β_{BC} are not known. The dependence of the radius of the loop should certainly be similar to that

The twist disclination loop (BV), source of electrical charge

$$\left\{ \begin{array}{l} R_{BV} = R_{BV0} e^{\alpha_{BV}\tau} \\ \Omega_{BV} = \Omega_{BV0} e^{\beta_{BV}\tau} \\ q_{\lambda BV} = q_{\lambda BV0} e^{(2\alpha_{BV} + \beta_{BV})\tau} \\ M_0^{BV} = M_{00}^{BV} e^{-7\tau/8} \end{array} \right\} \left\{ \begin{array}{l} \tau_{ext LD}^{BV}(r) \equiv -\frac{4G_{grav}}{c_t^2} \frac{M_0^{BV}}{r} \\ E_{dist}^{BV}(\tau^{externe}) \equiv M_0^{BV} c_t^2 e^{\tau^{externe}/8} \\ M_0^{BV} \equiv \frac{1}{2c_t^2} (K_2 + K_3) \zeta_{BV} R_{BV}^3 \Omega_{BV}^2 \equiv \left[\frac{1}{2c_{t0}^2} (K_2 + K_3) \zeta_{BV} R_{BV0}^3 \Omega_{BV0}^2 \right] e^{-7\tau_0/8} \end{array} \right.$$

The prismatic edge dislocation loop (BC), source of flexion charge

$$\left\{ \begin{array}{l} R_{BC} = R_{BC0} e^{\alpha_{BC}\tau} \\ \vec{B}_{BC} = \vec{B}_{BC0} e^{\beta_{BC}\tau} \\ q_{\theta BC} = q_{\theta BC0} e^{\beta_{BC}\tau} \\ q_{\theta BC} \begin{cases} > 0 \text{ if vacancy loop} \\ < 0 \text{ if interstitial loop} \end{cases} \\ M_{curvature}^{BC} \begin{cases} > 0 \text{ if vacancy loop} \\ < 0 \text{ if interstitial loop} \end{cases} \end{array} \right\} \left\{ \begin{array}{l} \tau_{ext LD}^{BC}(r) \equiv -\frac{4G_{grav}}{c_t^2} \frac{M_0^{BC}}{r} \\ E_{dist}^{BC}(\tau^{external}) \equiv M_0^{BC} c_t^2 e^{(\alpha_{BC} + 2\beta_{BC})\tau^{external}} \\ M_0^{BC} \equiv \left(\frac{K_2}{K_3} \right)^2 \frac{K_3 \zeta_{BC} R_{BC0} \vec{B}_{BC0}^2}{c_t^2} \equiv \left[\left(\frac{K_2}{K_3} \right)^2 \frac{K_3 \zeta_{BC} R_{BC0} \vec{B}_{BC0}^2}{c_{t0}^2} \right] e^{(\alpha_{BC} + 2\beta_{BC} - 1)\tau_0} \\ M_{curvature}^{BC} = -\frac{2\pi K_2 R_{BC}^2 \vec{n} \cdot \vec{B}_{BC}}{5c_t^2} = \left[-\frac{2\pi K_2 R_{BC0}^2 \vec{n} \cdot \vec{B}_{BC0}}{5c_{t0}^2} \right] e^{(2\alpha_{BC} + \beta_{BC} - 1)\tau_0} \end{array} \right.$$

The slip mixed dislocation loop (BM), source of an electric dipolar moment

$$\left\{ \begin{array}{l} R_{BM} = R_{BM0} e^{\alpha_{BM}\tau} \\ \vec{B}_{BM} = \vec{B}_{BM0} e^{\beta_{BM}\tau} \end{array} \right\} \left\{ \begin{array}{l} \tau_{ext LD}^{BM}(r) \equiv -\frac{4G_{grav}}{c_t^2} \frac{M_0^{BM}}{r} \\ E_{dist}^{BM}(\tau^{external}) \equiv M_0^{BM} c_t^2 e^{(\alpha_{BM} + 2\beta_{BM})\tau^{external}} \\ M_0^{BM} \equiv \frac{K_2 + K_3}{4c_t^2} \zeta_{BM} R_{BM} \vec{B}_{BM}^2 \equiv \left[\frac{K_2 + K_3}{4c_{t0}^2} \zeta_{BM} R_{BM0} \vec{B}_{BM0}^2 \right] e^{(\alpha_{BM} + 2\beta_{BM} - 1)\tau_0} \end{array} \right.$$

The macroscopic vacancy (L), analogous to a black hole

$$M_{grav}^{(L)}(\tau_0) \begin{cases} < 0 \Leftrightarrow \tau_0 < -1 \\ > 0 \Leftrightarrow -1 < \tau_0 < \tau_{0cr} \\ < 0 \Leftrightarrow \tau_0 > \tau_{0cr} \end{cases} \left\{ \begin{array}{l} R_L = \sqrt[3]{\frac{3N_L}{4\pi n_0 e}} \\ \tau_{ext}^{(L)}(r) \equiv -\left(1 + \tau_0 + \tau^{externe}\right) \frac{R_L}{r} \equiv -\frac{4G_{grav}}{c_t^2} \frac{M_{grav}^{(L)}}{r} \\ E_{grav}^{(L)} \equiv M_{grav}^{(L)} c_t^2 \left(1 + \frac{\tau^{externe}}{(1 + \tau_0)}\right) \\ M_{grav}^{(L)} \equiv \frac{R_{\infty}^2}{c_t^2} \sqrt[3]{\frac{6\pi^2 N_L}{n_0 e}} (K_0 - 4K_2/3 - 2K_1(1 + \tau_0))(1 + \tau_0) \\ \equiv \left[m R_{\infty 0}^2 \sqrt[3]{6\pi^2 e^{-1} n_0 N_L} \right] \frac{(K_0 - 4K_2/3 - 2K_1(1 + \tau_0))(1 + \tau_0)}{K_2 + K_3} e^{-\frac{\tau_0}{3}} \end{array} \right.$$

The macroscopic interstitial (I), analogous to a neutron star

$$M_{grav}^{(I)}(\tau_0) \begin{cases} > 0 \Leftrightarrow \tau_0 < \tau_{0cr} \\ < 0 \Leftrightarrow \tau_0 > \tau_{0cr} \end{cases} \left\{ \begin{array}{l} R_I \equiv \sqrt[3]{\frac{3N_I}{4\pi n}} \equiv \sqrt[3]{\frac{3N_I}{4\pi n_0}} e^{\frac{\tau_0}{3}} \\ \tau_{ext}^{(I)}(r) \equiv -\frac{4G_{grav}}{c_t^2} \frac{M_{grav}^{(I)}}{r} \\ E_{grav}^{(I)} \equiv M_{grav}^{(I)} c_t^2 e^{\tau^{external}} \\ M_{grav}^{(I)} \equiv \frac{N_I}{nc_t^2} (K_0 - 4K_2/3 - 2K_1(1 + \tau_0)) \equiv m N_I \frac{K_0 - 4K_2/3 - 2K_1(1 + \tau_0)}{K_2 + K_3} \end{array} \right.$$

Figure 8.8 - Dependence of the topological singularities of the lattice in the volume expansion of the lattice

of the twist disclination loop, either $\alpha_{BC} = 1/4$, but it could also be similar to the dependence of the lattice pitch, either $\alpha_{BC} = 1/3$. As for the dependence of the Burgers vector, which must be a vector of the lattice, it should in principle take on value $\beta_{BC} = 1/3$. But for the moment, we will not make a choice of these values, and we will keep the parameters α_{BC} and β_{BC} , because the exact values of these parameters are not called to play a crucial role for the rest of the theory. The expressions of R_{BC} , of \vec{B}_{BC} and of $\mathbf{q}_{\theta BC}$ thus obtained make it possible to write four important relationships for a prismatic edge dislocation loop in the presence of a background expansion field τ_0 and / or an external expansion field $\tau^{external}$ generated by other singularities, remembering that the charge of curvature and the gravitational mass associated with the charge of curvature can be positive or negative according to the nature of the charge, as indicated in the table of figure 8.8.

In the case of a slip mixed dislocation loop (**BM**), we also do not know a priori the dependencies in volume expansion of the radius of the loop and its Burgers vector. We therefore introduce expansion constants α_{BM} and β_{BM} allowing us to write the relationships shown in figure 8.8.

We have seen, from the dilation of time and the curvature of the wave rays in a weak gravitational field, that the values which must take the parameters α_{BV} and β_{BV} associated with the twist disclination loops cannot be determined in a simple and unequivocal manner, but they must at least satisfy the relationship $3\alpha_{BV} + 2\beta_{BV} = 1/8$. For the edge and mixed dislocation loops, there are again no known experimental effects which could make it possible to simply deduce the value of the parameters $\alpha_{BC}, \beta_{BC}, \alpha_{BM}, \beta_{BM}$. The values of the different parameters $\alpha_{BV}, \beta_{BV}, \alpha_{BC}, \beta_{BC}, \alpha_{BM}, \beta_{BM}$ are therefore not known to us, except for the relationship $3\alpha_{BV} + 2\beta_{BV} = 1/8$. But the actual values of these parameters should most likely have physical consequences which should be accessible by the experience.

But there is yet another much more confusing physical consequence of these parameters. Indeed, if the radius of the edge loops were to depend on a value different from $1/3$, therefore that $\alpha_{BC} \neq 1/3$, to ensure the existence of electron-like dispirations, this would mean that the number of lacunar or interstitial sites of the edge loop should vary if local expansion changes. However, the only possibility to vary this number of sites is that the edge loop behaves like a source or a pit of vacancies or interstitials in the presence of a variation of τ . And this effect would have very surprising consequences on Maxwell's equations, because in this case of divergent flow of vacancies or interstitials, Maxwell's equation $\text{div}(n\vec{p}^{rot}) = 0$ should be replaced by $\text{div}(n\vec{p}) \neq 0$, with for analog $\text{div}\vec{B} \neq 0$ in electromagnetism. In other words, in the case where $\alpha_{BC} \neq 1/3$ the edge dislocation loops behave like magnetic monopoles in the presence of variations in the expansion of the cosmological lattice. However, this effect should be observable and measurable by the **HS** observers, who should measure a very weak monopole magnetic component linked to the particles containing edge loops, and caused by the local variation of the expansion (which the **HS** cannot measure in principle). And this monopole component of particles containing edge loops should necessarily exist under the effect of the cosmological expansion of the universe, which could open up an exciting chapter in our approach.

In the case of a macroscopic vacancy, one can take again the relations obtained in figure 7.7a and transform them so as to obtain the various relations reported in table 8.8 in the

$$\begin{aligned}
& \left\{ \begin{aligned} F_{grav}^{BV-BV} &\equiv G_{grav} \frac{M_{0(1)}^{BV} M_{0(2)}^{BV}}{d^2} \\ F_{grav}^{BC-BC} &\equiv (\alpha_{BC} + 2\beta_{BC}) G_{grav} \frac{M_{curvature(1)}^{BC} M_{0(2)}^{BC} + M_{curvature(2)}^{BC} M_{0(1)}^{BC}}{d^2} + 2(\alpha_{BC} + 2\beta_{BC}) G_{grav} \frac{M_{0(1)}^{BC} M_{0(2)}^{BC}}{d^2} \\ F_{grav}^{BM-BM} &\equiv 2(\alpha_{BM} + 2\beta_{BM}) G_{grav} \frac{M_{0(1)}^{BM} M_{0(2)}^{BM}}{d^2} \end{aligned} \right. \\
& \left\{ \begin{aligned} F_{grav}^{BV-BC} &\equiv \frac{1}{2} G_{grav} \frac{M_{curvature}^{BC} M_0^{BV}}{d^2} + \left(\frac{1}{2} + 4(\alpha_{BC} + 2\beta_{BC}) \right) G_{grav} \frac{M_0^{BV} M_0^{BC}}{d^2} \\ F_{grav}^{BV-BM} &\equiv \left(\frac{1}{2} + 4(\alpha_{BM} + 2\beta_{BM}) \right) G_{grav} \frac{M_0^{BV} M_0^{BM}}{d^2} \\ F_{grav}^{BC-BM} &\equiv 4(\alpha_{BM} + 2\beta_{BM}) G_{grav} \frac{M_{curvature}^{BC} M_0^{BM}}{d^2} + 4(\alpha_{BC} + 2\beta_{BC} + \alpha_{BM} + 2\beta_{BM}) G_{grav} \frac{M_0^{BC} M_0^{BM}}{d^2} \end{aligned} \right. \\
& \left\{ \begin{aligned} F_{grav}^{BV-L} &\equiv \frac{1}{2} G_{grav} \frac{9 + \tau_0}{1 + \tau_0} \frac{M_0^{BV} M_{grav}^{(L)}}{d^2} \equiv \frac{c_t^2}{8} (9 + \tau_0) \frac{M_0^{BV} R_L}{d^2} \\ F_{grav}^{BC-L} &\equiv 4G_{grav} \frac{1}{1 + \tau_0} \frac{M_{curvature}^{BC} M_{grav}^{(L)}}{d^2} + 4G_{grav} \frac{1 + (\alpha_{BC} + 2\beta_{BC})(1 + \tau_0)}{1 + \tau_0} \frac{M_0^{BC} M_{grav}^{(L)}}{d^2} \\ &\equiv c_t^2 \frac{M_{curvature}^{BC} R_L}{d^2} + c_t^2 \left[1 + (\alpha_{BC} + 2\beta_{BC})(1 + \tau_0) \right] \frac{M_0^{BC} R_L}{d^2} \\ F_{grav}^{BM-L} &\equiv 4G_{grav} \frac{1 + (\alpha_{BM} + 2\beta_{BM})(1 + \tau_0)}{1 + \tau_0} \frac{M_0^{BM} M_{grav}^{(L)}}{d^2} \equiv c_t^2 \left[1 + (\alpha_{BM} + 2\beta_{BM})(1 + \tau_0) \right] \frac{M_0^{BM} R_L}{d^2} \end{aligned} \right. \\
& \left\{ \begin{aligned} F_{grav}^{BV-I} &\equiv \frac{9}{2} G_{grav} \frac{M_0^{BV} M_{grav}^{(I)}}{d^2} \equiv \frac{3c_t^2}{4R_{\infty}^2} \frac{M_0^{BV} R_I^3}{d^2} \\ F_{grav}^{BC-I} &\equiv 4G_{grav} \frac{M_{curvature}^{BC} M_{grav}^{(I)}}{d^2} + 4G_{grav} (1 + \alpha_{BC} + 2\beta_{BC}) \frac{M_0^{BC} M_{grav}^{(I)}}{d^2} \\ &\equiv \frac{2c_t^2}{3R_{\infty}^2} \frac{M_{curvature}^{BC} R_I^3}{d^2} + \frac{2c_t^2}{3R_{\infty}^2} (1 + \alpha_{BC} + 2\beta_{BC}) \frac{M_0^{BC} R_I^3}{d^2} \\ F_{grav}^{BM-I} &\equiv 4G_{grav} (1 + \alpha_{BM} + 2\beta_{BM}) \frac{M_0^{BM} M_{grav}^{(I)}}{d^2} \equiv \frac{2c_t^2}{3R_{\infty}^2} (1 + \alpha_{BM} + 2\beta_{BM}) \frac{M_0^{BM} R_I^3}{d^2} \end{aligned} \right. \\
& \left\{ \begin{aligned} F_{grav}^{L-L} &\equiv \frac{8G_{grav}}{(1 + \tau_0)} \frac{M_{grav(1)}^{(L)} M_{grav(2)}^{(L)}}{d^2} \equiv \frac{c_t^4}{2G_{grav}} \frac{(1 + \tau_0) R_{L(1)} R_{L(2)}}{d^2} \\ F_{grav}^{I-I} &\equiv 2G_{grav} \frac{M_{grav(1)}^{(I)} M_{grav(2)}^{(I)}}{d^2} \equiv \frac{c_t^4}{18G_{grav}} \frac{R_{I(1)}^3 R_{I(2)}^3}{d^2} \\ F_{grav}^{L-I} &\equiv 4G_{grav} \frac{2 + \tau_0}{1 + \tau_0} \frac{M_{grav}^{(L)} M_{grav}^{(I)}}{d^2} \equiv \frac{c_t^4}{6R_{\infty}^2} \frac{2 + \tau_0}{G_{grav}} \frac{R_L R_I^3}{d^2} \end{aligned} \right.
\end{aligned}$$

the gravitational interaction
it's not that simple!!




Figure 8.9 - The set of possible gravitational interaction forces between the various topological singularities of the lattice

presence of a background expansion field τ_0 and / or of an external expansion field $\tau^{external}$ generated by other singularities. We note that the gravitational mass of the vacancy has the property of changing sign for two values of the background volume expansion of the lattice, and we also remember that the macroscopic vacancy is the only singularity *which necessarily becomes a black hole* when the background volume expansion of the lattice satisfies the relationship $\tau_0 > 1 - \tau^{external}$.

In the case of a macroscopic interstitial, one can also take again the relations obtained in

figure 7.8 and transform them so as to obtain the various relations reported in table 8.8 in the presence of a background expansion field τ_0 and / or of an external expansion field $\tau^{external}$ generated by other singularities. We can see that the gravitational mass of the interstitial has

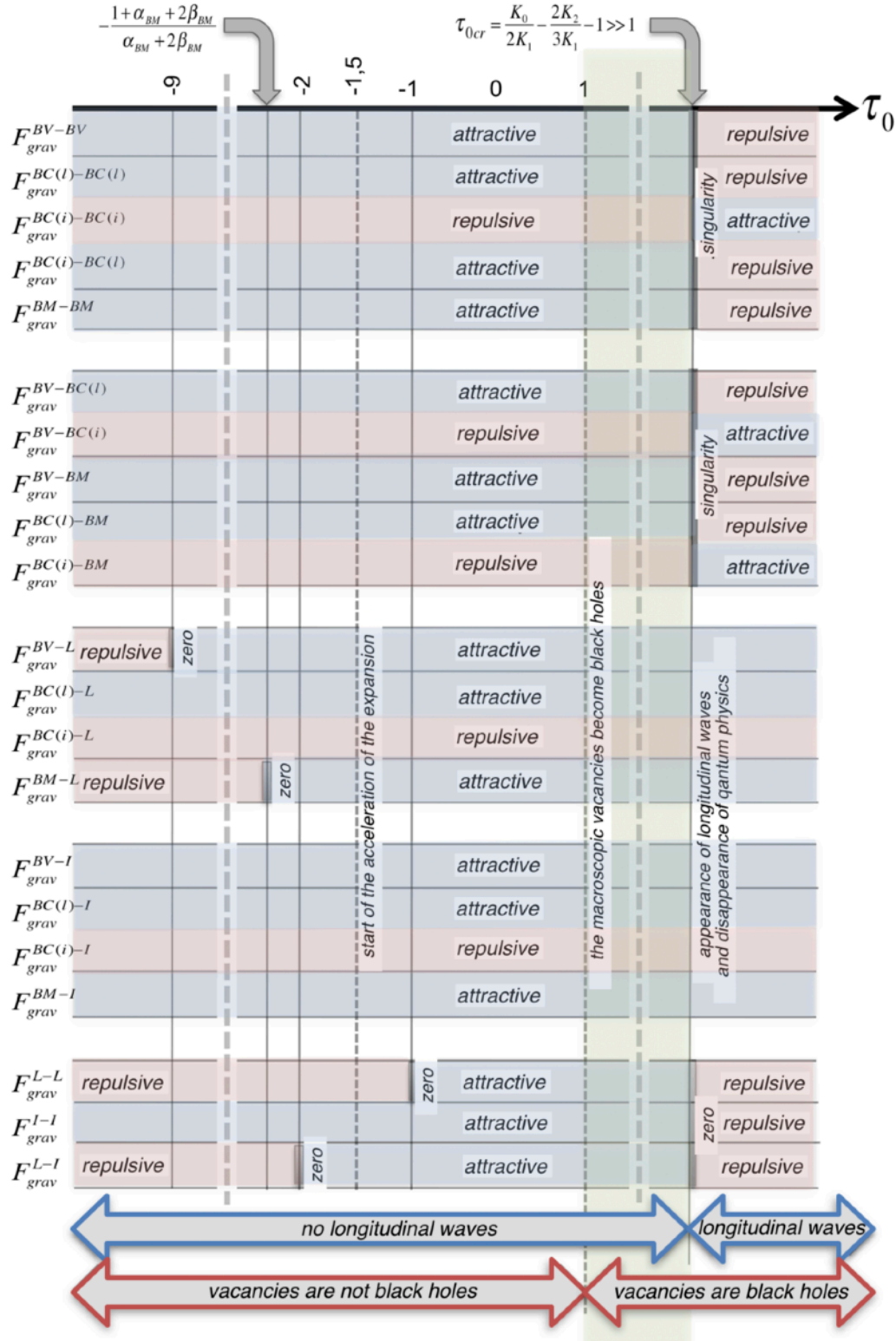


Figure 8.10 - Attractive or repulsive behaviors of "gravitational" interaction forces between singularities as a function of the background expansion of the cosmological lattice

the property of changing sign depending on the value of the background volume expansion of the lattice.

All of the gravitational interactions between the various singularities of the lattice

Using the relations obtained in table 8.8, we can then calculate the gravitational interaction forces that can appear between two of the singularities of the lattice, by calculating the energy increase of the two singularities by their interaction, as a function of the distance separating them. This increase therefore corresponds to the gravitational energy of interaction, and the derivative of this energy by the distance separating the two singularities corresponds to the force of gravitation between the two singularities. As five different topological singularities have been described in table 8.8, it is possible to calculate the gravitational interaction force in 15 different cases. By performing all these long and tedious calculations, we finally obtain all of these gravitational interaction forces as shown in figure 8.9. In this table, we see several important things:

- only the interaction between the twist disclination loops, carrying the "electric" charge of rotation, *exactly satisfies Newton's law of gravitation*. It should be noted that these loops have a much higher interaction energy than the other types of loops, and that *it is these loops which therefore very largely dominate the gravitational interactions between loops*,
- all the other interactions present a somewhat modified version of the gravitational interaction. Between the various loops, the interactions always depend on the "constant" of gravitation G_{grav} , but with an additional numerical factor which can contain the unknown parameters $\alpha_{BC}, \beta_{BC}, \alpha_{BM}, \beta_{BM}$,
- in the case where an edge dislocation loop occurs, there are always two interaction terms, one dependent on the mass of curvature $M_{curvature}^{BC}$ of the edge loop, and the other dependent on the mass of inertia M_0^{BC} of the edge loop. Since the curvature mass of the loop is much higher than its mass of inertia, the term containing the curvature mass largely dominates in the expression of the force of interaction. In addition, this dominant term can correspond to an attractive or negative interaction force since the mass of curvature of the corner loop is positive if the loop is of vacancy type and negative if the loop is of interstitial type,
- in the case where a macroscopic vacancy or a macroscopic interstitial intervenes, there are two possible formulations of the gravitational interaction force: the formulation which involves the masses of gravitation $M_{grav}^{(L)}$ and $M_{grav}^{(I)}$ and which resembles the formulation of Newton's law, but which has the disadvantage that the masses $M_{grav}^{(L)}$ and $M_{grav}^{(I)}$ strongly depend on the background expansion of the lattice, to the point of changing sign in certain domains of expansion. This is why we will prefer to use the second formulation which involves the radii R_L and R_I of the macroscopic singularities, and which has the advantage of being much simpler to analyze as regards the sign of the interaction (attractive or negative),
- on the basis of these expressions of "gravitational" interaction forces between singularities, we can deduce the attractive or repulsive behavior of all the interactions in table 8.8 as a function of the evolution of the background expansion τ_0 of the lattice. This behavior is reported in figure 8.10. In this figure, we did not respect the scale of values on the axis of expansion τ_0 , especially with regard to the value of τ_{0cr} which is in fact extremely higher ($\tau_{0cr} \gg 1$) since $K_0 \gg K_1$ in the case of the perfect cosmological lattice.

We see that the gravitational interactions evolve strongly under the effect of the background expansion of the cosmological lattice. There appear in particular changes of sign of the interactions, which pass from the attractive mode to the repulsive mode or vice versa for certain values of expansion. These changes in sign of the interaction correspond either to a *zero crossing of the interaction force*, or to the appearance of a *singularity of the attraction force*.

It is obvious that figure 8.10 implies very important consequences on the cosmological behavior of the singularities of the lattice, that is to say on the evolution of the singularities during the cosmological expansion of the lattice. We will return to this subject in a future chapter. In figure 8.10, we have also reported certain phenomena associated with the evolution of the background expansion of the cosmological lattice, namely:

- first of all, for $\tau_0 = \tau_{0cr}$, the transition from the expansion domain without transverse waves, dominated by localized longitudinal eigen modes (to which we will return later), to the expansion domain where the real propagation of longitudinal waves appears, and where quantum physics disappears as we will see later,
- then the expansion domains in which the macroscopic vacancies are or are not black holes, with a transition for the expansion value $\tau_0 = 1$,
- the expansion value $\tau_0 = -3/2$ for which the evolution of the perfect cosmological lattice (figure 3.10) passes from the domain of the end of inflation (with decrease in the speed of expansion) to the domain of expansion with a speed of increasing expansion (acceleration of expansion),
- it is quite clear that the domain which is concerned by our current Universe lies between the values $\tau_0 = 1$ and $\tau_0 = \tau_{0cr}$, because it is in this domain that there are no longitudinal waves and that the macroscopic vacancies are black holes,
- we will also notice that all the interactions which involve edge loops **BC** (i) of interstitial nature are repulsive in the domain between $\tau_0 = 1$ and $\tau_0 = \tau_{0cr}$, which will play a considerable role in the cosmological evolution of matter,
- finally, one did not represent in figure 8.10 the stages of the cosmological evolution which follow the critical value $\tau_0 = \tau_{0cr}$, namely the end of the acceleration of the expansion, the passage by a null value of the speed of expansion and finally the return to a contraction of the cosmological lattice (see figure 3.10).

Chapter 9

Cohesion of the edge-screw dispirations and the weak force

Considering topological singularities formed from the coupling of a twist disclination loop with an edge dislocation loop, which are called *dispiration loops*, an *interaction force similar to a capture potential* appears, with a very small range, which induces interactions between loops presenting a perfect analogy with the “weak interactions” between elementary particles of the Standard Model.

Previously, the notion of “mass of curvature” of the edge dislocation loops appeared, which corresponds to the equivalent mass associated with the gravitational effects of the charge of curvature of these loops, and which can be positive in the case of loops of vacancy nature or negative in the case of loops of interstitial nature. In fact, the charge of curvature and the mass of curvature associated with the edge dislocation loops do not appear in any other physical theory, nor in General Relativity, nor in Quantum Physics, nor in the Standard Model of elementary particles. But in our approach, it is precisely this mass of curvature which becomes responsible for the appearance of a *weak asymmetry between the particles* (hypothetically containing edge loops of interstitial nature) and the *anti-particles* (hypothetically containing edge loops of vacancy nature), and this weak asymmetry between matter and antimatter will be called upon to play a capital role in the cosmological evolution of topological singularities described in the following chapter.

While the previous chapter presented all of the long-range “gravitational” interactions between the various topological singularities of the cosmological lattice, this chapter is concerned with the very short-range “gravitational” interaction that occurs between a twist disclination loop (BV) and an edge dislocation loop (BC) due to the expansion perturbations associated with the curvature charge of the edge loop and the short-range perturbations associated with the rotation charge of the twist loop .

It is explained that this interaction between rotation and curvature charges corresponds to a very short-range repelling force in $1/d^5$ when the two loops are separated, but that it corresponds to a cohesive force when the two loops are joined in the form of a dispiration.

Long-range and short-range interactions between a twist disclination loop (BV) and an edge dislocation loop (BC)

If a twist disclination loop of radius R_{BV} is close enough to an edge dislocation loop of radius R_{BC} , as shown in figure 9.1, the total interaction energy between the two loops will involve the energies associated with the gravitational fields at long range, but also an interaction energy linked to the short-range expansion perturbation field of the twist disclination loop. By expressing the fields of long-range in $1/r$ and short-range in $1/r^4$ of the twist disclination loop (figure 7.10), the distortion energy of the edge dislocation loop can be calculated (figure

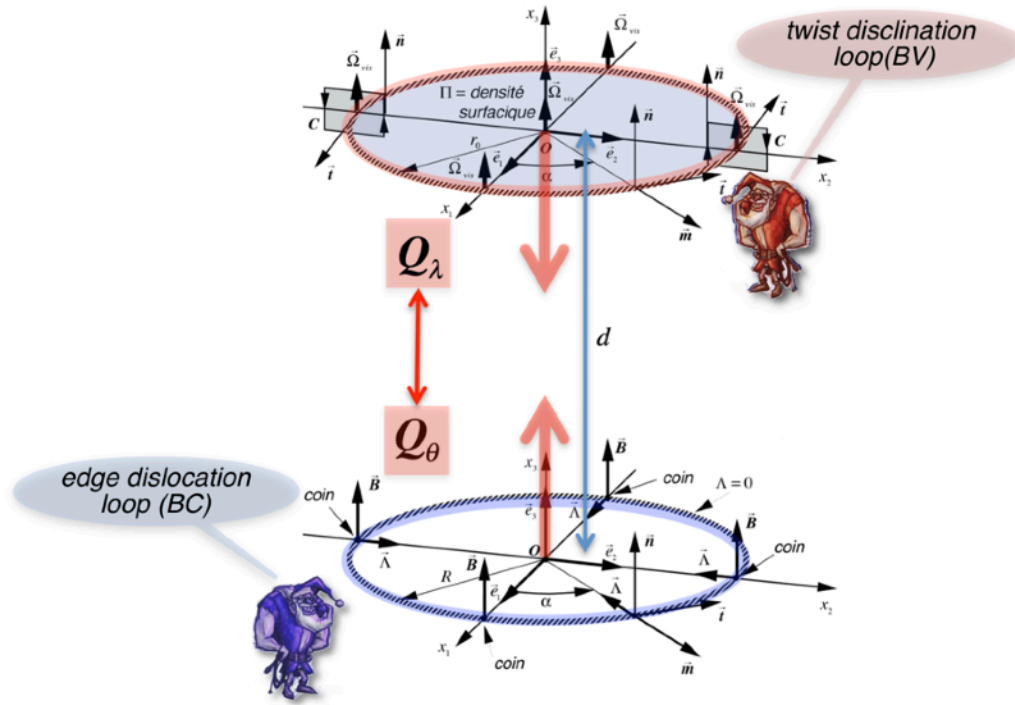


Figure 9.1 - Long and short range interactions between a loop of twist disclination (BV) and a loop of edge dislocation (BC)

8.8), and likewise by calculating the long-range field in $1/r$ of the edge dislocation loop (figure 7.11), the distortion energy of the screw loop can also be calculated (figure 8.8), so that the total gravitational interaction energy between the two loops is written as the sum of these distortion energies. Taking into account that the mass of curvature of the edge loop is much greater than its mass of inertia $|M_{curvature}^{BC}| \gg M_0^{BC}$, the total energy of the two loops can be simplified, and we can then find the increase ΔE_{inter}^{BV-BC} in energy compared to the sum of the energies of the two loops when they do not interact, corresponding to the interaction energy of the two loops. After some calculations, we obtain the relation for this increase ΔE_{inter}^{BV-BC} as expressed in figure 9.2.

At long distance, it is the term in $1/d^4$ which prevails, so that the interaction energy is negative if $M_{curvature}^{BC} > 0$, that is to say if the edge loop is of vacancy nature, and it is positive if $M_{curvature}^{BC} < 0$, that is to say if the corner loop is of interstitial nature (figure 9.2).

At a short distance, this is the term in $1/d^4$ that prevails, so that the energy of interaction necessarily becomes positive (figure 9.2). In the case of the vacancy type edge loop, we have $M_{curvature}^{BC} > 0$, so that the interaction energy goes through zero for $d = d_0$ whose value is given in figure 9.2

From the energy increase ΔE_{inter}^{BV-BC} , we can deduce the "gravitational" force of interaction $F_{grav}^{BV-BC}(d) = \partial E_{inter}^{BV-BC} / \partial d$ between the two loops thanks to the derivative with respect to the distance d . The expression of this force is also reported in figure 9.2, and we note that at long distance, it is the term in $1/d^2$ which prevails, so that the interaction force is negative, therefore repulsive, if $M_{curvature}^{BC} < 0$, that is to say if the edge loop is of interstitial nature, and it is positive,

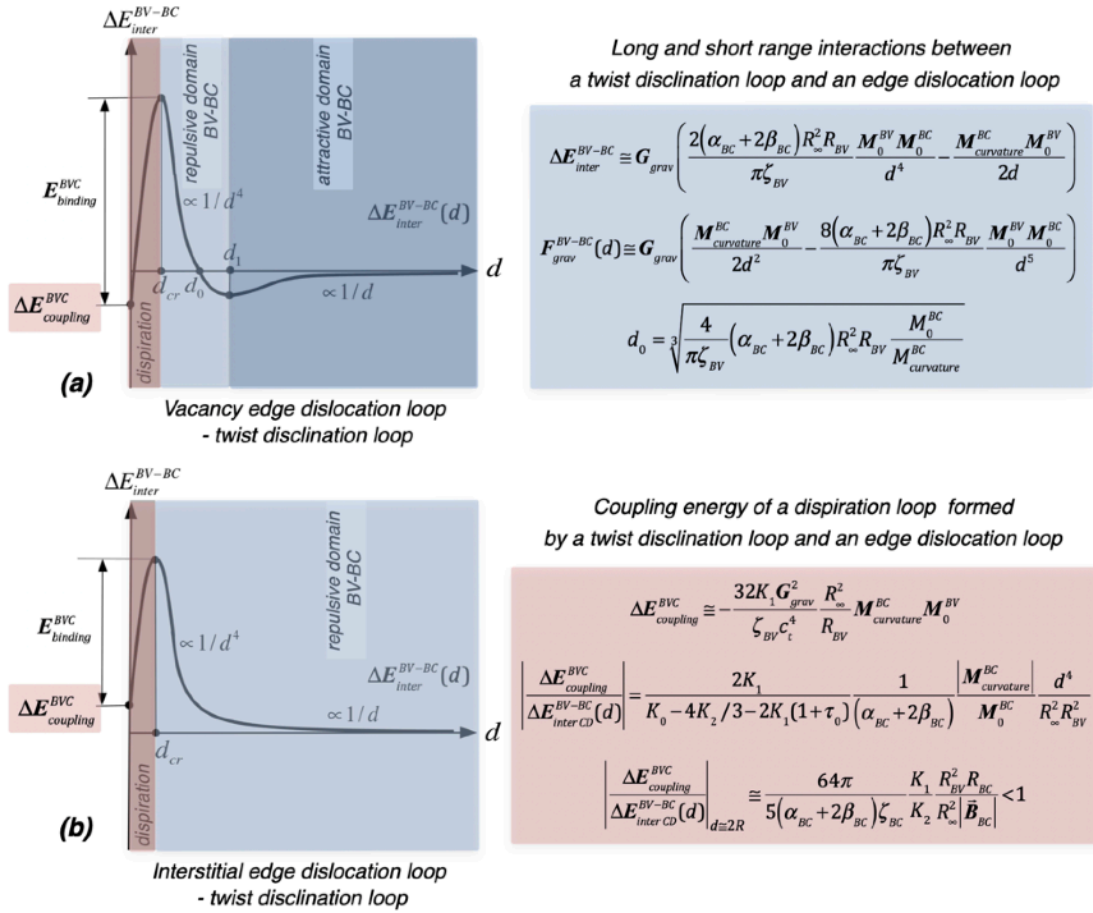


Figure 9.2 - Interaction (capture) potential between an edge dislocation loop BC, of vacancy type (a) or interstitial type (b) and a twist disclination loop BV to form an edge-screw dispiration loop BVC

therefore attractive, if $M_{curvature}^{BC} > 0$, that is to say if the edge loop is of vacancy nature.

At a short distance, this is the term in $1/d^5$ which prevails, so that the force of interaction becomes necessarily negative, therefore repulsive. In the case of the vacancy type edge dislocation loop for which $M_{curvature}^{BC} > 0$, the interaction force goes through zero for $d_1 = d_0 \sqrt[3]{4}$ and it presents a maximum for $d_2 = d_1 \sqrt[3]{10}$.

Coupling energy of a screw-edge dispiration loop (BVC) formed by a twist disclination loop (BV) and an edge dislocation loop (BC)

If a twist disclination loop (BV) of radius R_{BV} combines with an edge dislocation loop (BC) of radius $R_{BC} = R_{BV}$, we obtain a screw-edge dispiration loop (BVC). The elastic energy and the kinetic energy of this loop of dispiration is due to the field of rotation of the twist loop, to the fields of expansion and of shear of the edge loop and to the field of speed due to the two loops. As the various fields of the two loops are all orthogonal and contained in the torus surrounding the screw-edge dispiration loop, the relativistic energy of this one is the sum of the relativistic energies of the two loops, and is simply worth $E_v^{BVC} = (M_0^{BV} + M_0^{BC}) c_t^2 / \gamma$.

On the other hand, if we consider the external field of expansion perturbations associated with this dispiration loop, we will have the short and long distance fields of the screw loop (figure 7.10) and the fields of the edge loop (figure 7.11) which will overlap on the outside of the dispiration. The “gravitational” energy of this perturbation field can be calculated, and we then obtain the individual energies of the perturbation fields of each of the loops, but there is added a new coupling term between the two loops, due to the terms of interaction between the twist loop and the edge loop which occur in the square term $\left(\tau_{ext LD}^{BV}(r) + \tau_{ext CD}^{BV}(r) + \tau_{ext LD}^{BC}(r)\right)^2$. These coupling terms contribute to an increase $\Delta E_{coupling}^{BVC}$ in energy which, taking into account the fact that $M_0^{BC} \ll \left|M_{curvature}^{BC}\right|$ and keeping only the most important term, is represented by the value reported in figure 9.2.

In fact, this energy is due to the coupling of the external field of expansion perturbations at short range due to the rotation charge of the twist loop with the external field of expansion perturbations due to the charge of curvature of the edge loop. It is therefore an interaction between the rotation and curvature charges of the two loops of dispiration via their respective external gravitational effects. We also note that this coupling energy is negative if $M_{curvature}^{BC} > 0$, that is to say if the edge loop is of lacunar type, and positive if $M_{curvature}^{BC} < 0$, that is to say if the edge loop is of interstitial type.

We can now compare the energy $\Delta E_{inter CD}^{BV-BC}(d)$ of gravitational interaction at short distance between two loops distant of d with the energy $\Delta E_{couplage}^{DCV}$ of coupling within the loop of dispiration. It comes the relation for $\left|\Delta E_{coupling}^{BVC} / \Delta E_{inter CD}^{BV-BC}(d)\right|$ reported in figure 9.3. For a distance of the order of $d \approx 2R_{BV}$, we therefore have, if $\tau_0 \ll \tau_{0cr}$, and remembering that $K_3 = K_0$ in the perfect cosmological lattice that $\left|\Delta E_{coupling}^{BVC} / \Delta E_{inter CD}^{BV-BC}(d)\right|_{d \approx 2R} < 1$. Indeed, in the expression of figure 9.2, it appears the relation $R_{BV}^2 R_{BC} / R_\infty^2 \left|B_{BC}\right|$ which is very likely to be much smaller than the unit, so that the absolute value $\left|\Delta E_{coupling}^{BVC}\right|$ of the energy of coupling of the dispiration is undoubtedly clearly smaller than the interaction energy ΔE_{inter}^{BV-BC} between the two loops when separated by a distance $d \approx 2R_{BV}$.

It is deduced therefrom that the potential energy of interaction ΔE_{inter}^{BV-BC} between the two loops, as a function of the distance d between these two loops behaves in fact like a *capture potential* such as that represented in figure 9.2 in the domain “dispiration”. This potential keeps the two loops linked within the dispiration, with a binding energy $E_{binding}^{BVC}$ corresponding to the energy difference between the maximum of the potential energy ΔE_{inter}^{BV-BC} of interaction of the separate screw and twist loops and the coupling energy $\Delta E_{coupling}^{BVC}$ of the dispiration.

The potential energy of interaction ΔE_{inter}^{BV-BC} represents a repulsive force in $1/d^5$ between the two loops as soon as they separate from a distance greater than a certain critical distance of the order of $d_{cr} \approx 2R_{BV}$. To separate the two loops from the dispiration, it suffices:

- either of an energy fluctuation equal to or greater than the binding energy $E_{binding}^{BVC}$ of the dispiration loop, so that the two individual loops meet at a distance $d > d_{cr}$ and repel each other definitively,
- either that the edge loop crosses the potential barrier by *quantum tunnel effect*, and that the individual loops are found at a distance $d > d_{cr}$ and repel each other definitively.

About the analogy with the weak interaction of Standard Model of elementary particles

The short-range interaction that we have just described between the rotation and curvature

charges, respectively of a twist disclination loop and an edge dislocation loop, presents a remarkable analogy with *the weak interaction of the Standard Model of elementary particles*.

One of the four fundamental forces of nature is the weak interaction of the Standard Model. It is responsible for the radioactive decay of elementary particles and it affects all fermions, namely electrons, neutrinos and quarks. In the Standard Model, the weak interaction is linked to the exchange of massive bosons \bar{W}^+ , W^- and Z^0 , and it explains the weak lepton, semi-lepton and hadronic interactions. It is because this interaction is very short-range and weaker than the strong interaction and the electromagnetic interaction that it has been described as a weak interaction. On the other hand, it also has the property of breaking the **P** parity symmetry and the **CP** symmetry. It is also directly linked to the electric charge since electromagnetic interactions and weak interactions, which could be unified as two aspects of *an electroweak interaction*.

The analogy between the short-range interaction between an edge loop and a twist loop and the weak interaction of the Standard Model is literally obvious. Indeed:

- both are responsible for a weak bond within particles or loops,
- the two interactions have a very weak range,
- they both allow the decomposition of a particle or a loop into other particles or other loops,
- the decomposition of a particle or a loop of dispiration can be obtained by a local fluctuation of energy, or a quantum tunnel effect, which obviously intervenes in a random way, just like the radioactive decay associated with weak interaction is a statistical phenomenon,
- the weak interaction participates in the symmetry breaking **P** and **CP**, which agrees with the fact that it has asymmetry of the interactions between a twist loop and a lacunar or interstitial edge loop (figure 9.2).

As an example, consider the weak decay transforming the muon μ^- into an electron e^- shown in figure 9.3. This weak leptonic interaction presents an initial decomposition of the muon μ^- into a muonic neutrino ν_μ and a massive boson W^- , then the decomposition of the massive boson W^- into an electron e^- and an electronic anti-neutrino $\bar{\nu}_e$.

Let us then consider conjecture 8 which stipulates that *"the singularities of a vacancy nature correspond by analogy to anti-matter and the singularities of interstitial nature to matter"*. On this basis, let us suppose for example that the combination of a twist disclination loop BV^- with an interstitial edge dislocation loop $BC_{(1)}^{(i)}$ in the form of a loop of dispiration is the analog of the electron e^- , and imagine that the combination of a twist disclination loop BV^- with an interstitial edge dislocation loop $BC_{(2)}^{(i)}$ of slightly different topology (see chapter 13) forms a dispiration loop analog of a muon μ^- . The weak decay causing the muon μ^- to transform into an electron e^- shown in figure 9.3 (a) would then have a similar decay of the loops shown in figure 9.3 (b). The initial dispiration corresponding to the muon μ^- , and made up of the couple $BV^- + BC_{(2)}^{(i)}$ linked by the weak force, is broken down into a twist disclination loop BV^- carrying the rotation charge, and analogous to the massive boson W^- carrying the electric charge, and into an interstitial edge dislocation loop $BC_{(2)}^{(i)}$ analog to the of muonic neutrino ν_μ . Next, the twist disclination loop BV^- combines with an interstitial edge dislocation loop $BC_{(1)}^{(i)}$ to form a dispiration $BV^- + BC_{(1)}^{(i)}$ analog to an electron e^- , by emitting a vacancy edge dislocation loop $BC_{(1)}^{(i)}$, analog to the electronic anti-neutrino $\bar{\nu}_e$.

The weak interaction corresponding to the transformation of the anti-muon $\bar{\mu}^+$ into a

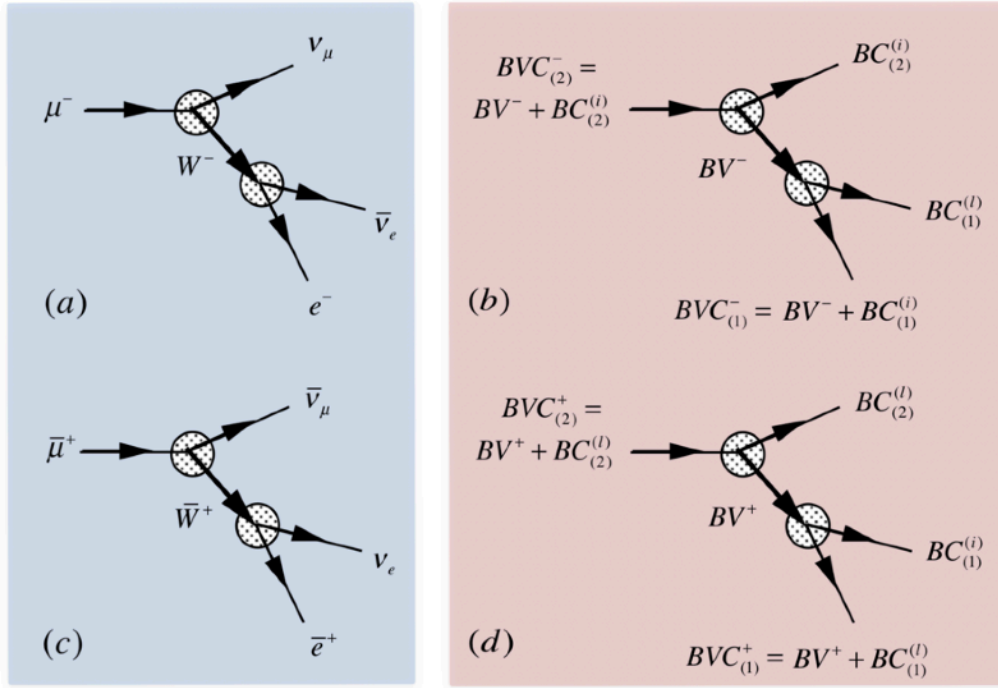


Figure 9.3 - Analogy between the weak leptonic interaction (a) and (c) and the decompositions and recompositions of dispiration loops (b) and (d)

positron \bar{e}^+ shown in figure 9.3 (c) also has its perfect analogue with loops shown in figure 9.3 (d). But this time, the twist disclination loop is replaced by the anti-loop BV^+ with an opposed rotation charge and the vacancy type edge loops are replaced by interstitial edge loops and vice versa. If we now consider the interactions between loops in figures 9.3 (b) and 9.3 (d), we immediately imagine that there is an asymmetry between these two reactions due to the slightly different interaction potentials in the case of lacunar and interstitial loops (figure 9.2). This asymmetry then becomes the analog of the violation of parity symmetry P and of symmetry CP in the case of weak interactions. We will return in detail in chapter 13 on the topological structures of the twist disclination loops and of the edge dislocation loops which could be involved in weak interactions.

Chapter 10

Matter-antimatter asymmetry and its cosmological evolution

Within the framework of our analogy with the great theories of physics, we begin in this chapter, *essentially qualitative and prospective*, by emitting some hypotheses concerning the constitution of the matter and the anti-matter by supposing that particles and anti-particles are made up of clusters of topological singularities in loops (of twist disclination, edge dislocation and mixed dislocation) of a perfect cosmological lattice. The weak asymmetry between matter and anti-matter is introduced by assuming that matter is based on edge loops of interstitial nature and that anti-matter is based on edge loops of lacunar nature. Using the results of chapter 8, we will see that the interactions of gravitational nature between particles and anti-particles of the Universe are almost all attractive, while presenting a weak gradation of the intensities of interaction according to the type of interacting particles. Only the interaction forces which involve a prismatic edge loop of interstitial nature, which will be interpreted as a neutrino, have a repulsive nature.

Based on the cosmological behaviors of lattice expansion and gravitational interactions between topological singularities, we can imagine a *very plausible scenario for the cosmological evolution of topological singularities* leading to the current structure of our Universe. This scenario is based entirely on the fact that, in the case of the simplest edge dislocation loops, analogously similar to *neutrinos*, *the mass of curvature dominates the mass of inertia*, so that neutrinos should be the only gravitational repellant particles, while the anti-neutrinos would be gravitatively attractive. This assertion then makes it possible to give a simple explanation to several facts still very poorly understood in the evolution of matter in the Universe. *The formation of galaxies* could correspond to a *phenomenon of precipitation* of matter and antimatter *within a sea of repellant neutrinos*. *The disappearance of anti-matter* could correspond to a *phenomenon of segregation* of particles and antiparticles within galaxies, due to their slight difference in gravitational properties, segregation during which the antiparticles would regroup in the center of the galaxies to finally form *gigantic black holes in the heart of galaxies*. Even the famous "*dark matter*" that astrophysicists had to invent to explain the abnormal gravitational behavior of the periphery of galaxies would then be very well explained in our approach. Indeed, "*dark matter*" would be in fact the sea of repellant neutrinos in which the galaxies have precipitated and bathed, which, by the compressive force which it exerts on the periphery of the galaxies, would explain the abnormal gravitational behavior of the stars in the galaxy peripheries. Finally, we also show how we can easily treat *the Hubble constant*, *the "redshift" of galaxies* and *the evolution of the cosmic microwave background* in the framework of our approach.

About the constitution and the asymmetry of matter and anti-matter

The existence of 15 different “gravitational” interaction forces depending on the nature of the singularities involved in the table in figure 8.9, as well as the behavior of these forces as a function of the background expansion of the lattice illustrated in the figure 8.10, allow us to develop a fairly simple and entirely plausible scenario of the cosmological evolution of our Universe.

Let's start from conjecture 8, which stipulated that the singularities of a vacancy nature correspond by analogy to anti-matter and the singularities of interstitial nature to matter, to introduce the following hypotheses:

- the particles of matter (electron e^- , neutrino ν^0 , neutron n^0 , proton p^+ , etc.) of the Universe would be made up of assemblies of loops of twist disclination, which give them their electrical charge, of loops of mixed dislocation, which give them their electric dipolar field, and prismatic edge dislocation loops of *interstitial* nature, which give them a *negative curvature charge*,
- the particles of anti-matter (positron \bar{e}^+ , anti-neutrino $\bar{\nu}^0$, anti-neutron \bar{n}^0 , anti-proton \bar{p}^- , etc.) of the Universe would be made up of assemblies of twist disclination loops, which give them their electrical charge, of loops of mixed dislocation, which give them their dipolar electric field, and of loops of prismatic edge dislocation of *vacancy* nature, which give them a *positive charge of curvature*.

If we accept this distinction between particles and anti-particles, the positive or negative curvature charge due to the component of edge loops of interstitial or vacancy nature, which appears neither in General Relativity, nor in the Standard Model of elementary particles, introduces a *weak asymmetry between particles and anti-particles which exists only in our approach*. This asymmetry is reminiscent of the asymmetry observed experimentally between particles and anti-particles in Particle Physics, without us knowing very well what cause attributed to it. This asymmetry affects certain properties of elementary particles (such as the violation of **CP** symmetry, combined action of a charge conjugation **C** and a symmetry by reflection **P**), but not the rest mass of these particles (linked to the non violation of **CPT** symmetry, combined action of charge conjugation **C**, reflection symmetry **P** and time inversion **T**). However, in current physics, whether it is Particle Physics or General Gravitation, there is never any mention of the property of curvature charge, since this can only appear by the approach of the topological singularities of a lattice that we have developed in this book. This property of curvature charge specific to lattice topological singularities could therefore be an excellent candidate to explain the asymmetry observed experimentally between particles and anti-particles of matter.

To simplify the rest of this talk, let's now call the various particles with a generic name according to their type:

- *particle X or Y* a particle of matter such as an electron e^- , a muon μ^- , a tauon τ^- , a neutron n^0 , a proton p^+ (or any other elementary particle composed of quarks) which involves twist disclination loops, therefore electrical charges, possibly loops of mixed dislocation in the event of a dipolar electric field and predominantly interstitial edge dislocation loops, therefore a *negative curvature charge*,
- *anti-particle \bar{X} or \bar{Y}* an anti-matter particle such as a positron \bar{e}^+ , an anti-muon $\bar{\mu}^+$, an anti-tauon $\bar{\tau}^+$, an anti-neutron \bar{n}^0 , an anti-proton \bar{p}^- (or any other particle composed of quarks)

which involves loops of twist disclination, therefore electrical charges, possibly mixed dislocation loops in the event of a dipolar electric field, and predominantly edge dislocation loops of a vacancy nature, therefore a *positive curvature charge*,

- *neutrino* ν^0 a particle of matter corresponding to the electron neutrino ν_e , to the muonic neutrino ν_μ or to the tau neutrino ν_τ , which does not involve any loops of twist disclination and loops of mixed dislocation, but only loops of prismatic edge dislocation of interstitial nature, therefore a *negative charge of curvature*,

- *anti-neutrino* $\bar{\nu}^0$ a particle of anti-matter corresponding to the electronic anti-neutrino $\bar{\nu}_e$, to the muonic anti-neutrino $\bar{\nu}_\mu$ or to the tau anti-neutrino $\bar{\nu}_\tau$, which does not involve loops of twist disclination and loops of mixed dislocation, but only loops of prismatic edge dislocation of a vacancy nature, therefore a *positive curvature charge*.

To these 4 types of particles or anti-particles, we can, thanks to the previous chapters, assign masses of inertia and equivalent masses of curvature, which satisfy the mass relationships indicated in figure 10.1 in the case of particles and anti-particles, and in the case of neutrinos and anti-neutrinos.

Thus, without first knowing the exact constitution in terms of singularity loops of the various particles and anti-particles, we can deduce thanks to these relationships between masses of inertia and masses of curvature, very relevant information about the behavior of gravitational forces of interaction between these various particles. Indeed, in the case of the interaction between particles X and anti-particles \bar{X} , we have, thanks to table 10.1, the following inequality relations $F_{grav}^{X-X} < F_{grav}^{X-\bar{X}} < F_{grav}^{\bar{X}-\bar{X}}$ between the gravitational interaction forces. As the mass of curvature is much lower than the mass of inertia $M_{curvature}^{\bar{X}} \ll M_0^{\bar{X}}$ in the case of a particle or an anti-particle which is not a neutrino, the difference between these interaction forces remains small, but it ensures still an asymmetry between particles and anti-particles (gravitationally, particles attract a little less strongly than anti-particles) which could play an important role in the cosmological evolution of the Universe, as we will see in the next section.

In the case of the interaction between particles X and Y , we have the following inequality relations $F_{grav}^{X-Y} < F_{grav}^{\bar{X}-Y} \equiv F_{grav}^{X-\bar{Y}} < F_{grav}^{\bar{X}-\bar{Y}}$ between the gravitational interaction forces which again show that particles attract a little less strongly than anti-particles.

As for the cases which involve only neutrinos, the following relationships are deduced for the interaction forces: $F_{grav}^{\nu^0-\nu^0} < 0$, $F_{grav}^{\bar{\nu}^0-\bar{\nu}^0} > 0$, $F_{grav}^{\nu^0-\bar{\nu}^0} \equiv 0$, $F_{grav}^{\bar{\nu}^0-\nu^0} = -F_{grav}^{\nu^0-\bar{\nu}^0}$. In other words, neutrinos repel each other with a force of the same magnitude as anti-neutrinos attract. As for the interaction between a neutrino and an anti-neutrino, it is extremely weak since it involves the product $(M_0^{\nu^0})^2$.

Finally, with regard to the interactions between particles and neutrinos, the following relationships are obtained: $F_{grav}^{X-\nu^0} < 0$, $F_{grav}^{X-\bar{\nu}^0} \equiv 0$, $F_{grav}^{\bar{X}-\nu^0} \equiv 0$, $F_{grav}^{\bar{X}-\bar{\nu}^0} > 0$. So the interaction between a neutrino and a particle is repulsive. Between an anti-neutrino and an anti-particle, it is attractive. And between a neutrino and an anti-particle, or between an anti-neutrino and a particle, the interaction can be slightly positive or negative, but of lesser magnitude than in the first two cases.

Effects of the cosmological expansion of the lattice on gravitational interactions

With the relations of inequality between gravitational interaction forces that we have just

**Mass relations
between particles
and anti-particles**

$$\begin{cases} M_0^X = M_0^{\bar{X}} > 0 \\ M_{curvature}^{\bar{X}} > 0 ; M_{curvature}^X < 0 \\ |M_{curvature}^X| = M_{curvature}^{\bar{X}} \ll M_0^X = M_0^{\bar{X}} \end{cases}$$

**Mass relations
between neutrinos
and anti-neutrinos**

$$\begin{cases} M_0^{\nu^0} = M_0^{\bar{\nu}^0} > 0 \\ M_{curvature}^{\bar{\nu}^0} > 0 ; M_{curvature}^{\nu^0} < 0 \\ |M_{curvature}^{\nu^0}| = M_{curvature}^{\bar{\nu}^0} \gg M_0^{\nu^0} = M_0^{\bar{\nu}^0} \end{cases}$$

$$\begin{cases} F_{grav}^{X-X} \equiv G_{grav} \frac{(M_0^X)^2}{d^2} + G_{grav} \frac{M_{curvature}^X M_0^X}{d^2} \equiv G_{grav} \frac{(M_0^X)^2}{d^2} - G_{grav} \frac{M_{curvature}^{\bar{X}} M_0^X}{d^2} \\ F_{grav}^{X-\bar{X}} \equiv G_{grav} \frac{M_0^X M_0^{\bar{X}}}{d^2} + \frac{1}{2} G_{grav} \frac{M_{curvature}^X M_0^{\bar{X}}}{d^2} + \frac{1}{2} G_{grav} \frac{M_{curvature}^{\bar{X}} M_0^X}{d^2} \equiv G_{grav} \frac{(M_0^X)^2}{d^2} \\ F_{grav}^{\bar{X}-\bar{X}} \equiv G_{grav} \frac{(M_0^{\bar{X}})^2}{d^2} + G_{grav} \frac{M_{curvature}^{\bar{X}} M_0^{\bar{X}}}{d^2} \equiv G_{grav} \frac{(M_0^X)^2}{d^2} + G_{grav} \frac{M_{curvature}^{\bar{X}} M_0^{\bar{X}}}{d^2} \end{cases}$$

$$\begin{cases} F_{grav}^{X-Y} \equiv G_{grav} \frac{M_0^X M_0^Y}{d^2} - \frac{1}{2} G_{grav} \frac{M_{curvature}^{\bar{X}} M_0^Y}{d^2} - \frac{1}{2} G_{grav} \frac{M_{curvature}^{\bar{Y}} M_0^X}{d^2} \\ F_{grav}^{\bar{X}-Y} \equiv G_{grav} \frac{M_0^X M_0^Y}{d^2} + \frac{1}{2} G_{grav} \frac{M_{curvature}^{\bar{X}} M_0^Y}{d^2} - \frac{1}{2} G_{grav} \frac{M_{curvature}^{\bar{Y}} M_0^X}{d^2} \\ F_{grav}^{X-\bar{Y}} \equiv G_{grav} \frac{M_0^X M_0^Y}{d^2} - \frac{1}{2} G_{grav} \frac{M_{curvature}^{\bar{X}} M_0^Y}{d^2} + \frac{1}{2} G_{grav} \frac{M_{curvature}^{\bar{Y}} M_0^X}{d^2} \\ F_{grav}^{\bar{X}-\bar{Y}} \equiv G_{grav} \frac{M_0^X M_0^Y}{d^2} + \frac{1}{2} G_{grav} \frac{M_{curvature}^{\bar{X}} M_0^Y}{d^2} + \frac{1}{2} G_{grav} \frac{M_{curvature}^{\bar{Y}} M_0^X}{d^2} \end{cases}$$

**Relations of forces
between a particle and
its anti-particle**

$$F_{grav}^{X-X} < F_{grav}^{X-\bar{X}} < F_{grav}^{\bar{X}-\bar{X}}$$

**Relations of forces
between a particle and
another particle**

$$F_{grav}^{X-Y} < F_{grav}^{\bar{X}-Y} \equiv F_{grav}^{X-\bar{Y}} < F_{grav}^{\bar{X}-\bar{Y}}$$

$$\begin{cases} F_{grav}^{\nu^0-\nu^0} \equiv 2(\alpha_{BC} + 2\beta_{BC}) G_{grav} \frac{M_{curvature}^{\nu^0} M_0^{\nu^0}}{d^2} \equiv -2(\alpha_{BC} + 2\beta_{BC}) G_{grav} \frac{M_{curvature}^{\bar{\nu}^0} M_0^{\nu^0}}{d^2} < 0 \\ F_{grav}^{\nu^0-\bar{\nu}^0} \equiv (\alpha_{BC} + 2\beta_{BC}) G_{grav} \frac{M_{curvature}^{\nu^0} M_0^{\bar{\nu}^0}}{d^2} + (\alpha_{BC} + 2\beta_{BC}) G_{grav} \frac{M_{curvature}^{\bar{\nu}^0} M_0^{\nu^0}}{d^2} + 2(\alpha_{BC} + 2\beta_{BC}) G_{grav} \frac{M_0^{\nu^0} M_0^{\bar{\nu}^0}}{d^2} \\ \equiv 2(\alpha_{BC} + 2\beta_{BC}) G_{grav} \frac{(M_0^{\nu^0})^2}{d^2} \\ F_{grav}^{\bar{\nu}^0-\bar{\nu}^0} \equiv 2(\alpha_{BC} + 2\beta_{BC}) G_{grav} \frac{M_{curvature}^{\bar{\nu}^0} M_0^{\bar{\nu}^0}}{d^2} \equiv 2(\alpha_{BC} + 2\beta_{BC}) G_{grav} \frac{M_{curvature}^{\nu^0} M_0^{\bar{\nu}^0}}{d^2} > 0 \end{cases}$$

**Relations of forces
between two neutrinos**

$$F_{grav}^{\nu^0-\nu^0} < 0 ; F_{grav}^{\bar{\nu}^0-\bar{\nu}^0} > 0 ; F_{grav}^{\nu^0-\bar{\nu}^0} \equiv 0 ; F_{grav}^{\bar{\nu}^0-\nu^0} = -F_{grav}^{\nu^0-\bar{\nu}^0}$$

$$\begin{cases} F_{grav}^{X-\nu^0} \equiv G_{grav} \frac{M_0^X M_0^{\nu^0}}{d^2} - \frac{1}{2} G_{grav} \frac{M_0^{\nu^0} M_{curvature}^{\bar{X}}}{d^2} - \frac{1}{2} G_{grav} \frac{M_0^X M_{curvature}^{\bar{\nu}^0}}{d^2} \equiv \frac{1}{2} G_{grav} \frac{M_0^{\nu^0} M_{curvature}^{\bar{X}}}{d^2} - \frac{1}{2} G_{grav} \frac{M_0^X M_{curvature}^{\bar{\nu}^0}}{d^2} \\ F_{grav}^{X-\bar{\nu}^0} \equiv G_{grav} \frac{M_0^X M_0^{\bar{\nu}^0}}{d^2} - \frac{1}{2} G_{grav} \frac{M_0^{\bar{\nu}^0} M_{curvature}^{\bar{X}}}{d^2} + \frac{1}{2} G_{grav} \frac{M_0^X M_{curvature}^{\nu^0}}{d^2} \equiv -\frac{1}{2} G_{grav} \frac{M_0^{\bar{\nu}^0} M_{curvature}^{\bar{X}}}{d^2} + \frac{1}{2} G_{grav} \frac{M_0^X M_{curvature}^{\nu^0}}{d^2} \\ F_{grav}^{\bar{X}-\nu^0} \equiv G_{grav} \frac{M_0^{\bar{X}} M_0^{\nu^0}}{d^2} + \frac{1}{2} G_{grav} \frac{M_0^{\nu^0} M_{curvature}^{\bar{X}}}{d^2} - \frac{1}{2} G_{grav} \frac{M_0^{\bar{X}} M_{curvature}^{\bar{\nu}^0}}{d^2} \equiv +\frac{1}{2} G_{grav} \frac{M_0^{\nu^0} M_{curvature}^{\bar{X}}}{d^2} - \frac{1}{2} G_{grav} \frac{M_0^{\bar{X}} M_{curvature}^{\bar{\nu}^0}}{d^2} \\ F_{grav}^{\bar{X}-\bar{\nu}^0} \equiv G_{grav} \frac{M_0^{\bar{X}} M_0^{\bar{\nu}^0}}{d^2} + \frac{1}{2} G_{grav} \frac{M_0^{\bar{\nu}^0} M_{curvature}^{\bar{X}}}{d^2} + \frac{1}{2} G_{grav} \frac{M_0^{\bar{X}} M_{curvature}^{\nu^0}}{d^2} \equiv +\frac{1}{2} G_{grav} \frac{M_0^{\bar{\nu}^0} M_{curvature}^{\bar{X}}}{d^2} + \frac{1}{2} G_{grav} \frac{M_0^{\bar{X}} M_{curvature}^{\nu^0}}{d^2} \end{cases}$$

**Relations of forces
between a particle and
a neutrino**

$$F_{grav}^{X-\nu^0} < 0 ; F_{grav}^{X-\bar{\nu}^0} \equiv 0 ; F_{grav}^{\bar{X}-\nu^0} \equiv 0 ; F_{grav}^{\bar{X}-\bar{\nu}^0} > 0$$

Figure 10.1 - Relations of masses and interaction forces between particles (X or Y), antiparticles (\bar{X} or \bar{Y}), neutrinos (ν^0) and antineutrino ($\bar{\nu}^0$)

obtained for the interactions between particles, anti-particles, neutrinos and anti-neutrinos, we can return to the cosmological evolution of the perfect cosmological network (figure 3.7 and 3.10), and integrate into it the behaviors of the gravitational forces of interaction between particles. We obtain the result of figure 10.2.

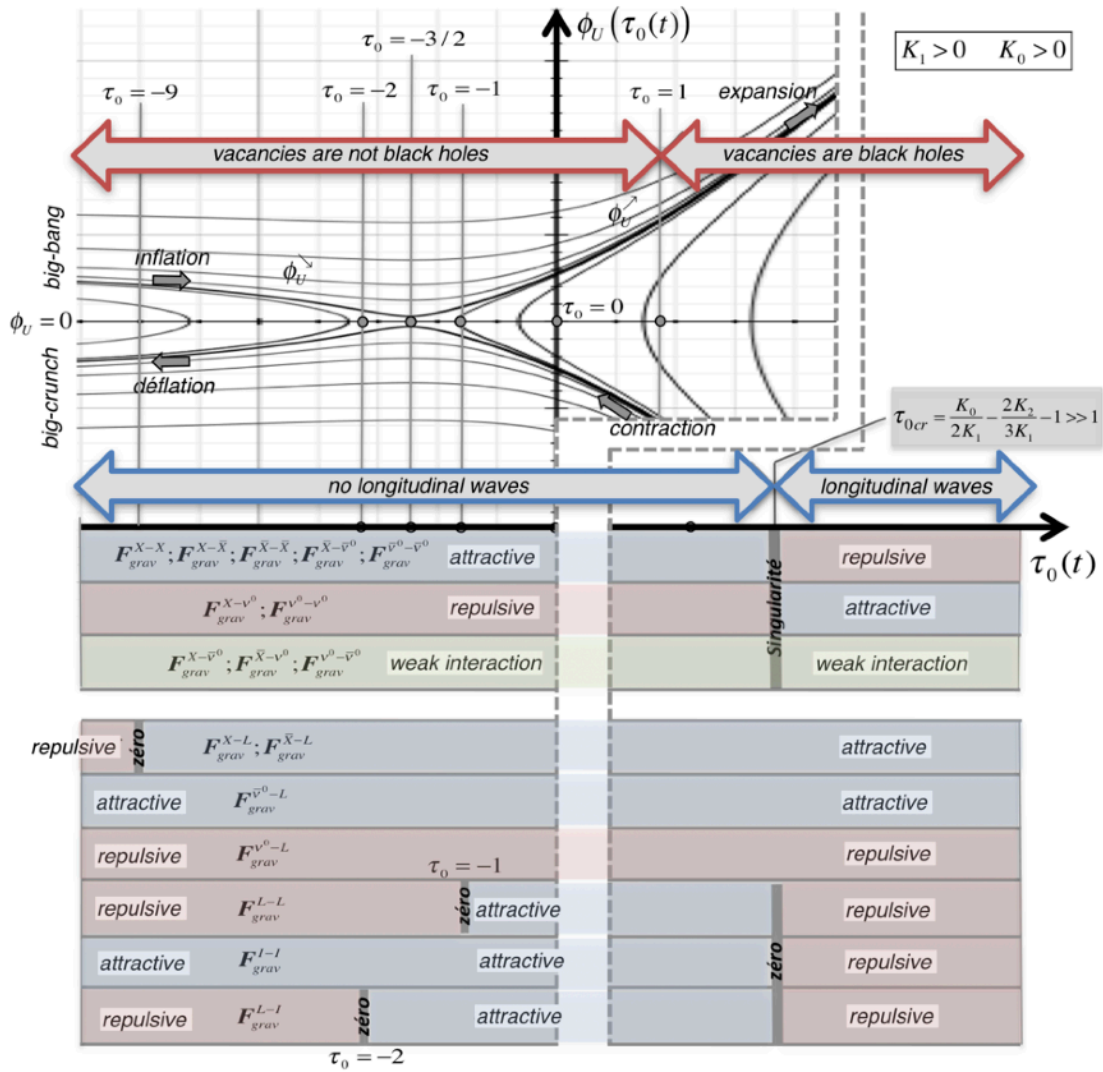


Figure 10.2 - Behavior of "gravitational" interaction forces as a function of the cosmological evolution of the lattice background expansion

As this figure shows, a series of values characteristic of expansion $\tau_0(t)$ appears for which there are sudden changes, either in the behavior of cosmological expansion, or in the behavior of the various gravitational interaction forces. In this figure, we have also reported the gravitational interaction forces involving macroscopic vacancies (black holes as soon as $\tau_0(t) \geq 1$) and macroscopic interstitials (neutron stars). Among the important characteristic values of the cosmological expansion of the lattice are:

- $\tau_0(t \rightarrow t_{init}) \rightarrow -\infty$, which represents the initial "big-bang" of the lattice over time t_{init} ,
- $\tau_0(t) = -9$, which represents the expansion value for which the interaction force between a macro vacancy and a particle or an anti-particle changes from repulsive to attractive,
- $\tau_0(t) = -2$, which represents the expansion value for which the interaction force between a macro vacancy and a macro interstitial changes from repulsive to attractive,
- $\tau_0(t) = -3/2$, which corresponds to the passage from the stage of inflation, during which

the speed $\phi_U(\tau_0(t))$ of expansion decreases, to *the stage of expansion* during which the speed $\phi_U(\tau_0(t))$ of expansion begins to increase again,

- $\tau_0(t) = -1$, which corresponds to the transition from the repulsion stage between macroscopic vacancies to the attraction stage between macroscopic vacancies,
- $\tau_0(t) = 1$, which represents the expansion value from which the macroscopic vacancies become black holes,
- $\tau_0(t) = \tau_{0cr}$, which represents *the critical expansion* from which longitudinal waves appear within the lattice to the detriment of localized eigen modes of vibration of the expansion, and which also represents the critical expansion for which several of the gravitational interaction forces change sign, either by passing through an infinite singularity, or by passing through a zero value.

Beyond τ_{0cr} , the cosmological evolution of the lattice passes from *the stage of expansion*, during which the speed $\phi_U(\tau_0(t))$ of expansion is positive, to *a stage of contraction* during which the speed $\phi_U(\tau_0(t))$ of expansion becomes negative, and which ends after *stages of contraction and deflation*, by a “big-crunch” followed by a new “big-bang” of the lattice, therefore by a “big-bounce” of the lattice due to the kinetic energy stored, as well show figures 3.7 and 3.10.

A plausible scenario of cosmological evolution of topological singularities in a perfect cosmological lattice

On the basis of figure 10.2, a plausible scenario of evolution of the topological singularities of the cosmological lattice can then be imagined, which implies several distinct stages to arrive at the current state of our Universe:

(1) *Hypothetical liquefaction and solidification of the lattice during the "big-bounce" and formation of an "initial hot soup" of loops of singularities.*

In the scenario of a “big-bounce” Universe represented in figures 3.7 and 3.10, the intense contraction of the lattice at the end of the “big-crunch” must certainly heat the lattice to an extreme since its compression becomes gigantic, which could lead to its “liquefaction”. It is obvious that such a phenomenon, modeled on our knowledge of usual matter, is not easy to imagine, and presupposes that the cells of the lattice are associated with “strange particles”, which would be responsible for the mass associated with lattice (and which would perhaps correspond to the famous Higgs particles of the Standard Model). For the lattice to effectively present a phase transition phenomenon by “liquefaction”, its complete state function should not only contain the terms of free energy for deformation, but also thermal terms leading to the phase transition .

Assuming therefore that the “big-bang” following the “big-crunch” occurs from a very hot liquid of massive “strange particles”, the inflation phase of cosmological evolution should lead to a cooling of the liquid (to a decrease in its thermal agitation) and to a sudden “solidification” of the liquid in the form of the perfect cosmological lattice which we introduced in chapter 3. During this phase transition, it could then appear *structural defects of the lattice*, in the form of dislocations, disclinations, loops, vacancies and interstitials, and even grain boundaries, very similar to what happens for example during the rapid solidification of a metal .

We could speak of an “initial hot soup” of singularity loops, the term soup including the fact of a homogeneous initial distribution of the various types of singularity loops and a very great mobility of these loops as in a liquid, then that the term hot includes the notion of a still extremely hot lattice, in other words containing a very large quantity of *transverse wave modes* (photons) and *localized longitudinal vibration modes* (gravitons), implying a very strong thermal agitation of the initial loops.

(2) *Inflation of the lattice and condensation of the loops of singularities into particles and anti-particles.*

During the inflation of the cosmological lattice, and therefore of its cooling, and as soon as the temperature has dropped sufficiently, the various dislocation and disclination loops will regroup within the “hot soup” to form complex and localized topological dispirations, formed by dislocation and disclination loops linked by the weak interaction force (chapter 9), and corresponding to the various elementary particles of matter (électron e^- , neutrino ν^0 , neutron n^0 , proton p^+ , etc.) and of anti-matter (positron \bar{e}^+ , anti-neutrino $\bar{\nu}^0$, anti-neutron \bar{n}^0 , anti-proton \bar{p}^- , etc.) of our Universe. The existence of such combinations of loops in localized form, which can correspond to the various elementary particles of our Universe, will be discussed in chapter 13 in this work.

(3) *Formation of galaxies by precipitation of matter and anti-matter in a sea of repulsive neutrinos.*

In the hot soup of lattice singularities, an initially homogeneous mixture of particles and anti-particles, there are particles and anti-particles whose gravitational interaction is attractive (electron e^- , neutron n^0 , proton p^+ , positron \bar{e}^+ , anti-neutrino $\bar{\nu}^0$, anti-neutron \bar{n}^0 , anti-proton \bar{p}^- , etc.), but there are also the various neutrinos ν^0 whose gravitational interaction with other particles (such as electron e^- , neutron n^0 , proton p^+ , positron \bar{e}^+ , anti-neutron \bar{n}^0 , anti-proton \bar{p}^- , etc.) is repulsive, or almost non-existent (with anti-neutrinos $\bar{\nu}^0$), and there is obviously also a sea of energetic photons interacting strongly with particles and anti-particles charged via the Compton scattering mechanism. This situation linked to the component of the edge dislocation loops with their curvature charge is completely original in our approach, and will necessarily lead to explain the phenomenon of *initial formation of galaxies*, which is very difficult to explain at present by other theories.

Indeed, it is possible to make an extremely simplified model of the initial and homogeneous hot soup of particles and anti-particles to describe the formation of galaxies. Consider that the initial hot soup forms a kind of liquid composed of attractive particles on the one hand (electron e^- , neutron n^0 , proton p^+ , positron \bar{e}^+ , anti-neutrino $\bar{\nu}^0$, anti-neutron \bar{n}^0 , anti-proton \bar{p}^- , etc.) and repulsive neutrinos ν^0 on the other part (electronic neutrino ν_e , muonic neutrino ν_μ and tau neutrino ν_τ), and let us try to express the free interaction energy $f^{interaction}$ per particle within this liquid mixture. By introducing the concentrations C_{ν^0} and $C_X = 1 - C_{\nu^0}$ of repulsive neutrinos ν^0 and attractive particles X into the mixture, the free energy of interaction can be written as the sum of an internal energy interaction term and an entropic mixing term¹, as shown in the first formula in figure 10.3, where z is the mean coordination number, which represents

¹ see section 7.6 in «Théorie eulérienne des milieux déformables: charges de dislocation et de désinclinaison dans les solides», G. Gremaud, Presses Polytechniques et Universitaires Romandes, Lausanne 2013, ISBN 978-2-88074-964-4 (751 pages).

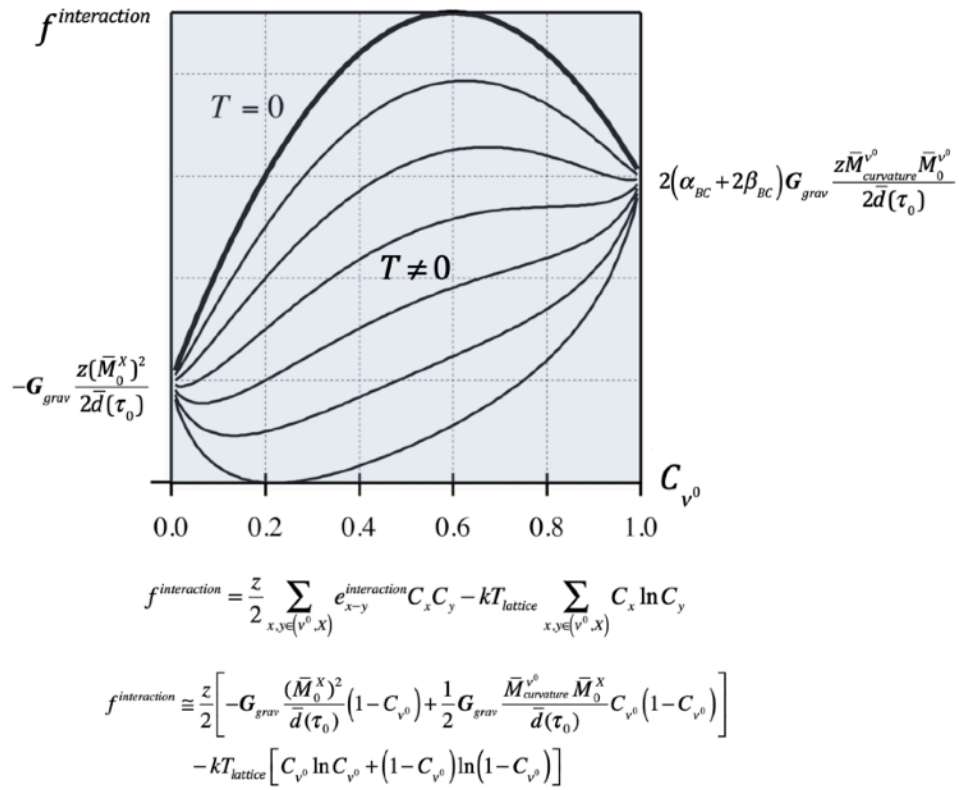


Figure 10.3 - The particle free interaction energy within the initial hot soup of particles as a function of the concentration C_{ν^0} of repulsive neutrinos and for different lattice temperatures

the mean number of neighboring particles with which a particle can form a pair interaction and where the factor 1/2 is introduced so as not to count each interaction twice.

By then introducing an average value of the mass of inertia of the attractive particles $\bar{M}_0^X > 0$ and neutrinos $\bar{M}_0^{\nu^0} > 0$, as well as the average mass of curvature $\bar{M}^{\nu^0}_{curvature} < 0$ of the matter neutrinos, and by supposing an average distance $\bar{d}(\tau_0)$ between the particles in the initial homogeneous hot soup, one can express very approximately the free energy of interaction per particle in the form of the second relation of figure 10.3. If we represent this interaction free energy as a function of the neutrino concentration C_{ν^0} for different lattice temperatures, as in the diagram in figure 10.3, we see that at high temperature the minimum free energy is obtained by a homogeneous mixture of attractive particles X and repulsive neutrinos ν^0 . But if the lattice temperature drops sufficiently, there appear two minima of free energy depending on the concentration C_{ν^0} : a minimum corresponding to a very low concentration of neutrinos and a minimum corresponding to a very high concentration of neutrinos. In fact, there appears a *phase transition by precipitation*, which tends to separate the attractive particles X and the repulsive neutrinos ν^0 , as represented in figure 10.4 (a). It will therefore appear *precipitates*, a kind of islands made up of attractive particles X , within a sea of repulsive neutrinos ν^0 . At low temperatures, the minimum free energy corresponds to the concentrations $C_{\nu^0} = 0$ and $C_{\nu^0} = 1$, which corresponds to a complete separation of the attractive particles and the repellent neutrinos.

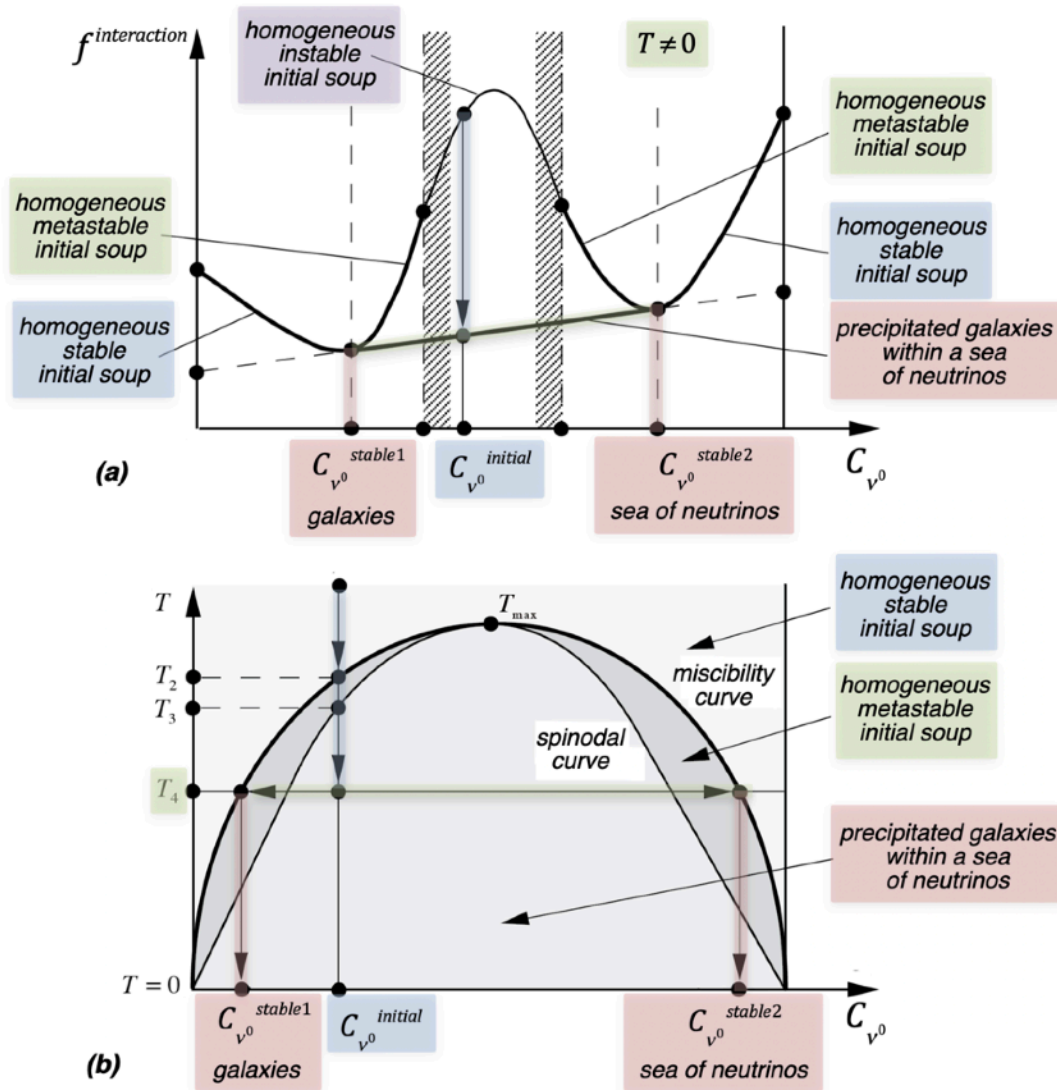


Figure 10.4 - (a) Precipitation of the galaxies within the initial hot soup of concentration $C_{v^0}^{initial}$ of neutrinos at a given temperature, (b) phase diagram of matter in the Universe as a function of temperature

The phase transition by precipitation of attractive particles and anti-particles in the form of localized clusters can be represented by a precipitation phase diagram as in Figure 10.4 (b), and it corresponds perfectly to the phenomenon of galaxy formation in our Universe. In this model, it is the existence of repulsive neutrinos that becomes the engine of galaxy formation. And it is very interesting to note that the repulsion of neutrinos of matter is due exclusively to the charge of curvature of neutrinos, a concept which does not exist in General Relativity nor in the Standard Model of elementary particles. On the other hand, we already know that the curvature charge is also at the origin of the weak asymmetry existing between matter and anti-matter, which confirms the strong link existing between this asymmetry observed experimentally and the initial formation of galaxies and structures of our current Universe.

(4) Formation and segregation of matter and anti-matter within galaxies.

Now let's take a look at what's going on in emerging galaxies, during the precipitation of

particles and anti-particles that attract each other. Within this precipitating liquid phase of particles, the attractive gravitational interaction forces have small differences depending on whether we are dealing with particles or anti-particles. Consider for example the family of particles X and anti-particles \bar{X} . The gravitational interaction forces between these particles are expressed in figure 10.1. With the mass of inertia M_0^X of these particles, we deduce, thanks to the classical Newton equation, the acceleration that these particles undergo during their various interactions $X - X$, $X - \bar{X}$ and $\bar{X} - \bar{X}$: $a_{grav}^{X-X} \equiv G_{grav} (M_0^X - M_{courbure}^{\bar{X}}) / d^2$, $a_{grav}^{X-\bar{X}} \equiv G_{grav} M_0^X / d^2$ and $a_{grav}^{\bar{X}-\bar{X}} \equiv G_{grav} (M_0^X + M_{courbure}^{\bar{X}}) / d^2$. We deduce that $a_{grav}^{X-X} < a_{grav}^{X-\bar{X}} < a_{grav}^{\bar{X}-\bar{X}}$, therefore anti-particles \bar{X} attract more strongly than particles X , and we must therefore see a *phenomenon of progressive segregation of anti-particles and particles* appear, during which anti-particles will tend to regroup towards the center of the emerging galaxy, leaving the particles in the periphery of the galaxy.

It is clear that this phenomenon of segregation must be accompanied by an intense activity of annihilation between particles and anti-particles, in an area located around the center of the galaxy, and which should necessarily be a source of intense gamma radiation. But there must also appear an activity of combinations between particles and between anti-particles to form matter and anti-matter (initially hydrogen and anti-hydrogen atoms and helium and anti-helium atoms). These annihilation and recombination processes must continue until there appears to be an effective separation between a galaxy core composed essentially of anti-matter and a galaxy periphery composed essentially of matter. We note again that this process of segregation of matter and anti-matter is to be associated with the charge of curvature of the dislocation edge loops, which is an exclusive property of our approach, since it is these charges which are responsible of the equivalent mass of curvature, itself responsible for the small difference in attractive gravitational interaction between matter and anti-matter.

(5) Formation of a cosmic radiation background.

Initially, all particles and anti-particles are in thermal equilibrium with a sea of photons, via interactions by Compton scattering, and as long as their temperature has not dropped enough to form atoms. But as soon as the temperature drops below around 3,000 K, helium, anti-helium, hydrogen and anti-hydrogen atoms are formed which ensures the electrical neutrality of matter and anti-matter. At this time there is also decoupling of photons from neutral matter and anti-matter. The Universe therefore becomes transparent to photons, which then fill all the space in the form of a *cosmic microwave background*. This cosmic radiation background has been observed and studied experimentally: it is almost *isotropic* and presents *the spectrum of a perfect black body*, that is to say a *Planck distribution of the energy density $U(\nu)$ of photons*, centered on a temperature T which is currently measured at 2.7 K (figure 10.5, with c the speed of light, h the Planck constant, k the Boltzmann constant, T the temperature of the black body and ν the photon frequency). We will come back to the process that leads to the “cooling” of this cosmic microwave background.

(6) Gravitational collapse and disappearance of anti-matter by the formation of gigantic black holes in the center of galaxies.

The formation by precipitation of galaxies composed of attractive particles and anti-particles within the sea of repulsive neutrinos will lead to enormous pressures in the heart of galaxies as they evolve. The appearance of a spinning movement of the galaxies makes it possible to

partially balance the gravitational pulling forces within the galaxies and the compressive forces of the neutrino sea. But at the very center of galaxies, the compressive forces could reach values sufficient to witness a gravitational collapse of their hearts. If such a collapse occurs, as the heart of the galaxies is formed essentially of anti-matter, it will be responsible for the appearance of macroscopic vacancies since during the collapse the loops of twist disclinations will annihilate (if the anti-matter was initially electrically neutral), while the vacancy edge dislocations loops specific to anti-matter combine to form macroscopic lattice vacancies in the center of the galaxies.

The macroscopic vacancy created in the center of a galaxy by the gravitational collapse of anti-matter is in fact nothing but a *gigantic topological singularity*, which becomes a *huge black hole* as soon as the bottom expansion of the lattice exceeds unity ($\tau_0 \geq 1$). This phenomenon of gravitational collapse of segregated anti-matter in the heart of galaxies would then explain perfectly, and quite simply, experimental observations of *the existence of gigantic black holes in the center of most galaxies* and of *the disappearance of the anti-matter in our current universe*.

(7) *Coalescence of matter in galaxies and formation of stars.*

The matter that composes the galaxies after the collapse of the anti-matter core in a central black hole will gradually coalesce under the effect of the gravitational attraction to form clouds of hydrogen and helium gases, various types of stars and planetary systems, such as those observed in our current universe.

(8) *Gravitational collapse of stars and formation of neutron stars.*

As the galaxies are then essentially made up of matter, based on *edge dislocation loops of interstitial nature*, any gravitational collapse of a very large star under the effect of its own gravity must lead to a *localized topological singularity of a macroscopic interstitial type*, and not of the macroscopic vacancy type. Consequently, *there cannot appear vacancy type black holes after the gravitational collapse of a massive star composed of matter*.

Experimentally, we sometimes and suddenly observe this phenomenon of gravitational collapse of massive stars of matter in the form of a *supernova* (a cloud of residual gases from the initial explosion of the star, which extends to very high speed), with, in the center of the supernova, a relatively small and very massive object, which should correspond to a residual macroscopic interstitial singularity, which we commonly describe as *pulsar* (by its properties of emission of electromagnetic pulses whose frequency corresponds to the very fast frequency of rotation of the object on itself) or as *neutron star* (due to the enormous mass density of the object).

The rest of the story is then well known and well described by astrophysicists, with the formation of atoms of increasing mass by the nuclear fusion of hydrogen and light elements in the heart of stars and by the dispersion of these elements by the supernovae, ultimately leading to the appearance of all the elements of Mendeleev's table and the formation of increasingly complex stars, planetary systems, etc.

(9) *The future of our universe.*

In the scenario of the *"big-bounce" universe* represented in figures 3.7 and 3.10, which in fact corresponds best to our own universe, the phase of expansion at increasing speed, under conditions where there is no propagation of longitudinal waves, is between the values $\tau_0 = -3/2$ and $\tau_0 = \tau_{0cr} \gg 1$. Our present Universe must therefore be situated in this field

of fundamental expansion since recent observations have shown that the expansion of the universe is most likely taking place at increasing speed. We can even say that the current background expansion should in fact be understood in the domain $1 < \tau_0 < \tau_{0cr}$, since massive black holes seem to have been observed in the center of most galaxies, especially in the center of our galaxy, the Milky Way.

Since this expansion range ($1 < \tau_0 < \tau_{0cr} \gg 1$) is very large, it is difficult to know where our Universe is currently located and how long it will take for it to reach the critical expansion τ_{0cr} . But we can on the other hand affirm that when this one approaches the critical value τ_{0cr} , it will inevitably appear titanic phenomena of reshaping of celestial objects, matter, black holes and the sea of repulsive neutrinos since at that moment we will have essentially that:

- the gravitational constant G_{grav} will become negative by passing through a singularity at τ_{0cr} ,
- the eigen modes of localized vibrations will disappear in favor of the propagation of longitudinal waves, which should in fact correspond to *the disappearance of quantum physics* as we will see in the rest of this work.

These two phenomena alone should be cataclysmic. But one could still push further by considering the phenomena which should intervene during the phase of re-contraction of the cosmological lattice, especially during the reverse passage by the critical value τ_{0cr} where the gravitational constant would become positive again and where it would reappear eigen modes of localized vibrations instead of the propagation of longitudinal waves. These predictions are most likely in the realm of the possible with our approach, although certainly very difficult and very rough. In fact, we are swimming there in full science-prediction, not to say in full science-fiction.

The fact remains that our approach goes much further in explanations and predictions than general relativity, and that a number of exotic phenomena such as instantaneous displacement in space and time via the famous wormholes described from general relativity, which are the delight of theoretical physicists and science fiction writers, should be nothing but pure ranting in the light of our approach.

About the famous «dark matter» of astrophysicists

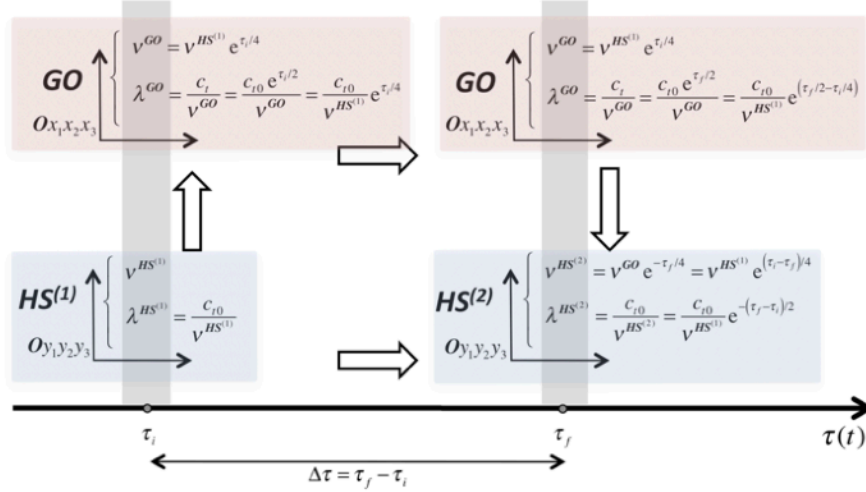
The formation of a “*sea of repelling neutrinos*” in which the galaxies are bathed perfectly explains the phenomenon attributed to “*dark matter*” by astrophysicists. Indeed, when we observe a galaxy and we measure experimentally the speeds of the stars composing it as a function of their distance from the center of the galaxy, we find that the speeds of the stars located on the periphery of the galaxy are too high compared to the speeds calculated by applying Newton's law of gravitation with the mass density of the stars (which can be measured experimentally by their brightness). Everything happens as if there was a halo of matter invisible to our eyes around the galaxy, which, by its gravitational effect, forces the stars to rotate faster to compensate for this attractive effect. This halo of invisible matter has been called *dark matter* by astrophysicists, and research into the very nature of this dark matter is currently one of the great subjects of basic research, having generated a plethora of diverse explanations, but none of which is satisfactory.

In our approach, the concept of dark matter is no longer necessary, because it is simply replaced by the concept of “*repulsive neutrino sea*” in which all the galaxies, globular clusters

Constante de Hubble

$$v = H_0 d$$

$$H_0(t) = \frac{1}{3} \left(\frac{\partial \tau}{\partial t} \right)_i + 2 \frac{\partial^2 \tau}{\partial t^2} \Big|_i$$

«Redshift» des galaxies

$$\Delta t_i^f \equiv \frac{6}{(\partial \tau / \partial t)_i} \ln \left(\frac{d_0}{2c_{t(i)}} \frac{\partial \tau}{\partial t} \right)$$

$$''\text{redshift}'' = e^{-\Delta \tau / 4} = e^{-\frac{3}{2} \ln \left(\frac{d_0}{2c_{t(i)}} \frac{\partial \tau}{\partial t} \right)} = \left(\frac{2c_{t(i)}}{(\partial \tau / \partial t)_i} \right)^{3/2} \frac{1}{d_0^{3/2}} \equiv \left(\frac{2}{3} \frac{c_{t(i)}}{H_0 d_0} \right)^{3/2} \frac{1}{v^{3/2}}$$

«Refroidissement» du fond diffus cosmologique

$$U(v) = \frac{8\pi h v^3}{c^3} \frac{1}{e^{h v / k T} - 1} dv$$

$$h v_{\text{mesurée}}^{HS(2)} / k T_{\text{mesurée}}^{HS(2)} = h v_{\text{émise}}^{HS(1)} / k T_{\text{émise}}^{HS(1)} \Rightarrow T_{\text{mesurée}}^{HS(2)} = T_{\text{émise}}^{HS(1)} e^{(\tau_i - \tau_f)/4}$$

$$\Delta \tau = 4 \ln(T_{\text{émise}}^{HS(1)} / T_{\text{mesurée}}^{HS(2)}) \cong 4 \ln(3'000) \cong 32$$

$$v^{HS(2)} / v^{HS(1)} = e^{\Delta \tau} \cong e^{32} \cong 8 \cdot 10^{13} \text{ (volume de la maille)}$$

Figure 10.5 - Constante de Hubble, «redshift» des galaxies et «refroidissement» du fond diffus cosmologique

and other structures of the visible Universe bathe. Indeed, let us consider a galaxy subjected to the repulsive force of the sea of neutrinos in which it bathes. This repulsive force actually corresponds to a compressive force which is applied to stars in the suburbs of the galaxy. To resist this compressive force, the stars on the periphery of the galaxy must force to rotate faster than what is calculated on the basis of the visible mass, so as to balance the compressive force of the neutrino sea by an additional centripetal force of rotation.

About the Hubble's constant

Experimentally, we see that the light from galaxies has a redshift (redshift of the spectral lines of emission of atoms). This offset was attributed by Hubble to the apparent recession

speed \mathbf{V} of the galaxies according to their distance d due to the expansion of the Universe, effect explained initially by the Doppler-Fizeau effect due to the flight movement of the galaxies in the space. The experimental relationship between the speed of recession and the distance d was measured by Hubble, who found that $\mathbf{V} = H_0 d$, where H_0 is the *Hubble constant* which is approximately 70 (km/s)/Mpc (70 km per second, per megaparsec). The initial interpretation of this observation as a Doppler-Fizeau effect due to the speed of separation of galaxies in space actually leads to galaxies which would be located at distances greater than 4,000 megaparsecs moving away from us at speeds higher than that of light, which is obviously nonsense from special relativity. The solution to this problem can be deduced from general relativity, for which the expansion of the universe should not be interpreted by a movement of galaxies in space, but rather by an inflation of space itself, which implies a progressive distancing of the objects which it contains (a little in the same way as in our approach where it is the perfect cosmological lattice which extends).

Let's take a look at the Hubble constant in our approach, which is very clearly distinguished from general relativity, by the existence of the scalar τ of volume expansion which is directly concerned by a cosmological expansion of the perfect cosmological lattice. Let us therefore suppose a cosmological evolution of the perfect cosmological lattice like that described in figures 3.7 and 3.10. In the course of evolution, suppose that the **GO** observes a certain region in graph 3.10, in which the cosmological lattice is expanding, and even expanding at increasing speed. Suppose that the **GO** observes galaxies that are initially distant from d_0 at the moment $t = 0$. If these galaxies *do not move in relation to the expanding cosmological lattice*, the initial distance d_0 will change over time, and the **GO** will observe that the distance between the two galaxies will increase exponentially as $d(t) = d_0 \exp\left[\left(\tau(t) - \tau_i\right)/3\right]$, so that the two galaxies will move away relative to each other with relative speed $\mathbf{v}(t) = \partial d(t) / \partial t$. The value of this speed can be approached by a second order development of the expansion $\tau(t)$ over time, which makes it possible to deduce the value $H_0 = \mathbf{v} / d$ of the Hubble constant reported in figure 10.5. If the **GO** then measures this speed at an instant $t \neq 0$, it will find that the Hubble constant becomes dependent on the instant at which it observes the universe during its cosmological evolution, and in particular that this increases if one is in a domain where the speed of expansion of the universe increases.

About the «redshift» of galaxies

Now consider two galaxies that were initially distant from d_0 at the instant $t = 0$ for the **GO**. If, at this instant $t = 0$, galaxy 1 emits a signal towards galaxy 2, the signal will travel a distance dx during the lapse of time dt such as $dx = c_t dt$. But as the lattice is expanding, and neglecting the acceleration of this expansion, we have that the speed of the transverse waves depends on the instant t , so that $c_t(t) = c_{t(i)} \exp\left[(\partial \tau / \partial t)_i t / 2\right]$, where $c_{t(i)}$ is the speed of the transverse waves at the instant $t = 0$. The distance d between the two galaxies will then be covered in the time lapse $\Delta t|_i^f$ shown in figure 10.5, which can be calculated approximately thanks to the relationship giving $c_t(t)$.

When the signal is received by galaxy 2, the expansion of the universe will then have reached a value τ_f worth $\tau_f \cong \tau_i + (\partial \tau / \partial t)|_i T$. Suppose that the signal emitted in galaxy 1 at the moment $t = 0$ is measured by a local observer **HS⁽¹⁾** at the frequency $\mathbf{v}_{emitted}^{HS^{(1)}}$ of a certain

spectral line of a given atom, the frequency $\nu_{received}^{HS(2)}$ of the signal received and measured by an observer $HS^{(2)}$ in galaxy 2 at the moment $t = T$ will be different because of the increase $\Delta\tau = \tau_f - \tau_i$ in expansion of the Universe during propagation. Thus, an observer $HS^{(2)}$ located in galaxy 2 will be able to compare the frequency $\nu_{received}^{HS(2)}$ of this signal received with the frequency $\nu_{emise}^{HS(2)}$ of the same spectral line of the same atom emitted in his own laboratory, and he will call "redshift" of galaxy 1 the ratio between these two frequencies: $redshift = \nu_{received}^{HS(2)} / \nu_{emitted}^{HS(2)}$. To calculate this redshift, we must schematically represent how the physical values measured by the observer $HS^{(1)}$ in galaxy 1 at the instant $t = 0$ with the same physical values measured by the GO at the instant $t = 0$ and at the instant $t = T$ as well as by the observer $HS^{(2)}$ in galaxy 2 at the moment $t = T$. For this, we remember that the time spans Δt_y measured by an HS in its own reference frame $Oy_1y_2y_3$ are perceived by the GO in its local reference frame $Ox_1x_2x_3$ as time spans Δt linked by the expression $\Delta t_y^{HS} = \Delta t^{GO} e^{\tau/4}$ in which τ is the expansion of the lattice at the location where is HS . This expression also makes it possible to link also the frequency measurements made by an HS and by the GO in the form $\nu_y^{HS} = \nu^{GO} e^{-\tau/4}$. With this relation, we can schematically represent in figure 10.5 how the frequency and wavelength measurements made during the signal transmission experiment between galaxies 1 and 2 behave.

We then observe that the "redshift" measured by the observe $HS^{(2)}$ is very simply related to the expansion increase $\Delta\tau = \tau_f - \tau_i$ of the Universe that occurred during the propagation since $redshift = \nu_{emitted}^{HS(1)} e^{(\tau_i - \tau_f)/4} / \nu_{emitted}^{HS(2)} = e^{-\Delta\tau/4}$. By calculating the value of $\Delta\tau$ thanks to the expression of the lapse of time Δt_i^f used by the light to traverse the distance separating the two galaxies, one obtains the expression reported in figure 10.5 for the "redshift" measured by the observer $HS^{(2)}$, which depends on both the instantaneous speed of expansion $\partial\tau / \partial t|_i$ and the initial distance d_0 between the two galaxies. But we can also connect the "redshift" to the instantaneous Hubble constant H_0 or to the relative speed \mathbf{V} of recession of the galaxies as reported in figure 10.5.

The "redshift" observed by the observer $HS^{(2)}$ will therefore be proportional to $1/d_0^{3/2}$ what means that the frequency ratio decreases if the initial distance d_0 between the galaxies increases, and therefore that the "red shift" of the spectral line increases with the increase in the initial distance d_0 . The "redshift" is also proportional to $1/(H_0)^{3/2}$, which means that it decreases if the Hubble constant increases. And finally it is also proportional to $1/\mathbf{V}^{3/2}$. However, the velocity of reciprocal remoteness of two galaxies is not limited by the speed of transverse waves in our approach since this speed is associated with *the speed of the lattice in the absolute space of the GO*, which satisfies a purely Newtonian dynamic. Thus, the measured "redshift" can tend towards 0 if the recession speed \mathbf{V} of expansion tends to infinity.

Note again that these calculations were made by making two restrictive assumptions:

- that we are in a limited region in graph 3.10 in which the cosmological lattice is expanding, and which can be approached by a second order development in time of expansion $\tau(t)$. For phenomena which would spread over much longer times, the calculations would be particularly complicated since it would then be necessary to know exactly the function of the cosmological expansion $\tau(t)$ of the lattice.
- that the galaxies do not move in relation to the expanding cosmological lattice. If this were not the case, for example because of the gravitational interactions between the galaxies, it would be

necessary to add to the "redshift" due to the expansion of the lattice a Doppler-Fizeau effect due to the displacements of the galaxies compared to the lattice, such than that described in figure 6.12.

About the «cooling» mechanism of the cosmic microwave background

The cosmic microwave background is currently observed as a *perfect black body spectrum*, very precisely following the *Planck distribution of the energy density* $U(\nu)$ of photons (figure 10.5), centered on a temperature T of 2.7 K. We assume that this radiation is fossil from the big bang, which formed during the decoupling of photons from particles during the formation of neutral atoms of helium and hydrogen, and that, therefore, it was originally emitted with a temperature of the order of 3'000 K. We can then ask ourselves what is the "cooling" mechanism of this radiation in the light of our approach. To do this, just look at figure 10.5. If we assume that the photon-matter decoupling occurred when the Universe had an expansion τ_i and that the current expansion of the Universe is τ_f , the emission frequency of the microwave background is given by $\nu_{emitted}^{HS(1)}$ and the frequency currently observed by an observer $HS(2)$ is worth $\nu_{measured}^{HS(2)} = \nu_{emitted}^{HS(1)} e^{(\tau_i - \tau_f)/4}$. From Planck's distribution (figure 10.5), there is the following relationship $h\nu_{measured}^{HS(2)} / kT_{measured}^{HS(2)} = h\nu_{emitted}^{HS(1)} / kT_{emitted}^{HS(1)}$ between the frequency of black body radiation and its color temperature, measured at the expansions τ_f and τ_i . We therefore deduce that $T_{measured}^{HS(2)} = T_{emitted}^{HS(1)} e^{-\Delta\tau/4}$, so that a numerical value of the variation in the expansion of the lattice between the moment of photon-matter decoupling and the current time can be calculated as $\Delta\tau = 4 \ln(T_{emitted}^{HS(1)} / T_{measured}^{HS(2)}) \cong 4 \ln(3'000) \cong 32$. This increase in expansion corresponds in fact to an *increase in the volume* \mathbf{v} of the elementary cell of the lattice worth approximately $\mathbf{v}^{HS(2)} / \mathbf{v}^{HS(1)} = e^{\Delta\tau} \cong e^{32} \cong 8 \cdot 10^{13}$, which must certainly take place during the inflation phase of the cosmological lattice (figure 3.10).

We therefore see that the apparent "cooling" of the cosmic microwave background is a direct effect of the expansion of the lattice, which dramatically changes the rulers and clocks of local reference frames $Oy_1y_2y_3$.

It is also interesting to note that, for the **GO**, the frequency $\nu_{measured}^{GO}$ of the cosmic microwave background does not change during the expansion since it is always worth the same value as at the time of its emission $\nu_{measured}^{GO} = \nu_{emitted}^{HS(1)} e^{\tau_i/4}$. But on the other hand, for the **GO**, it is the wavelength $\lambda_{measured}^{GO}$ which will change with the expansion, since this is then equal to $\lambda_{measured}^{GO} = c_t / \nu_{measured}^{GO} = c_{t0} e^{\tau(t)/2} / \nu_{measured}^{GO} = c_{t0} e^{\tau(t)/2 - \tau_i/4} / \nu_{emitted}^{HS(1)}$. The points of view of the local observers $HS(i)$ and of the external observer **GO** are therefore very different, and this is due to the fact that the speed of the transverse waves of rotation (speed of light) is a universal constant always valid for the observers $HS(i)$ whatever the state of expansion of the lattice in which they are placed, while the celerity of the transverse waves of rotation varies enormously according to the instantaneous expansion of the lattice for the external observer **GO**.

Chapter 11

Quantum Physics

In Figure 7.0, we have seen that when the mass density of a singularity or cluster of singularities exceeds a certain critical value, there are no static solutions for the field of internal expansion disturbances, *which means that these internal disturbances must necessarily become dynamic disturbances*. Intuitively, it is intuitively suspected that the existence of such dynamic solutions of Newton's second partial equation (figure 5.1) may well be related to the appearance of quantum physics, i.e. the existence of localized temporal fluctuations in the expansion field of the perfect cosmological lattice when it does not exhibit longitudinal wave propagation in the domain $\tau_0 < \tau_{0cr}$. We will show in this chapter that a wave function, deduced directly from Newton's second partial equation of the lattice expansion perturbations, is indeed intimately related to the mobile topological singularities of the lattice, whether these are clusters of elementary loops or isolated elementary loops.

We will thus be able to give a quite classical and rather simple "wave" interpretation of quantum physics: *the quantum wave function would in fact represent the amplitude and the phase of the gravitational fluctuations coupled to the topological singularities*. This interpretation then implies that the square of the amplitude of the normalized wave function is indeed related to the probability of the presence of the associated topological singularity.

In the wake of this, we also find *Heisenberg's uncertainty principle, the notions of bosons, fermions and indistinguishability, Pauli's exclusion principle*, and the path towards a physical understanding of intriguing phenomena such as *quantum entanglement and quantum decoherence*.

Thus, from figure 7.0, we deduce that the critical value of the mass density at which expansion perturbations become dynamic is nothing more than the quantum decoherence limit of this singularity or cluster of singularities.

Relativistic wave equation of gravitational expansion field fluctuations beyond the quantum decoherence limit

Above *the quantum decoherence limit*, i.e. for values of the mass density of a singularity or cluster of singularities greater than the critical mass density (figure 7.0), suppose the existence of dynamic longitudinal fluctuations in the cosmological lattice. These fluctuations must obviously satisfy the dynamic version of Newton's second partial equation in figure 5.1. We obtain at first order in $\tau^{(p)}$, by also taking into account the geometro-kinetic equation for $\tau^{(p)}$, and by emitting the hypotheses that $\tau_0 \ll \tau_{0cr}$, $K_2 \ll K_0$ and $2K_1(1 + \tau_0) \ll K_0$, the equation managing the gravitational fluctuations, represented in figure 11.1.

This equation is perfectly realistic, in that it is derived from Newton's equation of the lattice. However, it cannot be solved in this form because it would require to know the function

$F_{dist}^{ch}(\vec{r},t) + F_{pot}^{ch}(\vec{r},t)$ associated with the topological singularity, which depends in particular on the trajectory of the singularity within the network, a trajectory that we do not know a priori. We can therefore say that this function $F_{dist}^{ch}(\vec{r},t) + F_{pot}^{ch}(\vec{r},t)$ is in fact *a hidden variable of the problem*. It will thus be necessary, as we have already done in chapter 7 in the static case by introducing a mean value $\bar{\tau}_{int}^{(E)}$ of the static internal field, to find here again *a subterfuge* to find some form of solution to this dynamic equation.

Let us first propose a simple solution, localized and independent of the time of this equation for the wave function $\psi_{localisée}(\vec{r})$, assuming that it is a simple exponential decay with spans $\delta_1, \delta_2, \delta_3$ in the three directions of space, and that the pulsation ω_f is a real constant independent of time and space (figure 11.1). By introducing this solution into the wave equation that we have just established, we obtain the relation which must exist between the pulsation ω_f of the fluctuations and the ranges $\delta_1, \delta_2, \delta_3$ of these fluctuations. There then appears a localized gravitational fluctuation $\underline{\tau}_{localisée}^{(p)}$ which corresponds to a localized, non-damped and pulsating regime with a pulsation ω_f which decreases symmetrically and exponentially in the vicinity of the origin, with spatial ranges equal to δ_1, δ_2 and δ_3 along the 3 axes, which are correlated with each other and which decrease with the pulse frequency.

We therefore deduce that, in a perfect cosmological lattice satisfying the hypotheses that we have put forward, there can perfectly exist stable and localized fluctuations of vibrations of the volume expansion. We will return to this subject in more detail in chapter 14.

Let us imagine that mobile topological singularities within the lattice, such as clusters of elementary loops or isolated elementary loops as described in the previous chapters, are also associated with dynamic longitudinal gravitational fluctuations, which should obviously satisfy the dynamic version of Newton's second partial equation in the vicinity of the topological singularity.

It is known that, when the energy density of a singularity is lower than the critical value of the quantum decoherence limit, the second Newton partial equation reveals static gravitational perturbations of the expansion field within stationary clusters, perturbations that are directly dependent on the elastic distortion energy of these singularities. And in chapter 7, it was shown that this internal expansion disturbance field has a mean value $\bar{\tau}_{int}^{(E)}$ which is directly responsible for a static external gravitational field of expansion disturbances, in the form of $\tau_{ext LD}^{cluster}(r) \equiv -4G_{grav} M_0^{cluster} / c_t^2 r$, which also depends on the elastic distortion energy of the singularity or cluster of stationary singularities via the parameter $4G_{grav} / c_t^2$.

On the other hand, when the energy density of a singularity is *higher than the critical value of the quantum decoherence limit*, the gravitational disturbances can only be dynamic, and must then satisfy the Newtonian relationship shown in Figure 11.1, which also depends on the elastic and potential energy densities of the singularity.

There are therefore strong presumptions that, beyond the quantum decoherence limit, the field of dynamic gravitational perturbations $\tau^{(p)}$ of the expansion outside a moving singularity can be represented by *a subterfuge of imagining a similar pattern to that given for the isolated gravitational fluctuations in figure 11.1, but which this time also depends on the elastic distortion energy of the singularity, but probably also on the energy associated with the motion of the singularity*. Now we know that a moving topological singularity in the lattice is entirely characterized by a *total relativistic energy* E_v and a *total relativistic momentum* \vec{P}_v .

Therefore, the pulsation ω_f of the associated expansion fluctuations should certainly also depend on the relativistic energy $E_v(\vec{r}, t)$ of the singularity and its relativistic momentum $\vec{P}_v(\vec{r}, t)$. Let us therefore imagine that the topological singularities moving within the lattice, such as clusters of elementary loops or isolated elementary loops as described in the previous chapters, are also associated with dynamic longitudinal gravitational fluctuations, which should obviously satisfy the dynamic version of Newton's second partial equation outside the topological singularity.

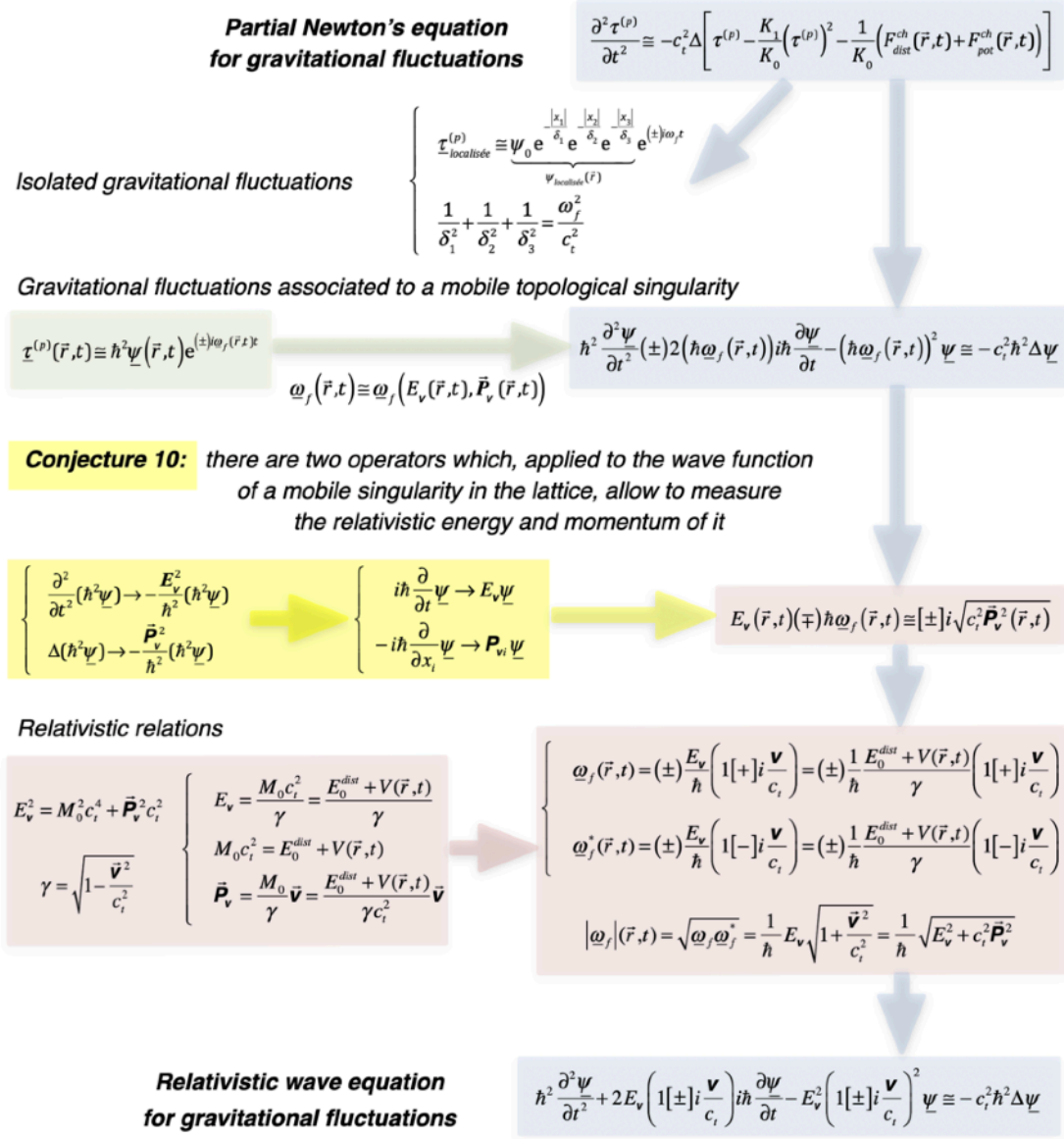


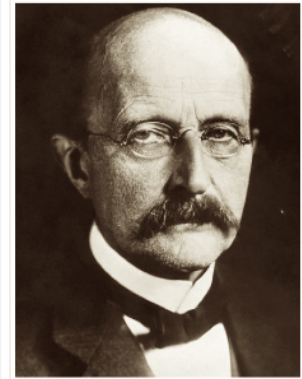
Figure 11.1 - From Newton's partial equation for gravitational fluctuations to the relativistic wave equation for the fluctuations associated with a moving singularity

We can then propose a solution of gravitational perturbations of complex pulsation ω_f , which we will write for convenience in complex formulation in the form $\tau^{(p)} \equiv \hbar^2 \psi e^{(\pm) i \omega_f t}$, where \hbar^2 is an arbitrary constant for the moment, $e^{(\pm) i \omega_f t}$ corresponds to the oscillation of the

fluctuation and the complex wave function $\underline{\psi}(\vec{r}, t)$ contains the phase and amplitude information for this oscillation. By introducing this solution into Newton's equation for lattice fluctuations, we obtain a wave equation for the complex function $\underline{\psi}(\vec{r}, t)$ in the form shown in figure 11.1.

If the frequency $\underline{\omega}_f(\vec{r}, t)$ of the gravitational fluctuations effectively depends on $E_v(\vec{r}, t)$ and $\vec{P}_v(\vec{r}, t)$, these two quantities must also be implicitly contained in the temporal and spatial behaviors of the complex wave function $\underline{\psi}(\vec{r}, t)$ associated with the mobile singularity. However, this wave function $\underline{\psi}(\vec{r}, t)$ associated with the wave equation in figure 11.1 actually recalls the wave function appearing in quantum physics, and quantum physics says that it is possible to define operators allowing to measure E_v and \vec{P}_v from the quantum wave function $\underline{\psi}(\vec{r}, t)$.

By analogy with quantum physics, we will therefore conjecture *a priori operators with similar properties*: this will be conjecture 10 of our approach, reported in figure 11.1. In fact, we are going to hypothesize that the second derivative with respect to the time of the envelope $\hbar^2 \underline{\psi}$ of the oscillations of $\underline{\tau}^{(p)}$ is directly correlated with the square of the total relativistic energy E_v of the singularity, and that the Laplacian (the second derivative with respect to space) of the envelope $\hbar^2 \underline{\psi}$ of the oscillations of $\underline{\tau}^{(p)}$ is directly correlated with the square of the total relativistic momentum \vec{P}_v . In the relations associated with this conjecture, we introduced, as in quantum physics, a constant \hbar allowing to normalize the partial derivatives of the wave function to energetic terms (and which is, in the case of quantum physics, nothing other than the Planck's constant). It is quite simple to verify that these operators, applied once to the wave function, provide the usual operators of quantum physics, as illustrated in figure 11.1.



Max Planck
(1858-1947)

Conjecture 10 that we have assumed here has a physical meaning that can be explained very simply. Indeed, suppose that the envelope $\hbar^2 \underline{\psi}$ of the oscillations of $\underline{\tau}^{(p)}$ is of oscillatory type, of the form $\hbar^2 \underline{\psi} = \hbar^2 \psi_0 \sin(\Omega t - kx)$. In this case, conjecture 10 simply implies that the pulsation $\Omega = 2\pi f = E_v / \hbar$ of the envelope is proportional to the total relativistic energy E_v of the singularity and that the wave number $k = 2\pi / \lambda = |\vec{P}_v| / \hbar$ of the envelope is proportional to the relativistic momentum $|\vec{P}_v|$ of the singularity, with a proportionality factor equal to the inverse of the Planck constant.

Thanks to the arbitrary constant \hbar^2 introduced into the solution for $\underline{\tau}^{(p)}(\vec{r}, t)$, the wave equation for $\underline{\psi}(\vec{r}, t)$ is then directly composed of terms corresponding to energy squares. We deduce that each term of this equation must represent the product of the square of an energy by the dimensionless wave function $\underline{\psi}(\vec{r}, t)$. We deduce in particular that the term $\hbar \omega_f$ has the dimension of an energy.

On the other hand, the second derivative operator of time provides the square of the total relativistic energy E_v that the singularity would have at the place where the operator is applied, and the Laplacian operator provides the square of the total relativistic momentum \vec{P}_v that the singularity would have at the place where the operator is applied. From this definition of the second derivative and Laplacian operators, we deduce the operators directly supplying the total

energy of the singularity and the components of the momentum of the singularity at a given location.

With these "a priori" conjectured operators based on quantum physics, we can try to apply them to the wave relation deduced from Newton's second partial equation. We thus obtain the relation which should exist between *the relativistic energy* E_v of the singularity, *the energy of movement* $\sqrt{c_t^2 \vec{P}_v^2}$ of the singularity and *the pulsation* $\underline{\omega}_f(\vec{r}, t)$ of the gravitational fluctuations associated with the singularity, which now really becomes a complex number, in the form $E_v(\vec{r}, t)(\mp)\hbar\underline{\omega}_f(\vec{r}, t) \equiv [\pm]i\sqrt{c_t^2 \vec{P}_v^2}(\vec{r}, t)$. It should be noted here that the double signs (\mp) and $[\pm]$ appearing in this relation are independent of each other because the first (\mp) comes from the expression $\underline{\tau}^{(p)} \equiv \hbar^2 \underline{\psi} e^{(\pm)i\underline{\omega}_f t}$ and the second is introduced by taking the square root of $-c_t^2 \vec{P}_v^2(\vec{r}, t)$.

In the case of a singularity which moves *at relativistic speed*, this one must satisfy the principal relativistic relations obtained in chapter 6 and reported in figure 11.1, in particular the important relation $E_v^2 = M_0^2 c_t^4 + \vec{P}_v^2 c_t^2$ which makes the link between *the total relativistic energy* E_v , *the relativistic momentum* \vec{P}_v and *the mass at rest* M_0 of the singularity. These relativistic expressions lead to the relation giving *the complex pulsation* $\underline{\omega}_f(\vec{r}, t)$ of the gravitational fluctuations associated with a topological singularity, either an elementary loop, or a cluster of elementary loops linked together, moving at speed \mathbf{v} . The complex relativistic pulsation $\underline{\omega}_f(\vec{r}, t)$ therefore presents two conjugate solutions shown in figure 11.1. It is interesting to note that there is indeed an expression justifying the hypothesis that we had put forward, namely that $\underline{\omega}_f(\vec{r}, t)$ is a direct function of E_v and \vec{P}_v . Indeed, by performing the product of the two combined values of the pulsation, we see that it is the norm $|\underline{\omega}_f|(\vec{r}, t) = (\underline{\omega}_f \underline{\omega}_f^*)^{1/2}$ of the complex pulsation $\underline{\omega}_f(\vec{r}, t)$ which is a simple and direct function of the quantities E_v and \vec{P}_v of the singularity.

The wave equation for $\underline{\psi}(\vec{r}, t)$ then has *two relativistic versions* shown in figure 11.1, because of the double sign $[\pm]$ that appears in $(1[\pm]i\mathbf{v}/c_t)$. On the other hand, in this expression of the wave equation, the double sign (\mp) no longer appears.

Gravitational perturbations of a massive singularity at relativistic speed

Let us take again the relativistic wave equation of figure 11.1 and try to find a solution for a rather massive singularity which would move *almost freely at relativistic speed* \mathbf{v} *more or less constant* in the direction $\mathbf{O}x_2$, which implies that $E_v(\vec{r}, t)$ *varies relatively slowly in time and space*. Under this hypothesis that the total relativistic energy of the singularity varies only slowly in time and space, we can admit that the function $\hbar^2 \underline{\psi}(\vec{r}, t)$, which represents the amplitude and the phase of the oscillation with a pulsation $\omega_f(\vec{r}, t)$ is in fact a function of the position x_2 along the axis $\mathbf{O}x_2$. Let us therefore pose a simple wave solution of the relativistic wave equation along the axis $\mathbf{O}x_2$, which does not explicitly depend on time, on the type $\underline{\psi}(\vec{r}, t) \equiv \psi_0 e^{i\mathbf{k}(\vec{r}, t)x_2}$, where the complex wave number $\mathbf{k}(\vec{r}, t)$ also varies very slowly over time and the space. By injecting this solution into *the relativistic wave equation*, we obtain the expression of figure 11.2 for the value of the complex wave number \mathbf{k} and we note that $\mathbf{k}(\vec{r}, t)$ in fact depends on \vec{r} and t only by the dependence of the relativistic energy $E_v(\vec{r}, t)$ in \vec{r} and t , which allows to express the wave function $\underline{\psi}(\vec{r}, t)$ as well as the expansion fluctuations

associated with the relativistic singularity. By introducing the value of $\omega_f(\vec{r}, t)$ obtained in figure 11.1, we get two solutions which really have a physical meaning among four possible solutions, so that, finally, the solution for $\tau^{(p)}(\vec{r}, t)$ can be written in the form represented in figure 11.2. We can therefore explain the real expansion fluctuations of a relativistic singularity, by taking the real part $\tau_{réel}^{(p)}(\vec{r}, t)$ of this expression.

$$\psi(\vec{r}, t) \cong \psi_0 e^{ik(\vec{r}, t)x_2} \rightarrow \hbar^2 \frac{\partial^2 \psi}{\partial t^2} + 2E_v \left(1[\pm] i \frac{\mathbf{v}}{c_t} \right) i \hbar \frac{\partial \psi}{\partial t} - E_v^2 \left(1[\pm] i \frac{\mathbf{v}}{c_t} \right)^2 \psi \cong -c_t^2 \hbar^2 \Delta \psi$$

$$\tau^{(p)}(\vec{r}, t) \cong \hbar^2 \psi_0 e^{\left\{ - \right\} \frac{E_v}{\hbar c_t} |x_2[\mp]| \mathbf{v} t} e^{i \frac{E_v}{\hbar} \left(t[\pm] \frac{\mathbf{v}}{c_t^2} x_2 \right)} \leftarrow \underline{k}(\vec{r}, t) \cong \left\{ \pm \right\} i \frac{E_v}{\hbar c_t} \left(1[\pm] i \frac{\mathbf{v}}{c_t} \right)$$

$$\tau_{réel}^{(p)}(\vec{r}, t) \cong \hbar^2 \psi_0 e^{\left(- \right) \frac{E_v}{\hbar c_t} |x_2[\mp]| \mathbf{v} t} \cos \left[\frac{E_v}{\hbar} \left(t[\pm] \frac{\mathbf{v}}{c_t^2} x_2 \right) \right] \quad \text{Relativistic gravitational perturbations}$$

$$f = \frac{E_v}{2\pi\hbar} = \frac{E_0^{dist} + V(\vec{r}, t)}{2\pi\hbar\gamma} = \frac{E_0^{dist} + V(\vec{r}, t)}{2\pi\hbar \sqrt{1 - \frac{\vec{v}^2}{c_t^2}}} \quad (\text{frequency of perturbations})$$

$$\lambda = \frac{2\pi\hbar c_t^2}{E_v \mathbf{v}} = \frac{2\pi\hbar c_t^2 \gamma}{(E_0^{dist} + V(\vec{r}, t)) \mathbf{v}} = \frac{2\pi\hbar c_t^2}{(E_0^{dist} + V(\vec{r}, t)) \mathbf{v}} \sqrt{1 - \frac{\vec{v}^2}{c_t^2}} \quad (\text{wave length of perturbations})$$

$$\delta = \frac{\hbar c_t}{E_v} = \frac{\hbar c_t \gamma}{E_0^{dist} + V(\vec{r}, t)} = \frac{\hbar c_t}{E_0^{dist} + V(\vec{r}, t)} \sqrt{1 - \frac{\vec{v}^2}{c_t^2}} \quad (\text{spatial range of perturbations})$$

Figure 11.2 - Associated gravitational perturbations to a massive singularity moving at relativistic speed

We see that this function $\tau_{réel}^{(p)}(\vec{r}, t)$ represents the product of oscillations in time and oscillations in space. Oscillations in time present a frequency f and oscillations in space a wavelength λ . We note that the frequency f of temporal oscillations is an increasing function of the speed \mathbf{v} and of the relativistic energy E_v of the singularity, and that it tends towards an infinite value for $\mathbf{v} \rightarrow c_t$. It depends indirectly on the position \vec{r} of the singularity and on time t via the dependence of the potential $V(\vec{r}, t)$ on these quantities. As for the wavelength λ of the spatial oscillations, it decreases as a function of the speed \mathbf{v} and of the relativistic energy E_v of the singularity, and it tends towards 0 for $\mathbf{v} \rightarrow c_t$. It is also modulated in space and time via the potential $V(\vec{r}, t)$.

The amplitude of these temporal and spatial oscillations is modulated by an exponentially decreasing envelope on both sides of the average position $x_2(t) = [\pm] \mathbf{v} t$ of the singularity

(which thus moves in the direction of the axis Ox_2 or in opposite direction according to the sign + or -). The speed of decrease of the envelope $e^{(-)|x_2[\mp]v|/\delta}$ is related to a range δ of the envelope of the oscillations, which decreases when the speed \mathbf{V} of the singularity increases and when its relativistic energy E_v increases, and it tends towards 0 for $\mathbf{V} \rightarrow c_t$. It, too, is modulated in space and time via the potential $V(\vec{r}, t)$ that the singularity undergoes. All this implies that the gravitational fluctuations associated with the total relativistic energy of the singularity are very short spans and certainly become negligible for massive singularities, such as clusters of linked elementary loops. For example, for an electron at non-relativistic speed, the range of gravitational perturbations associated with its rest energy E_0^{dist} is already tiny, of the order of $2 \cdot 10^{-12} m$.

Finally, we note that the dynamic expansion fluctuations associated with the relativistic singularity are contracted along the axis Ox_2 of the movement of the singularity, as a function of the speed \mathbf{V} of the singularity, as we can see on the wavelength λ of the spatial oscillations and on the range δ of the envelope of the oscillations. *These effects strictly correspond to the relativistic effect of contraction of the rulers of a mobile cluster of singularities* described in chapter 6.

Schrödinger's equation of gravitational perturbations of a massive singularity moving at non-relativistic speed in a variable potential

The treatment of the previous section applies to gravitational perturbations associated with a massive singularity which moves at relativistic speeds and which is not subject to a sufficiently strong potential to influence strongly its trajectory. But for a microscopic singularity (a loop of disclination or dislocation for example) in a non-relativistic regime $|\mathbf{V}| \ll c_t$, and subject to a potential $V(\vec{r}, t)$ large enough to influence strongly its trajectory, one can wonder what becomes its wave equation. To do this, let's rewrite the relativistic wave equation obtained in figure 11.1 by removing the very small terms in \mathbf{V}/c_t . This is the first step shown in figure 11.3.

Then using conjecture 10, the wave equation can transform into a "reduced form" containing only the first derivative of time. But the total energy $E_v(\vec{r}, t)$ of the non-relativistic singularity can be expressed as $E_v = M_0 c_t^2 / \gamma \cong M_0 c_t^2$ or as $E_v = (E_0^{dist} + V(\vec{r}, t)) / \gamma \cong E_0^{dist} + V(\vec{r}, t)$, which allows to rewrite approximately the wave equation in a third form, which we will call *the non-relativistic wave equation*. This wave equation then admits two distinct solutions for gravitational perturbations $\underline{\tau}^{(p)}(\vec{r}, t)$ which are distinguished by the sign of the rotating vector.

In this form, the non-relativistic wave equation is very similar to Schrödinger's equation of quantum physics, and it can be shown that it is possible to find this equation. Indeed, let's make a change in wave equation by introducing a wave function $\underline{\psi}_H(\vec{r}, t)$ such that it gives the initial wave function $\underline{\psi}(\vec{r}, t)$ when multiplied by the factor $\exp(-iE_0^{dist}t/\hbar)$. We then obtain a non-relativistic wave equation which is very well known, since it is *the famous Schrödinger's equation of quantum physics*.



Erwin Schrödinger
(1887-1961)

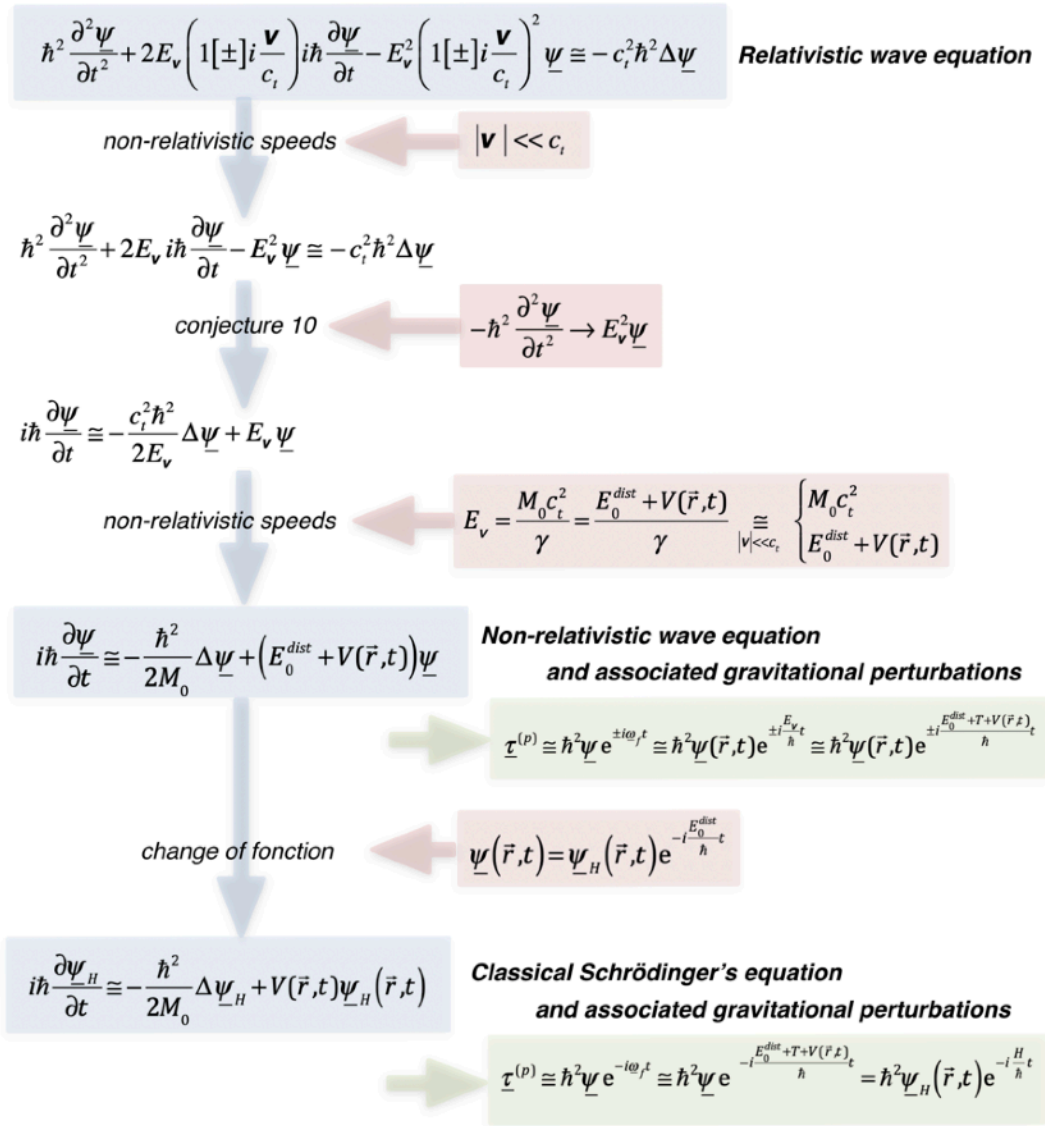


Figure 11.3 - Non-relativistic wave equation and Schrödinger's equation in the case of gravitational perturbations associated to a massive singularity moving at non-relativistic speed

By solving this wave equation for a singularity of mass M_0 subject to a potential $V(\vec{r}, t)$, we deduce the wave function $\psi_H(\vec{r}, t)$ which makes it possible to directly find the gravitational perturbations $\underline{\tau}^{(p)}(\vec{r}, t)$ associated with this singularity thanks to the relation reported in figure 11.3. But unlike the non-relativistic wave equation that precedes it, this equation, due to the change of the wave function $\psi(\vec{r}, t)$ by $\psi_H(\vec{r}, t)$, gives only one solution for the gravitational perturbations $\underline{\tau}^{(p)}(\vec{r}, t)$.

The wave function $\psi_H(\vec{r}, t)$ provided by the Schrödinger's equation is directly related to *the Hamiltonian of the singularity*, namely to the sum of its kinetic energy and its potential energy, since by using the operators defined by conjecture 10 in Schrödinger's equation, we get directly the relation $E_{\psi_H} \equiv \vec{P}_v^2 / 2M_0 + V(\vec{r}, t) = T + V(\vec{r}, t) = H$.

The wave equation that we have obtained for $\underline{\psi}_H(\vec{r}, t)$ corresponds in all points, very exactly, to the time-dependent Schrödinger's equation of quantum physics *for a non-relativistic particle*, provided that *the universal constant \hbar that we have conjectured is effectively the Planck constant of quantum physics*. This perfect similarity is obviously not fortuitous and allows *for the first time* to give a very understandable interpretation of quantum physics, by saying that «the Schrödinger's equation is a wave equation deduced from the second partial Newton equation of a perfect cosmological lattice, in the domain $\tau_0 \ll \tau_{ocr}$, which makes it possible to calculate the envelope $\underline{\psi}_H(\vec{r}, t)$ of the dynamic gravitational fluctuations $\underline{\tau}^{(p)}(\vec{r}, t)$ associated with a topological singularity of mass M_0 and subjected to a potential $V(\vec{r}, t)$ ».

The standing wave equation of a singularity placed in a static potential

If the potential in which the topological singularity is placed is a static potential $V(\vec{r})$, the left term of the non-relativistic wave equation reported in figure 11.4 is an operator giving the total energy E_v of the singularity, which must obviously be a constant since the singularity moves into a static potential. Using conjecture 10 to make the time derivative disappear, we obtain a time-independent wave equation.

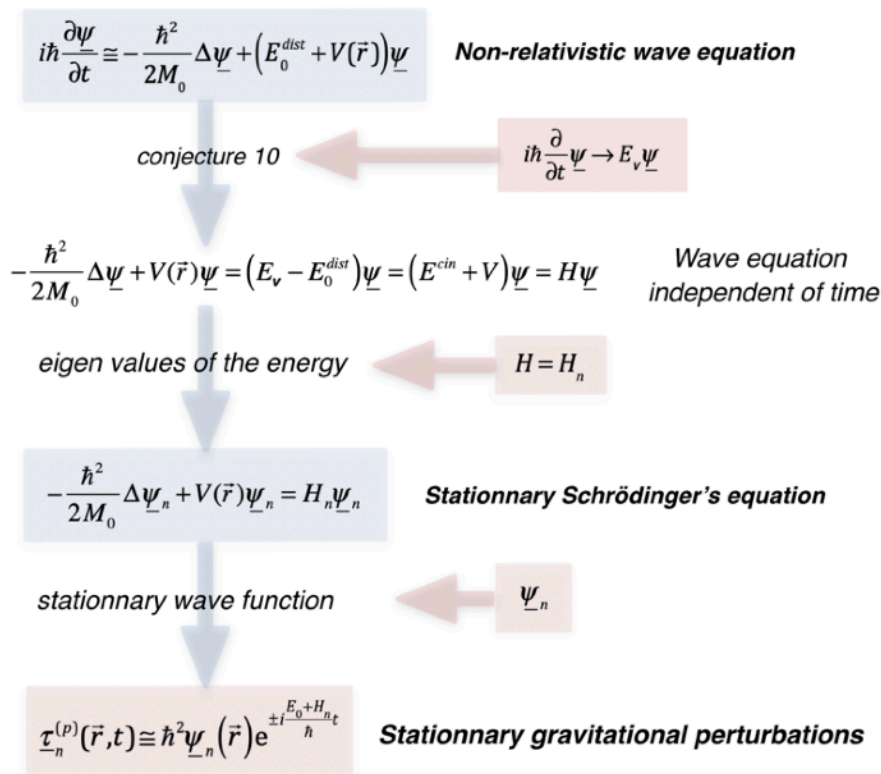


Figure 11.4 - Schrödinger's standing wave equation with eigenvalues for a massive singularity placed in a static potential

Here we find the expression of *the stationary Schrödinger's equation* of quantum physics, which is, as we know in quantum physics, a *problem with eigenvalues*, which means that the

Hamiltonian, that is say the sum of the potential energy and the kinetic energy associated with the movement of the singularity, given by $H = E^{cin} + V = E_v - E_0^{dist}$, is a constant which can take various eigenvalues H_n according to the potential $V(\vec{r})$, so that the wave function has eigenstates $\underline{\psi}_n$ satisfying the Schrödinger's equation with *eigenvalues* reported in figure 11.4.

On the basis of the solution $\underline{\psi}_n(\vec{r})$ of the wave equation, we deduce the true physical quantity, namely *the stationary expansion perturbations* associated with the singularity plunged in the stationary potential $V(\vec{r})$, given thanks to the relation of figure 11.3 by the expression $\underline{\tau}_n^{(p)}(\vec{r}, t) \equiv \hbar^2 \underline{\psi}_n(\vec{r}) \exp(\pm i(E_0 + H_n)t / \hbar)$, and it is the real part of $\underline{\tau}_n^{(p)}(\vec{r}, t)$ which will represent the real stationary expansion perturbations. This solution for stationary gravitational perturbations is then presented in the form of oscillations of fixed pulsation $|\omega_f| = (E_0 + H_n) / \hbar$ dependent on the eigen energy H_n , oscillations which are modulated by a stationary envelope $\hbar^2 \underline{\psi}_n(\vec{r})$ dependent on the potential $V(\vec{r})$ via the Schrödinger's stationary wave equation.

About the interpretation of the wave function of gravitational fluctuations

The power of the dynamic Schrödinger equation (figure 11.3) and the stationary Schrödinger equation (figure 11.4) is well known in quantum physics. Many consequences linked to Schrödinger's equations are obviously directly applicable in the case of our approach.

For example, *the operator commutators* and *the Heisenberg uncertainty principles* are deduced directly using the conjecture 10. Thus, the quantum operator of momentum $\hat{p}_k = -i\hbar \partial / \partial \xi_k$ does not commute with the position operator $\hat{\xi}_k = \xi_k$ of a particle, because the commutator $[\hat{p}_k, \hat{\xi}_k] = \hat{p}_k \cdot \hat{\xi}_k - \hat{\xi}_k \cdot \hat{p}_k = -i\hbar$ is not zero. Likewise, the energy operator $\hat{E} = i\hbar \partial / \partial t$ does not commute with the time operator $\hat{t} = t$ since the commutator $[\hat{E}, \hat{t}] = \hat{E} \cdot \hat{t} - \hat{t} \cdot \hat{E} = i\hbar$ is not zero. These two commuting relations are expressions of *the Heisenberg uncertainty principle*, which says that the measurements of certain pairs of observables disturb each other, so that the measurement uncertainties $\Delta \xi_k$, Δp_k , Δt , ΔE , ... are linked together by uncertainty relations.

Another example is the calculation of *the stationary eigenstates of a particle* in different types of potentials (harmonic oscillator, anharmonic oscillator, particle in a box, rotation of two linked particles, particle in a central potential, etc.), or the calculation of *the density of states in phase space*, and many others that are beyond the scope of this book, but found in all books dealing with quantum physics.

From this perfect correspondence between our approach of gravitational perturbations associated with mobile topological singularities and the Schrödinger wave equation of quantum physics, experimentally very well verified, we deduce *à posteriori* that our conjecture 10 turns out to be absolutely founded. Therefore, our "classical" interpretation of quantum physics, namely that quantum physics follows from Newton's second partial equation of the cosmic lattice, is undoubtedly correct, so that Newton's equation of the cosmic lattice seems more and more play a crucial role *at the heart of all known theories of the Universe*.



Werner Heisenberg
(1901-1976)

Even though the complex wave functions $\underline{\psi}(\vec{r}, t)$ do not give any indication concerning the position or the trajectory of the singularity, we can still find them a very interesting physical interpretation. As these wave functions correspond to a *complex representation of the amplitude and phase of the gravitational fluctuations of pulsation $\omega_f(\vec{r}, t)$ associated with the singularity*, it is entirely logical and probable that if there is locally no gravitational fluctuations, that is to say if the wave function is very small in certain places in space, there will be practically no chance of finding the topological singularity there, whereas if these fluctuations become maximum in some other places, there is a very good chance of finding the topological singularity there.

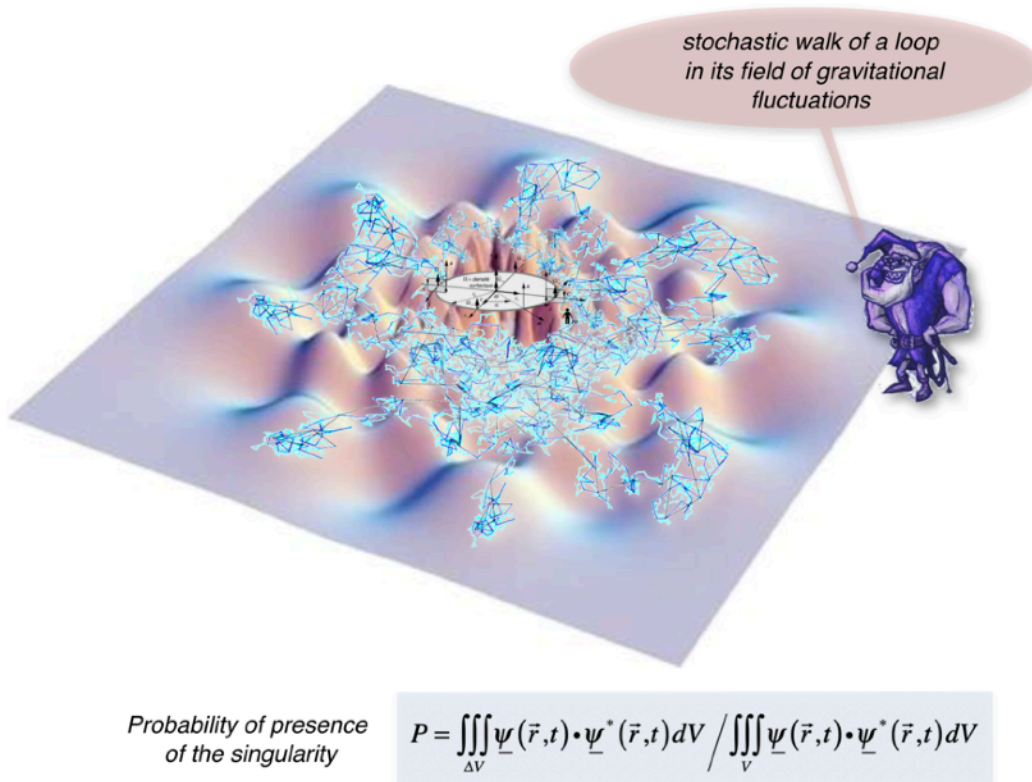


Figure 11.5 - Illustration of the "stochastic march" of a singularity loop in its stationary field of gravitational perturbations

We therefore come to a very interesting interpretation of this complex wave function $\underline{\psi}(\vec{r}, t)$: it must certainly be associated with the probability of the presence of the topological singularity with which the gravitational fluctuations $e^{i\omega_f t}$ are associated. The function $\underline{\psi}(\vec{r}, t)$ is in fact a complex mathematical object representing the amplitude and the phase of the gravitational fluctuations $e^{i\omega_f t}$, while a probability of presence is a positive scalar mathematical object whose sum over all the space must be equal to 1. Consequently, one possibility of extracting a quantitative value of probability of presence of the topological singularity from the function $\underline{\psi}(\vec{r}, t)$ is to use the fact that the square of an oscillating function does have a positive scalar. In the case of a complex quantity like $\underline{\psi}(\vec{r}, t)$, it is the product $\underline{\psi}(\vec{r}, t) \cdot \underline{\psi}^*(\vec{r}, t)$ of the complex function $\underline{\psi}(\vec{r}, t)$ by its complex conjugate $\underline{\psi}^*(\vec{r}, t)$ which represents the square of the amplitude of the function. It is therefore enough to normalize the product $\underline{\psi}(\vec{r}, t) \cdot \underline{\psi}^*(\vec{r}, t)$

taken over a portion ΔV of space by this product taken over all the space V likely to contain the singularity to obtain the probability P of finding the singularity in the portion ΔV of space, as illustrated in figure 11.5 . We therefore find the usual simple interpretation of the wave function in quantum physics, while giving it a conceptual explanation here.

The fact that the complex wave function $\underline{\psi}(\vec{r}, t)$ makes it possible to deduce, not the position of the singularities at a given instant, but their probability of presence in a given place and at a given instant, also means that the wave equations, which allow one to compute $\underline{\psi}(\vec{r}, t)$ or $\underline{\psi}_n(\vec{r})$ in the stationary case, and which are in fact nothing other than *emanations of the Newton's equation of the lattice* applied to the gravitational fluctuations, are at the same time *a new form of equations of the dynamics of microscopic topological singularities within the lattice*.

As the exact microscopic movements of topological singularities are not accessible and predictable via their complex wave function $\underline{\psi}(\vec{r}, t)$, but only the probability of the presence of singularities subject to a potential $V(\vec{r}, t)$ or $V(\vec{r})$ can be obtained, the real movements of microscopic singularities within the cosmological lattice must probably be stochastic and chaotic movements.

One can imagine for example that random gravitational fluctuations (see chapter 14), but of pulsations different from the pulsation $\underline{\omega}_f(\vec{r}, t)$ associated with the topological singularity, and which would appear and disappear in the vicinity of the singularity, could come to shake it enough by providing it random pulses. These impulses would then contribute to stochastic movements of the singularity. But as the stochastic walk of the singularity must also be strongly coupled with its proper gravitational fluctuations of frequency $\underline{\omega}_f(\vec{r}, t)$, this stochastic walk should present a statistical distribution of presence which would manifest itself via the probability of presence deduced from the wave function.

There are in fact two observable physical phenomena which present strong analogies with such a “stochastic march” of topological singularities:

- in solids, dislocations can exhibit a microscopic stochastic course under the effect of random thermal fluctuations (due to phonons) which can shake them up. There then appears a stochastic movement of dislocations, called *Brownian movement*, as described for example in the article «*overview on dislocation-point defect interaction: the brownian picture of dislocation motion*»¹.
- recent macroscopic experiments carried out in the laboratory with bouncing droplets on a vibrated liquid surface present fairly surprising results. The droplets move randomly on the liquid surface, which is why they have been called “walking drops”². This “walk” is attributed to a resonant interaction of the gout with its own wave field³. The measurement of the probability of distribution of the drop on a limited liquid surface can then have a regularity presenting

¹ G. Gremaud, *Materials Science and Engineering A* 370 (2004) 191-198

² Stéphane Perrard: “Une mémoire ondulatoire: états prores, chaos et probabilités”, thèse de doctorat, 2014, Université Paris Diderot (<https://tel.archives-ouvertes.fr/tel-01158368>)

³ D. M. Harris, J. Moukhtar, E. Fort, Y. Couder, J. W. M. Bush: “Wavelike statistics from pilot-wave dynamics in a circular corral” *Physical Review E*, 88, 011001(R), 2013

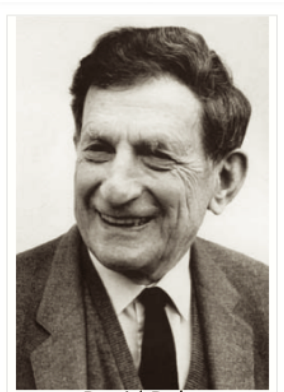
astonishing similarities with the probability of the presence of quantum microscopic particles confined in a well of potential ⁴.

In fact, the interpretation of quantum physics that emerges from our approach *comes close enough to the interpretation of Bohm, in its stochastic version, introduced in 1954 as a*



Louis de Broglie
(1892-1987)

development of the *pilot wave theory of Louis de Broglie of 1927*. Indeed, in our approach, the wave function $\underline{\psi}(\vec{r}, t)$ is a real and objective field, corresponding to the envelope of the gravitational fluctuations of the volume expansion of the cosmological lattice associated with topological singularities, while topological singularities are also, as for them, real particles (dislocation or disclination loops) which at all times have real coordinates in space and a given



David Bohm
(1917-1992)

momentum. These are indeed the main ideas of Bohm's interpretation. And the image of the world conveyed by our approach is clearly indeterministic as is the Bohmian image of quantum physics, in the sense that we do not have direct access to the positions of the singularities, but only to the notions of probabilities that we deduce from the wave function, which are only a reflection of our ignorance of the underlying history which determines the course of events for microscopic topological singularities.

Superposition of topological singularities, bosons, fermions and exclusion principle

One can legitimately wonder what becomes of the field of gravitational fluctuations when two topological singularities are close to each other. Imagine that we consider two singularities (a) and (b) which evolve in the same space, and therefore in the same potential $V(\vec{r})$. Let's look for the superimposed standing wave function, that is, how to write the volume expansion perturbations due to the two singularities at the same time. Assuming that in the state of stationary superposition, the stationary Schrödinger equations remain valid for the two singularities (figure 11.6), let us try to combine these two relations, by multiplying the first by $\underline{\psi}_m(\vec{r}_b)$ and the second by $\underline{\psi}_n(\vec{r}_a)$, and by summing the whole. We get a new equation which is nothing other than the Schrödinger equation for the superposition wave function $\underline{\psi}_n(\vec{r}_a)\underline{\psi}_m(\vec{r}_b)$. We therefore deduce that the oscillatory perturbations of the volume expansion due to the superposition of the two singularities are written as a product of the two wave functions multiplied by the oscillations $\exp(\pm i(E_0 + H_n)t/\hbar)$ and $\exp(\pm i(E_0 + H_m)t/\hbar)$. We note that there are then two types of possible superpositions, according to the signs of exponential exponents, which have very different global oscillation frequencies, related to the sum and the difference of the energies of the singularities, namely $\exp(\pm i(2E_0 + H_n + H_m)t/\hbar)$

⁴ R. Brady, R. Anderson: "Why bouncing droplets are a pretty good model of quantum mechanics", University of Cambridge Computer Laboratory, 2014 (arXiv:1401.4356v1)

and $\exp(\pm i(H_n - H_m)t/\hbar)$.

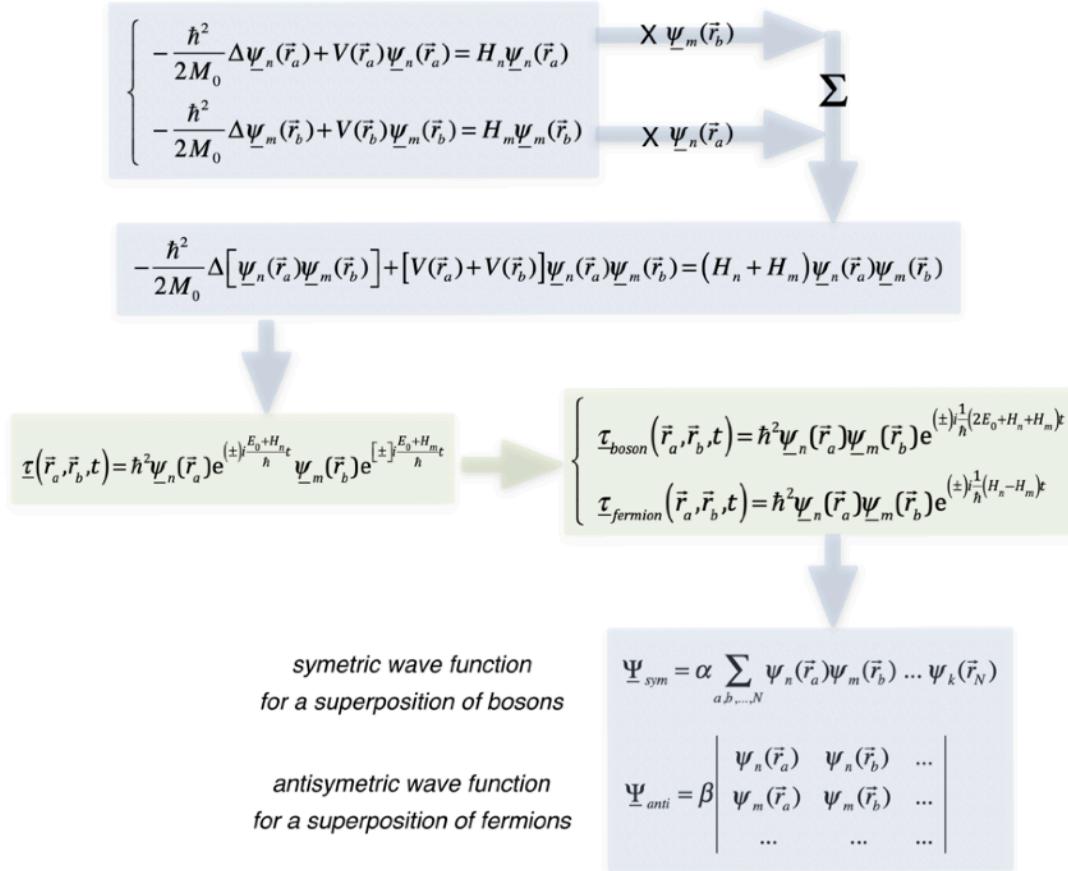


Figure 11.6 - Stationary equation for the superposition of topological singularities, gravitational fluctuations of bosons and fermions and symmetrical and anti-symmetrical wave functions

By analogy with quantum physics, we will call *bosons* the singularities corresponding to the first superposition solution, whose pulsation is $(2E_0 + H_n + H_m)/\hbar$, because the two singularities can occupy the same energy level without disappearance of the oscillatory perturbations of the expansion. As for the singularities which correspond to the second pulsation solution $|H_n - H_m|/\hbar$, they will be called *fermions* because they cannot be superimposed in the same energy level since in this case the oscillatory gravitational perturbations of the expansion disappear.

This observation on the way that the singularities are superimposed reveals therefore directly the famous *principle of exclusion of Pauli*: the singularities which combine according to



Wolfgang Pauli
(1900-1958)

the second possibility, namely the *fermions*, cannot be found in the same state of energy.

In usual quantum physics, where we only describe the wave functions, and where we ignore the real physical meaning of these wave functions in terms of amplitude and phase of oscillatory gravitational perturbations, we can show this difference between bosons and fermions directly in the superposition wave function $\underline{\psi}_n(\vec{r}_a)\underline{\psi}_m(\vec{r}_b)$. For this, we note that for the same value of the energy E of the system, there are two possible solutions of the equation for the superposition wave function $\underline{\Psi}$, which simply correspond to exchanging the two identical singularities, let $\underline{\Psi} = \underline{\psi}_n(\vec{r}_a)\underline{\psi}_m(\vec{r}_b)$ and $\underline{\Psi} = \underline{\psi}_n(\vec{r}_b)\underline{\psi}_m(\vec{r}_a)$. Now, one of the fundamental properties of linear and homogeneous differential equations is that any linear combination of particular solutions of this type of equation is also a solution, so that the most general solution of the Schrödinger equation can be written as a superposition $\underline{\Psi} = \alpha\underline{\psi}_n(\vec{r}_a)\underline{\psi}_m(\vec{r}_b) + \beta\underline{\psi}_n(\vec{r}_b)\underline{\psi}_m(\vec{r}_a)$. This expression would seem to indicate that there exists a large number of stationary states for a system of two singularities. However, it must now be taken into account that, because of the principle of uncertainty linked to the operator commutators, identical singularities lose their individuality. We say that identical singularities are indistinguishable, which quite simply means that it is not possible to follow the trajectory of a given singularity over time. If we consider the wave function $\underline{\Psi}$ of the system, we know that $\underline{\Psi}^2$ determines the probability of finding the two singularities in a certain portion of space. If we exchange the two singularities, it is clear that $\underline{\Psi}^2$ must remain unchanged. On the other hand, the phase of $\underline{\Psi}$ can be modified by this exchange, so that $\underline{\Psi} \rightarrow \underline{\Psi}e^{i\eta}$. If we proceed to a second exchange of singularities, we obviously have $\underline{\Psi} \rightarrow \underline{\Psi}e^{2i\eta}$ and we find ourselves in the initial state $\underline{\Psi}$, so that $e^{2i\eta} = 1$. To satisfy this last condition, it suffices that $e^{2i\eta} = +1$ or $e^{2i\eta} = -1$.

In the case where the wave function $\underline{\Psi}$ is transformed into $\underline{\Psi} \rightarrow +\underline{\Psi}$ during the exchange of the two singularities, the wave function is said to be *symmetrical*, and the singularities are called *bosons*. The wave function is written $\underline{\Psi} = \alpha(\underline{\psi}_n(\vec{r}_a)\underline{\psi}_m(\vec{r}_b) + \underline{\psi}_n(\vec{r}_b)\underline{\psi}_m(\vec{r}_a))$, where α is a normalization factor.

If the wave function $\underline{\Psi}$ changes to $\underline{\Psi} \rightarrow -\underline{\Psi}$, the wave function is said to be *antisymmetric*, and the singularities are called *fermions*. The wave function is written with a normalization factor β like $\underline{\Psi} = \beta(\underline{\psi}_n(\vec{r}_a)\underline{\psi}_m(\vec{r}_b) - \underline{\psi}_n(\vec{r}_b)\underline{\psi}_m(\vec{r}_a))$.

The indistinguishability of the two singularities then emerges clearly from the two previous expressions of the wave function $\underline{\Psi}$. We also note that, for the antisymmetric wave function, it is not possible that the two singularities are in the same state since $\underline{\Psi}$ would then be zero: this is indeed the mathematical expression at the level of the wave function itself of the *principle of exclusion of Pauli*, who says that two fermions cannot occupy the same state simultaneously because the gravitational perturbations disappear in this case.

In the case of a system of N identical singularities, the preceding concepts are easily generalized. In the case of bosons, the symmetric wave function $\underline{\Psi}_{sym}$ of the system is written in the form $\underline{\Psi}_{sym} = \alpha \sum \underline{\psi}_n(\vec{r}_a)\underline{\psi}_m(\vec{r}_b) \dots \underline{\psi}_k(\vec{r}_N)$, where the sum relates to the possible permutations of all the different states of the system. If the system has n_1 singularities in the energy state n , n_2 singularities in the energy state m , n_3 singularities in the energy state k , etc., the number of terms making up the wave function $\underline{\Psi}_{sym}$ is given by all the possible permutations, namely $P = N!/(n_1!n_2!n_3! \dots)$.

In the case of fermions, the antisymmetric wave function $\underline{\Psi}_{anti}$ of the system can be written

in the form of a determinant, as shown in figure 11.6. Indeed, the permutation of two columns of a determinant changes the sign of the determinant, which ensures the anti-symmetry of the wave functions under the exchange of two of the singularities. On the other hand, we also know that a determinant is zero if two lines are identical, which here corresponds to the expression of *the Pauli exclusion principle*, namely that a given state cannot be occupied by more than one fermion.

Demystifying quantum physics

It is quite remarkable that the wave function associated with the gravitational perturbations of the volume expansion is perfectly similar to the quantum wave function of a particle, and that it satisfies a wave equation identical to Schrödinger's equation. This obviously deserves further discussion.

We have shown in this chapter that *beyond the quantum decoherence limit*, i.e. for singularities whose mass density is above a certain critical value (figure 7.0), it is possible to link to this singularity a relativistic wave equation (figure 11.1) deduced by a "subterfuge" from Newton's second partial equation (figure 5.1). This equation made it possible to describe *the dynamic "gravitational" fluctuations of expansion* associated with a massive singularity moving at relativistic velocities within the network (figure 11.2). As for the non-relativistic wave equation of a singularity bound by a potential, it is absolutely identical to *the Schrödinger equation of quantum physics* (figure 11.3) since their respective interpretations in terms of the probability of the presence of a particle are *identical*. The key passages used to arrive at the Schrödinger equation of a singularity from Newton's second partial equation for gravitational expansion perturbations are, firstly, *the conjecture 10* postulating *the physical meaning of time and space operators applied to the wave function*, and secondly *the "reduction" of the wave equation* from the second-degree wave equation into spatial derivatives to the first-degree wave equation into spatial derivatives, again using *conjecture 10*. It is these two key passages that have made it possible to establish a physical theory quite similar to quantum physics to describe the microscopic behaviour of topological singularities within a cosmological network that does not exhibit longitudinal waves.

But our approach still lacks a deep physical explanation of these two key passages and their reason for being. In particular, we can legitimately ask the question of why the Planck constant exists, where its value comes from, and whether it is really a universal constant or if it is deductible from the other constants appearing in our approach. An answer to these questions would allow an even more in-depth and definitive understanding of quantum physics.

But in our approach, the complex wave function $\underline{\psi}(\vec{r}, t)$ and the Schrödinger wave equation are still physically demystified, since they become there the mathematical expressions of the envelope and of the phase of the vibratory fluctuations of the lattice expansion, therefore *gravitational fluctuations* correlated with topological singularities.

From this completely innovative interpretation of quantum physics, the possibility of having "bosons" and "fermions" type singularities, the fact that there is *indistinguishability* between topological singularities when they contribute to the same field of correlated gravitational fluctuations, and the fact that singularities of the "fermion" type must satisfy an exclusion principle similar to *the Pauli exclusion principle* is probably the most remarkable and astonishing

point of our calculations, because it demystifies a side that has always been most obscure in quantum physics.

Finally, it is equally remarkable to note that all these properties, such as for example *the properties of superposition* (the symmetry of the wave function Ψ_{sym} of singularities of bosons type and the anti-symmetry of the wave function $\Psi_{antisym}$ of singularities of fermions type, the *indistinguishability* of topological singularities and the principle of exclusion) are direct consequences of the fact that the gravitational fluctuations associated with one or more singularities must satisfy Newton's second partial equation of the cosmological network.

In fact, the image of a field of vibrational gravitational fluctuations correlated with a topological singularity has enormous potential to explain simply observed and / or calculated quantum phenomena, but still remains very mysterious in the framework of usual quantum physics. Just think of the following few examples:

- the concept of wave-particle duality of quantum physics, which finds an immediate and simple explanation here since the particle is the topological singularity, and that the wave is the field of the gravitational fluctuations which is correlated to it,
- the experiments of quantum interference obtained by the passage of particles through two slits, but by letting pass only one particle at a time, which can very well be explained now by the fact that each topological singularity has actually to go through only one of the slits. But the field of gravitational fluctuations associated with it crosses the two slits, hence the possibility of interference of these fluctuations at the exit of the two slits, resulting in their coupling with the singularity a modification of its trajectory, and finally a statistical distribution of the successive impact points of the particles on the screen placed after the two slits,
- the Heisenberg's uncertainty principle, which is obviously satisfied in our approach since it admits a fortiori the same interpretation of the operators acting on the wave function as quantum physics, and therefore satisfies all the relations of classical quantum physics. The uncertainty relationships are then directly linked to the existence of gravitational perturbations correlated to the singularity,
- the very mysterious experiments of quantum entanglement and quantum decoherence, since one can very well imagine that the entanglement is the fact for two or more topological singularities to have in common a single field of gravitational fluctuations, in which case the fact of acting on only one of the singularities will modify this common field of gravitational fluctuations, which will necessarily act on the other singularities which participate in the entanglement, and which can also cause quantum decoherence, in other words the decoupling of the topological singularities involved in the common field of gravitational fluctuations.

Einstein said "*God does not play dice*" when talking about quantum physics, meaning that the quantum physics of his time was not a complete theory, and that there had to be a rational and pragmatic explanation for the probabilistic aspect of quantum theory. This opinion of Einstein has been strongly contested, not to say highly criticized. It has been demonstrated that there could not be local hidden variables to explain quantum physics, but on the other hand nothing prevents there from being non-local hidden variables, and this is precisely the case of gravitational fluctuations correlated to topological singularities. It is therefore clear here that Einstein was indeed right, and that there is indeed a completely rational explanation of quantum physics.

There is, moreover, a highly ironic note in the famous Einstein sentence, since quantum physics would be explained by gravitational fluctuations of the volume expansion field and by a stochastic movement of topological singularities interacting with these gravitational fluctuations. And these are precisely the ingredients with which God, if he existed, could play dice, and that, oh ironic irony, it is precisely Einstein himself who is the inventor of the explanations of the General Gravitation and the Brownian Motion, which earned him the Nobel Prize in physics.

Thus, our explanation of quantum physics proves Einstein right, by showing that quantum physics is the expression of gravitational fluctuations at very small scales in a cosmological lattice without propagation of longitudinal waves. Consequently, all modern attempts to quantify gravitation are bound to fail since quantum physics is precisely the expression of dynamic gravitational fluctuations on a microscopic scale.

Chapter 12

Spin of the topological loops

In this chapter, we are going to be interested in finding the solution of Newton's second partial equation within the torus itself surrounding a twist disclination loop. At the very heart of a loop of topological singularity, one demonstrates that it cannot exist static solutions to Newton's second partial equation for longitudinal gravitational fluctuations. It therefore becomes imperative to find a dynamic solution to this equation, and the simplest dynamic solution that it is possible to envisage is that the loop turns on itself, in a quantified rotational movement of the loop around one of its axes. By solving this rotation movement with Newton's second partial equation, which is in this dynamic case nothing other than the Schrödinger's equation, one obtains the quantified solution of the internal gravitational fluctuations of the loop, which is in fact *the spin of the loop*, which can take several different values ($1/2$, 1 , $3/2$, etc.) and which is perfectly similar to the spin of the particles of the standard model. If the loop is composed of a twist disclination loop, there also appears *a magnetic moment of the loop*, proportional to the famous *Bohr magneton*.

On shows that, in the case of our approach, this rotation movement is very real, and that it does not infringe special relativity, contrary to what believed the pioneers of quantum physics. Indeed, the argument of the pioneers of quantum physics was that the spin of a particle can in no case be a real rotation of the particle on itself because of an equatorial speed of rotation greater than the speed of the light. This argument is swept away in our approach by the fact that the static expansion near the core of the loop is very high, which leads to celerities of light in the vicinity of the core of the loop much higher than the equatorial speed of loop rotation.

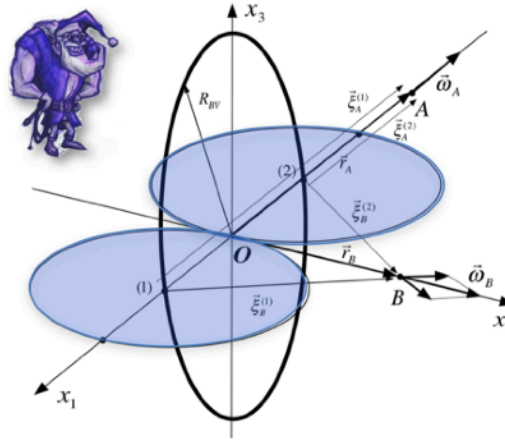
In this argument on the absolute necessity of a spin of singularity loops to satisfy Newton's second partial equation, only the exact value of the spin of a loop, namely the values $1/2$ or 1 , has no simple explanation yet.

About the non-existence of a static internal field of perturbations of expansion within a loop of twist disclination (BV)

We have already calculated the static external fields of gravitational perturbations of expansion of a twist disclination loop (figure 7.10), and we have seen that these fields are responsible for the effects of gravitational attraction at long distance from the loop via gravitation force (chapter 8), but also short-range coupling effects with other loops via the weak force (chapter 9).

On the other hand, we have not yet looked into the case of the expansionperturbation field in the immediate vicinity of the twist disclination loop. This field must be calculated within the torus surrounding the twist disclination loop. By using a simplified static version of Newton's second

partial equation of figure 5.1, in which one introduces the energy density $F_{dist}^{BV}(\vec{\xi})$ of distortion associated with the fields of rotation and shears of the screw pseudo-dislocation, one obtains an equation of the second degree whose solution $\tau_{int}^{BV}(\vec{\xi})$ within the torus is shown in figure 12.1, and in which $\vec{\xi}$ represents a point on a section of the torus relative to the center of this section.



$$\text{Static solution} \quad \tau_{int}^{BV}(\vec{\xi}) = \frac{4K_2/3 + 2K_1(1+\tau_0) - K_0}{2K_1} \left[-1 + \sqrt{1 - \frac{K_1(K_2+K_3)}{(4K_2/3 + 2K_1(1+\tau_0) - K_0)^2} \frac{q_{\lambda BV}^2}{2\pi^4 R_{BV}^2} \frac{1}{\xi^2}} \right]$$

$$\text{Condition of existence of a static solution} \quad \xi > \xi_{cr} = \sqrt{\frac{K_1(K_2+K_3)}{2\pi^4 (4K_2/3 + 2K_1(1+\tau_0) - K_0)^2}} \frac{|q_{\lambda BV}|}{R_{BV}} \cong \frac{1}{\pi^2} \sqrt{\frac{K_1}{2K_0}} \frac{|q_{\lambda BV}|}{R_{BV}}$$

Conjecture 11: K_1 satisfies the following relationship in the perfect cosmological lattice

$$K_1 > K_{1cr} = K_0 \frac{2\pi^4 R_{BV}^2}{q_{\lambda BV}^2} \longrightarrow \text{no static solution possible}$$

Figure 12.1 - Non-existence of static solutions for the internal gravitational perturbations of a twist disclination loop

So that this equation has a real solution, it would be necessary that the argument of the root is positive, therefore that the distance $\vec{\xi}$ in the middle of the loop satisfies the condition of existence reported in figure 12.1, which means that the distance $|\vec{\xi}|$ must be greater than a certain critical value ξ_{cr} for a static solution to exist. If this critical distance turns out to be greater than the radius R_{BV} of the loop, it is clear that a static solution becomes impossible. It is quite easy then to show that the condition for which $\xi_{cr} > R_{BV}$ is in fact a condition on the value of the module K_1 , which is expressed as $K_1 > K_{1cr} = 2\pi^4 K_0 R_{BV}^2 / q_{\lambda BV}^2$, and which means that, if K_1 is greater than the critical value K_{1cr} , there cannot exist a static solution for gravitational perturbations within the torus surrounding the disclination loop.

It is interesting to involve here numerical values which one can draw from the real world, by using for example the analogy with the electrons, namely that, for these, one has an electric charge being worth $|q_{\lambda BV}| = q_{electron} = 1.6 \cdot 10^{-19} [C]$, an estimated radius of the order of $10^{-18} [m]$ and that the elastic moduli $K_3 = K_0$ are in fact the analogs of the dielectric constant of vacuum, so that $K_3 = K_0$, the condition $K_1 > K_{1cr}$ would then imply that $K_{1cr} = K_0 2\pi^4 R_{BV}^2 / q_{\lambda BV}^2 \cong 10^{-21}$.

The condition that the module K_1 is greater than the critical value $K_{1cr} \cong 10^{-21}$ is very likely to be fulfilled in the presence of a twist disclination loop, which is strongly supported by the numerical application obtained thanks to the analogy with the electrons of the real world. Let us therefore admit a new conjecture, conjecture 11, which states that K_1 satisfies well the relation $K_1 \geq K_{1cr} = K_0 2\pi^4 R_{BV}^2 / q_{\lambda BV}^2$ in the perfect cosmological lattice.

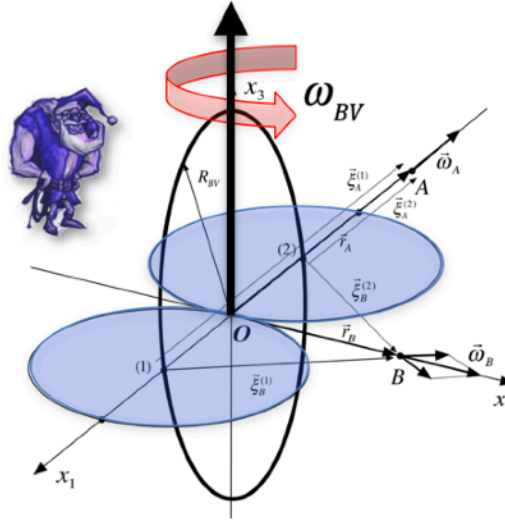
Admitting this conjecture, the “gravitational” perturbation field within the torus surrounding the twist disclination loop cannot be a solution of the static equation, and must therefore become a *dynamic internal “gravitational” perturbation field*, solution of Newton's second partial equation in figure 5.1. But around the loop, this Newton equation for dynamic perturbations is nothing other than the stationary Schrödinger equation in figure 11.4. It is therefore necessary to find a movement of the loop which is not a translation of it, but a movement confined to the same place in space. However, the only possible movement of the loop which is confined to the same place in space is actually a rotation of the latter on itself.

Classic rotation of a twist disclination loop (BV)

Let us therefore consider a twist disclination loop of radius R_{BV} as shown in figure 12.2, and imagine that it can rotate around a direction axis \vec{e}_{axis} contained in the plane of the loop *with a pulsation* ω_{BV} , which is not impossible since the loop actually corresponds to a *screw pseudo-dislocation*. If we first deal with this problem in a conventional way, we can use polar coordinates to define *the angular momentum* \vec{L}_{BV} of the loop around its axis of rotation, assuming the mass of the loop distributed uniformly over the surface of the loop, as illustrated in figure 12.2. As we know in fact only approximately the real distribution of the mass in the vicinity of the loop, we will introduce a numerical correction factor δ_1 such as $\delta_1 \cong 1$ in the calculation of \vec{L}_{BV} , as represented in figure 12.2.

We can then introduce *the moment of inertia of the loop* I_{BV} around the axis of rotation using the known relation $\vec{L}_{BV} \cong I_{BV} \omega_{BV} \vec{e}_{axis}$. As a twist disclination loop also has a rotation charge $q_{\lambda BV}$, analogous to the electric charge, it also has a «*magnetic moment*» $\vec{\mu}_{BV}$ in the direction of the rotation axis which is defined in figure 12.2, *assuming the charge distributed on the contour of the loop*. As we only know approximately the distribution of the charge in the vicinity of the loop, we will also introduce a numerical correction factor δ_2 such as $\delta_2 \cong 1$. And then we find a direct relationship between the «magnetic moment» $\vec{\mu}_{BV}$ and the kinetic moment \vec{L}_{BV} of this loop, which is called *the gyromagnetic ratio* g_{BV} which is roughly equal to $2\delta_2 / \delta_1 \cong 2$.

We can also calculate *the kinetic energy* $E_{rotationBV}^{cin}$ associated with this rotation movement around the axis of rotation, as shown in figure 12.2. With the corrective factor δ_1 on the distribution of mass within the loop, we obtain a value of the energy which is directly related to the angular momentum and the moment of inertia since $E_{rotationBV}^{cin} \cong \vec{L}_{BV}^2 / (2I_{BV})$.



Angular momentum ($\delta_1 \cong 1$)

$$\vec{L}_{BV} = \delta_1 \oint \vec{r} \wedge \vec{v} dm = \delta_1 \vec{e}_{axis} \int_0^{R_{BV}} 4 \int_0^{\pi/2} \underbrace{r \cos \theta}_{|\vec{r}|} \underbrace{r \cos \theta \omega_{BV}}_{|\vec{v}|} \underbrace{\frac{\delta_1 M_0^{BV}}{\pi R_{BV}^2} r d\theta dr}_{dm} = \delta_1 \frac{M_0^{BV} R_{BV}^2}{4} \omega_{BV} \vec{e}_{axis} \cong I_{BV} \omega_{BV} \vec{e}_{axis}$$

$$\Rightarrow I_{BV} = \delta_1 \frac{M_0^{BV} R_{BV}^2}{4} \quad (\text{moment of inertia})$$

Magnetic moment ($\delta_2 \cong 1$)

$$\vec{\mu}_{BV} = \delta_2 \frac{1}{2} \oint \vec{r} \wedge \vec{v} dq = \delta_2 \vec{e}_{axis} 2 \int_0^{R_{BV}} \underbrace{\cos \theta R_{BV}}_{|\vec{r}|} \underbrace{\cos \theta \omega_{BV}}_{|\vec{v}|} \underbrace{\frac{q_{\lambda BV}}{2\pi} d\theta}_{dq} = \delta_2 \frac{R_{BV}^2 q_{\lambda BV}}{4} \omega_{BV} \vec{e}_{axis} \cong g_{BV} \frac{q_{\lambda BV}}{2M_0^{BV}} \vec{L}_{BV}$$

$$\Rightarrow g_{BV} = 2 \frac{\delta_2}{\delta_1} \cong 2 \quad (\text{gyromagnetic ratio})$$

Kinetic energy

$$E_{rotationBV}^{cin} = \delta_1 \frac{1}{2} \oint \vec{v}^2 dm = \delta_1 \int_0^{R_{BV}} 2 \int_0^{\pi/2} \underbrace{r^2 \cos^2 \theta \omega^2}_{\vec{v}^2} \underbrace{\frac{M_0^{BV}}{\pi R_{BV}^2} r d\theta dr}_{dm} = \delta_1 \frac{M_0^{BV} R_{BV}^2}{8} \omega_{BV}^2 \cong \frac{2\vec{L}_{BV}^2}{\delta_1 M_0^{BV} R_{BV}^2} \cong \frac{\vec{L}_{BV}^2}{2I_{BV}}$$

Figure 12.2 - Classic solution of rotation of the twist disclination loop: angular momentum, magnetic moment and kinetic energy

Quantification of the angular momentum of the screw loop

Assuming that the twist disclination loop (BV) actually turns on itself, this microscopic movement of rotation will induce a field of gravitational fluctuations in the vicinity of the loop, depending on the second partial Newton equation of figure 5.1. Now we saw in the previous chapter that in the absence of a time-varying potential, Newton's second partial equation leads to the stationary Schrödinger equation in figure 11.4. The treatment of the rotation movement of a microscopic object around an axis by the stationary Schrödinger equation is succinctly summarized in figure 12.3.

For a particle subject to rotation, it is preferable to describe the operator \hat{H} linked to the classical Hamiltonian in spherical coordinates (θ, φ) . In the absence of a potential, this operator \hat{H} is linked to the square operator of the angular momentum \hat{L}^2 by the last relation

obtained in figure 12.2. With the expression of this operator in spherical coordinates, we deduce the stationary Schrödinger's equation in spherical coordinates, whose stationary solutions have quantified energy levels $\varepsilon_j = \hbar^2 j(j+1)/(2I_{BV})$ of rotation. For each value of the energy ε_j corresponding to a given angular speed, there are $2j+1$ different eigenstates corresponding conventionally to different orientations of the axis of rotation. It is said that the energy state ε_j has a degeneracy of $2j+1$.

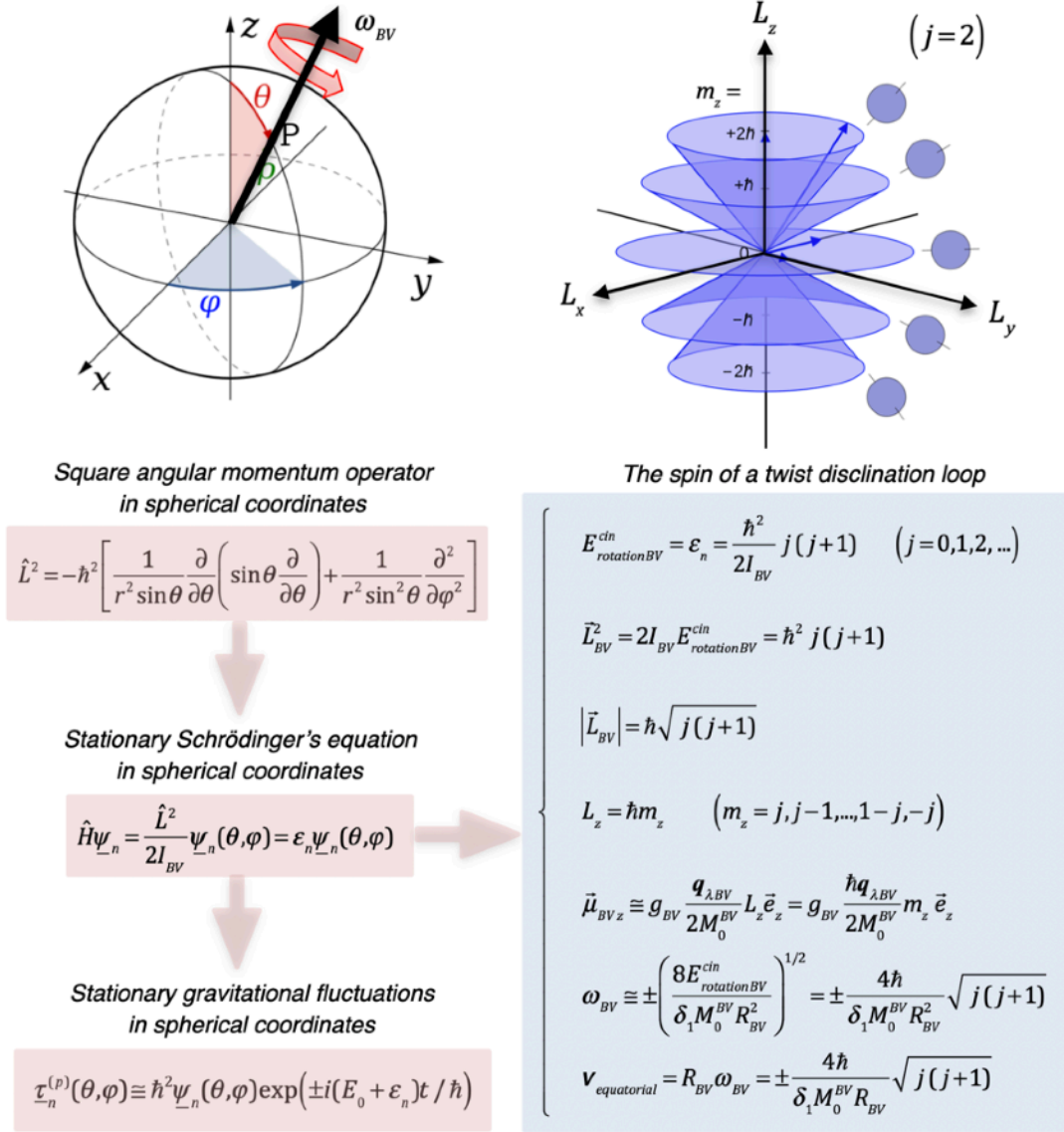


Figure 12.3 - Quantum solution of rotation of the twist disclination loop:
quantified rotational energy levels and magnetic quantum number m_z

It is the magnetic quantum number m_z that characterizes the quantification of the projection of the angular momentum along a certain axis z . It can take the $2j+1$ following values $m_z = j, j-1, \dots, 1-j, -j$, so that the projection L_z of the angular momentum on an axis Oz takes the values $L_z = \hbar m_z$. Apart from the kinetic energy and the kinetic momentum of the loop,

we still deduce *the quantized magnetic moment* of the loop along the axis Oz , which depends directly on the magnetic quantum number m_z , which also depends on *the Landé factor* g_{BV} of the screw loop, which is roughly equal to 2 in the case of the twist disclination loop, but which would depend on the distribution of mass and charge in the case of other types of topological singularities. We note that, in the expression of the quantified momentum, we then find the value of the famous *Bohr magneton*, namely $\hbar q_{\lambda BV} / 2M_0^{BV}$.

Finally, the resolution of the stationary Schrödinger equation in this case makes it possible to deduce the eigen wave functions $\psi_n(\theta, \varphi)$ correlated to the different energy levels ε_n , and to use them to obtain the stationary gravitational perturbations $\tau_n^{(p)}(\theta, \varphi)$ in the immediate vicinity of the loop under the form $\tau_n^{(p)}(\theta, \varphi) \equiv \hbar^2 \psi_n(\theta, \varphi) \exp(\pm i(E_0 + \varepsilon_n)t / \hbar)$.

About the completely classic interpretation of the spin of a particle

In quantum physics, the spin of a charged particle like the electron was initially attributed to a proper rotation of the particle. However, the fact that the electron is considered a spherical particle, which is extremely small, has raised doubts about this "classic" interpretation of spin. But the strongest argument for abandoning this "classic" interpretation, although the effects of spin like the magnetic moment of the electron correspond strictly to a proper rotation of the particle on itself, is the fact that calculating the equatorial speed of rotation of the electron gives a speed much higher than the speed of light, which does not at all fit with the theory of Special Relativity.

But it is quite different in our approach. Indeed, let us try to calculate the equatorial speed in the case of the twist disclination loop, which is obtained from its radius R_{BV} and the pulsation ω_{BV} of its rotation movement as $\mathbf{V}_{equatorial} = R_{BV} \omega_{BV}$. To determine the rotation pulsation ω_{BV} , we equal the classical kinetic energy of rotation of the loop to its kinetic energy determined via the Schrödinger equation, and we obtain the expressions for ω_{BV} and $\mathbf{V}_{equatorial}$ reported in figure 12.3. Numerically, let's use the known values of the electron, namely its mass $M_0^{BV} \equiv M_0^{electron} = 9,1 \cdot 10^{-31} [kg](\xi, t)$, its approximate radius on the order of $10^{-18} [m]$, the value of δ_1 equal approximatively to 1, the value of the Planck constant $\hbar \equiv 6,6 \cdot 10^{-34} [m^2 kg / s]$, and its known spin of $j = 1/2$, and it then comes the following approximative value of the equatorial speed $\mathbf{V}_{equatoriale} \cong 2,5 \cdot 10^{15} [m / s]$. We find that the equatorial speed of rotation of the loop is much greater than the speed of light $c_{t0} \equiv c = 3,3 \cdot 10^8 [m / s]$ within the lattice, as the pioneers of quantum physics had found.

But a completely new fact comes into our approach, which is the enormous static volume expansion in the immediate vicinity of the rotating loop. Indeed, let's express the static volume expansion at the limit of the torus where expansion perturbations can become static. At this limit, the static volume expansion is maximum, and it is given by the unique solution of the equation for $\tau_{int}^{BV}(\xi)$ in figure 12.1 when the term under the root is zero, and we obtain that $\tau_{static max}^{BV} = [K_0 - 4K_2 / 3 - 2K_1(1 + \tau_0)] / (2K_1) \cong K_0 / (2K_1)$. We therefore deduce that the actual speed of the transverse waves in the immediate vicinity of the loop is in fact worth $c_t|_{limite} \cong c_{t0} e^{\tau_{static max}^{BV}/2} \cong c_{t0} \exp(K_0 / 4K_1)$. Therefore, the speed $c_t|_{limite}$ is certainly much higher than $c_{t0} \equiv c = 3,3 \cdot 10^8 [m / s]$ since $K_0 / K_1 \gg 1$. In fact, it is enough that $c_t|_{limite} \cong c_{t0} \exp(K_0 / 4K_1) > \mathbf{V}_{equatorial} \cong 2,5 \cdot 10^{15} [m / s]$ for the equatorial speed of rotation of the loop to be possible. We can try to determine what is the limit value of the module K_1 so that

the rotation of the loop is possible. It's very easy to get that we need just to have that $K_1 / K_0 < 1,6 \cdot 10^{-2}$. Now this condition is always satisfied since we need, from conjecture 6, that $K_1 / K_0 \ll 1$. We are therefore assured that, *in our approach*, the rotation movement of the loop on itself is not only perfectly possible, but that it is *especially compulsory* since it is the only possible solution to Newton's second partial equation.

We therefore conclude that there is once again a completely "classic" explanation of the notion of spin of a particle, as a real quantified movement of rotation of the loop around an axis, which does not infringe in any way the principles of special relativity. This explanation removes on the one hand all the mysterious side of the notion of spin in quantum physics, and on the other hand perfectly explains the existence of a quantified magnetic momentum of spin of the electron, directly associated with the real rotation of the charged loop.

About the problem of the spin value of a topological loop

If the existence of a proper rotation of the loops is a necessity in our approach to satisfy Newton's second partial equation in the immediate vicinity of the loop, there is still a question to which we have no answer: what value must it attribute to the spin of the loop? Otherwise formulated, this question amounts to looking for the value to be assigned to the azimuthal quantum number j which characterizes the quantification of the energy of rotation and the angular momentum of the loop, as well as its magnetic moment (figure 12.3).

Experimentally, we know that the spin of the electron is worth $j = 1/2$ and that the spin of the intermediate boson W^- is worth $j = 1$. But the underlying reason why these particles have these particular values remains very mysterious. In our approach, the same goes: apart from the fact that the spin $j = 1/2$ and $j = 1$ are the weakest, and therefore correspond to the lowest possible kinetic energies, no reasonable argument allows for the moment to make a choice of the value of j to choose for a twist disclination loop. So let's look at the effect of a spin $j = 1/2$ or a spin $j = 1$ on a twist disclination loop:

- Loop of twist disclination with a spin 1/2

Consider a twist disclination loop of spin 1/2. Whatever the direction of the axis of rotation, there can only be two eigenstates of the loop, corresponding to a dextrorotatory or levorotatory rotation of the loop around the axis of rotation, since the state of degeneracy of the energy is in this case of $2j + 1 = 2$. The kinetic energy and the kinetic momentum of the loop become therefore $E_{rotationBV}^{cin} = 3\hbar^2 / (8I_{BV})$ and $|\vec{L}_{BV}| = \hbar\sqrt{3}/2$ in this case. As for the magnetic quantum number m_z , it can take the two values $m_z = \pm 1/2$ so that the projection L_z of the angular momentum on an axis Oz takes the values $\pm \hbar/2$. So here we find exactly the notion of spin of a particle of spin 1/2. The magnetic moment of the loop along the axis Oz is then written $\vec{\mu}_{BVz} \equiv \pm g_{BV} \hbar q_{\lambda BV} \vec{e}_z / (4M_0^{BV})$ with $g_{BV} \equiv 2$.

- Loop of twist disclination with a spin 1

Now consider a twist disclination loop of spin 1. Whatever the direction of the axis of rotation, there can then be only three eigenstates of the loop, corresponding to a dextrorotatory rotation, to a levorotatory rotation, or to no rotation of the loop around its axis of rotation, since the state of degeneracy of the energy is worth $2j + 1 = 3$ in this case. The kinetic energy and the kinetic momentum of the loop are worth $E_{rotationBV}^{cin} = \hbar^2 / I_{BV}$ and $|\vec{L}_{BV}| = \hbar\sqrt{2}$ respectively. As for the

magnetic quantum number m_z , it can take the following three values $m_z = -1, 0, +1$ so that the projection L_z of the angular momentum on an axis takes the values 0 and $\pm \hbar / 2$. We thus find here exactly the notion of spin of a particle of spin 1. The magnetic moment of the loop along the axis Oz is then written $\vec{\mu}_{BVz} \equiv 0, \pm g_{BV} \hbar q_{\lambda BV} \vec{e}_z / (2M_0^{BV})$ with $g_{BV} \equiv 2$.

About the link between the concepts of bosons, fermions and spin

The question of knowing if a loop of topological singularity behaves like a fermion or a boson in the event of superposition of several loops (see chapter 11) and the question of the value of the spin of a loop of topological singularity are undoubtedly very closely linked. Indeed, we know from quantum physics that fermions have a spin of 1/2 and that bosons have a spin of 1. From quantum physics, we also know that the spin component of the wave function Ψ of two particles is symmetric when the spins of the two particles are parallel, and antisymmetric if the spins are anti-parallel, and we therefore have the following possibilities for the wave function Ψ of two particles:

- *Fermions*: antisymmetric wave function \Rightarrow parallel spins and antisymmetric spatial component, or anti-parallel spins and symmetric spatial component.
- *Bosons*: symmetric wave function \Rightarrow parallel spins and symmetric spatial component, or anti-parallel spins and antisymmetric spatial component.

It would be very interesting to explore this problem further, and to see what topological interpretation to give it within the framework of our approach of topological loops. We will return to this problem in Chapter 13 dealing with the standard particle model.

About the very important consequences of the existence of spin on the cosmological behavior of the lattice

The fact that there is a spin of particles has very important consequences for the cosmological behavior of the lattice. Indeed, as the presence of the spin implies (i) that $K_1 > K_{1cr}$, with $K_{1cr} \equiv 10^{-21}$ for the electron, and (ii) that $K_1 / K_0 < 1,6 \cdot 10^{-2}$, we deduce that $K_1 > 0$, so that *the expansion of the lattice cannot be infinite* and that we find ourselves necessarily in one of the universe oscillating between big-bang and big-crunch. By adding to this condition on K_1 the conditions drawn from conjecture 6, in particular that $K_0 = K_3 \gg K_1 > 0$, we deduce that there is only one admissible behavior for the cosmological evolution of the lattice corresponding to figures 3.8 (g) and 3.10.

Chapter 13

Standard model of particles and strong force

We have previously shown that the perfect cosmological lattice presents strong analogies with all the major theories of modern physics, namely the equations of electromagnetism, special relativity, general relativity, black holes, cosmology, dark energy and quantum physics, including the notion of spin and magnetic moment, and that there can exist three types of loops of basic topological singularities respectively having the attributes of an electric charge, an electric dipolar moment or a load of curvature by bending (which is the exclusive prerogative of our approach of the perfect cosmological lattice, and which explains quite simply several mysterious phenomena at the present time, like the weak force of coupling of two topological loops, the dark matter, the galactic black holes and the disappearance of anti-matter).

In this chapter, we will focus on finding and describing the ingredients that could explain, on the basis of loops of basic topological singularities, the existence of the current standard model of elementary particles. In other words, we will try to find what mechanisms could generate the families of fundamental particles such as leptons and quarks, what could be the origins of the existence of three generations of these elementary particles, and where could the strong force come from with asymptotic behavior which binds quarks together to form baryons and mesons.

This chapter does not pretend at all to provide an elaborate theory or a definitive and quantitative solution to explain the standard model of particle physics, but rather to show by some specific arguments that it is certainly the choice of a particular microscopic structure of the perfect cosmological lattice which could provide an answer to the various questions which arise concerning the standard model. This chapter will therefore bring some elements of reflection by showing that it can appear in a solid of well chosen structure a whole "zoology" of loops of topological singularities which can have a strange family resemblance with the elementary particles of the standard model. It will also make it possible to present behaviors very similar to the behaviors of elementary particles, such as the presence of a strong asymptotic force which can participate in a coupling between topological loops.

The current Standard Model of elementary particles

At present, particle physics explains the intimate structure of matter using a model called the *Standard Model of Elementary Particles* (figure 13.1). This model reveals *fermions*, particles of matter that have two fairly different families, the *lepton family* and the *quark family*, as well as three types of interactions that can occur between these fermions: electromagnetic interaction, weak interaction and strong interaction.

The interactions between the fermions of matter take place through the exchange of particles called *gauge bosons*, corresponding to the quanta of the quantum fields of interaction concerned. The electromagnetic interaction uses the photon γ , the weak interaction with three gauge bosons Z^0 , W^+ et W^- , and the strong interaction with 8 gauge bosons called *gluons*.

As for the mass of particles, it is introduced into the standard model by a new interaction associated with the Higgs quantum field, the mediating particle of which is called the *Higgs boson*.

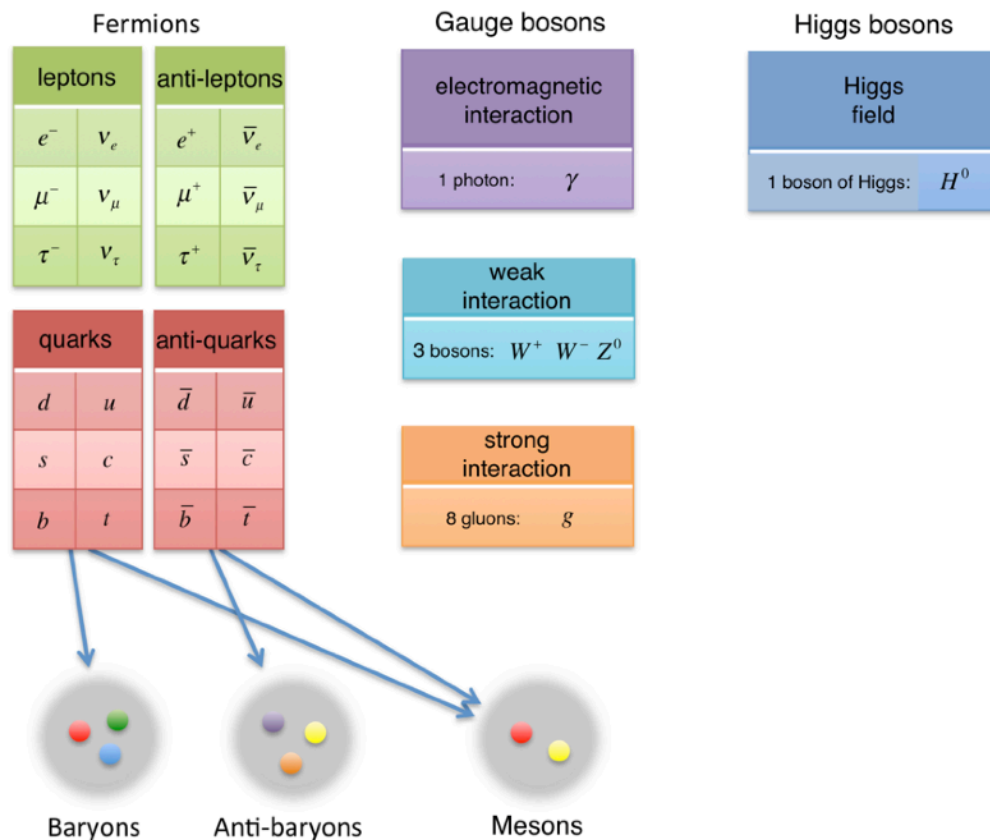


Figure 13.1 - The particles of Standard Model

Leptons and quarks

The *family of leptons* (figure 13.1) is made up of three generations of two types of particles: three electrically neutral particles called *electron neutrino* (ν_e), *muon neutrino* (ν_μ) and *tau neutrino* (ν_τ), and three electrically charged particles, called *electron* (e^-), *muon* (μ^-) and *tau* (τ^-). Each of these six particles has in principle an anti-particle ($\bar{\nu}_e$, $\bar{\nu}_\mu$, $\bar{\nu}_\tau$, e^+ , μ^+ and τ^+) which is essentially characterized by an opposite electric charge, which already raises a question regarding the existence of anti-particles of neutrinos. Leptons are quasi-point particles that are sensitive to electromagnetic interaction and weak interaction, but not strong interaction. It has long been thought that neutrinos do not have mass, but recent measurements show that this is not the case.

The *family of quarks* is also composed of three generations of two types of electrically charged particles: a first generation is formed of the quarks *down* (d) and *up* (u), respectively of electrical charges $-1/3$ and $+2/3$ of the electric charge of the electron, a second generation composed of the quarks *strange* (s) and *charm* (c), of electric charges $-1/3$ and $+2/3$ respectively of the electric charge of the electron, and a third generation composed of the

bottom (b) and *top* (t) quarks, respectively of electrical charges $-1/3$ and $+2/3$ of the electrical charge of the electron. Each quark has its electric charge anti-particle of opposite sign (\bar{d} , \bar{u} , \bar{s} , \bar{c} , \bar{b} and \bar{t}). The quarks are sensitive to both electromagnetic, weak and strong interaction. Quarks are not free particles, but they exist as a collection of quarks called *hadrons*. Quarks are linked within hadrons by strong force.

Hadrons come in two forms: *mesons* made up of a quark and an anti-quark, like particles $\Pi^+(u\bar{d})$, $\Pi^-(d\bar{u})$ or $\Pi^0(u\bar{u})$, and *baryons* made up of three quarks, like *proton* (uud) and *neutron* (ddu), or of three anti-quarks.

Each particle of matter, whether a lepton or a quark, has a non-zero mass and a spin $1/2$, which gives it the *fermion* status.

Fundamental interactions and gauge bosons

In the Standard Model, we consider the following three possible interactions between particles: *electromagnetic interaction*, *weak interaction* and *strong interaction*. These interactions are described by quantum field theories, except the gravitational interaction which could never be introduced in the Standard Model, despite an intensive search for the *graviton* gauge boson which would be associated with it. Each interaction therefore calls upon a field which is specific to it, and is then carried out by the exchange of a particle called a *gauge boson*, corresponding to the quantum of the field concerned. The electromagnetic interaction uses the *photon* (γ), a boson of zero mass gauge. The weak interaction uses the three gauge bosons Z^0 , W^+ and W^- , particles of non-zero mass and zero, positive or negative electrical charge respectively. As for the strong interaction, it uses 8 gauge bosons called *gluons*, in fact particles of zero mass.

The gauge bosons associated with these interactions are spin 1 particles, which explains their name as *bosons*.

Electromagnetic interaction and quantum electrodynamics

The quantum theory that describes electromagnetic interaction is called *quantum electrodynamics*. It is a quantification of the electromagnetic field: the charged particles interact there by the exchange of quanta of the field, the *photons*. It is a relativistic theory, because it takes into account the propagation time of the interaction, namely the speed of the vector boson, the photon. In this theory, we can represent an interaction in a simple and convenient way, thanks to *Feynman diagrams*. In figure 13.2, the example of the interaction between two electrons is represented by the exchange of a *virtual photon*, qualified here as virtual because it cannot be detected experimentally.

Weak interaction and electroweak theory

The weak interaction acts between all elementary fermions, whether they are leptons or quarks (Figure 13.3). This is the only interaction that acts on neutrinos. It is responsible for *nuclear decay*. This interaction has two aspects: the weak interaction by *charged currents*, whose vectors are the gauge bosons W^+ and W^- , and the weak interaction by *neutral*

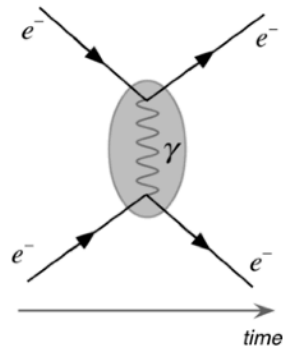
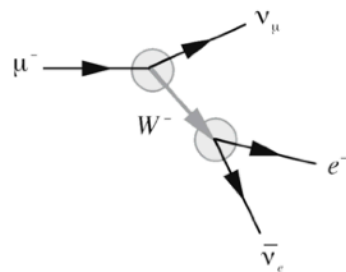
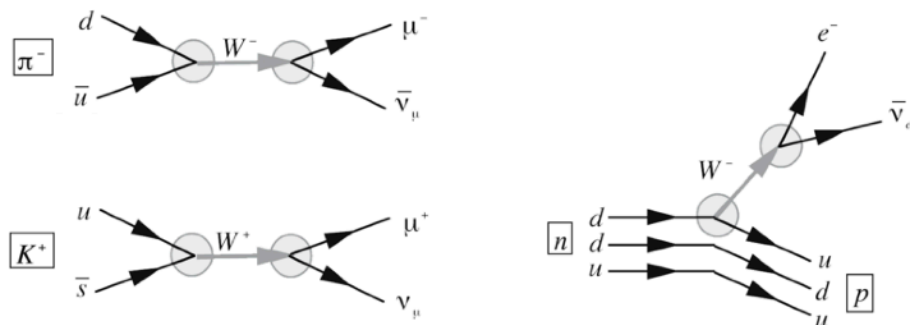


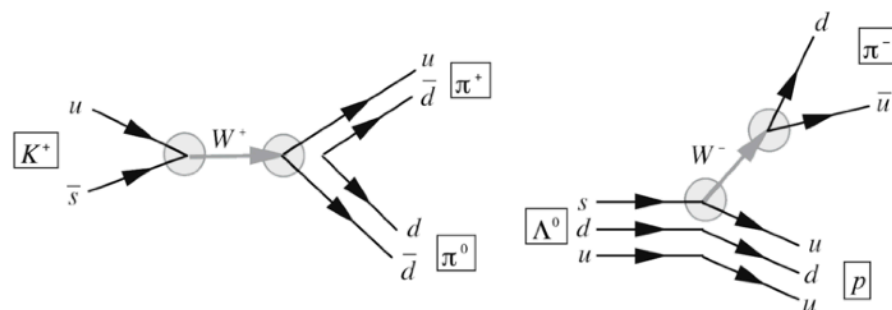
Figure 13.2 - Feynman diagram of the interaction between two electrons via a photon



(a) leptonic



(b) semi-leptonic



(c) hadronic

Figure 13.3 - Examples of Feynman diagrams leptonic, semi-leptonic and hadronic weak interactions

current, whose vector is the gauge boson Z^0 . The gauge bosons are the only ones which present masses, and these are very high, which imposes, by combining the relation $\Delta E \cdot \Delta t \approx \hbar$ of uncertainty of Heisenberg and the relation $\Delta E = mc^2$ of Einstein, a very short lifespan Δt of these bosons, and consequently, since the speed of light is an insurmountable limit, an extremely small range of the interaction via these bosons (of the order of $10^{-15} [m]$), which explains why this interaction does not manifest itself than at the scale of the atomic nucleus.

As the gauge bosons W^+ et W^- have a non-zero electric charge, fermions can change electric charge during an interaction by exchange of W^+ or W^- , which changes their *flavor* (we call flavor of a fermion its nature: electron, neutrino, quark u, quark d, etc.). For example, beta radioactivity is explained by the emission of a W^- by a quark d of the neutron, which then changes flavor and becomes quark u . Then, the W^- materializes in the form of an electron and an electronic anti-neutrino (figure 13.3, b).

The gauge boson Z^0 has no electrical charge, and therefore cannot induce a change in flavor during a weak interaction. The weak interaction by neutral current is quite similar to the exchange of a photon. Two fermions which can exchange a photon can also exchange a Z^0 , with the exception of the neutrino which can exchange a Z^0 but cannot exchange a photon since it is a neutral particle.

There are several types of weak interactions according to the fermions which interact: leptonic interactions, semi-leptonic interactions and hadronic interactions, of which examples of Feynman diagrams are reported in figure 13.3.

Note that the electromagnetic interaction and the weak interaction were unified in a quantum theory which was called *electroweak theory*.

Strong interaction and quantum chromodynamics theory

The strong interaction is a short-range interaction between quarks via gluons, gauge bosons that are vectors of this interaction. It is this interaction which explains not only the *mesons* composed of a quark and an anti-quark and the *baryons* composed of three quarks, but also how neutrons and protons can bond to form atomic nuclei.

To develop a quantum theory of strong interaction, it was necessary to call upon a new type of charges, called *charges of color*, from where the name of *theory of quantum chromodynamics*. Each quark has a charge of color, red ($R=rouge$), green ($V=vert$) or blue ($B=bleu$), and anti-quarks have a charge of one of the complementary colors (\bar{R}), (\bar{V}) or (\bar{B}).

The strong interaction is then explained by the exchange of "colored" gluons between elementary fermions with a color charge, which allows the color charges to be exchanged between fermions. There are 8 gluons of different colors, corresponding to 8 different combinations of a color and an anti-color. Thus, when exchanging a gluon between two quarks, they exchange their respective colors. In addition, since gluons carry a charge of color, they can also interact with each other, which is not the case with other gauge bosons. Leptons do not have a color charge and therefore do not undergo strong interaction.

Although the mass of the gluons is zero, the strong interaction is of very short range, of the order of $10^{-15} [m]$, and it has a rather strange characteristic: the more the quarks are distant from each other, the more the force of interaction between them is strong. And if they are

corresponding anti-color (anti-red, anti-green or anti-blue). The doublets formed by a quark and an anti-quark (among the quarks u , d , s or c) are represented in the diagram of figure 13.4 (b), in the case of global spin of 1 and 0, with the name given to the particle corresponding to this doublet.

Particle masses and Higgs boson

In a first version of the Standard Model, all the particles described (leptons and quarks) had to be of zero mass, which is obviously false as the table in figure 13.5 clearly shows. To make up for this gap in the initial Standard Model, theorists have imagined a fifth interaction, different from the other four (electromagnetic, weak, strong and gravitational), and calling on a field whose quantum is a particle of spin 0: *the boson of Higgs* H^0 (figure 13.1). It is then the

Fermions (spin 1/2)		Electric charge (q_e)	Mass (MeV/c^2)
lepton electron	e^-	-1	0,51
lepton muon	μ^-	-1	106
lepton tau	τ^-	-1	1777
lepton neutrino electron	ν_e	0	< 0,0000022
lepton neutrino muon	ν_μ	0	< 0,17
lepton neutrino tau.	ν_τ	0	< 15,5
quark Up	u	+2/3	2,55
quark Down	d	-1/3	5,04
quark Charm	c	+2/3	1270
quark Strange	s	-1/3	105
quark Top	t	+2/3	173100
quark Bottom	b	-1/3	4200

Jauge bosons (spin 1)		Electric charge (q_e)	Mass (MeV/c^2)
photon	γ	0	0
boson	W^+	-1	80398
boson	W^-	+1	80398
boson	Z^0	0	90187
8 gluons	g	0	0

Jauge bosons (spin 0)		Electric charge (q_e)	Mass (MeV/c^2)
boson Higgs	H^0	0	125000

Figure 13.5 - The charges and masses of the various particles

interactions between the elementary fermions of zero mass and the Higgs field via the Higgs bosons which provide a mass to the fermions of the Standard Model. The existence of the Higgs boson has been verified experimentally at CERN, quite recently.

***The problems of the standard model which already have solutions
in the theory of the perfect cosmological lattice***

The standard particle model, despite its undeniable success, leaves many questions unanswered. In the rest of this chapter, we will try to see if an approach to the standard model by our approach of the perfect cosmological lattice can provide an answer to these various questions. It will not be a question here of giving a complete and quantitative answer to all these problems, but of sketching, in a very qualitative way, in other words "with the hands", how the cosmological lattice could provide a solution to these problems. Some of the problems raised by the standard model already contain a sketch of an explicit solution in the previous chapters.

So let's take a tour of the problems posed by the standard model which already have an explanation in the approach of the cosmological lattice and explain how the cosmological lattice answers, at least partially, to these various problems:

- the absence of gravitational interaction in the standard model:

The gravitational interaction is directly part of the results obtained with the cosmological lattice, as a static solution of Newton's second partial equation, and it is moreover this same equation in its dynamic form which made it possible to introduce and give a simple explanation of quantum physics and the notion of spin of loop topological singularities.

- the need for the Higgs boson and the impossibility of calculating the masses of the various fermions and bosons in the standard model:

In the basic standard model, fermions have no mass, and theorists had to introduce an ad-hoc mechanism, the interaction with the Higgs field via the Higgs boson, which provides the mass of inertia to the elementary particles. However, in the standard model, it is not possible to obtain quantitative values of the inertia masses of the particles, which must therefore be "calibrated" on the values obtained experimentally. The theory of the cosmological lattice actually contains a mechanism fairly analogous to the Higgs field: it is the field of the masses of inertia of the "corpuscles" of the network (which are therefore a kind of analog of the spin 0 Higgs bosons) as well as the elastic energy of distortion of the lattice, which are responsible together for the relativistic properties of inertia of topological singularities, and which allow a quantitative calculation of the masses of inertia of topological singularities, without having to "calibrate" these values on results experimental.

- the physical nature of the electromagnetic interaction in the standard model:

The electromagnetic interaction, as well as its vector boson, the photon, with its various quantum properties, are an integral part of the theory of the cosmological lattice, and have there a simple and well-defined physical explanation based on the field of rotation within the cosmological lattice.

- the physical nature of the weak interaction in the standard model:

A weak interaction presenting an analogy with the weak interaction of the standard model has been obtained in the theory of the cosmological lattice (chapter 9), in the form of a very

short-range bonding force binding "topological fermions" between them (twist disclination loops to edge dislocation loops), by coupling their rotation and curvature charges.

- *violation of the CP invariance (charge / parity) in the standard model:*

In the current universe, there is a violation of the invariance **CP** (charge / parity) that theorists believe to be the probable cause of the matter / anti-matter asymmetry and of the matter / anti-matter imbalance in the current universe. In the theory of the cosmological lattice, this weak asymmetry between matter and anti-matter exists well, and is explained perfectly by the existence of the charge of curvature by bending of the edge dislocation loops, charge which has absolutely no equivalent in the standard particle model. This same phenomenon is also behind the explanation of the famous dark matter of astrophysicists and the disappearance of anti-matter during the cosmological evolution of the universe.

- *the absence of explanation of the dark energy and the dark matter in the standard model:*

These two concepts invented by theorists to provide explanations for the acceleration of cosmological expansion and the gravitational behavior of galaxies both have a direct explanation in the theory of the cosmological lattice: the energy of elastic distortion with regard to dark energy and the repulsive gravitational force of the neutrino sea with respect to black matter.

***The problems of the standard model which have not yet been explained
in the theory of the perfect cosmological lattice***

Among the problems of the standard model of elementary particles, there are some for which plausible explanations have not yet appeared in the theory of the cosmological lattice. These include:

- *the existence of fermions in the form of three generations of leptons and quarks:*

If the fermions correspond to topological singularities in the theory of the cosmological lattice, the existence of fermions in the form of leptons and quarks, as well as the existence of three generations of these fermions, should probably be explained by a judicious choice of the structure of the cosmological lattice and of the constitution of elementary particles as topological singularities in the form of dispiration loops, judicious assemblies of loops of twist disclination, of edge disclination, of edge dislocation and of mixed dislocation .

- *the existence of three massive gauge bosons in the weak interaction:*

Since the weak interaction has already appeared in our approach as the force linking the twist disclination loops to the edge dislocation loops, it remains to find out what the massive gauge bosons, vectors of this interaction, are in cosmological lattice theory.

- *the existence of a strong interaction linking quarks by a color confinement mechanism:*

The strong interaction, with its color confinement mechanism and its vector bosons, the gluons, is the only interaction that has not yet appeared in the framework of cosmological lattice theory. But we have already encountered mechanisms which could be very interesting potential candidates to explain this force and its asymptotic behavior, such as for example the mechanisms generating a fault energy within the lattice, such as the dissociation of a dislocation by example.

- *the existence of quantified electrical charges, of relative values 1, 1/3 and 2/3:*

The electrical charges of fermions have relative values 1, 1/3 and 2/3 between the charge of the electrons and the charges of the quarks. These quantified values have absolutely no explanation in the standard model, but it is a safe bet that the choice of a particular structure of the cosmological lattice could provide an explanation for this problem.

In the rest of this chapter, we will try to find answers and explanations to these questions of the standard model, playing exclusively on the structure of the cosmological lattice and on the properties of the topological singularities that it can contain. In the standard model, 26 different parameters are required in the case where the neutrinos are massive to obtain a functional theory, such as the masses of the particles and the intensities of the various forces, and these parameters must necessarily be “calibrated” on the values of experimental results. It is a safe bet that the model of the cosmological lattice can make it possible to greatly reduce the number of parameters to be adjusted, simply by the fact that it can provide new physical explanations for phenomena that do not have any in the standard model.

A "colored" face centered cubic lattice with specific stacking and rotation rules to explain the first family of quarks and leptons of the standard model

In the perfect cosmological lattice, we have seen that the simplest topological singularity for explaining the electric charge is the twist disclination loop. As we saw in chapter 8, for the gravitational interaction of twist disclination loops to satisfy behaviors similar to experimentally observed behaviors (time dilation, curvature of wave rays), it is sufficient that the coefficients α_{BV} and β_{BV} in the expressions $R_{BV} = R_{BV0} e^{\alpha_{BV}\tau}$ and $\Omega_{BV} = \Omega_{BV0} e^{\beta_{BV}\tau}$ giving the dependence of the radius and the torsion angle of the twist disclination loop as a function of the background expansion of the lattice satisfy the relation $3\alpha_{BV} + 2\beta_{BV} = 1/8$. This implies that the angle of twist Ω_{BV} could

- (i) either be a constant independent of the expansion, in which case $\alpha_{BV} = 1/24$ and $\beta_{BV} = cste$, which allows the existence of a topological reason for the explanation of the existence of discrete values, independent of the expansion, for the angle Ω_{BV} ,
- (ii) either depend in fact on the volume expansion, in which case Ω_{BV} cannot take a discrete

Conjecture 12 - the angle Ω_{BV} takes discrete values related to the symmetry of the lattice and independent of volume expansion ($\beta_{BV} = cste$)

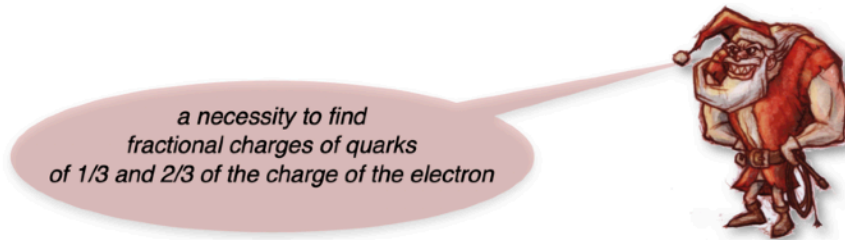


Figure 13.6 - The twelfth conjecture on the quantification of the angles of rotation of the twist disclination loop

value which is directly linked to the structure of the lattice since this angle would then depend continuously on the volume expansion.

Thus, so that it appears quantified charges like the charge of the electron, but also fractional charges of $1/3$ and $2/3$ of the charge of the electron as it is the case of the quarks of the standard model, the screw loops should be obtained by rotating the two planes inside the loop by an angle *corresponding to the symmetry of the lattice*, for example $\pi/2$, π , $3\pi/2$, ... in the directions perpendicular to the planes of a simple cubic lattice, or $\pi/3$, $2\pi/3$, π , ... in the directions perpendicular to the compact planes of a compact hexagonal or face-centered cubic lattice.

We will therefore choose hypothesis in the form of the conjecture 12 explained in figure 13.6 to try to find a cosmological lattice which could explain the standard model of elementary particles.

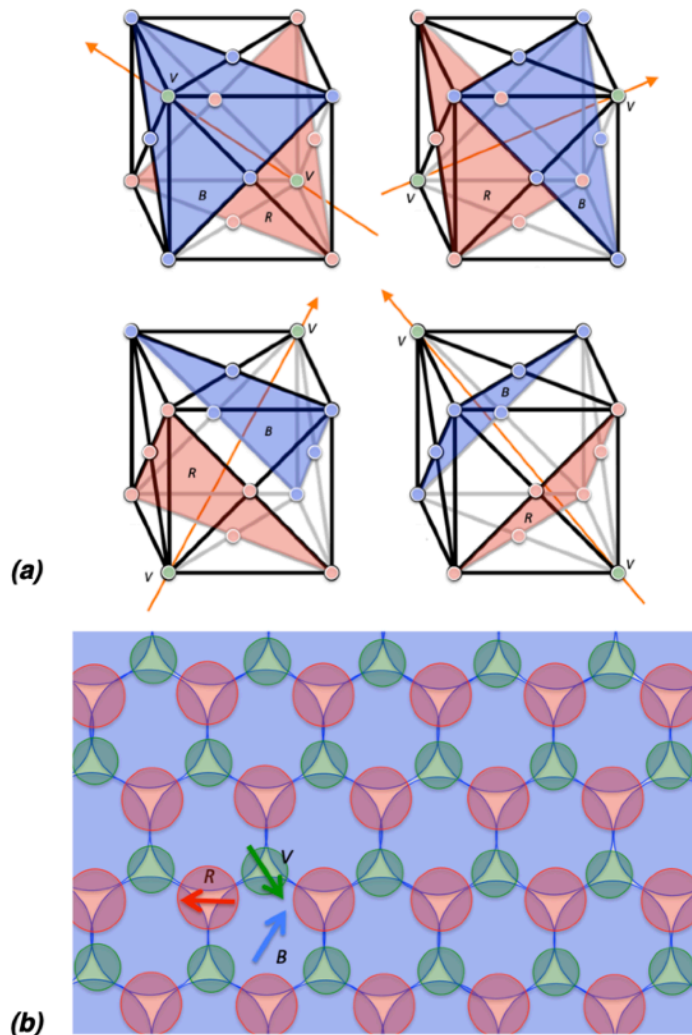


Figure 13.7 - An imaginary, "axial", face-centered cubic cosmological lattice:
(a) CFC cell with the dense planes **R,B,V** showing a regular compact stacking in the four directions of space perpendicular to the four families of dense planes,
(b) plane representation of the **R,B,V** stacking of three successive dense planes, with the preferred directions of the layers associated with the axial properties of the lattice.

To satisfy this assumption, it seems a priori preferable to choose a compact stacking lattice, namely a compact hexagonal lattice or a face-centered cubic lattice. For reasons that will be explained later, we will choose the face-centered cubic (FCC) lattice, as illustrated in figure 13.7.

In the FCC cell, there are four families of dense planes, shown in figure 13.7(a). The four axes perpendicular respectively to these four families of dense planes are third-order rotational symmetry axes passing through two opposite vertices of the FCC cell. Only rotations of $2\pi/3$, $4\pi/3$, 2π , ... about these axes respect the dense stacking of the FCC cell.

Let us imagine a priori that this FCC lattice is moreover an axial lattice, i.e. that each plane of "corpuscles" has a preferential direction represented in figure 13.7(b) by arrows making an angle of $2\pi/3$ between each dense layer. This axial property can be represented by "colored planes of corpuscles" with alternating three fundamental colors **R**, **B**, **V**. Each of these colors represents one of the three preferred directions of the dense planes, as shown in figure 13.7(b). These imaginary "colors" are chosen only for convenience, and so far have no relation to the

Conjecture 13 - the stacking of the **R**, **B**, **V** planes follows three basic rules with respect to the axial properties of the CFC lattice:

Rule 1: the alternation of the planes **R**, **B**, **V** cannot be broken, either by impossibility, or by penalty of an extremely high stacking fault surface energy γ_1 ,

Rule 2: there may appear a shift in the succession of **R**, **B**, **V** planes according to a connecting fault plane perpendicular to the dense planes, and this shift has a non-zero connecting fault surface energy γ_0 ,

Rule 3: if a plane of a given color is rotated by an angle $\pm 2\pi/3$, $\pm 4\pi/3$ ou $\pm 2\pi$, it changes color according to the table below

rotation angle Ω_{BV}	color change	colors R , V , B and anti-colors \bar{R} , \bar{V} , \bar{B}
$\begin{cases} +2\pi \\ 0 \\ -2\pi \end{cases}$	$\begin{cases} R \rightarrow R \\ V \rightarrow V \\ B \rightarrow B \end{cases}$	
$\begin{cases} +2\pi/3 \\ -4\pi/3 \end{cases}$	$\begin{cases} R \rightarrow V \\ V \rightarrow B \\ B \rightarrow R \end{cases}$	
$\begin{cases} +4\pi/3 \\ -2\pi/3 \end{cases}$	$\begin{cases} R \rightarrow B \\ V \rightarrow R \\ B \rightarrow V \end{cases}$	

three heuristic rules necessary to create an ad hoc "axial" cosmological lattice

Figure 13.8 - The thirteenth conjecture on the stacking and rotation rules of the **R**, **B**, **V** planes of the axial CFC cosmological lattice

"colors" used in the standard model to explain the color charge of quarks and gluons. Even if we do not know the physical reason for the existence of this axial property represented by these "colored planes", we can suppose that this alternation of colors of the corpuscular planes can be a condition for the existence of a perfect cosmological lattice in the absence of topological singularities, and that, if the **R**, **B**, **V** alternation of the lattice planes is broken by the presence of a topological singularity, fault energies can appear if a "corpuscular" plane does not follow the **R**, **B**, **V** arrangement. Let us then postulate *a priori* rules of stacking and rotation of the colored planes in this very particular lattice, in the form of a thirteenth conjecture reported in figure 13.8. In this conjecture, there are three rules which are all three associated with *the axial property of the FCC lattice* that we have postulated:

- *The first rule* stipulates that the **R**, **B**, **V** alternation of the dense planes of the lattice cannot be broken, under penalty of an important stacking fault energy, i.e. the preferential directions associated with the "corpuscles" must *if possible* alternate with an angle of $\pm 2\pi / 3$ from one dense layer to the other.
- *The second rule* states that there may be planes perpendicular to the dense planes that separate two domains of the lattice with a shift in the succession of planes **R**, **B**, **V**. These joints thus correspond to sorts of connecting fault planes, and it is assumed that these joints have a *non-zero connecting fault surface energy* γ_0 .
- *The third rule* states that if a dense plane is rotated by an angle $\pm 2\pi / 3$, $\pm 4\pi / 3$ or $\pm 2\pi$ about an axis perpendicular to this family of dense planes, and thus leaves the FCC structure intact, it is the preferred direction of this dense plane represented by the arrows in figure 13.7(b) that changes, and thus it is the "color" of this plane that changes since the color represents this preferred direction.

Existence of quarks due to combining a screw disclination loop with an edge dislocation loop

We can introduce a screw disclination loop in our particular lattice, shown symbolically in figure 13.10d, with a rotation angle of the lower plane of $\pm 2\pi / 3$ or $\pm 4\pi / 3$ or $\pm \pi$. But according to rule 3, a rotation of $\pm 2\pi / 3$ or $\pm 4\pi / 3$ will change the color of the inner plane of the screw disclination loop. In this way, rule 1 would no longer be satisfied. Therefore, on the one hand, an interstitial or lacunar edge loop must be added to satisfy rule 1 with the upper dense plane, and on the other hand, a cylinder must be induced in which all dense planes below the screw disclination loop change color to satisfy rule 1. Then, according to rule 2, *a cylinder of connecting faults with fault surface energy* γ_0 is generated, as schematically represented in figures 13.9a to 13.9d.

The intercalated plane in the case of the interstitial edge loop has one of the three colors **R**, **B**, **V** (red, blue, green), whereas the missing plane in the case of the lacunar edge loop has the anti-color of the color of the interrupted plane, namely one of the colors $\bar{\mathbf{R}}$, $\bar{\mathbf{B}}$ or $\bar{\mathbf{V}}$. One uses indeed in the figures the complementary colors of **R**, **B**, **G**, which are the colors cyan, magenta and yellow, as represented in figure 13.8. In the four cases (figures 13.9a to 13.9d), the screw disclination loop is obviously linked to the edge dislocation loop by the weak force described in chapter 9, but also by the necessity to introduce the edge loop to ensure the succession of the colors of the planes at the level of the screw disclination loop.

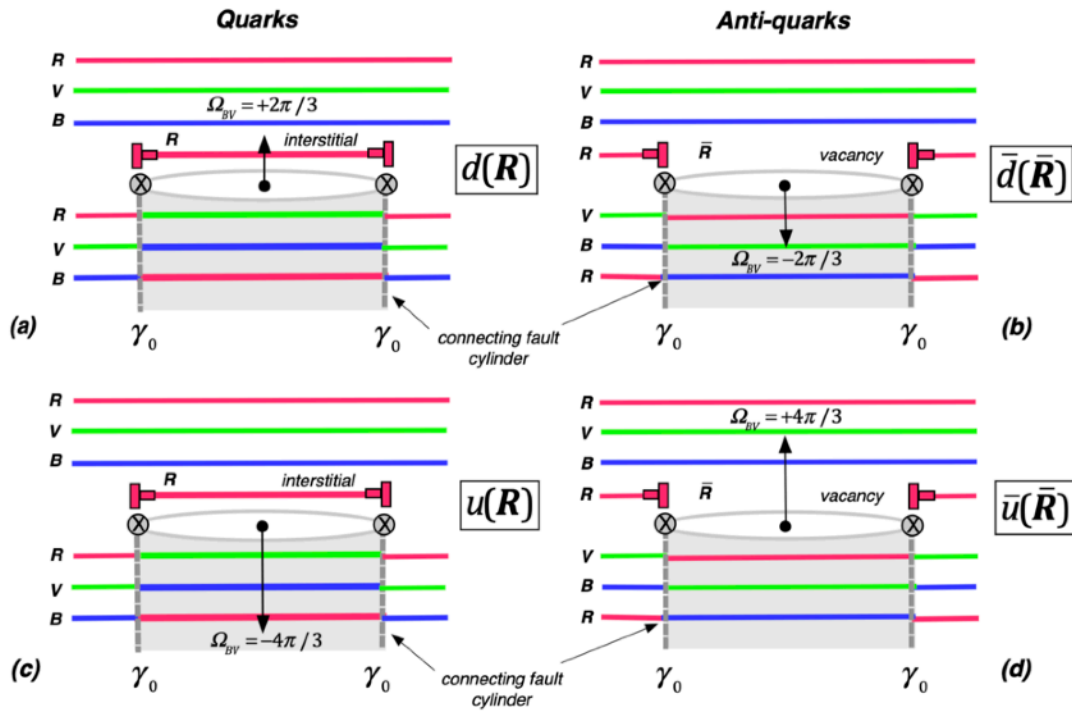


Figure 13.9 - quarks and antiquarks formed by combinations of screw disclination loops of quantized angles with edge dislocation loops which ensure the continuity of succession of planes R, B, V

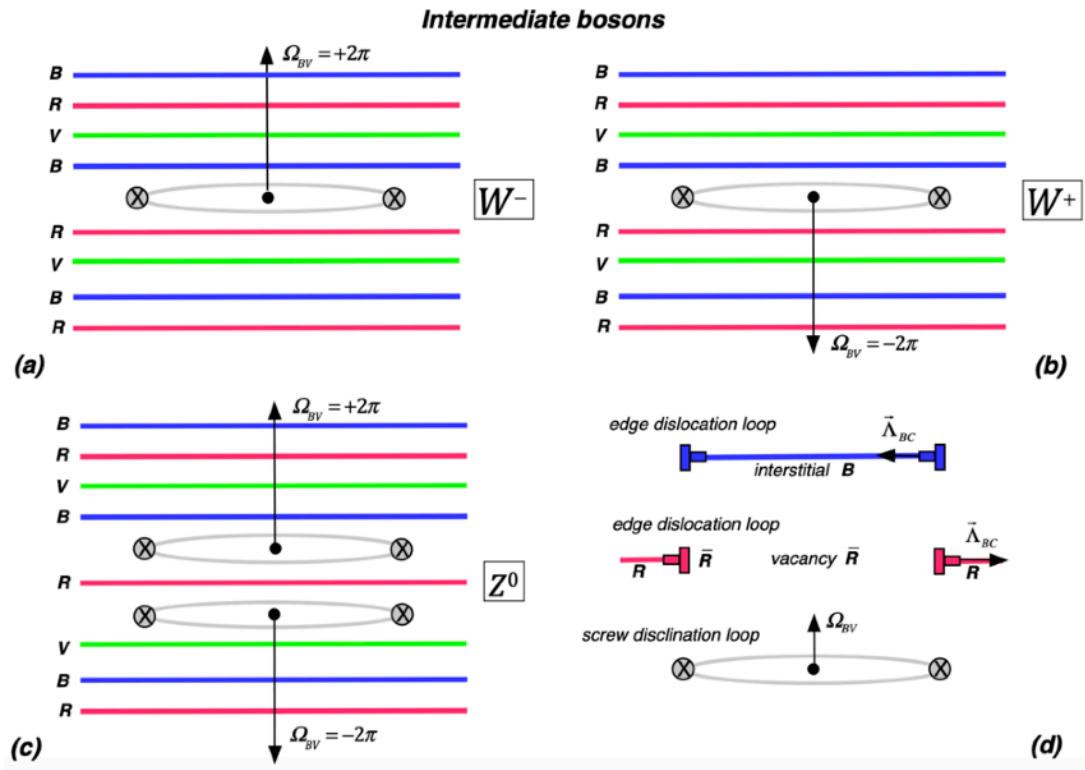


Figure 13.10 - Intermediate bosons formed by screw disclination loops of angle $\pm 2\pi$ which do not need edge dislocation loops to ensure the continuity of succession of R, B, V planes

The dispirations thus formed have a "color", which corresponds to the color of the interstitial loop plane or to the anti-color of the lacunar loop plane (the anti-color or complementary color of the corpuscular plane in which the lacunar loop appears).

Existence of intermediate gauge bosons

As for disclination loops of angle $\pm 2\pi$ (figures 13.10a to 13.10c), they do not need to be combined with edge loops since these rotations do not cause any color change in the lower planes, and therefore also no connecting fault cylinder below the loop.

In the table of figure 13.11, we have reported the properties of the different topological singularities thus formed, giving them, as in figures 13.9 and 13.10, a name chosen "by chance", and using the fact that the two dispirations on the right (a and c) in figure 13.9 are clearly the anti-loops of the loops on the left (b and d).

<i>name</i>	Ω_{BV}	$q_{\lambda BV}$	<i>edge loop</i>	$q_{\theta BC}$	<i>color</i>
<i>d</i>	$+2\pi/3$	$-2\pi^2 R_{BV}^2/3$	<i>interstitial</i>	$-2\pi a$	<i>R, V ou B</i>
<i>u</i>	$-4\pi/3$	$+4\pi^2 R_{BV}^2/3$	<i>interstitial</i>	$-2\pi a$	<i>R, V ou B</i>
\bar{d}	$-2\pi/3$	$+2\pi^2 R_{BV}^2/3$	<i>vacancy</i>	$+2\pi a$	\bar{R}, \bar{V} ou \bar{B}
\bar{u}	$+4\pi/3$	$-4\pi^2 R_{BV}^2/3$	<i>vacancy</i>	$+2\pi a$	\bar{R}, \bar{V} ou \bar{B}
W^-	$+2\pi$	$-2\pi^2 R_{BV}^2$	-	0	-
W^+	-2π	$+2\pi^2 R_{BV}^2$	-	0	-
Z^0	$(+2\pi)+(-2\pi)$	0	-	0	-

Figure 13.11 - The seven singularities composed of a screw disclination loop combined or not with interstitial or lacunar edge dislocation loops

In table 13.11, we then see that the rotation charges $q_{\lambda BV}$, analogous to the electric charge, have three different values, corresponding respectively to $1/3x$, $2/3x$ and $1x$ the charge of the loops W^- or W^+ . On the other hand, only the dispirations d , u , \bar{d} and \bar{u} present a non-zero curvature charge $q_{\theta BC}$, and the sign of these charges, positive in the case of the lacunar edge loop and negative in the case of the interstitial edge loop, implies, as we have already postulated with conjecture 8, that the particles d and u correspond by analogy to matter and that their anti-particles \bar{d} and \bar{u} correspond to anti-matter. The parameter a is in this

case the distance between two dense planes of the lattice. As for the particles W^- , W^+ and Z^0 which do not have a curvature charge, they must certainly have a large mass since they are loops of screw disclination with a very high rotation angle $\Omega_{BV} = -2\pi$.

Weak interaction between quarks via intermediate bosons

It is interesting to note here that the combination of two dispirations d and \bar{u} , or \bar{d} and u contributes to create a pure screw disclination loop W^- or W^+ , which can again be transformed into a pair d and \bar{u} , or \bar{d} and u . One can also imagine an exchange of an W^- or W^+ loop between two dispirations d and \bar{u} , or \bar{d} and u , which will change their nature, or to put it more colorfully or poetically, their "taste" or "flavor".

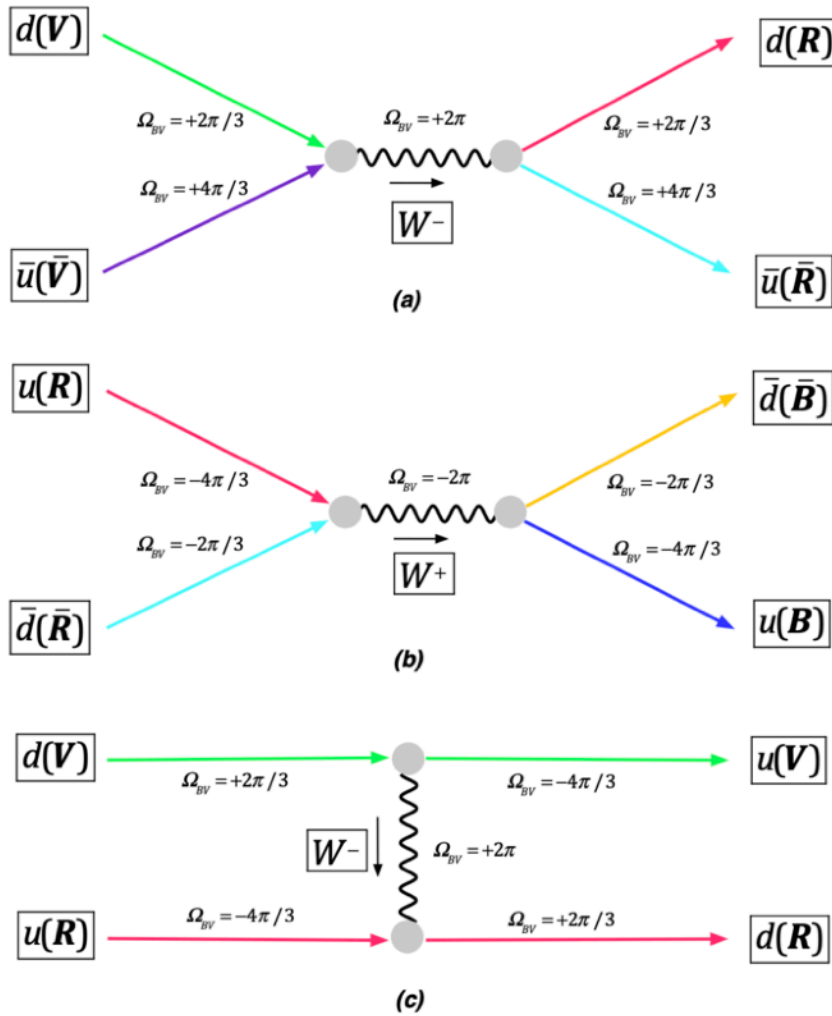


Figure 13.12 - Feynman diagrams of mechanisms of combinations and exchanges of intermediate bosons between quarks of the table 13.10

These combinations and exchanges are illustrated in figure 13.12 as *Feynman diagrams*. They are characterized by the fact that the total rotation Ω_{BV} is conserved, which ensures at the same time the conservation of the rotation charge $q_{\lambda BV}$. We also see that the total charge

$q_{\theta BC}$ is also conserved in these reactions. It is then undeniable that these reactions have a strange similarity with the weak interactions of the standard model reported in figure 13.3.

Existence of localized "baryons" and "mesons", formed by 3 and 2 dispirations

Each of the dispirations in figures 13.9a to 13.9d generates a connecting fault cylinder that has an energy proportional to the lateral surface of the cylinder. Consequently, it is impossible for these dispirations to appear in isolation, because the connecting fault cylinder would then be of gigantic length $\sim R_\infty$, and consequently of gigantic energy. One can then ask how to generate singularities composed of such dispirations, and which are of reasonable energy.

In fact, there are three ways to combine the four dispirations in figure 13.9 so that the resulting topological singularity is perfectly localized, namely that the connecting fault tube is of finite

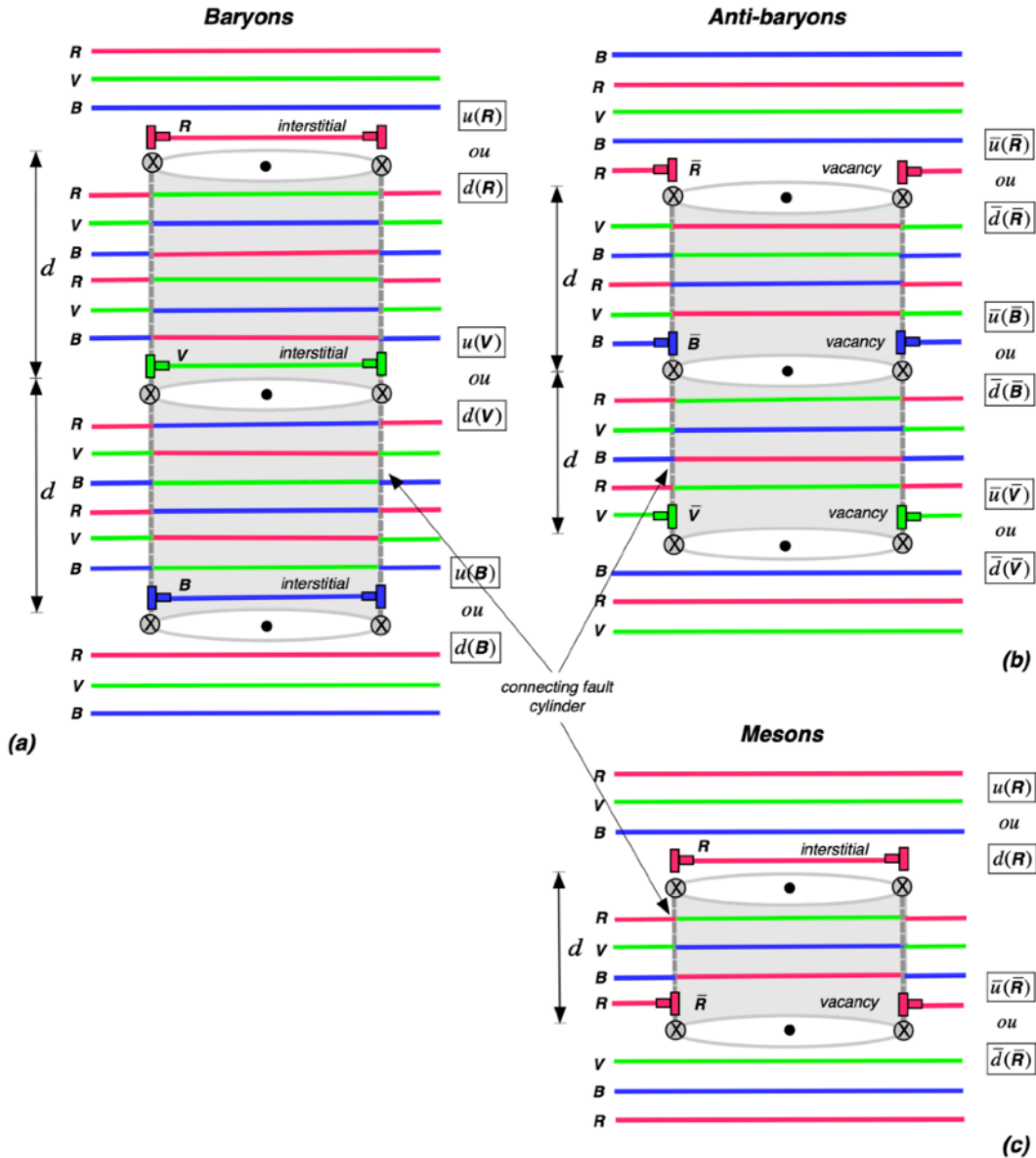


Figure 13.13 - The three possible combinations of 2 or 3 dispirations allowing to form perfectly localized topological singularities

length:

- the combination of three singularities u or d represented in figure 13.13a,
- the combination of three anti-singularities \bar{u} or \bar{d} represented in figure 13.13b,
- the combination of one singularity u or d with one anti-singularity \bar{u} or \bar{d} represented in figure 13.13c.

In order for the three rules previously stated to be all perfectly satisfied in these various combinations, it is necessary that:

- the sum of the angles of rotation Ω_{BV} of all the dispirations of the combination is zero or a multiple of 2π , which allows the connecting fault tube to be of finite length,
- the color of the assembly thus formed is "white", thus that the assembly presents the sum of the 3 colors R, G, B (figure 13.13a), or the sum of the 3 anti-colors $\bar{R}, \bar{V}, \bar{B}$ (figure 13.13b), or the sum of one of the colors R, G, B with its respective anti-color $\bar{R}, \bar{V}, \bar{B}$ (figure 13.13c).

In the table of figure 13.14, the 8 different possible combinations of 3 dispirations of the table

combinations	symbol spin 1/2	symbol spin 3/2	Ω_{BV}	$q_{\lambda BV}$	edge loop	$q_{\theta BC}$
ddd	e^- (?) electron	Δ^-	$+2\pi$	$-2\pi^2 R_{BV}^2$	interstitial	$-6\pi a$
dud	n neutron	Δ^0	0	0	interstitial	$-6\pi a$
udu	p proton	Δ^+	-2π	$+2\pi^2 R_{BV}^2$	interstitial	$-6\pi a$
uuu	e^{++} (???) lepton ?	Δ^{++}	-4π	$+4\pi^2 R_{BV}^2$	interstitial	$-6\pi a$
$\bar{d}\bar{d}\bar{d}$	e^+ (?) positron	$\bar{\Delta}^+$	-2π	$+2\pi^2 R_{BV}^2$	vacancy	$6\pi a$
$\bar{d}\bar{u}\bar{d}$	\bar{n} antineutron	$\bar{\Delta}^0$	0	0	vacancy	$6\pi a$
$\bar{u}\bar{d}\bar{u}$	\bar{p} antiproton	$\bar{\Delta}^-$	$+2\pi$	$-2\pi^2 R_{BV}^2$	vacancy	$6\pi a$
$\bar{u}\bar{u}\bar{u}$	e^{--} (???) anti-lepton ?	$\bar{\Delta}^{--}$	$+4\pi$	$-4\pi^2 R_{BV}^2$	vacancy	$6\pi a$

Figure 13.14 - The "white" baryons formed by 3 dispirations,
and the four leptons obtained by collapsing combinations of quarks
 ddd , $\bar{d}\bar{d}\bar{d}$, uuu and $\bar{u}\bar{u}\bar{u}$

of figure 13.11 have been reported with their property, giving them a symbol and calling them baryons by analogy with the standard model.

In this table, the analogy with the baryons of the standard model of elementary particles, composed of triplets of quarks u and d or triplets of anti-quarks \bar{u} and \bar{d} , is flagrant and perfect. Not only do we see particles composed of quarks with fractional rotation charges $q_{\lambda BV}$ corresponding to the electric charges of the standard model, but we also add here the curvature charge $q_{\theta BC}$ which has no equivalent in the standard model, and which corresponds perfectly with our conjecture 8, namely that *the singularities of lacunar nature correspond by analogy to anti-matter and the singularities of interstitial nature to matter*. The fact that the particles of the standard model appear with two different symbols in this table for the combinations dud , udu , $\bar{d}\bar{u}\bar{d}$ and $\bar{u}\bar{d}\bar{u}$ is explained by the notion of spin of the screw disclination loops, developed in chapter 12. Indeed, if each quark has a spin $\pm 1/2$, then the spin composition can create a global spin of $\pm 1/2$ in the case of particles (*neutron*) and (*proton*) and anti-particles (*anti-neutron*) and (*anti-proton*), or a spin $\pm 3/2$ in the case of particles Δ^0 and Δ^+ and anti-particles $\bar{\Delta}^0$ et $\bar{\Delta}^-$. In the case of the combinations ddd , uuu , $\bar{d}\bar{d}\bar{d}$ and $\bar{u}\bar{u}\bar{u}$, the spins of the 3 quarks are obligatorily aligned (for a reason which remains to be explained, but which is most probably linked with the exclusion principle) and the composition of the spins can then only provide a global spin of $\pm 3/2$ in the case of the particles Δ^- and Δ^{++} and anti-particles $\bar{\Delta}^+$ and $\bar{\Delta}^-$. In the case of the combinations ddd and $\bar{d}\bar{d}\bar{d}$, the complete collapse of the quarks with spin $\pm 1/2$ then presents exactly the configuration of the leptons "electron" and "positron" as represented in figure 13.17. We will come back to this subject in the rest of this chapter.

In the table of figure 13.15, the different possible combinations of 2 dispirations of the table of figure 13.11 have been reported with their property, giving them a symbol and calling them *mesons* by analogy with the standard model.

combina- tions	symbol spin 0	symbol spin 1	Ω_{BV}	$q_{\lambda BV}$	edge loop	$q_{\theta BC}$
$d\bar{d}$	π^0	ρ^0	0	0	-	0
$d\bar{u}$	π^-	ρ^-	$+2\pi$	$-2\pi^2 R_{BV}^2$	-	0
$\bar{d}u$	π^+	ρ^+	-2π	$+2\pi^2 R_{BV}^2$	-	0
$u\bar{u}$	η^0	ω^0	0	0	-	0

Figure 13.15 - The mesons of "white" color formed by 2 dispirations

In this table, the analogy with the mesons of the standard model of elementary particles, composed of quarks doublet u or d with anti-quarks \bar{u} or \bar{d} , is flagrant and perfect. One

can see particles composed of quarks with fractional rotation charges $q_{\lambda BV}$, which correspond to the mesons of the standard model, but with a zero curvature charge $q_{\theta BC}$, which means that these topological singularities cannot be catalogued as anti-matter (singularities of lacunar nature) or matter (singularities of interstitial nature).

The fact that the particles of the standard model appear with two different symbols in this table is also explained by the notion of spin of the screw disclination loops, developed in chapter 12. Indeed, if each quark has a spin $\pm 1/2$, then the spin composition can create a global spin of 0 in the case of particles π^0 , π^- , π^+ and η^0 , or a spin ± 1 in the case of particles ρ^0 , ρ^- , ρ^+ et ω^0 .

The strong force and its asymptotic behavior

The quarks composing the particles in the tables of figures 13.14 and 13.15 are bound by a cylinder of connecting faults, so that the energy of the topological singularity increases as $E_\gamma \sim \gamma_0 2\pi R_{BV} d$ if the distance d between two dispirations increases. The binding force of the dispirations is thus "*asymptotic in nature*", in the sense that it is a *strong force*, because *the binding force increases if one tries to separate the dispirations*. This is similar to the case of the stacking fault energy between two partial dislocations in a FCC lattice or the case of the connecting fault energy between three partial dislocations in an axial cubic lattice (see chapter 2). The equilibrium distance d between dislocations is then controlled by a competition mechanism between the interaction energy between the loops composing the particle and the connecting fault energy between the loops, a mechanism quite similar to that described in the case of figure 2.16.

Strong interaction between quarks via the gluon gauge bosons

In the standard model, the quantum treatment of the "colors" of quarks is provided by *quantum chromodynamics*, in which there are 8 colored gauge bosons, carriers of the strong force, called *gluons*.

And it is the exchange of a colored gluon between two quarks that allows then to exchange the color of these two quarks, by an interaction that can be represented, as in figure 13.16, in the form of a *Feynman diagram* illustrated by the configuration of the topological singularities involved.

The colored gluons then correspond to two associated edge dislocation loops, one of interstitial nature and one of lacunar nature, and their rotation charge $q_{\lambda BC}$ is zero. The edge loops are linked together by the existence of a connecting fault cylinder, and are therefore subject to the strong force. As for their curvature charge $q_{\theta BC}$, it is null since we have $q_{\theta BC} = (+2\pi a) + (-2\pi a)$, so that *the energy associated to the distortions of this pair of loops must be extremely low*, and that, consequently, *the mass of the gluons must be almost null, while it has a non null energy coming from the connecting fault cylinder*. From this point of view, gluons are similar to photons.

In quantum chromodynamics, it is thought that it is this mechanism of exchange of gluons between neutrons and protons of the atomic nucleus that explains the cohesion of atomic nuclei. It is therefore a side effect of the strong force since these exchanges of colored gluons dis-

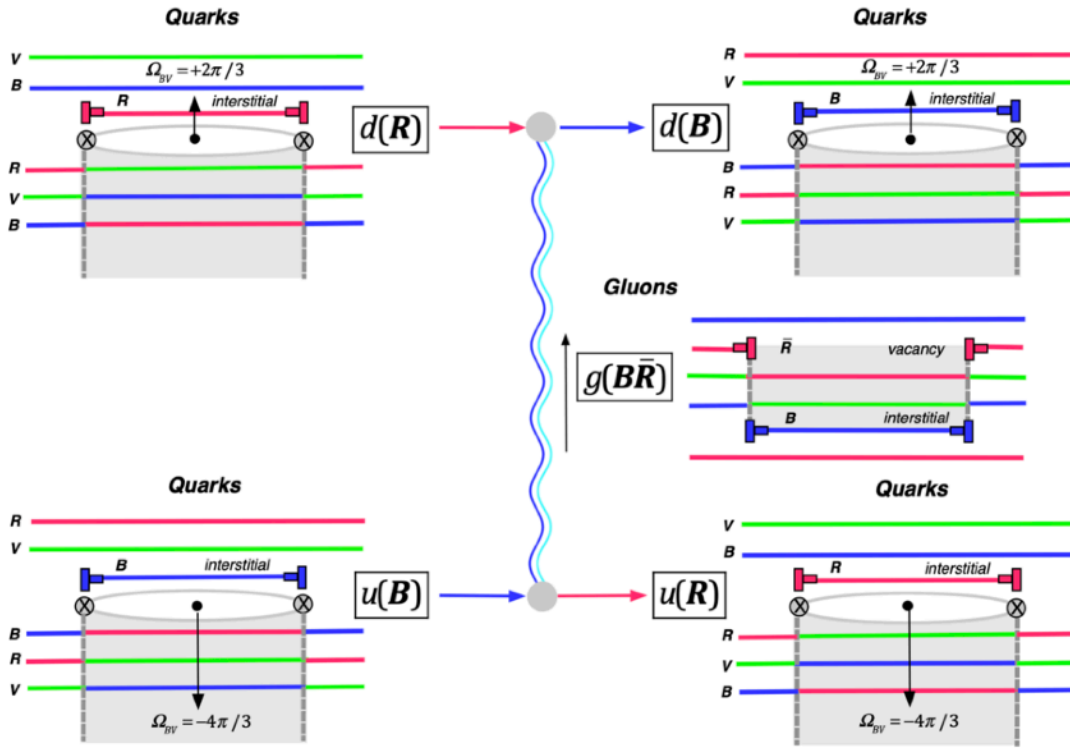


Figure 13.16 - Feynman diagram of the color exchange of two quarks by the exchange of a bicolor gluon

turb the distances between the dispirations composing the neutrons and protons, and consequently disturb the energies of the protons and neutrons.

The constitution of neutrino and anti-neutrino leptons

In the standard model, there is also a first family of quasi-punctual particles called leptons, represented by the electron e^- , the anti-electron or positron e^+ , the electron neutrino ν_e and the electron anti-neutrino $\bar{\nu}_e$.

In the cosmological lattice, we have already postulated the existence of the neutrino in the form of an edge dislocation loop of interstitial nature, while the anti-neutrino corresponded to an edge dislocation loop of lacunar nature. This is what allowed us to deduce exceptional repulsive gravitational properties for the neutrino, due to its curvature charge which largely dominates the attractive gravitational effects due to its inertial mass. In the case of the "colored cosmological lattice" of figure 13.7, in order to respect the three rules that this lattice must satisfy, the neutrino can only correspond to the insertion of three consecutive planes of color R, G, B , and the anti-neutrino to the subtraction of three consecutive planes $\bar{R}, \bar{V}, \bar{B}$, as represented in figures 13.17a and 13.17d, so as to form an inclusion or a hole that has no color, i.e. white color. In this form, neutrinos and anti-neutrinos have exactly the properties that we deduced in the previous chapters for prismatic edge dislocation loops, provided that their Burgers vector has a norm such that $|\vec{B}_{BC}| = 3a$, so that their curvature charge by flexion has a norm equal to $|\mathbf{q}_{\theta BC}| = 6\pi a$.

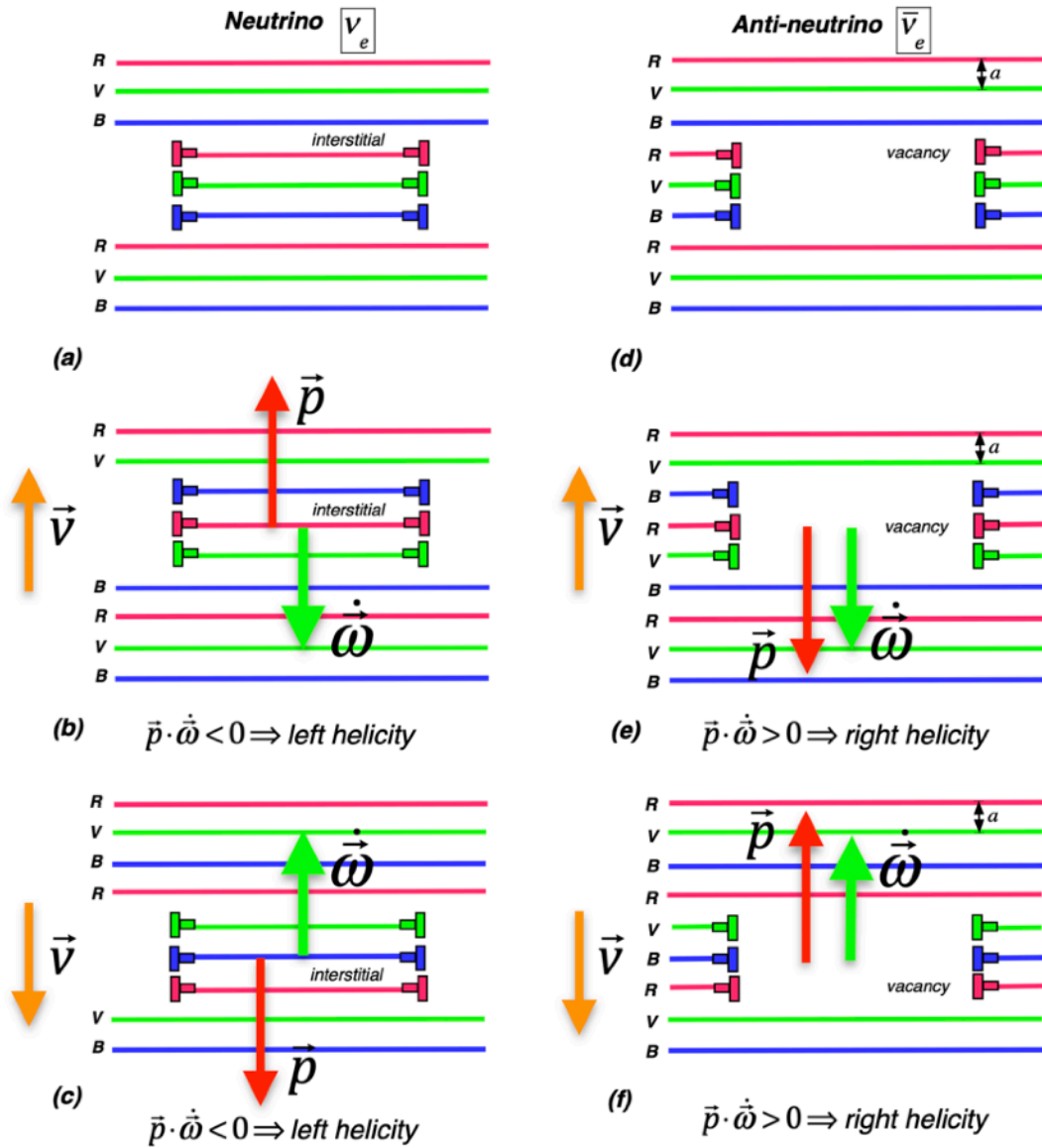


Figure 13.17 - The neutrino and the antineutrino and their negative and positive helicity as the scalar product of their momentum \vec{p} and the speed of rotation $\dot{\vec{\omega}}$ of their axial planes

In particle physics, the *helicity* $\vec{S} \cdot \vec{p} / |\vec{p}|$ of a particle is defined as the projection of its spin \vec{S} on the direction $\vec{p} / |\vec{p}|$ of its momentum \vec{p} (this projection corresponds to the component of the spin along the direction of propagation). We say that a particle's helicity is *right (positive)* or *left (negative)* depending on whether its spin is oriented in the same direction or in the opposite direction to its motion. In the case of the neutrino and the anti-neutrino, experimental observation shows that *all neutrinos always have a left helicity*, and that *all antineutrinos always have a right helicity*. And the fact that neutrinos are always left-handed is very important, because it explains *the phenomenon of parity violation in the weak interaction*.

An explanation of this helicity behavior can be given here by considering classically the motion of neutrinos and anti-neutrinos in figure 13.17. Indeed, if we consider that these particles

move in the lattice perpendicularly to the dense planes at velocity \vec{V} as illustrated in figures 13.17, we find that the direction of momentum \vec{p} associated with the displacements of the massive planes is in the direction of the neutrino's velocity \vec{V} , but in the opposite direction to the direction of the velocity \vec{V} of displacement in the case of the anti-neutrino. As for the direction of rotation of neutrinos and anti-neutrinos, represented by the angular velocity vector $\vec{\omega}$ of the "corpuscle" planes concerned, it can be seen that it is always opposite to the direction of the velocity \vec{V} . If we classically qualify the helicity of these motions by the sign of the scalar product $\vec{p} \cdot \vec{\omega}$ of the momentum \vec{p} and the angular velocity $\vec{\omega}$, we can see that the helicity of the neutrino is always negative, so that *the motion of the neutrino is always of left-handed helicity*, while this same product in the case of the anti-neutrino is always positive, so that *the motion of the anti-neutrino is always of right-handed helicity*.

The constitution of electron and positron leptons

As for the electron and the anti-electron or positron, we have already hypothesized that the screw disclination loop is a good candidate to represent them. In this case, to ensure that the rotation charge matches well, the rotation angle Ω_{BV} between two consecutive planes must be equal to $\pm 2\pi$, so that the norm of the rotation charge satisfies the relation $|\mathbf{q}_{\lambda BV}| = 2\pi^2 R_{BV}^2$. However, in this pure form, the screw disclination loop has already been identified as the particle W^- or W^+ in figures 13.10a and 13.10b. Moreover, the electron and the positron must present the dissymmetry between matter and anti-matter, and they must satisfy the weak leptonic interactions of figure 13.3. To satisfy these desiderata, one must again use a combination of a screw disclination loop of angle $\pm 2\pi$, which satisfies rule 3 and therefore has no color, with an edge dislocation loop corresponding to the insertion of three consecutive planes of color \mathbf{R} , \mathbf{G} , \mathbf{B} , or the subtraction of three consecutive planes $\bar{\mathbf{R}}$, $\bar{\mathbf{V}}$, $\bar{\mathbf{B}}$.

In principle, there should thus be four different electrons, of charges $\mathbf{q}_{\lambda BV} = \pm 2\pi^2 R_{BV}^2$ and $\mathbf{q}_{\theta BC} = \pm 6\pi a$ as represented in figures 13.18c to 13.18f. But in reality, one observes in nature only *the electron e^- and the anti-electron or positron e^+* . The "unknown leptons" represented in figures 13.18e and 13.18f could be considered in fact as a positive electron of matter and a negative anti-electron, but they are not observed in nature, whereas nothing seems a priori to show the reason in figures 13.17.

However, there could be a rather simple explanation, although difficult to justify. One could imagine that the charged leptons are in fact the results of collapses of three-quark baryons. Let us consider the simplest case, namely the compression of assemblies of quarks ddd and $\bar{d}\bar{d}\bar{d}$, so as to collapse the three screw loops into one, and to collapse the three edge loops into one. We then obtain directly the electron and the positron represented in figures 13.18c and 13.18d. But it would be necessary that these collapses lead to leptons of spin 1/2 since the electron and the positron are of spin 1/2. However, in table 13.14, we see that the assemblies of quarks ddd and $\bar{d}\bar{d}\bar{d}$ lead exclusively to baryons Δ^- and $\bar{\Delta}^+$ of spin 3/2, and that there are no baryons ddd and $\bar{d}\bar{d}\bar{d}$ with a spin 1/2. One can therefore imagine that the assemblies of quarks ddd and $\bar{d}\bar{d}\bar{d}$ with spin 1/2 must necessarily become leptons, thus electrons and positrons, as suggested in table 13.14.

By admitting this explanation, it becomes quite simple to explain the non observation of the

"unknown leptons" of figures 13.18e and 13.18f. Indeed, it is enough to note that there is no assembly of three quarks in the table 13.14 which could lead by collapse to the two "imaginary" leptons of figures 13.18e and 13.18f, hence the explanation of the non-existence of these two leptons.

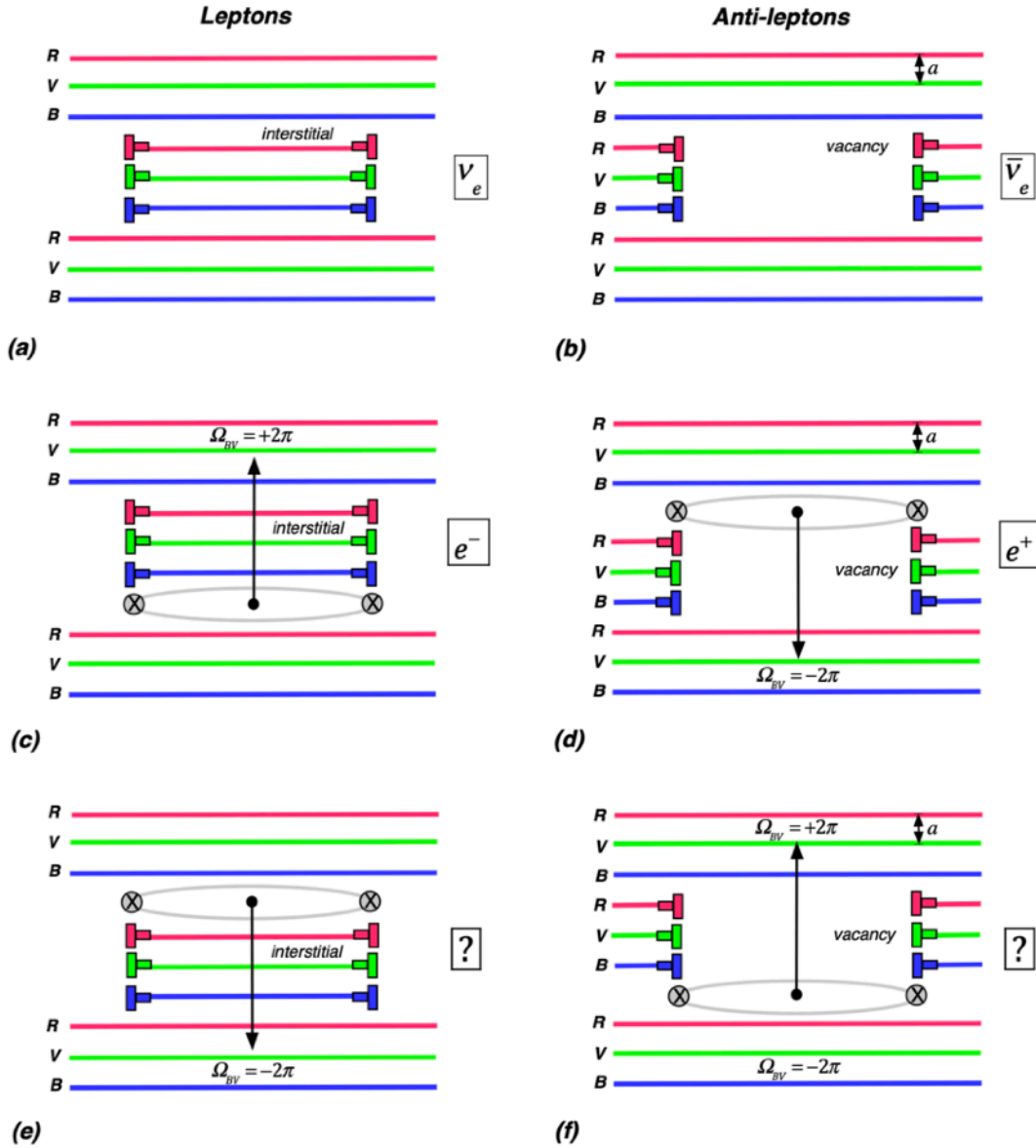


Figure 13.18 - Structure of the neutrino, the anti-neutrino, the electron, the positron, and two "unknown leptons", as assemblies of edge dislocation loops and screw disclination loops

Looking at the table of figure 13.14, we also see that there are no spin 1/2 baryons obtained by combining quarks uuu and $\bar{u}\bar{u}\bar{u}$, and we could then ask ourselves if there would not exist a positive lepton e^{++} of spin 1/2 and double charge coming from the collapse of the quark assembly uuu and a negative anti-lepton \bar{e}^{--} of spin 1/2 and double charge coming from the collapse of the quark assembly $\bar{u}\bar{u}\bar{u}$. The existence of these two leptons would have the ad-

vantage of filling the two gaps left in table 13.14. Note that in the literature¹, doubly charged leptonic states appear in type II flip-flop mechanisms, in strong electroweak symmetry breaking models, in some extensions of supersymmetric models, in models of flavors in extra distorted dimensions, and in even more general models, in string theory inspired models and in 3-3-1 models. In addition, doubly charged stable leptons are also considered by some as an acceptable candidate for cold dark matter.

Weak interaction of leptons and intermediate bosons of the standard model

In the standard model, the weak interactions correspond to exchange of intermediate bosons W^\pm ou Z^0 , which allow to exchange the electric charge between two particles, as reported in figures 13.3 and 13.11. For the Feynman diagrams of these figures to work with the dispirations of our model, it is necessary that the intermediate bosons are pure screw disclination loops of rotation angles Ω_{BV} worth respectively $\pm 2\pi$ or 0 , as represented in figure 13.9e to 13.9g.

The intermediate bosons are then the only massive gauge bosons, which is understandable if they are indeed pure loops of screw disclination. Experimentally, it has been found that their mass is much higher than that of the electron and the positron, which could be explained by the

symbol	Ω_{BV}	$q_{\lambda BV}$	edge loop	$q_{\theta BC}$
ν_e	0	0	<i>interstitial</i>	$-6\pi a$
e^-	$+2\pi$	$-2\pi^2 R_{BV}^2$	<i>interstitial</i>	$-6\pi a$
$\bar{\nu}_e$	0	0	<i>vacancy</i>	$6\pi a$
e^+	-2π	$+2\pi^2 R_{BV}^2$	<i>vacancy</i>	$6\pi a$
W^-	$+2\pi$	$-2\pi^2 R_{BV}^2$	-	0
W^+	-2π	$+2\pi^2 R_{BV}^2$	-	0
Z^0	$(+2\pi) + (-2\pi)$	0	-	0

Figure 13.19 - The leptons of the first family and the intermediate gauge bosons

¹ A. Ozansoy, «Doubly Charged Lepton Search Potential of the FCC base Energy-Frontier Electron-Proton Colliders», *Advances in High Energy Physics*, Volume 2020, Article ID 9234130, 13 pages, <https://doi.org/10.1155/2020/9234130>

fact that the rotation of $\pm 2\pi$ must be entirely done on a distance of a in the case of the intermediate bosons, whereas in the case of the electron and the positron, the rotation of $\pm 2\pi$ can be distributed on 3 successive planes, thus on a distance of $3a$, which must decrease very considerably the local distortions of the lattice, and thus the energy of the particle. This could also be the reason why a gauge boson would associate extremely quickly with 3 interstitial or lacunar edge loops to strongly decrease its energy, which would perfectly explain the weak interactions of figure 13.3.

Note also that, in the standard model of particles, the gauge bosons W^+ and Z^0 are of spin 1, and therefore they do not satisfy the exclusion principle, which means that two gauge bosons can occupy the same state, and thus superimpose, which creates a loop of screw disclination of angle Ω_{BV} equal to for example $\pm 4\pi$. On the other hand, the electron and the positron are particles of spin 1/2, which satisfy the Pauli exclusion principle. They cannot therefore occupy the same state, which means that they cannot be superimposed, which becomes naively almost an evidence if we consider the loop structure of electrons and positrons represented in figure 13.15. One can then plot the properties of the leptons and the gauge bosons in the table of figure 13.19.

An attempt to explain the three families of quarks and leptons of the standard model

In the Standard Model, there are not only the quarks and leptons just described, but there

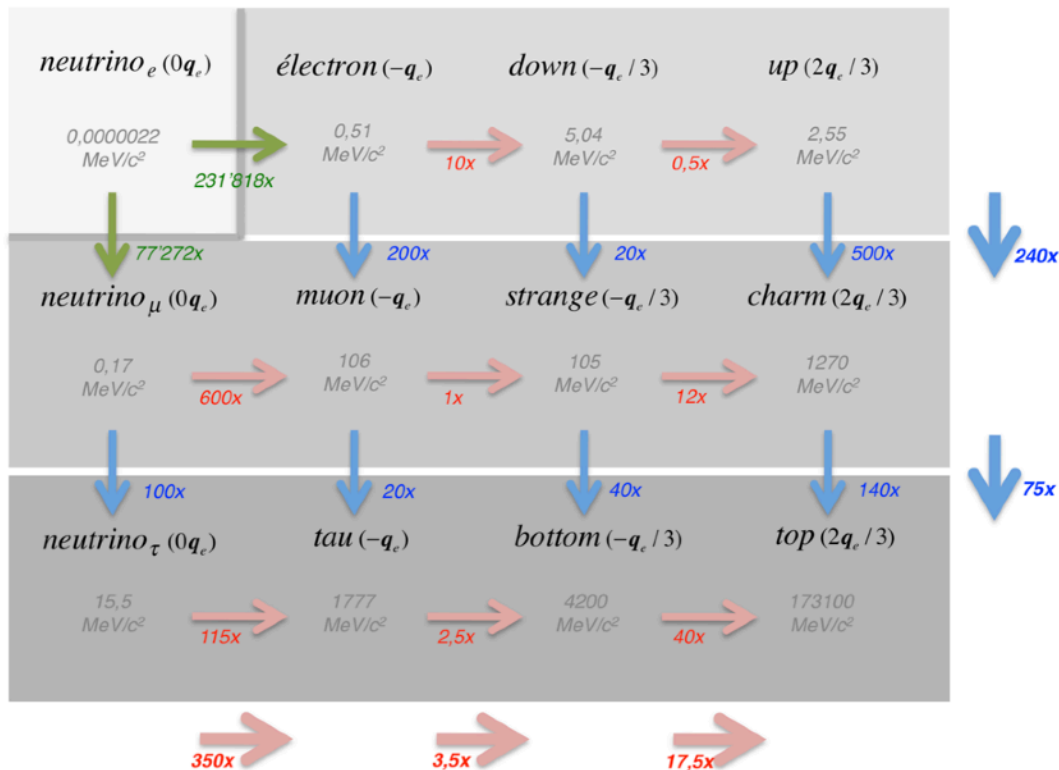


Figure 13.20 - The masses of the particles of the standard model, measured experimentally and expressed in MeV/c², with the approximate multiplicative factors

are also two additional families of quarks and leptons (figure 13.1), distinguished mainly by the much higher masses observed experimentally each time one moves from one family to the next. The progression of masses within the table of elementary particles of the standard model is plotted in figure 13.20, giving the approximate multiplicative factor of the masses, in the horizontal direction of the table and in the vertical direction of the table. It can be seen that the average multiplicative factors reported outside the table are indeed very high when moving from one family to another, while the multiplicative factors for moving from one particle to another within each family are not so high, except in the case of the neutrino to electron transition, which would tend to suggest that the topological structure responsible for the large mass increase most likely changes from one family to another but most likely remains the same within the same family. It is also remarkable that the multiplicative factors associated with the neutrino V_e are colossally higher than all other factors, which tends to make one think that it is probably the structure of the edge loops that change from one family to another.

As for the colossal multiplicative factor to go from neutrino V_e to electron e^- , it is explained by the huge energy difference between an edge dislocation loop and a screw disclination loop, as we have explained in chapter 5.

About the possibility of involving the stacking fault energy between axial dense planes

The fact that there are two additional families with much higher energies could perhaps be attributed to the appearance of stacking faults between axial dense planes, faults that were ini-

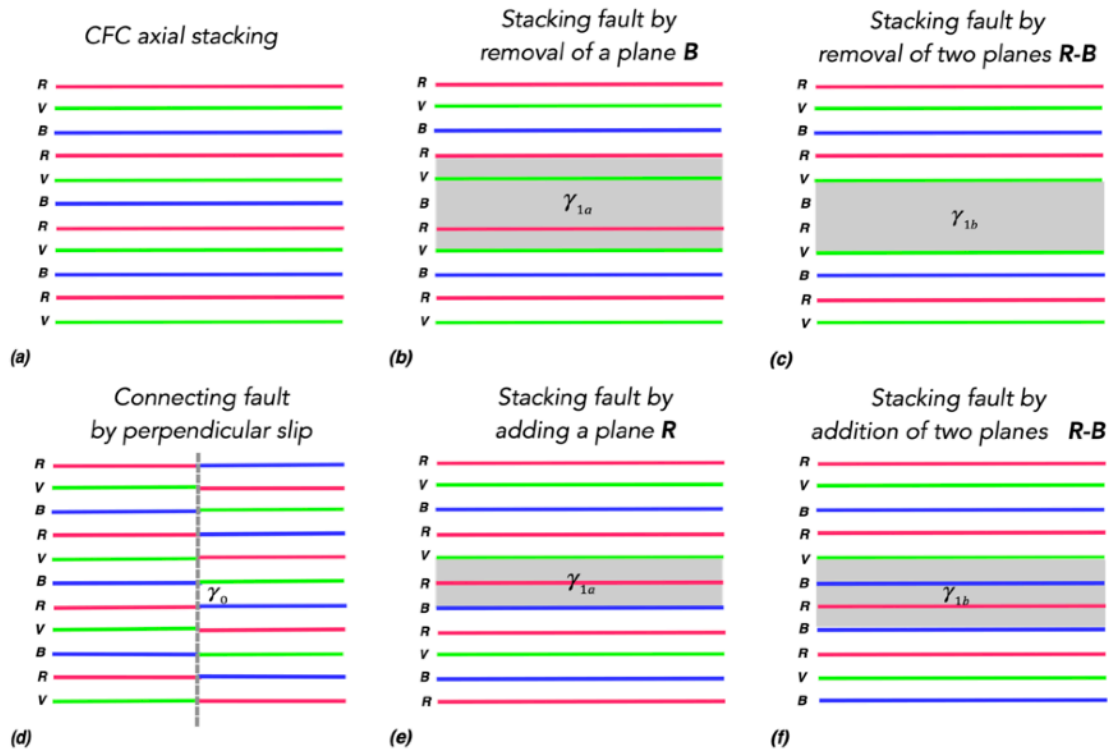


Figure 13.21 - The three types of faults between axial dense planes, by perpendicular slip (d), by removal (b,c) or addition (e,f) of one or two dense planes, with respectively fault energies γ_0 , γ_{1a} and γ_{1b}

tially eliminated by rule 1 in conjecture 13. Indeed, we have built the first family of particles taking into account this rule, i.e. making sure that the **R**, **V**, **B** succession of dense planes is never faulty. To do so, we had to introduce edge dislocation loops of the right color to describe quarks, and introduce a triple edge loop of three colors to describe leptons.

Let us imagine, then, that stacking faults can exist between the dense planes of the lattice, as we have described them in figure 13.21. There are only two types of stacking faults that can be realized, either by shrinking a dense plane (figure 13.21b), or by shrinking two successive dense planes (figure 13.21c). Assume that the fault energies associated with these two types of stacking faults are primarily due to the axial properties of these planes, and thus have axial surface fault energies γ_{1a} and γ_{1b} respectively. The fault energy γ_{1a} associated with the shrinkage of a single dense plane is related to a **V-R-V-R** type stacking fault, while the fault energy γ_{1b} due to the shrinkage of two successive dense planes is associated with a **V-V** type stacking fault. The fault energy is therefore related to a stacking error with the second neighboring plane, whereas is related to a stacking error with the first neighboring plane. There is therefore a good chance that *the energy γ_{1b} is significantly higher than the energy γ_{1a}* , and therefore that $\gamma_{1b} \gg \gamma_{1a}$. One can also consider the stacking errors associated with the addition of a dense plane (figure 13.21e), or with the addition of two successive dense planes (figure 13.21f). As these operations by addition correspond in fact to the inverse of the operations by withdrawal, it is likely that the fault energies are the same for the case of withdrawals as for that of additions, thus γ_{1a} for the addition of a dense plane and γ_{1b} for the addition of two successive dense planes.

The constitution of neutrino families

Let us take the case of neutrinos, which are known to exist in three different states or three "flavors", as physicists say: electronic, muonic and tauic. By removing or adding one or two planes to the electron neutrino and anti-neutrino in figures 13.18a and 13.18b, we can construct the six neutral leptons shown in figure 13.22. By comparing the stacking faults of these leptons with the faults reported in figure 13.21, we see that the addition or removal of three planes does not lead to any stacking faults of the axial dense planes, and thus correspond to the electron neutrinos and anti-neutrinos of the 1st family. The addition or removal of 1 axial dense plane corresponds to a fault energy γ_{1a} and could therefore correspond to muonic neutrinos and anti-neutrinos of the 2nd family, while the addition or removal of two axial dense planes corresponds to fault energy γ_{1b} and could therefore correspond to tauic neutrinos and anti-neutrinos of the 3rd family.

Experimentally, it has been observed, surprisingly, that neutrinos are capable of spontaneously changing from one flavor to another during their movement. They are even the only elementary particles endowed with this property, called "oscillation". The major result of these experiments is that this transformism of neutrinos can only be explained by the fact that they have different masses, which is the case since they differ from one family to another (from one flavor to another) by their lattice deformation energy and by their axial dense plane stacking fault energy.

As for the mechanism that leads to this oscillation, it is assumed that at the moment of creation and emission of neutrinos or antineutrinos by the weak interaction (for example in beta de-

cays of radio-active nuclei), one cannot separate the mass states. A coherent superposition of defined mass states is formed, and the wave function now contains all types of neutrinos. There is then a probability of observation of each type of neutrino which can be deduced from the wave function, and this probability function exhibits a beautiful oscillatory behavior. Neutrino oscillations can only be observed if the masses m_1 , m_2 and m_3 are not all identical, which leads to slightly different velocities from one flavor to another, hence the oscillation phenomenon, and if the initial neutrino (emitted in a weak interaction process) is created in a coherent superposition of mass eigenstates.

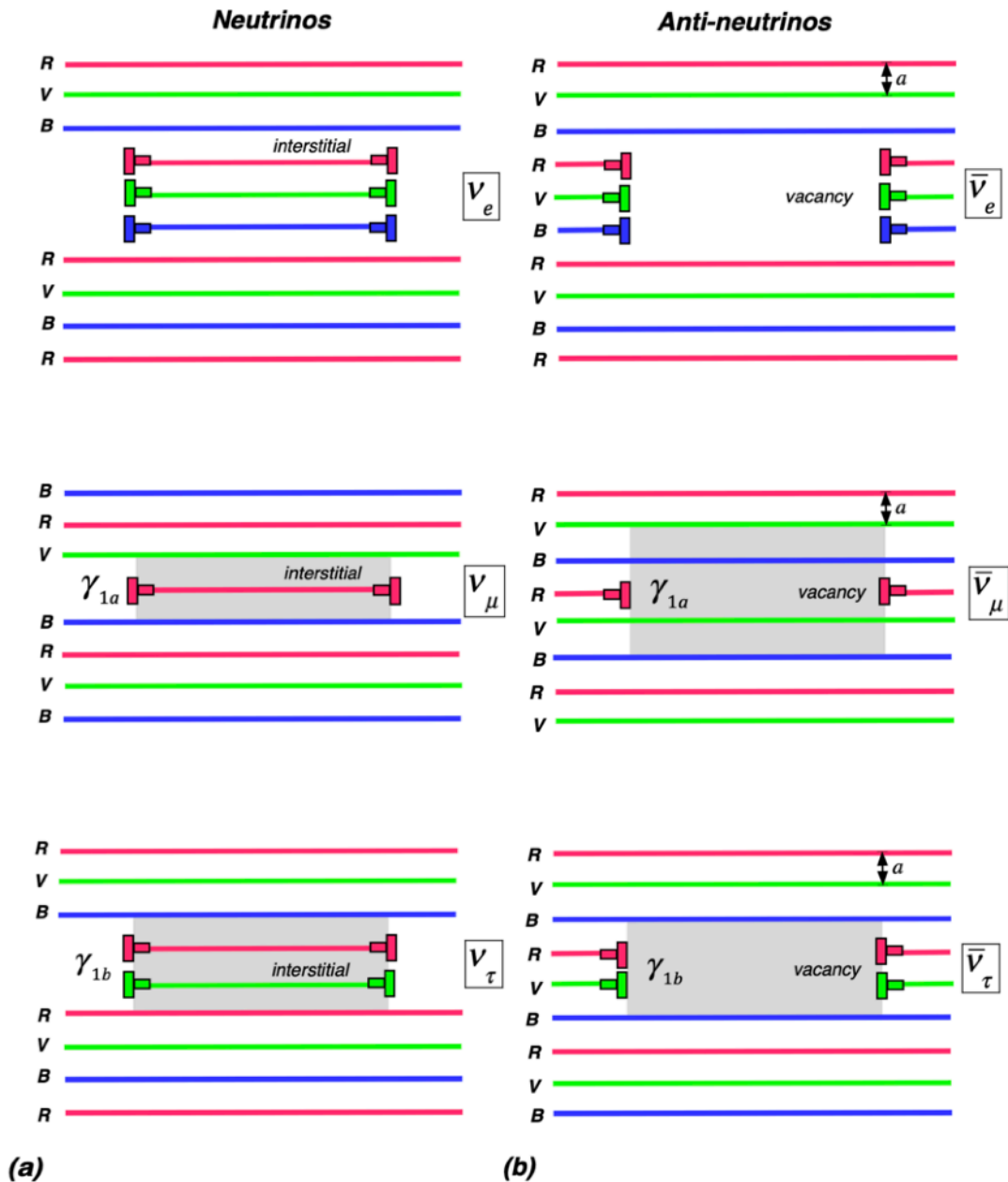


Figure 13.22 - the three families of neutrinos and anti-neutrinos, by adding and removing one, two or three dense planes

The constitution of electron families

In the case of the electrons and anti-electrons of figure 13.18c and 13.18d, it is enough to add to the neutrinos of figure 13.22 the loops of screw disclination with an angle of rotation Ω_{BV} worth respectively $\pm 2\pi$. We obtain in these cases respectively the electrons and anti-electrons of the 1st family, the muons and anti-muons of the 2nd family, and the taus and anti-taus of the 3rd family represented in figure 13.23.

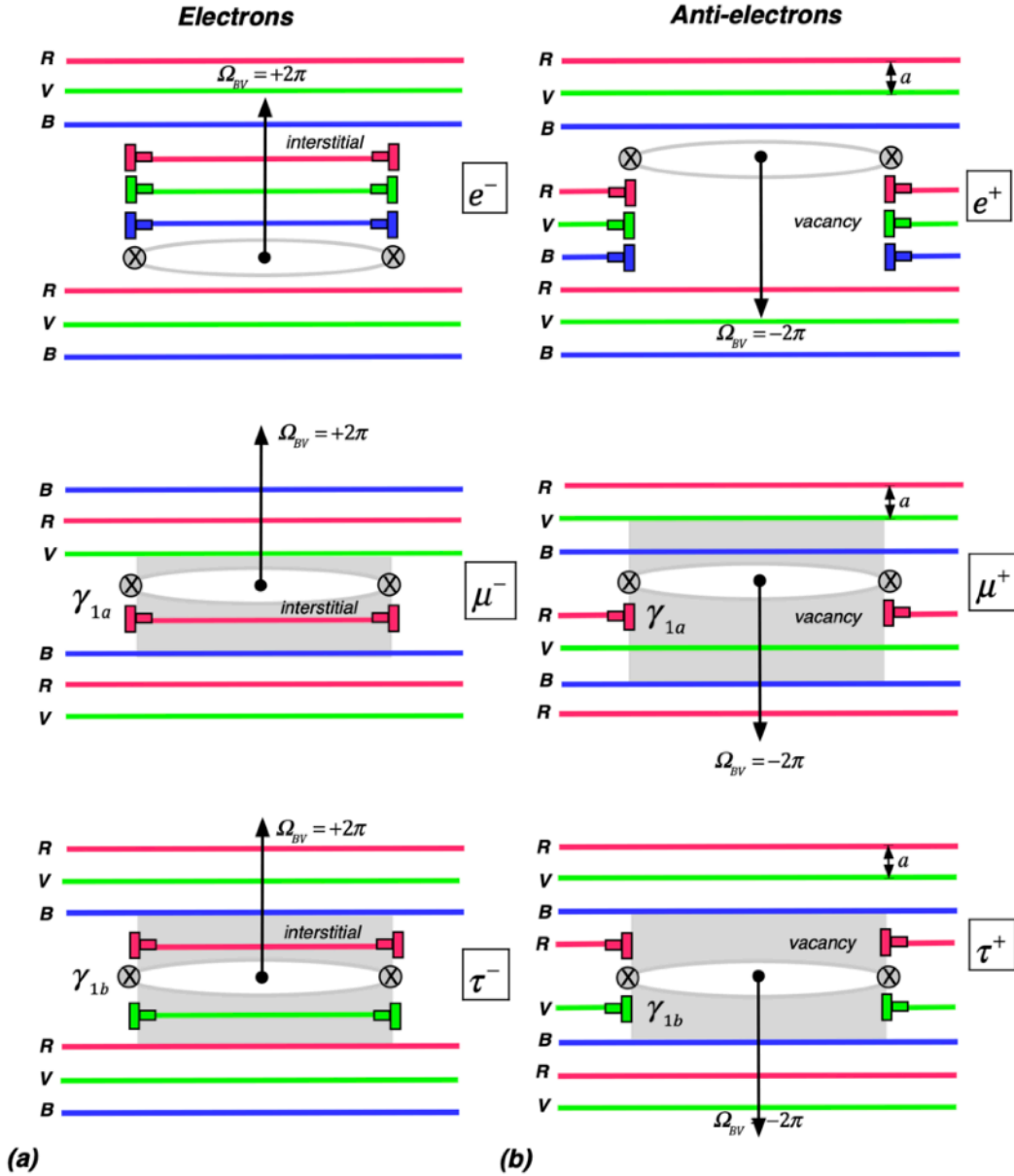


Figure 13.23 - the three families of electrons and anti-electrons, by adding and removing one, two or three dense planes, in combination with the screw disclination loop

The constitution of the quark families

In the case of quarks, one can add or subtract 1 or 2 axial dense planes to the quarks u

and d or to the anti-quarks \bar{u} and \bar{d} , so as to make appear stacking errors of the axial dense planes with energies γ_{1a} or γ_{1b} . We then obtain the family of quarks represented in figure 13.24, which is also composed of three generations of two types of electrically charged particles: a first generation is formed of the *down* (d) and *up* (u) quarks, respectively of electric charges $-1/3$ and $+2/3$ of the electric charge of the electron, a second generation composed of the *strange* (s) and *charm* (c) quarks, respectively of electric charges $-1/3$ and $+2/3$ of the electric charge of the electron, and a third generation composed of the *bottom* (b) and *top* (t) quarks, respectively of electric charges $-1/3$ and $+2/3$ of the electric charge of the electron. And each quark also has its anti-particle of electric charge of opposite sign (\bar{d} , \bar{u} , \bar{s} , \bar{c} , \bar{b} and \bar{t}).

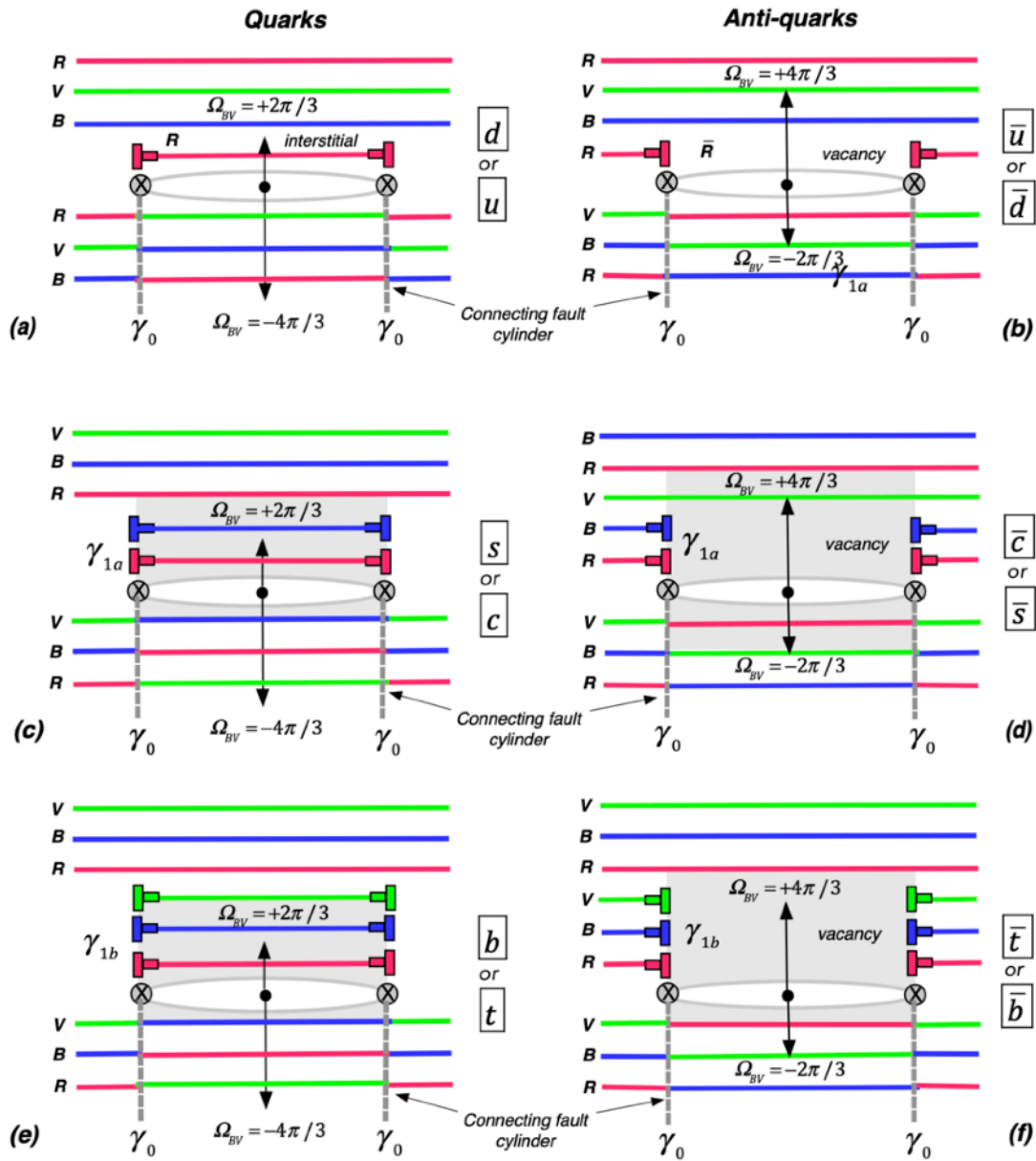


Figure 13.24 - the three families of quarks and anti-quarks, by adding and removing one, two or three dense planes, in combination with a screw disclination loop

About the interest of the analogy between the "colored" cosmological lattice and the standard model

The analogy between our "colored" cosmological lattice model, with the elementary topological singularities it may contain, and the standard model of elementary particles is excellent, and it is very fruitful to provide explanations to several rather mysterious facets of the standard model that we are going to list here.

- The structure of the Standard Model particles in three families of quarks and leptons:

The topological structures of edge dislocation loops and screw disclination loops introduced in a "colored" FCC lattice having strict rules of arrangement and rotation of the "colored" corpuscular planes, with connecting and stacking fault energies γ_0 , γ_{1a} and γ_{1b} , allow to reconstitute all the particles of the standard model of elementary particles, namely quarks and leptons. These particles present a structure in three families whose very different masses can be explained by the stacking fault energies γ_{1a} and γ_{1b} . These various quarks and leptons also satisfy *all the properties of the weak interaction and the strong interaction* using respectively the intermediate gauge bosons W^\pm and Z^0 and the gluons, which also have their own topological structures in the "colored" cosmological lattice. As for the strong force, it has good asymptotic properties due to the fact that it is generated by a cylinder of connecting faults whose fault energy γ_0 increases if it is lengthened, and it is responsible for the existence of baryons and mesons, which are localized and "uncolored" topological structures that it is possible to form on the basis of quarks. In this way, one can reconstruct all the particles of the standard model, such as the baryons and mesons of figure 13.4, composed of the quarks and anti-quarks u, d, s and/or c.

- The weak and strong force interaction fields:

As for the force fields acting between the topological loops, they have simple topological explanations:

(i) *the weak force* is essentially due to the decrease in the formation energy of a dispiration loop when an edge dislocation loop is associated with a screw disclination loop, as discussed in chapter 9. It is the very weak range of the capture interaction potential of this force that then explains the radio-active decay of elementary particles, by the crossing of the interaction potential by quantum tunneling. In fact, *the weak force is an interaction between the rotation charge of a screw disclination loop with the curvature charge of an edge dislocation loop.*

And there are indeed gauge bosons exchanged during the weak interaction: these are the intermediate bosons W^\pm et Z^0 , which have a well defined topological structure, reported in figure 13.10.

(ii) *the strong force*, which binds two or three quarks together, is due to *the connecting fault cylinder generated by the fact that the screw disclination loops associated with the quarks have charges $q_{\lambda BV}$ that are only 1/3 or 2/3 of the charge of the perfect screw disclination loop associated with the electron.* The dissociation distance between loops of a doublet or a triplet of quarks depends essentially *on the energy of connecting faults per unit area.* If this energy is very high, one can imagine that the loops will be very close, as illustrated in the figures of this chapter. But if this energy is low, one could also imagine fault tubes constituting membranes whose diameter (equal to the diameter of the topological loops) is much smaller than their

length, so that the topological singularities in doublet and triplet could then have the aspect of "long strands" terminated at each end by topological loops.

And there are indeed gauge bosons exchanged during the strong interaction: these are the bicolor gluons, which have a well-defined topological structure, shown in figure 13.16.

- *The possibilities of calculating the energy of the particles of the standard model:*

A first very interesting consequence of this explanation of the Standard Model particles is related to the fact that, in the case of dispiration loops and their interactions via the weak and strong forces, the energies involved in the formation of loop multiplets has a known origin since it is in fact the sum of the following various energies:

- (i) the formation energies associated with the very strong local lattice distortions generated by these objects, and stored in the lattice in the vicinity of these objects,
- (ii) the energies of connection faults (related to) and stacking faults (related to and) appearing due to the fact that the imaginary cosmological lattice considered here is a "colored" lattice which must have axial properties,
- (iii) the energies involved by *the weak force* in the gravitational couplings between the edge dislocation loops and the screw disclination loops, as described in chapter 9,
- (iv) the longer range stored energies, which are due to the long range distortions of the lattice related to the global charge q_θ of curvature by flexion and the global charge q_λ of rotation by torsion of loop multiplets, which are contained in the calculations of energies that we made in the previous chapters, as well as the proper vibration and proper rotation energies of the loops that we obtained in chapters 11 and 12, respectively.

The total energy of formation of the loop multiplets could thus be calculated in a rigorous way, provided that the exact elastic properties (the moduli K_0 , K_1 , K_2 and K_3) as well as the surface energies of fault γ_0 , γ_{1a} and γ_{1b} of the cosmological lattice in which these objects appear are known. This energetic aspect is very important because, in the case of the standard model of particles, the origin and the value of the energy of elementary particles (their mass) still remain very mysterious, and are introduced as parameters of the standard model, which must be measured experimentally.

- *The "elementarity" of the particles of the standard model:*

Another interesting consequence of our conception of the standard model is the existence of a difference in "elementarity" between the topological loops of dispiration of our imaginary cosmological lattice and the leptons and quarks of the standard model. Indeed, the dispiration loops that we have described, contrary to the elementary leptons and quarks of the standard model, are not strictly speaking elementary particles, but are already assemblies of screw disclination loops and lacunar or interstitial edge dislocation loops.

To judge the other potentialities of this idea of the constitution of the Standard Model particles, one would have to check whether this approach would allow to justify and explain the complicated set of selection rules that had to be introduced in particle physics to describe all the experimentally observed interactions. This is obviously only a suggestion, and its detailed development is beyond the scope of this treatise. Note that other similar approaches to decompose the Standard Model particles have already been proposed in particle physics, but in different forms, such as the model based on pre-quarks called "rishons". But these models have proved to be unsuccessful.

- *The role of the curvature charge in the standard model:*

The curvature charge q_θ plays an important role in the development of a model of "elementary topological singularities" to explain the standard model of particles. It is quite easy to see that this charge, for which we do not see a direct analogy in the standard model, satisfies a conservation principle during the interactions between loops, both during weak and strong interactions.

But this charge has another major interest related to the bosonic or fermionic nature of particles. Indeed, we find that *all particles with a curvature charge (leptons, quarks and baryons) are fermions with a half-integer spin, which satisfy the Pauli exclusion principle, while all particles without a curvature charge (photons, gauge bosons, gluons and mesons) are bosons with an integer spin, not subject to the Pauli exclusion principle.* There is most probably a crucial role played by the curvature charge, which remains to be elucidated, but which is not within the scope of this treatise.

The question is also to know if the charge q_θ , which is conserved during the loop interactions, has a correlation with one of the characteristic quantities or with one of the conservation relations of the standard model, such as the Gell-Mann-Nishijima relation for example. The answer to this question could certainly present very important potentialities for particle physics, especially since we have already shown many times that *it is the curvature charge q_θ that is responsible for the weak asymmetry between matter and anti-matter*, and consequently for the cosmological evolution of matter and anti-matter in the universe, and for the presence of a "dark mass" in the form of a sea of repulsive neutrinos surrounding the galaxies.

***Still open questions about the "colored" cosmological lattice model
and its analogy with the standard model***

The analogy developed in this chapter between the topological loops of dispiration in an imaginary "colored" cubic cosmological lattice and the standard model of elementary particles proves to be very fruitful to try to understand some points still unclarified in particle physics, such as the topological nature of elementary particles, as well as of the strong and weak forces, or the origin of the mass of elementary particles.

However, there are still several unanswered questions, which deserve to be studied in detail, among which the main ones are the following:

- *The application of the concept of spin:*

As we have already mentioned in chapter 12, the notion of spin seems to correspond to a real rotation of topological loops. But there are still many questions that need to be studied in detail.

The first question is obviously to try to imagine how an edge dislocation loop, and/or a screw disclination loop can rotate on itself in a "colored" FCC cosmological lattice, knowing moreover that there is a stacking fault tube responsible for the strong force in the case of baryons and mesons. Is there a possible topological explanation for such a spinning motion, or should we imagine a lattice with "even stranger" properties?

The second question is obviously related to the value to be assigned to the spin of a topological loop. For example, why does the electron, which would correspond to a weak coupling

between an edge dislocation loop and a screw disclination loop, have a spin 1/2, while the gauge boson, which would correspond to an isolated screw disclination loop, has a spin 1? This is where the important observation that we have made is likely to play an essential role in explaining the value of the spin of a particle, namely that all particles with a curvature charge (leptons, quarks and baryons) are fermions with a half-integer spin, while all particles without a curvature charge (photons, gauge bosons, gluons and mesons) are bosons with a whole spin.

The third question would be how to apply more carefully the concept of spin developed in chapter 12 to the "colored" cosmological lattice model that we described in this chapter. The answer to this question could allow to find an explanation for the existence of particles composed of the same quarks, but of different spins, like mesons π^+ and ρ^+ composed both of quarks $u\bar{d}$, but of respective spins 0 and 1, or baryons p (proton) and Δ^+ composed both of quarks uud , but of respective spins 1/2 and 3/2. Such a study would perhaps also make it possible to explain the exact origin of the spin 1/2 of the baryons and the spin 1 of the mesons, which is still a rather obscure point of the standard model of the particles, but which could perhaps find an explanation in the case of the "colored" cosmological lattice by supposing that it is the existence or not of a curvature charge which imposes a behavior of boson or fermion to a given particle.

- *The theory of quantum chromodynamics:*

It would obviously be very instructive and interesting to develop a much more detailed study of the application of the wave equation calculations, of the concepts of bosons and fermions, of the Pauli exclusion principle developed in chapter 11, as well as of the notion of spin introduced in chapter 12, to the topological loop singularities analogous of the particles of the standard model, and to try to see if such a study would not finally lead us to a comprehensible physical explanation of the famous theory of "quantum chromodynamics"?

- *The existence of supersymmetric models:*

A more detailed study of the existence of the curvature charge could not only (perhaps) explain why there are fermions (spin 1/2 particles like quarks and leptons) and bosons (spin 1 particles like intermediate gauge bosons and gluons) in the Standard Model, but it could also answer the question of whether (by chance) it would be possible to create a zoology of particles identical to those we have obtained in this chapter, but whose spins 1/2 and 1 would be inverted, which could lead to a "supersymmetric model". But we note that in the framework of our model of particles, it appears very difficult, if not impossible, to imagine such supersymmetric particles.

- *The existence of "exotic" leptons:*

In our description of the quarks of figure 13.24, the fact that the quarks possess electric charges $-1/3$ and $+2/3$ of the charge of the electron, whereas the anti-quarks possess electric charges $+1/3$ and $-2/3$ of the charge of the electron is easily explained by the rules of succession of the colors of the corpuscular planes that we have emitted. On the other hand, for the leptons that we have introduced in figures 13.22 and 13.23, we have chosen arbitrarily to associate to the neutrino an electric charge -1 to obtain *the electron of matter* and to associate to the anti-neutrino an electric charge $+1$ to obtain *the positron of anti-matter*. But in fact the rules of color that we introduced would not prevent a priori to associate an electric charge $+1$ to the neu-

trino to obtain *an exotic positron of matter* and an electric charge -1 to the anti-neutrino to obtain *an exotic electron of anti-matter*, as reported in figure 13.18. There is a subject of reflection there that we have already approached by commenting on the table 13.14, where we proposed that the electron and the positron could be considered as the result of the compression of assemblies of quarks ddd and $\bar{d}\bar{d}\bar{d}$, which would explain the existence of the electrons of matter and the positrons of anti-matter and the absence of the electrons of anti-matter and the positrons of matter. But this "explanation" of being able to collapse the assemblies of three identical quarks ddd and $\bar{d}\bar{d}\bar{d}$ to form electrons and positrons also led us to wonder if it was also possible to collapse in the same way three identical quarks uuu and $\bar{u}\bar{u}\bar{u}$, to form exotic leptons, namely *a positive lepton* e^{++} of spin 1/2 and of double charge and *a negative anti-lepton* \bar{e}^{--} of spin 1/2 and of double charge. The existence of these two exotic leptons would have the advantage of filling the two gaps left in table 13.14.

There is matter to think about to confirm or deny the formation of leptons by collapse of three identical quarks.

- *Conclusion :*

To conclude this section, we must note that our model of a "colored" cosmological FCC lattice still raises many unresolved questions, and that it could thus be the origin of a new exciting field of research, especially if we try to elucidate the preponderant role that the new and original element of our approach, namely the curvature charge, must surely play.

Chapter 14

Photons, Vacuum Fluctuations, Multiverses and Gravitons

This chapter is to be taken with caution, because it will deal with some very speculative consequences, but also very interesting, of our approach of the perfect cosmological network.

The first part of this chapter is dedicated to *a discussion of pure transverse waves*, quantified in the form of photons. In chapter 3, we have shown that the propagation of a linearly polarized transverse "electromagnetic" rotation wave is accompanied by a longitudinal "gravitational" wavelet. In this chapter, we will focus on what happens in the case of localized wave packets. We will show that these wave packets can only appear with *a non-zero helicity* so that their total energy does not depend on time. Assuming that these wave packets are emitted when a topological singularity suddenly changes state, it becomes quite understandable that they present *a quantification of their energy*. These wave packets then behave like energetic quasi-particles of "electromagnetic" fluctuations which one could qualify as "*photons*" and which actually have properties very similar to the quantum properties of photons: circular polarization, zero mass, non-zero momentum, non-locality, wave-corpuscle duality, entanglement and phenomenon of decoherence.

The rest of the chapter is dedicated to some very hypothetical consequences of the perfect cosmological lattice, associated with *pure gravitational fluctuations*. One can imagine the existence of pure longitudinal fluctuations within the cosmological lattice which can be treated, either as random gravitational fluctuations which could have an analogy with "*quantum vacuum fluctuations*", or as stable gravitational fluctuations, which could lead on a macroscopic scale to a "*cosmological theory of Multiverses*", and on a microscopic scale to the existence of a form of stable quasi-particles which one could call "*gravitons*", by analogy with photons, but which in fact have nothing in common with the gravitons usually postulated in the context of General Relativity.

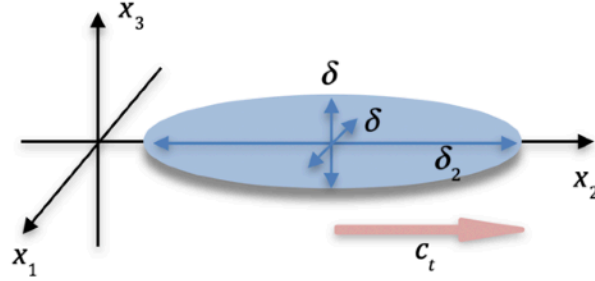
Transverse rotation wave packets: the photons

We saw in chapter 3 that the propagation of a linearly polarized transverse wave within the cosmological lattice is bound to the existence of a correlated perturbation of the expansion of the lattice, and that only the circularly polarized rotation waves are pure transverse waves, without associated expansion wavelets. One can reasonably wonder if this astonishing property could not be at the origin of the existence of *quantified "electromagnetic" fluctuations*, like the famous *photons* of quantum physics?

Let us consider transverse waves of pulsation Ω propagating along the axis Ox_2 , with a polarization of the fields of rotation $\underline{\omega}_1(x_2, t)$ and $\underline{\omega}_3(x_2, t)$ and of the fields of velocity $\underline{\phi}_1(x_2, t)$ and $\underline{\phi}_3(x_2, t)$ along the axes Ox_1 and Ox_3 . We then try to form a bundle of transverse waves, of pulsation Ω , of exponential envelopes of range δ_2 along the axis Ox_2 and of equal ranges $\delta_1 = \delta_3 = \delta$ along the axes Ox_1 et Ox_3 . By applying linearized field equations for these

fluctuations in the domain $\tau_0 < \tau_{0cr}$, there appears a volume expansion component $\underline{\tau}^{(p)}(x_2, t)$ associated with the wave packet, of frequency 2Ω . If one calculates the energy density of this fluctuation by oscillations of the field of rotation and the field of expansion, it contains terms in $\cos^2 \Omega t$, in $\cos^2 2\Omega t$ and in $\cos 2\Omega t$, so that it is not independent of time, whereas it should be in principle. To make these terms in $\cos^2 \Omega t$, in $\cos^2 2\Omega t$ and in $\cos 2\Omega t$ disappear, so that the energy density of the fluctuation does not depend on time, and to make disappear the volume expansion component of the wave packet, a rather tedious calculation leads to the real solution of the wave packet proposed in figure 14.1.

This wave packet represents in fact, in the analogy with electromagnetism, a packet of electromagnetic waves, which *MUST* present a right or left helicity so that its energy is independent of time, and especially so that it is not accompanied by a "gravitational" disturbance of expansion. Knowing that $mnc_t^2 = K_3$ in the perfect cosmological lattice for $\tau_0 < \tau_{0cr}$, the energy density of this packet of wave is given by the relation reported in figure



Wave packet of circular polarization transverse waves
not coupled with gravitational fluctuations

$$\begin{cases} \omega_1(x_2, t) = \omega_{10} e^{-\frac{|x_1|}{\delta}} e^{-\frac{|x_3|}{\delta}} e^{-\frac{|x_2 - c_t t|}{\delta_2}} \cos\left[\frac{\Omega}{c_t}(x_2 - c_t t)\right] \\ \omega_3(x_2, t) = (\mp) \omega_{10} e^{-\frac{|x_1|}{\delta}} e^{-\frac{|x_3|}{\delta}} e^{-\frac{|x_2 - c_t t|}{\delta_2}} \sin\left[\frac{\Omega}{c_t}(x_2 - c_t t)\right] \\ \phi_3(x_2, t) = -2c_t \omega_{10} e^{-\frac{|x_1|}{\delta}} e^{-\frac{|x_3|}{\delta}} e^{-\frac{|x_2 - c_t t|}{\delta_2}} \cos\left[\frac{\Omega}{c_t}(x_2 - c_t t)\right] \\ \phi_1(x_2, t) = (\mp) 2c_t \omega_{10} e^{-\frac{|x_1|}{\delta}} e^{-\frac{|x_3|}{\delta}} e^{-\frac{|x_2 - c_t t|}{\delta_2}} \sin\left[\frac{\Omega}{c_t}(x_2 - c_t t)\right] \end{cases}$$

Energy density

$$e^{fluctuation} = \underbrace{2K_3(\omega_1^2 + \omega_3^2)}_{e^{rot}} + \underbrace{\frac{1}{2}mn(\phi_1^2 + \phi_3^2)}_{e^{in}} = 4K_3\omega_{10}^2 e^{-\frac{|x_1|}{\delta}} e^{-\frac{|x_3|}{\delta}} e^{-2\frac{|x_2 - c_t t|}{\delta_2}}$$

Total energy of the wave packet

$$E_{wave\ packet} = 8 \int_0^\infty dx_1 \int_0^\infty dx_3 \int_0^\infty dy \left(4K_3\omega_{10}^2 e^{-\frac{x_1}{\delta}} e^{-\frac{x_3}{\delta}} e^{-2\frac{y}{\delta_2}} \right) = 4K_3\omega_{10}^2 \delta^2 \delta_2$$

Figure 14.1 - Wave packet of circular polarization transverse waves
not coupled with gravitational fluctuations

14.1. And by making a change of variable $x_2 - c_t t = y$, we can quite easily calculate the total energy of this fluctuation of the field of rotation, which is worth $E_{\text{wave packet}} = 4K_3 \omega_{10}^2 \delta^2 \delta_2$. It can therefore be seen that this expression of the energy of the wave packet only depends on the maximum amplitude ω_{10} of the oscillations of the field of rotation and of the spans δ_2 along the axis Ox_2 and $\delta_1 = \delta_3 = \delta$ along the axes Ox_1 et Ox_3 , and that the pulsation ω of the wave does not intervene in this expression of energy.

If we consider that the perfect cosmic lattice is indeed a theoretical representation of the real Universe, then the rotation wave packets that we have just described must probably correspond to photons. Assuming therefore that these wave packets are emitted when a topological singularity suddenly changes state (such as for example the level transition of an electron in an atom), it becomes very simple to explain that they present a quantification of their energy. Indeed, suppose a singularity which passes from a high energy level (a) to a lower energy level (b), as illustrated in figure 14.2. Using the relations of figure 11.1 for the pulsation of the gravitational fluctuations, and by expressing these relations in the non-relativistic case, one has $\hbar \omega_f^{(a)} = E_0^{\text{dist}} + V^{(a)}$ and $\hbar \omega_f^{(b)} = E_0^{\text{dist}} + V^{(b)}$, so that the loss of energy of the singularity during its transition from level of energy is expressed as $\Delta E_{\text{lost}} = V^{(a)} - V^{(b)} = \hbar(\omega_f^{(a)} - \omega_f^{(b)})$.

This energy ΔE_{lost} is dissipated in the form of a photon, therefore of a packet of transverse waves transporting this energy lost by the singularity. By equalizing the dissipated energy ΔE_{lost} with the total energy $E_{\text{wave packet}}$ of the transmitted wave packet, we obtain a relation between the parameters $\omega_{10}, \delta, \delta_2$ of the wave packet and the pulsation $\Omega_{\text{wave packet}}$ of the wave packet, in the form $E_{\text{wave packet}} = 4K_3 \omega_{10}^2 \delta^2 \delta_2 = \hbar(\omega_f^{(a)} - \omega_f^{(b)}) = \hbar \Omega_{\text{wave packet}}$.

This relation is then quite remarkable, because it shows that *the energy of the transverse fluctuation is quantified with the value $\hbar(\omega_f^{(a)} - \omega_f^{(b)})$* , and that *the frequency $\Omega_{\text{wave packet}}$ of the transverse fluctuation emitted is nothing other than the difference of the frequencies of the*

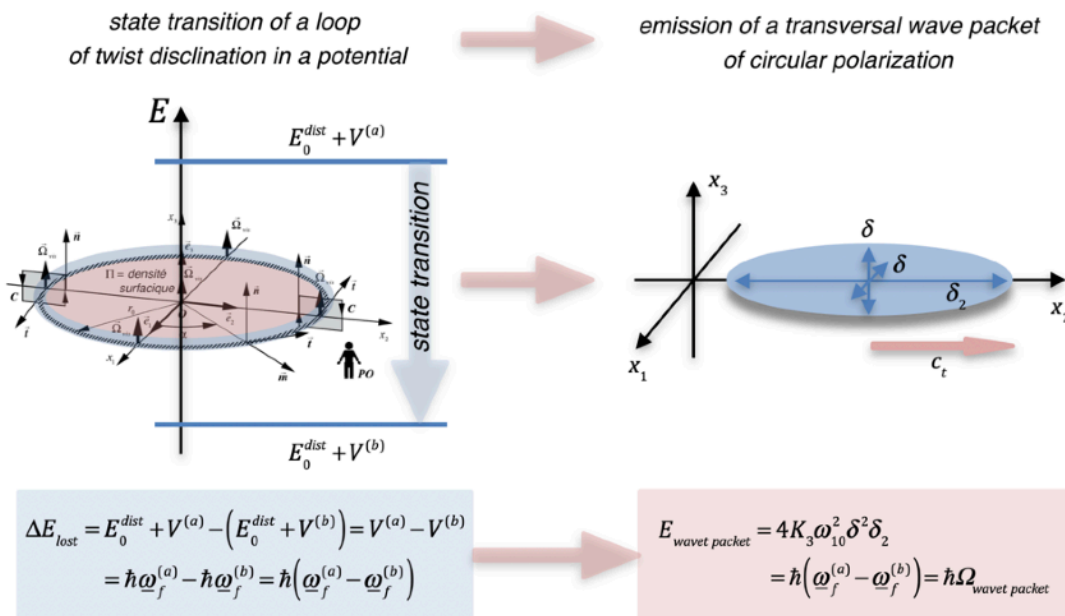


Figure 14.2 - Emission of a packet of transverse waves of circular polarization by the state transition of a twist disclination loop in a potential

gravitational perturbations of the singularity in states (a) and (b). We therefore find the experimental observation that the energy of photons is quantified, as Einstein initially proposed, and that the energy of a photon has a well-determined value proportional to its pulsation $\Omega_{\text{wave packet}}$ via the Planck constant.

About the possible properties of transverse rotation wave packets

- About the non-locality of the rotation wave packet:

The wave packet thus formed has a "volume" $\delta^2\delta_2$, an amplitude ω_{10} and an energy $E_{\text{wave packet}} = \hbar\Omega_{\text{wave packet}}$. As its energy is required to remain constant, this implies that neither the amplitude ω_{10} nor the "volume" $\delta^2\delta_2$ are predetermined, but that they are simply linked by the relationship $4K_3\omega_{10}^2\delta^2\delta_2 = \hbar\Omega_{\text{wave packet}}$. The wave packet thus presents a kind of "malleability", or "plasticity". It can for example lengthen or shrink along its axis of propagation Ox_2 , or extend or compress along the axes Ox_1 and Ox_3 perpendicular to the direction of propagation, or else extend or contract isotropically in the lattice, provided that the product $\omega_{10}^2\delta^2\delta_2$ remains a constant equal to $\hbar\Omega_{\text{wave packet}} / 4K_3$.

If the wave packet is very picked up on itself, that is to say that its «volume» $\delta^2\delta_2$ is very small and that its amplitude ω_{10} is very large, it will then behave like a *localized quasi-particle of energy* $E_{\text{wave packet}} = \hbar\Omega_{\text{wave packet}}$. But during its propagation, it can also very well extend and occupy a very large «volume» $\delta^2\delta_2$, with a very low amplitude ω_{10} , and behave in this case rather like a wave, capable of all phenomena of interference and diffraction of a usual wave. We find here *the non-locality property* of the quasi-particle during its propagation, in the same sense as in quantum physics.

- About the momentum of the quasi-particle "photon":

In the form of a quasi-particle, that is to say when the wave packet is very contracted, therefore of very low "volume", it obviously has no mass of inertia, but it does have a non-zero momentum. We deduce this peculiarity from the fact that this wave packet moves at the speed c_t and therefore that it must satisfy *the relativistic equation of the energy* of figure 11.1, with a mass of inertia $M_0 = 0$, namely $(E_{\text{photon}})^2 = (\vec{P}^{\text{photon}})^2 c_t^2$, which implies a non-zero momentum $\vec{P}^{\text{photon}} = \pm E_{\text{photon}} \vec{e}_2 / c_t = \pm \hbar\Omega \vec{e}_2 / c_t$ in the propagation direction.

- About the wave-particle duality of the rotation wave packet:

These wave packets actually have a *wave-particle duality* similar to that observed in quantum physics. The only restriction imposed on this wave packet by the fact that it propagates in a cosmological lattice satisfying $\tau_0 < \tau_{0cr}$ is that it is obliged to remain a *single entity* of given energy and helicity, so that its energy $\hbar\Omega$ remains constant and that there is no expansion perturbations.

This implies that such a wave packet, if it is very large and that it must, for example, pass through a slot, must necessarily contract sufficiently to pass through the slot in the form of a single entity. But nothing prevents that during this crossing, the wave side of this entity interacts with the edges of the slit so that the entity is diffracted during this crossing, and therefore that the "trajectory" of this quasiparticle can be modified.

Similarly, if this extended wave packet encounters a double slit, it can cross the two slits by contracting locally, and recombine after this crossing, provided that its entity integrity has not

been modified during this crossing. But the recombination of the wave entity after the passage of the two slits is subject to wave interference, so that the probability of finding the quasi-particle in space after the slits presents fringes identical to conventional interference fringes for a plane wave passing through two slits.

This also implies that if the wave packet, very large during its propagation, begins to be absorbed by an obstacle, the maintenance of a constant energy over time forces it to contract again so that the absorption of its energy is a very localized phenomenon. We could reasonably speak here of the *"materialization" of the wave packet in the form of a "quasi-particle"*. It must therefore behave like a very localized quasi-particle during its creation or its annihilation.

Note that what is called *the "measurement problem" in quantum physics* corresponds exactly to this type of phenomenon. Any attempt to "touch" the wave packet will force it to change so that it remains an energy entity independent of time. Thus, a measurement on this wave packet is necessarily an action which will disturb this wave packet and modify its characteristics.

- *About the creation of pairs of "photon" quasi-particles:*

As the quasi-particle "photon" has a momentum due to its relativistic behavior, the creation of a single photon would violate the principle of momentum conservation. This implies that photons can only be created in pairs of photons of the same frequency, propagating in two opposite directions so that their overall momentum is zero.

- *About the entanglement phenomenon of two virtual quasi-particles "photons":*

Initially, when creating a pair of photons, there may well be only one locally created wave packet, in which case it must lengthen at the speed c_t on either side of the axis of propagation of the two virtual quasi-particles in order to ensure zero global momentum. You could say that the single wave packet of energy $2\hbar\Omega$ representing the two quasi-particles of momentum $\vec{P}^{photon} = \pm(\hbar\Omega/c_t)\vec{e}_2$ then corresponds to *an entangled state of the two virtual quasi-particles*. But if one end of this wave packet is suddenly "materialized" in the form of a quasi-particle (photon 1) transferring energy $E_{déposée} = \hbar\Omega$ to an "object" interacting with it, the second end of the wave packet will regroup and own the energy $E^{fluctuation} = \hbar\Omega$ and the momentum $\vec{P}^{photon} = \pm(\hbar\Omega/c_t)\vec{e}_2$. It will therefore necessarily transform into a wave packet representing photon 2, which can be "materialized" in the form of a quasi-particle.

But it should be noted that the initial wave packet had, at the time of the "materialization" of the first quasi-particle, a polarization and a helicity which could be measured, and that this polarization and this helicity measured then become the prerogative of the residual wave packet. This is exactly what quantum physics predicts when it talks about *the entanglement of two photons*. And there is therefore no instantaneous "transmission" of information from one quasi-particle (photon 1) to the other quasi-particle (photon 2) since it is during the "materialization" of the first quasi-particle (photon 1) that the wave packet associated with the second quasi-particle (photon 2) forms and necessarily acquires the characteristics complementary to the first quasi-particle (photon 1), characteristics which will be observed during of the "materialization" of the second quasi-particle (photon 2).

- *About the phenomenon of decoherence:*

As we have just said, a wave packet of energy $E^{fluctuation} = \hbar\Omega$ representing the two photons created initially can extend along a single axis over great distances. But this lengthening is obviously done at the expense of the amplitude ω_{10} of the wave packet. As the

wave packet lengthens, it will become more and more sensitive to its environment, that is to say to the other field fluctuations it encounters, until it encounters a sufficiently strong fluctuation to "break" the initial wave packet and divide it into two independent wave packets, which will therefore no longer be entangled. From this moment, the two wave packets become independent. We can then speak of a *phenomenon of decoherence*, in the sense that the "materialization" of the two wave packets in the form of two individual photons will no longer exhibit the entanglement effect described in the previous section.

This phenomenon is absolutely similar to the phenomenon of decoherence that quantum physics invokes to explain the passage from the microscopic quantum world to the classical macroscopic world.

Although quite speculative, the results obtained here are quite interesting, because they mean that the cosmological lattice which does not present longitudinal waves for $\tau_0 < \tau_{0cr}$ may contain localized disturbances of pure transverse waves of circular polarization which seem to have all the characteristics of photons (quantification, wave-particle duality, entanglement, etc.).

Localized longitudinal gravitational fluctuations

In figure 11.1, we have seen that, in a lattice in which the propagation of longitudinal waves is not possible, there can appear localized longitudinal vibrations, which one could call *localized gravitational fluctuations* $\tau_{localized}^{(p)}(\vec{r}, t)$ since they are field fluctuations of the volume expansion. We can try to dig a little deeper into this subject, by describing these longitudinal fluctuations in a cosmological lattice containing neither topological singularities nor transverse waves.

In the absence of topological singularities and transverse waves, imagine the existence of fluctuations $\tau^{(p)}(\vec{r}, t)$ of the volume expansion field of a cosmological lattice in the domain $\tau_0 < \tau_{0cr}$, of type $\tau(\vec{r}, t) = \tau_0 + \tau^{(p)}(\vec{r}, t)$. These fluctuations $\tau^{(p)}(\vec{r}, t)$, if they exist, must obviously satisfy Newton's equation of the volume expansion field. In the absence of topological singularities and transverse waves, and neglecting the effects of vacancies and interstitials ($\vec{p} \equiv m\vec{\phi}$), Newton's second partial equation for longitudinal perturbations is given by the relation of figure 5.1 in which we neglect all the fields apart $\tau^{(p)}$ and $\vec{\phi}^{(p)}$, and from which we take directly the divergence. By considering sufficiently small fluctuations $\tau^{(p)}(\vec{r}, t)$, it is possible to linearize the equation, by completely neglecting the term $(\tau^{(p)})^2$ and by extracting the density n from the divergence term. We can also introduce a parameter α with value $\alpha = K_0 - 4K_2/3 - 2K_1(1 + \tau_0)$, which is positive if the cosmological lattice does not present longitudinal waves, that is to say if $\tau_0 < \tau_{0cr}$, and replace the material derivative by the partial derivative of time, so that the equation is reduced to the first equation of figure 14.3. Still using the geometro-kinetic equation for volume expansion, assuming zero lattice sources, and neglecting the material derivative, we obtain the second equation in figure 14.3. By combining these two relations, we obtain the linearized Newton's equation of weak gravitational fluctuations in the cosmological lattice without propagation of longitudinal waves, in the domain $\tau_0 < \tau_{0cr}$.

If we dissociate the spatial behavior and the temporal behavior of these fluctuations $\tau^{(p)}(\vec{r}, t)$, we can write them as the product of a spatial function $\hbar^2\psi(\vec{r})$ by an oscillating term $e^{-i\omega t}$ in time, in the form $\tau^{(p)}(\vec{r}, t) \equiv \hbar^2\psi(\vec{r})e^{-i\omega t}$. By introducing this writing of fluctuations into

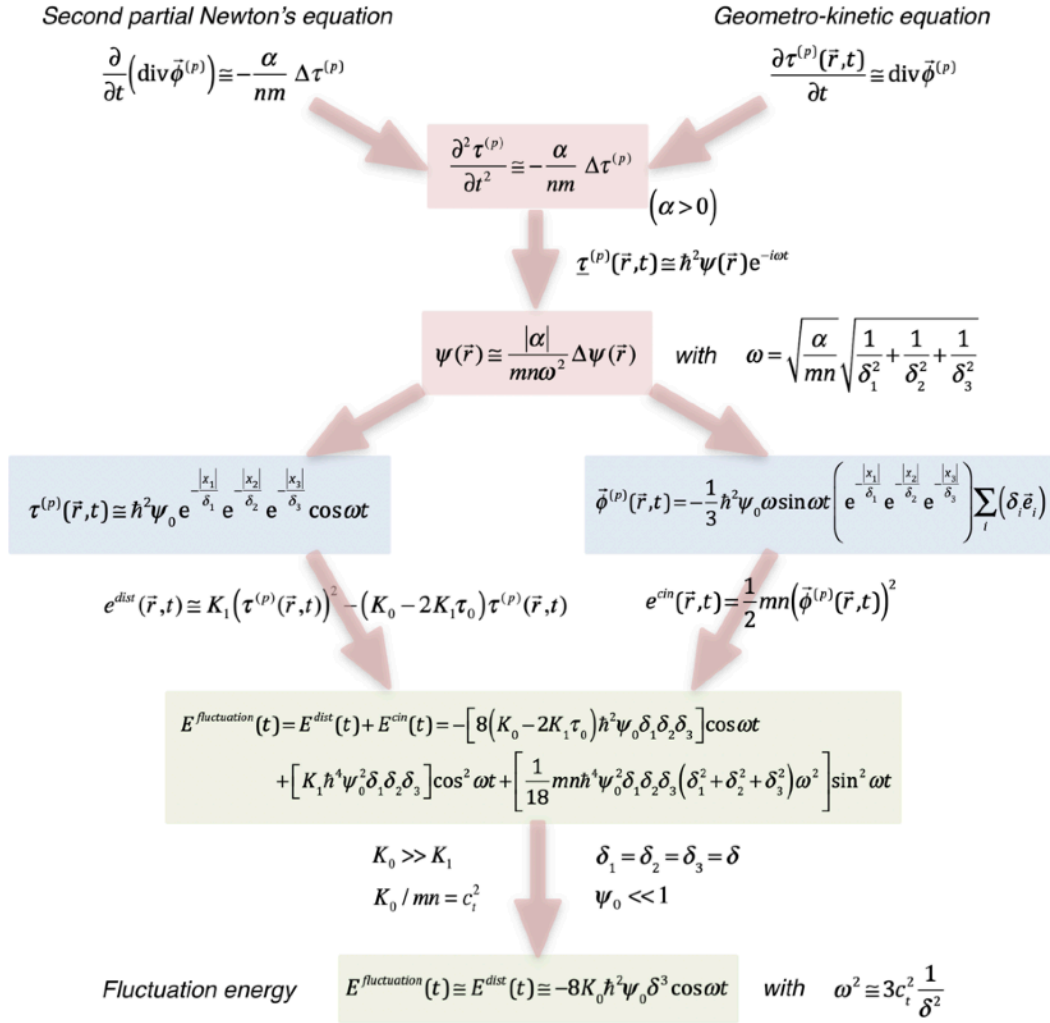


Figure 14.3 - Energy of a localized gravitational fluctuation

Newton's equation, we obtain the equation which governs the spatial component $\psi(\vec{r})$ when the fluctuations present a pulsation ω .

For example, suppose a fluctuation which is located in the vicinity of the origin, along the three axes of space. For such a fluctuation to satisfy the previous Newton's equation, the spatial component $\hbar^2 \psi(\vec{r})$ must be written in the form of a symmetrical exponential decay on either side of the origin, which, introduced into the equation of Newton, makes it possible to connect the pulsation ω of the fluctuation to its spatial ranges δ_i according to the three directions of space. We therefore see that the pulsation of a gravitational fluctuation is then inversely proportional to its spatial ranges. We can easily deduce the spatial fluctuation $\tau^{(p)}(\vec{r}, t)$, as well as the velocity fluctuation $\vec{\phi}^{(p)}(\vec{r}, t)$ within the lattice.

Let's try to calculate the elastic energy stored by this perturbation in the lattice. The elastic energy density $e^{dist}(\vec{r}, t)$ is given by the expression in figure 14.3 if the background expansion τ_0 of the cosmic lattice is not zero. The total elastic energy $E^{dist}(t)$ of the fluctuation is obtained by integrating $e^{dist}(\vec{r}, t)$ over all of the space. The kinetic energy density $e^{cin}(\vec{r}, t)$ of the fluctuation is given by the expression in figure 14.3, and the total kinetic energy $E^{cin}(t)$ of

the fluctuation is obtained by integrating $e^{cin}(\vec{r}, t)$ over all of the space. We deduce the total energy of the fluctuation $E^{fluctuation}(t) = E^{dist}(t) + E^{cin}(t)$ reported in figure 14.3.

Random microscopic fluctuations and quantum vacuum fluctuations

Now consider microscopic longitudinal fluctuations, that is to say "gravitational" fluctuations for which the amplitude ψ_0 is extremely small. Let's discuss here the very simple case of an isotropic "gravitational" fluctuation, that is to say such that the ranges in the three directions of space are equal. In the case of the perfect cosmological lattice, for $\tau_0 < \tau_{0cr}$, we have that $K_0 \gg K_1$ and $K_0 / mn = c_i^2$, so that, if this fluctuation is of very small magnitude $\psi_0 \ll 1$, it is the energy of distortion associated with K_0 which largely dominates the others, and therefore that $E^{fluctuation}(t) \cong E^{dist}(t) \cong -8K_0 \hbar^2 \psi_0 \delta^3 \cos \omega t$.

This result of a fluctuating energy which is symmetrically positive or negative over time is quite interesting and intriguing. It indeed means that a lattice not presenting longitudinal waves could be subjected to a *superposition of local fluctuations* of various pulsations ω_k , various

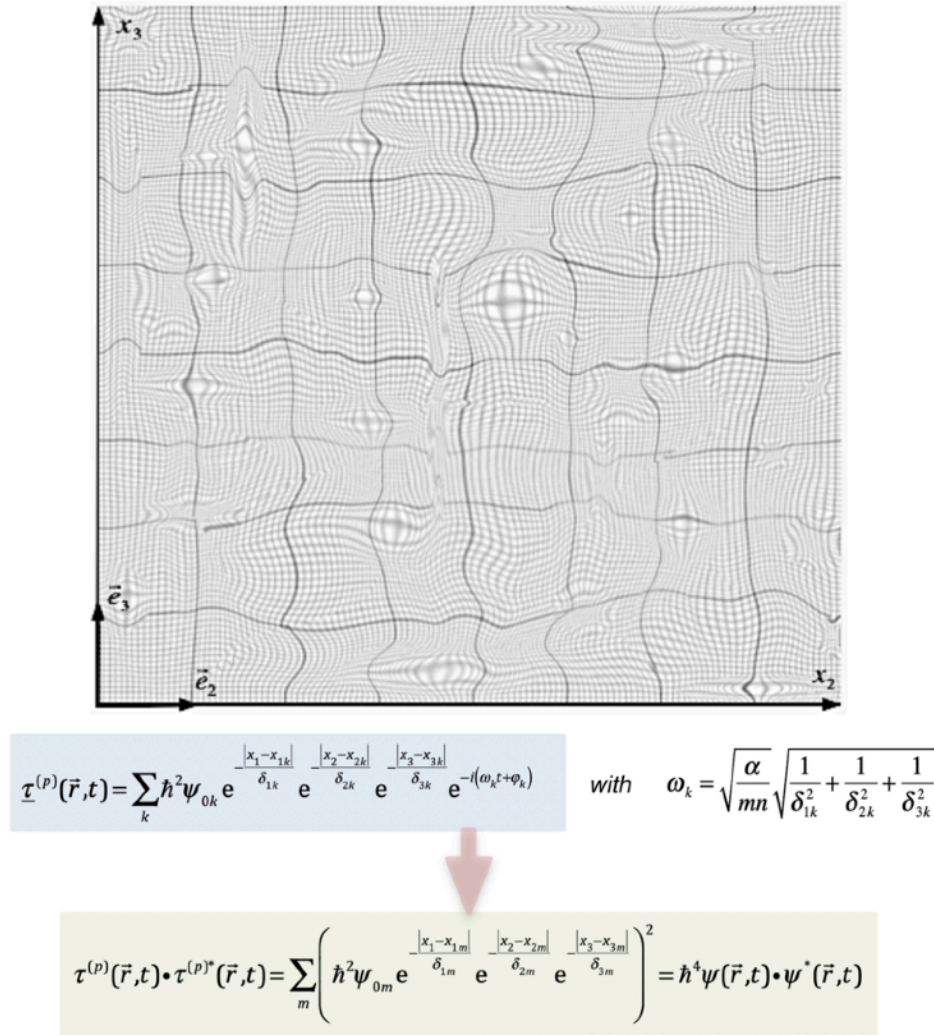


Figure 14.4 - Schematic representation of the field $\tau^{(p)}(\vec{r}, t)$ of elementary "gravitational" fluctuations

phases φ_k and various amplitudes ψ_{0k} , and whose centers would be located randomly at the positions \vec{r}_k , so as to take instantly the mathematical look shown in figure 14.4.

And since the energy of each of these fluctuations can be positive or negative over time, with a zero average, the instantaneous global energy of *this field would always have zero energy on average*. We can try to schematically represent this situation in the lattice, as we did in figure 14.4.

This field of microscopic "gravitational" fluctuations is obviously not formed of stable fluctuations in time since their energy is not a constant. It is in fact made up of "evanescent" fluctuations, which appear and disappear spontaneously, while maintaining a zero global energy of the cosmological lattice. As such, this field of "gravitational" fluctuations is the perfect analog of *the field of quantum fluctuations of the vacuum*, also composed of quantum fluctuations on the microscopic scale, of positive and negative energies, but whose average energy remains zero.

In the presence of such a superposition of fluctuations, we can calculate the product of $\tau^{(p)}(\vec{r}, t)$ by its complex conjugate. When expressing this product, it appears many terms, some having a zero value because of the positive and negative random values of the products $e^{i(\omega_n - \omega_m)t} e^{i(\varphi_n - \varphi_m)}$ and some having a non-zero value because they represent the sum of the squares of the amplitudes of each fluctuation. We thus obtain a nonzero product which is nothing other than the instantaneous product of the wave function $\psi(\vec{r}, t)$ by its complex conjugate as illustrated in figure 14.4. In chapter 1, we interpreted the product $\psi(\vec{r}, t) \cdot \psi^*(\vec{r}, t)$ as the probability of the presence of a topological singularity responsible for the wave function $\psi(\vec{r}, t)$. We can therefore apply this probabilistic concept here and imagine that the nonzero instantaneous value of $\psi(\vec{r}, t) \cdot \psi^*(\vec{r}, t)$ corresponds to *a probability of the presence of a virtual topological singularity*, in other words a topological singularity which does not really exist, which perfectly matches the usual interpretation of the quantum vacuum fluctuations in quantum physics.

Is it possible to form stable oscillatory gravitational fluctuations?

To form stable gravitational fluctuations presenting themselves as localized and lasting longitudinal oscillations within the cosmological lattice, the total energy $E^{fluctuation}(t)$ of the single fluctuation in figure 14.3 poses a serious problem. Indeed, if the fluctuation must be a stable localized vibration of frequency ω , it should in principle have an oscillation energy $E^{fluctuation}(t)$ independent of time, which is obviously not the case of the expression of figure 14.3, since this expression depends at the same time on $\cos \omega t$, on $\cos^2 \omega t$ and on $\sin^2 \omega t$.

It is therefore necessary to imagine an *ad hoc* mechanism which can ensure the independence of the total energy $E^{fluctuation}(t)$ over time. In fact, it can be shown by fairly long and tedious calculations that the total fluctuation must be composed of at least four individual elementary fluctuations a , b , c and d , of the same frequency ω , and located in different places of the lattice, respectively in $\vec{r}_a(t)$, $\vec{r}_b(t)$, $\vec{r}_c(t)$ and $\vec{r}_d(t)$, as described in figure 14.5. And so that these four fluctuations together present a total energy independent of time, the various ranges of the four fluctuations must satisfy conditions which are reported in figure 14.5, where the product ABC of any three numbers is in fact proportional to *the "volume" occupied by each fluctuation within the lattice*. In this case only, we obtain a fairly simple expression of the total

energy independent of the time of the four fluctuations, which is essentially composed of *kinetic energy*, and this global fluctuation is then stable over time.

**Stable macroscopic gravitational oscillations
in an infinite cosmological lattice and Multiverses**

In the domain of the cosmological lattice in which there are no longitudinal waves, there is thus the possibility of seeing a *stable macroscopic fluctuation* appear formed of a quadruplet of elementary fluctuations, like that represented in figure 14.5, which represent local longitudinal vibrations at a given frequency ω , and in such a way that the total energy of the global fluctuation, essentially of kinetic nature, does not depend on time.

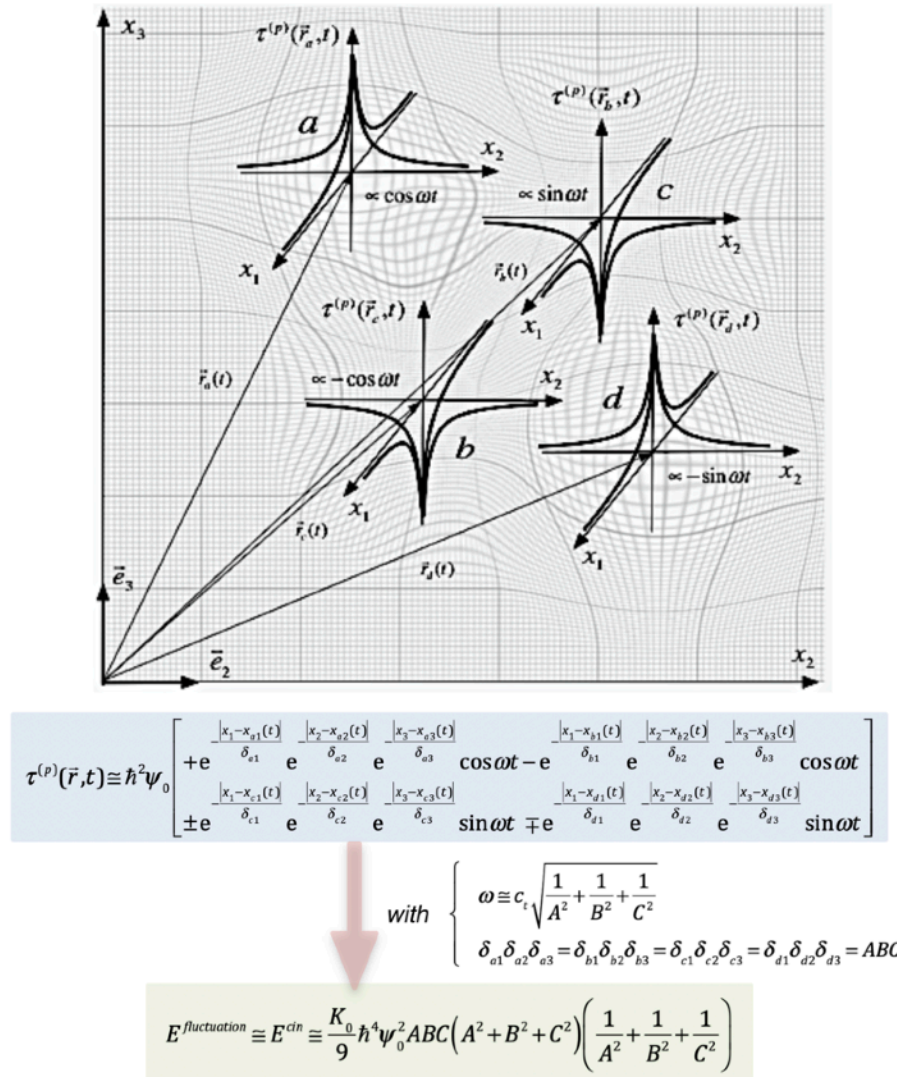


Figure 14.5 - Schematic representation of the four elementary fluctuations, components of a gravitational fluctuation with kinetic energy independent of time

Consider then the case of a macroscopic fluctuation composed of a quadruplet of elementary quasi-isotropic fluctuations, that is to say with $\delta_{x1} \equiv \delta_{x2} \equiv \delta_{x3} \equiv \delta$. From the relationships in figure 14.5 we deduce the pulse frequency $\omega \equiv c_t \sqrt{3} / \delta$ of this macroscopic fluctuation, which is inversely proportional to the range δ , as well as the energy $E^{fluctuation} \equiv E^{cin} \equiv K_0 \hbar^4 \psi_0^2 \delta^3$ of the fluctuation which is essentially kinetic in nature. We deduce that macroscopic gravitational fluctuations of large amplitudes ψ_0 in the domain $\tau_0 < \tau_{0cr}$ would have a frequency of pulsation ω proportional to the inverse of their range δ and that their overall energy would be proportional to the product of the square ψ_0^2 of their amplitude and to their volume δ^3 , and independent of their pulsation ω .

In a perfect cosmological lattice which *would be of infinite size*, it is not possible to envisage a cosmological expansion like that which we described in chapter 3 (figures 3.7 to 3.10) in the case of a finite perfect cosmological lattice. On the other hand, one could imagine the appearance of a macroscopic fluctuation like that which we have just described in figure 14.5, which would be of gigantic volume δ^3 , so that its frequency ω of oscillation would be extremely low. And if its amplitude ψ_0 were also high enough, for tiny **HS** observers who would be placed within one of these elementary fluctuations, this one would have all the characteristics of a Universe which would oscillate between a maximum expansion and a maximum contraction with the pulsation ω . Thus, the set of the four elementary fluctuations could represent a *Multiverse*. And within each of these elementary fluctuations, that is to say of each of the four universes, the observations of **HS** would be very similar to those made by **HS** who would be placed within a Universe such as those described in chapter 3 in the case of a finite perfect cosmological lattice.

But for that, there are necessary conditions which can be deduced from figure 14.6 and which would be essentially the following:

- (i) that the infinite cosmological lattice has a background expansion τ_0 such that $\tau_0 \gg 1$ in order to ensure that the formation of lacunar black holes occurs in the gray area (in figure 14.6) where the expansion of this Universe takes place at increasing speed,
- (ii) that the amplitude ψ_0 of the oscillation around $\tau = \tau_0$ is sufficient for the oscillation to pass through the range of values situated around $\tau \approx 0$ so that the cosmology scenario presented in chapter 10 is also applicable to these Multiverses.

Under these two conditions, each of these multi-universes then presents an expansion starting with a kind of "big-bounce", but which no longer implies that the volume expansion passes through a singularity such that $\tau \rightarrow -\infty$, with, in the vicinity of its center, a cosmological evolution similar to that described in chapter 10, presenting a phase with an expansion at increasing speed during which the lacunar black holes are formed, then a phase with expansion at decreasing speed leading to the maximum expansion, which can or not go through an expansion domain located beyond the critical expansion value τ_{0cr} where longitudinal waves appear at the expense of localized longitudinal fluctuations. Then this universe would go through a phase of contraction leading it to a new "big-bounce". However, it is clear that the complete calculation of the behavior of such Multiverses is not as simple as the calculation which we have just presented, if only by the fact that we adopted the assumption that $\tau_0 \ll \tau_{0cr}$ in our calculations, which would obviously not be an appropriate hypothesis in the case of gigantic gravitational fluctuations that can form such multiverses.

associated with longitudinal "gravitational" vibrations of expansion of the lattice. We could therefore speak in this case of

In fact, these gravitons have nothing to do with the gravitons sought in the context of quantification tests of general relativity. The gravitons postulated in our approach are stable energetic quasi-particles, which can travel within the lattice, but which are not required to move at the speed of transverse waves, unlike the gravitons of general relativity which are supposed to be moving at the speed of light. In addition, our gravitons are not carriers of the gravitational interaction between two singularities, but only localized and quantified energy fluctuations of the expansion field, unlike the gravitons of general relativity, which are considered as the mediating particles of gravitational interaction.

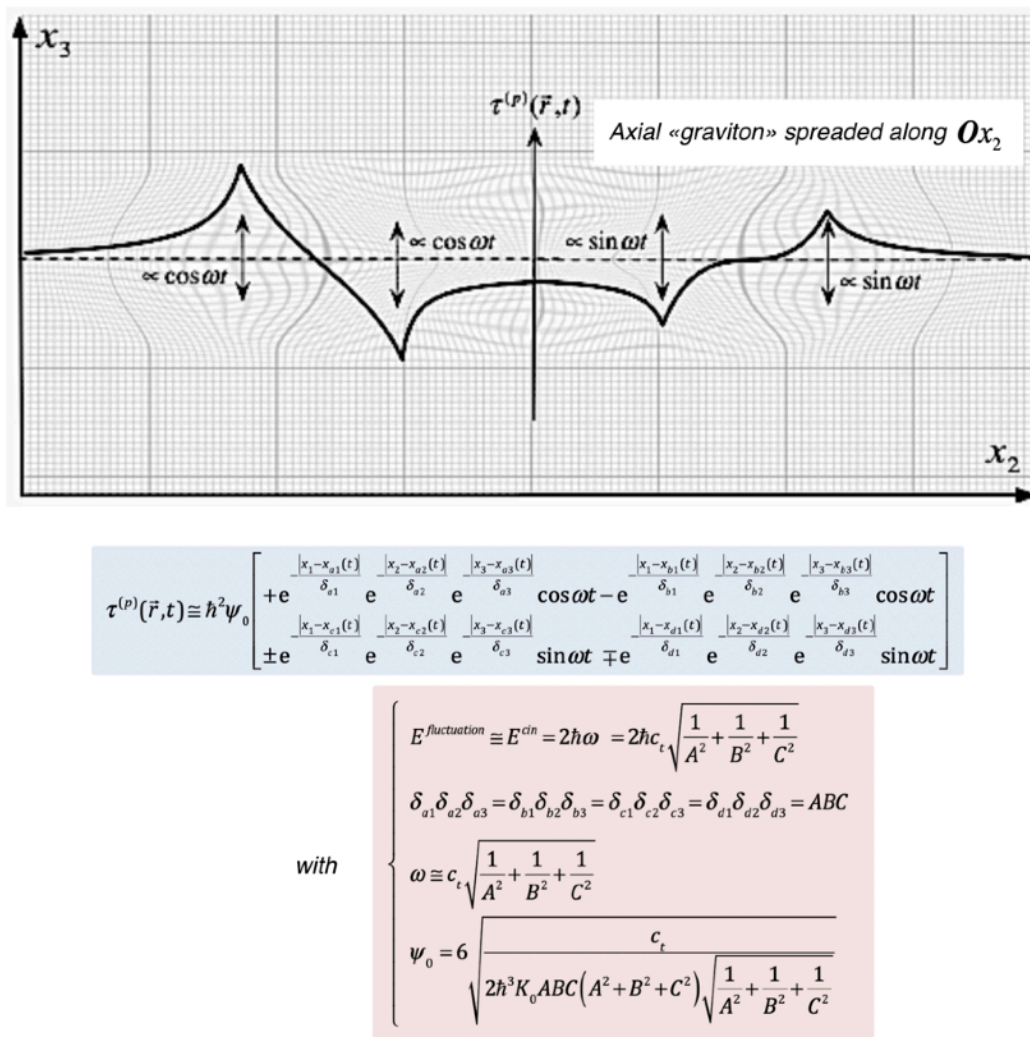


Figure 14.7 - Very schematic equations and representation of a quasi-particle "graviton"

The configuration of the four elementary fluctuations making up the "graviton" quasi-particle can be very complex. The only condition obviously being that the four elementary fluctuations can exchange energy between them in order to keep the total kinetic energy constant. One could for example imagine axial "gravitons", that is to say quasi-particles for which the four

elementary fluctuations would be aligned along a preferential axis, an illustration of which is shown in figure 14.7. There is shown very schematically the case of a hypothetical axial "graviton" in the case where it is very spread out along the axis Ox_2 . In this representation, we have graphically reported the instantaneous local volume expansion of the "graviton", by specifying the oscillations of the four components in $\cos \omega t$ and $\sin \omega t$.

It can be seen that the spreads δ_{ij} of the fluctuation along the different axes are constrained so that the products for each of the partial fluctuations are constant and equal. But each spread is not fixed, so that this quasi-particle can deform by spreading or shrinking along all the axes. For example, an axial "graviton" of pulsation ω , and therefore of kinetic energy $2\hbar\omega$, can very well oscillate between a very condensed form along the axis Ox_2 and very extended along the axes Ox_1 and Ox_3 , and an opposite shape, very extended along the axis Ox_2 and very condensed along the axes Ox_1 and Ox_3 . This effect is again clearly an aspect of the famous non-locality of quantum physics, as it has been described in the case of photons.

Finally, note that these hypothetical "graviton" quasi-particles are very different from the hypothetical evanescent gravitational fluctuations analogous to the quantum vacuum fluctuations described in figure 14.4. Indeed, in the case of evanescent gravitational fluctuations, the energy of the fluctuation is essentially *an energy of elastic distortion* associated with the modulus K_0 of the cosmological network, oscillating between a positive and negative value, and of zero mean value, while the energy of the hypothetical quasi-particles "gravitons" is *essentially kinetic in nature* and has a constant and not zero value, which ensures their long-term stability. And to obtain this stability, the quasi-particle must be composed of four strongly correlated and indissociable fluctuations which ensure the constancy of energy, in the same way as the quasi-particles "photons" must be composed of two perpendicular rotation fluctuations and out of phase, giving them their helicity and thus ensuring the constancy of their energy. There is therefore a strong analogy between quasi-particles "photons" and "gravitons", not only by their constitution ensuring the constancy of their energy, but also by their non-locality, namely their ability to spread in space while preserving their identity and their energy, a property which is a typical prerogative of quantum physics.

Conclusion

As already said in the introduction, this essay does not pretend to present a perfectly elaborated *Theory of Everything*, but rather to show that a rigorous approach to elastic solid lattices by an Euler coordinate system, as we developed in this essay, provides a much simpler framework for investigation than differential geometries such as those used for example in general relativity, but which are very rich and fertile since it has been shown quite simply that it is possible (i) to make very strong and often perfect analogies appear with all the major physical theories of the macrocosm and the microcosm, such as Maxwell's equations, special relativity, general relativity, Newtonian gravitation, modern cosmology, quantum physics and the standard model of elementary particles, and (ii) reveal strong unifying bridges between these various theories.

About the central role of Newton's equation of the cosmological lattice

Since the beginning of this essay, we note that Newton's equation (figure 3.1) that we presented in chapter 3 for the *imaginary isotropic cosmological lattice* has everywhere played a central and capital role, and that it is at the basis of most of the amazing properties of the perfect cosmological lattice, including:

- *the propagation of transverse waves* coupled to longitudinal wavelets, managed by the Newton equation, which implies that pure transverse waves can only exist with circular polarization (which is a fundamental property of photons),
- *the existence of domains of expansion* ($\tau_0 < \tau_{0cr}$) in which there are no solutions of longitudinal waves to Newton's equation, but only *quasi-static solutions* which are the basis of the phenomena of gravitational interaction between topological singularities, or *localized longitudinal vibration modes*, which are the basis of *the quantum dynamics* and *the spin of localized topological singularities*,
- *the curvature of the wave rays* in gradients of the volume expansion, which is also a direct consequence of Newton's equation, and which predicts the possibility of the existence of black holes which irrevocably capture transverse perturbations,
- *the complete Maxwell's equations* for the rotation vector $\vec{\omega}$ when the volume expansion field is homogeneous, which show that the electromagnetism equation $\partial \vec{B} / \partial t = -\vec{\text{rot}} \vec{E}$ is nothing other than the expression of Newton's equation of the cosmological lattice applied to this particular case,
- *special relativity*, with the contraction of rulers and the dilation of time for an observer moving within and with respect to the lattice, which is a direct consequence of Newton's first partial equation,
- *Newtonian gravitation* and *general relativity*, which are direct consequences of the quasi-static solution of Newton's second partial equation, in the case where the topological singularity considered has an energy density or rotation charge density below a certain critical value,

- *the spatial curvature of space for the **GO** observer situated outside the lattice and the space-time curvature for local observers **HS** within the lattice itself*, which implies a direct analogy between the divergence of Newton's equation and the famous *Einstein equation of zero divergence* $\vec{\nabla} \cdot \mathbf{T} = 0$ *for the energy-momentum tensor* which ensures that the laws of conservation of energy and angular momentum are respected,
- *the black holes*, static solutions of Newton's second partial equation in the presence of macroscopic vacancies in the lattice when $\tau_0 > 1$,
- *the neutron or pulsar stars*, static solutions of Newton's second partial equation in the presence of macroscopic interstitial clusters in the lattice,
- *the weak interaction force* between the edge dislocation loops and the twist disclination loops, which is also a consequence of Newton's second partial equation,
- *the quantum physics, the wave functions, the Schrödinger wave equation, and the notion of spin*, which are consequences of Newton's second partial equation in the dynamic case of gravitational perturbations associated with localized topological singularities of the cosmological lattice, when these have an energy density or rotation charge density that is above a certain critical value. This critical value of the energy density or of the rotation charge density then becomes an extremely important quantity since it actually corresponds to *a quantitative value which defines the famous quantum decoherence limit*, i.e. the limit of passage between a classical behaviour and a quantum behaviour of a topological singularity,
- *the photons*, quanta of the transverse solution of circular polarization of the Newton equation,
- *the pure and hard quantum concepts*, such as *bosons, fermions and the indistinguishability of topological singularities*, as well as *the Pauli exclusion principle*, which are all deduced directly from the application of the second partial equation of Newton to several localized topological singularities.

About the perfectly innovative role of the curvature charge

In our approach of the cosmological lattice, a perfectly innovative concept appears, *the charge of curvature of the edge dislocation loops*, which is an unavoidable consequence of the treatment of a solid lattice and its topological singularities in Euler coordinates. This concept does not appear absolutely in all modern theories of physics, whether in general relativity, in quantum physics or in the Standard Model, while in our approach this concept provides explanations for many obscure points of these theories, among which the main ones are:

- *the weak force associated with the cohesion of the corner-screw dispirations:*

Considering topological singularities formed by the coupling of a twist disclination loop with an edge dislocation loop, which are called dispiration loops, *an interaction force similar to a capture potential* appears, *with a very weak range*, which induces interactions between loops presenting a perfect analogy with the weak interactions between elementary particles of the Standard Model.

- *the matter-antimatter asymmetry:*

In our approach, the matter-antimatter asymmetry has no more mystery because it is precisely the charge of curvature which becomes responsible for the appearance of *a weak*

asymmetry between the particles (hypothetically containing edge loops of interstitial nature) and anti-particles (hypothetically containing edge loops of a lacunar nature).

- *the mass of curvature associated with the curvature charge and its consequences:*

Each topological singularity is associated with a mass of curvature due to the curvature charge which is added to its mass of inertia, and which induces slight differences in the behavior of the gravitational interaction forces between matter and anti-matter, and which provides simple explanations for several still mysterious phenomena of the cosmological evolution of matter, such as (i) *the segregation between matter and antimatter within galaxies*, (ii) *the formation of gigantic black holes* (macroscopic lacunar singularities) at the heart of galaxies by gravitational collapse of antimatter, (iii) *the apparent disappearance of antimatter* in the Universe following the formation of the black holes in the heart of galaxies, and (iv) *the formation of neutron stars* (macroscopic interstitial singularities) by gravitational collapse of stars of matter within galaxies.

- *the appearance of neutrino antigravity and its consequences:*

The negative mass of curvature dominates the positive mass of inertia in the case of the pure edge dislocation loop, which we associate with the neutrino of the standard model. This phenomenon leads to the fact that the neutrino is gravitationally repellant for other particles, which provides simple explanations for several still mysterious phenomena in the cosmological evolution of matter, such as (i) *the formation of galaxies* by precipitation of matter and antimatter in the form of aggregates within a sea of repellant neutrinos, and (ii) *the concept of dark matter* which is replaced by the concept of "sea of repellant neutrinos" in which are immersed all galaxies, globular clusters, and other structures of the visible Universe. This sea of neutrinos exerts a compressive force on the stars of the periphery of the galaxies, which must necessarily rotate faster to compensate for this compressive force by an additional centripetal force of rotation.

- *the bosonic or fermionic nature of the particles:*

The curvature charge has another major interest linked to the bosonic or fermionic nature of the particles. Indeed, we note that *all the particles with which a charge of curvature is associated (leptons, quarks and baryons) are fermions with a half-integer spin, which satisfy the Pauli exclusion principle*, while *all particles which do not have a curvature charge (photons, gauge bosons, gluons and mesons) are bosons with an integer spin, not subject to the Pauli exclusion principle*. There is very probably here a crucial role played by the curvature charge, which could impose a boson or fermion behavior on a given particle.

About the importance of the microscopic structure of the cosmological lattice

The structure of the cosmological lattice also plays a major role in the analogies we have developed, but it is especially at the level of the structures of microscopic topological singularities in loops that it plays a crucial role. Indeed, it was necessary to imagine *a face-centered cubic lattice with an axial property of dense planes, imaginary "colored" in red, green and blue, and satisfying some simple rules concerning their arrangement*, to find topological loops surprisingly analogous to all particles, leptons, quarks, intermediate bosons and gluons of the first family of elementary particles of the Standard Model. And the existence of a connecting

fault energy between dense planes has allowed to explain the appearance of a force with asymptotic behavior between the quark-like singularities, quite similar to the strong force of the Standard Model, and which forces the formation of doublets or triplets of singularity loops similar to the mesons and baryons of the Standard Model.

And it was also necessary to imagine *the existence of two types of stacking faults between the dense planes of this axial CFC lattice*, to try to explain the existence of the three families of the Standard Model of elementary particles.

From this enumeration of the important roles of Newton's equation and the structure of the cosmological lattice, we can conclude that *the Newtonian inertia of the lattice in absolute space, its elasticity by shear, by rotation and by volume expansion, its microscopic structure and the existence of the curvature charge associated with the edge dislocation loops* are the main ingredients of the cosmological lattice theory and are the keys to explain all the properties of this particular lattice, and thus, by analogy, of the real Universe, even if there are still many obscure points in this analogy.

Still unclear points about the Crystalline Ether

It is clear that *the Crystalline Ether* that we have developed throughout this book, in spite of the undeniable success it has brought us, is by no means perfect. There are still many obscure points which deserve to be studied and, if possible, clarified. Among them, we will mention the most important ones, in the order of their appearance during the presentation, and in the form of questions:

- does a "crystalline ether" really exist, i.e. a cosmological lattice of CFC structure with axial properties, what are the "corpuscles" that compose it, which would possess a purely Newtonian mass of inertia in absolute space, and what are the relations existing between these "corpuscles" and the Higgs boson of the Standard Model?
- what is the physical nature of the isotropic elasticity of the cosmological lattice constituting the crystalline ether, which leads to the moduli $K_0 = K_3 > 0$, $0 < K_1 \ll K_0$, $0 \leq K_2 \ll K_3$ allowing to express the elastic free energy of the lattice per unit volume?
- what is the origin of the kinetic energy of the lattice necessary for the behaviors of the cosmological expansion of the lattice?
- what role could the "corpuscles" of the cosmological lattice play in hypothetical diffusion phenomena within the cosmological lattice (which could very well explain some properties of magnetism)?
- would it be possible that there are still vector electric charges?
- what exactly are the parameters ζ_{BV} , ζ_{BC} , ζ_{BM} introduced to calculate the energy of the loops, and are they really independent of the background expansion of the lattice?
- what could be the role of *the slip mixed dislocation loops* in our analogy with elementary particles?
- what is the relevance of the analogy between macroscopic vacancies and black holes, as well as between macroscopic interstitial and neutron stars?
- what physical explanation and which numerical values should be given to the parameters α_{BV} , β_{BV} , α_{BC} , β_{BC} , α_{BM} , β_{BM} used for the calculation of the energy dependence of the loops in the background expansion of the lattice?

- how to explain physically the fact that the parameters a and b used to find the clock and the rulers of the observer **HS** must be worth exactly $1/4$?
- what is the thermal dependence of the free energy of the cosmological lattice, and could this justify a kind of “liquefaction” of the lattice for extremely small values of the volume expansion, in the vicinity of the “big-bang” ?
- how, from a topological point of view, can a dislocation loop or a disclination loop turn on itself to explain the spin?
- what makes a certain topological loop have a spin $1/2$ or a spin 1 , and what is the exact role of the charge of curvature in the value of the spin and the bosonic or fermionic behavior of a particle?
- what exactly are the structure of the cosmological lattice and the nature of the colored planes of this lattice, and what is the link between these colored planes and the "corpuscles" composing the lattice?
- how can topological singularities analogous to quarks have a spin when they are linked to others by a connecting fault energy tube?
- and many other questions, of a purely physical, or even philosophical nature which are not within the scope of this book, but which are very intriguing.

About the unifying power of our Crystalline Ether Theory

In fact, even if there are still many obscure points, it appears that our Crystalline Ether Theory contains strong analogies with all the great theories of modern physics, and that in this it has *an enormous unifying power*. And this approach by the cosmological lattice is *very simple*, on the contrary of the theories of superstrings or of the theory M which the theorists propose to unify “of force” the physical theories by *quantifying gravity* and by independently introducing into it the four elementary interactions, which leads to *extremely complicated mathematical theories*, in very complex spaces with n dimensions ($n = 11$ for theory M), and which have so far shown no predictive power.

It is interesting to note here that the superstring theories use cords and branes in complicated multidimensional spaces to quantify gravity, while our approach also uses cords, loops and membranes, but which are then simple topological singularities of a purely three-dimensional lattice, with an additional dimension of absolute time completely decoupled from the dimensions of space, since time can be measured there by the universal clock of an imaginary observer **GO** external to the lattice in absolute space .

And if the quasi-static volume expansion of this lattice on the macroscopic scale is the expression of the phenomena attributed to gravitation, the dynamic fluctuations of the expansion of this lattice on the microscopic scale are nothing other than the expression of the phenomena attributed to quantum physics. It is therefore wrong to try to quantify the theory of gravitation, since quantum physics in the Crystalline Aether Theory is precisely the expression of the dynamic fluctuations of gravitation at the microscopic scale.

About the epistemology and the consequences of this essay

It is true that, in this essay, nothing comes yet to give a definitive explanation to the existence of the Universe, to the reason of being of the big-bang, and why the universe could

be constituted by *a crystalline ether*. These points remain, at least for now, within the purview of each individual's philosophy or beliefs. But, from an epistemological point of view, this essay shows that it is possible to find a very interesting framework to unify the various current physical theories, a framework in which there would no longer be many mysterious phenomena other than the reason to be of the universe. And this approach is based in fact on a single concept absolutely essential, but of a disarming simplicity, which one could state in the following way, while being inspired by a famous quotation of the great physicist that was Richard P. Feynman:

"It is possible to observe and measure from the outside, with an absolute Eulerian reference frame endowed with fixed and immutable rulers and a universal clock, the spatio-temporal evolutions of a solid lattice having both a certain microscopic structure, specific elastic properties and Newtonian inertia properties. This one sentence contains, as you'll see, a huge amount of information about the universe, as long as you put a little imagination and thought into it. "



Richard Feynman
(1918-1988)

Glossary

Average local velocity $\vec{\phi}(\vec{r}, t)$: velocity of particles in a liquid or a solid at the coordinates of space \vec{r} and time t in the absolute reference frame $Ox_1x_2x_3$ of the laboratory of the **GO** observer.

Average volume $v(\vec{r}, t)$: average volume occupied by a solid lattice cell, defined as the inverse of n , that is to say $v = 1/n$.

Average volume density $n(\vec{r}, t)$: average volume density of particles in a fluid or of elementary substitutional sites in a lattice with space \vec{r} and time t coordinates.

Contorsions: set of curvatures of a solid lattice by flexion and torsion.

Euler coordinates: the Euler coordinate system is based on the description of the evolution in space and time of the vectors $\vec{\phi}(\vec{r}, t)$ of the velocity field of the points of the fluid or solid medium located at the space \vec{r} and time t coordinates in the absolute coordinate system of the **GO** observer laboratory (figure 1.2).

Disclinations: topological singularities corresponding to discontinuities $\vec{\Omega}$ (*Frank vector*) of the field of rotations by deformation within the medium.

Dislocations: topological singularities corresponding to discontinuities \vec{B} (*Burgers vector*) of the field of displacements within the medium.

Dispirations: topological singularities formed by the combination of a dislocation and a disclination.

Distorsions: set of deformations, global rotations and local rotations of a solid lattice. Only the global translations of the lattice are not included in the distortions.

Eulerian thermokinetics: set of two principles of continuity of the total energy and the entropy, absolutely essential in Euler coordinates and deduced from the first two laws of thermodynamics and the Newtonian kinetic energy.

Geometro-kinetics: set of equations which relate *the temporal variations of the distortions of the solid*, which are calculated along the trajectory of the particles of the medium using a *mathematical operator of time called the material derivative*, with *the spatial variations of the velocity field* $\vec{\phi}(\vec{r}, t)$ of the medium, which are calculated using *mathematical space operators from vector analysis* applied to the velocity field.

Geometro-compatibility: set of equations which assure, from a topological point of view, that it does not exist, or that it exists, discontinuities \vec{B} in the field of displacements, called dislocations, within the medium

Great Observer GO: the person outside the medium who observes, describes and analyzes the continuous medium from his observatory, which is provided with a frame of reference composed of an orthonormal Euclidean frame of reference $Ox_1x_2x_3$, i.e. three rulers of

unit length , oriented perpendicularly to each other and represented by three arrows called the base vectors $(\vec{e}_1, \vec{e}_2, \vec{e}_3)$ of the coordinate system, and a universal clock ensuring that time t is measured identically everywhere in the laboratory.

Homo Sapiens HS: a person situated inside the lattice, et composed of topological singularities of the lattice, who observes, describes and analyzes the phenomena from his observatory, which is provided with a frame of reference composed of an orthonormal Euclidean frame of reference $Ox_1'x_2'x_3'$, i.e. three rulers of unit length , oriented perpendicularly to each other and represented by three arrows called the base vectors $(\vec{e}_1', \vec{e}_2', \vec{e}_3')$ of his reference frame, and a clock measuring his own time t in his reference frame. Measured by the **GO** observer, the lengths of the rulers and the speed of the clock of the **HS** observer depend strongly on the velocity of the observer **HS** relative to the lattice, and also on the local volume expansion of the lattice.

Lagrange coordinates: the Lagrange coordinate system is based on the description of the evolution in space and time of the vectors of a displacement field $\vec{u}(\vec{r}, t)$, knowing the coordinates \vec{r} of all the points of the initial solid in the fixed frame $Ox_1x_2x_3$ of the laboratory of the observer (figure 1.1).

Newtonian dynamics: dynamics of the particles of the medium which satisfy the law of Newton $\vec{f} = m\vec{a}$, and which implies that the acceleration \vec{a} of a particle is related to the force \vec{f} which one applies to it via the mass of inertia m of the particle.

Non-Markovian process: physical process within a system which depends not only on the present conditions acting on the system, but also on the history of the system which undergoes it.

Operator material derivative: it is a mathematical operator of time used to calculate the temporal variations of a physical quantity along the trajectory of the particles of a medium moving at velocity $\vec{\phi}$. This operator is represented by a straight derivative defined as $d/dt = \partial/\partial t + (\vec{\phi}\vec{\nabla})$.

Operator divergence: the divergence of a vector field \vec{u} is a mathematical space operator of vector analysis providing a scalar field g . The scalar g represents the limit of the flow of the field \vec{u} through a closed surface S around a point A and can be different from zero only if the field \vec{u} "diverges locally around the point A ". The divergence is an invariant of the field \vec{u} , that is to say that it does not depend on the coordinate system chosen.

Operator gradient: the gradient of a scalar field f is a mathematical space operator of vector analysis providing a vector field \vec{u} . The direction of the vector \vec{u} is perpendicular to the level surfaces of the function f in space. Its norm is proportional to the speed of variation of the function f in this direction, and is therefore different from zero only if the value of the function f "varies in a direction of space". The gradient is an invariant of the field f , that is to say that it does not depend on the chosen coordinate system.

Operator curl (rotational): the curl (rotational) of a vector field \vec{u} is a mathematical space operator of vector analysis providing another vector field \vec{v} . The direction of the vector \vec{v} is perpendicular to the maximum circulation area of the vector \vec{u} around a point A . Its norm is proportional to the speed of circulation of \vec{u} around A in this direction, and is

different from zero only if the field \vec{u} "turns around the point A ". The rotational is *an invariant* of the field \vec{u} , that is to say that it does not depend on the chosen coordinate system.

Scalar: a scalar is a mathematical object corresponding to a physical quantity described by a *single number*. We speak of a *scalar field* when a scalar physical quantity takes different values at all points in space and over time.

Scalar of volume expansion $\tau(\vec{r}, t)$: scalar defined as $\tau(\vec{r}, t) = -\ln(n/n_0) = \ln(v/v_0)$, depending on the space \vec{r} and time t coordinates within the lattice, and perfectly measuring the concept of volume expansion of the lattice since $\tau \rightarrow \infty$ for intense expansions (when $v \rightarrow \infty$), $\tau \rightarrow -\infty$ for intense contractions (when $v \rightarrow 0$) and $\tau \rightarrow 0$ when $v \rightarrow v_0$. This scalar represents also the trace of the distortion tensor $\vec{\beta}_i$ or the strain tensor $\vec{\varepsilon}_i$.

Solid medium: a medium will be said to be *solid* when, on a microscopic scale, it corresponds to a collection of particles such that *the identity of the nearest neighbors of a given particle does not change over time*.

Source of Frank-Read: mechanism for creating dislocations by a dislocation segment anchored at two points and subjected to a force exceeding a certain limit value.

String model: mathematical model used to describe the movement of a dislocation that moves and curves within a lattice.

Tensor of order two: a tensor of order two is a mathematical object represented by an array 3 of 3 of *nine different numbers*. A tensor of order two actually represents a physical quantity described by *nine numbers*. It can be very convenient to represent a tensor of order two using three vectors in the Euler coordinate system. We speak of a tensor field of order two when a tensorial physical quantity takes different values at all points in space and over time.

Tensor of shear strain $\vec{\alpha}_i$: symmetric tensor of order two, without trace, deduced from the strain tensor $\vec{\varepsilon}_i$ from which we subtract the trace, and which represents the set of shears of the medium, without taking into account the volume expansion of the lattice.

Tensor of contortion $\vec{\chi}_i$: spatial variations of the deformation field $\vec{\varepsilon}_i$ which can be decomposed by symmetries into a vector of flexion $\vec{\chi}$ and a transverse symmetric tensor (without trace) of torsion $[\vec{\chi}_i]^s$.

Tensor of deformation $\vec{\varepsilon}_i$: symmetric tensor of order two deduced from the symmetrical part of the distortion tensor $\vec{\beta}_i$, which represents all the deformations of the medium, but without the global rotations of the medium.

Tensor of distortion $\vec{\beta}_i$: array of nine numbers β_{ij} sufficient to describe perfectly the set of global and local rotations and deformations of the solid lattice. The lattice distortion tensor field β_{ij} will be represented for convenience by a field of three vectors $\vec{\beta}_1, \vec{\beta}_2, \vec{\beta}_3$, remembering that a vector is a space-oriented arrow composed of three numbers.

Tensor of torsion $[\vec{\chi}_i]^s$: symmetric transverse tensor (without trace) deduced from the contortion tensor $\vec{\chi}_i$, and representing the torsions of the medium, as illustrated in figure 1.18.

Thermal activation: activation process of a mechanism given by localized thermal fluctuations, due to the temperature within the medium.

Vector: a vector is a mathematical object corresponding to *an arrow oriented in space*. A vector actually represents a physical quantity described by *three numbers* which correspond respectively to the lengths of the three projections of the arrow on the axes of the coordinate system $Ox_1x_2x_3$. We speak of a *vector field* when a vector physical quantity takes different values at all points in space and over time.

Vector of flexion $\vec{\chi}$: vector deduced from the anti-symmetrical part of the contortion tensor $\vec{\chi}_i$, and representing the flexions of the medium, as illustrated in figure 1.17.

Vector of rotation $\vec{\omega}$: axial vector deduced from the anti-symmetrical part of the distortion tensor $\vec{\beta}_i$, and which represents all the local and global rotations within the medium.

Mathematical and physical symbols

Mathematical operators

$\vec{\text{grad}}$ = gradient operator of the vector analysis

rot = curl (rotational) operator of the vector analysis

div = divergence operator of the vector analysis

$\vec{\nabla}$ = «del» operator of the vector analysis

$\partial/\partial t$ = time derivative to measure the time variations of a physical quantity at a given location in space in the Euler coordinate system

$d/dt = \partial/\partial t + (\vec{\phi}\vec{\nabla})$ = material derivative to measure the temporal variations of a physical quantity along the trajectory of the particles of a medium

Coordinate system

\vec{r} = vector position in the coordinate system $Ox_1x_2x_3$

$\vec{u}(\vec{r}, t)$ = field of displacement in Lagrange coordinates

$\vec{u}_E(\vec{r}, t)$ = field of displacement in Euler coordinates

$\phi(\vec{r}, t)$ = local average velocity of the medium

$n(\vec{r}, t)$ = average volume density

$v(\vec{r}, t)$ = average volume of a lattice cell

$\tau(\vec{r}, t)$ = scalar of volume expansion

Distortions et contortions

$\vec{\beta}_i$ = distortion tensor

$\vec{\varepsilon}_i$ = symmetric deformation (strain) tensor

$\vec{\alpha}_i$ = symmetric transverse shear strain tensor

$\vec{\omega}$ = rotation vector

τ = scalar of volume expansion

$\vec{\omega}^{(e)}$ = field of rotation $\vec{\omega}^{(e)}$ deduced from the deformation tensor

$\vec{\beta}_i^{el}, \vec{\varepsilon}_i^{el}, \vec{\alpha}_i^{el}, \vec{\omega}^{el}, \tau^{el}$ = tensors of elastic distortions

$\vec{\beta}_i^{an}, \vec{\varepsilon}_i^{an}, \vec{\alpha}_i^{an}, \vec{\omega}^{an}, \tau^{an}$ = tensors of anelastic distortions

$\vec{\beta}_i^{pl}, \vec{\varepsilon}_i^{pl}, \vec{\alpha}_i^{pl}, \vec{\omega}^{pl}, \tau^{pl}$ = tensors of plastic distortions

$\vec{\chi}_i$ = tensor of contortion

$[\vec{\chi}_i]^S$ = tensor of torsion

$\vec{\chi}$ = tensor of flexion

Physical quantities

$\rho(\vec{r}, t)$ = mass density of the medium

S_m = mass volume source

\vec{J}_m = mass transport surface flux

S_n = volume source of lattice sites

e_{cin} = average kinetic energy per lattice site

s = average entropy per lattice site

u = average internal energy per lattice site

S_w^{ext} = volume source of external work

\vec{J}_w = surface work flow

\vec{J}_q = heat flux

S_e = volume source of entropy

T = local medium temperature

$\Delta\vec{\phi}_L$ = relative velocity of a vacancy compared to the lattice

$\Delta\vec{\phi}_I$ = relative velocity of an interstitial compared to the lattice

$n_L(\vec{r}, t)$ = number of vacancies per unit of lattice volume

$n_I(\vec{r}, t)$ = number of self-interstitials per unit of lattice volume

$C_L = n_L / n$ = atomic concentrations of vacancies relative to the site density n

$C_I = n_I / n$ = atomic concentrations of self-interstitials relative to the site density n

\vec{J}_L = surface flow of diffusion of vacancies with respect to the lattice

\vec{J}_I = surface flow of diffusion of self-interstitials with respect to the lattice

S_L = volume source of vacancies within the lattice

S_I = volume source of self-interstitials within the lattice

State functions and state equations

$u(\vec{\alpha}_i^{el}, \vec{\alpha}_i^{an}, \vec{\omega}^{el}, \vec{\omega}^{an}, \tau^{el}, C_L, C_I, s)$ = internal energy state function of an elastic, anelastic and self-diffusing solid

$\vec{\Sigma}_k, \vec{\sigma}_k, \vec{s}_k, \vec{m}, p, \vec{\Sigma}_k^{cons}, \vec{\sigma}_k^{cons}, \vec{s}_k^{cons}, \vec{m}^{cons}$ = mechanical potentials conjugated with elastic and anelastic distortion tensors respectively $\vec{\beta}_i^{el}, \vec{\varepsilon}_i^{el}, \vec{\alpha}_i^{el}, \vec{\omega}^{el}, \tau^{el}, \vec{\beta}_i^{an}, \vec{\varepsilon}_i^{an}, \vec{\alpha}_i^{an}$

$\vec{\Sigma}_k$ = stress tensor conjugated with the elastic distortion tensor $\vec{\beta}_i^{el}$

$\vec{\Sigma}_k^{cons}$ = stress tensor conjugated to the tensor of anelastic distortions $\vec{\beta}_i^{an}$

$\vec{\sigma}_k$ = symmetric stress tensor conjugated to the elastic strain tensor $\vec{\varepsilon}_i^{el}$

$\vec{\sigma}_k^{cons}$ = symmetric stress tensor conjugated to the tensor of anelastic deformations $\vec{\varepsilon}_i^{an}$

\vec{s}_k = symmetric transverse stress tensor conjugated with the elastic shear tensor $\vec{\alpha}_i^{el}$

\vec{s}_k^{cons} = symmetric transverse stress tensor conjugated with the anelastic shear tensor $\vec{\alpha}_i^{an}$

\vec{m} = torque vector conjugated to the elastic rotation vector $\vec{\omega}^{el}$

\vec{m}^{cons} = torque vector conjugated to the anelastic rotation vector $\vec{\omega}^{an}$

p = pressure conjugated with the scalar of volume expansion τ^{el}

μ_L = chemical potential conjugated with the atomic concentration C_L of vacancies

μ_I = chemical potential conjugated with the atomic concentration C_I of self-interstitials

T = thermal potential combined with the entropy s of the medium, called the local temperature

Dislocations et disclinations

\vec{B} = Burgers vector

$\vec{\Omega}$ = Frank vector

$\vec{\lambda}_i$ = tensor density of dislocation charge

$\vec{\lambda}$ = vector density of flexion charge, deduced from the anti-symmetrical part of $\vec{\lambda}_i$

λ = scalar density of rotation charge, deduced from the trace of $\vec{\lambda}_i$

$\vec{\lambda}_i - \vec{e}_i \wedge \vec{\lambda} - \vec{e}_i \lambda$ = tensor density of contortion charge

$\vec{\lambda}_i - (\vec{e}_i \wedge \vec{\lambda}) / 2 - \vec{e}_i \lambda$ = tensor density of torsion charge

$\vec{\theta}_i = \text{rot} [\vec{\lambda}_i - \vec{e}_i \wedge \vec{\lambda} - \vec{e}_i \lambda]$ = tensor density of disclination charge

$\theta = \text{div } \vec{\lambda}$ = scalar density of curvature charge

$\vec{\Lambda}_i$ = linear tensor charge of dislocation of a dislocation line

$\vec{\Lambda}$ = linear vector charge of dislocation of an edge dislocation line

Λ = linear scalar charge of dislocation of a screw dislocation line

$\vec{\Pi}_i$ = surface tensor charge of dislocation of a thin membrane

$\vec{\Pi}$ = surface vector charge of flexion of a thin membrane of flexion or disorientation

Π = surface scalar charge of rotation of a thin membrane of torsion

q_θ = global scalar charge of curvature of a prismatic dislocation loop

q_λ = global scalar charge of rotation of a twist disclination loop

Q_λ = global scalar charge of rotation of a localized cluster of topological singularities

Q_θ = global scalar charge of curvature of a localized cluster of topological singularities

\vec{J}_i = tensor surface flux of dislocation charges

\vec{J} = vector surface flux of rotation charges, deduced from the anti-symmetrical part of \vec{J}_i

S_n = scalar volume source of lattice sites, deduced from the trace of \vec{J}_i

\vec{V} = relative velocity of a singularity compared to the lattice

\vec{Y}_i = linear tensor flow of dislocation charges per unit of dislocation length

\vec{Y} = linear vector flow of flexion per unit of dislocation length

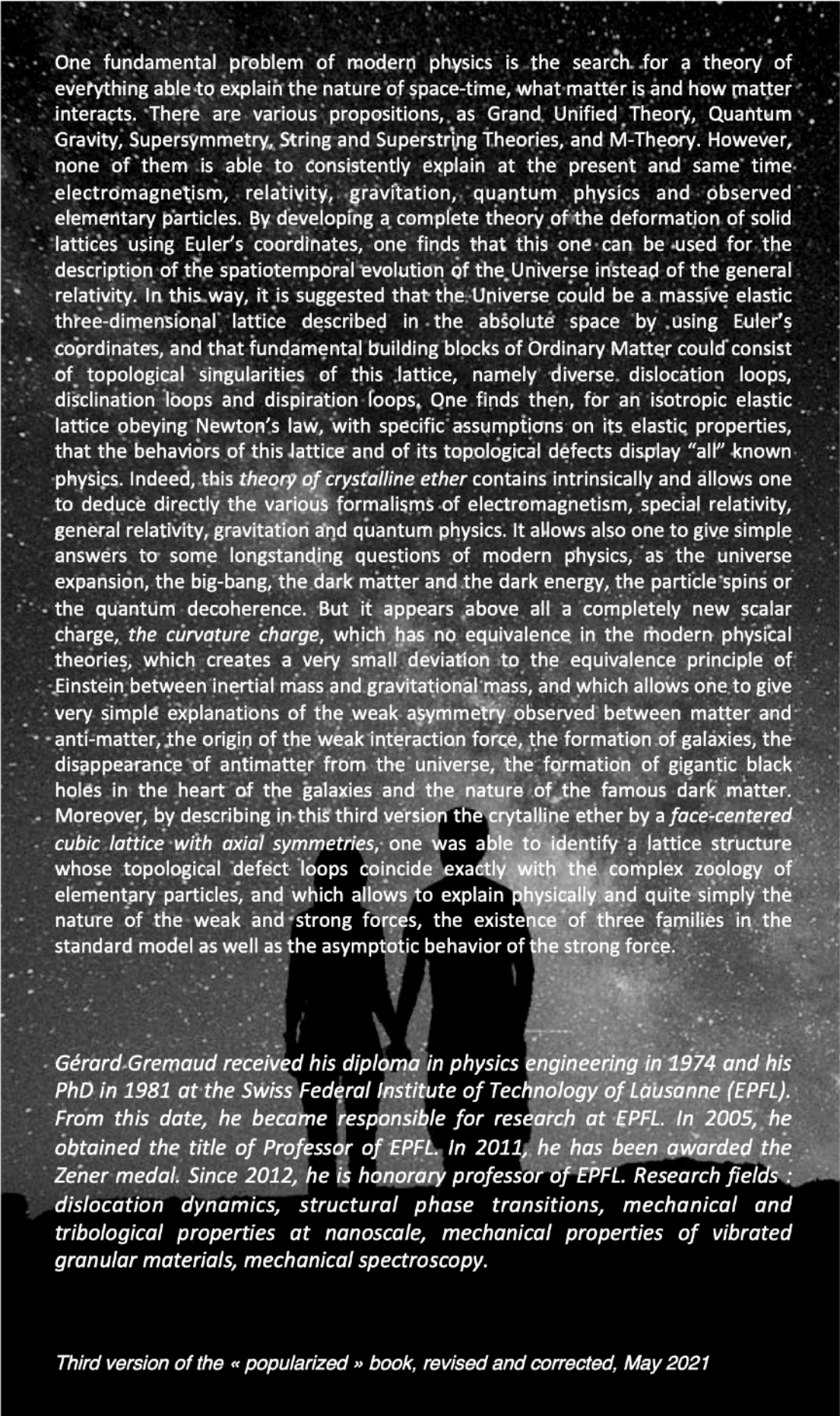
Y = linear source of lattice sites per unit of dislocation length

\vec{F}_{PK} = Peach and Koehler force acting per unit length on a dislocation

$E_i(d) = \gamma d + E_d(d)$ = total energy of dissociation of a dislocation into two partials, according to the distance d separating them

$E_d(d)$ = interaction energy of two partials as a function of the distance d between them, per unit of dislocation length

γ = stacking fault energy per unit area



One fundamental problem of modern physics is the search for a theory of everything able to explain the nature of space-time, what matter is and how matter interacts. There are various propositions, as Grand Unified Theory, Quantum Gravity, Supersymmetry, String and Superstring Theories, and M-Theory. However, none of them is able to consistently explain at the present and same time electromagnetism, relativity, gravitation, quantum physics and observed elementary particles. By developing a complete theory of the deformation of solid lattices using Euler's coordinates, one finds that this one can be used for the description of the spatiotemporal evolution of the Universe instead of the general relativity. In this way, it is suggested that the Universe could be a massive elastic three-dimensional lattice described in the absolute space by using Euler's coordinates, and that fundamental building blocks of Ordinary Matter could consist of topological singularities of this lattice, namely diverse dislocation loops, disclination loops and dispiration loops. One finds then, for an isotropic elastic lattice obeying Newton's law, with specific assumptions on its elastic properties, that the behaviors of this lattice and of its topological defects display "all" known physics. Indeed, this *theory of crystalline ether* contains intrinsically and allows one to deduce directly the various formalisms of electromagnetism, special relativity, general relativity, gravitation and quantum physics. It allows also one to give simple answers to some longstanding questions of modern physics, as the universe expansion, the big-bang, the dark matter and the dark energy, the particle spins or the quantum decoherence. But it appears above all a completely new scalar charge, the *curvature charge*, which has no equivalence in the modern physical theories, which creates a very small deviation to the equivalence principle of Einstein between inertial mass and gravitational mass, and which allows one to give very simple explanations of the weak asymmetry observed between matter and anti-matter, the origin of the weak interaction force, the formation of galaxies, the disappearance of antimatter from the universe, the formation of gigantic black holes in the heart of the galaxies and the nature of the famous dark matter. Moreover, by describing in this third version the crystalline ether by a *face-centered cubic lattice with axial symmetries*, one was able to identify a lattice structure whose topological defect loops coincide exactly with the complex zoology of elementary particles, and which allows to explain physically and quite simply the nature of the weak and strong forces, the existence of three families in the standard model as well as the asymptotic behavior of the strong force.

Gérard Gremaud received his diploma in physics engineering in 1974 and his PhD in 1981 at the Swiss Federal Institute of Technology of Lausanne (EPFL). From this date, he became responsible for research at EPFL. In 2005, he obtained the title of Professor of EPFL. In 2011, he has been awarded the Zener medal. Since 2012, he is honorary professor of EPFL. Research fields : dislocation dynamics, structural phase transitions, mechanical and tribological properties at nanoscale, mechanical properties of vibrated granular materials, mechanical spectroscopy.

Third version of the « popularized » book, revised and corrected, May 2021